Novel Approaches to Piperidine and Hydropyridine Derivatives

PAUL RICARDO GIRLING

Novel Approaches to Piperidine and Hydropyridine Derivatives

A thesis submitted in partial fulfilment of the requirements
for the degree of
DOCTOR OF PHILOSOPHY
At the Chemistry Department of Durham University

By Ricardo Girling

Supported by:

Declaration

The work described in this thesis is the work of the author unless indicated otherwise and has not previously been submitted to this or any other university for any other degree. The research was carried out between October 2009 and September 2012, under the supervision of Professor Andy Whiting.

Statement of Copyright

Ricardo Girling
September 2012

Abstract

Three new modes of reactivity are reported between the reaction of an imine, but-3-en-2-ones and a Lewis acid. These are formal [2+2+2]-, [1+2+1+2]- and [4+2]-cycloadditions, deriving 1,1'-(1,2-dihydropyridine-3,5-diyl)diethanones **A**, 1,1'-(1,4-dihydropyridine-3,5-diyl)diethanones **B** and piperidin-4-ones **C** and **D** respectively. The [2+2+2]- and [1+2+1+2]-cycloadditions proceed when R^3 = LG (leaving group), with the [1+2+1+2]-pathway dominating when the imine is easily hydrolysed within the reaction conditions. When $R^3 \neq$ LG, the cycloaddition proceeds through different [4+2]-mechanistic pathways, dependent on how good a Michael acceptor the enone is.

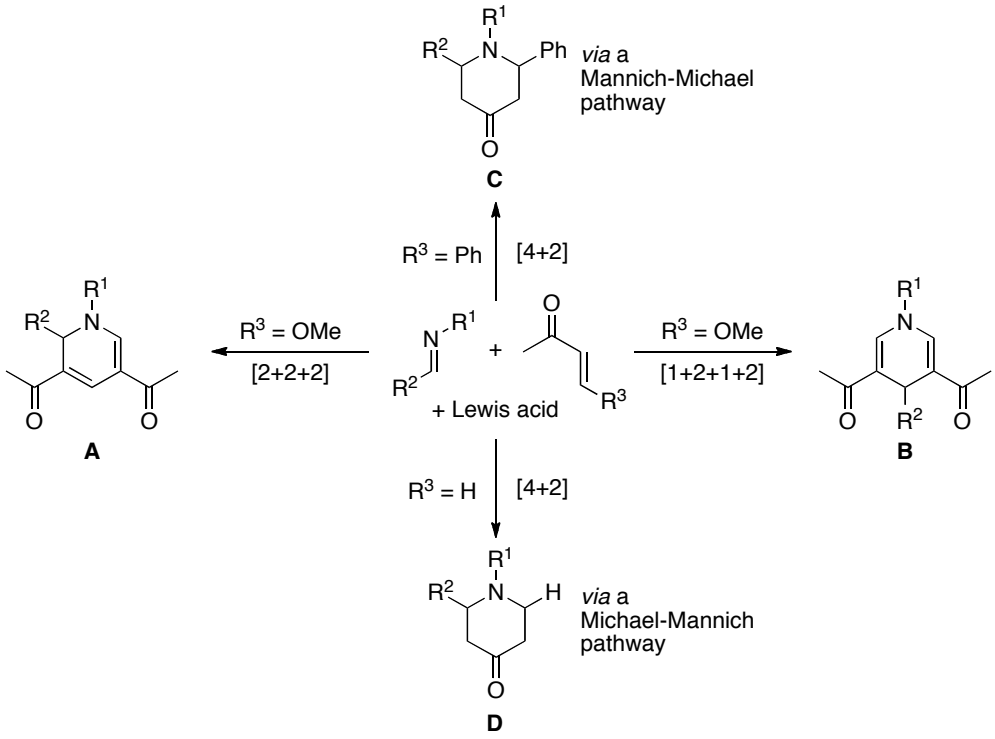

In addition, this work presents the asymmetric synthesis of aminoboronic acid **E**. Its activity as a bifunctional organocatalyst was explored and it was found that partly due to boron-nitrogen chelation, this catalyst was inactive within the aza-Diels-Alder, aldol and Mannich reactions, although active within the Michael reaction. Nonetheless, this catalyst was found to be active when performing the aldol reaction in high concentrations, in order to predominantly afford double aldol products.

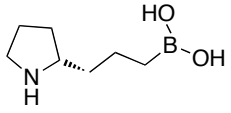

E

Acknowledgements

I would first like to sincerely thank my academic supervisor Prof. Andy Whiting for taking me on this exciting project and for his continued enthusiasm, motivation and support during my PhD.

Secondly, I would like to thank Merck & Co. (formerly Schering-Plough, Newhouse, UK) for funding this project, and in particular my respective industrial supervisors Dr. Hong Shen and Dr. Takao Kiyoi for their eager support and assistance along the way.

In addition, I am grateful for the analytical services, both at Durham University and Merck (Rahway, US), including NMR spectroscopy, mass spectrometry, chromatography and elemental analysis. In particular, I would like to thank Dr. Andrei Batsanov for performing the X-ray crystallography, Dr. Paul Yeo for running the biological experiments, and the EPSRC National Mass Spectrometry Service at Swansea for performing mass spectrometry on some of the more sensitive samples.

A special recognition goes to everyone in the Whiting group and Merck labs past and present, along with all the friends I have made during my PhD, for making my time at Durham an enjoyable experience and for all the help I have received. This includes (although not limited to) Fathia, Andy, Ben, Vicki, Hayley, Nim, Garr-Layy, Adam, Farhana and Hesham. In particular, I would like to express thanks to Craig and Irene for sharing their experience and knowledge, with a big thank-you going to Dr. Alex Gehre for proofreading this thesis.

Finally, I am forever indebted to my family for their unwavering love and support throughout my studies.

Para Abuela
y Nanny

Contents

ABBREVIATIONS

Å	angström(s)
Ac	acetyl
aq	aqueous
Ar	aromatic
ASAP	atmospheric solids analysis probe
BINAP	2,2'-bis(diphenylphosphino)-1,1'-binaphthyl
BINOL	1,1'-bi-2-naphthol
Bn	benzyl
Boc	*tert*-butoxycarbonyl
bp	boiling point
br	broad
Bz	benzoyl (not benzyl)
t-Bu	*tert*-butyl
°C	degrees Celsius
CH_2Cl_2	dichloromethane
CI	chemical ionisation
cod	*cis,cis*-1,5-cyclooctadiene
d	doublet
de	diastereomeric excess
DEPT	distortionless enhancement by polarisation transfer
dppe	1,2-bis(diphenylphosphino)ethane
DMSO	dimethyl sulfoxide
dr	diastereomeric ratio
DSD	dodecyl sulphate
ee	enantiomeric excess
EI	electron ionisation
ES	electrospray
Et	ethyl
Et_2O	diethyl ether
EtOAc	ethyl acetate
g	gram(s)
GC	gas chromatography
h	hour(s)
HMQC	heteronuclear multiple quantum correlation

HPLC	high performance liquid chromatography
HSQC	Heteronuclear single quantum correlation
HRMS	high resolution mass spectroscopy
Hz	hertz
IPA	isopropanol
IR	infra-red
J	coupling constant (in NMR spectroscopy)
k	kilo
K	Kelvin(s) (absolute temperature)
L	liter(s)
LA	Lewis acid
LCMS	liquid chromatography-mass spectrometry
LG	leaving group
lit.	literature
LRMS	low resolution mass spectroscopy
LW	long-wave
M	molar
m	multiplet; milli
M+	parent molecular ion
Me	methyl
MeCN	acetonitrile
MeOH	methanol
min	minute(s); minimum
mol	mole(s)
m.p.	melting point
M.S.	molecular sieves
MS	mass spectrometry
NMI	*N*-methylimidazole
NMR	nuclear magnetic resonance
NOE	nuclear Overhauser effect
NOESY	nuclear Overhauser effect spectroscopy
Ph	phenyl
piv	pivaloyl
PMP	*para*-methoxyphenol
PNP	*para*-nitrophenol
ppm	part(s) per million
Pr	propyl
i-Pr	isopropyl

n-Pr	normal (primary) propyl
psi	pound(s) per square inch
q	quartet
quin	quintet
R_f	retention factor (in chromatography)
RSV	respiratory syncytial virus
rt	room temperature
s	singlet
sat.	saturated
SDS	sodium dodecyl sulphate
t	triplet
TBAF	tetrabutylammonium fluoride
TBAT	tetrabutylammonium triphenyldifluorosilicate
TBPA+	tris(4-bromophenyl)-aminium hexachloroantimonate
TFA	trifluoroacetic acid
THF	tetrahydrofuran
TLC	thin layer chromatography
TMEDA	tetramethylethylenediamine
TMG	tetramethylguanidine
TMS	trimethylsilyl
TMSCl	chlorotrimethylsilane
TOCSY	total correlation spectroscopy
TOF	time-of-flight
t_R	retention time (in chromatography)
triflate	trifluoromethanesulfonate
Ts	*para*-toluenesulfonyl (tosyl)
UV	ultra violet
wt	weight

Chapter 1:
INTRODUCTION

1. INTRODUCTION

The piperidine ring system[1] is widely found within nature[2] with the natural products possessing these ring systems showing a wide range of biological activities.[3] Consequently, there is considerable interest in these types of compounds[4] due to their medicinal properties[5] and as a result, many analogues have been developed as therapeutic agents.[6] One way of constructing these six-membered rings is *via* an aza-Diels-Alder reaction involving an imino dienophile and a conjugated diene. The cycloaddition can be either a relatively concerted process with less polarised dienes.[7] However, when using more electron rich dienes (*i.e.* oxygenated dienes or enone equivalents), only a formal Diels-Alder process occurs, generally assisted by an activating agent such as a Lewis acid[8] or an organocatalyst.[9] In this introduction, we investigate the development of the formal cycloaddition of imino dienophiles with highly electron rich dienes and enones to derive tetrahydropiperidine frameworks and compare the different reaction conditions, reagents and applications as well as the mechanisms which are operating.

1.1 aza-Diels-Alder Reaction

The Diels-Alder reaction is a classic example of a concerted pericyclic cycloaddition between a conjugated diene **1** and a dienophile **2** in order to form a cyclohexene ring **3** (Equation 1). Otto Diels and his student Kurt Alder first documented this simple reaction in 1928, which instantaneously opened up new gateways in organic synthesis and quickly became widely used. As a result, they were awarded the 1950 Nobel Prize in Chemistry "for their discovery and development of the diene synthesis" (Nobel Foundation).

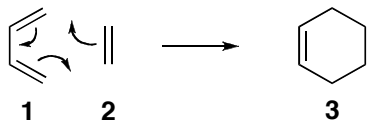

Equation 1

The fundamental difference in the aza-Diels-Alder reaction is the exchange of a carbon for a nitrogen atom (typically in the dienophile), resulting in the formation of a six-membered nitrogen-containing tetrahydropyridine (or equivalent). The aza-Diels-Alder reaction may occur in a concerted manner, however, in many cases, the reaction may be better thought of as a step-wise Mannich followed by an intramolecular Michael reaction. Both concerted and Mannich-Michael processes might be assisted by the use of catalysts, including Lewis acids and organocatalysts, and this is the subject of this project.

The Lewis acid-catalysed approach to achieving overall aza-Diels-Alder addition relies upon activating the imine, which in turn activates the initial Mannich reaction to proceed. In contrast, the organocatalytic approach is generally based upon activating the diene (in the form of an α,β-unsaturated ketone) through the formation of an enamine. As such, the organocatalytic process tends to involve chiral pyrrolidine-derived systems which permit asymmetric induction to be developed, with the simplest and most commonly available catalyst being L-proline.[10]

Earlier research has tended to concentrate on Lewis acid-catalysis[11] due to their relative availability and versatility. However, in recent years there has been a shift towards organocatalysis because it is possible to achieve high enantioselective transformations.[12] This shift in concentration has been brought about by the increasing importance of organocatalysis in the last decade,[13] and our understanding of the underlying concepts that has enabled application on different systems,[14] including the aza-Diels-Alder reaction.

1.2 Asymmetric Construction using Lewis acids

In 1974, Danishefsky *et al*. reported on "a useful diene for the Diels-Alder reaction", where they explained the formation of an electron rich diene in the form of a silyl enol ether **4**, suggesting that it can be used as an activated diene in the Diels-Alder reaction to mask carbonyl groups. This compound has ever since been known as the Danishefsky diene **4**.[15] Over the years, Danishefsky *et al.* have successfully investigated the use of this diene in the concerted Diels-Alder reaction, including the use of enones **5** as dienophiles carried out under thermal (uncatalysed) conditions.[16] They went on to find that aldehydes **6** could undergo "cyclocondensation" with the Danishefsky diene **4** in the presence of Lewis acids (Scheme 1).[17]

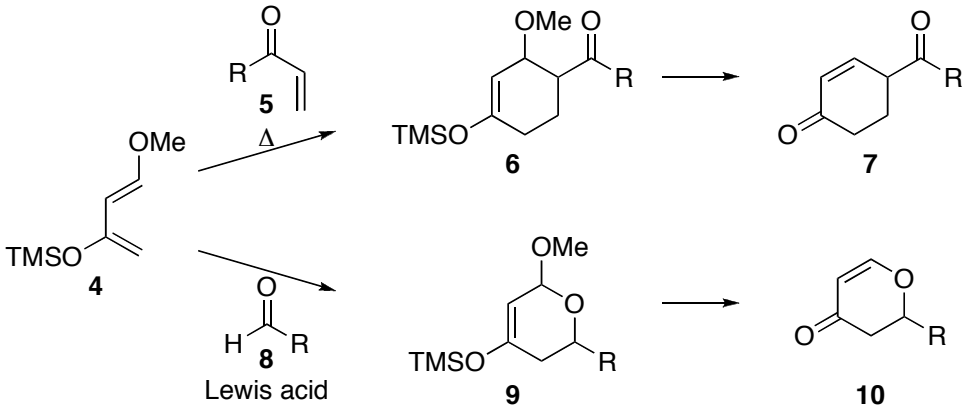

Scheme 1. The Diels-Alder reaction between Danishefsky's diene **4** and an enone **5** or an aldehyde **8**.

In the early 1980s, Danishefsky *et al.* reported the first general cycloadditions involving simple, unactivated imines **11**, catalysed by Lewis acids to form piperidine rings **12**.[18] This formal aza-Diels-Alder reaction was shown to work between diene **4** and α,β-unsaturated imines **11** in the presence of zinc(II) chloride ($ZnCl_2$)[19] (Equation 2). The reactions were relatively slow (1-2 days), with stoichiometric amounts of Lewis acid and a large excess (4 equivalents) of the diene being required.

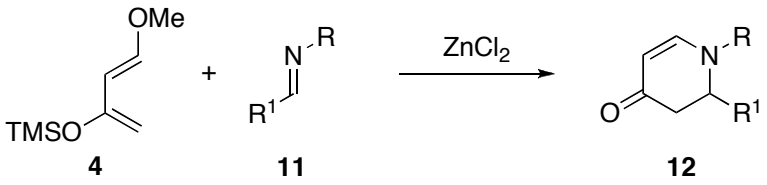

Equation 2

This methodology was later used in the synthesis of various alkaloids.[20] Analogously to the use of aldehydes **8** over imines **11**, it was mentioned that the mechanism went through either a concerted or Mannich-Michael process.[21] However, with the lack of evidence to disprove the concerted theory, Danishefsky *et al*. went on to describe Lewis acid catalysed aza-Diels-Alder reactions as a "cyclocondensation reaction". [22]

This aza-Diels-Alder procedure was subsequently tried and tested by numerous research groups. Some groups followed the procedure without focusing on the mechanism,[23] whilst others questioned the presence of a Mannich product **13**, acknowledging the possibility of two conceivable mechanisms for this reaction.[24] The observation of Mannich products led some to believe that this Diels-Alder process is probably a "non-synchronous concerted one".[25] It was also found that instead of the Danishefsky diene, the silyl enol ether of acetyl cyclohexene **14** could also be used.[26]

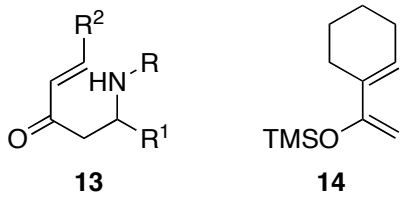

Meanwhile, Raithby *et al*. formed bicyclic ring **19** from an electron deficient imine **16** and an electron rich diene **15** in the presence of a Lewis acid, during which they observed the minor Mannich product **20**. They proposed that the mechanism could either be: a) concerted; b) stepwise; or c) even occur simultaneously in competition with each other (Scheme 2).[27] They also suggested that varying the reaction conditions (such as solvent and temperature) makes the reaction proceed through a different process.[28]

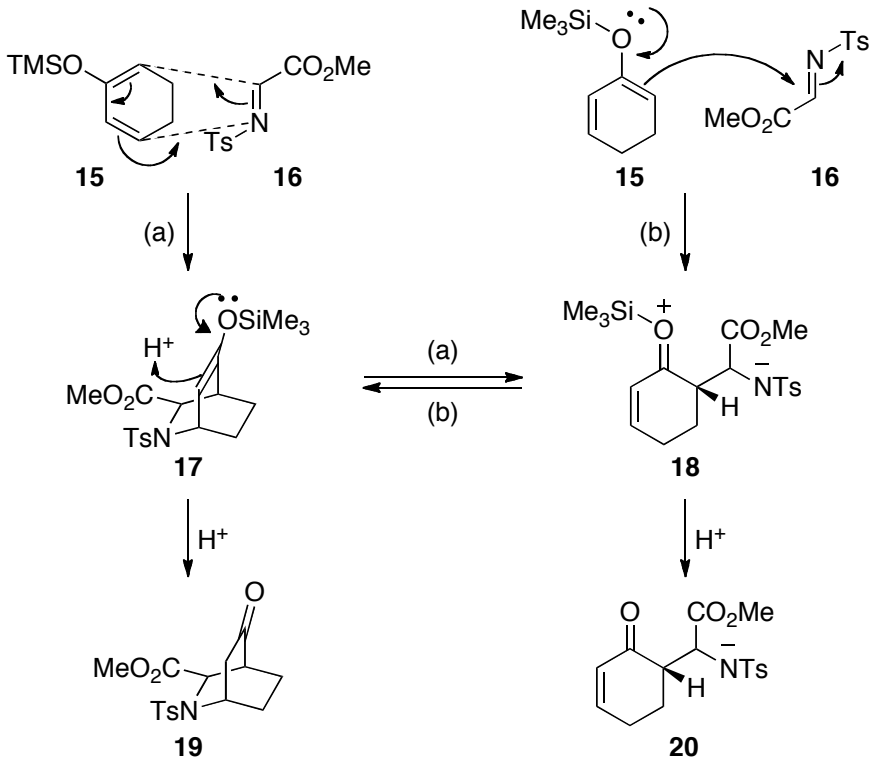

Scheme 2. Proposed competing mechanism for the formation of products **19** and **20**.

In their aza-Diels-Alder reactions, Kunz *et al.* used the more active $ZnCl_2$ etherate as their Lewis acid and have argued that this process initially proceeds *via* a Mannich reaction followed by a cyclisation *via* nucleophilic intramolecular attack of the intermediate amine **23**. In their examples, imines attached to a sugar acting as a chiral auxiliary **22** were reacted highly selectively with the Danishefsky diene **4** in the presence of stoichiometric amounts of $ZnCl_2$ to give high yields of the piperidine ring **24**. They showed that if the reaction was stopped after 2-12 hours with aqueous ammonium chloride solution, the Mannich compounds **23** could be isolated. After direct acid hydrolysis of either the reaction mixture or isolated Mannich products **23**, the subsequent Michael addition occurs immediately. This is followed by elimination of methanol to give the desired unsaturated piperidine ring **24**; thus proving the reaction proceeds *via* a Mannich-Michael mechanism (Scheme 3).[29] It was also shown that the Mannich product **23** governs the diastereoselectivity of the Michael product **24**.

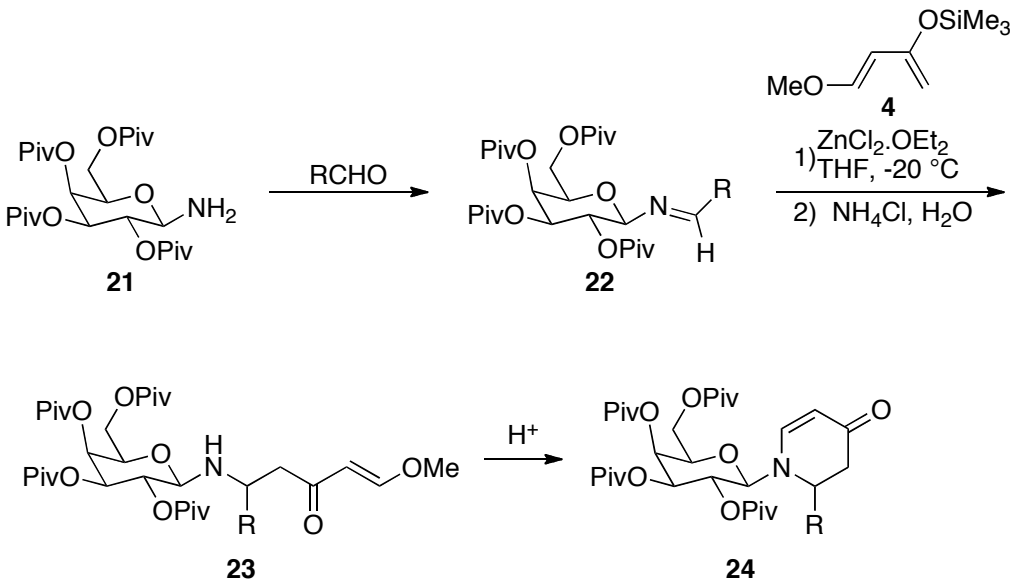

Scheme 3. Kunz's procedure for piperidine ring formation using sugars as chiral auxiliaries.

Changing the R substituent of the imine did not make a difference to the reaction unless R was a large group; in such cases the yields started to diminish.[30] The sugar **29** was subsequently recovered almost quantitatively after acidic cleavage of the *N*-glycosidic bond. Through this method the tobacco alkaloid (*S*)-anabasin **28** was successfully synthesised in a few steps (Scheme 4).[31]

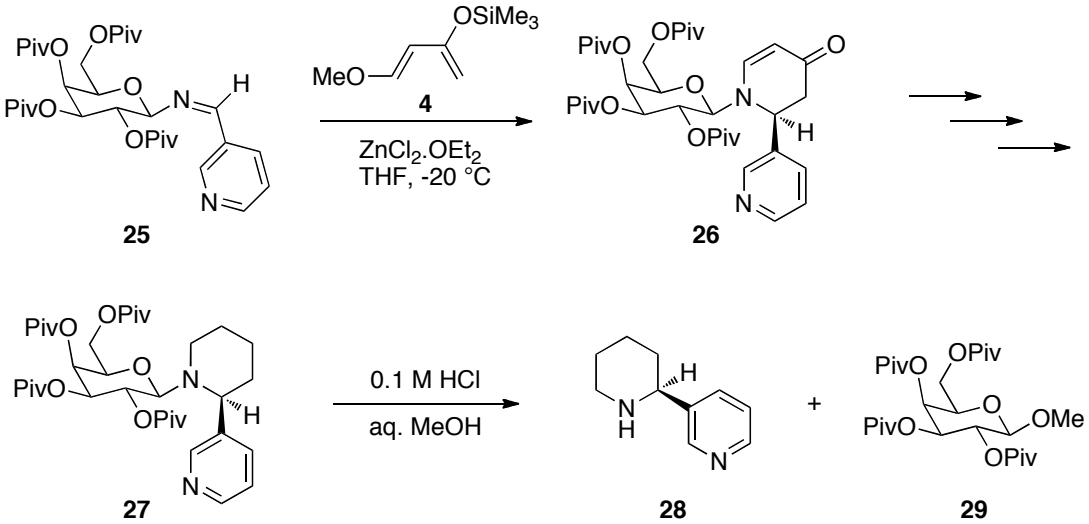

Scheme 4. The route taken for the formation of (*S*)-anabasin **28**.

With the rise of resin-bound solid phase chemistry in the last decade, resin-bound aryl dialkylsilyl ethers have been used in numerous syntheses of oligosaccharides,[32]

glycopeptides,[33] polyketides[34] and prostaglandins[35] to name but a few. Accordingly, Kunz *et al*. bound their chiral auxiliaries to dialkylsilyl resins **30** in order to facilitate the isolation of their subsequent piperidine ring products **32** (Scheme 5). In this case, five equivalents of $ZnCl_2$ were used in THF at rt, the reaction taking two days.[36]

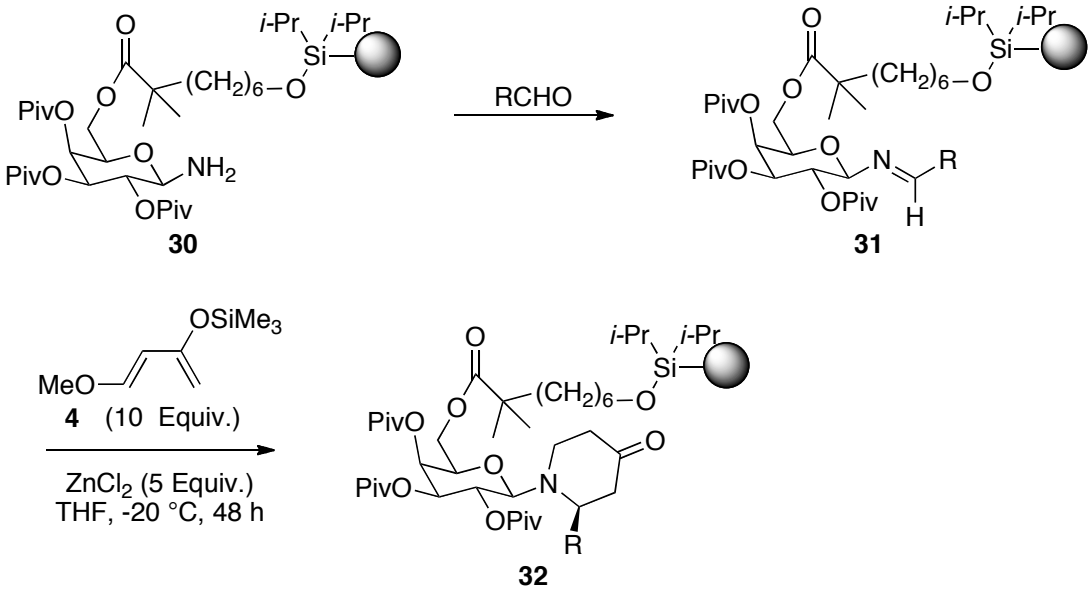

Scheme 5. Kunz *et al*.'s procedure using sugars bound to a resin.

Through the use of amino acids as chiral auxiliaries on the imine **33**, Waldmann *et al*. have shown that in the presence of stoichiometric amounts of $ZnCl_2$, the electron rich Danishefsky's diene **4** was sufficiently reactive to react with unactivated imines **33** to form unsaturated piperidine ring structures **36** and **37**. The chiral auxiliary was subsequently removed in a few steps.[37] Depending on the imine used, poor to moderate yields were obtained with good enantioselectivity. When performing this reaction with different imines, it was noticed that the electronics of the imine substituent (R^1) did not influence the reaction outcome. Additionally, if the reaction were concerted, it would have proceeded *via* intermediate **34**. However, by-product **38** from one of the reaction mixtures was isolated, most probably formed by nucleophilic attack of a free amino acid ester, meaning the reaction must have gone through intermediate **35**. This suggested that the reaction proceeded *via* a Mannich-Michael process (Scheme 6).

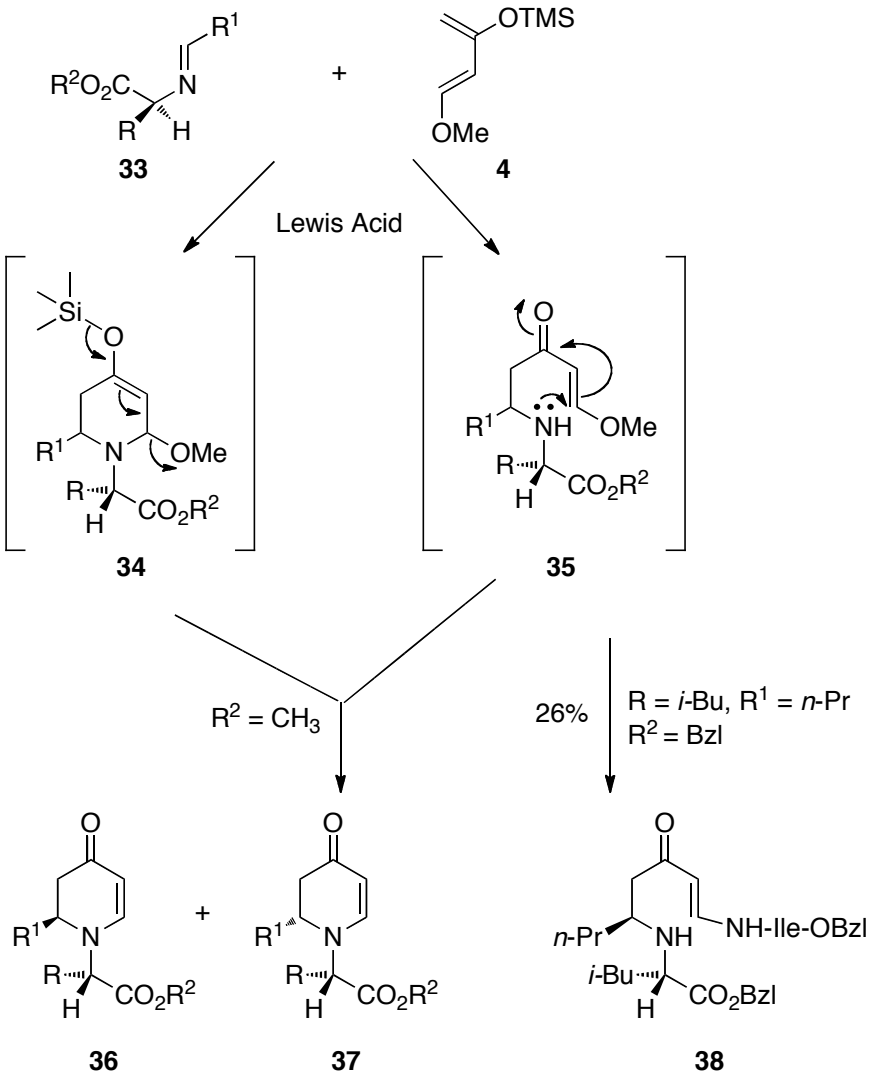

Scheme 6. aza-Diels-Alder reaction using amino acids as chiral auxiliaries.

It was also found that chelating Lewis acids (such as $ZnCl_2$ and $TiCl_4$) afforded the same stereoisomers as non-chelating Lewis acids (such as boron and aluminium). The non-chelating Lewis acids would coordinate with the nitrogen of the imine **41** to form the conformation **42** as explained in the Felkin-Anh model[38] for nucleophilic addition to carbonyl groups. According to this model, attack of the diene happens on the *re*-face. The opposite would then be expected with chelating Lewis acids as they can also chelate to the oxygen of the carbonyl group. However, under the reaction conditions ($ZnCl_2$: 0 °C to -20 °C; $TiCl_4$: warming from -78 °C to rt) the imine double bond is isomerised as previously reported by Ojima *et al.*,[39] and hence, the diene also attacks from the *re*-face to give the same diastereoisomer **40**. Conversely, having two equivalents of $ZnCl_2$ affords the opposite diastereoisomer **39** (Scheme 7).

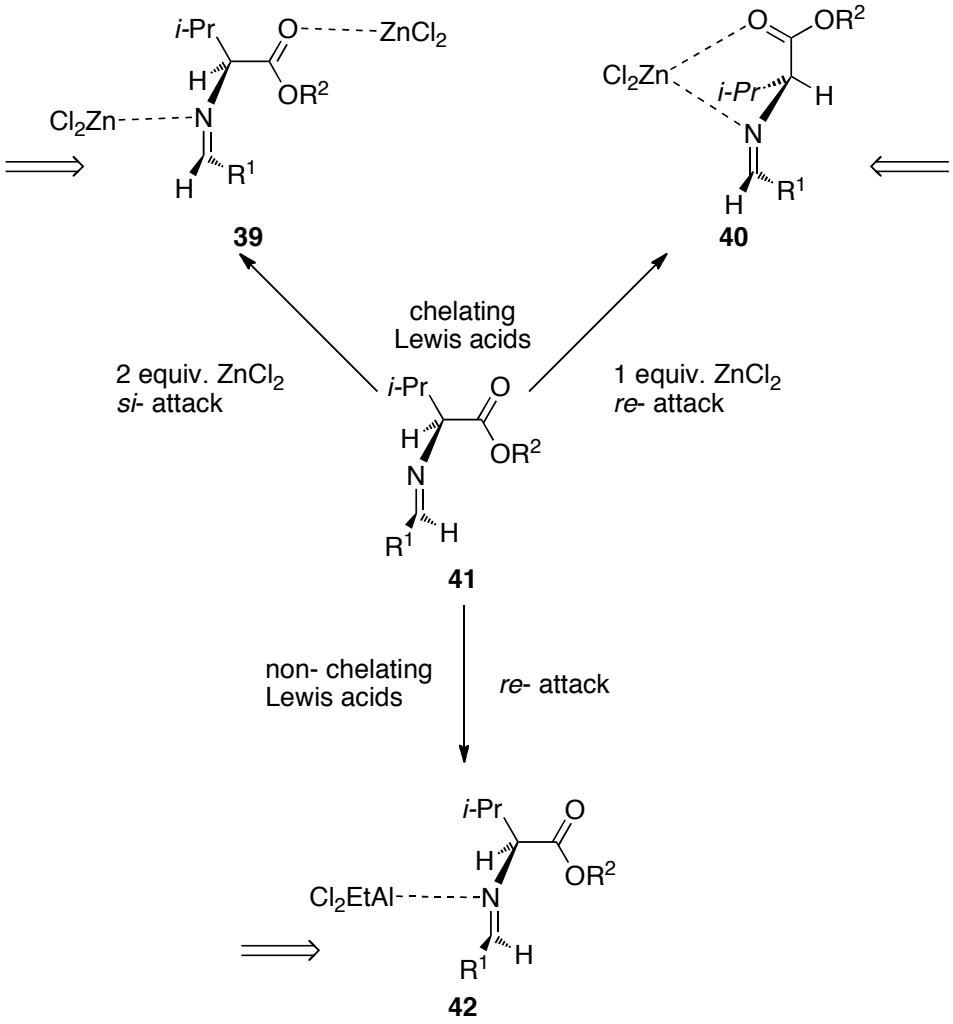

Scheme 7. The different sides of attack to **41**.

Weinreb *et al*. have shown the imine **44** can also cyclise with silyl enol ether **43** to give unsaturated piperidine rings **45** and **46** in moderate yields.[40] When using catalytic amounts of $ZnCl_2$, the *syn*-piperidine ring **45** was obtained in a ratio of 22:1 to *trans*-**46**, which was a higher dr than when using $AlCl_3$ as a Lewis acid. If needed, the *syn*-product **45** could be isomerised to the *anti*-product **46** by refluxing with *p*-TsOH in benzene (Scheme 8).

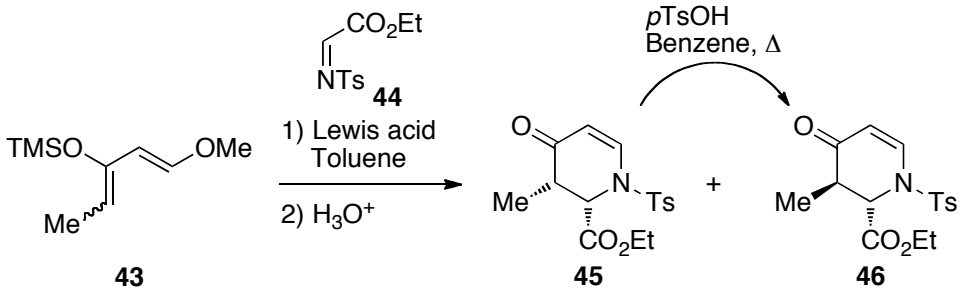

Scheme 8. Formation of **46** from **43**, showing improved yield from conversion of **45**.

By screening multiple Lewis acids, Gálvez *et al*. further demonstrated that the Lewis acid catalysed aza-Diels-Alder reaction between **4** and **47** showed good stereoselectivity towards diastereoisomer **48**, regardless of the complexing properties (Equation 3). The best selectivity was observed with stoichiometric amounts of ZnI_2, followed by Et_2AlCl and $BF_3.Et_2O$, whilst the Lewis acids $MgBr_2$, $Eu(fod)_3$, $SnCl_4$ and $TiCl_4$ seemed to be inactive.[41] Various solvents were also screened with the best results being obtained using acetonitrile followed by dichloromethane, tetrahydrofuran, diethyl ether, and lastly, toluene. This suggested that polar solvents may be important in stabilising the chelated intermediate. However, the diastereoisomers proved challenging to separate, whilst higher temperatures were needed when using less reactive imines in order to obtain acceptable yields. Mannich intermediates were also observed, suggesting the aza-Diels-Alder reaction proceeds *via* a Mannich-Michael process.

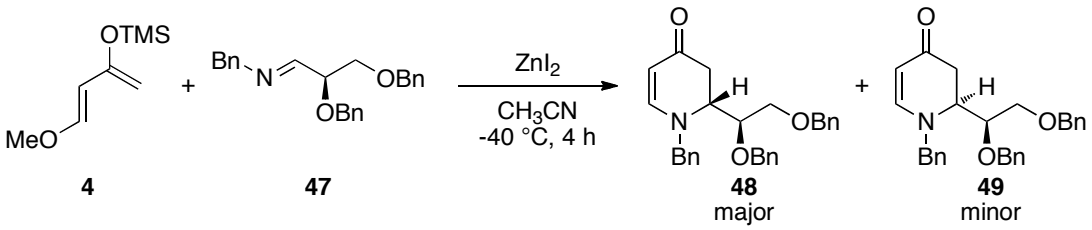

Equation 3

Imines with the nitrogen attached to an aromatic ring such as compound **50** can undergo a Lewis acid catalysed imino-Diels-Alder reaction with an alkene **51** to form a ring fused piperidine **52** (Equation 4). Hence, the imine **50** acts as a heterodiene, which is activated by the Lewis acid.[42]

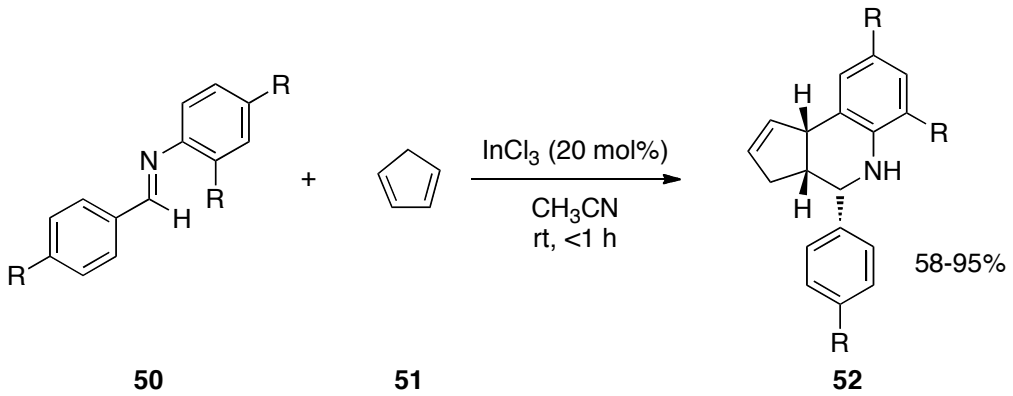

Equation 4

This high-yielding reaction is completed in under an hour with the Lewis acid $InCl_3$ present in 20 mol%. However, when changing the alkene **51** to a cyclohexenone **54**, Perumal *et al*. observed that bicyclic rings **56** and **57** were formed with poor selectivity instead of **55**. This shows that when enones **54** are present, these are activated over the imines **53** by the Lewis acid (Scheme 9). Despite the poor selectivity, it was thus serendipitously shown that the aza-Diels-Alder reaction could be performed in the presence of catalytic amounts of Lewis acid using unactivated diene equivalents, such as enone **54**.

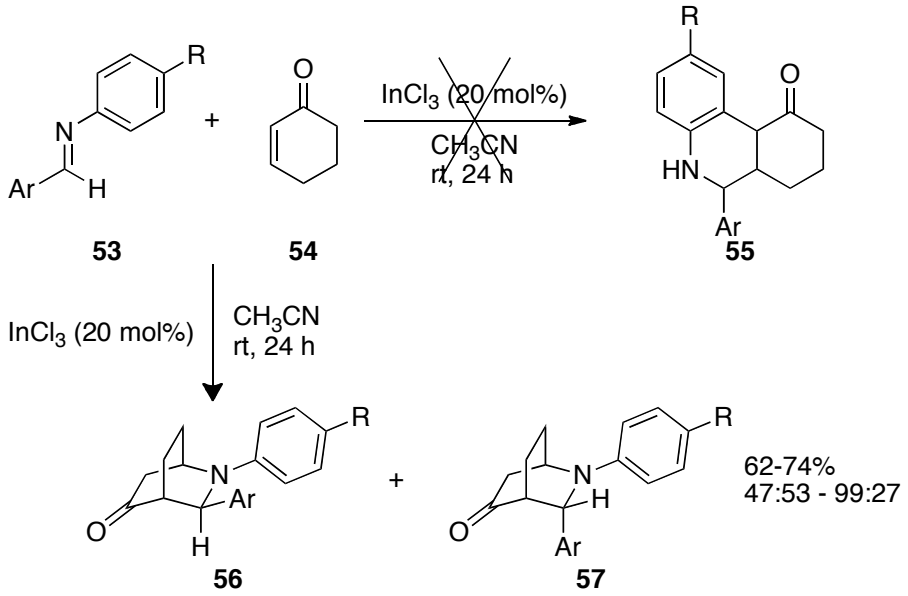

Scheme 9. Imine **53** acting as a dienophile, as opposed to a diene.

Enantioselective reactions of carbonyl compounds catalysed by chiral Lewis acids have been known for some time[43] although the analogous asymmetric reactions with imines took longer to be established.[44] This is partly due to the flexible (*E*,*Z*)-conformational structure of the imine double bond, the tendency to form enamines if an α-acidic proton is present, as well as the fact that some imines are highly unstable and cannot be isolated. However, the main reason is that the imine nitrogen is more Lewis basic than the oxygen of the carbonyl group, thus Lewis acids tend to strongly coordinate to the nucleophilic nitrogen atom of the reactants or product, which can result in inhibition or decomposition of the chiral Lewis acid complex and low catalyst turnover. Hence, for a long time, stoichiometric amounts of Lewis acids have been needed.[45]

In 1998 Kobayashi *et al*. reported the first catalytic use of a chiral Lewis acid for the enantioselective aza-Diels-Alder reaction between an imine **11** and the Danishefsky diene **4**. They used 20 mol% of a chiral zirconium catalyst based on complexes with substituted 2,2`-binaphthol (BINOL), obtaining ee as high as 93%.[46] From Zr(IV)[47] they subsequently went on to investigate chiral niobium Lewis acids.[48] Their preferred catalyst **58** was formed *in situ* from ligand **59** and $Nb(OMe)_5$ in the presence of *N*-methylimidazole (NMI).

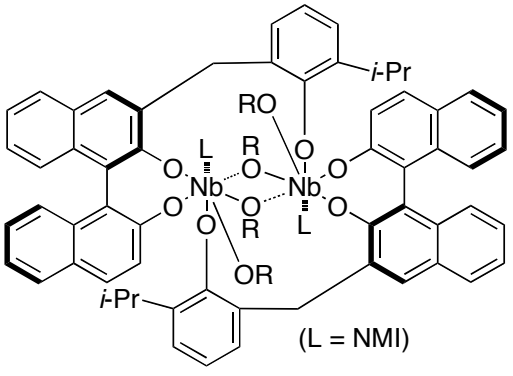

58

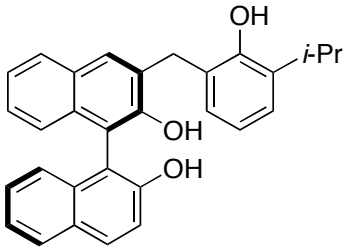

59

The catalyst **58** has been shown to give highly enantioselective unsaturated piperidine rings **61** from a silyloxy diene **60** and an aromatic or aliphatic imine **11** (Equation 5).

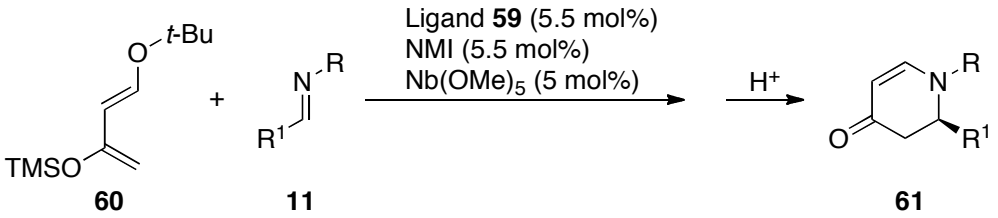

Equation 5

Meanwhile, Jørgensen *et al*. have formed piperidine ring **62** from imine **44** and the Danishefsky diene **4** with the aid of catalytic amounts (10 mol%) of Lewis acid.[49] The catalyst was made up of a metal Lewis acidic salt and a chiral ligand to induce asymmetry. Different metal salts that were screened include $CuClO_4 \cdot 4MeCN$, $2CuOTf \cdot C_6H_6$, $CuPF_6 \cdot 4MeCN$, $Cu(OTf)_2$, AgOTf, $AgSbF_6$, $AgClO_4$, $Pd(SbF_6)_2$, $Pd(ClO_4)_2$, $Pd(OTf)_2$, $RuSbF_6$ and $Zn(OTf)_2$. The chiral ligands were either BINAP **64** or phosphino-oxazoline systems, which were individually synthesised.[50] The best combination was found to be a phosphino-oxazoline-copper(I) catalyst, which afforded up to 96% yield and 87% ee. X-ray analysis suggests that the reaction proceeds *via* a Mannich-Michael process, evidence that was further supported by the detection of Mannich product intermediate **63** in some reactions (Equation 6).

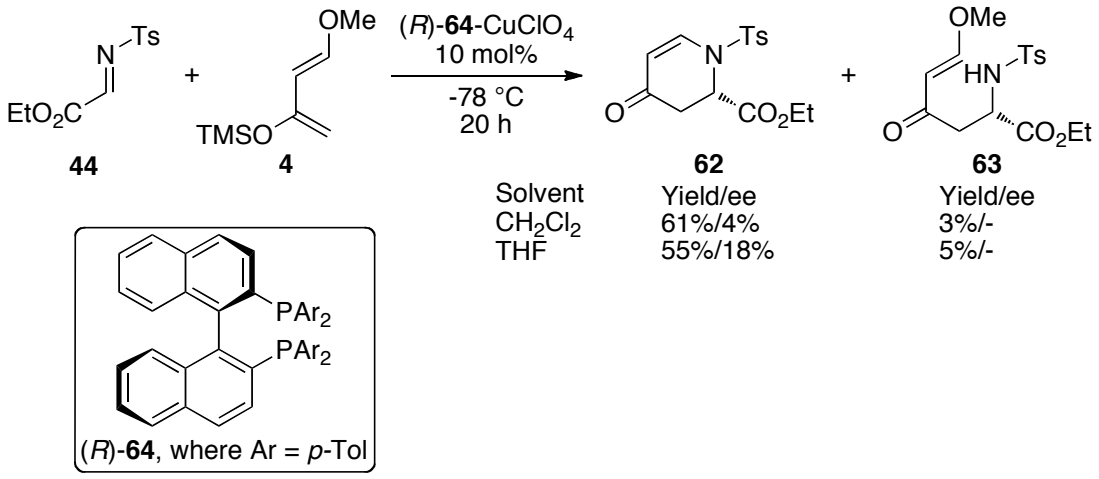

Equation 6

Within the aza-Diels-Alder reaction, isoquinolines **66** have been shown by Langer *et al*. to act as a *N*-dienophile when reacted with electron rich dienes **65** and stoichiometric amounts of Lewis acids. The reaction proceeds in a stepwise fashion, with the Lewis acid activating the imine to **68**. Hence, nucleophilic attack by the

Brassard's type diene **65**[51] affords intermediate **69**. Treatment of **69** with two equivalents of trifluoroacetic acid (TFA) aids in the tautomerisation of the carbonyl to the enol, as well as activation of the imine **70** for a subsequent intramolecular Michael addition. The result was a new piperidine ring **71** exhibiting an enol over a ketone (Scheme 10). The enol form is more stable by 3.3 kcal mol^{-1}, which is partly due to the adjacent electron withdrawing ester group.[52] This methodology has been used to form simple structural analogues of morphine.

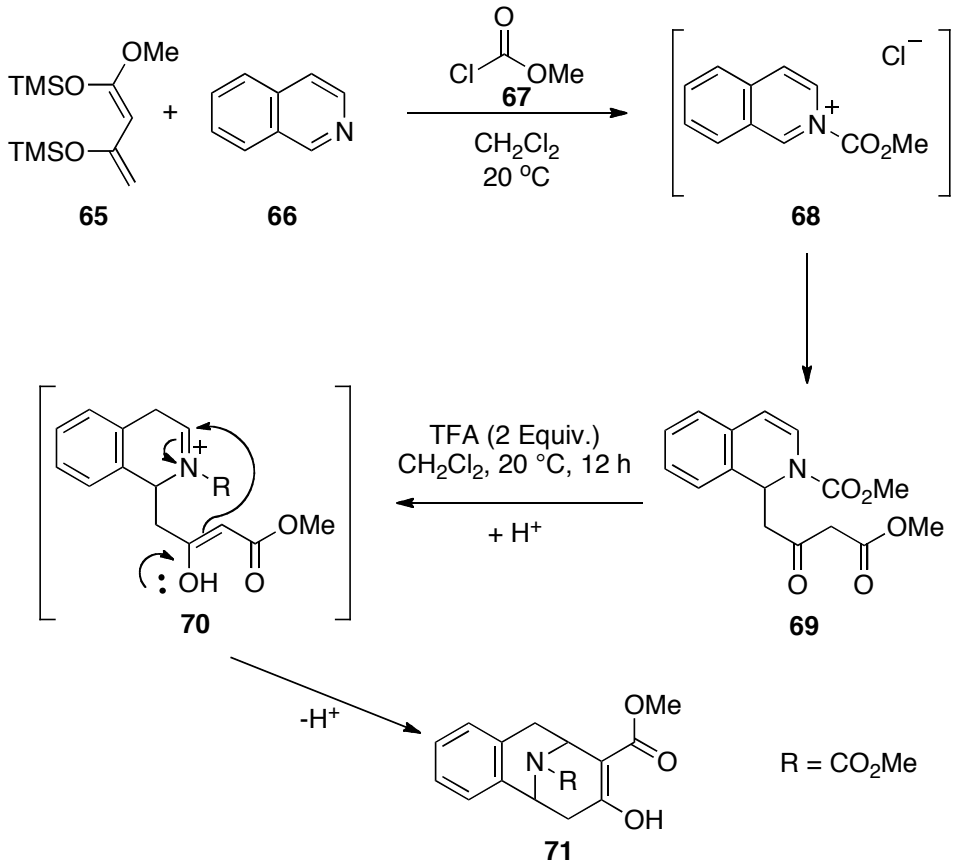

Scheme 10. Using of Brassard's diene **65** for the formation of new piperidine rings.

The use of ytterbium(III) triflate[53] was shown by Whiting *et al*. to catalyse the aza-Diels-Alder reaction asymmetrically.[54] However, as with many aza-Diels-Alder examples, these reactions proved difficult to reproduce and scale up,[55] which prompted the development of robust catalytic asymmetric methods. Prior to this, it was necessary to clearly understand the reaction mechanism as it was generally accepted that the aza-Diels-Alder reaction could either proceed through a concerted (either standard or inverse electron-demand Diels-Alder cycloadditions) or a stepwise

process. Indeed, after screening various dienes against electron-deficient imines in the presence of Lewis acid under different conditions, the isolated piperidine ring products gave evidence towards all three reaction pathways. However, the intermediates that were subsequently isolated showed that a stepwise addition-cyclisation process derived by imine activation of the Lewis acid could explain all the reactions.[56] Further investigations into this reaction to gather evidence for and against the different plausible mechanisms resulted in findings that disproved a concerted mechanism, thus suggesting that a stepwise Lewis-acid catalysed process was occurring.[57]

Zinc(II)-BINOL has been shown to be an efficient asymmetric catalyst in the Diels-Alder reaction[58] as well as the hetero-Diels-Alder reaction between dienes and aldehydes.[59] Subsequently, Whiting *et al*. showed that zinc(II)-BINOL could also be used in the asymmetric aza-Diels-Alder reaction between electron deficient imine **72** and the electron rich Danishefsky's diene **4**.[60] Following on from this finding, they observed that this reaction, along with efficient asymmetric induction, was dependent upon the formation of a bidentate zinc-imine complex **74** (Scheme 11).[61]

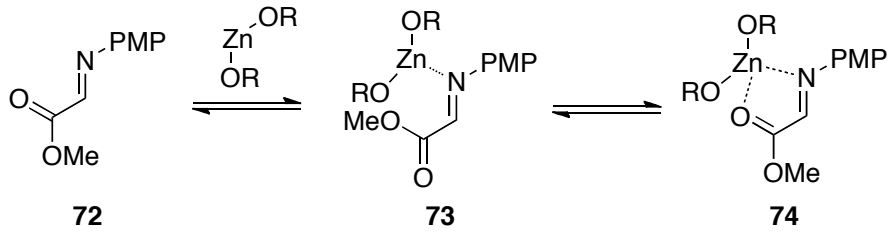

72 **73** **74**

Scheme 11. Binding of zinc(II)-BINOL to imine **72**.

As expected, the cycloaddition proceeds *via* a two-step process. The imine must be suitably activated for the initial Mannich-like step, which means that, when possible, the zinc(II)-BINOL forms a bidentate ligand with the imine (Scheme 11 and Scheme 12) (aromatic imines would form monodentate ligands).

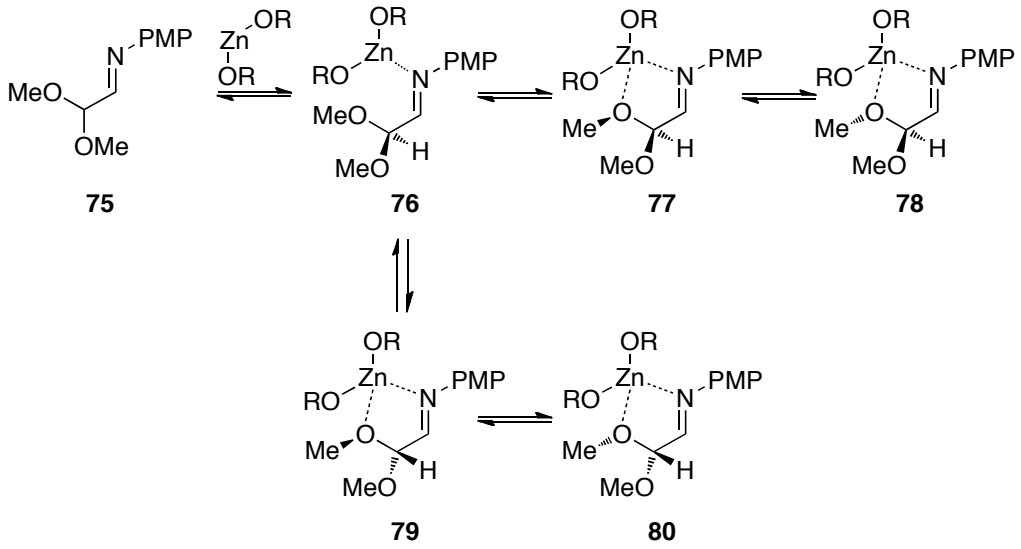

Scheme 12. Binding of Zn(II)-BINOL to imine **75**.

After formation of the bidentate ligand **80**, addition of the diene **4** to the imine **80** can take place. Ring closure of **83** is a slow process that can be accelerated with an acidic work up. As *S*-BINOL is used in this case, the *S*-enantiomer product **84** is obtained. However, a competing reaction of the activated iminium ion **82** with diene **4** forms the racemic product **84** through intermediate **85** (Scheme 13).

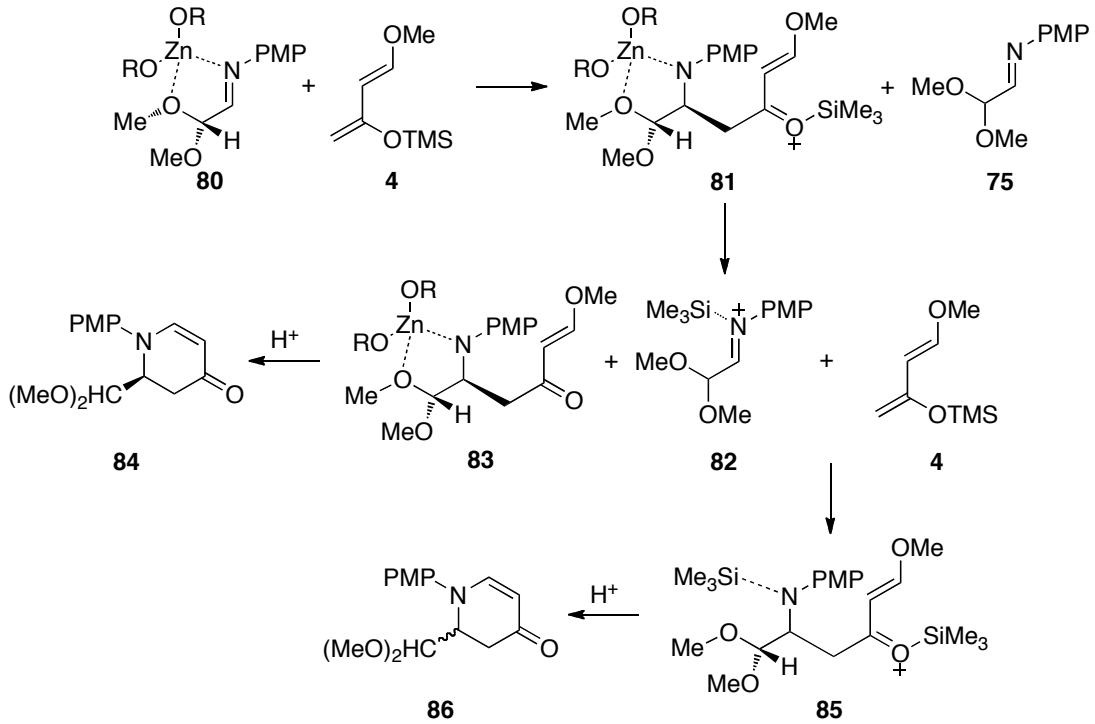

Scheme 13. Piperidine ring formation between Danishefsky's diene **4** and the imine-Lewis acid complex **80**.

For these reactions, there seem to be two competing effects. Firstly, the presence of a catalytic equilibrium between monomer and dimer complexes in solution is important, and secondly, low catalyst loadings seems to be less effective due to the likelihood of competing silicon transfer effects.

Iodine has been shown by Yao *et al*. to be effective as a Lewis acidic catalyst in the aza-Diels-Alder reaction.[62] These iodine-catalysed reactions can either be performed neat or at high concentrations. Additionally, as iodine is a strong Lewis acid, the reaction can be performed without the need of an electron rich diene such as Danishefsky's diene **4**. The best results were also obtained with the use of 0.5 equivalents of iodine. Hence, it was shown that aldehydes **8**, amines **86** and cyclic enone **87** react together in the presence of iodine to form fused piperidine rings **88** in 55-95% yield; the best yields were obtained when R^1 was electron withdrawing (Equation 7).

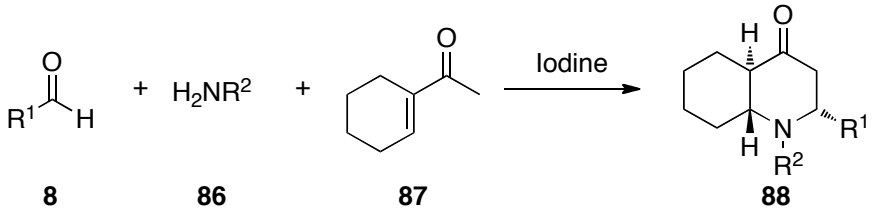

8 **86** **87** **88**

Equation 7

Similar results were observed when using cyclohexenone **54** as the diene source to form bicyclic compounds **93** and **94**. However, when using the 5-membered ring acetylcyclopentene **91** as opposed to the six-membered cyclohexenone **54**, the yields obtained for **92** were drastically diminished to less than 10% (Scheme 14). This may suggest that the spatial alignment of the enone is important in order for the aza-Diels-Alder reaction to proceed effectively.

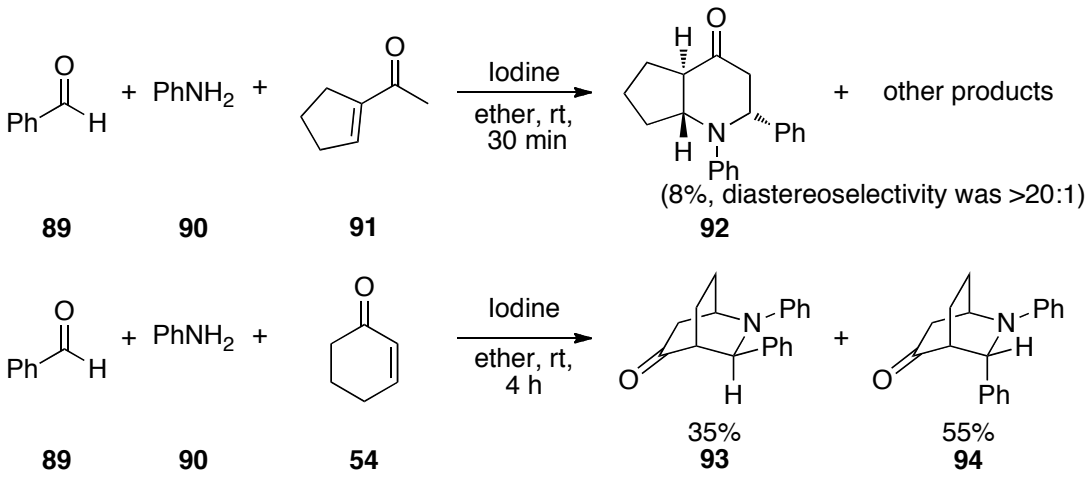

Scheme 14. Comparing acetylcyclopentene **91** and cyclohexenone **54** as the enone within the aza-Diels-Alder reaction.

Understanding that the aza-Diels-Alder reaction proceeds *via* a Mannich-Michael process, Hoveyda *et al*. optimised their silver catalysed Mannich reactions prior to performing the aza-Diels-Alder reaction between imines and the Danishefsky diene **4**.[63] These silver catalysed reactions required an additive (*i*-PrOH) and performed well in an atmosphere of air using THF as solvent. This was subsequently optimised into a three-component, one-pot synthesis using 5 mol% of the silver Lewis acid and 5 mol% of the chiral ligand **96** to give the desired piperidine ring **97** in good yield and high diastereo- and enantio-selectivity (Equation 8).

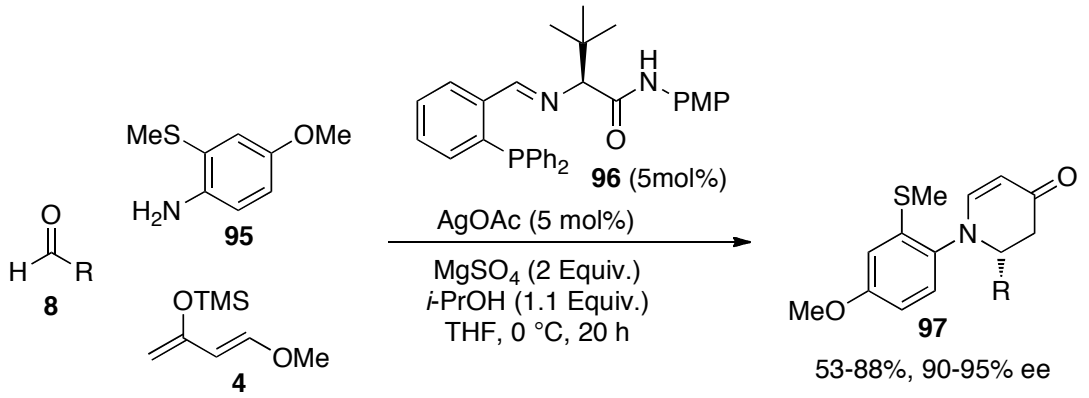

Equation 8

The Lewis acid catalysed aza-Diels-Alder reaction has also been shown to be useful in the formation of indolizidines **103**, an important biologically active class of alkaloids found in numerous natural products.[64] An imine such as **101** derived from

allylsilane amine[65] has been shown by Furman *et al*. to be necessary to react smoothly with Danishefsky's diene **4** in the presence of 10 mol% $Yb(OTf)_3$ in order to form the piperidine ring **102** in good yields.[66] Nonetheless, it was subsequently found that the best chiral Lewis acid at their disposal was the chiral boron complex **100**, which was used in stoichiometric amounts. This boron complex was formed *in situ* from **98** and **99** (Equation 9).[67]

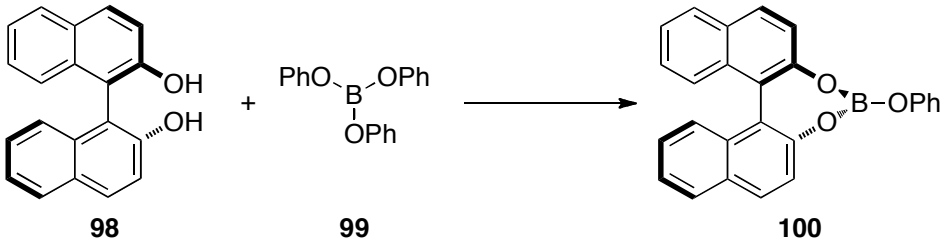

98 **99** **100**

Equation 9

The key step to form the indolizidine **103** involves a cyclocondensation reaction in the presence of tetrabutylammonium triphenyldifluorosilicate (TBAT).[68] This reaction is stereospecific, the stereochemistry subsequently proved through circular dichroism spectroscopy (Scheme 15);[67] a technique first used on such systems by Whiting *et al*.[57]

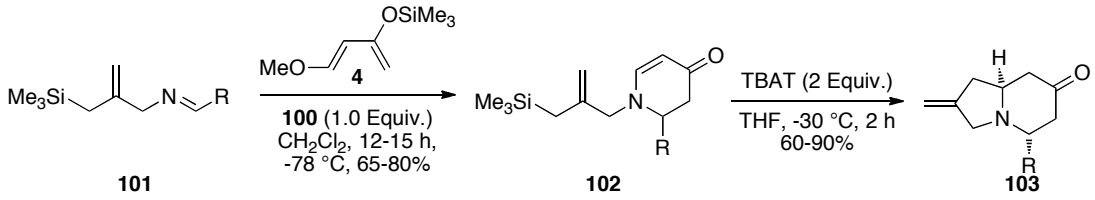

101 **102** **103**

Scheme 15. A route to indolizidines *via* the aza-Diels-Alder reaction.

The use of silicon Lewis acids within the aza-Diels-Alder reaction between hydrazone **105** and Danishefsky's diene **4** has been investigated by Leighton *et al*.. Good yields and high enantioselectivities (up to 85% and 92 % respectively) were generally observed with these reactions.[69] There seems to be a strong solvent effect when using silicon Lewis acids, shown by the observation that using dichloromethane instead of toluene gives the opposite enantiomer of the aza-Diels-Alder product (Scheme 16).

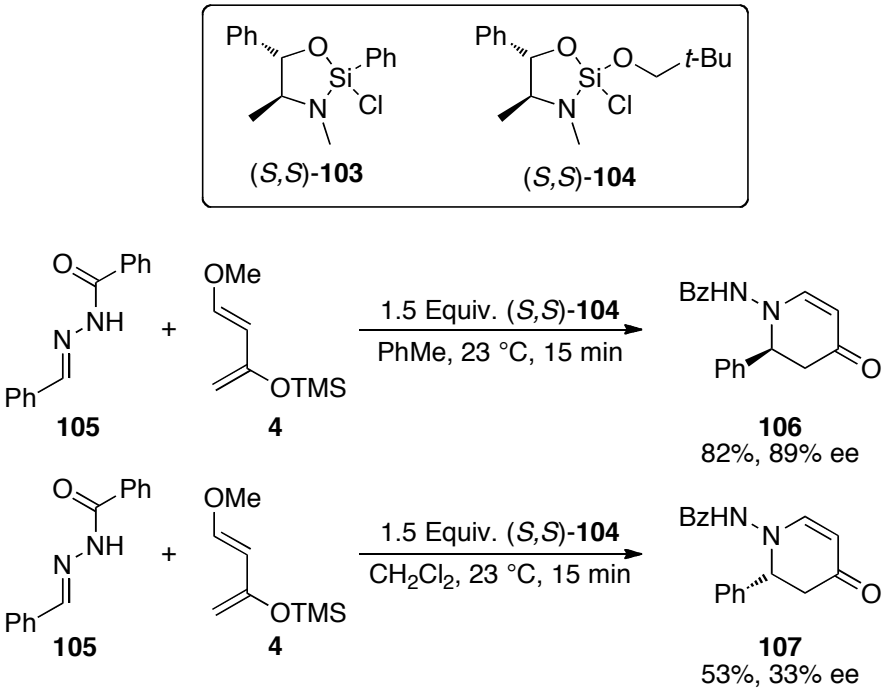

Scheme 16. Silicon Lewis acids and their use within the aza-Diels-Alder reaction.

It is also mechanistically interesting to note that two silicon catalysts were synthesised and tested: **103** and **104**. Catalyst **103** had previously been proven to be effective for a variety of transformations of acylhydrazones.[70] However, it proved to be ineffective in the Mannich reaction.[71] Consequently, when catalyst **103** was used as the Lewis acid in the aza-Diels-Alder reaction, the reaction did not proceed. Instead, catalyst **104** had been shown to perform well in enantioselective Mannich reactions[71] and when subsequently used within the aza-Diels-Alder reaction, the reaction proceeded efficiently. These findings suggest that the aza-Diels-Alder reaction could be proceeding through a Mannich reaction, thus adding evidence that the aza-Diels-Alder reaction goes through a two-step process *via* a Mannich-Michael pathway as opposed to being concerted. Armed with these findings, Leighton *et al.* went on to synthesise casopitant **111**, a neurokin 1 receptor antagonist,[72] after forming the core piperidine ring **108** *via* an aza-Diels-Alder reaction using their silicon Lewis acid **104** (Scheme 17).

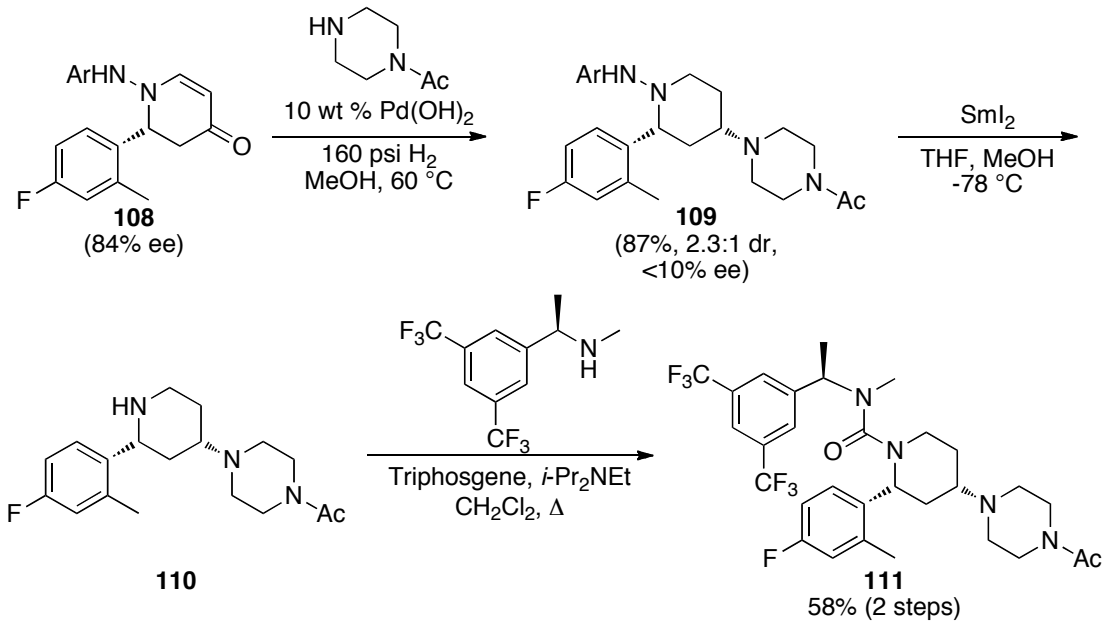

Scheme 17. Synthesis of casopitant **111** from the aza-Diels-Alder product **108**.

If one wants to bring down the reaction time for the aza-Diels-Alder reaction, then activation by microwave irradiation is a viable option as demonstrated by Török *et al*. when using silicotungstic acids as catalysts.[73] After screening different heteropolyacids[74] they were able to show that their one-pot, three-component system forms the aza-Diels-Alder product **114** in good yields and diastereoselectivities within 10 min when performed in a microwave at 100 °C, using $H_4[SiW_{12}O_{40}]$ as the catalyst (Equation 10).

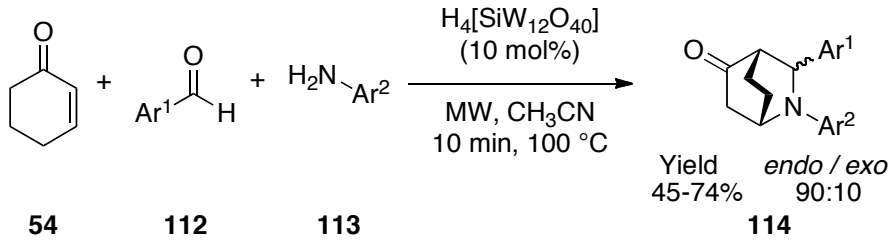

Equation 10

1.3 Asymmetric Construction using Brønsted Acids

The use of Brønsted acids in the aza-Diels-Alder process can be simply explained in the context of the reaction between a cyclic enone **54** and an imine **11**, whereby the Brønsted acid activates both these reagents. As seen in Scheme 18, under acidic conditions, the ketone tautomerises to enol **115**. This then undergoes a Mannich reaction with the protonated imine **116**, followed by an intramolecular aza-Michael addition to give the *endo*-**118** and *exo*-**119** bicyclic products and regenerating the acid catalyst at the same time.

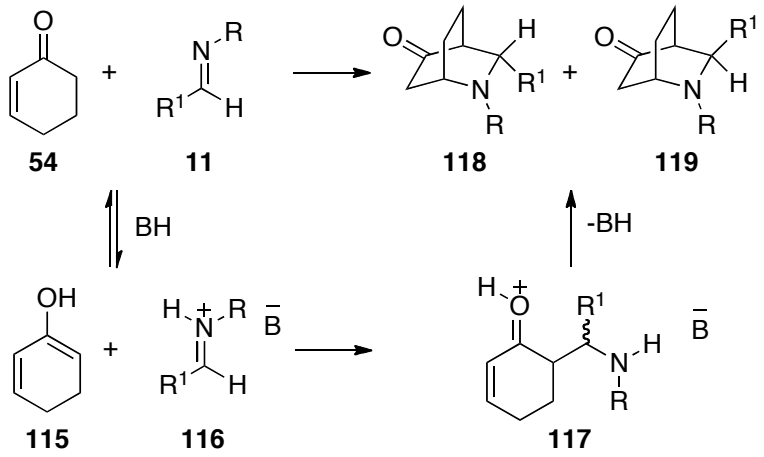

Scheme 18. General procedure for the Brønsted acid catalysed aza-Diels-Alder reaction.

The success of this reaction depends on the proton-donating capacity of the catalyst (acidity) and on the experimental conditions, particularly the solvent. Piermatti *et al.* have been able to perform such reactions in water using *α*-zirconium hydrogen phosphate (*α*-$Zr(HPO_4)_2 \cdot H_2O$) as the Brønsted acid to give yields of 70-90%, although with hardly any selectivity between the *endo*-**118** and *exo*-**119** products (50:50 – 55:45).[75]

Prior to this finding, Akiyama *et al.* made significant progress in this field of green chemistry by demonstrating that the three-component, one-pot aza-Diels-Alder reaction between an aldehyde **8**, amine **120** and Danishefsky's diene **4** can be performed solely in water, using sodium dodecyl sulphate (SDS) as a surfactant.[76]

This reaction proceeds giving the racemic product **121** in good yield, using fluoroboric acid (10 mol%) as a catalyst (Equation 11).

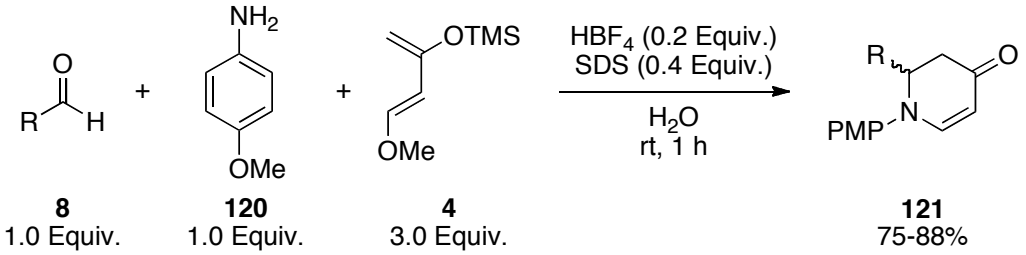

Equation 11

Following on from this work, Kobayashi *et al*. carried on experimenting with the aza-Diels-Alder reaction in water. In one set of reactions, amines **86**, aldehydes **8** and the Danishefsky diene **4** were reacted together in the presence of catalytic AgOTf at room temperature for two-three hours (Equation 12).[77] The use of Danishefsky's diene **4** in this reaction using water as a solvent was believed to be beneficial because it was thought that Danishefsky's diene **4** probably hydrolyses slower under these heterogeneous reaction conditions, thus preventing formation of side products. However, only the racemic product was obtained. It was subsequently found that the slow addition of the diene **4** over a period of an hour dramatically helped to improve yields. Yields were subsequently increased by up to 20% through the use of non-ionic surfactants such as 'Triton X-100'. It was thought that the role of this surfactant was to help the formation of the imine, as no improvements were observed in the two-component reaction. Higher equivalents of diene **4** also gave higher yields of up to 90%.

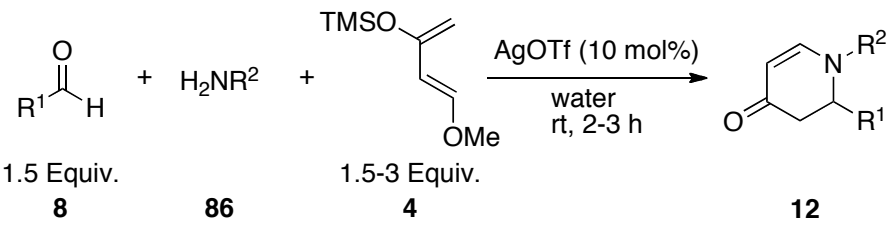

Equation 12

Through the use of α,β-unsaturated esters over ketones, the Mannich reaction can be investigated and optimised independently in order to give a greater understanding of

the Mannich-Michael ring forming process. Hence, Mannich reactions between imines **122** and acyclic silyl dienolate **123** using catalytic amounts of Brønsted acids have been optimised by Schneider *et al*..[78] This they achieved with 5 mol% of their BINOL-based phosphoric acid catalyst **124** in a solvent mixture at -50 °C. The low temperature was necessary in order to improve enantioselectivity; a lower temperature would have frozen the solvent mixture (Equation 13).

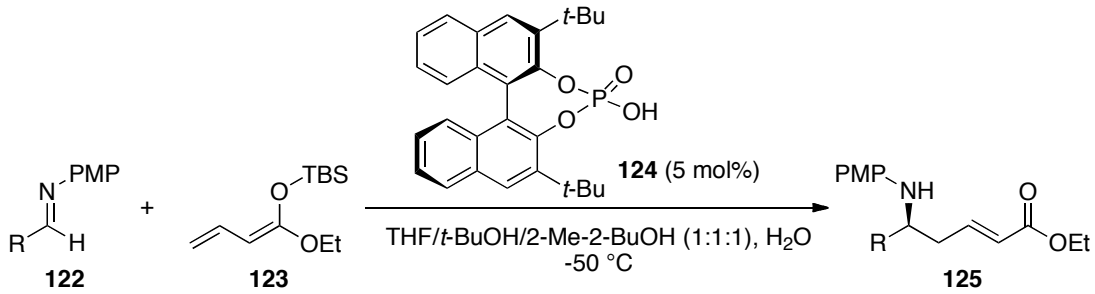

Equation 13

After optimisation of their chiral Brønsted acid, Schneider *et al.* found that higher enantioselectivities were observed when the R group on the ester **125** was small. When using aromatic protecting groups on the imine, having electron-donating groups on the *para*-position afforded high enantioselectivities, whereas the reaction became non-selective when this group was on the *ortho*-position. The main effect that the R-substituent of the imine had on this reaction was to slow the reaction down. Hence, the reaction times ranged from twelve hours to a week, with most reactions going to completion within two days; increasing the low catalytic concentration would undoubtedly speed up the reaction. When using γ-substituted silyl dienolates, it was found that an *E*-geometry **126** would mainly afford the *anti*-product **127** (Equation 14), whilst the *Z*-geometry **128** would mainly afford the *syn*-product **129**, although with lower yield and poor diastereoselectivity (Equation 15).

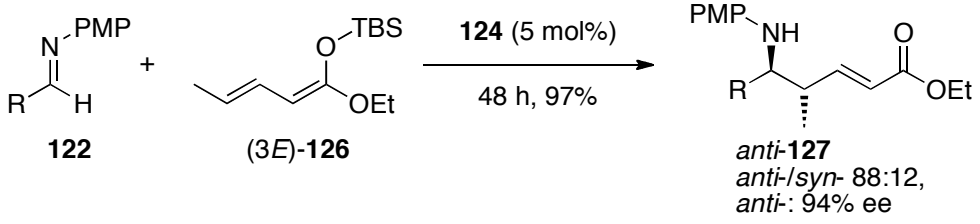

Equation 14

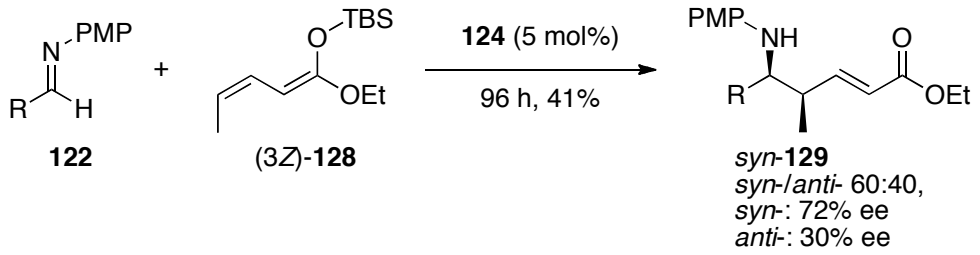

Equation 15

Mechanistic investigations were carried out to explain the role of the solvent system (equal amounts of *t*-BuOH, 2-methyl-2-butanol and THF with one equivalence of water) as well as the reaction mechanism. Hence, the alcohol component was shown to be important for the rate of the reaction, with the water content further accelerating the reaction. 2-Methyl-2-butanol was needed in order to decrease the allowed reaction temperature, whilst THF had a beneficial effect on the selectivity of the reaction. This solvent system is thought to trap the cationic silicon species as silanol and regenerate the chiral Brønsted acid catalyst through protonation. Thus, in the proposed catalytic cycle, the Brønsted acid **124** protonates the imine **122** whilst shielding the *Re*-face, making the protonated imine **130** sufficiently activated to undergo the Mannich reaction with the silyl dienolate **123** from the opposite side. The intermediate **132** was subsequently hydrolysed to give the Mannich product **125** (Scheme 19). This reaction was also shown to proceed well in a one-pot, three-component manner by forming the imine *in situ*.

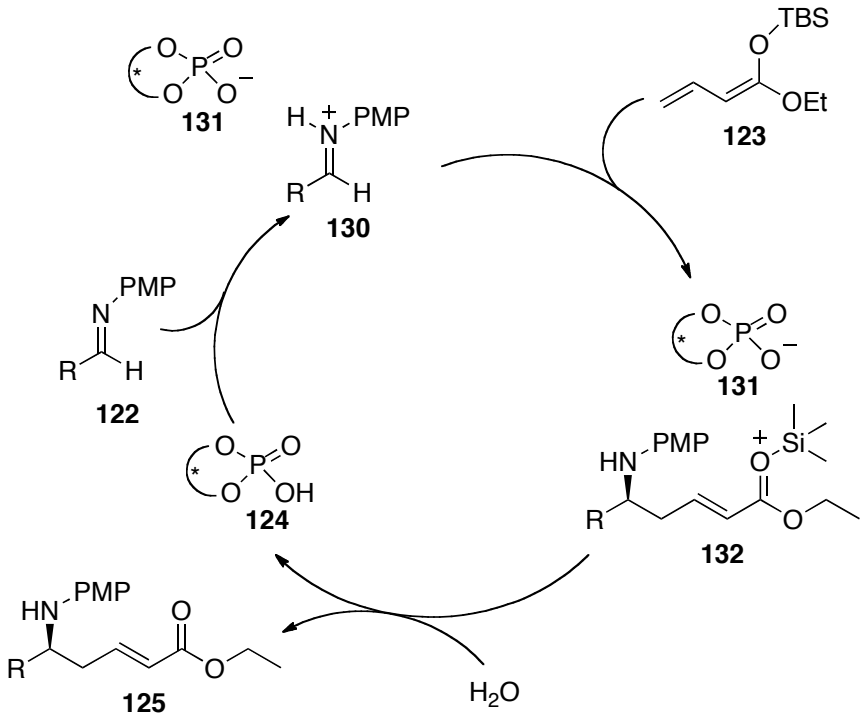

Scheme 19. Proposed catalytic cycle for the formation of **125** from **122** and **123**.

The first Brønsted acid catalysed aza-Diels-Alder reaction using unactivated cyclohexenone **54** as opposed to the activated Danishefsky diene **4** was reported by Gong *et al*. through their use of chiral phosphoric acids.[79] The reaction relies on the acid enolising the carbonyl group of **54** in order to generate an electron-rich diene **115** *in-situ*, and thus, attack the protonated imine **116** in order to undergo a Mannich reaction, followed by an intramolecular Michael addition (Scheme 20).

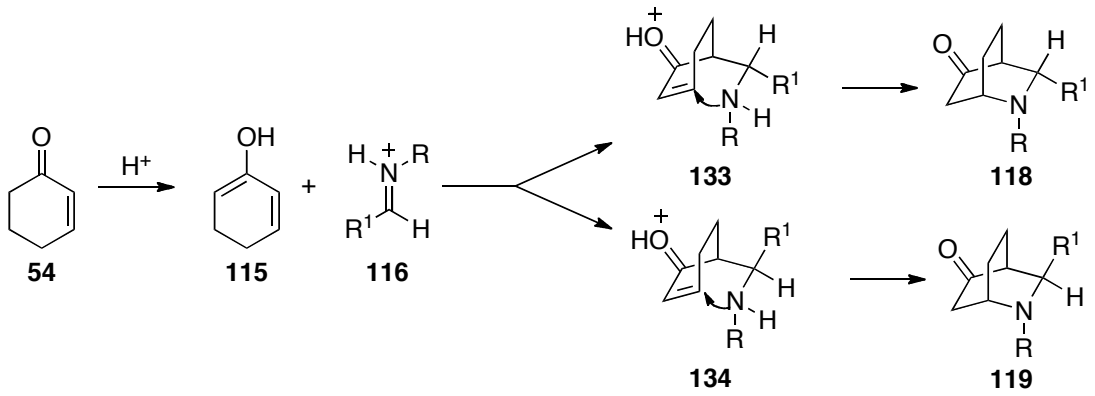

Scheme 20. The route to bicyclic piperidine rings **118** and **119** from a cyclic enone **54**.

The reaction shown in Scheme 20 took six days with two equivalents of enone **54** and 5 mol% of optimised chiral phosphoric acids **135** at room temperature. It was found that lower temperatures gave higher enantioselectivites; nevertheless the overall yields were notably decreased. The use of different solvents only affected the yields, with non-polar solvents such as toluene affording the highest yields. Dichloromethane follows this, with polar solvents such as THF exhibiting the lowest yields. Similar results in terms of yields and stereoselectivites were observed when the aromatic electronics of the nitrogen-protecting group were changed. Finally, the optimised reaction was effectively performed in a three-component one-pot fashion (Equation 16).

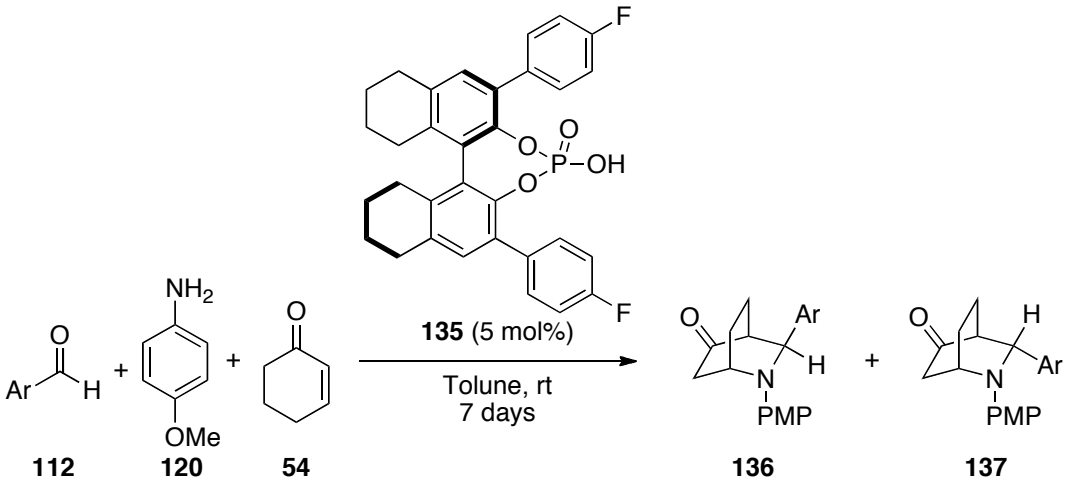

Equation 16

A double Brønsted acid catalysed reaction using the chiral BINOL-phosphoric acid **138** (10 mol%) and acetic acid as an achiral acid (20 mol%) was successfully performed to form bicyclic piperidine rings **140** from imines **11** and cyclohexenone **54**. Rueping *et al.*[80] have shown that both catalytic acids need to be of different strengths, with the achiral catalyst having a much higher pK_a so that it would not be able to compete with the chiral acid **138** in activating the imine **11**, which would have resulted in reduced enantioselectivity. Hence, the chiral acid **138** activates the imine **11** generating the more electrophilic **116**, whilst the achiral acid tautomerises the ketone **54** into a nucleophilic enol **115**. Consequently, the imine and enone are able to

cyclise *via* a Mannich-Michael process (Scheme 21) to give **140** in moderate yields and high enantioselectivity.

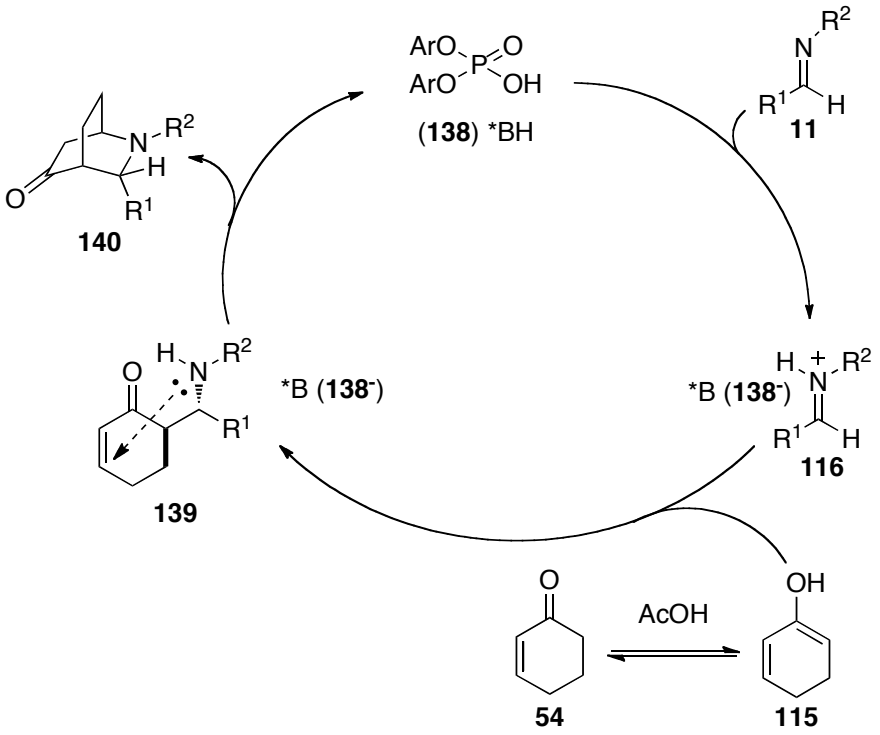

Scheme 21. Proposed catalytic cycle for piperidine ring formation using two acid catalysts.

Work done by Feng *et al.* have also shown that ytterbium is the Lewis acid of choice when performing the aza-Diels-Alder reaction; scandium, samarium, yttrium and lanthanum all gave lower yields than ytterbium.[81] Furthermore, Brassard's diene **65** was used instead of the Danishefsky diene **4**; the use of Brassard's diene **65** using chiral Brønsted acid catalysts had only been mentioned once before within the literature.[82] The double substitution at the terminus of Brassard's diene **65** makes this diene less enantioselective, which can explain the previous low usage of this diene.[83] It was observed that after reacting Brassard's diene **65** with an imine **141** in the presence of the Brønsted acid, the Mannich product **143** was obtained. **143** was subsequently cyclised by heating it with benzoic acid to form the piperidine ring **144**, thus suggesting that the overall mechanism of the cycloaddition is stepwise as opposed to being concerted (Scheme 22). The use of ligand complexes was shown to greatly increase the enantioselectivities (up to 81% ee), with yields of up to 58% being obtained. Feng *et al*. have also shown that with their aza-Diels-Alder reactions,

higher yields are also obtained when the reaction is performed in solvent-free conditions and that this also applies to the one-pot, three-component reactions.[84] Hence, these findings suggest that it may be best to use the minimum amount of solvent within the aza-Diels-Alder reactions.

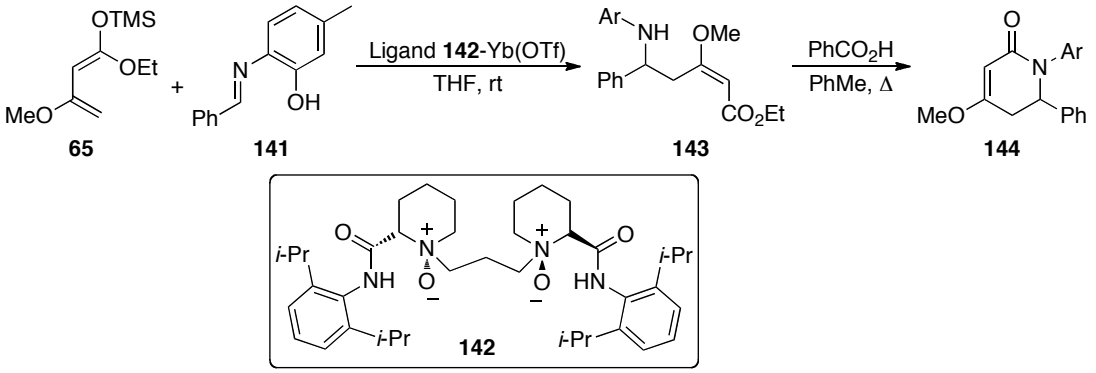

Scheme 22. The use of chiral Yb complexes within the aza-Diels-Alder reaction.

If one wants to perform the aza-Diels-Alder reaction in water, Vaccaro *et al*. have shown that this is possible when using zirconium hydrogen phosphate alkyl and/or aryl phosphonates $[Zr(PO_3OH)_{2-(x+y)}(PO_3R)_x(PO_3R')_y]$ as heterogeneous Brønsted acids.[85] They report that a high concentration of hydrophobic groups (Me, Ph and Pr) on their solid catalyst favours reagent diffusion towards the acidic sites in order to aid proton transfer to the reagents. As a result, no additives are needed in their system and both the Mannich (**149** and **150**) and aza-Diels-Alder (**147** and **148**) products were obtained in good conversion (Scheme 23).

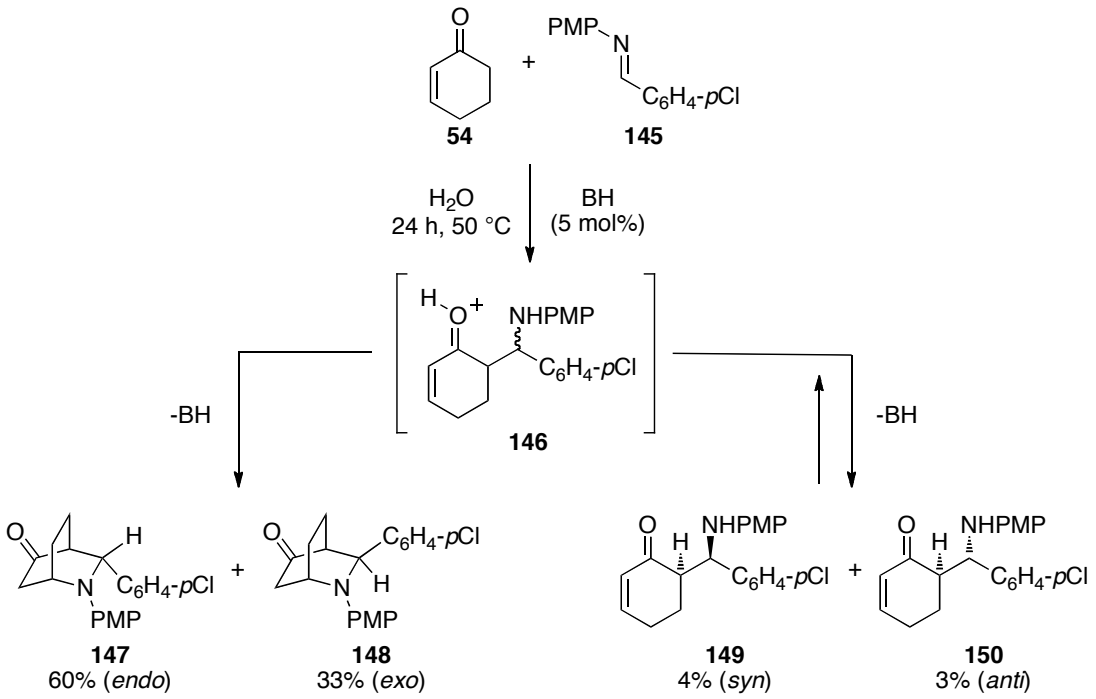

Scheme 23. An aza-Diels-Alder reaction performed in water, where BH = $Zr(PO_3OH)_{0.37}(PO_3Me)_{0.65}(PO_3Ph)_{0.98}$-$0.7H_2O$.

1.4 Asymmetric Construction using Organocatalysis

As it is generally accepted that the aza-Diels-Alder reaction proceeds *via* a Mannich-Michael process, understanding each of these processes is highly important. Asymmetric Mannich reactions can afford high diastereo- and enantio-selectivities with the use of pyrrolidine derived catalysts.[86] It has been widely shown that having an (*R*)-carboxylic acid group on the 2-position of pyrrolidine **152** (i.e. L-proline) makes the Mannich reaction *syn*-selective **154** (Scheme 24).[87]

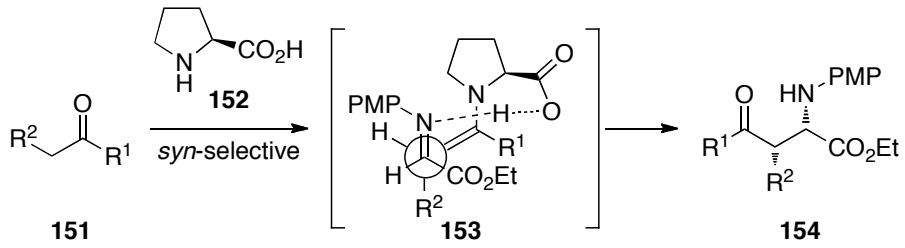

Scheme 24. *syn*-Selectivity of the L-proline **152** catalysed Mannich reaction between an imine and a ketone or an aldehyde compound.

Conversely, Tanaka *et al.* have shown that having the (*S*)-carboxylic acid group on the three-position of pyrrolidine **154** makes this an *anti*-Mannich catalyst, thus giving the *anti*-product **160** (Scheme 25).

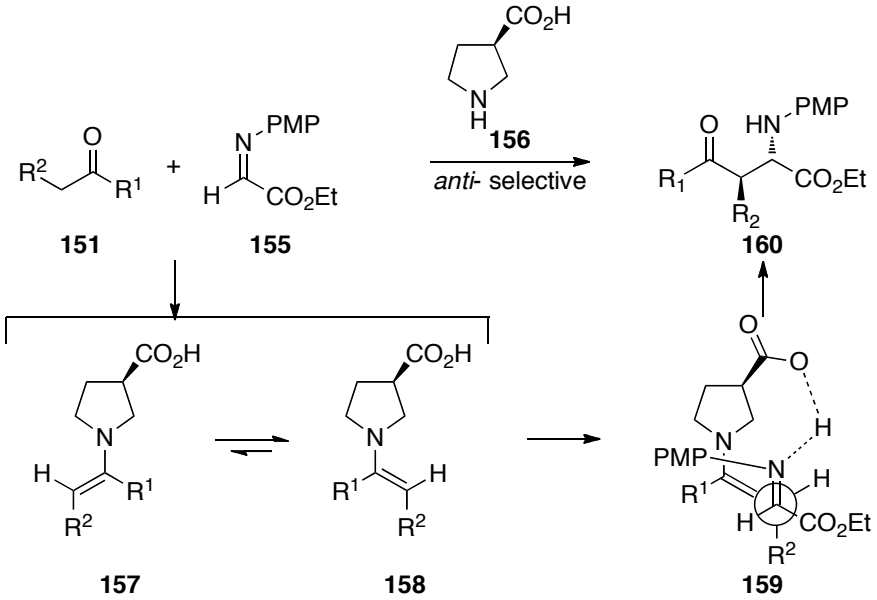

Scheme 25. *anti*-Selectivity of the catalyst **156** between imines and ketones.

Condensation of the catalyst with the ketone would afford an enamine interconverting between conformations **157** and **158**. However, only conformation **158** will react further with the imine **155** *via* a preferred transition state **159** whereby the acid and the nitrogen of the imine are H-bonding with each other. Hence, stereoselective Mannich product **160** is formed.

When exploring the L-proline catalysed Mannich reaction between methyl-ketones **162** and imines **161**, Ohsawa *et al*. found that at room temperature with 5 mol% of catalyst, high yields (up to 99%) of Mannich product **163** were obtained after three days when 50 equivalents of water were present in the reaction mixture; under dry conditions almost no stereoselectivity was observed, whilst too much water drastically decreased the reaction rate (Equation 17).[88]

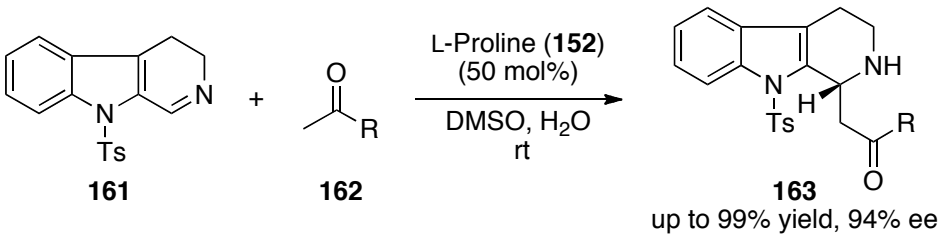

Equation 17

Lower temperatures also greatly decreased the rate of reaction. However, the stereoselectivity was improved. When the same reaction was performed using methyl vinyl ketone **164**, dry conditions were necessary in order to sufficiently increase the rate of reaction, with 50 mol% of catalyst **152** being used. Even then, the reaction took a week to proceed (Equation 18). This work was published in 2003, and was one of the first to show that L-proline **152** can be used in the aza-Diels-Alder reaction.

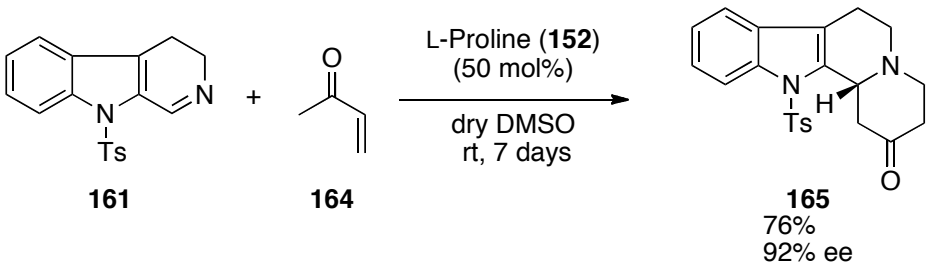

Equation 18

The unprotected **165** is a precursor for the synthesis of indole alkaloids such as deserpidine[89] and yohimbine.[90] In 2006, Ohsawa *et al*. reported their findings (to access one of these alkaloids) using different enones catalysed with 30 mol% of L-proline **152**.[91] Despite the reaction taking a week to go through to completion, using 30 equivalents of enone **166**, high yields and enantio- and diastereo-selectivities were obtained. With three further steps, the alkaloid *ent*-dihydrocorynantheol **168** was synthesised asymmetrically (Scheme 26). Seeing as this reaction was proceeding in the same manner as when simple methyl ketones **162** were used as a reagent over enones, it was thought the reaction was proceeding *via* a Mannich-Michael process. Hence, the large excess of enone **166** that was needed would suggest that the initial Mannich reaction was the rate-determining step.

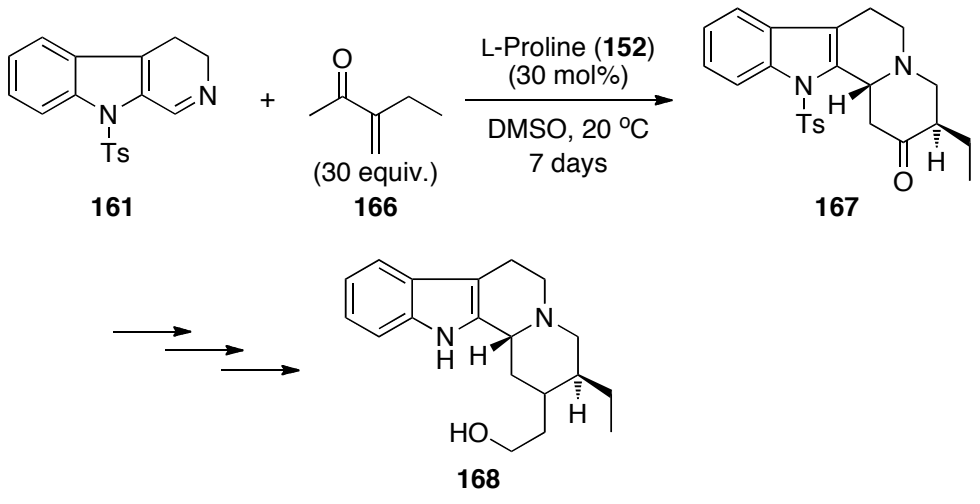

Scheme 26. The aza-Diels-Alder reaction for the formation of the alkaloid *ent*-dihydrocorynantheol **168**.

Córdova *et al*. first mentioned the use of cyclohexenones **169** within the aza-Diels-Alder reaction with pyrrolidine derived organocatalysts in 2005, in order to produce

enantioselective bicyclic piperidine rings **171** in moderate yields. This reaction was performed in a three-component one-pot manner using enones **169**, formaldehyde **170** and *p*-anisidine **120** (Equation 19).[9]

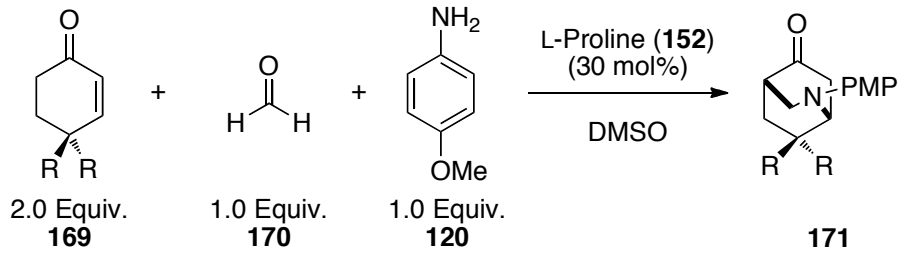

Equation 19

Different solvents were used, and it was found that after 24 hours at 50 °C, DMSO gave better yields (52%), followed by DMF (35%), NMP (10%) and toluene (<5%). High ee of 99% was obtained from L-proline **152** and the Ley catalyst **172**, with slightly lower ee (94%) obtained with the amide catalyst **173**. When performing the reaction at room temperature, a lower yield of 30% was obtained when using catalyst **152**. However, at room temperature, catalyst **172** gave a slightly higher yield of 61%. After deciding to use the cheaper L-proline **152** catalyst, the reaction was performed using various enones to give a range of bicyclic piperidines in similar ee and yield. In one example, when using enone **174**, only the α,β-unsaturated Mannich product **175** was obtained.

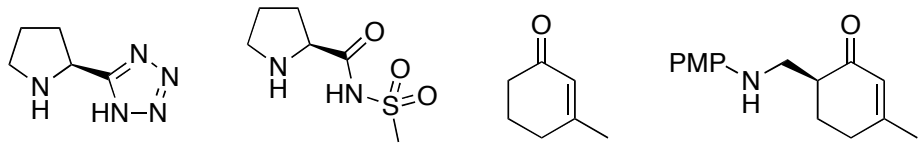

172 **173** **174** **175**

Formation of **175** was used as evidence to propose that the aza-Diels-Alder reaction was proceeding *via* a Mannich-Michael, as opposed to a concerted process; presumably the methyl group on the enone was blocking the amine's access to the Michael receptor. Various aromatic amines were also screened and it was found that neutral aromatic rings gave lower yields than the electron donating PMP ring, with *p*-halogenated aromatics giving the lowest yields. Furthermore, trace amounts of Mannich adduct were also observed when using the *p*-halogenated aromatic amines,

which is further proof that this reaction proceeds *via* a Mannich-Michael process. Hence, a chiral enamine **177** is first formed; with the *in-situ* generated imine **178** attacking it from the *Si*-face *via* transition state **182** (Scheme 27). The trace amounts of *p*-halogenated aromatic amines observed could be attributed to the lower nucleophilicity of the secondary amine intermediate in the Michael step.

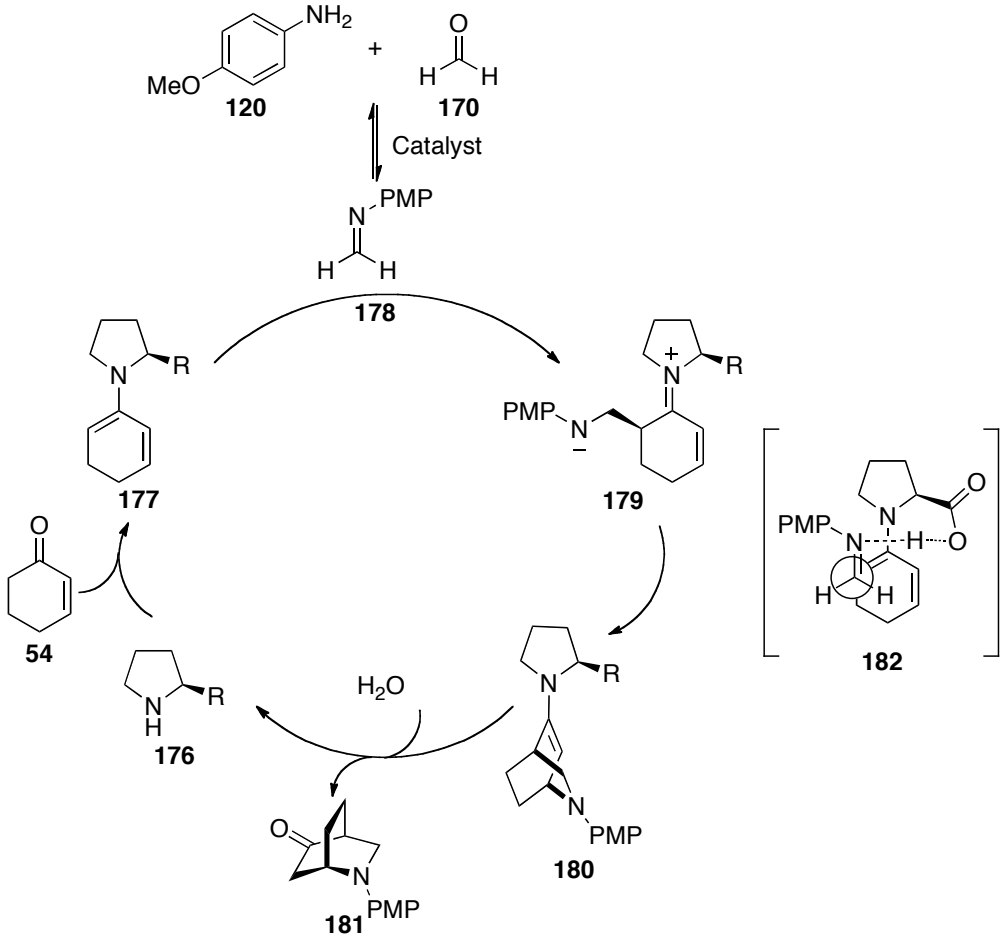

Scheme 27. Proposed catalytic cycle for the formation of bicyclic piperidine rings *via* the aza-Diels-Alder reaction.

When using L-proline **152** as the organocatalyst, the *syn*-selectivity of the Mannich reaction can be used to form *cis*-2,6-diarylpiperidin-4-ones **185** from their corresponding enones **183** and imines **184**.[92] However, the advantages of using L-proline are limited by the fact that four equivalents of the enone were needed to produce a moderate yield, as well as the limited number of solvents this reaction was effective in. Despite this, high diastereoselectivity was observed with these reactions,

although no enantioselectivity was obtained when the R substituents on the ring were different (Scheme 28).

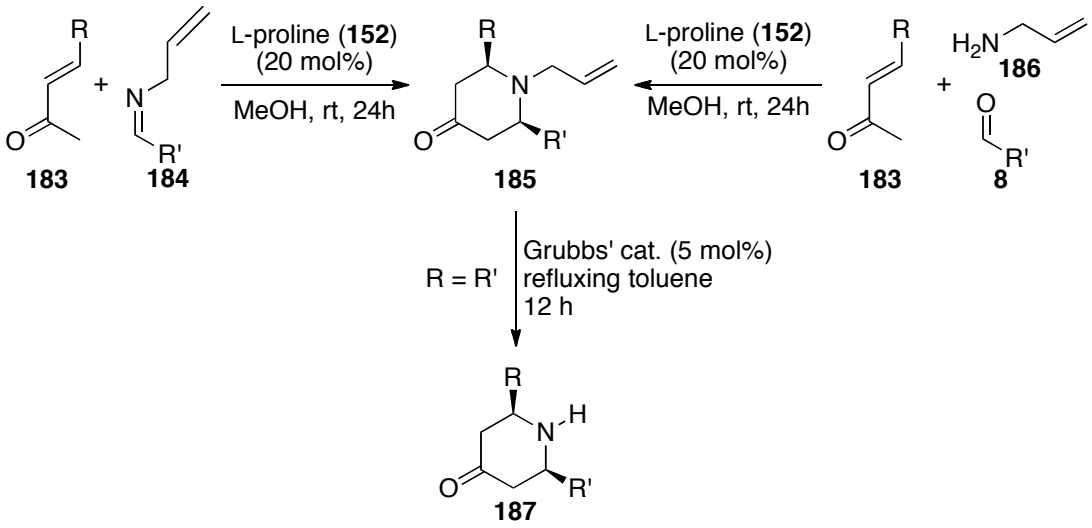

Scheme 28. Different routes for the formation of the deprotected piperidine ring **187**.

It is also interesting to note that the reaction only seems to proceed efficiently with an aliphatic protecting group on the nitrogen of imine **184**. Low conversions were obtained when this protecting group was aromatic, meaning more traditional nitrogen protecting groups such as *p*-methoxyphenyl could not be used. Aznar *et al.* have shown that a convenient aliphatic protecting group in such cases would be an allyl group as this group could easily be removed after the cycloaddition using Grubbs' catalyst, the methodology of which was serendipitously discovered in Madrid by Alcaide *et al*.[93] In their quest for synthesising bioactive β-lactams **188**, Alcaide *et al*. found that in some cases, isomerisation of the internal double bond in a *N*-allyl amide **189** was favoured over ring-closing metathesis (Scheme 29).

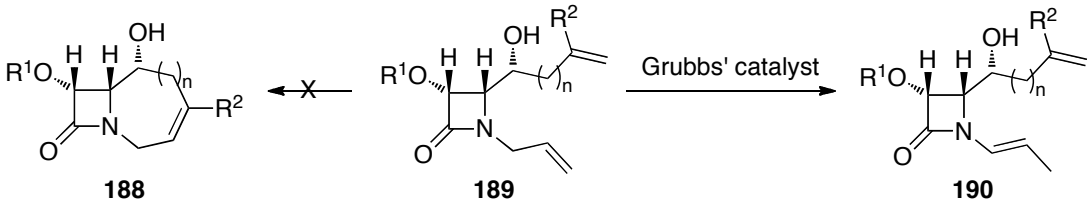

Scheme 29. An observed ring-closing anomaly with Grubbs' catalyst.

Consequently Alcaide *et al.* looked into this phenomenon using different *N*-allyl amines and found that Grubbs' catalyst efficiently catalysed the deprotection of tertiary amines **191**. Mechanistic studies showed that the reaction proceeds *via* a ruthenium-catalysed isomerisation to a more stable olefin **194**, followed by hydrolysis to afford the amine **195** (Scheme 30).

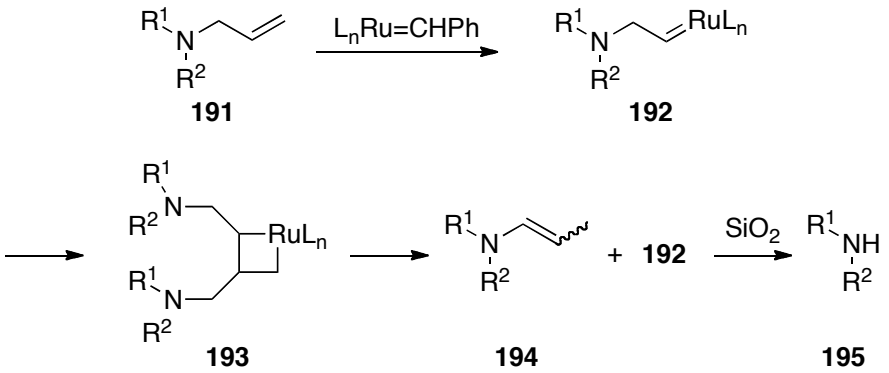

Scheme 30. Deprotection of allylic tertiary amines using Grubbs' catalyst.

Regarding the organocatalyst, Aznar *et al*. also screened the aza-Diels-Alder reaction against the pyrrolidine derived catalysts **196** and **197**.[94] Both of these catalysts were ineffective by themselves in the reaction between enone **183** and imine **184**. However, in the presence of 20 mol% of *p*-toluenesulfonic acid, piperidine ring **185** was formed in 58% and 61% yields respectively. These results suggested that some acidic source is required to promote formation and equilibration of the initial iminium ion to the reactive enamine. In the case of L-proline **152**, the acid was incorporated into the organocatalyst. Hence, no extra acidic source was needed to promote the aza-Diels-Alder reaction, unlike with the pyrrolidines **196** and **197**.

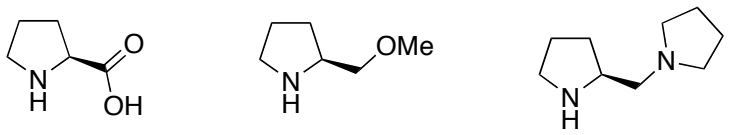

When looking into organocatalysed methods for accessing nitrogen-containing bicyclic rings **119** in a highly enantioselective and diastereoselective manner, Carter *et al.*[95] suggested that the initial Mannich reaction proceeds *via* the transition state put forward by Houk (Scheme 31).[96] In this system, the *syn*-zwitterionic product **200**

governs the subsequent aza-Michael cycloaddition in order to form the enamine **203**. This mechanism would explain the strong *exo*-preference observed in these reactions. However, higher catalyst loadings of **198** (30 mol%) compared to standard aldol[97] and Mannich reactions[98] were necessary because cleavage of the enamine **203** in this example was slow due to increased steric congestion.

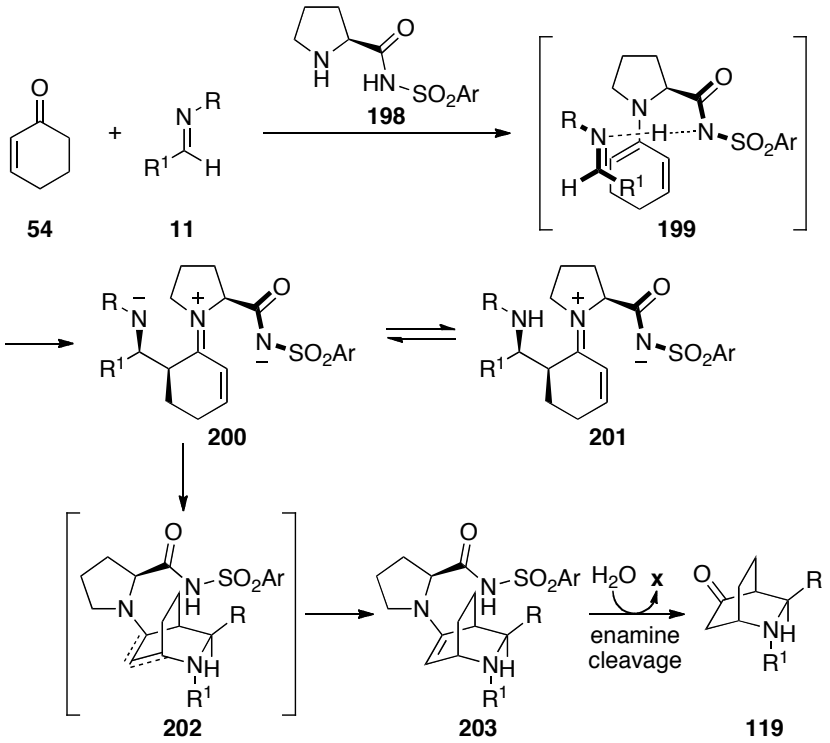

Scheme 31. The aza-Diels-Alder reaction using the organocatalyst **198**.

Franzén *et al*. have found proline-derived organocatalysts **205** to be useful in the direct synthesis of quinolizidine skeletons **211**-**214**, with the formation of three new stereocentres (Scheme 32).[99]

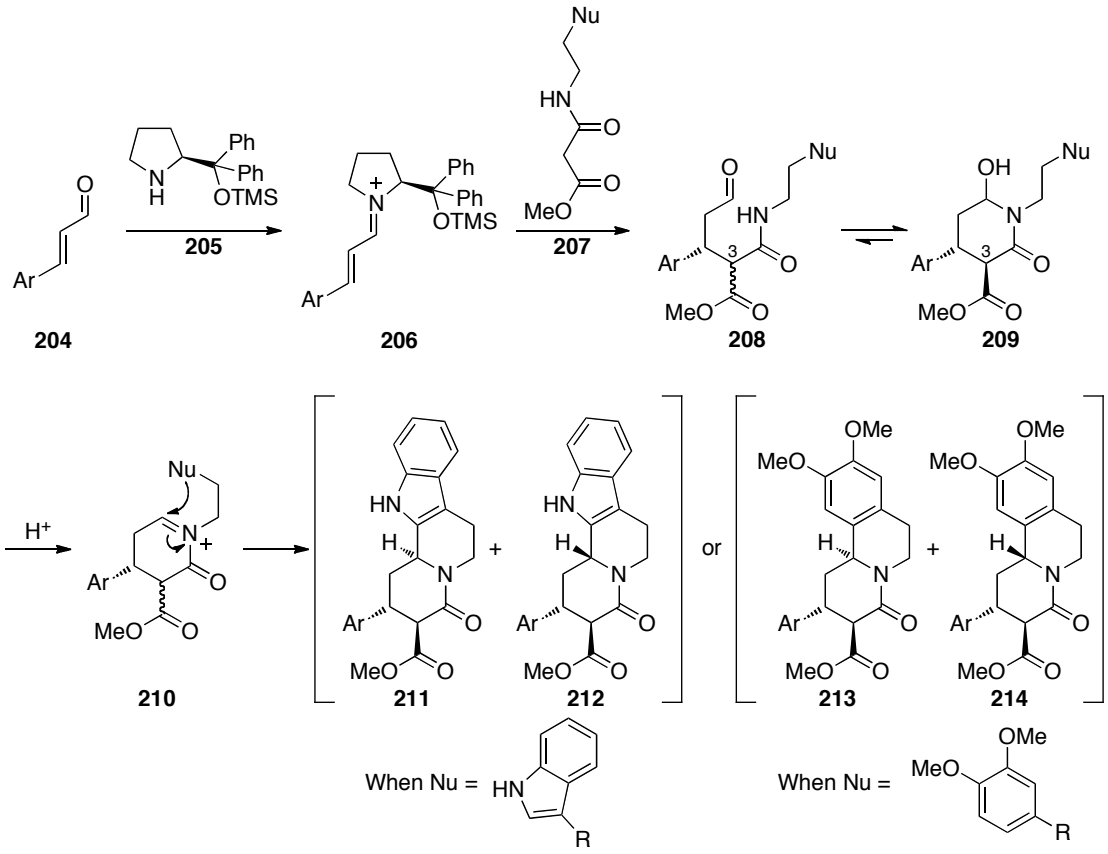

Scheme 32. The use of the aza-Diels-Alder reaction for the formation of fused-piperidine ring compounds.

Thus, catalyst **205** attacks the enone **204** to form the chiral iminium intermediate **206**. This shields the *Re*-face and hence, conjugate addition of the amide would happen on the *Si*-face. After the addition of **207**, the compound **208** cyclises spontaneously to form the hemiacetal **209**. This compound was observed to be in the thermodynamically stable 2*R*,3*S*-*trans*-configuration due to epimerisation of the stereochemically labile stereocentre at C3. In the presence of catalytic amounts of acid, the hemiacetal **209** then converted into the acyliminium ion **210**, which could then undergo aromatic substitution to give the quinolizidine products **211**-**214**. This reaction is noted to be under kinetic control, with high to excellent enantioselectivity and moderate diastereoselectivity. This was thought to be due to less steric hindrance from the equatorial α-proton in the transition state **215** (Scheme 33).

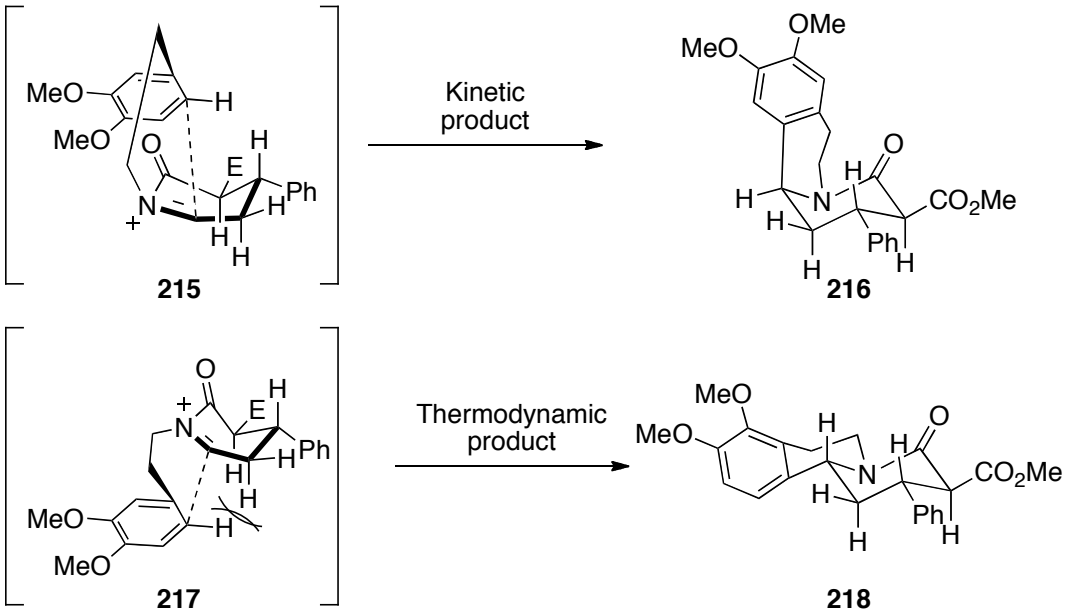

Scheme 33. The transition states for the kinetic **216** and thermodynamic **218** products.

Recently, a one-pot three-component tandem reaction has been shown by Chen *et al.* to form piperidine containing spirocyclic oxindoles **224**.[100] They had previously found that with the aid of a chiral organocatalyst **205**, achiral bifunctional compound **221** could be formed from the asymmetric Michael addition of aliphatic aldehydes **219** to electron-deficient olefinic oxindoles **220**. They subsequently found that *N*-Boc-imines **222** could be used as electrophiles in the reaction with intermediate **221**, with tetramethylguanidine (TMG) catalysing this highly diastereoselective Mannich reaction to afford the hemiaminal **223** in the same pot. This hemiaminal **223** was directly dehydroxylated to afford the piperidine derivatives **224** in moderate yields with high enantioselectivities (Scheme 34). Thus, by altering the aromatic groups, spirocyclic oxindoles such as **225** may be synthesised; **225** is a potent non-peptide MDM2 inhibitor, which may be useful as an anticancer agent.[101]

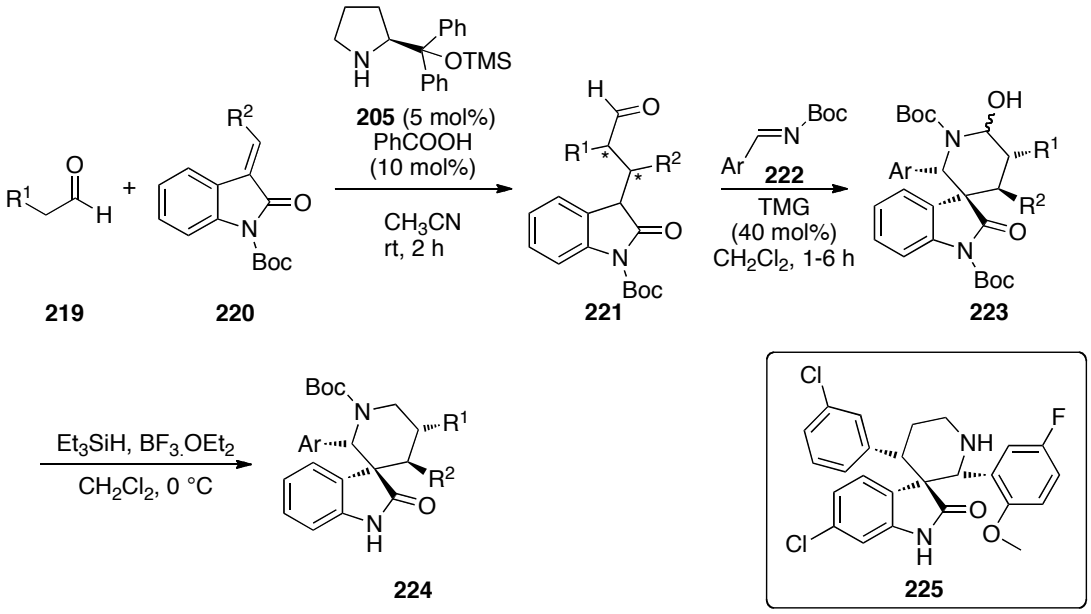

Scheme 34. The use of the aza-Diels-Alder reaction to form spirocyclic piperidine ring compounds.

Interestingly, Schneider *et al.* have recently shown that Mannich-Michael reactions can be performed from imines **155** and an aldehyde tethered to an enone **226** in the presence of catalytic amounts of L-proline **152** (20 mol%); the tether forming part of the synthesised piperidine ring **227**.[102] The enone group in **226** has a chiral auxiliary attached to it; hence, it contains no acidic α-protons. Thus, the organocatalyst **152** solely formed an enamine with the aldehyde group in **226**, through which a Mannich reaction occurred with the imine **155**. The Mannich adduct subsequently underwent an intramolecular aza-Michael reaction with the enone, thus forming the highly substituted piperidine ring **227** in moderate yields and good stereocontrol after subsequent aldehyde reduction (Equation 20). Small amounts (<5%) of the uncyclised Mannich product were also observed. Reaction time was 24 hours at -20 °C and it was found that if the imine was not reactive enough, no reaction was observed as the initial Mannich reaction did not precede. The reaction was also performed using D-proline as the catalyst, which afforded the piperidine ring with opposite configuration at the two- and three-positions. This demonstrated that the initial Mannich step was catalyst-controlled, whereas the subsequent Michael addition was substrate controlled, hence the need for a chiral auxiliary in this case.

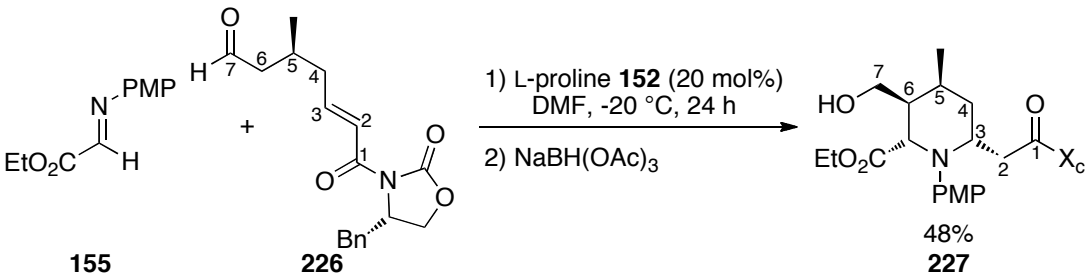

Equation 20

The use of enzymes to catalyse organic transformations[103] is becoming more prevalent within the chemistry community,[104] with an aza-Diels-Alder example recently being published by Guan *et al*..[105] In their system, they found that Hen Egg White Lysozyme (HEWL) efficiently promotes the one-pot, three-component reaction between an amine **113**, aldehyde **112** and 2-cyclohexen-1-one **54** in order to form the aza-Diels-Alder product **228** in good yield and stereoselectivity (Equation 21).

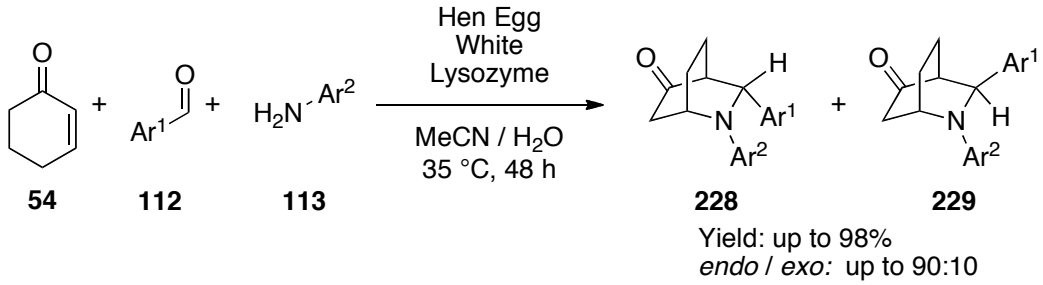

Equation 21

1.5 Other aza-Diels-Alder reactions using imines as the dienophile

To overcome the need to protect the amine in the aza-Diels-Alder reaction, Edwards *et al*. have shown that piperidine rings can be formed in a one-pot, three-component fashion when using ammonia as the nitrogen source. However, low yields of 20-35% were generally observed.[106] This methodology was subsequently used in the synthesis of frog alkaloids such as the biologically active piperidine 241D (**235**).[107] Hence, reaction of an enone **230** and aldehyde **232** with NH_4OAc (**231**) in methanol predominantly afforded the *cis*-isomer of the piperidine ring **234** (80:1, *cis* to *trans*) in 25% yield. Subsequent reduction of the carbonyl group using sodium borohydride gave *cis,cis*-4-hydroxy-2-methyl-6-nonylpiperidine (**235**) as the major product (Scheme 35). Edwards *et al*. noted that the one-step ring-closing reaction most probably goes *via* Mannich and Michael condensations.

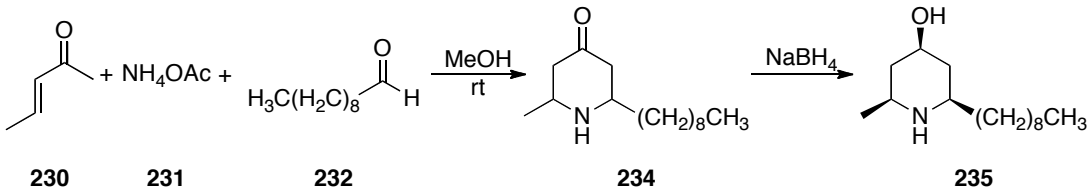

Scheme 35. Synthesis of the frog alkaloid **235** *via* an aza-Diels-Alder reaction.

Ding *et al*. have shown that *N*-aryl imines undergo an acid-free aza-Diels-Alder reaction with Danishefsky's diene **4** in MeOH, where it was suggested that the reaction goes through a Mannich-type pathway due to the regioselectivity of the reaction and the observance of the Mannich product in the crude mixture.[108] Following on from this work with an aim of synthesising imines through an alternative method, Yan *et al*. have shown a method to perform metal-free aerobic oxidative coupling of amines to form imines by refluxing aerated suspensions of water and benzylamines **236**. After extracting the imines from the aqueous solvent, followed by concentration *in vacuo*, the imines were mixed with a methanol solution of Danishefsky's diene **4** to form the aza-Diels-Alder products **237** in moderate yields (Equation 22).[109]

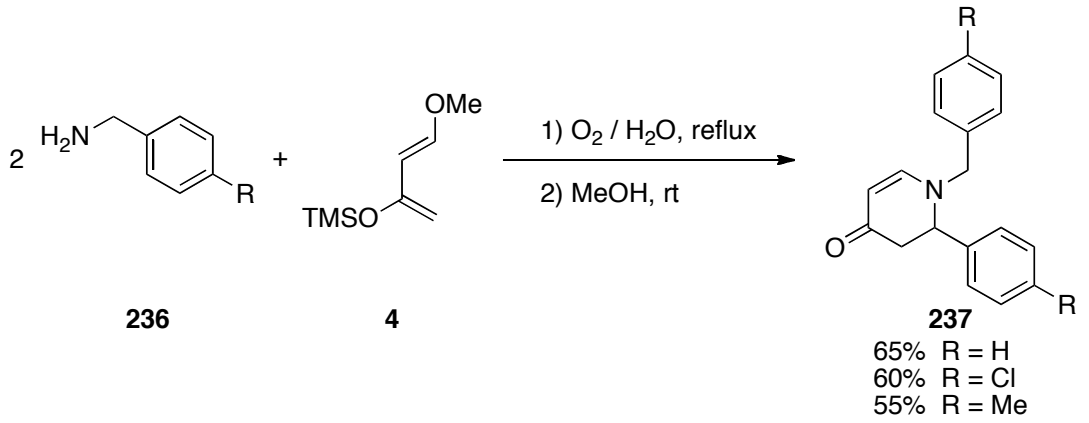

Equation 22

The use of chiral ionic liquids within the aza-Diels-Alder reaction has been explored by Vo-Thanh *et al.*.[110] Interestingly, in this case the ionic liquid **239** was also being used as the solvent, which removed the need for acids or any other catalyst within the reaction mixture.[111] It was noted that these chiral ionic liquids were recycled, with their efficiency being preserved, thus making this a green alternative to the traditional Lewis acid mediated aza-Diels-Alder reaction between Danishefsky's diene **4** and imines **238**. It was thought that the reaction proceeds though intermediate **241**, with yields of up to 66% and de of 60% of **240** being obtained at room temperature. Higher yields were obtained at lower temperatures due to a reduction in decomposition of Danishefsky's diene **4**. However, in such cases only the racemic product was obtained. Thus in order to reduce decomposition of Danishefsky's diene **4** at room temperature, the diene **4** was added in three phases at equal intervals, consequently improving the yield by 20% compared to when the diene **4** was added all at once (Scheme 36).

Cinchona-derived catalysts[112] have been developed and used since the late 1970s. Using this methodology, Park *et al*. have recently shown that these *cinchona*-derived ammonium catalysts **242** can also be prepared and applied to the aza-Diels-Alder reaction between an imine **11** and Danishefsky's diene **4** in order to form different dihydropyridones **12**.[113] After optimisation of the catalyst **242**, they were able to achieve the racemic product **12** in good yield (Equation 23).

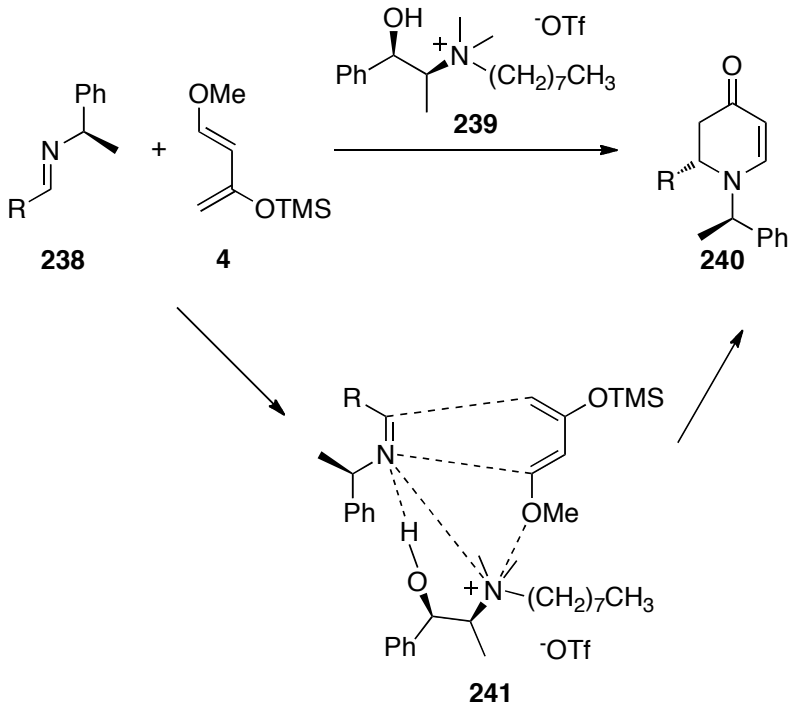

Scheme 36. The use of Ionic liquid **239** within the aza-Diels-Alder reaction, showing its possible interaction with the substrates **238** and **4**.

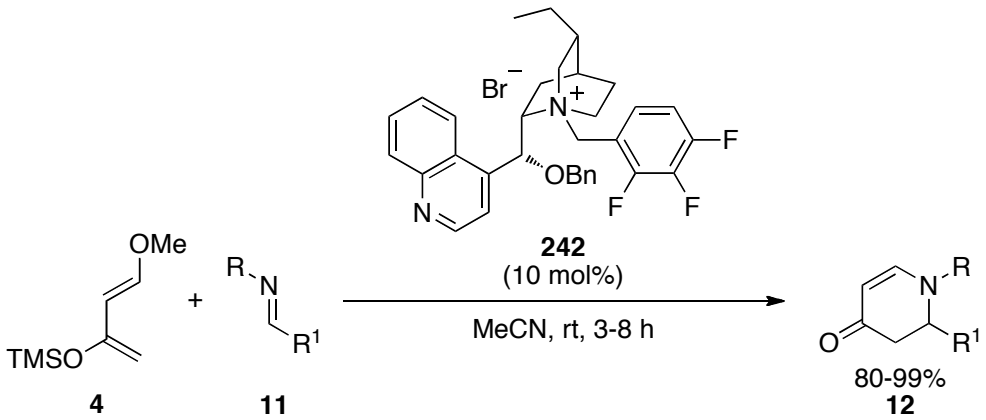

Equation 23

Subsequently, Park *et al*. tried to increase their substrate scope by reacting cyclic arylimines **243** with Danishefsky's diene **4** in the presence of their catalysts **242**. In doing so, they were able to synthesise polycyclic-dihydropyridones **244** and **247**, which are essentially the skeletons for the medical drug tetrabenazine **245**[114] (used to treat chorea associated with Huntington's disease) and the alkaloid tangutorine **248**[115] respectively (Scheme 37). However, lower yields of 50-54% were obtained for these

cyclisations, presumably because the conjugation between the imine and the aromatic rings significantly lowers the reactivity of the system. Despite their moderate yields, this was the first time that the synthesis of polycyclic-dihydropyridones *via* an aza-Diels-Alder pathway had been reported.

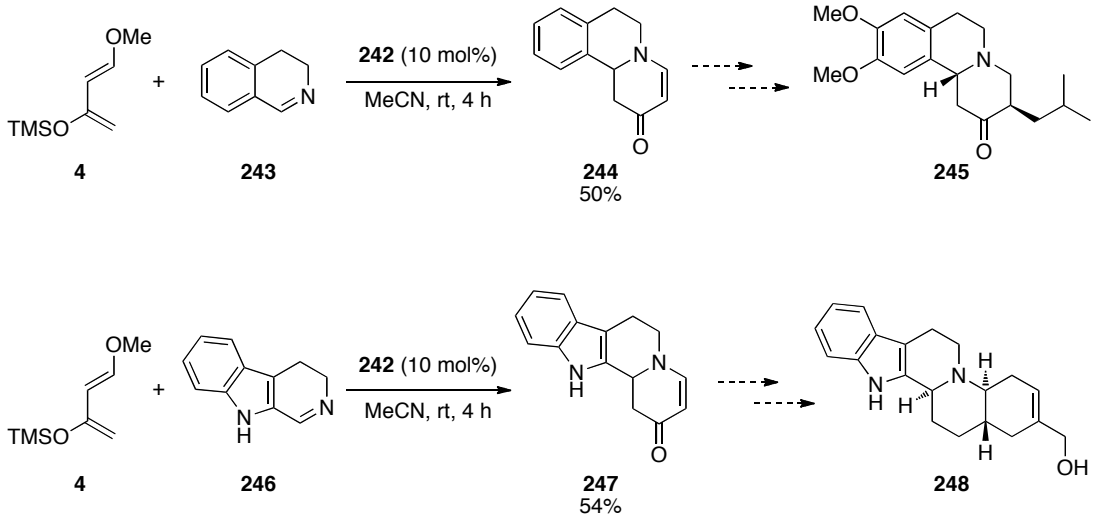

Scheme 37. The use of cyclic arylimines within the aza-Diels-Alder reaction.

As can be seen in the literature, the evidence suggests that when using electron rich dienes within the aza-Diels-Alder reaction, the process can be thought of as going through a Mannich-Michael reaction.[116] Using this Mannich-Michael principle, Raabe *et al.* have shown an example to form five-membered ring *N*-heterocycles **253** instead of 6-membered ones.[117] They performed this by reacting imines **249** with γ-malonate-substituted α,β-unsaturated esters **250** in the presence of bifunctional thioureas as catalysts. In their studies, they found that the Mannich product **252** was only formed when R = H. In order to make the intramolecular Michael addition proceed with the generated secondary amine, they found that they needed to make the Michael acceptor more electrophilic, which they achieved by adding an additional ester function to the double bond. Hence, when R = CO_2Me, they were able to obtain the cyclised product **253** in good yield. This example shows the importance of the electronics of the system in order to make the Mannich-Michael reaction proceed in the way one wishes.

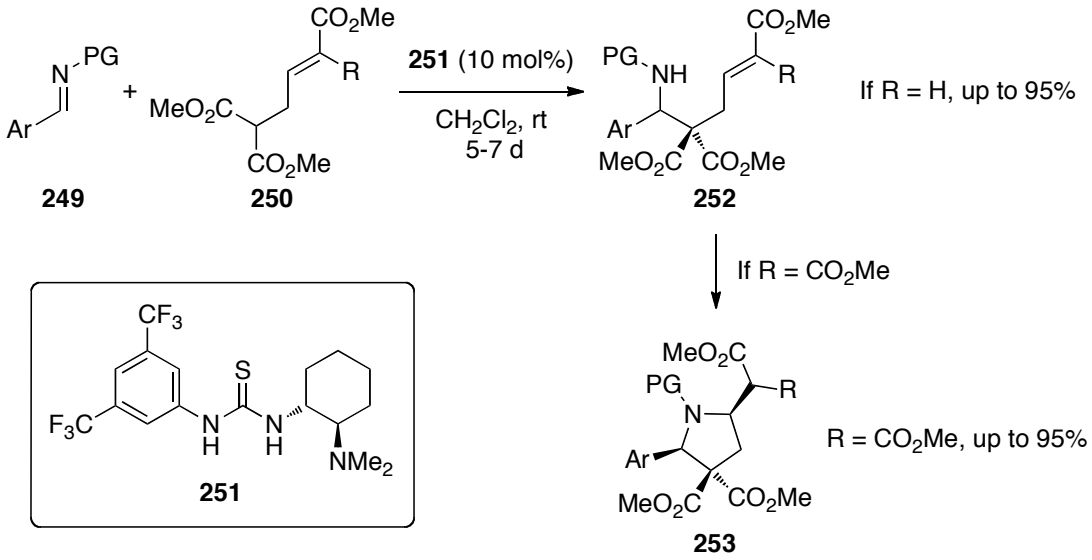

Scheme 38. A Mannich-Michael cycloaddition to form five-membered *N*-heterocycles **253**.

1.6 Other aza-Diels-Alder reactions using azadienes

When the nitrogen component is located within the diene, different piperidine ring derivatives are obviously formed compared to when the nitrogen is located within the dienophile,[118] and below are a few of the more recent examples found within the literature. For example, Palacios *et al*. have shown that 1-azadienes (i.e. α,β-unsaturated imines) **254** can react with an enamine **256** as the dienophile in order to form the desired piperidine ring in good regio- and stereo-selectivity (Scheme 39).[119] Indeed, the enamine **256** can also be formed *in situ* by using an aldehyde and a proline-derived organocatalyst.[120]

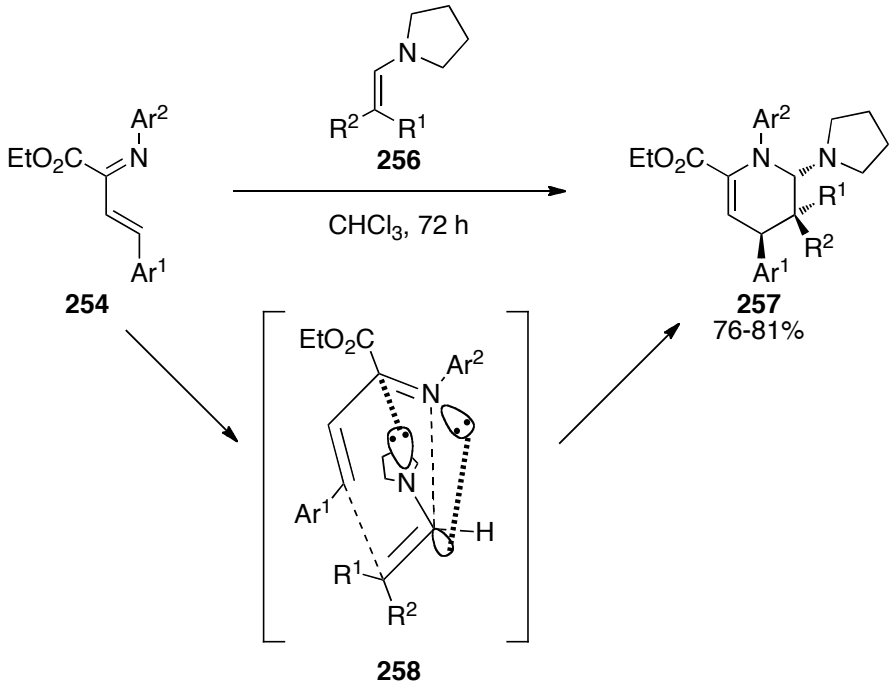

Scheme 39. An aza-Diels-Alder reaction between an azadiene **254** and an enamine **256**.

A further example of the use of organocatalyst **205** has been shown by Chen *et* al. in the presence of benzoic acid within the aza-Diels-Alder reaction of aldehydes **259** and aza-dienes **260**.[121] The piperidine ring product **261** subsequently undergoes an intramolecular hemiacetal formation to **262**, which can then be oxidised to give the lactone **263** (Scheme 40). High yields of 90% were obtained using MeCN as the

solvent, whilst THF gave low yields of 30%. MeOH, toluene and CH_2Cl_2 gave similar high yields of 81-83%, with good efficiency and excellent stereocontrol.

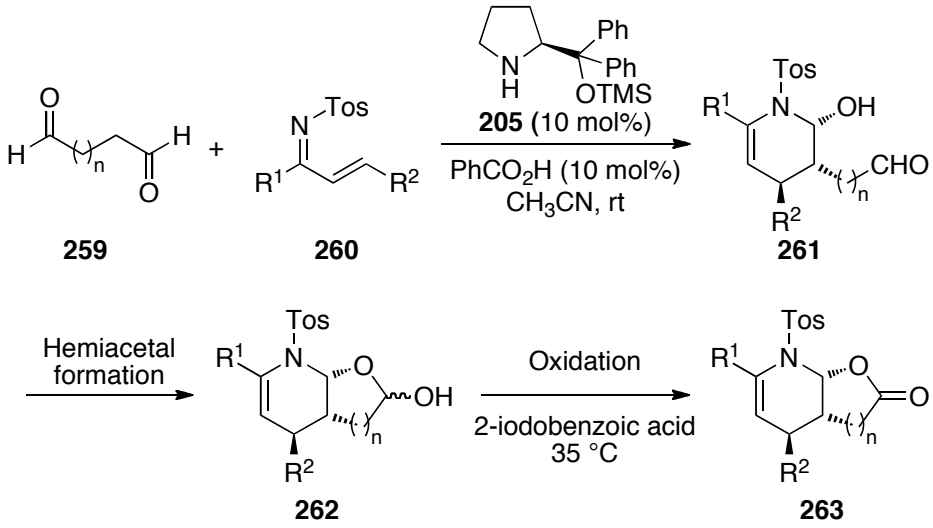

Scheme 40. Formation of lactones **263** *via* the aza-Diels-Alder reaction.

These types of lactone-piperidine containing compounds are frequently observed within natural products. Examples include the biologically active marine natural product class of zoanthamines **264**,[122] and the alkaloid lycojapodine A **265**, which acts as an inhibitor towards acetylcholinesterase and HIV-1.[123]

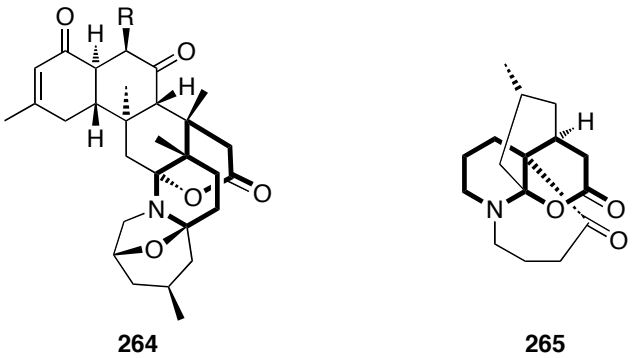

264 **265**

The direct cycloaddition of **267** onto activated enamines is not normally an effective strategy *via* enamine activation.[124] Reasons are given that this may be due to self-condensation, oligomerisation, as well as poor stereocontrol.[125] Despite this, Chen *et al*. have also demonstrated that acetaldehyde **267** can be used in the inverse-electron-demand aza-Diels-Alder reaction with azadiene coumarin derivative **266** to form piperidine rings **269**.[126] This reaction was catalysed by proline-type organocatalyst

268 (20 mol%) and benzoic acid (20 mol%) and gave good yield and high ee after 24 hours. The newly formed piperidine ring **269** was subsequently dehydroxylated to **270** to aid with the analysis (Scheme 41). Hence, this reaction used the coumarin skeleton **266**, a natural product first isolated in 1830 from tonka beans.[127] Its derivatives exhibit broad biological activities, ranging from anti-inflammatory agents[128] and coronary vasodilators,[129] to tautomerase inhibitors[130] and selective FXIIa inhibitors.[131]

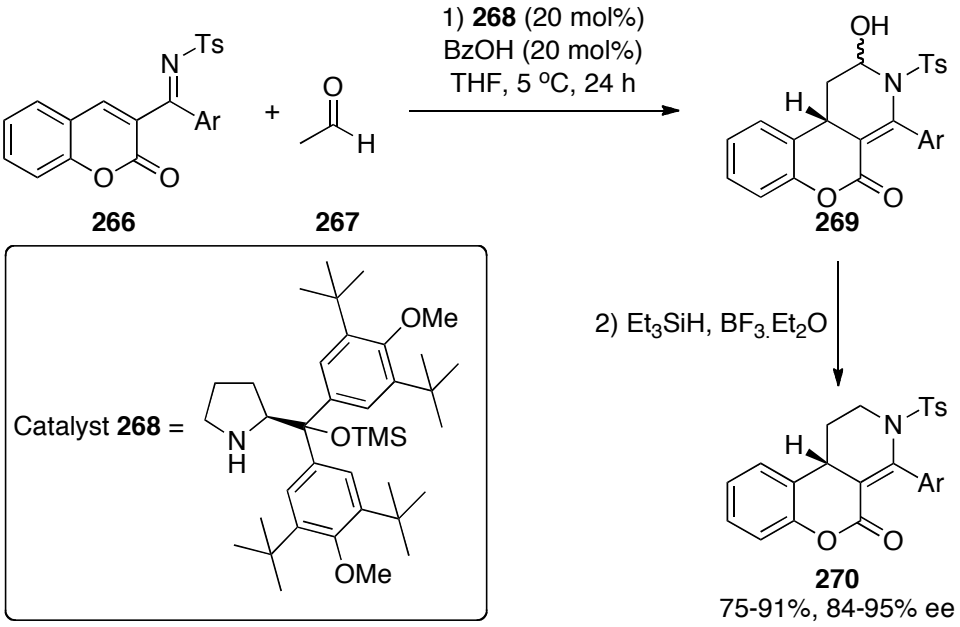

Scheme 41. The use of coumarin derivatives **266** within the aza-Diels-Alder reaction.

If the carbonyl double bond of an aldehyde **8** is specifically used as the dienophile, 1,3-oxazinan-4-ones **273** can be formed with electron-rich azadienes **271** in the presence of a Rhodium catalyst. Hashimoto *et al*. have shown that this reaction proceeds exclusively in an *endo* mode to give the desired product in high yields and high levels of enantioselectivity.[132] Only 1 mol% of Rh_2(*S*-BPTPI)$_4$ (dirhodium(II) tetrakis[*N*-benzene-fused-phthaloyl-(*S*)-piperidinonate]) was necessary to catalyse the reaction (Scheme 42).

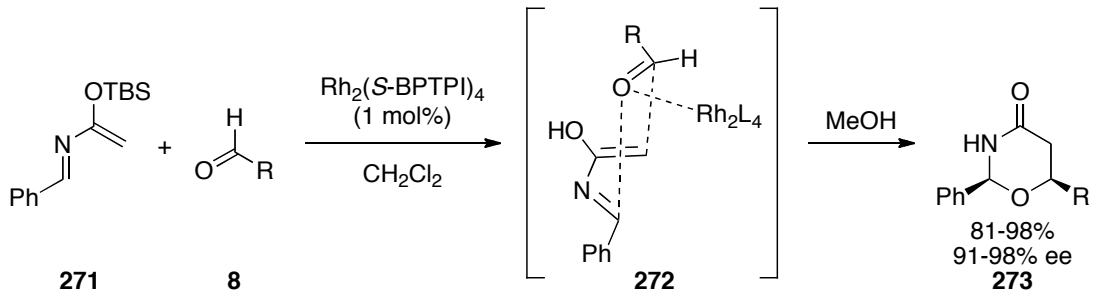

Scheme 42. Catalytic asymmetric hetero-Diels-Alder reaction between azadiene **271** and aldehydes **8**.

If an alkyne is used as the dienophile instead of an olefin, no extra catalysts are normally needed to make the reaction cyclise.[133] For example, Kim *et al*. have shown that 1,4-dihydropyridine **276** can be formed either by heating the reaction mixture under reflux[134] or by microwave irradiation.[135] Through these methods, they were able to synthesise Amlodipine[136] **277** after four extra steps. This is a compound that acts as a Ca^{2+} blocker[137] and hence, is currently used as an antihypertensive drug.[138]

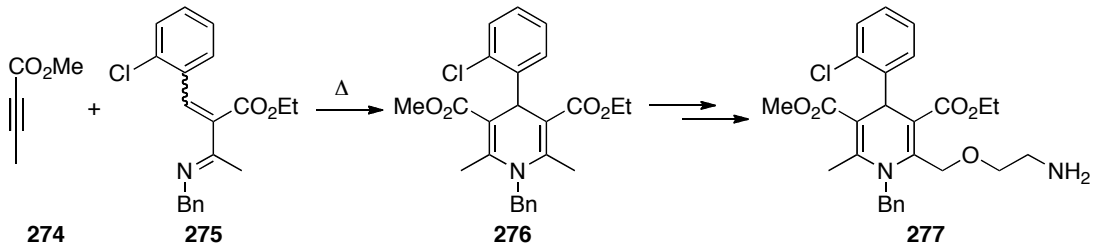

Scheme 43. Synthesis of amlodipine **276** *via* an aza-Diels-Alder reaction between 1-azadiene **275** and alkyne **274**.

A further interesting example using an alkyne **281** as a dienophile is shown by Singh *et al*. through a three-component one-pot reaction, whereby the 1-azadiene **280** is formed *in situ* by reacting pyrido[2,3-*d*]pyrimidine **279** with an aldehyde **8** in the presence of catalytic amounts of L-proline **152**. Through this method, the organocatalyst **152** forms an iminium ion **278** with the aldehyde **8**, thus making it sufficiently electrophilic for a conjugate addition to take place with the enamine **279** in order to form the 1-azadiene **280.** Reaction with the alkyne **281** subsequently affords the aza-Diels-Alder product **282** (Scheme 44).[139] These compounds containing the pyrido[2,3-*d*] framework are biologically important, with numerous examples known to show different pharmacological properties, such as antibacterial,[140]

antitumour,[141] cardiotonic,[142] antialergic,[143] antimalarial,[144] analgesic,[145] antifungal properties[146] and as a CNS depressant.[147]

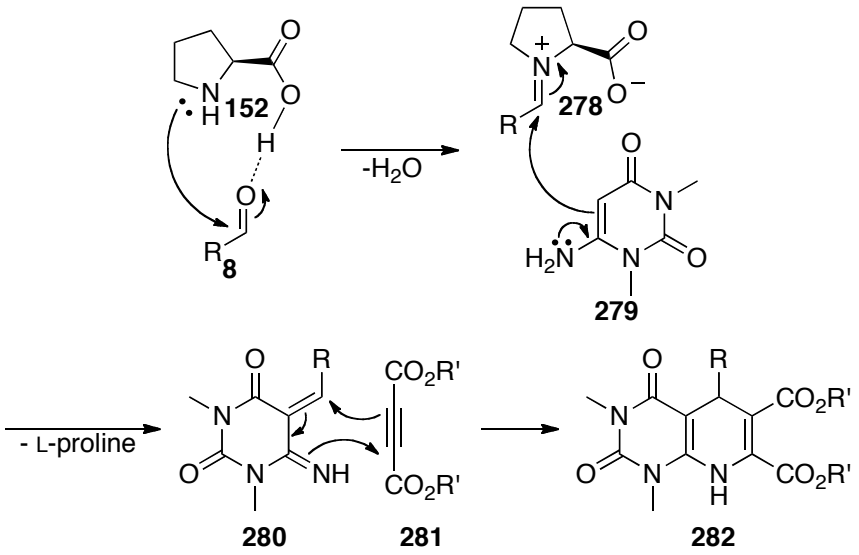

Scheme 44. An organocatalysed route to construct the pyrido[2,3-*d*] framework **282**, the reaction being performed at reflux.

2-Azadienes have also been reported to undergo inverse electron demand aza-Diels-Alder cycloadditions when using a suitably active dienophile species in the presence of an appropriate acid. These 2-azadiene species are typically an imine where the nitrogen is protected with an aromatic group and thus, one double bond within the aromatic ring forms part of the diene (**283**). Examples of the dienophile include 3,4-dihydro-2*H*-pyran **284**[148] or 2,3-dihydrofuran **285**[149] as the dienophile (Scheme 45) and hence, this method effectively synthesises a fused tricyclic compound (**286-288**) with good regioselectivity. Interestingly, varying the temperature can also control the stereoselectivity (compare **286** with **287**). Additionally, the diene can also be formed *in situ* by reacting an aldehyde with a primary amine attached to an aromatic ring, such as aniline.[150]

Similar reactions are observed when using an alkyne **289** as the dienophile, either intermolecularly[151] or intramolecularly,[151, 152] with the piperidine ring **290** being formed in good yield and regioselectivity. Interestingly, where an alkyne is used instead of an olefin **284** or **285**, the ring containing the nitrogen aromatises to give the observed product **290** (Scheme 45).

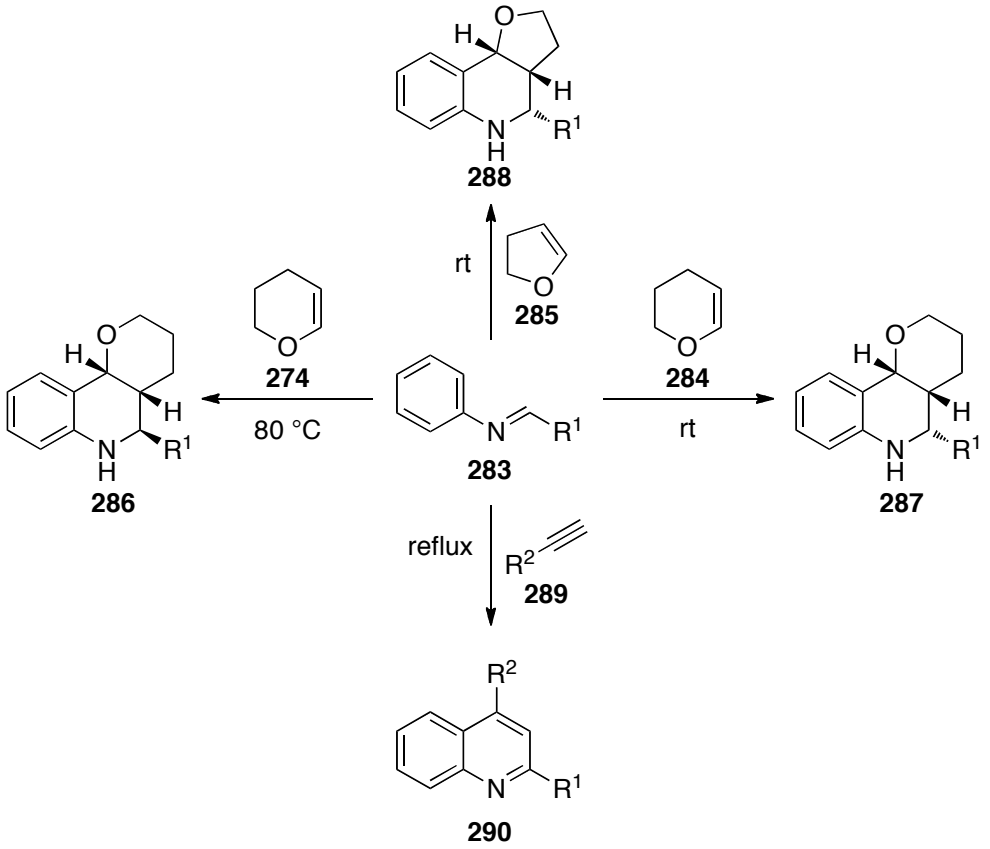

Scheme 45. Aza-Diels-Alder reactions using 2-azadienes.

Boronates **293** derived from imines have also been shown to be effective in the formation of piperidine rings in order to access functionalised dihydroquinolines **295**, whereby the imine is essentially part of a 2-azadiene unit.[153] In these cases, the imine nitrogen **293** coordinates to and polarises the C=N bond. This, in turn, increases the reactivity of the arylamine towards the imino-Diels-Alder reaction (However, this route is limited to specific imines that are capable of forming the boronate) (Scheme 46).

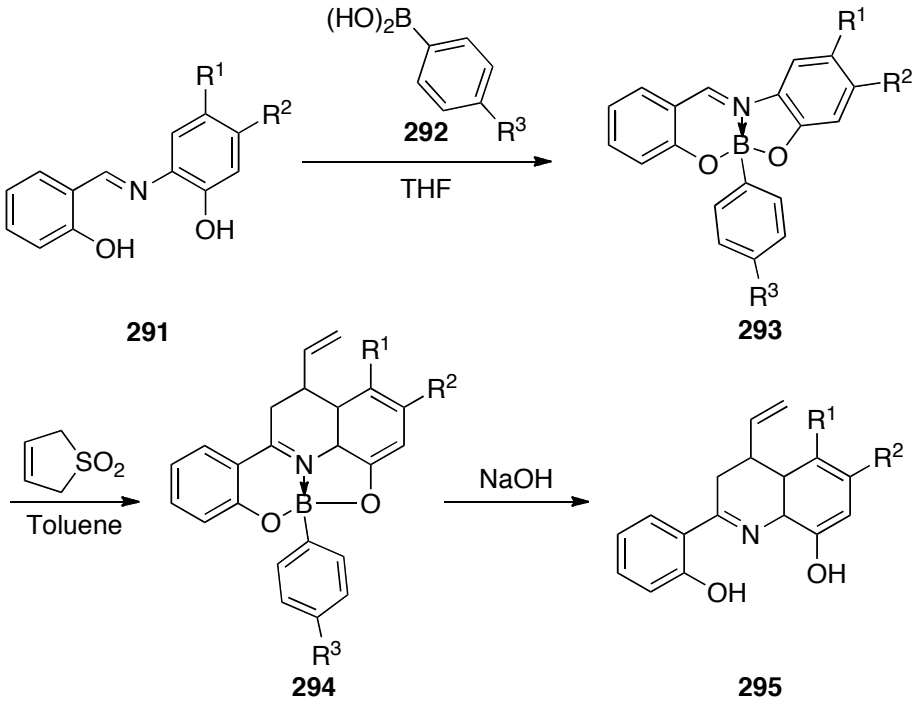

Scheme 46. Piperidine ring formation using boronic acids.

Once the boronate complex **293** was formed, a diene could cyclise with the activated imine bond, thus forming the unsaturated piperidine ring **296** (Scheme 47). This reaction proceeded by inverse electron demand, because the 2-azabutadiene system present in the boronates was electron deficient and it reacted with butadiene as the dienophile. Subsequent hydrolysis under basic conditions afforded the desired dihydroquinolines **295**.

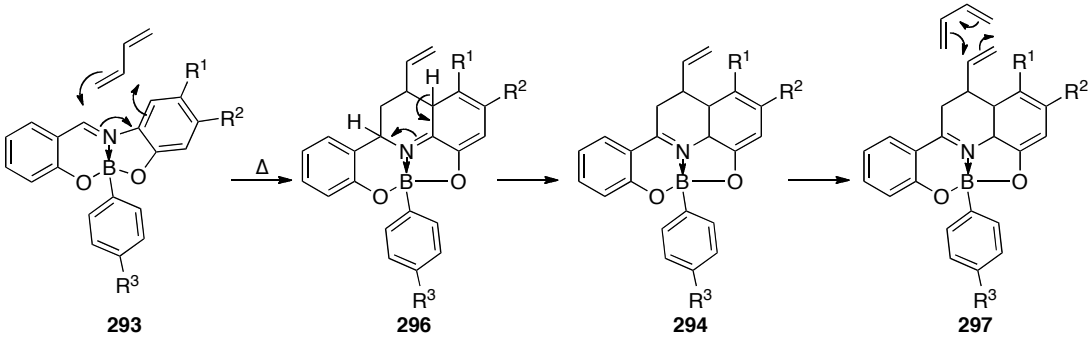

Scheme 47. Mechanism for the formation of piperidine rings *via* a boronate complex.

1.7 Other ways of forming piperidine rings

Whilst looking into the formation of β-amino ketones from ketones and aromatic imines *via* a Mannich reaction induced by radicals, Wang *et al*. found that piperidine rings **307** could also be formed by this method.[154] To form their β-amino ketones **303**, the imine **300** was activated by a radical cation salt (TBPA+), whilst the tautomerisation of the ketone **298** to the enol **299** was aided with a Lewis acid. Hence, the activated starting materials reacted with each other to give the desired β-amino ketone **303**. Depending on the aromatic substituent of the imine, **303** could react further to form piperidine **307**. Formation of this ring structure was dependent on having a *p*-NO_2 group on Ar^1. This was thought to be due to the increased electrophilicity of the radical cation intermediate **301** that the electron-withdrawing group brings, thus making the second addition to the enol tautomer of **303** more favourable. Electron transfer followed by intramolecular substitution then afforded the piperidine ring **307** in mild yields of 18-48% (Scheme 48).

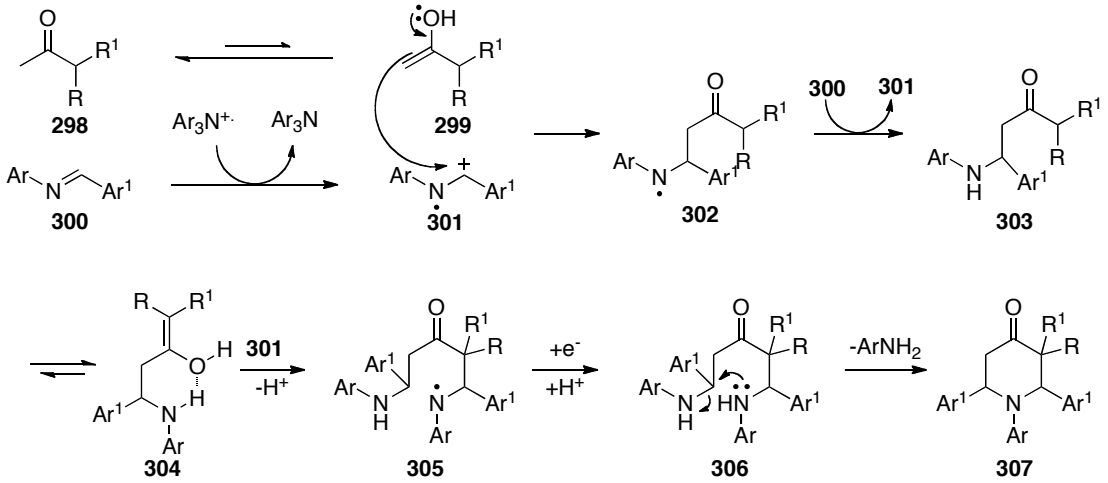

Scheme 48. A radical initiated aza-Diels-Alder reaction.

Through the use of azomethine ylids **309**, aza-Diels-Alder cyclisation reactions are also possible in an intramolecular fashion, where the imine and enone are tethered together as one starting material **308**. Hence, the stereochemistry of the product **310** is locked in place from the start. Gin *et al*. have used this idea in their quest for the first non-racemic synthesis of stemofoline,[155] a biologically active alkaloid first isolated in 1970 by Irie and co-workers.[156] Thus, in the presence of trifluoromethanesulfonic

anhydride (Tf_2O) and tetrabutylammonium triphenyldifluorosilicate (TBAT), the carbonyl oxygen conjugated with the amine in **308** was activated, followed by desilylation with the anhydrous fluoride source to form the azomethine ylid **309**. It was thought that this was followed by an intramolecular [3+2]-cyclisation in order to stereoselectively afford the desired polycyclic alkaloid **310** in good yield (71%) (Scheme 49). Equation 24 shows the proposed interaction prior to cyclisation.

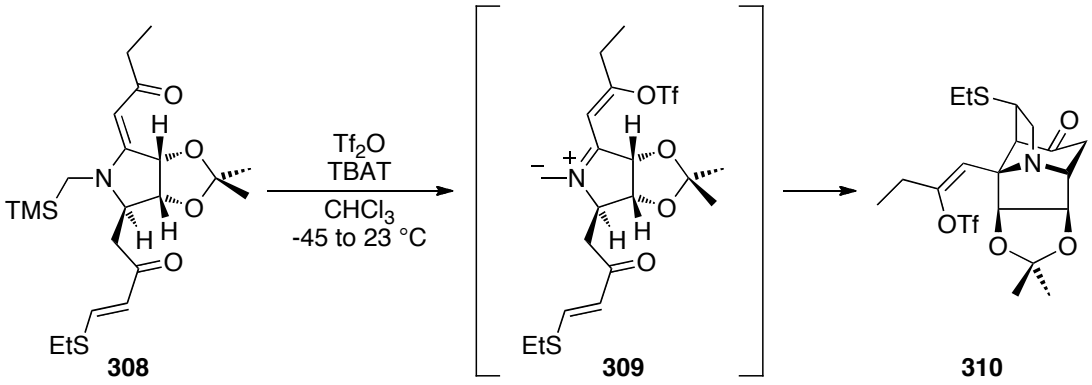

Scheme 49. An aza-Diels-Alder reaction going *via* an azomethine ylid intermediate.

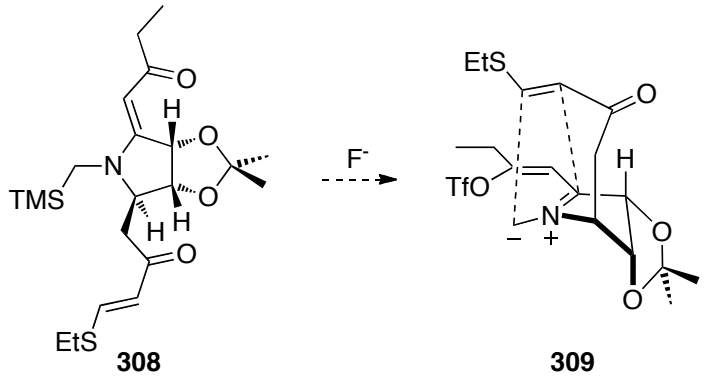

Equation 24

Additionally, piperidine rings can also be formed *via* routes that do not involve the Mannich reaction. These include: 1) ring formation *via* alkylation of a nitrogen centre with an acyclic precursor containing pre-established stereogenic centres; 2) asymmetric generation of stereocentres and substitution patterns on an existing six-membered heterocycle; 3) ring expansion of pyrrolidine or furan derivatives; and 4) ring closing-metathesis on dialkyl substituted nitrogen derivatives where each alkyl group contains an appropriately positioned alkene functional group.[157]

1.6 Summary

In summary, the present evidence suggests that the aza-Diels-Alder reaction of electron rich dienes with imino dienophiles proceeds *via* a Mannich-Michael process as opposed to a concerted mechanism. This is largely supported by the presence of Mannich-intermediates, which have been isolated within reaction mixtures. Generally, Lewis acids or organocatalysts catalyse this reaction.

With the use of Lewis acids, activated enones in the form of the Danishefsky's diene have traditionally been necessary, along with stoichiometric amounts of the Lewis acid. However, with more recent optimised examples, the Lewis acids have been shown to be effective in catalytic amounts using enones as the diene, although a secondary acid is sometimes needed to activate the enone to the enol. With regards to the reaction conditions, a lower temperature in general gives higher stereoselectivity. Conversely, a lower temperature also lowers the yield obtained, hence a compromise is usually reached between 0 °C to room temperature. Depending on the Lewis acid used, different polarities of solvent are effective. For example, Zn(II) catalysts tend to operate more effectively in polar solvents, whereas phosphoric acid catalysts prefer non-polar solvents. Additionally, the diene used seems to be limited to the electron rich Danishefsky diene or cyclic enones.

The use of organocatalysts in the aza-Diels-Alder reaction has only been investigated in the last decade. Higher catalyst loadings are needed compared to their individual Mannich and Michael reaction counterparts and this is due to the increased steric congestion. Proline-derived organocatalysts seem to work well here, although if the catalyst has no acidic character, then an additional catalytic amount of acid tends to be needed in the reaction. The main disadvantages of using organocatalysts are the necessity of including a large excess of enone (typically 4 equivalents, although sometimes as much as 30), as well as their low reactivity; many days are required for the reactants to cyclise. As a result, the reactions are normally carried out at room temperature. Additionally, it seems to be of preference to abstain from having aromatic groups on the nitrogen of the imine.

Nonetheless, the field of the aza-Diels-Alder reaction is still in its infancy, and no doubt the same advances will be seen with the use of organocatalysts as have been seen with Lewis acids. [116] After all, industry is always looking into new ways of constructing these rings asymmetrically to make the synthesis of highly functionalised piperidines more efficient and versatile.

Chapter 2:

AIMS AND OBJECTIVES

2. Aims and Objectives

The piperidine ring is an important moiety found in countless natural products, many of which are biologically active. Examples include: nicotine **310**;[158] the fire ant toxin solenopsin **311**;[159] and the alkaloid (*S*)-scoulerine **312**,[160] a natural medicinal compound acting as an adrenoceptor and 5-HT receptor antagonist (Figure 1). An atom-economical route for the formation of these biologically active piperidine ring systems could be *via* an aza-Diels-Alder pathway.

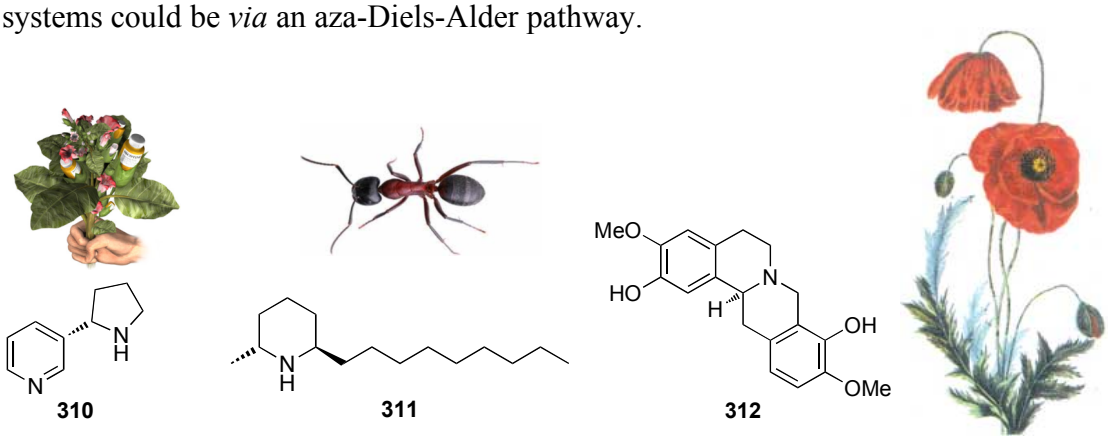

Figure 1. Examples of different biologically active piperidine rings.

By using metal- or organo-catalysis in an aza-Diels-Alder reaction, different piperidine ring systems could be synthesised and subsequently manipulated to form the biologically active compound of ones choice (Scheme 50). The metal catalysed aza-Diels-Alder reaction has been known for some time,[116] whilst the more recent organocatalytic route is currently a slower and less efficient process, requiring a large excess of enone (4-30 equivalents)[9] and long reaction times (1-7 days),[91] with varying yield ranges of isolated compound obtained. Hence, there is a need to make the aza-Diels-Alder reaction cleaner, greener and more robust.

For the aza-Diels-Alder reaction, current procedures mainly rely on using Lewis or Brønsted acids as catalysts, with limited procedures available for the use of organocatalysts. Hence, a main objective of this research was to investigate, with the aim of improving, the organocatalysed aza-Diels-Alder reaction.

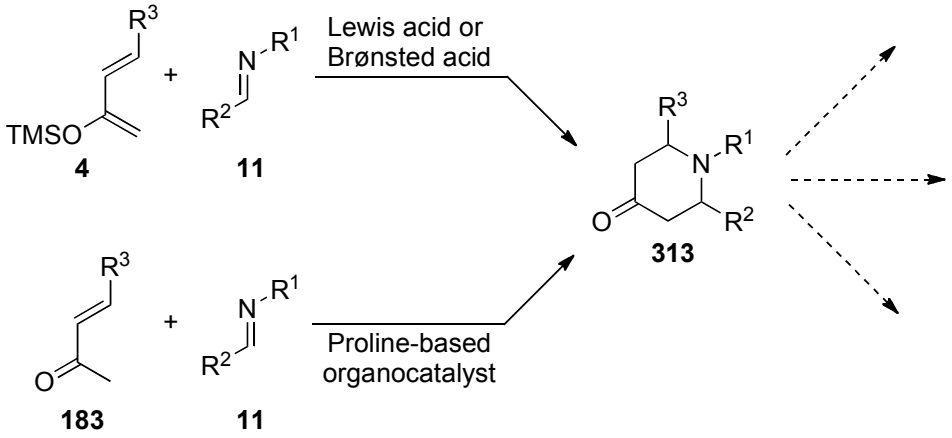

Scheme 50. aza-Diels-Alder routes using different catalysts.

A desired method to perform an atom-economical aza-Diels-Alder reaction would be to react an amine, aldehyde and ketone together in a one-pot, three-component system; thus eliminating the need to pre-form the imine and saving time and money in the process. Hence, the first aim in this project was to probe how viable this method was by determining whether a broad selection of amines, aldehydes and ketones could react together in this way. Further investigations would determine what reaction conditions and substrate limitations were important within the aza-Diels-Alder reaction.

The approach towards the development of an asymmetric organocatalytic aza-Diels-Alder reaction was based on imminium catalysis and Lewis acid activation through boronic acids **315**. These bifunctional aminoboronic catalysts have recently been shown to give high asymmetric induction for the aldol reaction (Scheme 51).[161] Hence, a further aim of this project was to synthesise and compare these bifunctional aminoboronic acids with other more established pyrrolidine-derived organocatalysts to see if these acids could be better suited for the aza-Diels-Alder reaction.

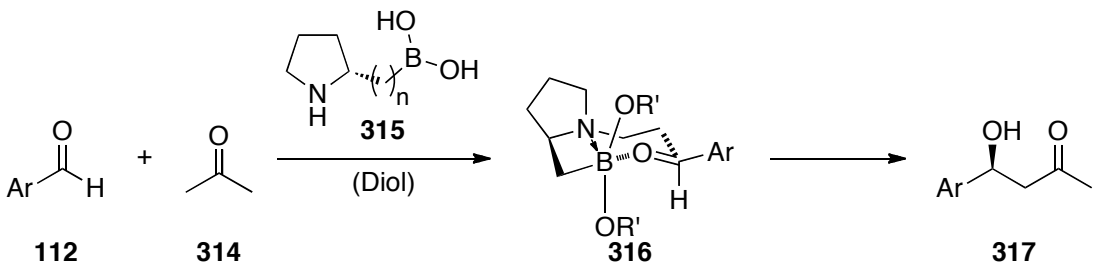

Scheme 51. Example of aminoboronic acid reactivity in the aldol reaction.

For the aza-Diels-Alder reaction, it was believed that the reaction would go through a stepwise Mannich-Michael process *via* transition state **321** (Scheme 52). Hence, the Mannich and Michael reactions would be individually investigated in order to determine what characteristics of the aminoboronic acid would be important in order to make this a successful catalyst for the aza-Diels-Alder reaction.

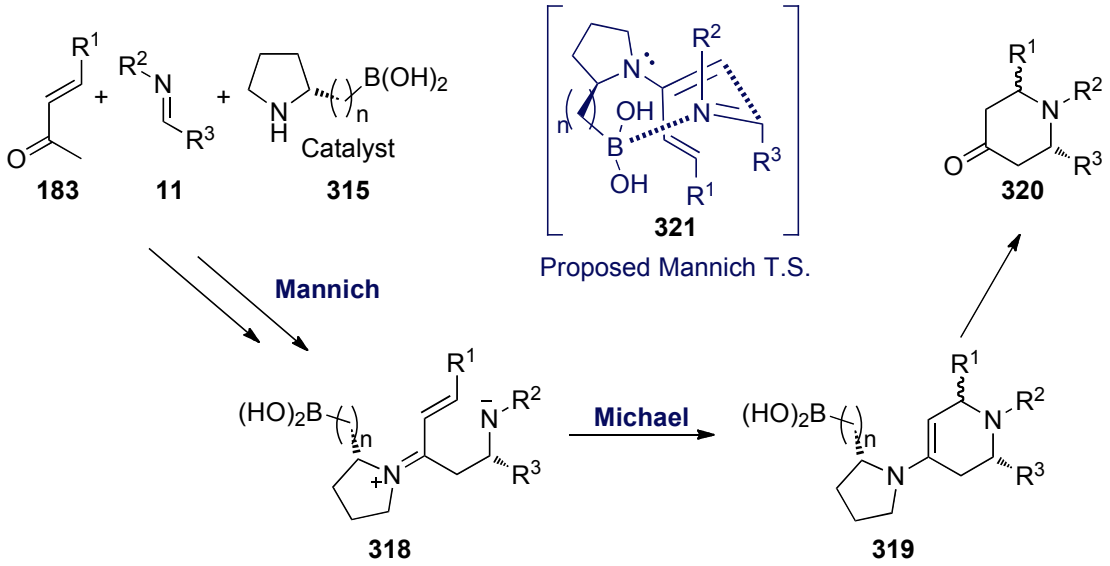

Scheme 52. Proposed aza-Diels-Alder reaction using bifunctional aminoboronic acids as catalysts.

There is substantial industrial interest in advancing the field of piperidine ring formation, due to the medicinal properties that such piperidine ring-containing compounds possess. Hence, the development of a robust, efficient and general organocatalytic aza-Diels-Alder process has the potential to make a considerable impact within industry by lowering costs, saving time and improving on their green ratings through following procedures that are more environmentally friendly.

Chapter 3:
RESULTS AND DISCUSSION

3. Results and Discussion

3.1 Synthesis of Precursor Reagents

3.1.1 Imine Formation

Imines are typically synthesised by the condensation of primary amines and aldehydes. In terms of mechanism, such reactions proceed *via* a nucleophilic addition giving a hemiaminal intermediate, followed by elimination of water to afford the imine. A catalyst and/or a drying agent is typically used to help drive the equilibrium in favour of imine formation.

A selection of different imines were synthesised from their aldehyde and amine starting components in the presence of a drying agent, with the results tabulated in Table 1.

Imines **323**, **324**, **326**, **75** and **328** were relatively straightforward to synthesise and purify following literature procedures.[162] However, the synthesis of imine **330** proved to be unsuccessful (Table 1, Entry 7), whilst a low yield of 23% was obtained with imine **155** (Table 1, Entry 6). This can be attributed to one of the side-products of this reaction, **331**; a solid that was isolated from the crude oil reaction mixture and which was subsequently characterised. Two *p*-anisidine **120** units were consumed for every aldehyde **329** unit in order to make **331**. In the ^{1}H NMR of **331**, it is interesting to note that the N*H* proton is located in the 9 ppm region, which is further downfield than is expected for a simple amide. To confirm this assignment, a D_2O shake was performed on **331** in $CDCl_3$ to form **332** (Equation 25), whereby the N*H* peak at $\delta = 9$ ppm disappeared, showing that hydrogen to deuterium exchange had taken place confirming the ^{1}H NMR spectrum of **331**.

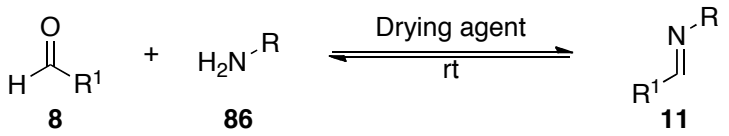

8 **86** **11**

Table 1. Synthesis of different imines.

Entry	Aldehyde	Amine	Solvent	Drying Agent	Product	Yield
1	 **322** 1.5 Equiv.	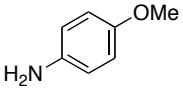 **120** 1 Equiv.	CH_2Cl_2	$MgSO_4$	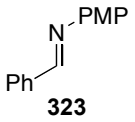 **323**	75%
2	 **322** 1 Equiv.	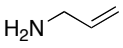 **186** 1.1 Equiv.	CH_2Cl_2	$MgSO_4$	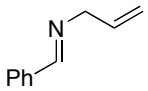 **324**	72%
3	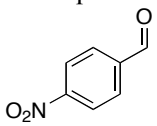 **325** 1 Equiv.	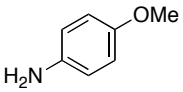 **120** 1 Equiv.	CH_2Cl_2	$MgSO_4$	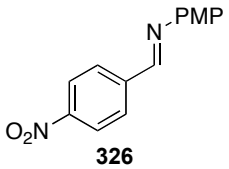 **326**	99%
4	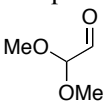 **327** 1.5 Equiv.	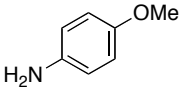 **120** 1 Equiv.	CH_2Cl_2	3 Å M.S.	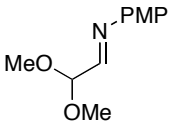 **75**	94%
5	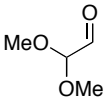 **327** 1 Equiv.	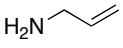 **186** 1.1 Equiv.	CH_2Cl_2	3 Å M.S.	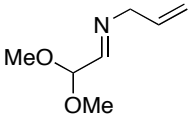 **328**	97%
6	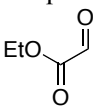 **329** 1 Equiv.	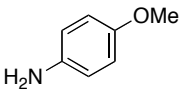 **120** 1 Equiv.	Toluene	$MgSO_4$	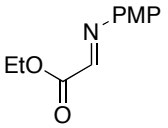 **155**	23%
7	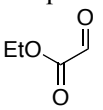 **329** 1 Equiv.	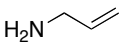 **186** 1 Equiv.	Toluene	$MgSO_4$	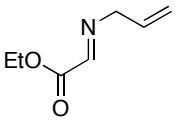 **330**	0%

It is also interesting to note that compound **331** had only been mentioned once before in the literature.[163] This was in a 1976 Russian paper looking into the association and mesomorphism of amido nitrones using infrared (IR) spectroscopy, in which only the IR and melting point of **331** were reported.

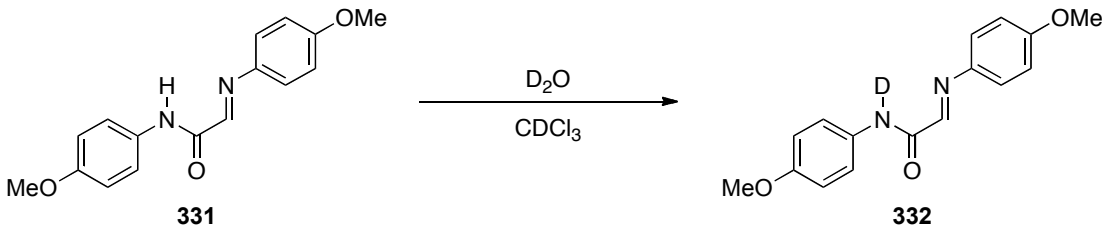

Equation 25

In order to compare configurationally locked imines to acyclic ones, the synthesis of cyclic imines **243**, **246**, **333** and **334** were also explored.

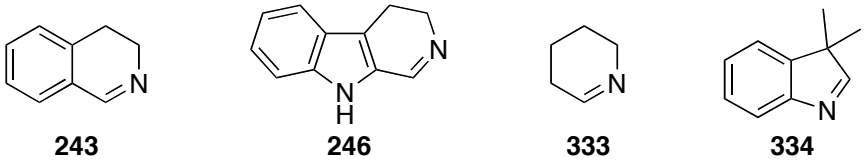

Imine **243** was synthesised in two steps in accordance with literature methods (Scheme 53).[164] Hence, 2-phenylethylamine **335** was heated neat with excess ethyl formate **336**, after which the excess ethyl formate was evaporated *in vacuo* to give the crude product. Purification using Kugelrohr distillation gave pure formamide **337** as a mixture of rotamers (around the amide bond) in the ratio 5:1 (^{1}H NMR). ^{1}H NMR experiments carried out in DMSO were performed at rt, 50 ºC and 100 ºC in an attempt to determine whether the rotameric species would interconvert. However, this did not occur, although the amide N*H* and C*H*$_2$ resonances did change chemical shift at different temperatures. Subsequent intramolecular cyclisation of formamide **337** was straightforward in polyphosphoric acid to give the pure imine **243**.

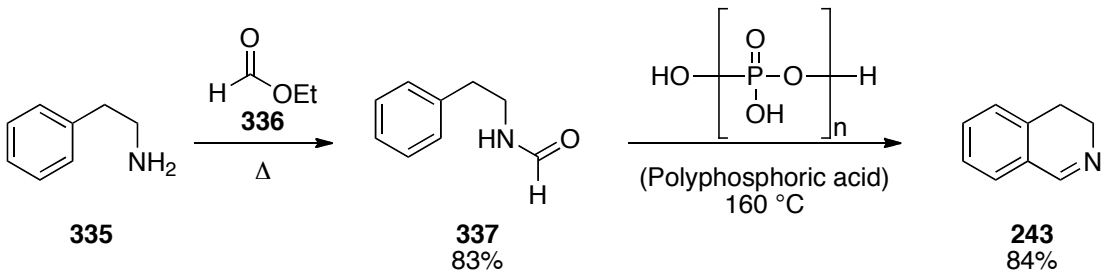

Scheme 53. Synthesis of cyclic imine **243**.

Imine **246** was synthesised in a similar fashion whereby formamide **339** was formed after refluxing tryptamine **338** with excess ethyl formate **336**.[165] However, cyclisation of formamide **336** using polyphosphoric acid at elevated temperatures proved challenging. Hence, phosphorus(V) oxychloride was used instead, in accordance with a procedure reported by O'Rell *et al.*,[166] in order to afford the desired imine **246**.

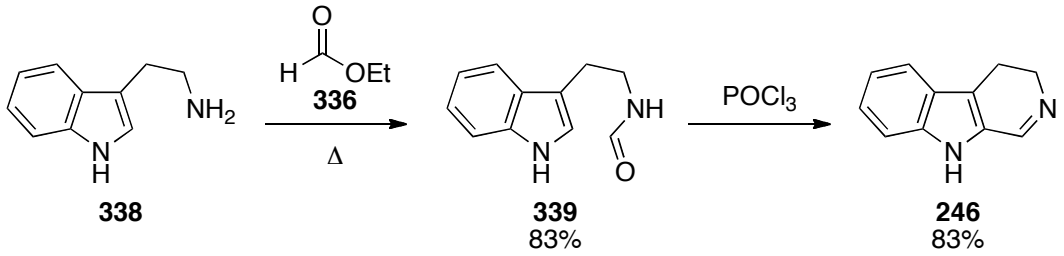

Scheme 54. Synthesis of cyclic imine **246**.

The synthesis of imine **333** was also straightforward following literature procedures, *i.e.* by reacting piperidine **340** with *N*-chlorosuccinimide (NCS), followed by treatment of the obtained chlorinated amine **341** with a base.[167] However, the product **333** was obtained as part of a mixture with its dimer **342** and trimer **343** forms; these species were confirmed by MS, IR and NMR.

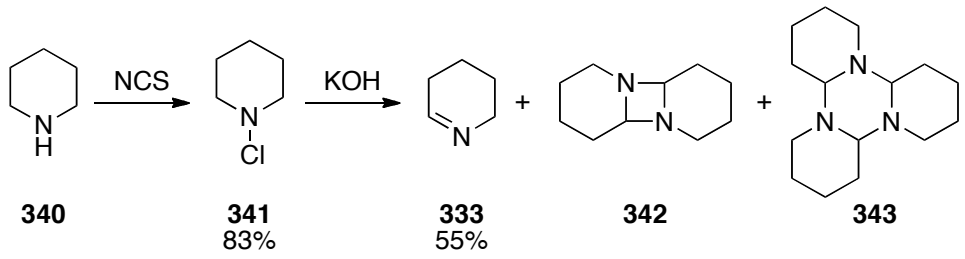

Scheme 55. Synthesis of cyclic imine **333**.

In order to compare six-membered cyclic imines with five-membered ones, the synthesis of imine **334** was also attempted. Imine **334** with the di-methyl group on the 3'-position was chosen, as this would prevent the imine tautomerising to the aromatic indole. Hence, the synthesis of **334** was attempted following a patent procedure starting with phenylhydrazine **344** and isobutyraldehyde **345**, with the intermediate **346** being cyclised in the presence of methanesulfonic acid (Scheme 56).[168] LCMS of

the crude reaction mixture showed the presence of the imine **334**. However, attempts to purify this compound proved futile and the imine **334** was not isolated.

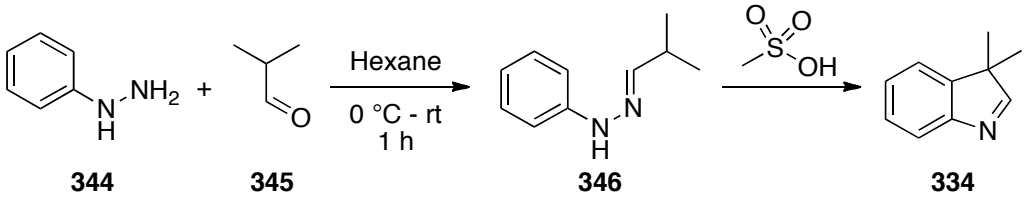

344 **345** **346** **334**

Scheme 56. Attempted synthesis of imine **334**.

3.1.2 Electron-Rich Diene Formation

Electron-rich dienes were needed for the comparison of the organocatalytic aza-Diels-Alder reaction with the Lewis-acid catalysed reaction. Hence, these dienes **347** were synthesised from their corresponding enones **183** (Table 2).[15, 169]

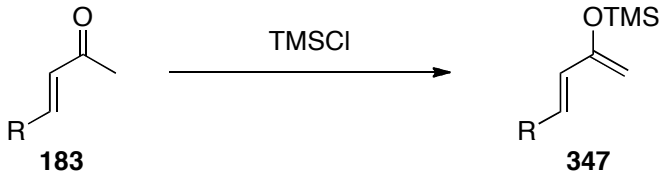

183 **347**

Table 2. Synthesis of electron-rich dienes.

Entry	Enone	Conditions	Diene (% Isolated Yield)	Main Impurity
1	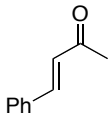 **348**	DBU rt, CH_2Cl_2	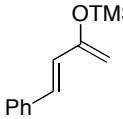 **349** 56%	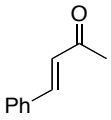 **348**
2	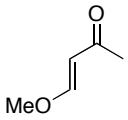 **350**	NEt_3, dry $ZnCl_2$ 40 ºC, Diethyl ether	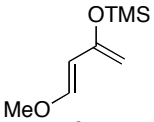 **4** 65%	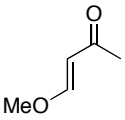 **350**
3	 **164**	NEt_3, dry $ZnCl_2$ 40 ºC, Diethyl ether	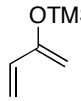 **351**	NEt_3

These reactions were found to be challenging; the dienes were easily hydrolysed to their corresponding enones, meaning care was needed to prevent this happening. In

addition, the dienes and their corresponding enones had very similar properties, making it a challenge to separate them from each other. These problems were partly circumvented by performing the reaction under inert conditions using anhydrous reagents, and by purifying by vacuum distillation.

Synthesis of diene **351** from enone **164** was attempted under inert conditions (Table 2, entry 3). However, purification proved to be challenging; the boiling point of diene **351** was too high for atmospheric distillation and too low for a facile reduced pressure distillation (lit. bp = 25-28 °C, 16 mbar).[170] Control of the vacuum was attempted using a bleed in the apparatus. Despite this, diene **351** was obtained contaminated with triethylamine.

3.1.3 Chalcone Formation

In order to determine whether the electronics of the enone may have a significant effect within the aza-Diels-Alder reaction, chalcones **169** with different electronics were synthesised from acetone **314** and their corresponding aldehydes **112** *via* an aldol condensation reaction (Table 3).[171]

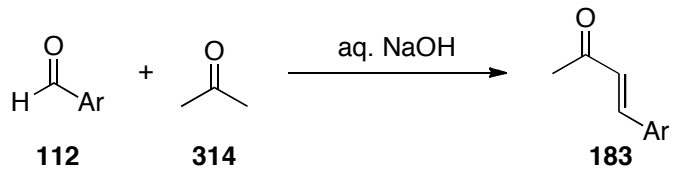

112 **314** **183**

Table 3. Synthesis of different chalcones.

Entry	Aldehyde	Temperature (°C)	Product	Yield (%)
1	 **322**	40	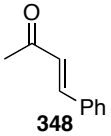 **348**	88
2	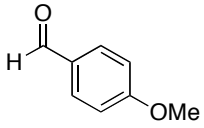 **352**	40	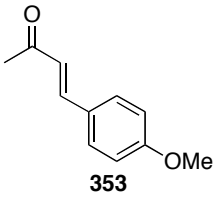 **353**	88
3	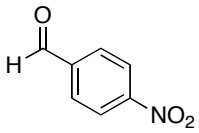 **354**	rt	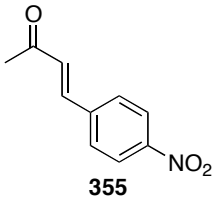 **355**	41

Thus, in addition to the electronically neutral enone **348**, the electron-donating enone **353** and the electron-withdrawing enone **355** were synthesised from aldehydes **322**, **352** and **354** respectively, with excess acetone **314** in (aq) NaOH (Table 3).

3.2 Aza-Diels-Alder Screening Studies

3.2.1 Screening of the One-Pot, Three-Component aza-Diels-Alder Reaction

A straightforward way to synthesise piperidine rings *via* an aza-Diels-Alder reaction would be to react a ketone with an amine and an aldehyde in the presence of a suitable catalyst. In order to help determine the robustness of this methodology, sets of different enones **183**, aldehydes **8** and amines **86** were screened in the presence of an organocatalyst in different solvents (Table 4).

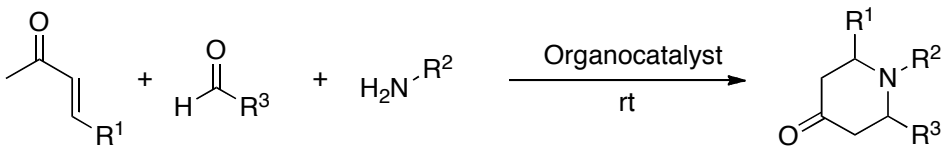

Table 4 (a). Tabulated results for the one-pot, three-component screening reactions.

Enone 4 mmol	Aldehyde 1 mmol	Amine 1.1 mmol	Catalyst 0.2 mmol	Solvent 2 mL
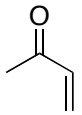 **164**	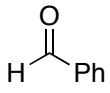 **322**	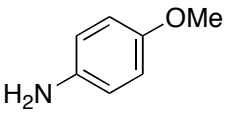 **120**	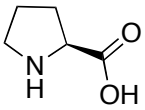 **152**	MeOH
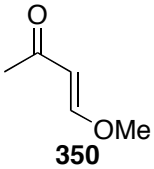 **350**	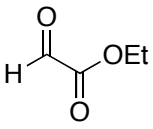 **329**	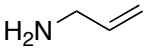 **186**	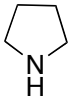 **356**	THF
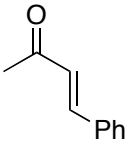 **348**	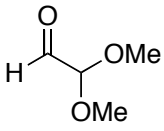 **327**			CH_2Cl_2

Table 4 (b). Tabulated results for the one-pot, three-component screening reactions.*

Aldehyde and Amine	Enone:	R^1 = H **164**						R^1 = OMe **350**						R^1 = Ph **348**					
	Catalyst:	Pyrrolidine **356**			L-Proline **152**			Pyrrolidine **356**			L-Proline **152**			Pyrrolidine **356**			L-Proline **152**		
	Solvent	**A**	**B**	**C**	**A**	**B**	**C**	**A**	**B**	**C**	**A**	**B**	**C**	**A**	**B**	**C**	**A**	**B**	**C**
322 (R^3 = Ph) + **120** (R^2 = Ar)	MeOH	0	0	N	0	0	N	0	1	N	0	1	N	0	0	N	0	0	N
	THF	0	0	N	0	0	N	0	1	N	0	1	N	0	0	N	0	0	N
	CH_2Cl_2	0	0	N	0	0	N	0	1	N	0	1	N	0	0	N	0	0	N
322 (R^3 = Ph) + **186** ($R^2 \neq$ Ar)	MeOH	0	0	N	0	0	N	0	0	N	0	1	N	0	0	N	0	1	N
	THF	0	0	N	0	0	N	0	0	N	0	1	N	0	0	N	0	0	N
	CH_2Cl_2	0	0	N	0	0	N	0	0	N	0	1	Y	0	0	N	0	1	N
329 (R^3 = CO_2Et) + **120** (R^2 = Ar)	MeOH	0	0	N	0	0	N	0	0	N	1	0	N	1	1	N	0	0	N
	THF	0	0	N	0	0	N	0	0	N	1	0	N	1	0	N	0	0	N
	CH_2Cl_2	0	0	N	0	0	N	0	0	N	1	0	N	1	0	N	0	0	N
329 (R^3 = CO_2Et) + **186** ($R^2 \neq$ Ar)	MeOH	0	0	N	0	2	N	0	0	N	0	0	N	0	0	N	0	0	N
	THF	0	0	N	0	0	N	0	2	N	0	0	N	0	2	N	0	1	N
	CH_2Cl_2	0	0	N	0	2	N	0	0	N	0	0	N	0	0	N	0	0	N
327 [R^3 = $CH(OMe)_2$] + **120** (R^2 = Ar)	MeOH	0	0	N	0	0	N	0	0	N	0	0	N	0	0	N	0	0	N
	THF	0	0	N	0	0	N	0	0	N	0	0	N	0	0	N	0	0	N
	CH_2Cl_2	0	0	N	0	0	N	0	0	N	0	0	N	0	0	N	0	0	N
327 [R^3 = $CH(OMe)_2$] + **186** ($R^2 \neq$ Ar)	MeOH	0	0	N	0	0	N	0	0	N	0	0	N	0	0	N	0	0	N
	THF	0	0	N	0	0	N	0	0	N	0	0	N	0	0	N	0	0	N
	CH_2Cl_2	0	0	N	0	0	N	0	0	N	0	1	N	0	0	N	0	0	N

***A** = the number of starting reagents completely consumed
B = the number of prominent/interesting new spots observed
C = TLC analysis suggesting a good, clean reaction (Y = yes, N = no).

Enones **164**, **350**, and **348** were chosen due to their ability to form piperidine rings with different degrees of saturation and substitution. Aldehydes **322**, **329**, and **327** were chosen for their electronic properties to form imines with varying levels of electronics. Amines **120** and **186** were chosen to determine how aromatic amines compare versus allylic ones. The organocatalysts **152** and **356** were chosen in order to compare the default organocatalyst of choice: L-proline **152**, against its un-functionalised analogue, pyrrolidine **356**. These compounds were screened against each other in small vials at room temperature, monitoring the reactions over a period of 24 and 48 hours by thin layer chromatography (TLC).

From these screening reactions (Table 4), it was apparent that most of the combinations of reactants afforded either multiple products or none at all; they did not form clean, robust, kinetically controlled reactions. This suggested that formation of

the imine beforehand could have been a better approach for the study of this reaction. Indeed, the one-pot, three-component reactions in the literature are usually performed after optimisation with the pre-formed imine.[92]

From the complex array of spots on the TLC plates, it was possible to deduce some further findings. The reactions using L-proline **152** as catalyst tended to consume the starting materials more rapidly than those using pyrrolidine **356**. This suggested that the acidic character of L-proline **152** was important. Regarding solvents, better reactivity was observed when using CH_2Cl_2, the opposite being true when using THF. Allylamine **186** gave cleaner reactions compared to aromatic amine **120**, as did the use of benzaldehyde **322** over ethyl glyoxylate **329**. In terms of the enones used, methyl vinyl ketone **164** was the least reactive, whereby most of the TLC spots observed were starting material spots. The Ph **348** and OMe **350** enones seemed to be similarly reactive to each other.

In order to determine whether the two-component reaction between an imine and an enone was cleaner than the three-component reaction, a further screening study was carried out whereby the imines were formed *in situ* prior to addition of the enone and catalyst. 3 Å Molecular sieves (M.S.) were used to aid with the imine formation by helping to remove water. After 48 hours, an enone and catalyst **152** (20 mol%) were added to the reaction mixture (Table 5). These reactions were monitored by TLC, whereby fewer minor spots were observed compared to the one-pot, three-component system. These results further suggested that pre-formation of the imine did lead to cleaner reaction outcomes.

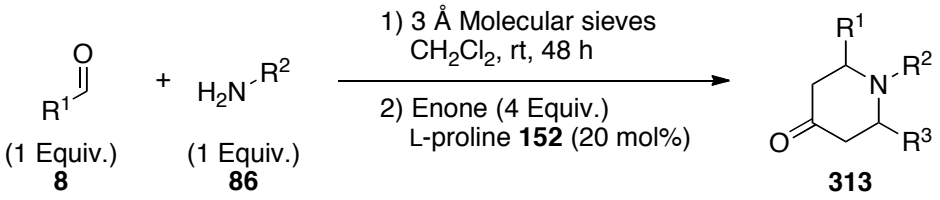

Table 5. Screening reactions where the imine was formed *in situ* prior to addition of the enone and catalyst.

Entry	Aldehyde (1 Equiv.)	Amine (1 Equiv.)	Enone (4 Equiv.)	Cleaner Reactions?
1	 **322**	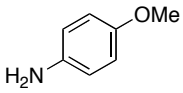 **120**	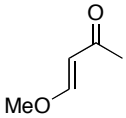 **350**	Slightly
2	 **322**	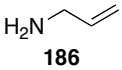 **186**	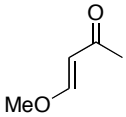 **350**	Slightly
3	 **322**	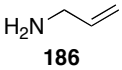 **186**	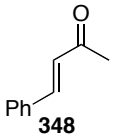 **348**	Yes

3.2.2 Screening Using Imines

Through the previous screening studies (Table 5), it was determined that the study of the aza-Diels-Alder reaction was better approached through the use of imines in a two-component reaction. Hence, the pre-formed acyclic imines **11** (Table 1) were screened in the aza-Diels-Alder reaction with enones **183** in order to determine if a combination of these would afford clean reactions to the desired piperidine ring product **313**. The reactions were performed in the presence of 3 Å molecular sieves in order to limit the amount of imine **11** hydrolysing back down to its corresponding amine **86** and aldehyde **8**. These screening reactions were performed in small vials at room temperature, with each reaction being monitored after 24 and 48 hours *via* TLC. The different combinations of enone to imine, catalyst and solvent used are tabulated in Table 6. In this set of screening reactions, THF was not used because this solvent had proved to be less effective for the one-pot, three-component screening reactions (Table 4).

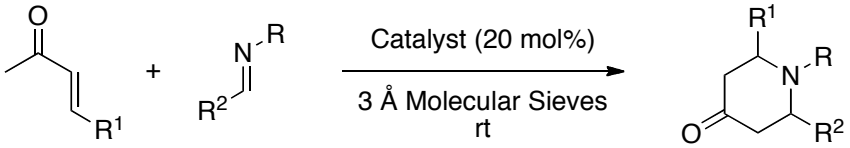

183 **11** **313**

Table 6. Tabulated results for imine screening reactions.*

	Enone:	R^1 = H **164**						R^1 = OMe **350**						R^1 = Ph **348**					
	Catalyst:	Pyrrolidine **356**			L-Proline **152**			Pyrrolidine **356**			L-Proline **152**			Pyrrolidine **356**			L-Proline **152**		
Imine	Solvent	**A**	**B**	**C**	**A**	**B**	**C**	**A**	**B**	**C**	**A**	**B**	**C**	**A**	**B**	**C**	**A**	**B**	**C**
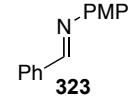 **323**	MeOH	0	0	N	0	1	N	0	0	N	0	1	N	0	0	N	0	0	N
	CH_2Cl_2	0	0	N	0	0	N	0	0	N	0	0	N	0	0	N	0	0	N
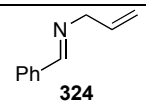 **324**	MeOH	0	0	N	0	0	N	0	1	N	0	1	N	0	1	N	0	1	N
	CH_2Cl_2	0	0	N	0	0	N	0	1	N	0	1	N	0	1	N	0	1	Y
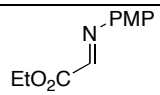 **155**	MeOH	1	0	N	0	1	N	0	0	N	0	1	N	0	0	N	0	0	N
	CH_2Cl_2	0	0	N	0	1	N	0	0	N	0	0	N	0	0	N	0	1	N
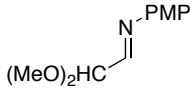 **75**	MeOH	0	0	N	0	1	N	0	0	N	0	1	N	0	1	N	0	1	N
	CH_2Cl_2	0	0	N	0	1	N	0	0	N	0	0	N	0	1	N	0	1	Y
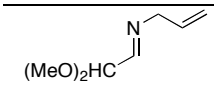 **328**	MeOH	0	0	N	0	0	N	0	0	N	0	1	N	0	0	N	0	0	N
	CH_2Cl_2	0	1	N	0	1	Y	0	0	N	0	1	N	0	1	N	0	1	Y

***A** = the number of starting reagents completely consumed
B = the number of prominent/interesting new spots observed
C = TLC analysis suggesting a good, clean reaction (Y = yes, N = no).

The results obtained from the imine screening reactions (Table 6) generally showed that cleaner reactions were taking place *via* TLC analysis, compared to the one-pot, three-component reactions. However, it was also observed that these reactions were slow, none of which went through to completion (single spot) after 48 h. These screening results also seemed to agree with the one-pot, three-component screening results, *i.e.* that CH_2Cl_2 seemed to be a better solvent to use compared with MeOH, and that L-proline **52** seemed to be a more active catalyst than pyrrolidine **356**. Methyl vinyl ketone **164** was the least reactive of the enones, whilst the most promising results seemed to be obtained when the allylic imines **324** and **328** were used.

The main challenge in analysing these screening reactions *via* TLC analysis was in determining which of the newly observed spots was the desired piperidine ring product **313**, if any. Hence, it was immediately apparent that the piperidine rings **313**

needed to be individually synthesised to obtain a set of standards, which could be used as a references in order to aid in the identification of the product. It was decided to synthesise the piperidines using two methods: a) an organocatalytic pathway using enones and L-proline; and b) a more traditional Lewis acid-catalysed pathway using electron-rich dienes.

3.3 Initial Piperidine Ring Formation Attempts

3.3.1 Attempted Piperidine Ring Formation Using Organocatalysts

Having all the starting materials at hand, the synthesis of piperidine standards **313** was attempted from their corresponding imines **11** and enones **183** and the readily accessible L-proline **152** was used as an organocatalyst. This was carried out in order to aid with product identification by having the pure compound at hand. Hence, R_f values could be compared whilst the NMR spectrum could be used to assist in identifying and isolating these products from the organocatalysed reaction attempts.

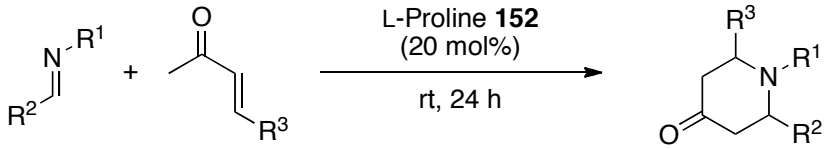

11 **183** **313**

Table 7. Piperidine ring formation attempts using organocatalysts.

Entry	Imine	R^1	R^2	Enone	R^3	Solvent	3 Å M.S.	Products
1	**324**	Allyl	Ph	**348**	Ph	MeOH	No	**357** 43%
2	**323**	PMP	Ph	**348**	Ph	MeOH	No	-
3	**324**	Allyl	Ph	**350**	OMe	MeOH	No	Mannich + Michael
4	**323**	PMP	Ph	**350**	OMe	CH_2Cl_2	No	Michael
5	**328**	Allyl	$(MeO)_2CH$	**164**	H	CH_2Cl_2	Yes	-
6	**328**	Allyl	$(MeO)_2CH$	**348**	Ph	CH_2Cl_2	Yes	Mannich
7	**324**	Allyl	Ph	**353**	PMP	CH_2Cl_2	Yes	-
8	**324**	Allyl	Ph	**355**	PNP	CH_2Cl_2	Yes	-

Synthesis of piperidine **357** (Table 7, entry 1) was chosen because it was the example in the literature that gave the highest yields (77%).[92] Hence, **357** was synthesised with an adequate yield of 43%, with the ^{1}H NMR spectra confirming the relative stereochemistry: the proton peak at Ph*H*CN was a clear doublet of doublets [δ = 3.94 (dd, *J* = 12.0, 3.0 Hz, 2H)], which suggested that it was symmetric, *i.e.* both the Ph groups being *cis* to each other (Figure 2).

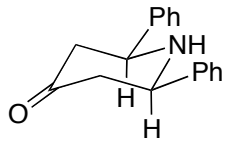

Figure 2. Proposed relative stereochemistry of compound **357**.

The use of aromatic group PMP on the R^1 position of the imine was also explored (Table 7, entries 2 and 4). It was known in the literature that these groups were relatively simple to remove from the nitrogen at a later stage.[61] However, the desired piperidine ring products could not be isolated. The difficulty in obtaining these piperidine compounds through this method was re-enforced in the literature,[92] where it was noted that the piperidine was often a minor product, with only 21% yield being obtained. This may be due to the imine being too electron-rich due to the methoxy group in the *para* position of the R^1 aromatic, and hence, not sufficiently nucleophilic to go through with the initial Mannich reaction.

The examples shown in Table 7, entries 3 and 4, were chosen due to the interesting LW UV active spots observed by TLC analysis when screening the one-pot, three-component screening reactions (Table 4). However, neither of the piperidines were isolated. Instead, the major new compound in both sets of reactions was the vinylogous amide **358**. It was proposed that in order to form **358**, the imine **324** had to have hydrolysed to the corresponding aldehyde **322** and amine **186** units, with the free amine **186** subsequently performing a Michael addition to the enone **350** and elimination of methanol to form the vinylogous amide **358**.

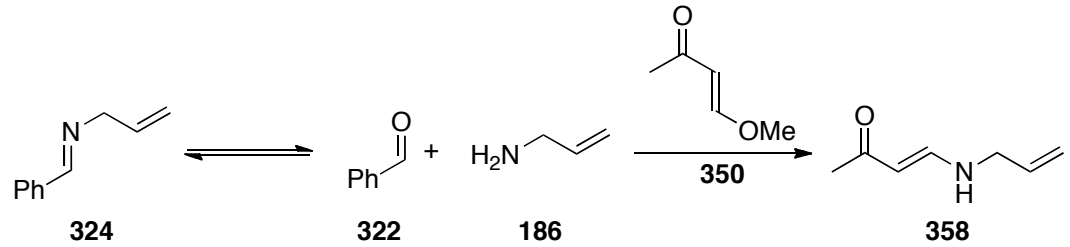

Scheme 57. Proposed route for the formation of **358**.

In order to confirm that the vinylogous amide **358** was formed from amine **186** and enone **350**, **186** and **350** were dissolved in $CDCl_3$ in an NMR tube. After 20 hours, it

was observed by ^{1}H NMR that amine **186** had reacted quantitatively with enone **350** to form **358** (Equation 26). These results showed the importance of keeping these reactions dry, a process that could be performed through the use of molecular sieves.

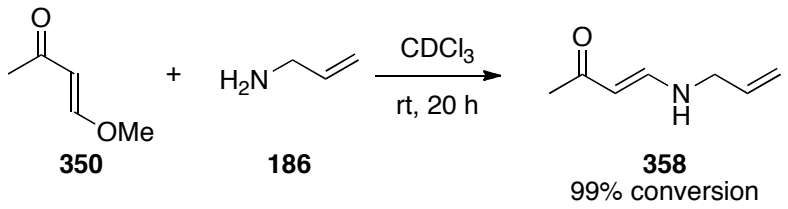

Equation 26

Table 7, entry 3 also showed a minor compound that was believed to be **360** (3% yield). It was thought that imine **324** was sufficiently nucleophilic to perform a Mannich reaction with the enone **350** to form the adduct **359**, with this Mannich adduct subsequently performing a Michael vinyl ether addition with methanol (solvent) in order to form **360** (Scheme 58). This result demonstrated the challenge of having an active catalyst that is able to efficiently perform a Mannich followed by an intramolecular Michael reaction to form a piperidine ring, without stalling in the middle of the reaction sequence.

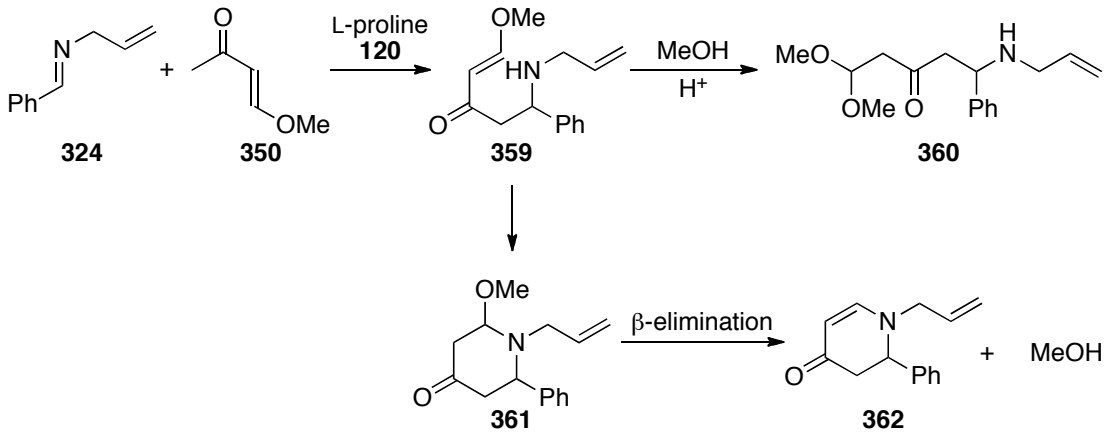

Scheme 58. Possible reactions from the Michael adduct **359**.

From the imine screening experiments (Table 6), it was thought that methyl vinyl ketone **164** could give promising results when reacted with imine **328**. However,

when imine **328** was reacted with methyl vinyl ketone **164**, no piperidine product **313** was isolated (Table 7, entry 5).

The reactions between imines **75** and **328** with enone **347** also seemed promising (Table 6). However, when the reactions were scaled up (Table 7, entry 6), again no piperidine product **313** was isolated. Instead, in the reaction with imine **328**, the main intermediate observed was a highly polar compound where spectroscopic evidence suggested this was the uncyclised product **363**. This was proposed due to: a) high solvent polarities that were needed to flush the mixture containing **363** when purifying by silica gel chromatography (11% yield); and b) the ^{1}H NMR showed an AB conjugated *trans*-alkene system [δ 6.53 (d, J = 16.3 Hz, 1H), 6.26 (d, J = 16.3 Hz, 1H)]. Apart from some allylic peaks, it was hard to tell what the rest of the peaks in the spectra belonged to. This result again hinted at the challenge of making the catalyst sufficiently reactive to catalyse the intramolecular cyclisation to the piperidine.

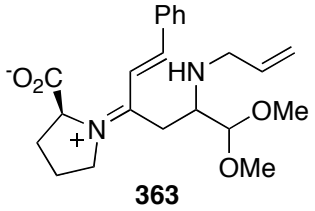

363

In the attempted formation of **313** from **353** (Table 7, entry 7), the electron-rich enone **353** seemed to be inactive and did not react with imine **324**. Indeed, after 1 week of stirring at room temperature, only the starting materials **353** and **324** were observed in the reaction mixture. This might be due to the electron-donating methoxy group of **353** stabilising the iminium ion that the catalyst would have formed with the enone.

In the attempted formation of piperidine **313** from electron-deficient enone **355** (Table 7, entry 8), two new minor spots were observed after 48 hours by TLC analysis. However, after subsequent purification *via* silica gel chromatography, it was found that neither of these new spots were **313,** as there was no characteristic allylic peaks observed in the ^{1}H NMR spectrum. However, it could not be determined what these

minor spots corresponded to because of the large array of complex peaks present in their ^{1}H NMR's.

3.3.2 Attempted Piperidine Ring Formation Using Lewis Acids

Building up a library of piperidine standards **313** using L-proline **152** as a catalyst had proved challenging. Hence, it was decided to follow the more traditional Lewis acid approach for the formation of systems **313** and **12**, using electron rich dienes and imines in the presence of Lewis acids (Table 8).[31, 84]

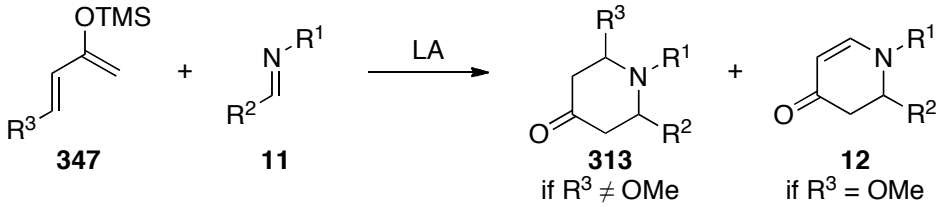

Table 8. Piperidine ring formation attempts using Lewis acids.

Entry	Diene	R^3	Imine	R^1	R^2	LA	Solvent	Product
1	**349**	Ph	**324**	Allyl	Ph	$ZnCl_2$•Et_2O (4 Eq.)	CH_2Cl_2	-
2	**349**	Ph	**323**	PMP	Ph	$Yb(OTf)_3$ (20 mol%)	Toluene	-‡
3	**349**	Ph	**324**	Allyl	Ph	$Yb(OTf)_3$ (20 mol%)	Toluene	-‡
4	**4**	OMe	**323**	PMP	Ph	$Yb(OTf)_3$ (20 mol%)	Toluene	**364** 99%*
5	**4**	OMe	**324**	Allyl	Ph	$Yb(OTf)_3$ (20 mol%)	Toluene	**362** 99%*
6	**4**	OMe	**324**	Allyl	Ph	$Yb(OTf)_3$ (20 mol%)	CH_2Cl_2	**362** 37%
7	**4**	OMe	**328**	Allyl	$(MeO)_2CH$	$Yb(OTf)_3$ (20 mol%)	Toluene	-
8	**4**	OMe	**75**	PMP	$(MeO)_2CH$	$Yb(OTf)_3$ (20 mol%)	Toluene	-
9	**4**	OMe	**155**	PMP	CO_2Et	$Yb(OTf)_3$ (20 mol%)	CH_2Cl_2	-

‡ Unable to isolate the product from the crude reaction mixture.
* These compounds were not isolated 100% pure.

When using diene **349** and $ZnCl_2$•Et_2O as Lewis acid, this being the catalyst of choice used by Kunz *et al*. in their aza-Diels-Alder reactions,[30] the reaction seemed to be inactive with the substrates used (Table 8, entry 1). Hence, the reaction was attempted using $Yb(OTf)_3$ (Table 8, entries 2 and 3). Through comparing the crude ^{1}H NMRs

with the literature examples,[49, 61] it was found that piperidine products had been formed, however, they were mixed with starting enone **348**. Purification by silica gel chromatography was challenging since enone **348** had a similar R_f to the piperidine products, and hence, the piperidines were not isolated cleanly.

In the literature, there were only a few examples where the dienes such as **349** were used in the aza-Diels-Alder reaction;[172] most of the Lewis acid catalysed aza-Diels-Alder reactions seemed to use the more electron-rich Danishefsky's diene or a cyclic enone as the diene source.[29] Hence, different imines were reacted with Danishefsky's diene with the aim of forming piperidines of type **12** (Table 8, entries 4 - 9).

Despite obtaining some of the desired piperidines, it was again challenging to purify and obtain them 100% pure (Table 8, entries 4 - 6). The use of more electron-rich imines (Table 8, entries 7 - 9) and an electron-deficient imine (Table 8, entry 9) were also investigated. However, mixtures of compounds were again formed, and the isolation of the corresponding products proved unsuccessful.

The difficulties encountered in synthesising piperidine standards confirmed the need to develop a more robust methodology for the efficient assembly of these heterocyclic rings *via* an atom-economical, aza-Diels-Alder pathway. In addition, it was observed that the pharmaceutical industry was particularly interested in the synthesis of piperidines that were fused to other aromatic rings, due to the special biological activities that they can exhibit. Examples include the VMAT2 inhibitor **365** that is used to diagnose Parkinson's disease,[173] and the multi-cyclic compound **366** used to cleave DNA plasmids.[174]

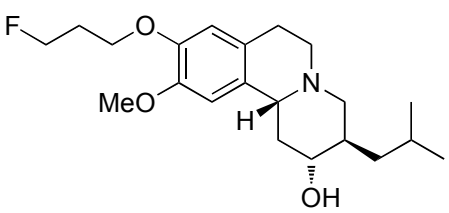

365

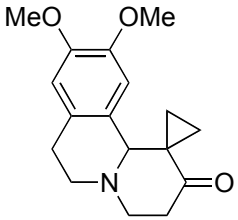

366

As a result, it was decided to concentrate investigation efforts on forming the building block **244** as a simplified example of such multi-cyclic compounds *via* an aza-Diels-Alder reaction, starting from the fused bi-cyclic imine **243** (Equation 27).

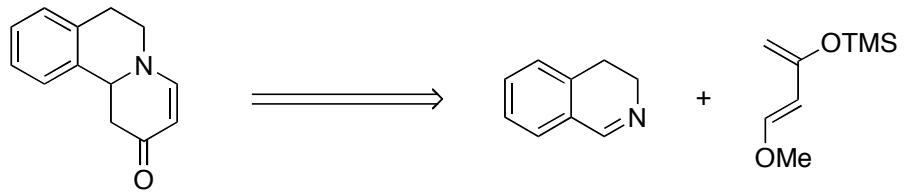

244 **243** **4**

Equation 27

3.4 Formal [4+2]-Cycloadditions Using Dienes

Having experienced the challenges of synthesising piperidine standards from acyclic imines, it was deemed sensible to investigate the aza-Diels-Alder reaction using cyclic imines. This would produce fused-multicyclic piperidine rings, which are a class of compound the pharmaceutical industry is particularly interested in due to the biological activities they can exhibit. Hence, it was decided to explore the synthesis of polycyclic nitrogen heterocycles **368** starting from cyclic imines of type **367** (Equation 28). As a result, aza-Diels-Alder methodology was investigated in an attempt to find a general approach to dihydroisoquinoline-derived dihydropyridinones from formal aza-Diels-Alder adducts.

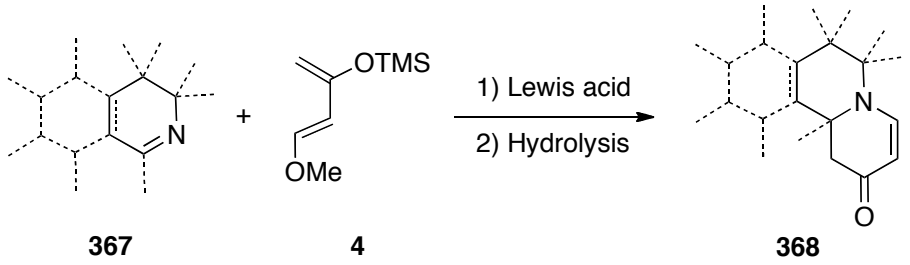

367 **4** **368**

Equation 28

Initially, 3,4-dihydroisoquinoline **243** was used as the imine equivalent of **367**. This imine **243** was synthesised according to literature methods[164] and subsequently reacted with Danishefsky's diene **4** in the presence of catalytic ytterbium(III) triflate in CH_2Cl_2, with the aim of forming piperidenone **244**. When this reaction was performed under air, there was no evidence that piperidenone **244** had been formed. However, when the reaction was performed under inert conditions, piperidenone **244** was formed and isolated, albeit in poor yield (Equation 29).

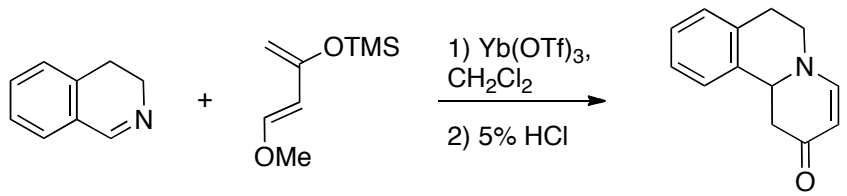

243 **4** **244**
14%

Equation 29

However, when imine **243** was reacted with one equivalent of Danishefsky's diene **4**, it was observed that another compound was being formed which had an almost identical R_f value to the piperidenone **244**. In addition, it was observed that when more of the same batch of Danishefsky's diene **4** was used in the reaction shown in Equation 29, more of the mixture seemed to be contaminated with the side-product. MS and NMR studies suggested that the side-product was being formed from two enones and one imine. It was later confirmed by X-ray crystallography that the side-compound being produced was the diacetyl-dihydropyridine **369** (Figure 3), arising from a formal [2+2+2]-cycloaddition; it was seen that its formation versus that of piperidenone **244** (a [2+4]-cycloaddition product) depended on the purity of Danishefsky's diene **4** and how easily hydrolysed it was under the reaction conditions. Hence, in order to fully understand what was happening, further studies were undertaken using both Danishefsky's diene **4** and the 4-methoxy-3-buten-2-one **350** (Table 9).

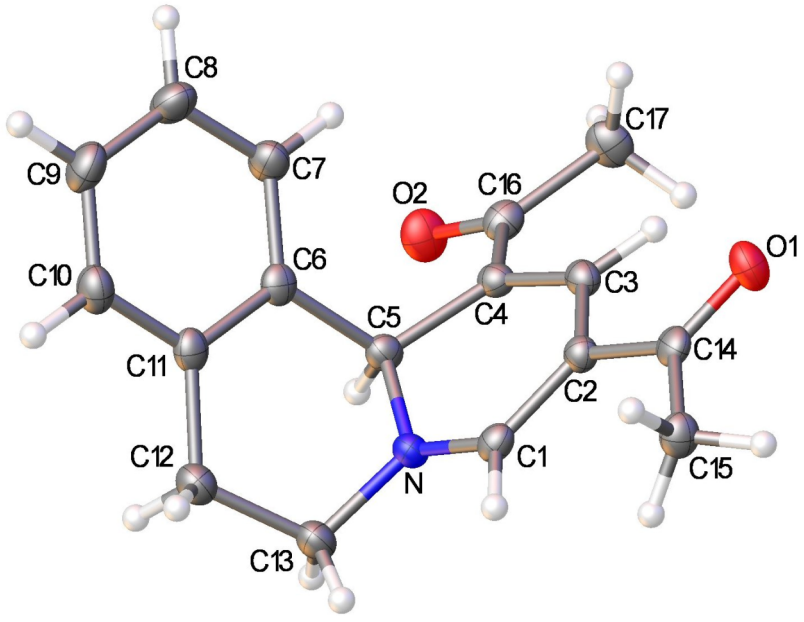

Figure 3. X-ray molecular structure of compound **369**.

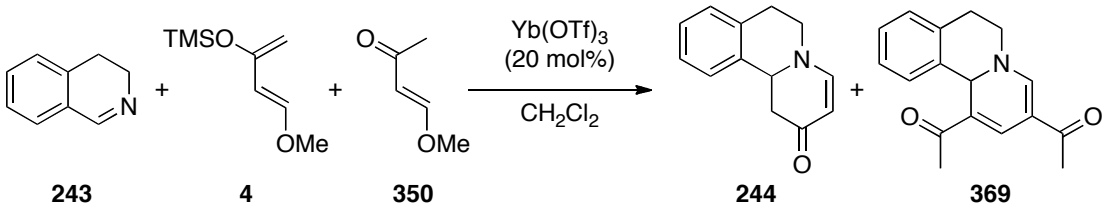

Table 9. Reaction of the imine **243** with the diene **4** and enone **350**.

Equivalents of **243**	Ratio of **244**/**369** (total = 1.2 equivalents)	Yield of **244** (%)	Yield of **369** (%)
1	1/0	14	None isolated pure
1	1/0.25	None isolated pure	20
1	0/1	0	20

When using pure Danishefsky's diene **4** from a new commercial source, piperidenone **244** was obtained in 14% yield, with no diacetyl-dihydropyridine **369** being isolated (Table 9, entry 1). However, when Danishefsky's diene **4** was contaminated with 4-methoxy-3-buten-2-one **350** (6/1), piperidine ring **244** was obtained contaminated with the by-product **369** (20% yield) (Table 9, entry 2). In contrast, use of 4-methoxy-3-buten-2-one **350** in place of Danishefsky's diene **4** under identical reaction conditions (Equation 30) did not provide piperidenone **244**. Instead, the only cleanly isolated product proved to be the diacetyl-dihydropyridine **369**, clearly derived from the reaction of two equivalents of the 4-methoxy-3-buten-2-one **350** *via* an overall formal [2+2+2]-cycloaddition process.

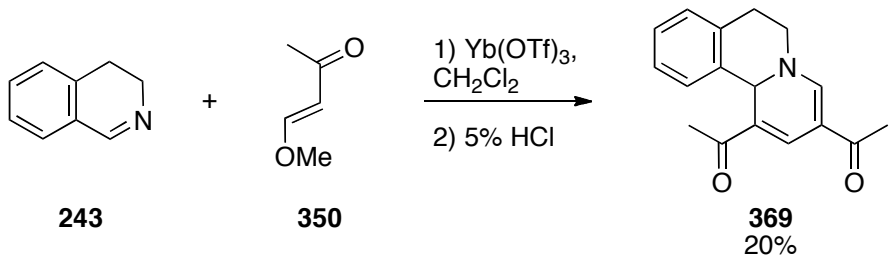

Equation 30

Thus, it was seen that the prevalence of side-product **369** over piperidenone **244** occurred due to the facile hydrolysis of Danishefsky's diene **4** to 4-methoxy-3-buten-

2-one **350**; the enone **350** being responsible for the formation of side product **369**. Hence, in order to improve on the yield of piperidenone **244** (Equation 29), it was immediately apparent that the system needed to be as dry as possible in order to prevent hydrolysis of Danishefsky's diene **4**. Thus, the reaction was screened using different Lewis acids in the presence of 3 Å molecular sieves and 2-ethyl-2-oxazoline (to aid in solubility) in an attempt to determine which Lewis acids were more likely to catalyse the synthesis of piperidenone **244**, and which were more likely to hydrolyse Danishefsky's diene **4** (Table 10). In all cases, the imine **243** was fully consumed within 72 h.

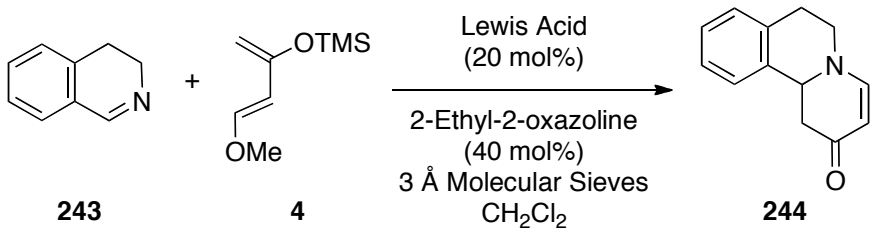

243 **4** **244**

Table 10. Catalyst screening for the [4+2]-reaction, analysed by TLC after 72 h.

Entry	Lewis Acid	Presence of Enone	Formation of [2+2+2] product	Clear formation of **244** in good amounts
1	Cu(II) $(OTf)_2$	Yes	Yes	Yes
2	Cu(I) Cl	Yes	No	No
3	Cu(II) Cl_2	Yes	No	Yes
4	$ZnCl_2 \bullet OEt_2$	No	No	No
5	Fe(III) Cl_3	No	Yes	Very little
6	In(III) Cl_3	Yes	No	Yes-little
7	Sn(II) Cl_2	Yes	Yes	Yes
8	Ru(III)Cl_3	Yes	No	Yes
9	Rh(III) Cl_3	Yes	No	Yes
10	Sc(III) $(OTf)_3$	No	Yes	Yes
11	Ce(III) Cl_3	Yes	No	Yes
12	In(III) $(OTf)_3$	No	Yes	Yes

Collectively, it was observed that the triflate-based catalysts (Table 10, entries 1, 10, 12) favoured the [2+2+2]-cycloaddition. This was not too surprising because even though these catalysts were more active compared to the chloride-based catalysts, they were very hygroscopic, meaning it was almost impossible to obtain them completely anhydrous; hence, these catalysts were discarded for use in the [4+2]-cycloaddition reaction.

$RuCl_3$ and $RhCl_3$ gave similar results (Table 10, entries 8, 9). However, considering rhodium was around 1000x more expensive than Ruthenium, the $RhCl_3$ catalyst was also discarded.

The most promising catalysts that were chosen were: $CuCl_2$, $CeCl_3$, and $RuCl_3$ (Table 10, entries 3, 11, 8). These were taken forward to a further set of screening reactions where different phosphine ligands were used to see whether these ligands would have any significant effect over 2-ethyl-2-oxazoline in terms of helping to catalyse the reaction (Table 11). The phosphine ligands used (Figure 4) were chosen due to them representing a range of mono- and bi-dentate systems.

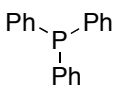

370
Triphenylphosphine

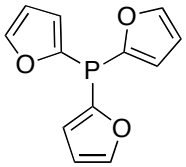

371
Tri(2-furyl)phosphine

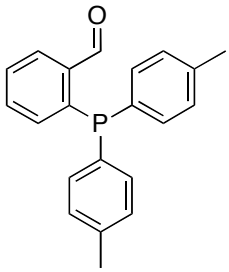

372
2-(Di-*p*-tolyphosphino)-benzaldehyde

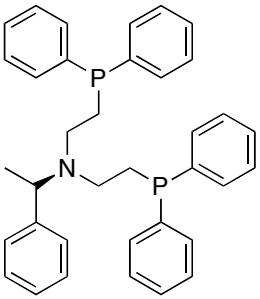

373
(R)-(+)-*N,N*-Bis(2-diphenylphosphinoethyl)-1-phenylethylamine

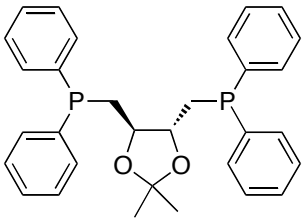

374
(-)-2,3-*O*-Isopropylidene-2,3-dihydroxy-1,4-bis(diphenylphosphino)butane

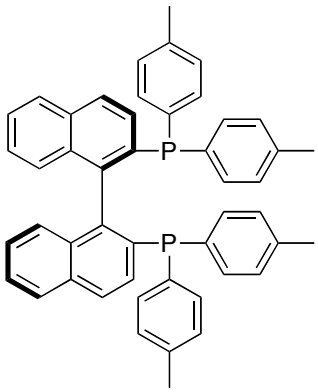

375
(R)-T-BINAP

Figure 4

CuCl, $InCl_3$ and $ZnCl_2$ were also taken forward to the next set of screening reactions (Table 11), as these were catalysts that had previously been used in similar reactions in the literature (using acyclic imines).[116] It was also thought wise to include one triflate-based catalyst for comparison, thus $Sc(OTf)_3$ was chosen as this catalyst

formed the least amount of [2+2+2]-product compared to the other triflate-based Lewis acid systems.

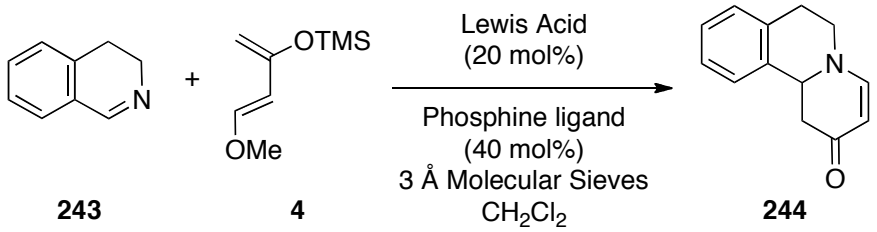

243 **4** **244**

Table 11. Catalyst screening with phosphine ligands for the [4+2]-reaction, analysed by TLC after 48 h.

Entry	Lewis Acid	Phosphine Ligand	Presence of enone	Formation of [2+2+2] product	Clear formation of **244** in good amounts	Other Points
1	CuCl	**370**	Yes	No	Unclear	Unreacted imine
2	$CuCl_2$	**370**	Little	No	Unclear	Unreacted imine
3	$CeCl_3$	**370**	Little	No	Unclear	Unreacted imine
4	$InCl_3$	**370**	Yes	No	Unclear	Unreacted imine
5	$RuCl_3$	**370**	Little	No	Unclear	Unreacted imine
6	$ZnCl_2$	**370**	Yes	No	Unclear	Unreacted imine
7	$Sc(OTf)_3$	**370**	No	Yes	Unclear	-
8	CuCl	**371**	Yes	No	No	Unreacted imine
9	$CuCl_2$	**371**	Little	Yes	No	Unreacted imine
10	$CeCl_3$	**371**	Yes	No	No	Unreacted imine
11	$InCl_3$	**371**	Yes	No	No	Unreacted imine
12	$RuCl_3$	**371**	Little	No	No	-
13	$ZnCl_2$	**371**	Yes	No	No	Unreacted imine
14	$Sc(OTf)_3$	**371**	No	Yes	No	-
15	CuCl	**372**	Yes	No	Unclear	Unreacted imine
16	$CuCl_2$	**372**	Little	Yes	Unclear	Unreacted imine
17	$CeCl_3$	**372**	Little	No	Unclear	Unreacted imine
18	$InCl_3$	**372**	Yes	No	Unclear	Unreacted imine
19	$RuCl_3$	**372**	Little	No	Unclear	Prominent high *Rf*

20	$ZnCl_2$	**372**	Yes	No	Unclear	point -
21	$Sc(OTf)_3$	**372**	No	Yes	Unclear	Very clean
22	CuCl	**373***	Yes	No	Yes	Unreacted imine
23	$CuCl_2$	**373***	Yes	Yes	Yes	Unreacted imine
24	$CeCl_3$	**373***	Yes	No	Yes	Unreacted imine
25	$InCl_3$	**373***	Little	No	Yes	Unreacted imine
26	$RuCl_3$	**373***	Little	No	Yes	-
27	$ZnCl_2$	**373***	Yes	No	Unclear	Unreacted imine
28	$Sc(OTf)_3$	**373***	No	Yes	Yes	-
29	CuCl	**374**	Yes	No	Little	Unreacted imine
30	$CuCl_2$	**374**	Little	No	Yes	Unreacted imine
31	$CeCl_3$	**374**	Little	No	Yes	Unreacted imine
32	$InCl_3$	**374**	Yes	No	Yes	Unreacted imine
33	$RuCl_3$	**374**	Little	No	Yes	Prominent high *Rf* point
34	$ZnCl_2$	**374**	Yes	No	Yes	Unreacted imine
35	$Sc(OTf)_3$	**374**	No	Yes	Yes	-
36	CuCl	**375**	Yes	No	Yes	Unreacted imine
37	$CuCl_2$	**375**	Little	No	Yes	-
38	$CeCl_3$	**375**	Yes	No	Yes	Unreacted imine
39	$InCl_3$	**375**	Yes	No	Yes	-
40	$RuCl_3$	**375**	Little	No	Yes	Prominent high *Rf* point
41	$ZnCl_2$	**375**	Yes	No	Little	-
42	$Sc(OTf)_3$	**375**	No	Yes	Little	Very clean

*Due to limited amount of material, only 20 mol% of this ligand was used.

From these results (Table 11), one can deduce that the bidentate phosphine ligands seemed to perform better than the monodentate ones. In particular, ligands **374** and **375** seemed to be better in terms of clearly forming piperidenone **244** (as judged by TLC analysis). In contrast, the triflate-based catalyst always produced [2+2+2]-product, whilst $CuCl_2$ also formed the [2+2+2]-product when using certain phospine ligands. Interestingly, the $RuCl_3$ catalyst gave a distinct new high R_f spot by TLC

analysis, despite also giving the cleanest [4+2]-product spot. CuCl seemed to be the least active Lewis acid catalyst, and $InCl_3$ seemed to give the most complex mixtures, as determined by TLC analysis.

On the whole, these reactions showed more spots by TLC analysis compared to using 2-ethyl-2-oxazoline as ligand. Hence, it was decided to take the most promising Lewis acids forward by scaling up the cleaner 2-ethyl-2-oxazoline methodology (Table 12). The Lewis acids taken forward were $CuCl_2$, $CeCl_3$ and $RuCl_3$. For comparison, the reaction was also performed neat, with and without 3 Å molecular sieves.

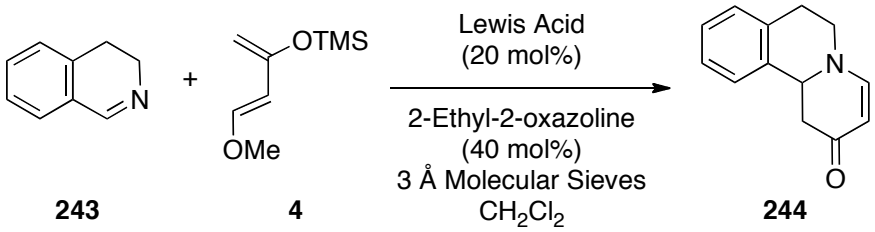

Table 12. Scaled up [4+2]-reactions (performed on a 1 mmol scale).

Entry	Lewis Acid	After 24 h	After 48 h	Yield (%)
1	$CuCl_2$	A lot of imine and enone still present	Mostly enone and product, some imine present	28
2	$CeCl_3$	A lot of imine and enone still present	Mostly enone and product, some imine present	49
3	$RuCl_3$	No imine and little enone. Cleanest product.	Same as before	44
4	Neat with molecular sieves	Some imine, enone, diene and product present	Imine consumed: mainly product	47
5	Neat without Molecular sieves	Two prominent new spots along with enone, diene and imine present: no product	Two prominent new spots, along with a lot of enone, present: little product	-

The slowest reaction seemed to be when $CuCl_2$ was used (Table 12, entry 1), whilst the quickest reaction to go to completion seemed to be achieved with $RuCl_3$ (Table 12, entry 3). However, after purification by silica gel chromatography, the isolated product (Table 12, entry 3) was black and clearly not clean, despite the ^1H NMR

showing a clean spectrum; a common problem with ruthenium systems and likely due to metal contamination.

When performing the reaction neat, the use of molecular sieves seemed to be essential because without them, the diene **4** quickly hydrolysed to the enone **350**, and thus the diacetyl product **369** was formed instead of piperidenone **244** (Table 12, entry 5). When molecular sieves were used, a similar yield of **244** was obtained compared to when $CeCl_3$ was used as the catalyst (Table 12, entries 4 and 2). These results suggest that it is essential to perform these reactions under inert conditions with the use of molecular sieves, and that many Lewis acids hinder the reaction instead of catalysing it.

Each of the reactions shown in Table 12 were purified directly after being quenched. This was important because if a significant amount of time lapsed after the quench and prior to the purification, then the unwanted [2+2+2]-product **369** would form. This was especially undesirable as the [2+2+2]-product **369** was challenging to separate from the desired piperidenone **244**, and hence, lower isolated yields would be obtained (Table 13).

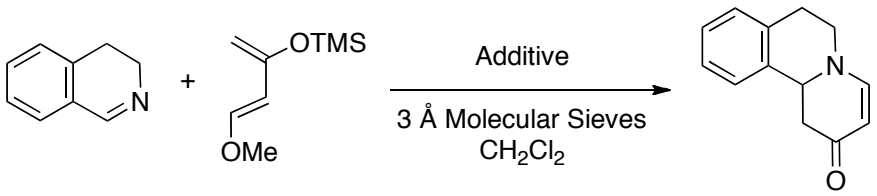

243 **4** **244**

Table 13. [4+2]-reactions where the product **244** was not purified directly after quenching.

Entry	Additive 1 (mol%)	Additive 2 (mol %)	[2+2+2]-product **369** observed	[2+2+2]-product **369** observed 24 h after quench	**244** (%)
1	$CeCl_3$ (20)	Ethyl oxazoline (40)	No	Yes	23*
2	-	-	No	Yes (little)	47*
3	$Fe(OTf)_3$ (20)	Ethyl oxazoline (40)	Yes	Yes (a lot)	-‡
4	$Ga(OTf)_3$ (20)	Ethyl oxazoline (40)	Yes (very little)	Yes	-‡

*After the compounds were quenched and concentrated *in vacuo*, they were left overnight (without molecular sieves) before purifying by silica gel chromatography. During this time, a noticeable amount of [2+2+2]-product was formed, which lowered the isolated yield of the [4+2]-product as they have almost identical R_f values.

‡Despite being relatively clean directly after quenching, these reactions were not purified as they were contaminated by too much [2+2+2]-product 24 h after the quench.

From these studies, it was evident that in order to optimise the formation of the aza-Diels-Alder adduct **244**, it was essential to perform these cycloadditions under anhydrous conditions. In addition, it is necessary for the diene **4** to be pure, with no enone **350** present. Otherwise, the unwanted diacetyl-piperidine ring **369** would be formed instead. Both these compounds arise through a different formal cycloaddition pathway: a [4+2]-cyclisation to give the aza-Diels-Alder adduct **244**, and a [2+2+2]-cyclisation to give the diacetyl-piperidine **369**.

3.5 [2+2+2]-Cycloaddion Reaction

The unexpected observation of the formation of the [2+2+2]-cycloaddition product **369** was almost unprecedented,[175] and therefore, this reaction required further investigation and optimisation. Initially, catalyst loading was investigated (Table 14), during which a new side-product **376** was observed. The side-product **376** was identified as the trimer because it was formed by the reaction from three equivalents of enone **350**, followed by elimination of three equivalents of methanol.

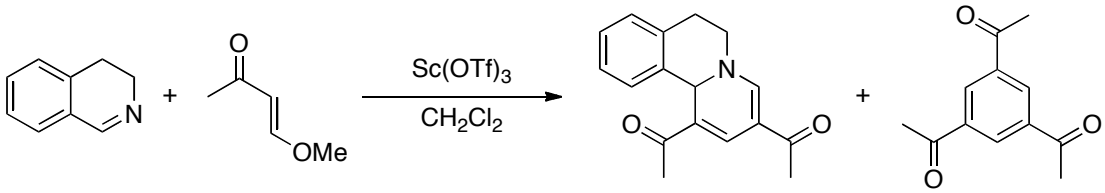

243 **350** **369** **376**

Table 14. Investigating catalyst loadings in the formal [2+2+2]-cycloaddition reaction.

Entry	Lewis Acid (mol%)	Yield of dihydropyridine **369** (%)	Yield of trimer **376** (%)
1	0	0	-
2	5	<10	-
3	10	61	-
4	20	48	<5*
5	100	0	>55

* Conversion estimated from the crude ^{1}H NMR spectrum.

From these results (Table 14), one can deduce that the formation of trimer **376** was favoured over the formation of dihydropyridine **369** with increasing amounts of Lewis acid. However, with no Lewis acid present, no reaction occurred (Table 14, entry 1), which showed that the Lewis acid was important in terms of activating the enone **350**. If the Lewis acid concentration was too low (5%), very little activity was observed (Table 14, entry 2). Hence, a sensible compromise, where maximum amounts of dihydropyridine **369** was synthesised, with no trimer **376** being produced, was when 10 mol% of the Lewis acid was used (Table 14, entry 3).

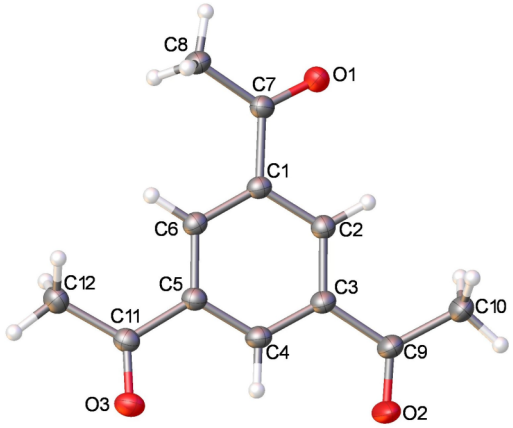

Figure 5. X-ray molecular structure of compound **376**.

Due to the unusual aromatic downfield ^{1}H NMR peak of trimer **376** (8.7 ppm), the structure of **376** was determined only after its crystal structure had been obtained (Figure 5). Examining the literature showed that other groups had isolated this compound when reacting 4-methoxy-3-buten-2-one **350** under acidic conditions.[176] This transformation was confirmed by reacting enone **350** alone in the presence of a Lewis acid (Equation 31).

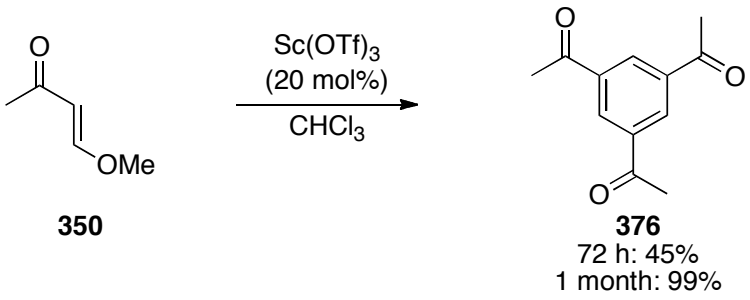

350 **376**
72 h: 45%
1 month: 99%

Equation 31

When performing the reaction shown in Equation 31 in $CHCl_3$ at room temperature for three days, purification by silica gel chromatography afforded the trimer **376** in 45% yield. The reaction shown in Equation 31 was also performed in $CDCl_3$ in an NMR tube to monitor how long it took for enone **350** to completely convert into trimer **376**. Within one day, **376** appeared. However, peaks corresponding to intermediates were also present. By the end of seven days, the signals in the ^{1}H NMR corresponding to **376** were more prominent compared to the intermediate peaks. After a month, the only peaks observed in the ^{1}H NMR spectrum were those corresponding

to the trimer **376**, showing that the transformation was slow, although surprisingly efficient.

Having understood that catalyst concentration affects the formation of trimer **376** or otherwise, optimisation of dihydropyridine **369** was explored by examining the effect of catalyst, enone equivalents, drying agent, solvent and inert atmosphere. It was immediately apparent that different ranges of isolated yields were obtained depending on the purification process. Relatively low yields in the 20-40% range were generally observed when the reaction was purified by trituration (Table 15).

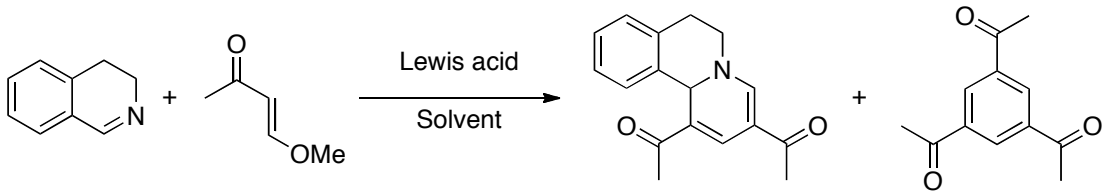

243 **350** **369** **376**

Table 15. Optimisation studies of the [2+2+2]-cycloaddition reaction, the product **369** being purified by trituration.

Entry	Enone Equiv. **350**	Catalyst (mol%)	Solvent	Time (Days)	Ar	Addi-tives	Yield of **369** (%)	Yield of **376** (%)
1	5	$Yb(OTf_3)$ (20)	CH_2Cl_2	2	P	-	40	<5*
2	2	$Yb(OTf_3)$ (20)	$CDCl_3$	1	P	-	30	<5*
3	2	$Sc(OTf)_3$ (10)	$CHCl_3$ (1.5)	2	P	-	41	0
4	2	$Sc(OTf)_3$ (10)	$CHCl_3$	2	P	4 Å M.S.	42	0
5	2	$Yb(OTf_3)$ hydrate (10)	$CHCl_3$	2	P	-	40	0
6	3	$Sc(OTf)_3$ (10)	$CHCl_3$	1-2	P	-	40	0
7	4	$Sc(OTf)_3$ (10)	$CHCl_3$	2	P	-	50	0
8	5	$Sc(OTf)_3$ (10)	$CHCl_3$	2	F	-	20	0
9	4	$Sc(OTf)_3$ (10)	EtOAc	3	N	-	20	0
10	4	$Sc(OTf)_3$ (10)	MeOH	3	N	-	15	0
11	4	$Sc(OTf)_3$ (10)	CH_3CN	3	N	-	15	0
12	4	$Sc(OTf)_3$ (10)	THF	3	N	-	30	0
13	4	$Sc(OTf)_3$ (10)	Diethyl Ether	3	N	-	21	0
14	4	$Sc(OTf)_3$ (10)	Hexane	3	N	-	19	0
15	4	$Sc(OTf)_3$ (10)	CH_2Cl_2	3	N	-	21	0
16	4	$Sc(OTf)_3$ (10)	Toluene	3	N	-	20	0
17	4	$Sc(OTf)_3$ (10)	$CHCl_3$	3	N	3 drops of water	15	0
18	4	$Sc(OTf)_3$ (10)	$CHCl_3$	3	N	4 Å M.S.	25	
19	4	$Sc(OTf)_3$ (10)	$CHCl_3$	3	N	-	20	0
20	4	$Sc(OTf)_3$ (10)	$CHCl_3$	2	F	-	Normal	0

21	4	$Sc(OTf)_3$ (10)	(1 mL) $CHCl_3$ (0.5 mL)	2	F	-	TLC Normal TLC	0
22	4	$Sc(OTf)_3$ (10)	$CHCl_3$ (min.)	2	F	-	Clean TLC	0
23	4	$Sc(OTf)_3$ (10)	neat	2	F	-	20 (Normal TLC)	0

Note: P means that the flask was sealed with a septum, through which argon was pumped; F means the flask was flushed with argon before being sealed with a stopper; N means that the flask was sealed with a stopper without being flushed with argon; * means that the yield was not isolated, the amount being estimated from the crude ^{1}H NMR spectra.

Despite the low yields obtained, these results (Table 15) provided some added, useful information. For example, the use of $Sc(OTf)_3$, $Yb(OTf)_3$ or its hydrate as a catalyst gave little difference in yield (Table 15, entries 1, 3, 5), with or without molecular sieves (Table 15, entries 3, 4). When comparing solvents, no significant difference was observed except when using methanol and acetonitrile, in which cases the yields tended to be lower (Table 15, entries 9-16). The concentration of the reaction mixture was also investigated (Table 15, entries 20-23) and it was observed by TLC analysis that the cleanest reaction was when the minimum amount of solvent was used (Table 15, entry 22), sufficient only for complete solution of reagents.

Higher yields of **369** were typically obtained when the reaction mixture was purified by silica gel chromatography using EtOAc as eluent (Table 16, entries 1-3). This purification procedure was subsequently optimised by including CH_2Cl_2 in the eluent mixture (4:1, EtOAc:CH_2Cl_2) to help with the solubility of **369** (Table 16, entries 6-10).

These results (Table 16) showed the importance of optimising the purification procedure in order to maximise yields. The Lewis acids that afforded the highest yields were $Fe(OTf)_2$ and $Ga(OTf)_3$ (Table 16, entries 7, 8), whilst the chiral Lewis acid $Eu(hfc)_3$ seemed to be inactive, even at higher temperatures (Table 16, entry 4, 5). Overall, the highest yields obtained of pure product **369** were a very satisfactory 88% (Table 16, entries 7-8). Considering the very low yields obtained initially and the complexity of the reactions, this shows that the reaction could be very usefully optimised. In addition, three new bonds are formed in sequence, showing that each one can be formed with greater than 96% efficiency.

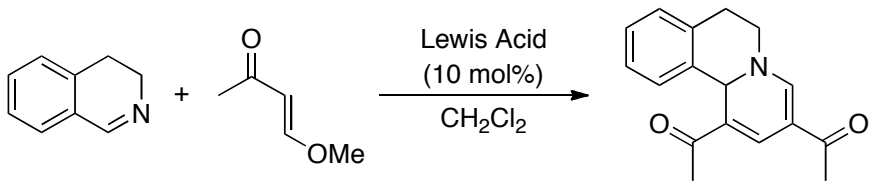

243 **350** **369**

Table 16. Optimisation studies of the [2+2+2] cycloaddition reaction, the product **369** being purified by silica gel chromatography.

Entry	Lewis acid	Purification Eluent	**369** (%)
1	$Yb(OTf)_3$	EtOAc	61
2	$Sc(OTf)_3$	EtOAc	46
3	$In(OTf)_3$	EtOAc	49
4	$Eu(hfc)_3$	-	-
5	$Eu(hfc)_3$ (60 ºC)	-	-
6	$Sc(OTf)_3$ (+Pybox 10 mol%)	4:1, EtOAc:CH_2Cl_2	82
7	$Fe(OTf)_2$	4:1, EtOAc:CH_2Cl_2	88
8	$Ga(OTf)_3$	4:1, EtOAc:CH_2Cl_2	88
9	$Yb(OTf)_3$	4:1, EtOAc:CH_2Cl_2	87
10	$In(OTf)_3$	4:1, EtOAc:CH_2Cl_2	81

Similar results were observed when using enone synthons of **350**, such as the alkyne 3-butyn-2-one **377** (Equation 32), demonstrating that the interaction of the corresponding ynone might be involved in the reaction.

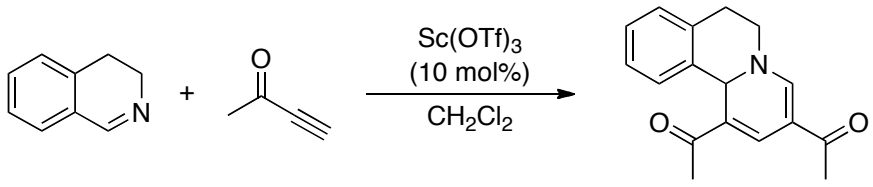

243 **377** **369**
58%

Equation 32

Compound **369** is a very polar, yellow solid that is extremely long wave (LW) UV active. As determined by crystallography experiments, **369** is highly delocalised between the nitrogen and the first conjugated acetyl group, with both acetyl groups being in the same plane.

X-ray diffraction experiments (Table 17) were carried out on a 3-circle Bruker diffractometer with a SMART 6000 CCD area detector, using graphite-monochromated Mo-K_α radiation ($\bar{\lambda}$=0.71073 Å) and a Cryostream 700 (Oxford

Cryosystems) open-flow N_2 cryostat. The structure was solved by direct methods and refined by full-matrix least squares against F^2 of all reflections, using SHELXTL 6.14[177] and OLEX2[178] software. Dr. Andrei Batsanov performed both the X-ray diffraction experiments and the DFT calculations.

Table 17. Crystal data for compounds **369** and **376**.

Compound	**369**	**376**
CCDC dep. no.	828903	828904
Formula	$C_{17}H_{17}NO_2$	$C_{12}H_{12}O_3$
Formula weight	267.32	204.22
T, K	120	120
Symmetry	orthorhombic	monoclinic
Space group	*Pbca* (# 61)	$P2_1/c$ (# 14)
a, Å	10.5511(4)	8.3010(3)
b, Å	8.8537(3)	16.2516(6)
c, Å	28.6974(10)	7.5205(3)
β, °	90	95.38(1)
V, Å^3	2680.8(2)	1010.08(7)
Z	8	4
D_x, g cm^{-3}	1.325	1.343
Reflections total, unique	25682, 2369	11734, 2315
2θ max. (º)	50	55
R_{int}	0.088	0.040
Refls with $I>2\sigma(I)$	1510	1806
R_1, wR_2	0.038, 0.095	0.044, 0.128

Table 18. Bond distances (Å) in molecule **369** from X-ray diffraction and DFT calculations

Bond	X-ray	DFT	Bond	X-ray	DFT
N-C(1)	1.328(2)	1.344	C(6)-C(11)	1.399(3)	1.408
N-C(5)	1.473(2)	1.479	C(9)-C(10)	1.379(3)	1.392
N-C(13)	1.465(2)	1.460	C(10)-C(11)	1.395(3)	1.401
C(1)-C(2)	1.380(3)	1.380	C(11)-C(12)	1.510(3)	1.521
C(2)-C(3)	1.445(2)	1.439	C(12)-C(13)	1.529(3)	1.533
C(3)-C(4)	1.346(3)	1.358	C(2)-C(14)	1.439(3)	1.471
C(4)-C(5)	1.518(3)	1.524	C(14)-O(1)	1.242(2)	1.227
C(5)-C(6)	1.527(3)	1.541	C(14)-C(15)	1.517(3)	1.526
C(6)-C(7)	1.389(3)	1.401	C(4)-C(16)	1.465(3)	1.472
C(7)-C(8)	1.383(3)	1.393	C(16)-O(2)	1.232(2)	1.231
C(8)-C(9)	1.388(3)	1.396	C(16)-C(17)	1.503(3)	1.523

The molecular structure of **369** is shown in Figure 6; bond distances are listed in Table 18. Ring *A* adopts a sofa conformation, the C(5) atom is displaced by 0.37 Å from the mean plane of the remaining five atoms (which are coplanar with the mean deviation of 0.03 Å). The latter plane forms dihedral angles of 78.0º with the arene

ring *B*, 3.0º and 14.2º with the acyl groups bonded to C(2) and C(4). The nitrogen atom has an almost planar geometry (the sum of bond angles 358.1º) and there is a significant π-delocalisation along the (nearly planar) NC(1)C(2)C(14)O(1) path. Thus, the N–C(1) and C(2)–C(14) bonds are shorter than the standard single bonds (1.355 and 1.464 Å, respectively) and C(1)=C(2) and C(14)=O(1) are longer than the standard double bonds (1.340 and 1.222 Å) in similar moieties.[179]

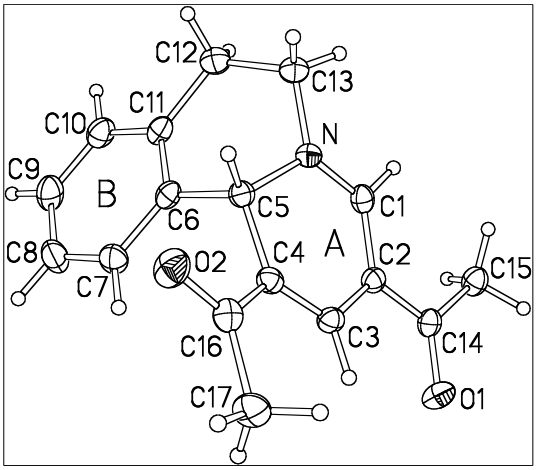

Figure 6. X-ray molecular structure of compound **369**.

The DFT calculation failed to reproduce this delocalisation fully, although other bond distances are in reasonable agreement with the observations (Table 18) and the conformation of ring *A* is identical within experimental error. The angles between the NC(1)C(2)C(3)C(4) plane and the two acyl groups (2.0º and 15.2º) reproduce the observed conformation accurately; the angle of the former with ring *B* (69.8º) is smaller than the observed by 8º, although this difference can be due to crystal packing effects.

The crystal structure of **376**, studied at 120 K (Figure 7), is essentially the same as determined earlier by X-ray[180] and neutron diffraction[181] at room temperature. This molecule **376** has a nearly planar conformation: the acetyl substituents in positions 1, 3 and 5 are twisted with respect to the benzene ring plane by 6.6º, 7.7º and 9.2º, respectively. Molecules in crystal are stacked in slightly puckered layers (Figure 8). At room temperature, the O(1) atom showed large thermal vibrations in the direction perpendicular to the molecular plane, much larger than the other two oxygen atoms. Interestingly, this situation persists at low temperature (attempts to rationalise it as

static disorder were unsuccessful). It is probably due to the crystal packing allowing more leeway for O(1) than for O(2) and O(3). Thus, the shortest inter-layer O…C distances on either side of the molecular plane, equal 3.65 and 3.83 Å for O(1), 3.41 and 3.57 Å for O(2), 3.21 and 3.30 Å for O(3).

Table 19. Final atomic coordinates (orthogonal, in Å) in **369** calculated by DFT method.

Atom	x	y	z	Atom	x	y	z
O(1)	-4.002	-0.057	-1.543	C(17)	-1.099	-3.847	0.101
O(2)	0.835	-3.038	1.250	H(1)	-1.720	2.323	0.712
N	-0.277	0.950	1.216	H(3)	-2.373	-1.673	-0.641
C(1)	-1.390	1.301	0.549	H(5)	0.865	-0.681	1.836
C(2)	-2.115	0.422	-0.230	H(7)	1.855	-1.934	-0.813
C(3)	-1.681	-0.950	-0.222	H(8)	3.818	-1.410	-2.208
C(4)	-0.516	-1.338	0.359	H(9)	4.786	0.890	-2.179
C(5)	0.457	-0.293	0.893	H(10)	3.751	2.633	-0.756
C(6)	1.659	0.052	-0.008	H(12A)	1.109	3.188	0.172
C(7)	2.257	-0.928	-0.811	H(12B)	2.386	3.026	1.370
C(8)	3.372	-0.634	-1.592	H(13A)	-0.065	2.771	2.230
C(9)	3.914	0.652	-1.576	H(13B)	1.052	1.488	2.714
C(10)	3.332	1.629	-0.774	H(15A)	-4.749	2.310	-1.483
C(11)	2.210	1.348	0.016	H(15B)	-4.100	2.527	0.160
C(12)	1.600	2.469	0.844	H(15C)	-3.095	2.929	-1.242
C(13)	0.564	1.959	1.853	H(17A)	-2.077	-3.804	0.593
C(14)	-3.361	0.785	-0.922	H(17B)	-1.270	-3.760	-0.978
C(15)	-0.177	-2.748	0.612	H(17C)	-0.634	-4.811	0.317
C(16)	-3.852	2.229	-0.867				

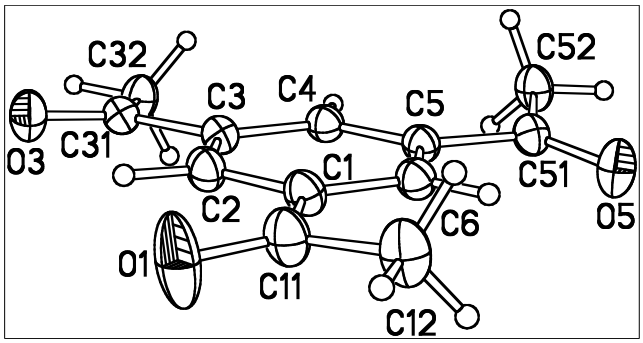

Figure 7. X-ray molecular structure of compound **376**.

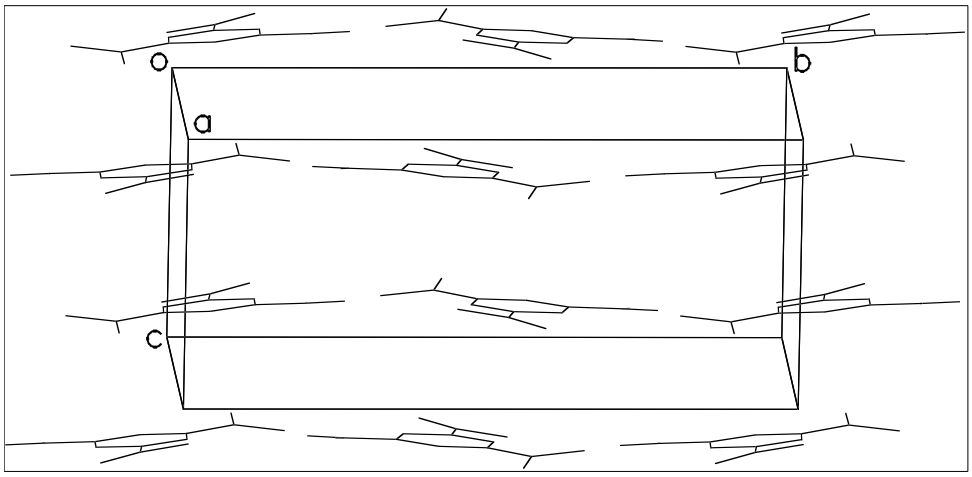

Figure 8. Crystal packing of **376**.

The mechanism for the formal [2+2+2]-cycloaddition reaction has been proposed below (Scheme 59). It was thought that the Lewis acid could initially coordinate to the carbonyl oxygen of the enone (**378**), which would in turn make it sufficiently electrophilic for a second enone **350** to perform a conjugate addition in order to form the first enolate-oxonium intermediate **379**. At high Lewis acid concentrations, this enolate-oxonium intermediate **379** would most likely interact with a third Lewis-acid activated enone molecule **378** in order to undergo a second conjugate addition to form **381**, followed by cyclisation (to **382**) and elimination of methanol to afford the trimer **376**. However, with lower Lewis acid concentrations, it was believed that there would be less Lewis acid activated enone and hence, the initial enolate-oxonium intermediate **379** would more likely interact and cyclise with the imine **243**, most probably through a step-wise Mannich–Michael pathway, and then eliminate methanol in order to form the dihydropyridone **369** (Scheme 59).

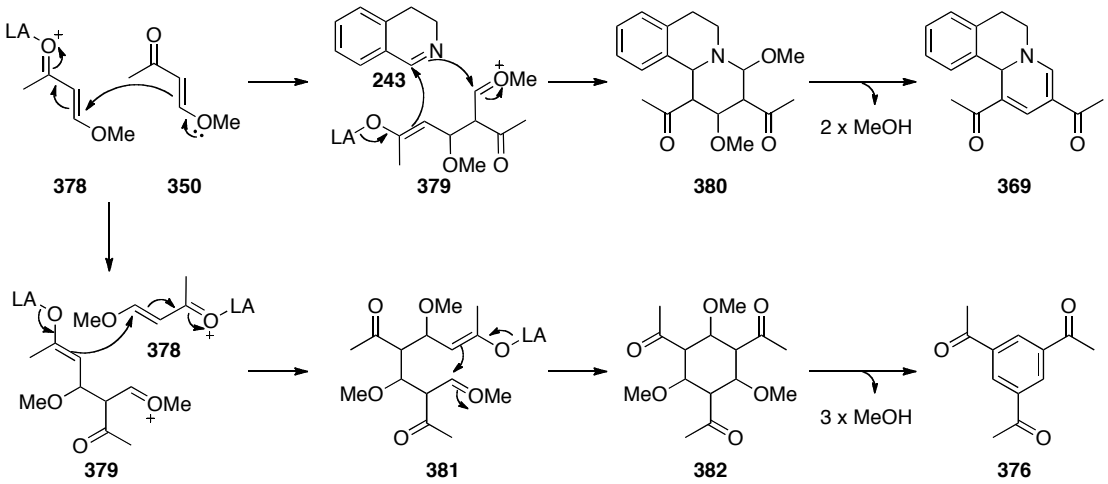

Scheme 59. Proposed mechanisms for the formation of the dihydropyridine **369** and the trimer **376**.

In order to test the scope of the formal [2+2+2]-cycloaddition reaction, enone **350** was reacted with different cyclic imines **383** with the aim of forming different dihydropyridines **384** (Table 20). However, isolation of other desired dihydropyridines **384** proved challenging in both cases.

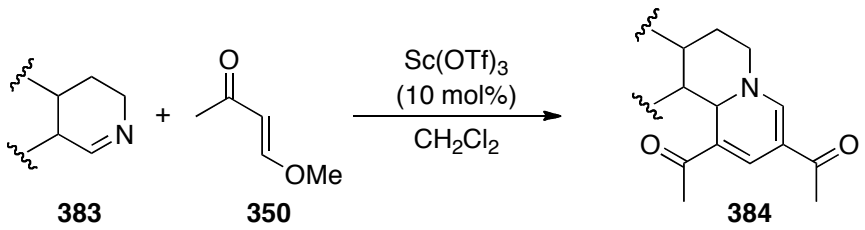

Table 20. [2+2+2]-Cycloaddition attempts between cyclic imines **3383** and enone **350**.

Entry	Imine	Cycloadduct obtained?
1	 **333**	No (mixture of products)
2	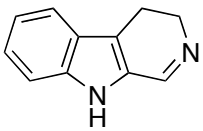 **246**	A promising new LW UV active spot observed by TLC. However, this was in very close proximity to two other spots, making it challenging to isolate.

To summarise, in all of the sets of reactions relating to the formal [2+2+2]-cycloadditions, it was observed that the Lewis acid concentration was important: too low and no reaction occurred; too high and the trimer **376** formation would compete

with dihydropyridine **369** formation. Optimising the purification procedure was important to maximise on yield, though this could be achieved in nearly 90% yield. These dihydropyridines were only obtained when specifically using 4-methoxy-3-buten-2-one **350** or similar synthons. However, this formal [2+2+2]-cycloaddition reaction still needs to be tested on a larger array of cyclic imines to see how general it is. To date, no other imines have reacted equally successfully to **243**.

3.6 Formal [1+2+1+2]-Cycloaddition Reactions

It had been observed that if an aza-Diels-Alder reaction between a cyclic imine and an enone with a leaving group on the β-position, such as 4-methoxy-3-buten-2-one, is carried out, then a formal [2+2+2]-cycloaddition would take place to afford diacetyl-dihydropyridine derivatives, as opposed to a formal [4+2]-cycloaddition to form dihydropyridones. In order to further test the scope of the formal [2+2+2]-cycloaddition reaction, the use of acyclic imines was explored.

Initially, acyclic imine **324** was reacted with two equivalents of enone **350** in the presence of 20 mol% $Yb(OTf)_3$ in the expectation of forming the diacetyl product **385**. However, after purification by silica gel chromatography, the isomer **386** and the [4+2]-cycloaddition product **362** were isolated in 20% and 2% yields respectively (Equation 33). No [2+2+2]-product **385** was observed.

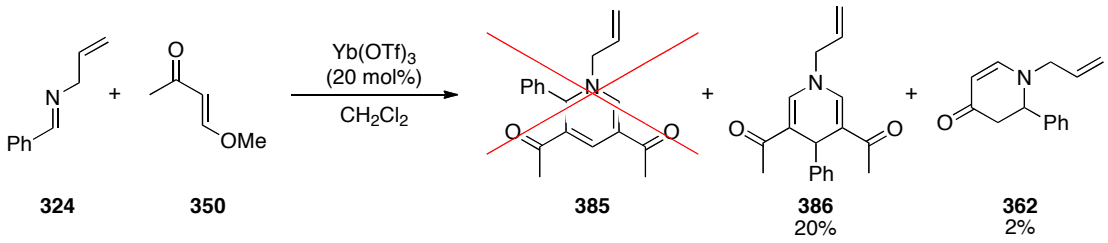

324 **350** **385** **386** 20% **362** 2%

Equation 33

Dihydropiperidine **386** was an interesting and unexpected product because it was formed by a formal [1+2+1+2]-cyclisation pathway, *i.e. via* a four-component reaction. Evidence for the isomer obtained came from the ^{1}H NMR, which showed the two acetyl methyl groups as one singlet (δ = 2.15 ppm), with an integral of six protons indicating the symmetric nature of the structure. Compound **385** however, would show two distinct singlets. The structure of compound **386** was also confirmed by single crystal X-ray structure (Figure 9).

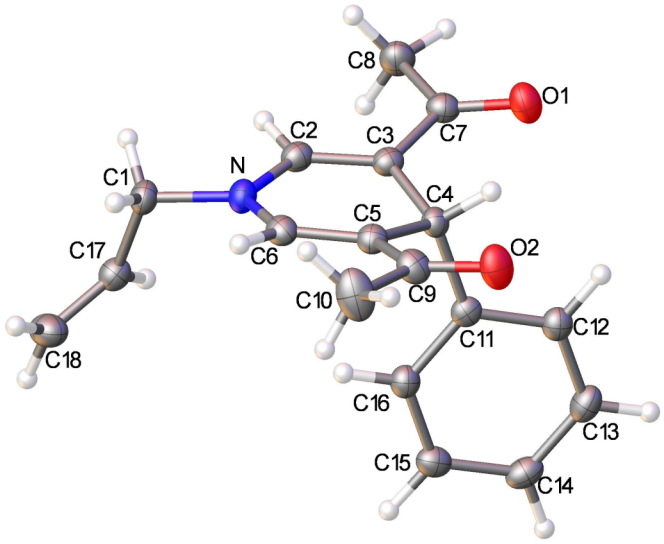

Figure 9. X-ray molecular structure of compound **386**.

In light of this novel result, a selection of acyclic imines **11** were reacted with 4-methoxy-3-buten-2-one **350** at room temperature with a lower catalyst loading (10 mol%), in order to determine the scope of this reaction with different acyclic imines **11**. As well as accessing a number of new adducts **387**, a number of unexpected compounds were also formed, as outlined in Table 21.

These reactions (Table 21) were generally more complex than expected and after purification by silica gel chromatography, many compounds were isolated. It was challenging to isolate them, and those that were isolated (Table 21, entries 1-2) were only retrieved in low yields (20-31%). Indeed, many of the crude ^{1}H NMRs showed mainly starting materials, which could explain some of the low yields. However, from this set of reactions, it was obvious that the imine **11** was hydrolysing to the amine and aldehyde components and reacting separately. This showed that in order to form compounds such as **385**, it was important to have imines that do not easily hydrolyse, such as cyclic systems.

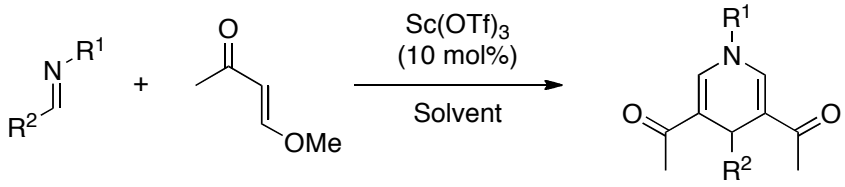

11 **350** **387**

Table 21. Reactions between acyclic imines **11** and enone **350**.

Entry	Imine	Enone Equiv.	Solvent	Major product (yield)	Minor product (yield)
1	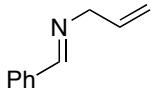 **324**	4	$CHCl_3$	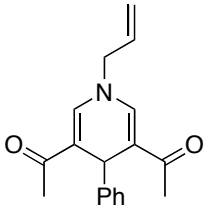 **386** (31%)	
2	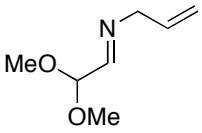 **328**	4	$CHCl_3$	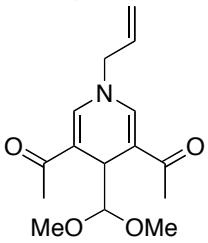 **388** (20%)	
3	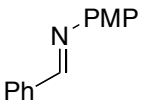 **323**	2.5	$CHCl_3$	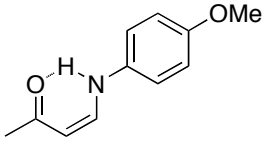 **389** (25%)	
4	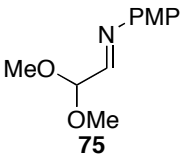 **75**	2.5	$CHCl_3$	Complex mixture	
5	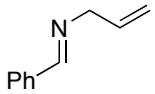 **324**	2.5	MeOH	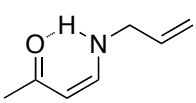 **358** (40%)	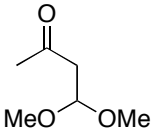 **390** (20%)

In addition, main side-products that were observed were the Michael adducts **389** and **358**, resulting from reaction between the amine and enone **350** (Table 21, entries 3 and 5). This suggested that the mechanism for the formation of the [1+2+1+2]-

adducts could involve formation of a vinylogous amide intermediate; a hypothesis that could be readily tested.

The alkene conformation of the Michael adducts **389** and **358** were determined to be *cis* due to the low alkene and high amine proton J coupling constants (J = 7 and 12 Hz, respectively), values that are expected for *cis* vinylogous amides.[182] In addition, the N*H* signal on the ^{1}H NMR (10 ppm) was less shielded than is expected for a normal N*H* peak (*ca*. 6.5 ppm). This suggests there is an intramolecular H-bond to the carbonyl oxygen, which is in agreement with the literature.[183]

In Table 21, entry 5, there was an example where use of methanol inhibited piperidine product formation compared with chloroform, which agrees with the results observed for the [2+2+2]-cycloaddition reactions (Table 15). This could be due to the formation of side-product **390** resulting from methanolysis of the vinyl ether of **350**, or stalling of the rest of the cascade reaction due to intermediate H-bonding in the polar, protic solvent.

A TLC spot corresponding to compound **358** (Table 21, entry 5) was also observed in the reaction mixture of entry 1. However, this compound was not isolated (in entry 1) since it was not present in sufficiently high concentration according to TLC.

Considering that the imine **324** almost certainly had to be hydrolysed to the amine and aldehyde components in order to access isomer **386** through a formal [1+2+2+1]-cycloaddition pathway, it was realised that this may have been due to the presence of water in the reaction mixture. Hence, the reaction was attempted under anhydrous conditions (argon, 3 Å molecular sieves, dried solvents and dried reagents). Despite these precautions, TLC analysis confirmed that isomer **386** was still being formed, suggesting that some water was still present in the reaction mixture. It was thought that the Lewis acid [$Sc(OTf)_3$] might be too hygroscopic to completely dry and indeed, other groups have gone to extreme measures in vain attempts to completely remove all water coordinated to triflate-based Lewis acids.[184] Similar results were observed (where isomer **386** was preferentially formed over **385**) when using $In(OTf)_3$, $Yb(OTf)_3$, $TiCl_4$, $ZnCl_2$ etherate and BF_3 as the catalyst (Equation 34).

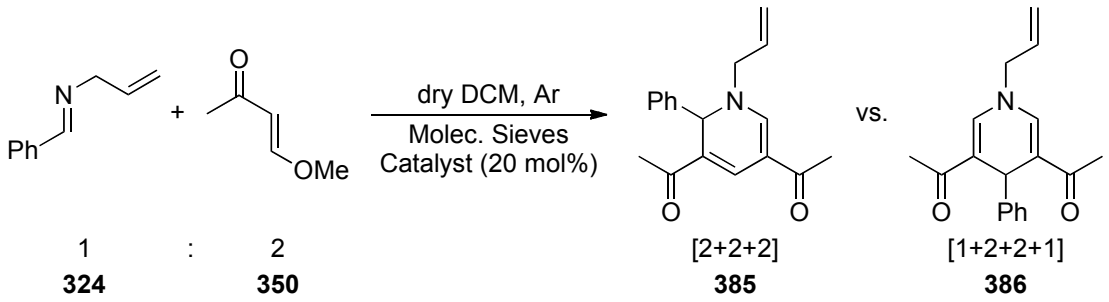

324 **350** **385** **386**

Equation 34

A closer investigation involving the reaction of one equivalent of both amine **86** and aldehyde **8** with two equivalents of 4-methoxy-3-buten-2-one **350** in the presence of a Lewis acid formed the corresponding diacetyl dihydropyridines **387** (Table 22) with low to high efficiency, revealing the generality of the reaction.

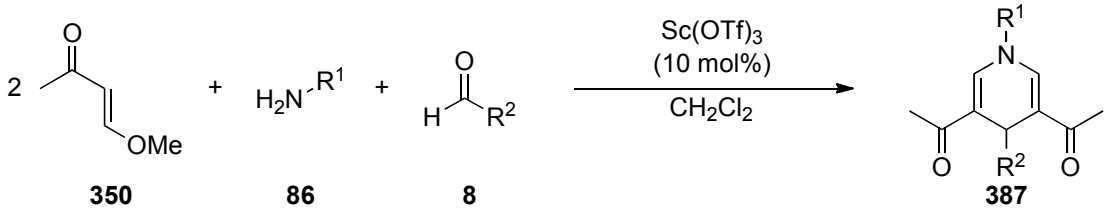

350 **86** **8** **387**

Table 22. [1+2+1+2] Cycloadditions to form dihydropyridines **387**.

Entry	Amine	Aldehyde	Time (d)	Isolated Cycloadduct	Other Isolated Products
1	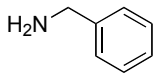 **391**	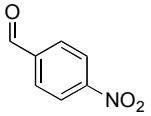 **354**	11	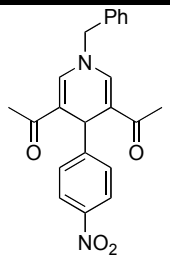 **392** (86%)*	-
2	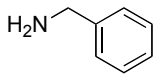 **391**	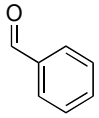 **322**	10	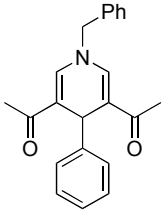 **393** (59%)	-

3	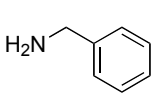 **391**	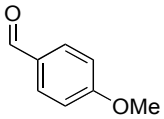 **351**	13	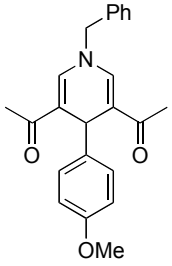 **394** (59%)	-
4	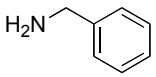 **391**	 **395**	19	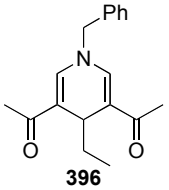 **396** (13%)*	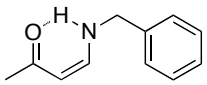 **397** (28%)
5	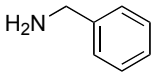 **391**	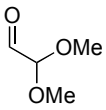 **327**	4	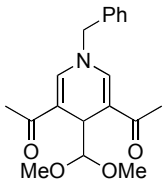 **398** (42%)*	-
6	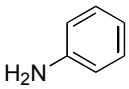 **90**	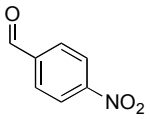 **354**	11	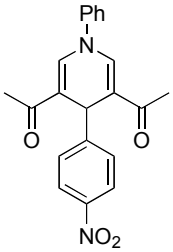 **399** (31%)*	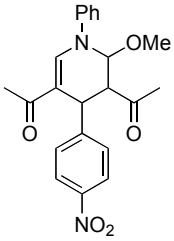 **400** (27%)*
7	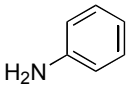 **90**	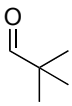 **401**	14	-	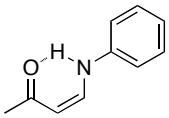 **402** (45%)
8	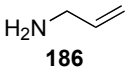 **186**	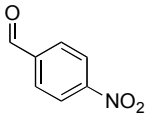 **354**	8	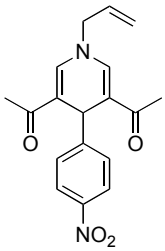 **403** (62%)*	-
9	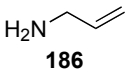 **186**	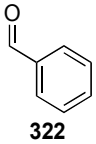 **322**	2	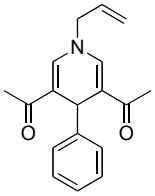 **386** (58)*	-

10	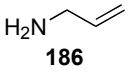 **186**	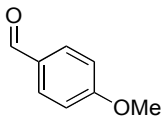 **351**	8	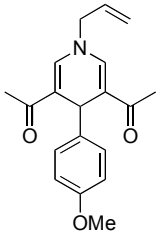 **404** (34%)*	-
11	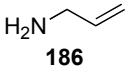 **186**	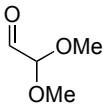 **327**	2	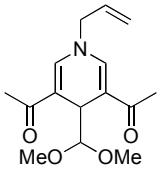 **388** (20%)	-
12	 **405**	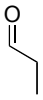 **395**	20	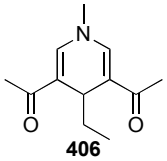 **406** (28%)*	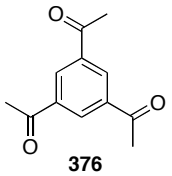 **376** (12%)
13	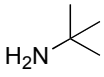 **407**	 **395**	17	-	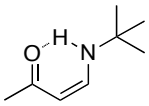 **407** (99%)
14	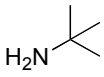 **407**	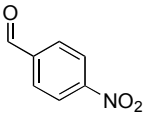 **354**	7	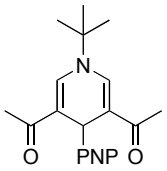 **408** (30% at 60 ºC in toluene)	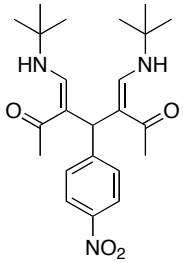 **409** (59%)*
15	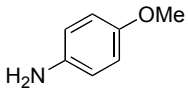 **120**	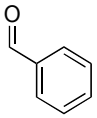 **322**	2	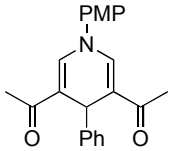 **410**[#]	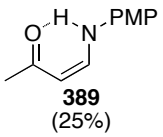 **389** (25%)

* Single X-ray structures obtained.

[#] An inseparable mixture of cycloadduct and its MeOH adduct was obtained in *ca*. 3:1 ratio in an estimated yield (by ^{1}H NMR) of 39%.

NB: The reactions could have gone to completion before the times stated in the table, the table merely states when they were purified by silica gel chromatography.

At first glance, this reaction looks similar to the Hantzsch pyridine synthesis;[185] however, it almost certainly proceeds through a novel and different mechanism in order to give rise to the different dihydropyridines. The use of an enone instead of an α-ketoester to form these types of dihydropyridines is almost unprecedented; to our knowledge, only Inouye *et al*. reported in the late 1950s the only related example,[186,

[187] where 4-chloro-3-buten-2-one was employed instead of 4-methoxy-3-buten-2-one **350**.

In terms of use of different aldehydes (Table 22), higher yields were generally obtained with aromatic aldehydes, whereas, for amines, lower yields were obtained with either less nucleophilic amines (such as aniline, Table 22, entries 6 and 7) or more bulky amines (such as *tert*-butylamine, Table 22, entries 13 and 14). In these cases, the reactions tended to stall at the initial Michael-addition step to form the vinylogous amides, *i.e.* resulting in the isolation of compounds **397**, **402**, **407** and **389**. This could generally be overcome to some extent by heating the reaction to 60 °C (Table 22, entry 14). However, this also resulted in the formation of the doubly vinylogous amide product **409** being the major product.

The highest yield was obtained when using benzylamine **391** and *p*-nitrobenzaldehyde **354** (Table 22, entry 1). Interestingly, when the role of the solvent was examined by running the reaction in different solvents and monitoring by TLC, CH_2Cl_2 appeared to provide the cleanest reaction mixtures after 48 h compared with other solvents. The preferred order of reactivity was CH_2Cl_2 > THF > EtOAc > MeOH > toluene. Many of the products were also crystalline and hence, their structures were confirmed by single crystal X-ray diffraction studies (Figure 10).

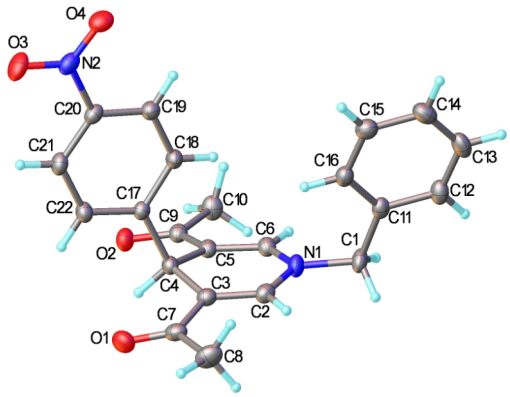

392

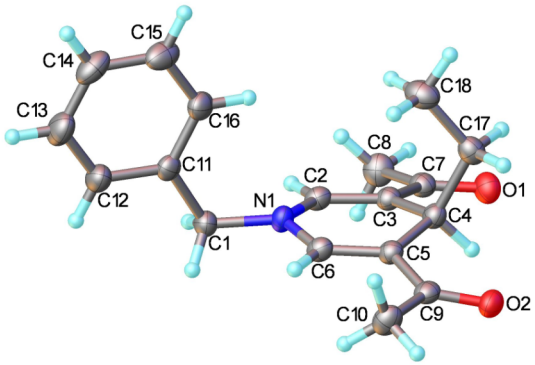

396

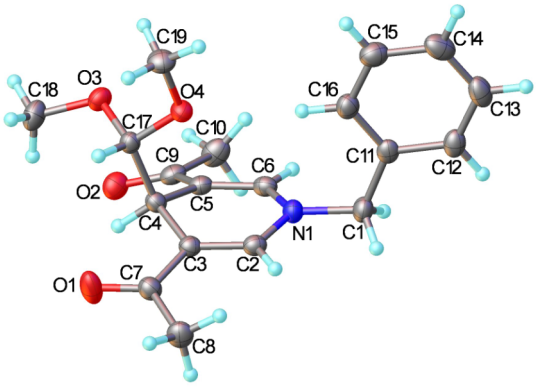

398

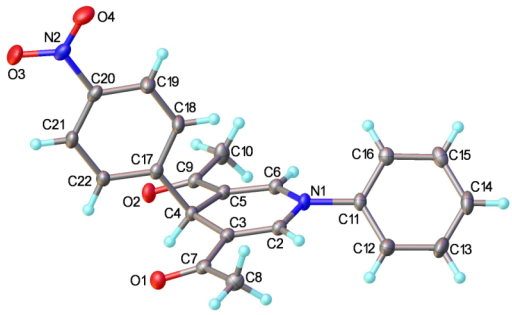

399

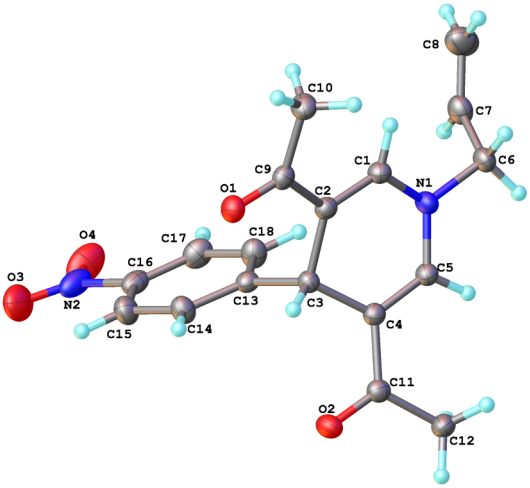

403

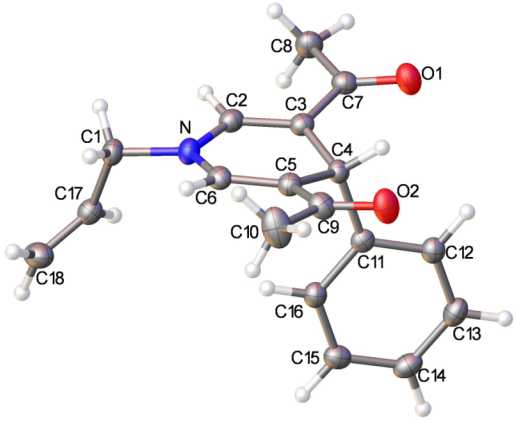

386

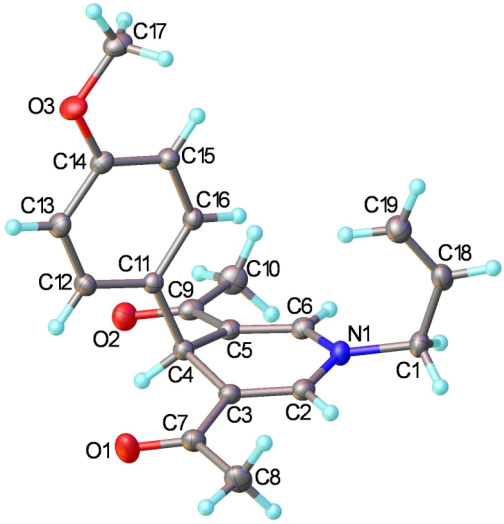

404

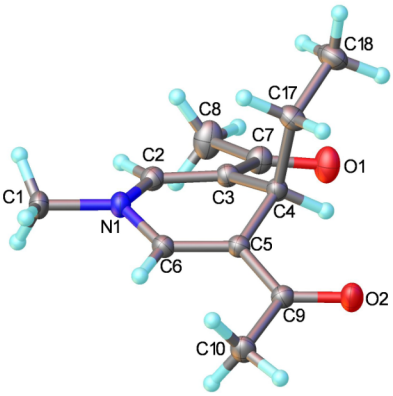

406

Figure 10. X-ray molecular structures of diacetyl dihydropyridines.

The biological activity of the compounds shown in Figure 10 were explored by Dr. Paul Yeo, along with that of the [2+2+2]-cycloaddition product **369**. They were tested against the cell line A549 infected with the Respiratory Syncytial Virus (RSV), which causes respiratory disease. The main individuals at risk from this virus are infants less than six months of age, with RSV being the major cause of hospitalisation for severe respiratory disease in this age group. After this, 'flu' becomes the major cause of respiratory disease towards individuals until they reach 70+ years of age, after which RSV becomes a major cause of mortality due to respiratory disease (although no one knows why this is). For most people, about one third of the events we normally attribute as colds is due to RSV, so finding a cure also has an economic impact due to days taken off work. No effective vaccine or drug treatment is currently available and the potential of a new drug against RSV would be worth up to £2 billion a year. When the compounds were tested between the 100 μM and 1 nM level, these alkaloids were found to be very insoluble when added to the aqueous solution. However, no cells were observed, suggesting these compounds could be very potent on this cell line and that future tests should be done with solutions below the 1 nM level. In addition, it was noted that these alkaloids should be tested again to obtain solubility levels.

It was also interesting to note that the isolated MeOH adduct **411** slowly converted to the more thermodynamically favourable dihydropyridine **410** when left in solution (Equation 35). This suggests that probably the last step in the mechanism involves elimination of methanol. This step would be slower when using relatively less nucleophilic amines, such as aniline **90** and *p*-anisidine **120**.

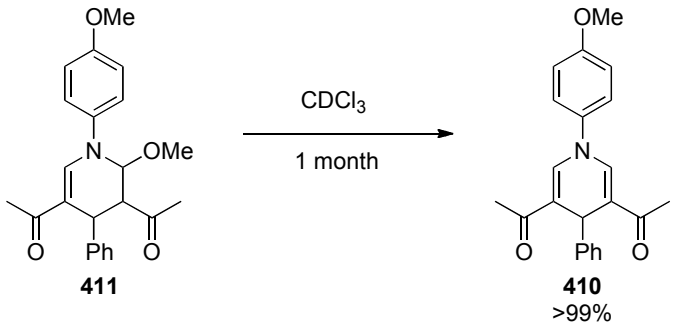

Equation 35

In order to probe the mechanism of the formal [1+2+1+2]-cycloaddition reaction further, the ^{1}H NMR studies outlined in Table 23 were carried out. This involved attempts to follow each stage of the reaction by varying the ratio of reagents and orders of addition, followed by NMR examination. The results are summarised in Table 23.

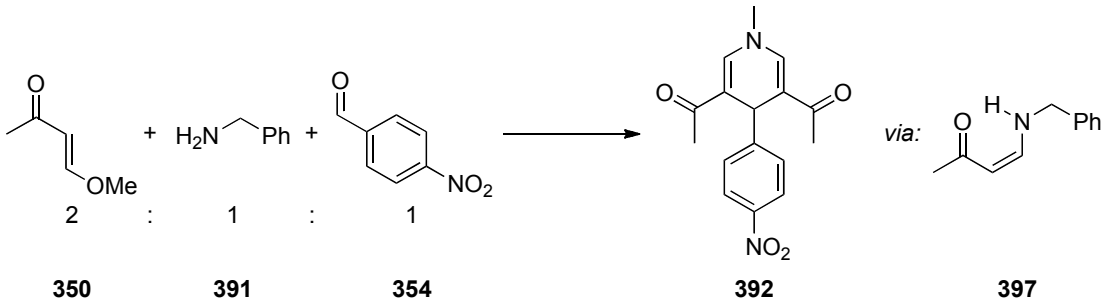

350 **391** **354** **392** **397**

Table 23. Mechanistic studies towards the [1+2+1+2]-cycloaddition reaction.

Entry	Reaction
1	**350** + **391** (2 : 1) $\xrightarrow[CDCl_3,\ 1\ d]{Sc(OTf)_3\ (10\ mol\%)}$ **397** + **391** (50%* : 50%*) $\xrightarrow[2\ d]{\mathbf{354}}$ **392** (60%*) (: 1)
2	**350** + **391** (2 : 2) $\xrightarrow[CDCl_3,\ 1\ h]{Sc(OTf)_3\ (10\ mol\%)}$ **397** (100%*) $\xrightarrow[5\ d]{\mathbf{354}}$ **392** (32%*) (: 1)
3	**350** + **391** (2 : 2) $\xrightarrow[1\ h]{CDCl_3}$ **397** (100%*) $\xrightarrow[5\ d]{\mathbf{354},\ Sc(OTf)_3\ (10\ mol\%)}$ **392** (33%*) (: 1)
4	**350** + **391** + **354** (1 : 1 : 1) $\xrightarrow[CDCl_3,\ 1\ d]{Sc(OTf)_3\ (10\ mol\%)}$? $\xrightarrow[5\ d]{\mathbf{350}}$ **392** (97%*) (: 1)

5	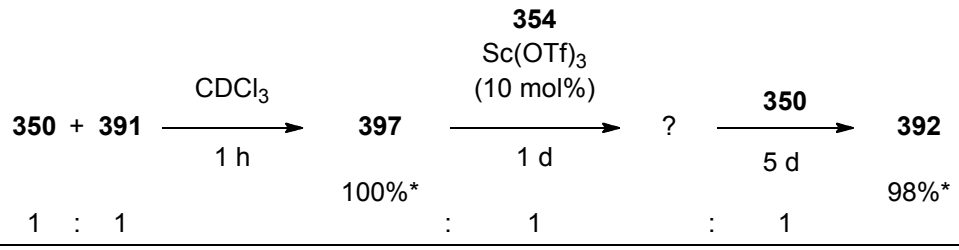

* Conversions estimated with respect to the amount of MeOH produced in the reaction, by 1H NMR integration.

It was possible to be reasonably certain that the initial intermediate formed in these formal [1+2+1+2]-cycloaddition reactions was the vinylogous amide **397**, for several reasons:

1) this intermediate was isolated several times in the reactions in Table 22, *i.e.* entries 4, 7, 13 and 15;

2) reaction of enone **350** (2 Equiv.) with amine **391** (1 Equiv.) in the absence of aldehyde **354** gave the vinylogous amide **397** and unreacted enone **350** (Table 23, entry 1), and subsequent addition of aldehyde **354** gave rapid conversion to the cycloadduct **392** (*ca*. 60%);

3) if the enone **350** (2 Equiv.) was reacted with the amine **391** (2 Equiv.), only the intermediate vinylogous amide **397** was formed. Subsequent addition of the aldehyde **354** (1 Equiv.) resulted in the less efficient formation of the dihydropyridine **392** (32%) (Table 23, entry 2);

4) the vinylogous amide **397** was formed just as efficiently in the absence of the Lewis acid (Table 23, entry 3) and subsequent addition of aldehyde **354** and a Lewis acid provided the cycloadduct **392** with a similarly low conversion as in entry 2 (32%) (Table 23);

5) the dihydropyridine **392** was formed most efficiently and cleanly by reaction of enone **350** (1 Equiv.), amine **391** (1 Equiv.) and aldehyde **354** (1 Equiv.), followed by the addition of another equivalent of enone **350** (Table 23, entry 4);

6) Similarly high conversion rates (98%) to the dihydropyridine **392** were obtained when the vinylogous amide **397** (1 Equiv.) was pre-formed *in situ* prior to addition of the aldehyde **354** (1 Equiv.) (Table 23, entry 5), suggesting this intermediate **397** formed quickly and selectively, regardless of the other reagents in the reaction mixture.

By taking all of the results in Table 23 into account, an array of potential mechanisms (Scheme 60) could be considered and some discarded. Hence, enone **350** and amine **86** must first react together to form vinylogous amide **412**. This can then react *via* pathways A, B or C to produce the final product **387**. However, when path C was probed, where the vinylogous amide **412** reacts initially with the enone **350** followed by the aldehyde (98%) **8** (Scheme 60), a moderate conversion of 60% was obtained (Table 23, entry 1). When path B was probed, where two vinylogous amides **412** react with one aldehyde **8** to form a doubly vinylogous amide **415** prior to cyclisation (Scheme 60), a low conversion of 32-33% was obtained (Table 23, entries 2 and 3). However, when path A was probed, where the vinylogous amide **412** initially reacts with the aldehyde **8** followed by the enone **350** (Scheme 60), high conversion to **387** (97-98%) was obtained (Table 23, entries 4 and 5), suggesting the order of events is as outlined in this pathway. This differs from the related process reported by Inouye,[186] who claimed that two equivalents of a vinylogous amide reacted with one equivalent of aldehyde.

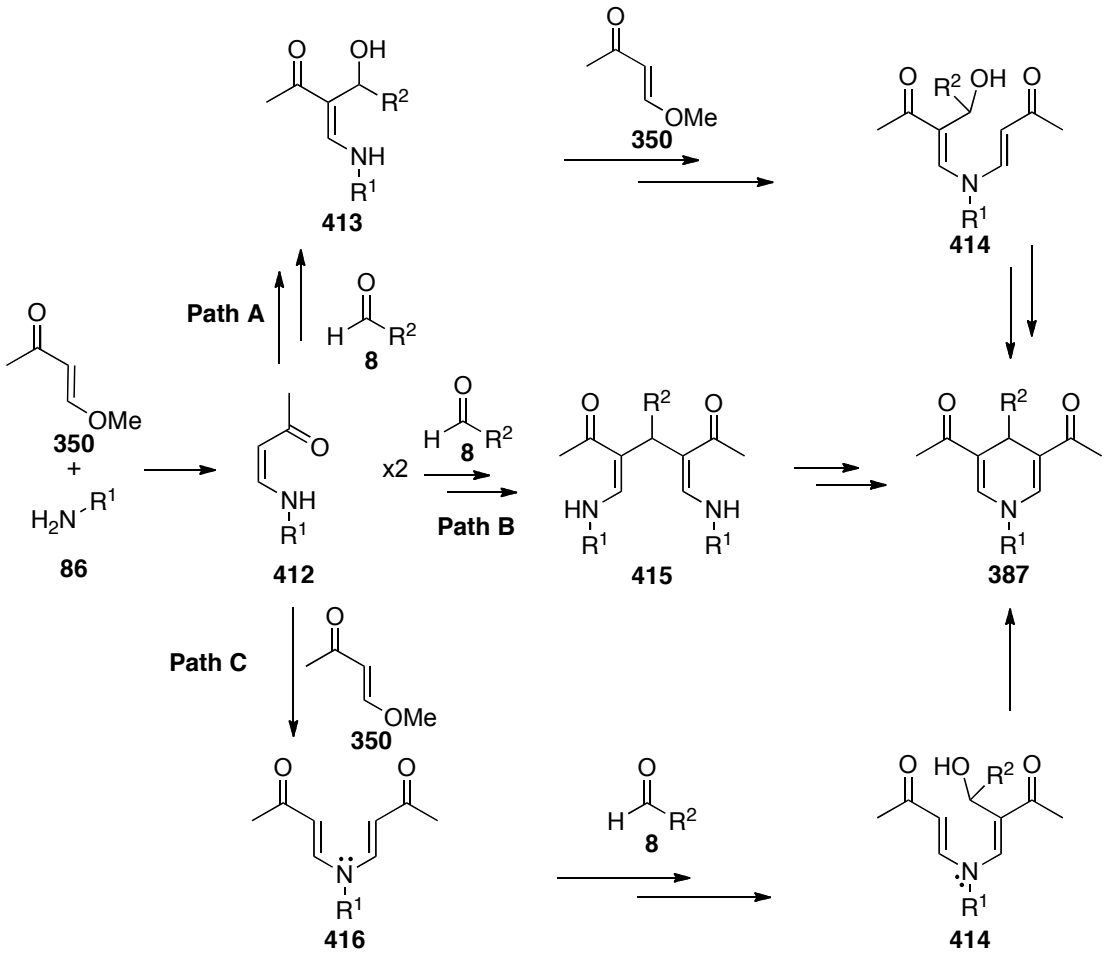

Scheme 60. Probing the mechanistic pathway of the formal [1+2+1+2]-cycloaddition.

Hence, these results strongly suggest that the mechanistic order of events is as outlined in Scheme 61, *i.e*. that intermediate **412** formed quickly and reacted with an aldehyde **8** to give species **417** assisted by the Lewis acid. It is believed that from this intermediate **417**, it is likely that two possible pathways may operate. Either a Diels–Alder cycloaddition pathway can occur *via* scandium-assisted elimination to derive electron deficient aza-diene **418**, which could undergo inverse electron demand Diels–Alder cycloaddition with further enone **350** to derive **419**. This can then eliminate; or, the enamine intermediate **417** could protonate (to give **413**) and react with the enone **350** in a Lewis-acid assisted Michael addition process to derive **420**. This species then requires cyclisation, presumably *via* an enolate equivalent cyclising onto an unsaturated iminium ion such as **421**, to derive the same intermediate **419**, from which methanol elimination can occur to afford the product **387**.

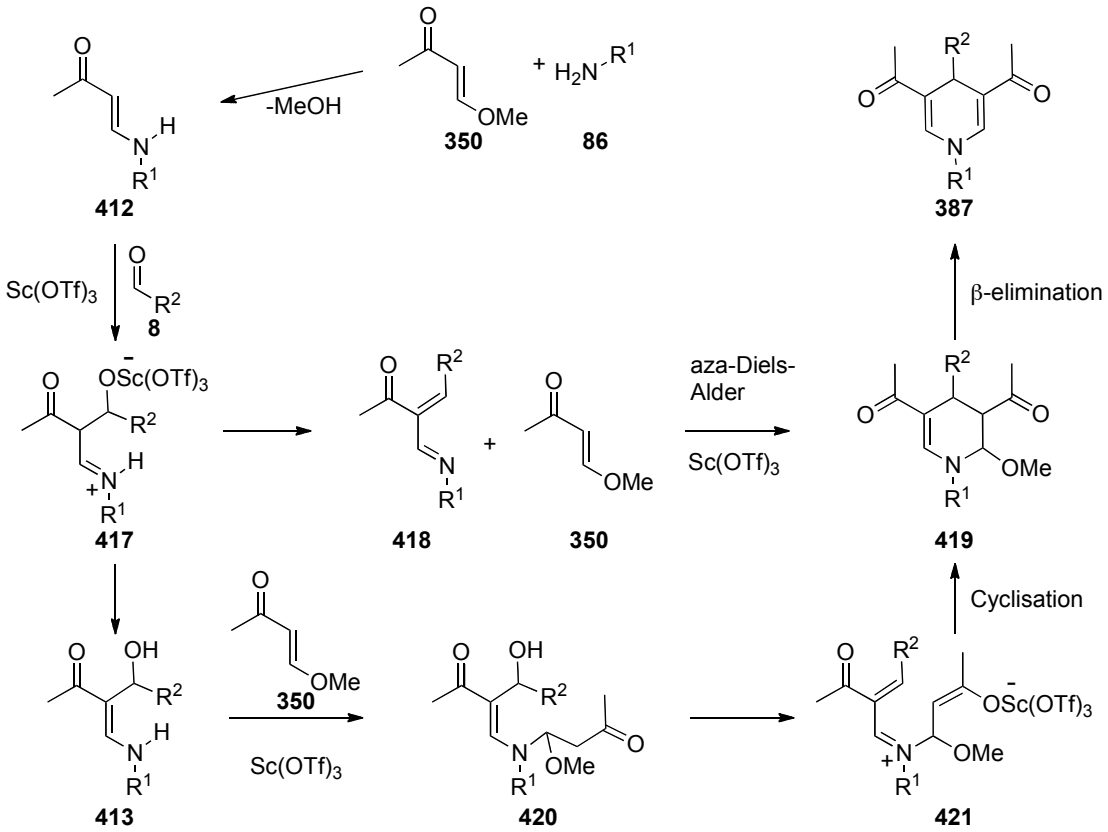

Scheme 61. Proposed mechanism for the formal [1+2+1+2] cycloaddition reaction.

Further evidence for the process outlined in Scheme 61 came from the isolation of the MeOH adduct **400** in 27% from the reaction involving aniline **90** and *p*-nitrobenzaldehyde **354** (see Table 22, entry 6).

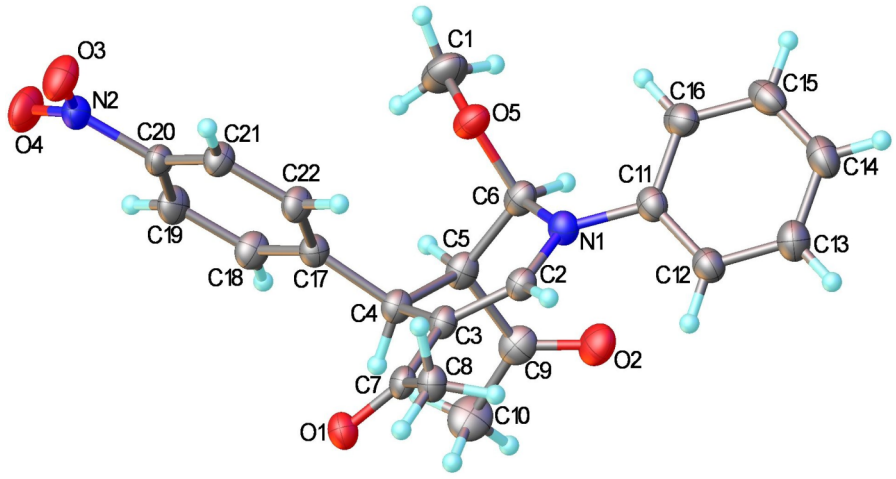

Figure 11. X-ray molecular structure of the MeOH adduct **400**.

Isolation of compound **400** is a clear example of the importance of species **419** in Scheme 61. Single crystal X-ray analysis clearly revealed that this compound **400** was as shown in Figure 11 and must correspond to the last intermediate before β-elimination occurs, to give the dihydropyridine **387**, as outlined in Scheme 61.

It is interesting to note that similar dihydropyridine reactions using vinylogous amides **422** (instead of enones with a leaving group on the β-position) are thought to go through doubly vinylogous intermediate **424** (Equation 36),[188] similar to the one shown in Path B of Scheme 60. This suggests that this reaction could be going through a different mechanistic pathway, *i.e*. *via* a doubly vinylogous amide **424**. Liu *et al*. have demonstrated that this particular reaction needs to be heated to 80-90 °C for the reaction to go through this pathway (Equation 36).[188]

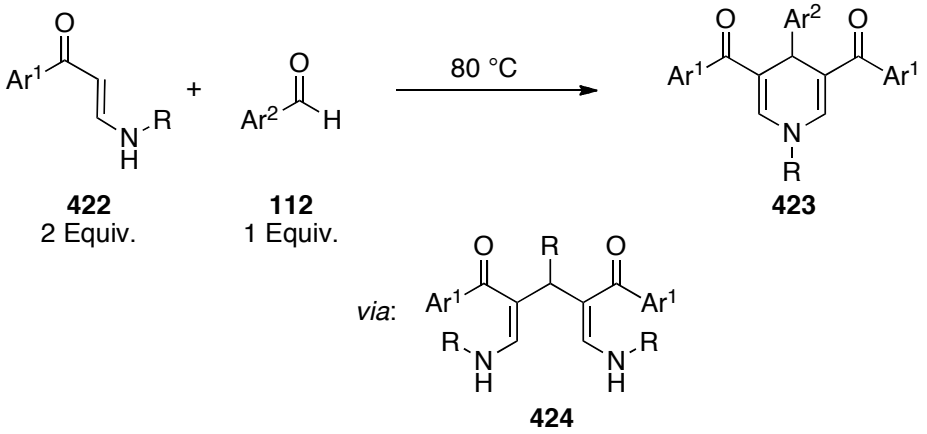

Equation 36

The need for heating in order for the cyclisation to occur for systems involving intermediate **424** (Equation 36) can be understood from examination of the obtained X-ray crystal structure of the doubly vinylogous compound **409** (Figure 12). As explained in Table 22, entry 14, the dihydropyridine product **408** was only obtained (in low yield) after heating the mixture at 60 °C; only the vinylogous amide **407** was obtained when the reaction was performed at room temperature (Table 22, entry 13). The major product from heating at 60 °C was the doubly vinylogous compound **409**, showing that heat was needed in order to form these compounds. However, X-ray crystal structure of **409** showed this compound was particularly stable due to two sets

of intramolecular H-bonds (Figure 12). Hence, it was presumed that additional energy (80 - 90 °C) would be needed in order for the doubly vinylogous amide **424** to break these H-bonds and cyclise. This could explain why such doubly vinylogous amides **424** were not observed when the reaction was performed at room temperature, and why high temperatures of 80-90 °C were necessary when using vinylogous amides **422**, where the mechanism is proposed to go through the doubly vinylogous intermediate **424** (Equation 36).

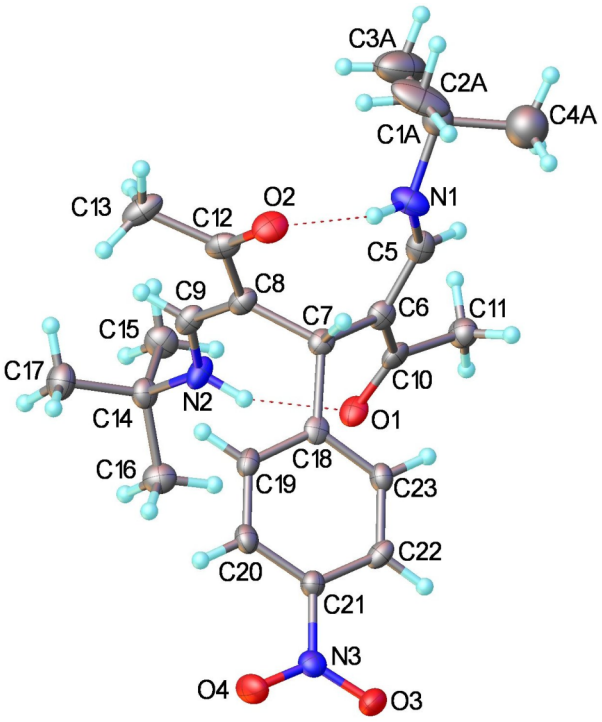

Figure 12. X-ray molecular structure of the double vinylogous amide **409**.

Referring back to the attempts where an imine **11** was reacted with the enone **350** under anhydrous conditions (Equation 34), it was presumed that the imine was being hydrolysed to its amine and aldehyde components. However, if it was believed that the system was completely free from water, then one cannot ignore a different initial mechanism whereby the imine could react with a Lewis acid activated enone compound. The subsequent elimination of methoxide ion could hydrolyse the imine **425**, and in turn lead to the formation of intermediate **429**. Subsequent β-elimination of the MeOH would afford the diene **418** (Scheme 62). As shown in Scheme 61, diene

418 could undergo a formal aza-Diels-Alder reaction with a second enone **350** in order to afford the dihydropyridine **387**, after elimination of MeOH.

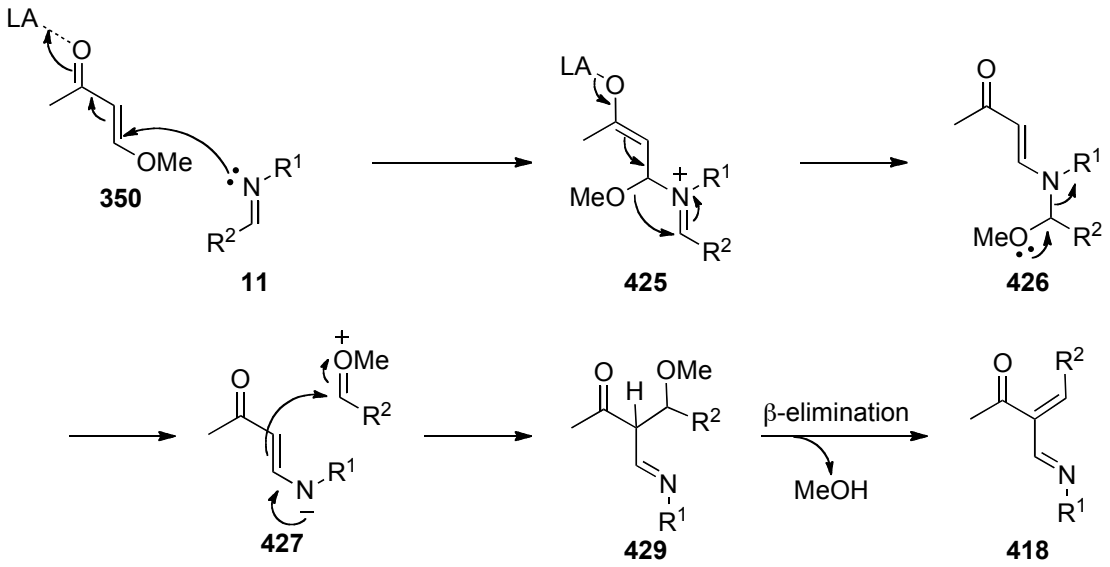

Scheme 62. Alternative mechanism to intermediate **418** from imine **11**.

Understanding that the reaction intermediate **418** could potentially undergo an aza-Diels-Alder reaction with a second enone in order to afford a piperidine of type **419**, the reaction scope with different enones **183** to form substituted piperidines **430** was investigated (Table 24). In this case, the initial enone **350**, amine **391** and aldehyde **354** were allowed to react in the presence of the Lewis acid prior to addition of the second enone **183**. The enones investigated were methyl vinyl ketone (Table 24, entry 1) and 4-phenyl-3-buten-2-one (Table 24, entry 2). However, on each occasion, TLC analysis mainly showed the presence of dihydropyridine **400** and unreacted starting materials; there was no clear evidence that piperidines **430** were being formed.

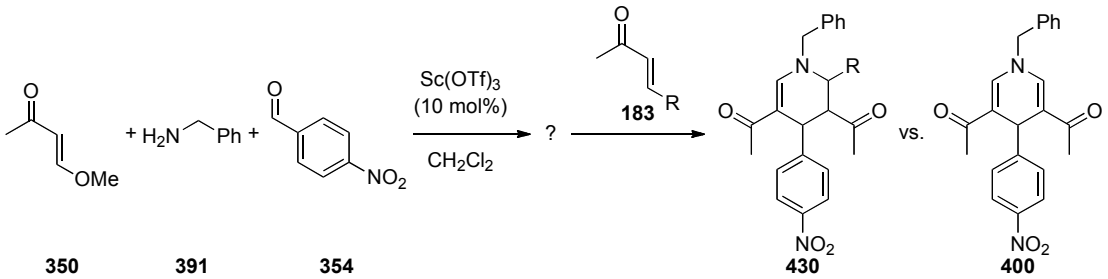

Table 24. The use of different enones in the [1+2+1+2]-reaction.

Entry	R	Cycloadduct **430** obtained?
1	H	No
2	Ph	No

In summary, it has been deduced that under these reaction conditions (Table 21), imines hydrolyse to amine and aldehyde components, after which the amine can react with a methoxy enone to form a vinylogous amide. In the presence of a Lewis acid, this can then react with an aldehyde and a second methoxy enone to form a new dihydropyridine. The reaction goes through a formal [1+2+1+2]-cycloaddition pathway in a novel one-pot, four-component cyclisation reaction. The mechanism has not been fully determined, however, evidence for these studies involves the isolation of intermediates within the reaction mixture, as well as high conversion when the reagents were reacted in the proposed order.

3.7 Formal [4+2]-Cycloadditions Using Enones

It was observed that when cyclic imines were reacted with 4-methoxy-3-buten-2-one, a [2+2+2]-formal cycloaddition occurred to form diacetyl-dihydropyridines. If acyclic imines were used, then the reaction went through a formal [1+2+1+2]-cyclisation pathway forming a different class of dihydropyridine.[189] Hence, it was realised that cyclic imines that do not easily hydrolyse are essential for a formal [2+2+2]-cyclisation pathway to proceed.

In order to determine the scope of the formal [2+2+2]-cyclisation reaction by using enones **183** that do not contain a leaving group (LG) on the β-position, the cyclic imine **243** was reacted with 2 equivalents of two different enones: 4-phenyl-3-buten-2-one **348** and methyl vinyl ketone **164** (Table 25).

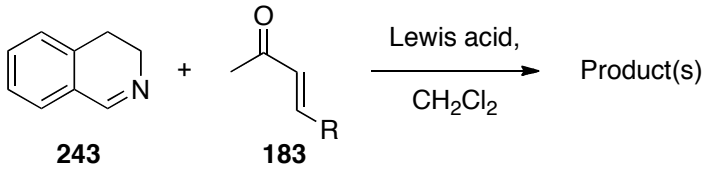

243 **183**

Table 25. Reaction of an enone **183** with imine **243**, where R ≠ LG.

Entry	Enone	Lewis acid	Time	Major product (yield)	Minor product (yield)
1	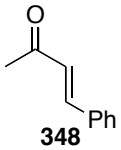 **348**	$Sc(OTf)_3$ (10 mol%)	72 h	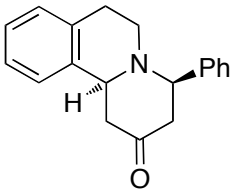 **431** (61%)	-
2	**348**	$Sc(OTf)_3$ (10 mol%)	24 h	Mixture mainly consists of starting materials	
3	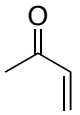 **164**	$Yb(OTf)_3$ (20 mol%)	24 h	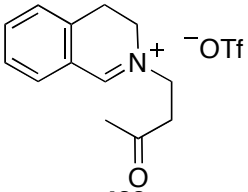 **432** (37%)	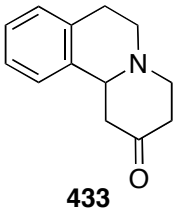 **433** (25%)

When using 4-phenyl-3-buten-2-one **348** (Table 25, entry 1), the aza-Diels-Alder product **431** was obtained in moderate yield and seemingly a single diastereoisomer. It was found that this reaction was slow (72 h) and that the use of excess enone **348** made identification and purification by silica gel chromatography challenging because the product **431** and enone **348** had almost identical R_f values. Hence, the product **431** was only isolated analytically pure after purification using reverse phase chromatography. The stereochemistry of this product was determined to be as shown in Table 25, entry 1, with both the methine protons presumed axial, as shown by a strong NOE between them, suggesting **431** exists as shown in Figure 13. It was thought that in order to form this product, the reaction would probably have gone through a Mannich–Michael pathway (*vide supra*).

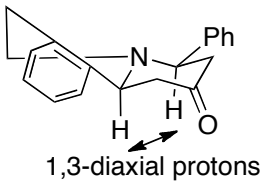

Figure 13. Proposed conformation of compound **431**.

When using methyl vinyl ketone **165** as the enone (Table 25, entry 3), the aza-Diels-Alder product **433** was obtained in low yields within 24 hours. However, the isoquinolium salt **432** was predominantly obtained; this structure was attributed in part due to a low field N=C*H* resonance of 9.20 ppm in the ^{1}H NMR spectrum, with the connectivity confirmed by analysing the HSQC and HMBC spectra. This implied that the initial attack of the imine **243** on the enone **183** was likely to have been *via* a Michael-type reaction when using methyl vinyl ketone as the enone, followed by a Mannich cyclisation to form the aza-Diels-Alder product **433**.

In order to further confirm the structure of the isoquinolium salt **432**, the reaction between imine **243** and methyl vinyl ketone **164** was performed in the presence of trifluoromethanesulfonic (triflic) acid in an attempt to compare the salt formed with the isoquinolium salt **432**. However, the crude ^{1}H NMR indicated that instead of forming the isoquinolium salt **432**, the salt **434** had been formed instead (Equation 37). Considering triflic acid is a strong superacid, it is believed that protonation takes

place because the acidic proton from triflic acid is more electrophilic (harder) than the methyl vinyl ketone **164**.

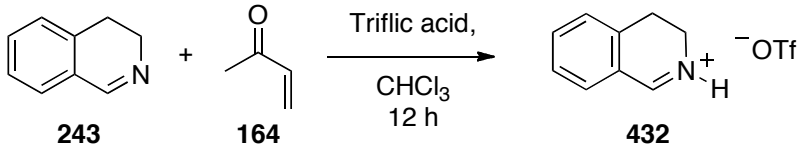

Equation 37

Evidence for the formation of **432** includes the observance in the ^{1}H NMR of: 1) the imine *Ha* peak was split into a doublet; 2) the *Hb* peak was a multiplet as opposed to being a clear t; 3) a br s peak that would account for the N*H* [^{1}H NMR (400 MHz, $CDCl_3$) δ 8.54 (d, *J* = 8.5 Hz, 1H, *Ha*), 8.11 (br s, 1H *NH*), *7*.84 (d, *J* = 7.5 Hz, 1H, *Hg*), 7.78 (t, *J* = 7.5 Hz, 1H, *Hf*), 7.53 (t, *J* = 7.5 Hz, 1H, *He*), 7.40, (d, *J* = 7.5 Hz, 1H, *Hd*), 4.11-4.05 (m, 2H, *Hb*), 3.24 (t, *J* = 8.2 Hz, 2H, *Hc*)].

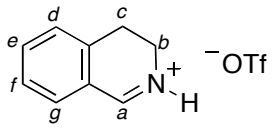

432

Considering that the methyl vinyl ketone **164** had to be acting as a Michael acceptor for the formation of isoquinolium salt **432**, the reaction between imine **243** and methyl vinyl ketone **164** was explored further using different oxy-philic Lewis acid catalysts. These reactions were screened using LCMS, with the crude reaction mixtures of the more promising Lewis acids being subsequently analysed by ^{1}H NMR (Table 26).

From the screening studies (Table 26), it was found that the formation of the isoquinolium salt **432** was most favourable when using $In(OTf)_3$ as catalyst (Table 26, entry 7).

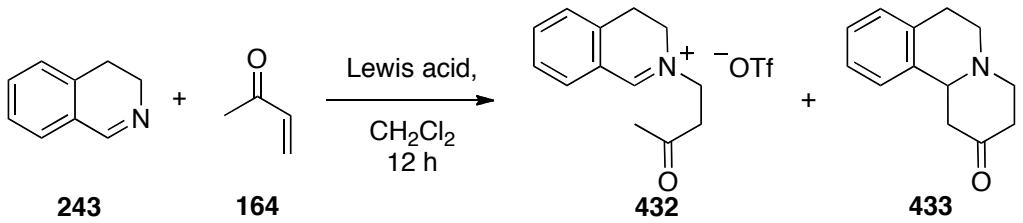

Table 26. Lewis acid screening.

Entry	Lewis Acid	Was product **432**/**433** observed by LCMS?	Was the reaction clean enough to take further?	Crude ^{1}H NMR result
1	$AuCl_3$	No	No	-
2	$HAuCl_4 \cdot 3H_2O$	Yes	Yes	Complex spectrum
3	$Ag(OTf)_3$	Yes	No	-
4	$Cu(OTf)_3$	Yes	No	-
5	$Eu(hfc)_3$	Yes	No	-
6	$La(OTf)_3$	Yes	Yes	Both **432** and **433** observed
7	$In(OTf)_3$	Yes	Yes	**432** cleanly observed
8	$Sc(OTf)_3$	Yes	Yes	Complex spectrum, difficult to see either **432** or **433**

The isoquinolium salt **432** could probably subsequently be cyclised *in situ* by treatment with base, including NaOH, diisopropylamine and L-proline (Table 27). Indeed, simultaneously using catalytic amounts of both $In(OTf)_3$ and L-proline afforded the aza-Diels-Alder product **433** (Table 27, entry 4), albeit in racemic form. Reacting imine **243** and methyl vinyl ketone **164** in the presence of L-proline with no $In(OTf)_3$ afforded negligible amounts of product **433**, as determined by crude ^{1}H NMR after 72 h; mostly starting material remained unreacted under these conditions (Table 27, entry 5). A similar transformation was found in the literature and the procedure followed,[190] whereby mixing imine **243** and methyl vinyl ketone **164** in acid (such as HCl), followed by a base quench (such as NH_4OH) afforded the aza-Diels-Alder product **433** in good yield of 74% (Table 27, entry 6). Interestingly, when a reducing agent such as $NaBH(OAc)_3$ was used (Conditions B), the product **433** was obtained as the major product after basic work up (Table 27, entry 2).

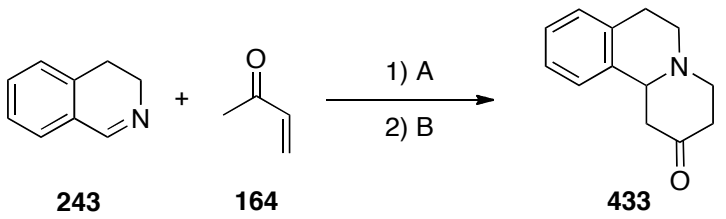

243 **164** **433**

Table 27. Synthesis of the piperidinone **433**.

Entry	Solvent	Conditions A (24 h)	Conditions B (24 h)	Yield **433** (%)	ee (%)
1	$CHCl_3$	$In(OTf)_3$ (20 mol%)	Diisopropylamine	>50*	-
2	$CHCl_3$	$In(OTf)_3$ (20 mol%)	$NaBH(OAc)_3$ followed by NaOH	>60*	-
3	$CHCl_3$	$In(OTf)_3$ (20 mol%)	L-proline (30 mol%)	>50*	0
4	$CHCl_3$	$In(OTf)_3$ (20 mol%) and L-proline (30 mol%)	Left for an extra 48 h	49	3
5	$CHCl_3$	L-proline (30 mol%)	Left for an extra 48 h	<5*	-
6	Ethanol	HCl	NH_4OH	74	-

*Values estimated from crude ^1H NMR

Considering that the cycloadduct **433** was only being synthesised in moderate yields, the different species in the reaction mixture were monitored in an attempt to determine why this was (Table 28).

From these reactions (Table 28), it was observed that the use of $NaBH(OAc)_3$ reduced the isoquinolium salt **432** to **435**, and hence, gave lower yields of cycloadduct **433** (Table 28, entries 2, 10). It was also observed that both NaOAc and $NaBH(OAc)_3$ acted as a mild base to cyclise **432** to **433** (Table 28, entry 3). However, NaOH base was needed for higher conversion of **432** to **433** (Table 28, *cf*. entry 3 with entries 4-5, 10).

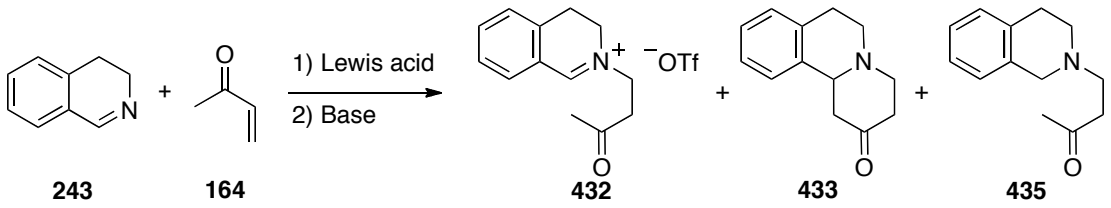

243 **164** **432** **433** **435**

Table 28. Further studies into the reaction between imine **433** and methyl vinyl ketone **164**.

Entry	Lewis Acid (mol %)	Base	Quench	Solvent	**432** (%)	**433** (%)	**435** (%)
1	$In(OTf)_3$ (20)	NaOH	-	DCM	-	62	-
2	$In(OTf)_3$ (20)	$NaBH(OAc)_3$	NaOH	DCM	-	12	NM
3	$In(OTf)_3$ (20)	NaOAc	Brine	DCM	-	11	-
4	$In(OTf)_3$ (20)	NaOAc	-	DCM	-	45	-
5	$In(OTf)_3$ (40)	NaOAc	-	DCM	-	59	-
6	$In(OTf)_3$ (40)	NaOH	-	EtOAc	-	37	-
7	$In(OTf)_3$ (40)	NaOH	-	MeOH	-	37	-
8	$In(OTf)_3$ (40)	NaOH	-	MeCN	-	27	-
9	$In(OTf)_3$ (40)	NaOH	-	THF	-	5	-
10	$In(OTf)_3$ (40)	$NaBH(OAc)_3$	NaOH	DCM	-	11	34
11	$Sc(OTf)_3$ (10) Pybox (10)	NaOH	-	DCM	-	39*	-
12	$Fe(OTf)_2$ (10)	NaOH	-	DCM	-	35	-
13	$Ga(OTf)_3$ (10)	NaOH	-	DCM	-	18	-

NB.: NM = not measured
Entries 6 onwards were performed using a purer imine.
*0% ee

In terms of the solvents used, the preferred order in terms of achieving the cycloadduct **433** most efficiently was CH_2Cl_2>EtOAc/MeOH/MeCN>THF (Table 28, entries 1, 6-9). Similarly, the order of Lewis acid reactivity towards preferred formation of the cycloadduct **433** was $In(OTf)_3$>$Sc(OTf)_3$>$Fe(OTf)_2$>$Ga(OTf)_3$ (Table 28, entries 1, 11-13). Unfortunately, the use of a chiral ligand, Pybox, did not induce asymmetric induction; cycloadduct **433** was obtained as a racemic mixture as determined by HPLC analysis (Table 28, entry 11). The results shown in Table 28 were partly confirmed when the reaction was monitored by ^1H NMR (Table 29).

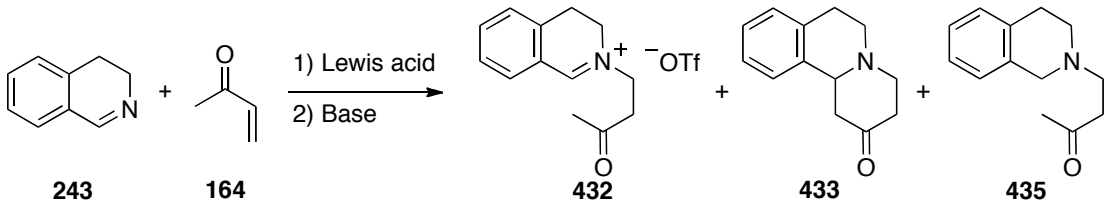

243 **164** **432** **433** **435**

Table 29. Monitoring the reaction by NMR.

Entry	Time	Ratios of compounds			
		242	**432**	**433**	**435**
1	1 h	0.2	1	0.2	0.06
2	3.5 h	0.13	1	0.7	0.08
3	12 h	-	1	1.4	-
4	After NaOAc addition	-	1	3	-
5	After NaOH addition	-	1	11	-

Hence, it was observed from Table 29 that when imine **243** was reacted with methyl vinyl ketone **164** in the presence of a Lewis acid, then after one hour the isoquinolium salt **432** was formed as the major product, with a small proportion of the salt **432** also cyclising to product **433** (Table 29, entry 1). Over time, the amount of cyclised product **433** relative to the isoquinolium salt **432** increases (Table 29, entry 2). By the time all of the imine **243** has been consumed, the amount of cyclised product **433** observed is greater than that of the isoquinolium salt **432** (Table 29, entry 3). It was also confirmed that usage of NaOAc as a mild base cyclised **432** to **433** (Table 29, entry 4), whilst usage of NaOH base afforded higher conversion of **432** to **433** (Table 29, entry 6).

Thus, in terms of mechanism, it was proposed that the formal [4+2]-aza-Diels-Alder reaction using imine **243** and enones **183** (where R ≠ LG) in the presence of a Lewis acid goes through a different mechanism depending upon how strong a Michael acceptor the enone **183** was. Because methyl vinyl ketone **164** is a good Michael acceptor, the mechanism is believed to go through a Michael-Mannich pathway. Evidence for this included the fact that the isoquinolium salt **432** (the Michael product) was isolated, which in turn cyclised most effectively in the presence of a base in order for the subsequent Mannich reaction to occur (Scheme 63).

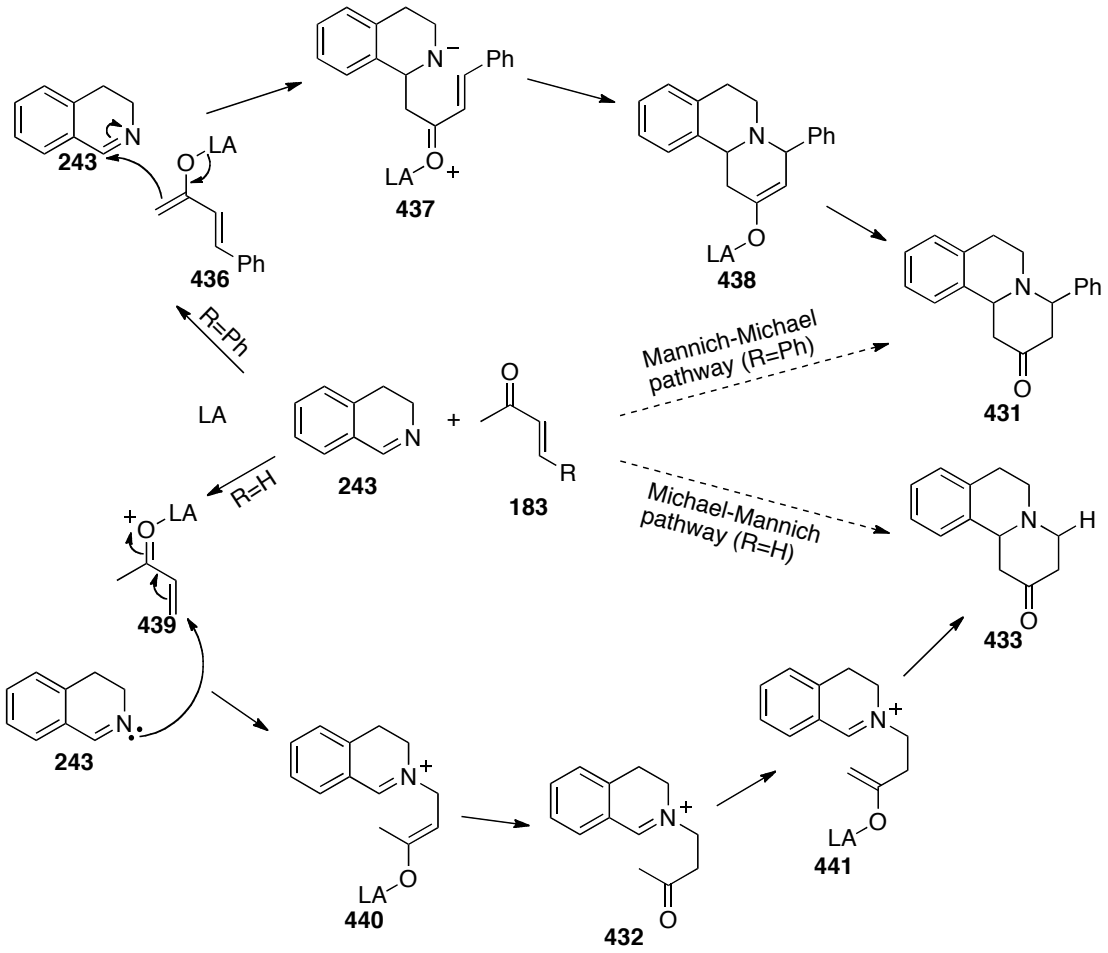

Scheme 63. Proposed Mechanisms for the formal [4+2]-cycloaddition using different enones (where R≠LG).

In the case of 4-phenyl-3-buten-2-one **348**, it was believed that the mechanism of formation of **431** involves a Mannich-Michael pathway (Scheme 63). This was further attributed to the fact that no isoquinolinium salt was isolated, and no base was needed to help with the cyclisation. Hence, the reaction is likely to involve an activated enone of type **436** in order to perform a Mannich reaction with imine **243** to form the Mannich product **437**. This would then cyclise to form a species of type **438**, where compound **431** would be formed after tautomerisation.

The scope of this reaction was further investigated using different cyclic and acyclic imines. This was monitored by TLC and ^{1}H NMR analysis over a period of a week. However, no cycloadduct was isolated form the reaction mixtures (Table 30).

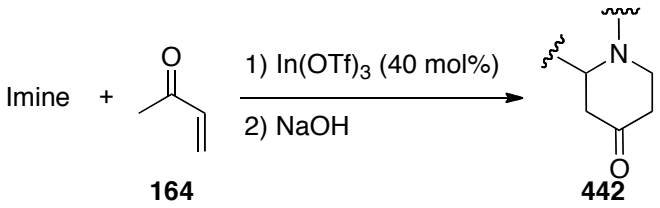

Table 30. Reaction of methyl vinyl ketone **164** with different imines.

Entry	Imine	Cycloadduct obtained?
1	 **333**	No
2	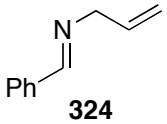 **324**	No

Interestingly, when the imine **324** was reacted with methyl vinyl ketone **164** in the presence of a Lewis acid without any subsequent treatment with base, a new compound **443** was isolated (Equation 38).

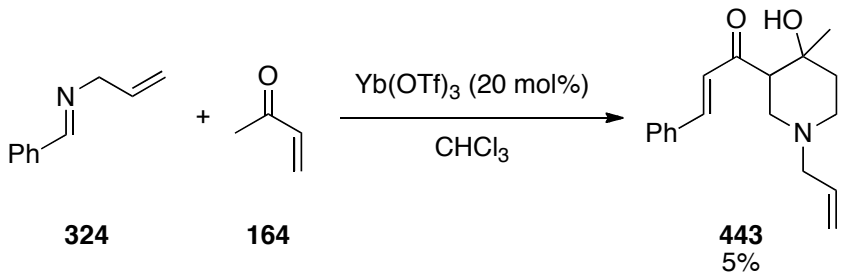

Equation 38

Compound **443** was only isolated in very small amounts (5%) and confirmed by HSQC and HMBC. In order for **443** to have been formed, the imine **324** would have hydrolysed to its amine **186** and aldehyde **322** components, with these reacting with two equivalents of methyl vinyl ketone **164**; a proposed mechanism has been laid out in Scheme 64. The other components observed in the reaction mixture were starting materials and allylamine **186**.

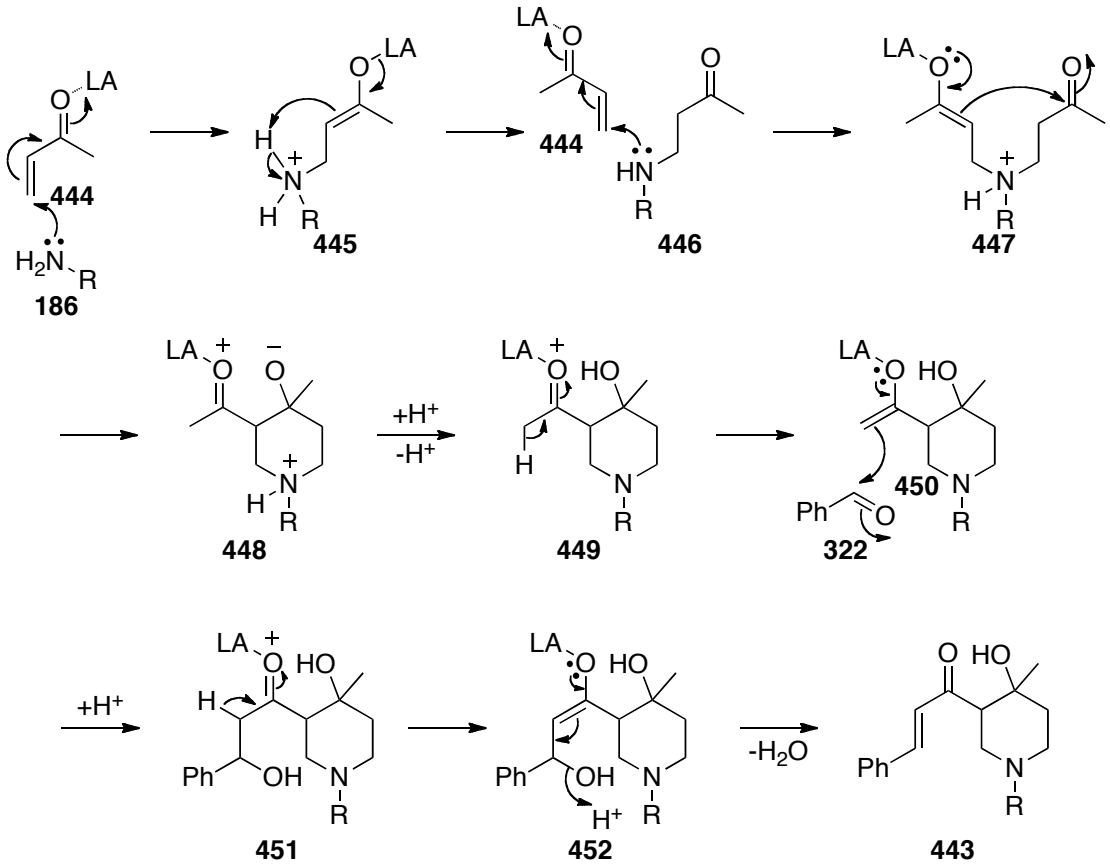

Scheme 64. Proposed mechanism for the formation of compound **443**, where R=allyl and LA=Yb(OTf)$_3$.

It was also deemed interesting to directly compare the methyl vinyl ketone **164** results for the [2+2+2]-reaction. Hence, it was decided to see if different bis-methyl-ketone-substituted products could be formed with varying degrees of saturation by employing the addition of imines to different enones. This was investigated by reacting imine **243** with enones **164** and **350** in order to determine if this formed the bis-methyl-ketone **453** (Equation 39).

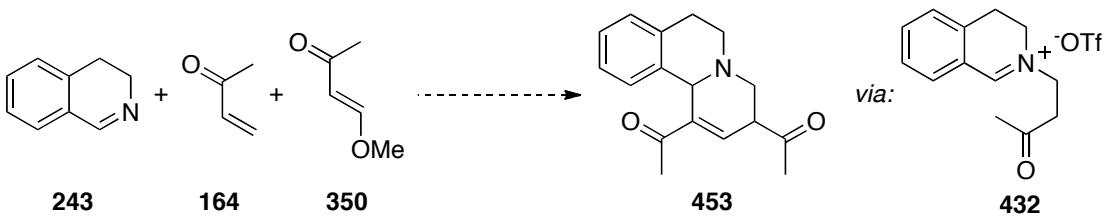

Equation 39

The reasoning behind Equation 39 was that enone **164** (lacking an electron-donating methoxy group) would act as a better Michael acceptor towards imine **243** compared to enone **350**, hence, forming the isoquinolinium salt **432**. Subsequently, enone **350** would act as a better electrophile than **164** towards attacking the isoquinolinium salt **432** *via* a Mannich reaction. Subsequent cyclisation and elimination of methanol could afford **453**.

In order to be certain that imine **243** attacked enone **164** first, enone **350** was added to the reaction mixture one hour after the first enone **164** (Equation 40). After purification by silica gel chromatography, it was observed that only methyl vinyl ketone **164** had reacted with imine **243** to form the iminium salt **432** as the major product, along with some cyclised product **433**. From the crude ^{1}H NMR, it was observed that the enone **350** was unreacted, showing that diacetyl-piperidines of type **453** cannot be formed by this method.

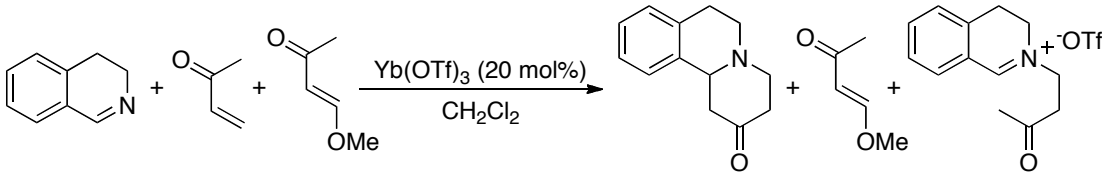

243 **164** **350** **433** 21% **350** >99% **432** 40%

Equation 40

In summary, it has been observed that when reacting cyclic imines with enones that do not have a leaving group in the β-position, in the presence of a Lewis acid, a formal [4+2]-aza-Diels-Alder cyclisation takes place in order to form piperidine derivatives. The cyclisation goes through a stepwise Mannich-Michael or Michael-Mannich pathway, depending on how strong a Michael acceptor the enone is. When the reaction goes through the Michael-Mannich pathway (*e.g.* when using methyl vinyl ketone), a base is needed to promote the cyclisation after the initial Michael addition reaction. No extra additives are necessary in the Mannich-michael pathway.

3.8 Synthesis of new bifunctional aminoboronic acid catalysts

Through exploring traditional Lewis acid-catalysed aza-Diels-Alder reactions, two novel cycloaddition reactions were serendipitously discovered: formal [2+2+2]- and [1+2+1+2]-cyclisation pathways. For the formal [4+2]-cycloaddition using enones without a leaving group on the β-position, the aza-Diels-Alder reaction was deemed to proceed through a stepwise Mannich-Michael mechanism (depending on the enone used). In order to advance this aza-Diels-Alder methodology, it was decided to investigate the use of aminoboronic acids as catalysts;[191] variances of these catalysts have been shown successfully catalyse a range of reactions, from asymmetric direct amide formation[192] to asymmetric aldol reactions.[193] In particular, the aminoboronic acids of type **454** used in the asymmetric enamine-based aldol reaction have been shown to catalyse the aldol reaction in high yield and enantiomeric excess (ee), with greater ee being obtained when making the boron more Lewis acidic through *in situ* esterification of the boronic acid.[194] We were interested in examining the reactivity scope of these aminoboronic acids that work through enamine activation.

Similar to L-proline, these bifunctional aminoboronic acid catalysts **454** consist of a basic amine group and a Lewis acidic boron group (carboxylic acid group for L-proline), with the advantage of circumventing the solubility problems associated with L-proline. Hence, the first aim was to synthesise these aminoboronic acids in order to investigate their activity as chiral catalysts, especially in the Mannich-Michael (or *vice versa*) formal cycloaddition reaction.

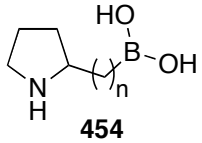

454

Previously, the aminoboronic acids of type **454** with side chains of n = 0-2 had been synthesised and investigated in the aldol reaction.[161] Hence, it was decided to synthesise the n = 3 catalyst in order to compare it with the shorter chain analogues and study their potential for accessing piperidine derivatives.

3.8.1 Racemic catalyst synthesis

In order to determine how the chain length between the nitrogen and boron atoms affected catalyst properties in the aza-Diels-Alder reaction, aminoboronic catalyst **457**, with the nitrogen and boron atoms separated by four carbon atoms, was synthesised, initially using the procedure outlined in Scheme 65.

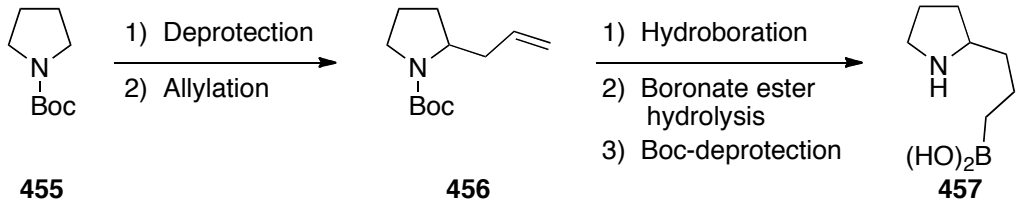

Scheme 65. Proposed synthetic route to catalyst **457**.

Protection of pyrrolidine **356** was straightforwardly performed with di-*tert*-butyl-dicarbonate in ethanol, affording *N*-boc-pyrrolidine **455** in good 86% yield (Scheme 66).

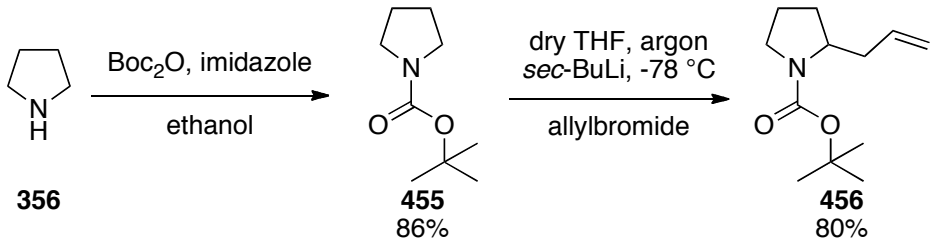

Scheme 66. Synthesis of catalyst pre-cursor **456** from pyrrolidine.

The deprotonation of *N*-Boc pyrrolidine **455** was then performed using *sec*-BuLi followed by allylation with allylbromide to give product **456** in 80% yield (Scheme 66). This reaction could be performed on gram quantities.

It was interesting to observe from the ^{13}C NMR spectrum of **456**, that the product was a mixture of two carbamate rotamers. When ^{13}C NMR analysis was performed at room temperature, two carbon peaks were observed for the carbons denoted with an asterisk in Figure 14. When the ^{13}C NMR was performed at a higher temperature (50 °C), the two peaks for each of the individual carbon atoms merged into one, confirming the rotameric effects.

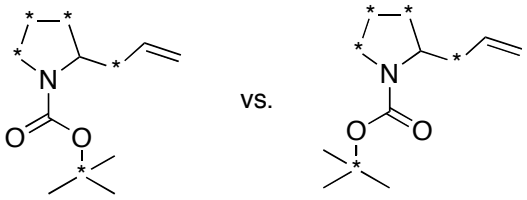

Figure 14. The two rotamers of **456**, where the asterisks signify the carbons exhibiting two peaks by ^{13}C NMR at rt.

In order to access the potential aminoboronic catalyst **456**, a catecholborane hydroboration of **456** was attempted under standard reaction conditions.[195] Heating catecholborane **458** with allyl derivative **456** at 100 ºC for 1 h gave, after workup, a major crude product. ^{1}H NMR suggested that this major component was the deprotected starting material, *i.e.* **466**, on the basis of the allylic peaks (5.4 and 4.9 ppm) being present, along with a lack of a Boc peak at 1.4 ppm. This suggested that catecholborane **458** was too Lewis acidic to hydroborate **456**; instead interacting with the carbonyl oxygen of the Boc group and triggering cleavage. A plausible mechanism explaining this is shown in Scheme 67.

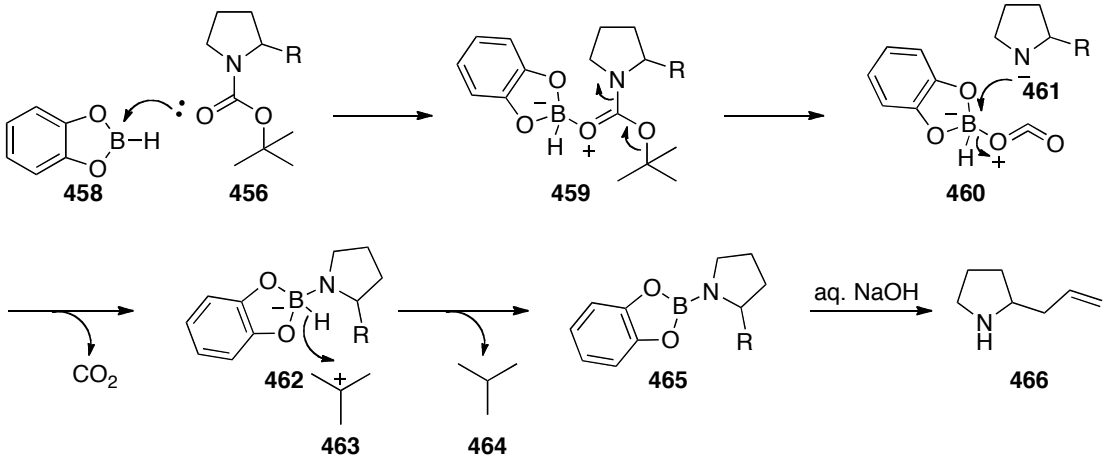

Scheme 67. Boc deprotection using catecholborane, where R = allyl.

Because catecholborane appeared to be too Lewis acidic for the hydroboration reaction of **456**, the borane (BH_3•THF) was employed instead (Scheme 68).[195] This reaction was performed in THF at 0 ºC, and was subsequently quenched with MeOH. A prominent new spot by TLC analysis showed that a major new compound was

formed. ^{1}H NMR suggested this was compound **467** on the basis of: 1) no allylic peaks being observed at 5.4 and 4.9 ppm; 2) the Boc group being present at 1.4 ppm; and 3) upfield BC*H*$_2$ and BCH$_2$C*H*$_2$ peaks at 0.8 and 1.3 ppm respectively. However, the peaks were not completely clean, and it was obvious that some minor material was present. The ^{11}B NMR peak was in the expected region (32 ppm) for a boronate derivative.

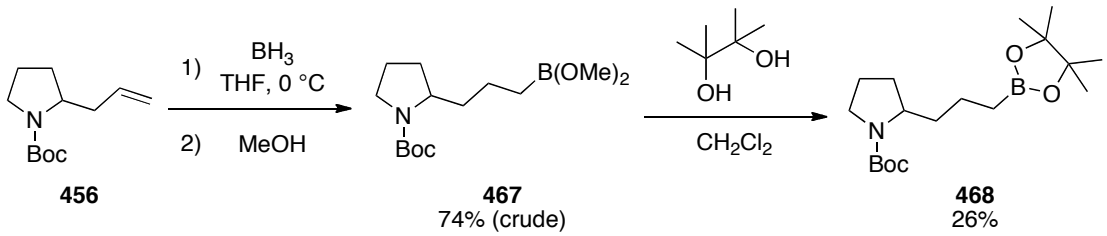

456 **467** 74% (crude) **468** 26%

Scheme 68. Hydroboration of compound **456** using borane.

The crude **467** was protected with pinacol to form **468**, in order to make the compound more stable and easier to handle and characterise (Scheme 68). After purification by silica gel chromatography, compound **468** was isolated (26%) along with a second compound, which was proposed to have structure **469**. This was on the basis of the Boc and pinacol peaks being observed at 1.4 and 1.2 ppm respectively by ^{1}H NMR, along with no upfield BC*H*$_2$ peaks observed. Instead, a lower field 3.6 ppm signal was observed, which would account for the BOC*H*$_2$ protons. The ^{1}H NMR of **469** also gave a higher integration than expected in the 1.4-1.9 ppm region, possibly due to H-bonding with water. Hence, the integration was approximately in line with what was expected, especially when a D_2O exchange was performed.

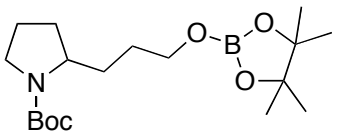

469

Synthesis of **468** was also performed from **456** in a one-pot reaction without evaporating the MeOH prior to the pinacol protection (Equation 41). This strategy also gave a similarly low yield of **468** (20%).

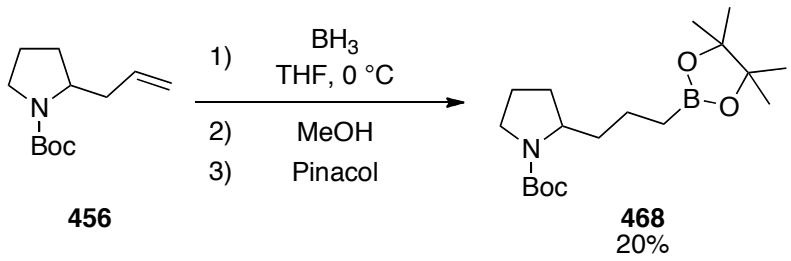

Equation 41

Hence, it was decided to try the hydroboration reaction using IPC-borane **470**. Commercial IPC-borane as the TMEDA complex **469** was used, however, no reaction occurred if the TMEDA was not removed beforehand. Hence, the IPC-borane **469** was treated with BF_3 etherate in order to complex the TMEDA and release the free IPC-borane **470**. The resulting TMEDA•2BF_3 complex was unreactive and could be left in the reaction mixture.[196] Thus, it was thought that subsequent hydroboration of **456** with **470** would give **471**, following literature procedures.[197] After treating **471** with acetaldehyde this would give the boronate ester **472**, whereby the boronic acid **473** could be retrieved after work up (Scheme 69).

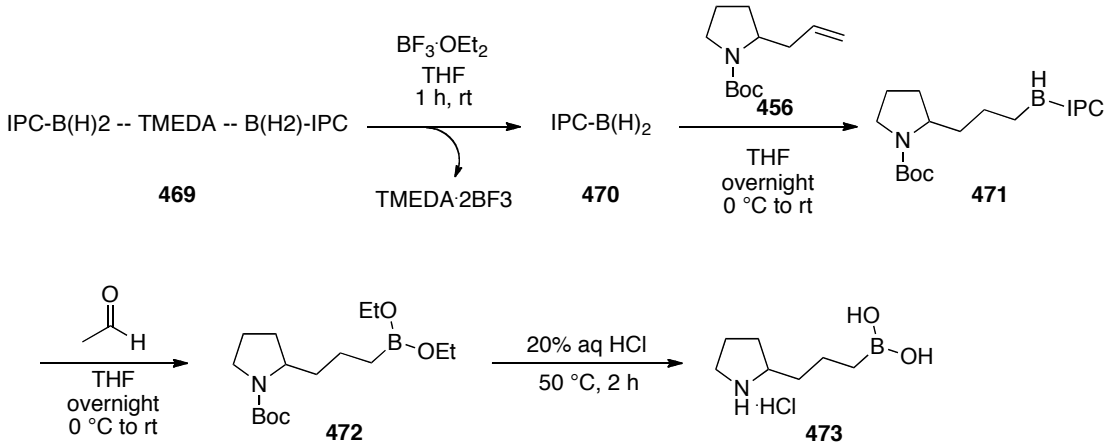

Scheme 69. Hydroboration of compound **456** using IPC-borane.

In practice, the steps to form the boronic acid **473** were not straightforward. Isolation of boronic acid **473** was attempted by separating **473** in the aqueous layer from the organic layer as a salt. However, the combined aqueous extracts also contained other salts, including TMEDA•2BF_3. Hence, compound **473** could not be isolated through this method. Not knowing how stable the boronate ester **472** was, it was refrained from purifying at this stage in case **472** would decompose.

At the same time, hydroboration of **456** with pinacol borane **474** was attempted using metal catalysis. Literature conditions were followed using Wilkinson's catalyst ($RhCl(PPh_3)_3$)[198] and an iridium complex ($[Ir(cod)Cl]_2$)[199] respectively (Scheme 70).

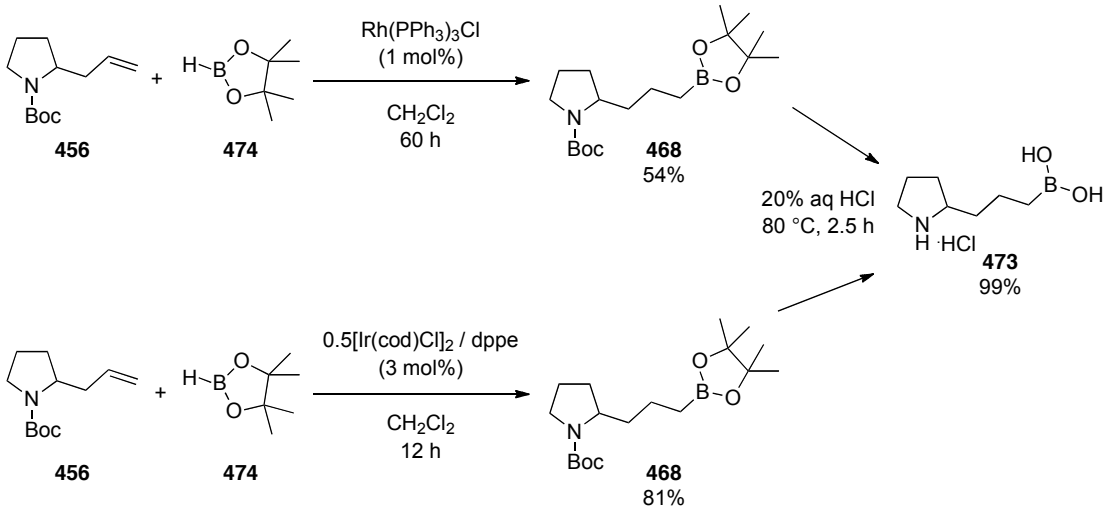

Scheme 70. Hydroboration of **456** using metal catalysis.

Through these methods, it was found that the pinacol protected boronate ester **468** was stable to isolation after purification by silica gel chromatography by either catalytic process. The iridium catalyst was the superior catalyst, being higher yielding and faster reacting. Subsequent heating of **468** for 2.5 hours in 20% (aq) HCl gave both boronate and Boc deprotection, and afforded aminoboronic acid salt **473** in quantitative yields.

Through a combination of ^{1}H, ^{13}C, COSY, HSQC and TOCSY NMR, it was confirmed that the product was indeed compound **473**, with the ^{11}B NMR showing a broad peak at 35-36 ppm. The ^{1}H NMR peak of the CH_2 group next to the boron was very shielded, showing a triplet at 0.6 ppm.

Compound **473** was also obtained when directly heating the crude **468** in acid followed by evaporation and azeotropic removal of volatile components, and thereby preventing the need to purify **468**. Through this method (Scheme 71), **468** was obtained in equally high yields, although with slightly lower purity than the method shown in Scheme 70. Boronic acid **473** was found to be harder to handle than

boronate ester **468**. Hence, it was preferred to store **468** and convert the necessary amounts to 4**73** as required.

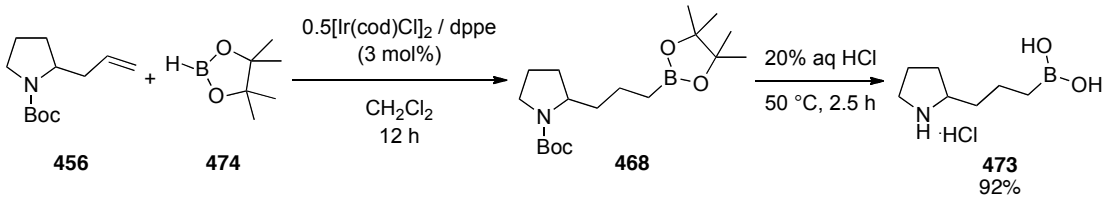

Scheme 71. Isolation of aminoboronic acid **473** without purification of the precursor **468**.

3.8.2 Asymmetric Synthesis of the Aminoboronic Acid Catalyst

Having synthesised the racemic aminoboronic acid **473**, it was decided to use this as a standard for its asymmetric synthesis in order to test if this compound could induce asymmetry into the aza-Diels-Alder reaction. Hence, an asymmetric synthesis of **475** using a sparteine-mediated lithiation was attempted from *N*-boc-pyrrolidine **455**. The results are shown in Table 31.

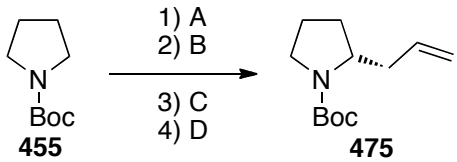

Table 31. (-)-Sparteine mediated lithiations of **455**, carried out under argon at -78 °C.

Entry	Condition A	Condition B	Condition C	Condition D	Yield (%)	ee (%)
1	Dry ether, *sec*-BuLi, (-)-sparteine, 1 h	Allyl bromide	-	-	64	19
2	Dry ether, *sec*-BuLi, (-)-sparteine, 1 h	CuCN•2LiCl in dry THF, 1 h	Allyl bromide	-	63	69
3	Dry ether, (-)-sparteine, *sec*-BuLi (**455** added 30 min after) 6 h	$ZnCl_2$, dry THF, 30 min	CuCN•2LiCl in dry THF, 30 min	Allyl bromide	96	82
4	Dry ether, (-)-sparteine, *sec*-BuLi (**455** added 30 min after) 1 h	$ZnCl_2$, dry THF, 30 min	CuCN•2LiCl in dry THF, 30 min	Allyl bromide	80	82

When performing the lithiation reactions with *N*-Boc pyrrolidine **455** in the presence of (-)-sparteine, compound **475** was obtained with a low ee (19%) (Table 31, entry 1). In an attempt to improve on this, the literature reported by Dieter *et al*. was followed, involving a solution of CuCN•2LiCl in THF which was added to the reaction mixture after the lithiation step, prior to addition of the electrophile.[200] However, this method only raised the ee of **475** to 69% (Table 31, entry 2). In order to try and develop on this further, the literature procedure reported by Coldham *et al*. was followed whereby a solution of $ZnCl_2$ in THF was added to the reaction mixture prior to the CuCN•2LiCl solution.[201] A further difference with this method involved the lithiation step: the *N*-boc pyrrolidine was added dropwise to a solution of (-)-sparteine in *sec*-BuLi, as opposed to the *sec*-BuLi being added dropwise to a stirred solution of *N*-boc pyrrolidine and (-)-sparteine. By following this procedure, compound **475** was obtained with 82% ee (Table 31, entries 3 and 4). It was also observed that the time spent stirring the reaction mixture prior to the addition of $ZnCl_2$ affected the overall yield. Hence, a 96% yield was obtained when the reaction mixture was stirred for six hours prior to the addition of the $ZnCl_2$, compared to a yield of only 80% when the reaction mixture was stirred for 1 hour (Table 31, entries 3 and 4 respectively).

*3.8.2 Structural Studies on the Bifunctional System **478***

After synthesising **475**, the aminoboronic acid salt **477** was formed following the procedure shown in Scheme 72, with **477** giving a ^{11}B NMR signal at 35 ppm. Neutralisation of **477** with equimolar amounts of triethylamine was carried out in order to determine the structural effects of the boron-nitrogen functions in **478**, *i.e.* the extent of the nitrogen-boron chelation **479** (Scheme 72).

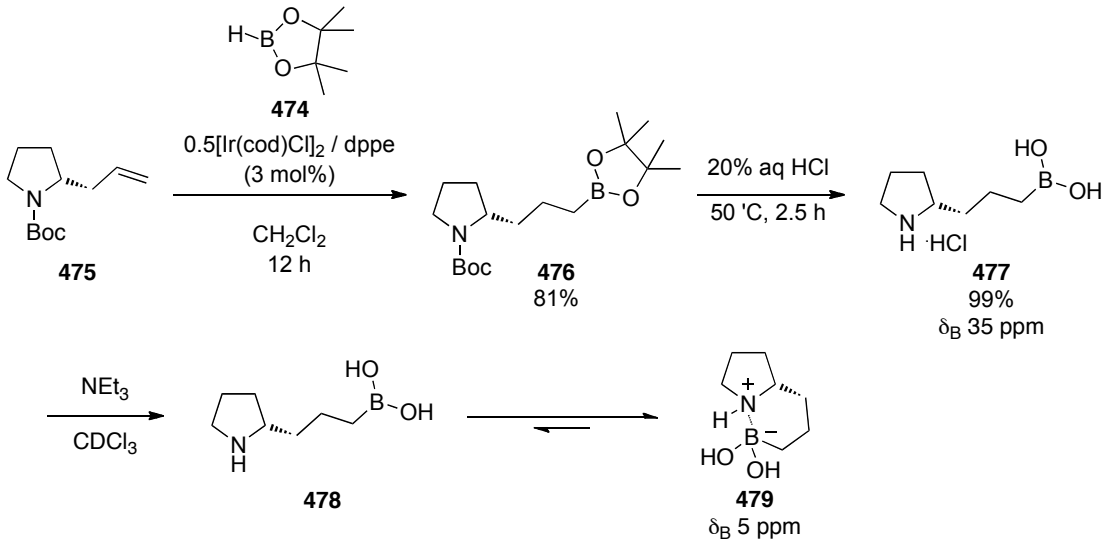

Scheme 72. Synthesis of the neutral aminoboronic acid **478**.

Thus, after stirring **477** (n = 3) in the presence of triethylamine for five minutes, the ^{11}B NMR showed two signals: one at 35 ppm and another at 5 ppm; the 35 ppm signal being free boronic acid **477**, presumably still as the HCl salt. When repeating the ^{11}B NMR after 24 hours, the signal at 35 ppm disappeared, leaving only the signal at 5 ppm due to the neutral aminoboronic acid. The single upfield signal was indicative of complete nitrogen-boron chelation, resulting in six-membered ring formation (**479**). It was thought the same chelation might occur when the tether distance between the nitrogen and the boron was shortened by one carbon atom (n = 2) as then a stable five-membered chelate ring would be formed, *i.e.* **481**. Thus, it was thought that the more active aminoboronic acid catalyst would be the one where the tether distance between the boron and the nitrogen was reduced by a further carbon atom (n = 1) since in this case, the chelation between the boron and the nitrogen would be unfavourable due to a strained four-membered ring needing to be formed (**483**) (Figure 15).

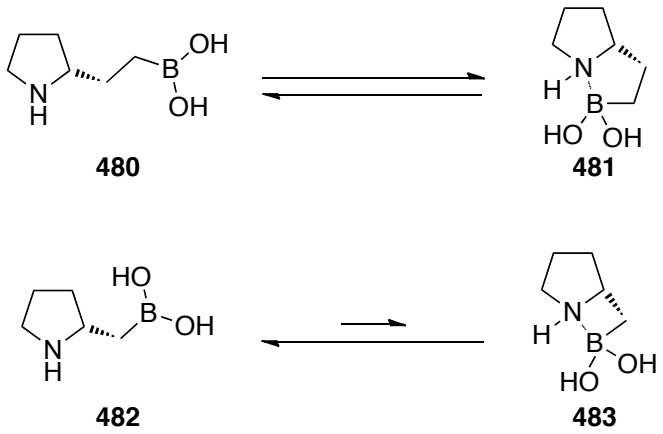

Figure 15. Aminoboronic acid chelation.

3.8.3 Homoboroproline Synthesis (n = 1)

The homoboroproline (n = 1 system) was synthesised according to procedures developed by Whiting *et al.*[202] in order to compare this catalyst with the n = 3 system **477** and see how the chain length affects the reactivity of the reaction. The *S*-enantiomer **488** was synthesised from *N*-Boc pyrrolidine **455** and electrophile **486** through a sparteine-mediated lithiation reaction. Subsequent deprotection of **487** afforded the desired aminoboronic acid salt **488** (Scheme 73).

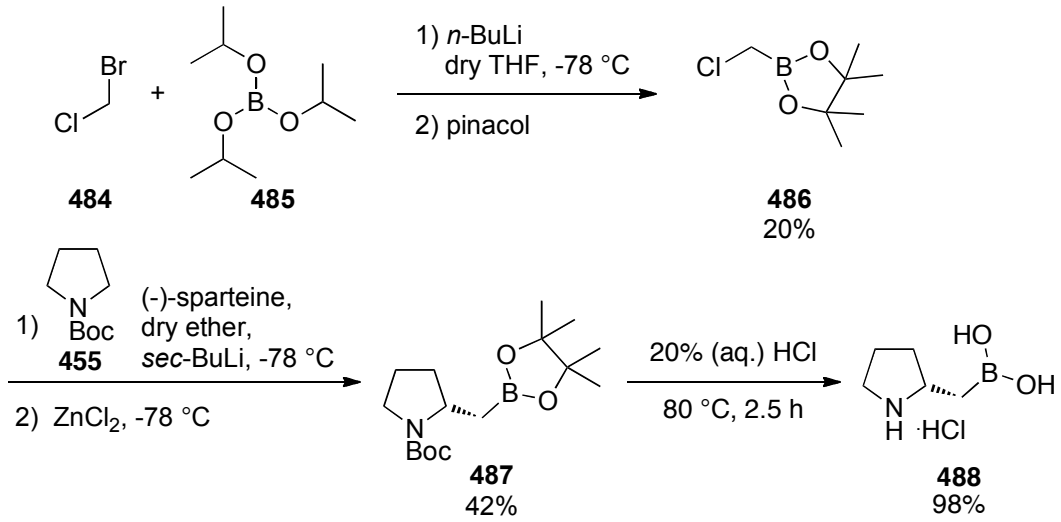

Scheme 73. Synthesis of the *S*-enantiomer **488**.

The *R*-enantiomer **493** was synthesised from L-proline **152**,[202] whereby after *N*-Boc protection to **489**, the carboxylic acid was reduced to the alcohol **490**, this

being iodinated to **491** in order to borylate the compound to **492**. Hence, the free aminoboronic acid **493** was obtained in its HCl salt after deprotection of **492** (Scheme 74).

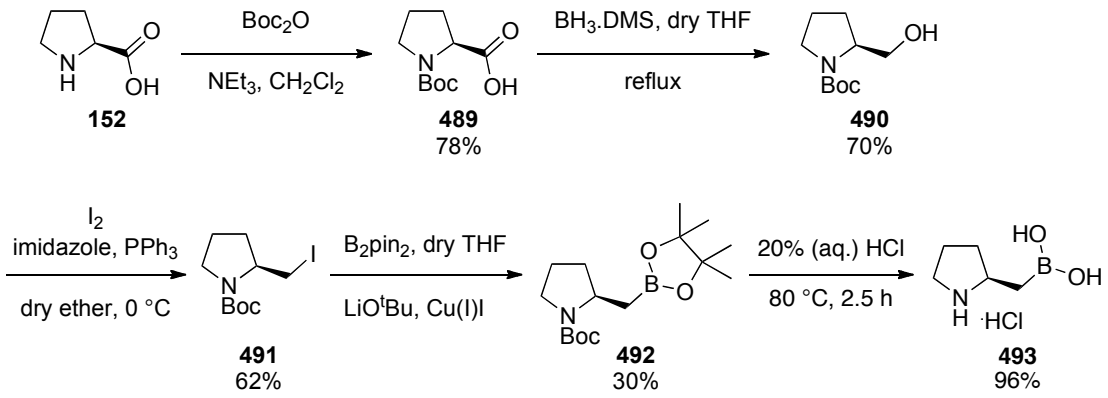

Scheme 74. Synthesis of the *R*-enantiomer **493**.

In summary, the aminoboronic acid catalyst **477** (n = 3) and the homoboroproline **488** and **493** (n = 1) were synthesised in order to determine how the chain length of the aminoboronic acid affects the reactivity of the aza-Diels-Alder reaction. For a complete comparison, the n = 2 system **10** was obtained from Irene Georgiou. The n = 3 system was asymmetrically synthesised in an asymmetric manner using a (-)-sparteine-mediated lithiation procedure, followed by hydroboration using iridium catalysis; the n = 1 system was synthesised following literature procedures.[202]

3.9 Examination of the Catalytic Potential of Bifunctional Catalysts

Having synthesised the n = 3 and n = 1 aminoboronic acid systems (see previous section), the next aim was to test their catalytic activities in different reactions, and in particular, the aza-Diels-Alder reaction in order to use the best catalyst for the synthesis of biologically important piperidine systems.

3.9.1 Catalysis of the aza-Diels-Alder reaction

The synthesis of **356** was attempted using the aminoboronic acid salt **488** in order to compare and test the aminoboronic acid in a formal aza-Diels-Alder reaction (Equation 42). However, after a week of stirring at room temperature, only starting materials **348** and **324** were observed in the reaction mixture, suggesting that a more Lewis acidic catalyst may be needed.

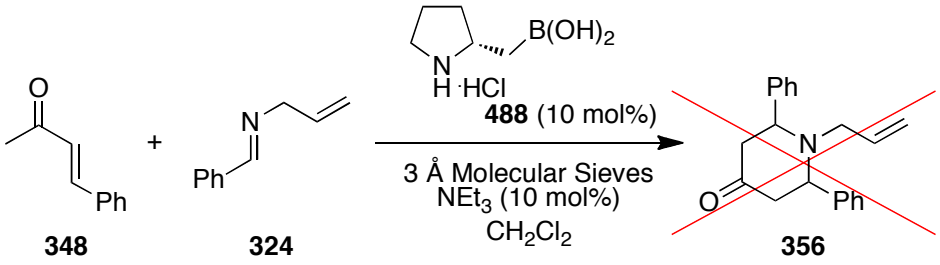

Equation 42

Formation of the dihydropyridone **244** was also attempted using organocatalysis. In particular, catalysts **473** and **494** were compared, and the crude reaction mixtures analysed by TLC and LCMS. However, neither reaction showed any dihydropyridone **244** formation. Instead, small amounts of the [2+2+2]-derived dihydropyridine **369** adduct were detected by TLC and LCMS analysis (Table 32).

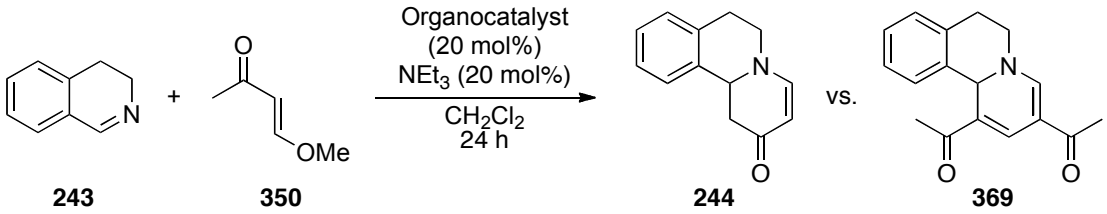

Table 32. Reaction attempts between imine **243** and methoxy enone **350** using different organocatalysts.

Entry	Organocatalyst	LCMS analysis of crude	TLC analysis of crude
1	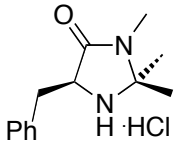 **494**	Imine **243** and dihydropyridine **369** were clearly present	**369** was clearly present
2	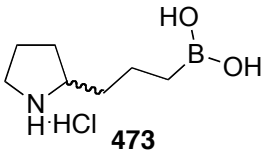 **473**	Imine **243** was clearly present	**369** was present, although not to the same extent as in entry 1

It was also found that the aminoboronic acid **473** was not sufficiently active to catalyse the Michael-Mannich formal [4+2]-cycloaddition between imine **243** and methyl vinyl ketone **164** (Equation 43). This was probably due to no imminium ion formation to encourage Michael addition, or enamine formation to assist in the Mannich process.

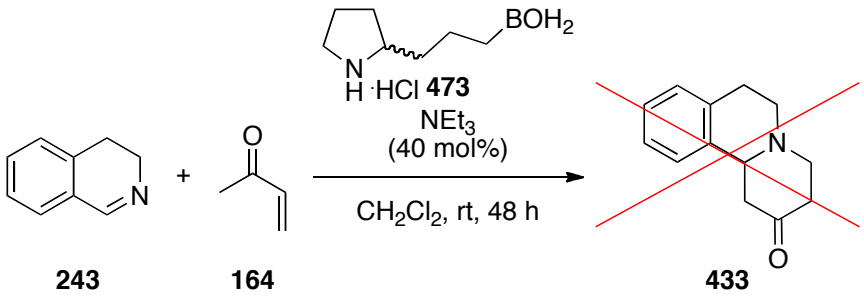

Equation 43

Examination of the literature[116] revealed that organocatalytic aza-Diels-Alder reactions generally tend to work best when using electron-deficient imines; examples include *N*-sulfonamido imines such as **495**. Hence, it was decided to attempt the aza-Diels-Alder reaction between imine **495**, using the aminoboronic acid **473**. To begin with, a standard was prepared using Danishefsky's diene **4** (Table 33). However,

when this reaction was attempted using Lewis acid catalysis, the dihydropyridone **496** was not observed (Table 33, entry 1). Instead, when this reaction was heated without a Lewis acid, the dihydropyridone **496** was successfully formed and isolated after purification by silica gel chromatography (Table 33, entry 2). Interestingly, product **496** was not observed by LCMS analysis when the reaction was heated in the presence of a Lewis acid (Table 33, entry 3).

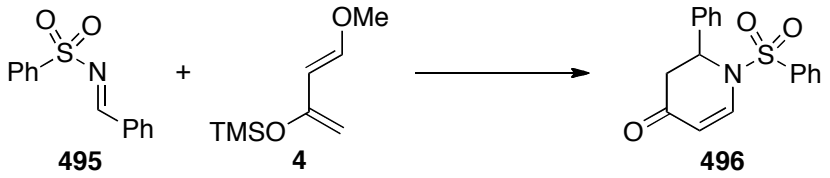

Table 33. aza-Diels-Alder reaction for the formation of dihydropyridone **469**.

Entry	Conditions	Yield (%)
1	$Yb(Otf)_3$ (20 mol%), rt, $CHCl_3$	0
2	100 °C, toluene	62
3	$Sc(Otf)_3$ (10 mol%), 100 °C, toluene	0

Having obtained the racemic standard **496**, an organocatalytic aza-Diels-Alder reaction was subsequently tested between imine **495** and the enone **350** (the enone equivalent of diene **4**). The organocatalysts tested were the aminoboronic acid **473** and the imidazoline-based catalyst **494**.[203] The reactions were monitored by LCMS and TLC. The neutral organocatalysts were formed *in situ* by neutralising their HCl salts with an equimolar amount of triethylamine. However, the dihydropyridone **496** was not observed on any of these attempts (Table 34).

Table 34. Organocatalytic attempts for the synthesis of dihydropyridone **496**.

Entry	Organocatalyst (20 mol%)	Conditions	Yield (%)
1	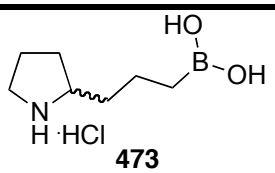 **473**	Toluene, rt	0
2	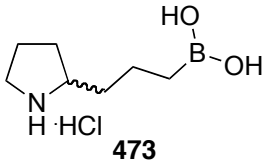 **473**	CH_2Cl_2, reflux	0
3	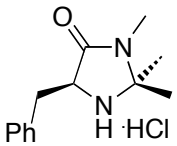 **494**	Toluene, rt	0

Since the desired product was not observed in the above reactions (Table 34) when using 4-methoxy-3-buten-2-one **350** as the enone, the reaction was investigated using different enones to determine if this had an impact on the reaction. Hence, the substrates shown in Table 35 were examined, and again monitored by LCMS. However, in all cases, LCMS showed only starting materials and even when the reactions were at reflux, LCMS analysis did not show any product formation. TLC analysis showed complex mixtures, with no clear single products being formed.

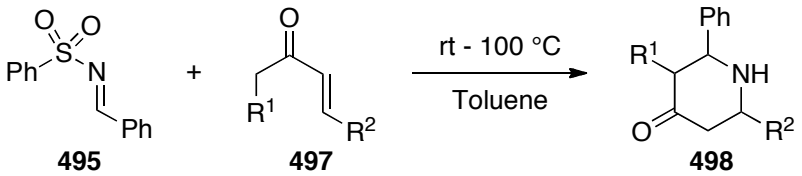

495 **497** **498**

Table 35. aza-Diels-Alder attempts between enones and *N*-sulfonamido imine **10**.

Entry	Enone	Catalyst (20 mol%)	Desired Product	Observed by LCMS
1	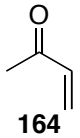 **164**	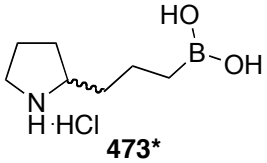 **473***	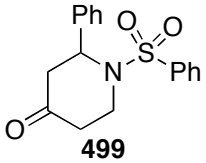 **499**	No
2	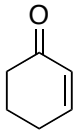 **54**	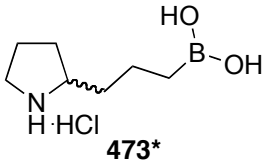 **473***	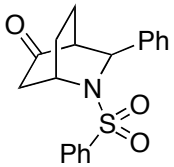 **500**	No
3	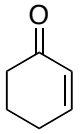 **54**	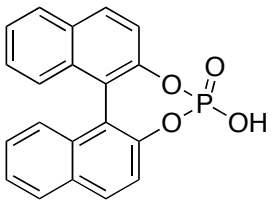 **138** (5 mol%)	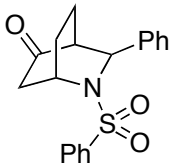 **500**	No
4	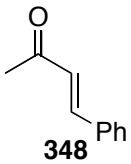 **348**	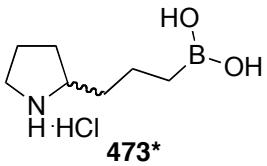 **473***	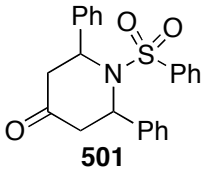 **501**	No

*Equimolar amounts of NEt_3 were added to neutralise the catalyst.

These reactions suggest that the aminoboronic acid **473** may not be sufficiently Lewis acidic (in its present form) to catalyse the aza-Diels-Alder reaction or more likely that boron-nitrogen chelation prevents reactivity. Hence, it was decided to probe the reactivity of these different aminoboronic acids in reactions that have already been shown to be catalysed by aminoboronic acids, such as the aldol reaction.[161]

3.9.2 Catalytic Studies on the Aldol Reaction

Discovered in 1838,[204] the aldol reaction[205] is perhaps one of the oldest named reactions in organic synthesis, and has been extensively researched. The reaction combines two carbonyl compounds (originally aldehydes) to form a new β-hydroxy

carbonyl compound. The term *aldol* was derived from the *ald*ehyde and alcoh*ol* functional groups that were observed in many of the products.

Considering that the aldol reaction has been extensively studied, it was deemed sensible to test the reactivity of to aminoboronic acid **473** within this reaction, and at the same time compare it against other proline-based catalysts,[206] *i.e.* L-proline **152** and the imidazoline based catalyst **494** (Figure 16).[207] Aminoboronic acids **493** and **508** with varying chain lengths were also used to compare their reactivity with that of **473**. (Table 36).

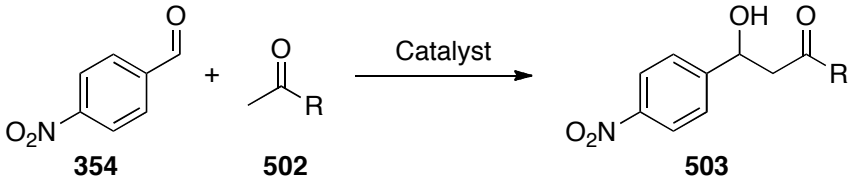

354 **502** **503**

Table 36. Organocatalytic aldol reactions, using 1 mmol of reagents.

Entry	Ketone	R group	Catalyst (20 mol%)	Solvent (1 mL)	Time (h)	Aldol product (%)	Double aldol product (%)	Other isolated product (%)
1	**314**	Me	**473***	Acetone	72	**505 (**27) (0% ee)	**506 (**69)	**507** (4)
2	**314**	Me	**493***	Acetone	1.5†	**505** (36) (21% ee)		**355** (8)
3	**314**	Me	**493***	Acetone	72	**505** (63) (18% ee)	**506 (**6)	**355** (22)
4	**314**	Me	**508***	Acetone	3	**505** (83) (30% ee)		**355** (17)
5	**314**	Me	**508***	Acetone	72	**505 (**61) (23% ee)		**355** (39)
6	**314**	Me	**152**	Acetone	48	**505 (**77)		
7	**314**	Me	**494***	Acetone	72	-		
8	**314**	Me	**152**	DMSO	48	**505 (**74)		
9	**509**	*p*-ClPh	**473***	DMSO	216	**510** (<5)	**511 (**5)	
10	**509**	*p*-ClPh	**152**	DMSO	120	**510** (<1)		
11	**509**	*p*-ClPh	**152**	Acetone	120	Aldol product **505** from acetone only		

†Not all of the catalyst was in solution.
* Equimolar amounts of NEt_3 were added to neutralise the catalyst.

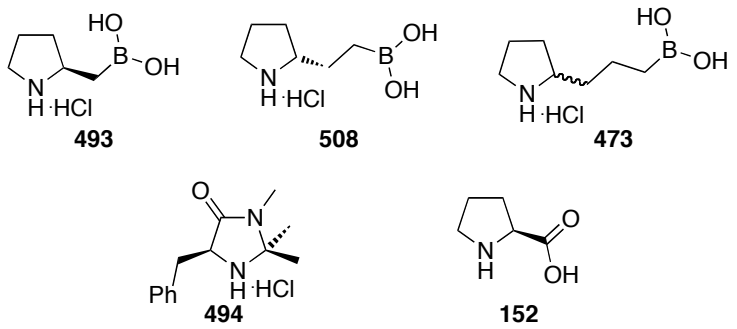

Figure 16. Organocatalysts used within the aldol reaction in Table 36.

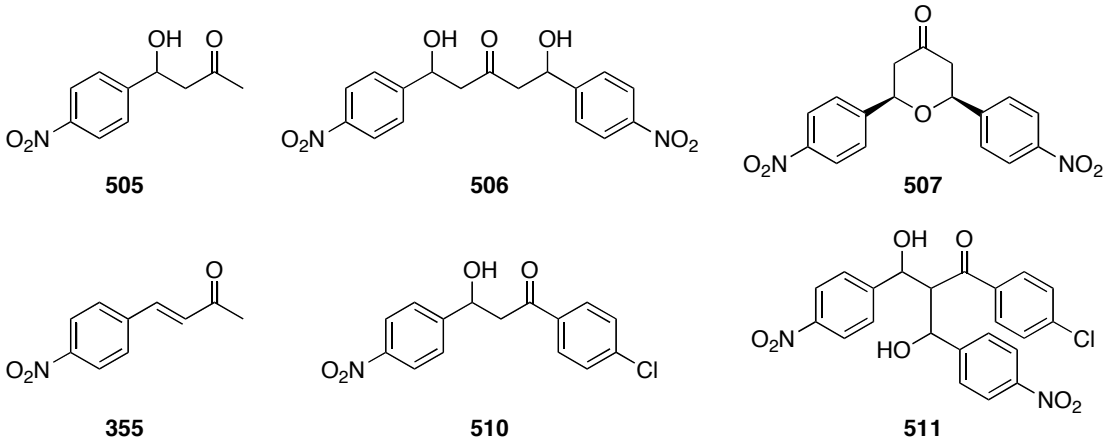

Figure 17. Isolated compounds from Table 36.

The aldol reaction between *para*-nitrobenzaldehyde **354** and acetone **314** (R = Me) was initially carried out (Table 36, entries 1-8) and it was found that having some Lewis acidic character in the organocatalyst was important. Without it (*i.e.* catalyst **494**) the reaction did not proceed (Table 36, entry 7). As expected,[206] L-proline **152** gave good yields of the aldol product, with similar results obtained when using acetone or DMSO as the solvent (Table 36, entries 6 and 8).

It had previously been found by Irene Georgiou (PhD student, Whiting group) that the optimum conditions to perform the aldol reaction using aminoboronic acids as the catalyst was with the n =1 system **493** in DMF at 0.2 M, where high yields and enantiomeric excess of the aldol product **505** were obtained over six hours (88%, 95% ee).[194] Nonetheless, under these diluted reaction conditions, the n = 3 system **473** showed no reactivity after 24 hours. However, having a concentrated reaction (2 M vs. 0.2 M) gave interesting results when using the aminoboronic acids (Table 36).

With catalyst **473** (n = 3), the reaction went to completion after 72 hours and interestingly, the major product obtained was the racemic double aldol product **506** (Table 36, entry 1). The formation of the double aldol product was confirmed by obtaining its X-ray crystal structure (Figure 18).

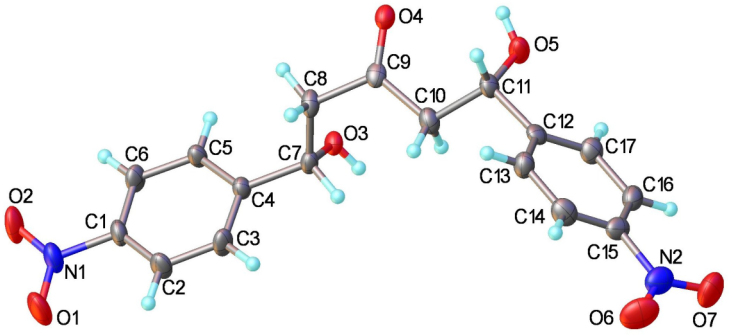

Figure 18. X-ray molecular structure of compound **506**.

When using the catalyst **493** (n = 1) or **508** (n = 2), however, the aldol reaction was completed within a few hours, with the major product obtained as the single aldol product **505** (Table 36, entries 2 and 4 respectively). The catalysts **493** and **508** were also reacted for 72 hours to see if the double aldol product could be formed to a greater extent if the reaction was left for longer. However, on both occasions the major product was still the aldol product **505**, followed by the condensation product **355** (Table 36, entries 3 and 5). No double aldol product **506** was observed with catalyst **508** (n = 2) (Table 36, entry 5). Interestingly, small amounts of the double aldol product **506** were observed with catalyst **493** (n = 1) when the reaction was left to react for 72 hours (Table 36, entry 3). Additionally, when catalyst **473** (n = 3) was used, small amounts of the tetrahydropyran **507** were isolated as a single diastereoisomer, which presumably arose from the elimination of the double aldol product **48** followed by cyclisation (Scheme 75).

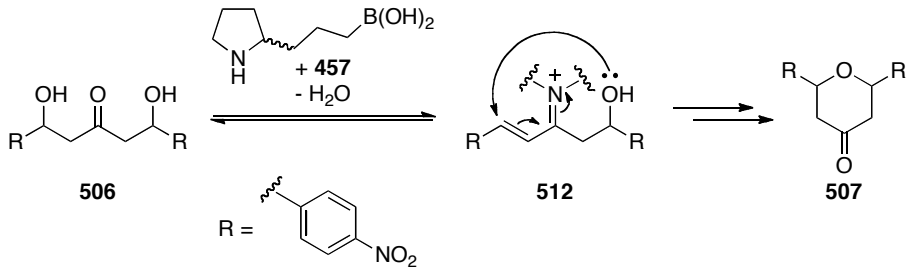

Scheme 75. Formation of the tetrahydropyran **507** from the double aldol product **506**.

In order to see if the aminoboronic acid **473** (n = 3) would preferentially form the aldol product **510** when the ketone could only enolise in one direction, the aldol reaction was performed between *p*-nitrobenzaldehyde **354** and *p*-chloroacetophenone **509** (R = *p*-ClPh) following procedures laid out by Wang *et al*.[208] (Table 36, entries 9-11) (Equation 44). The aminoboronic acid **473** (n = 3) was shown to be the more active catalyst compared with L-proline **152** since some of the aldol product **510** was isolated (< 5%). Interestingly, ^{1}H NMR and MS analysis suggested that some of the double aldol product **511** was formed in a slightly higher amount (5%). However, not enough product **511** was isolated to allow confirmation of the structure by ^{13}C NMR (Table 36, entry 9).

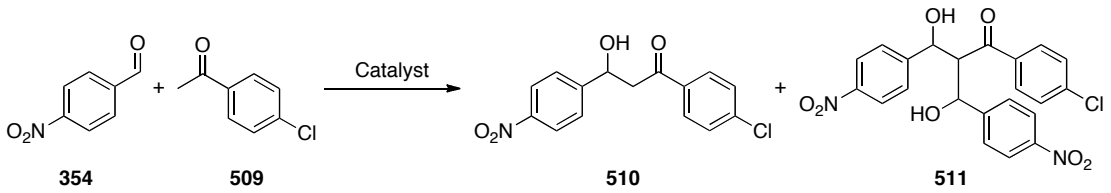

Equation 44

When using L-proline **152**, the aldol reaction (Equation 44) was slow, with minimal amounts of the aldol product **510** being obtained (Table 36, entry 10). Unsurprisingly, when using acetone as the solvent instead of DMSO, only the aldol product **505** between *p*-nitrobenzaldehyde **354** and the more reactive ketone (acetone) was observed; *p*-chloroacetophenone **509** (R = *p*-ClPh) remained unreacted (Table 36, entry 11). This aldol reaction was significantly less reactive than when using acetone as the ketone, probably due to the aromatic ring stabilising the initial iminium ion that would be formed between the ketone and the catalyst (**513** and **514**), thus preventing the enamine formation **515** with the methyl group (Scheme 76).

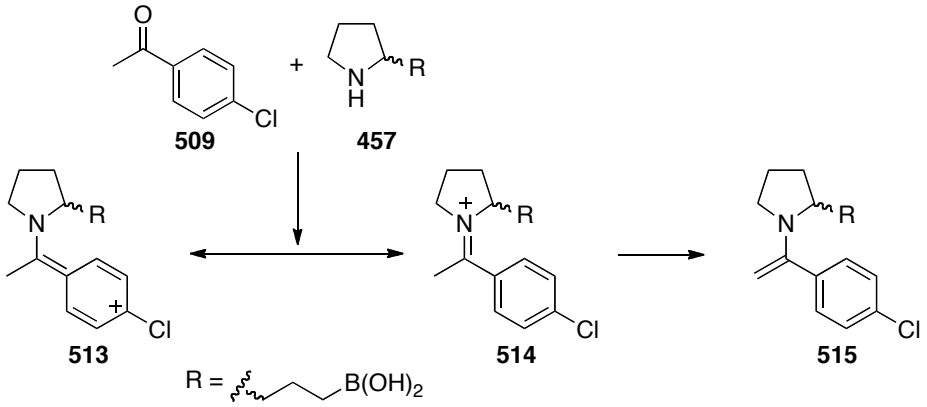

Scheme 76. Resonance stabilisation of the imminium species **514**.

Overall, these results (Table 36) suggest that the aminoboronic catalyst **473** (n = 3) is oddly only active when used under highly concentrated reaction conditions (2 M), whilst still being slower than catalysts **493** (n = 1) and **508** (n = 2). When applied to the aldol reaction, this catalyst **473** (n = 3) is the only one to favour formation of the double aldol products **506** and **511** over the single aldol products **505** and **510** respectively. Higher conversions were obtained when using the more reactive ketone acetone **314** over *p*-chloroacetophenone **509**. In addition, the fact that no reactivity was observed when using the imidazoline catalyst **14** confirms the probable need to have a Lewis acidic section on the organocatalyst for the aldol reaction to proceed smoothly.

3.9.3 Examination of the Mannich Reaction

Considering a main aim of this work was to develop an aminoboronic acid to act as an organocatalyst in the aza-Diels-Alder reaction, and that the formal aza-Diels-Alder reaction is generally accepted to go through a Mannich-Michael pathway, the Mannich reaction was explored using the aminoboronic acids. If these catalysts could not catalyse a Mannich reaction, it meant that they would not be able to catalyse the aza-Diels-Alder reaction either. Such a study would aid in determining which of the reaction steps, *i.e.* the Mannich or Michael reaction, was the most problematic step for aminoboronic acids to catalyse. Fully understanding the Mannich *versus* Michael reactions would also assist in understanding what necessary properties the

organocatalyst needed to enable the Mannich-Michael reaction to occur and hence, this could be applied to the efficient formation of piperidine systems.

A Mannich reaction was reported by Bella *et al*. in which cyclic imine **333** was reacted with acetone **314** in the presence of L-proline **152** to form the Mannich product **516** in reasonable yield and ee (Equation 45).[167]

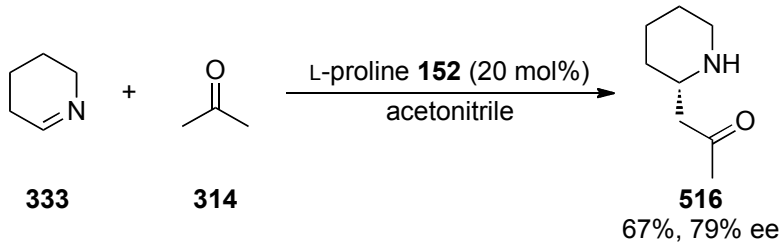

333 **314** **516**
67%, 79% ee

Equation 45

In order to test the scope of this procedure, the Mannich reaction between cyclic imine **243** and acetone **314** in the presence of L-proline **152** was performed in an attempt to form the Mannich product **517** (Equation 46). However, the Mannich product **517** was not formed under these conditions.

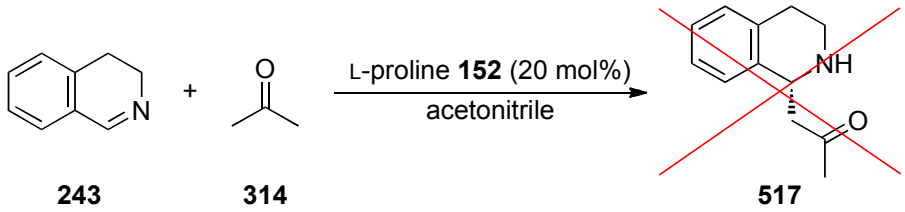

243 **314** **517**

Equation 46

Hence, it was decided to investigate a more developed Mannich reaction between hydroxyacetone **518**, *p*-anisidine **120** and *p*-nitrobenzaldehyde **354**, in the presence of L-proline **152**, following a procedure reported by List *et al*.[209] The Mannich product **519** was obtained in 83% yield (Equation 47) and according to List *et al*., **519** was obtained with 20:1 dr and 99% ee.[209] However, under these dilute reaction conditions (0.2 M), no reaction occurred when the aminoboronic acid **473** (n = 3) was used as catalyst.

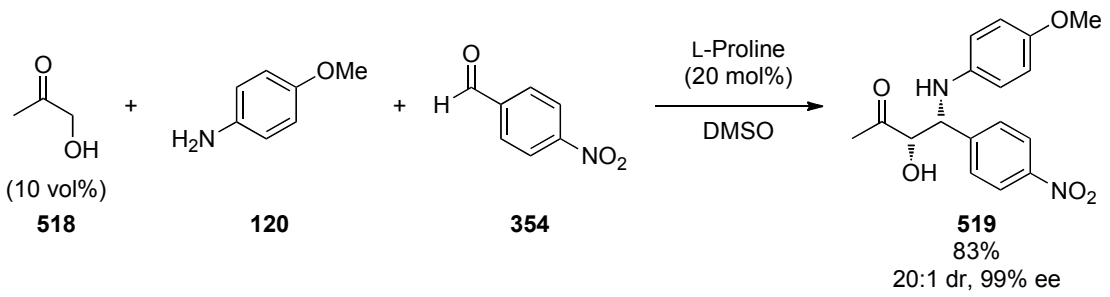

Equation 47

Nonetheless, aminoboronic acid **473** (n = 3) was tested to see if it worked on a Mannich reaction between *p*-nitrobenzaldehyde **354**, acetone **314** and *p*-anisidine **120** (Equation 48). Monitoring this reaction by TLC revealed that after 24 hours, all of the *p*-nitrobenzaldehyde **354** had been consumed, with the *p*-anisidine **120** being unreacted. After 72 h, TLC analysis showed that most of the *p*-anisidine **120** was still unreacted. Despite this, the reaction mixture was purified by silica gel chromatography and it was revealed that the major component was the imine **326** (29%). The aldol reaction between *p*-nitrobenzaldehyde **354** and acetone **314** had also taken place, although small amounts of these products (**355**, **505** and **506**) were obtained. The Mannich adduct **520** was a minor product, being isolated in low yield (6%).

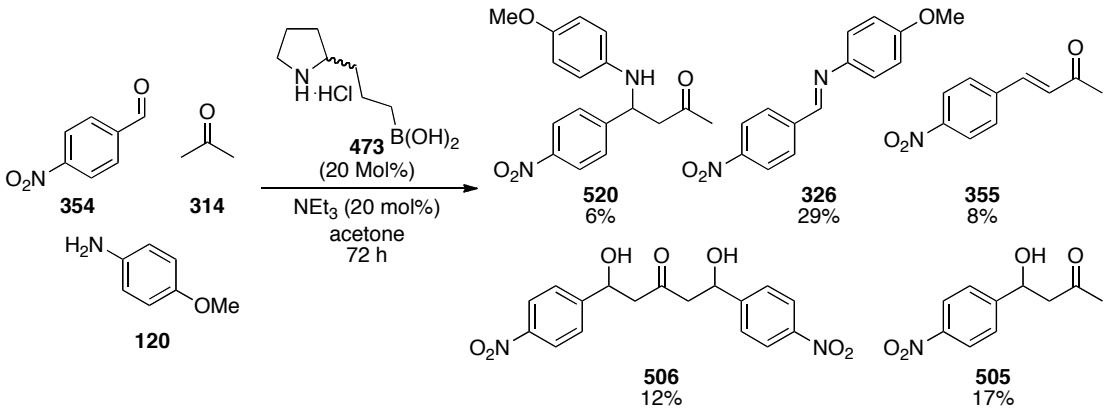

Equation 48

Turning our attention to more electron-deficient imines, the Mannich reaction between imine **495** and acetophenone **89** was also attempted. However, no product **521** was detected by LCMS, neither after reacting at room temperature or heating up to 70 °C (Equation 49). Instead, the starting materials were observed amongst other

peaks by LCMS analysis, while TLC analysis showed a mixture of starting materials and products.

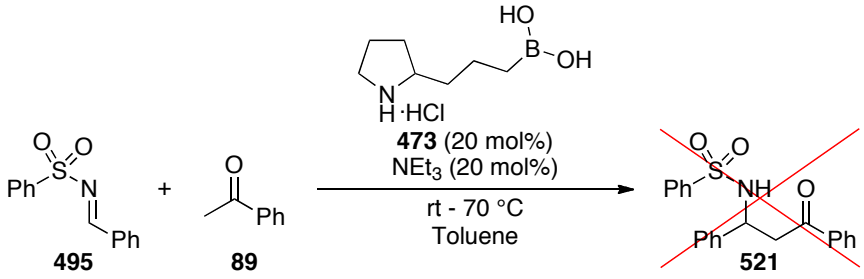

Equation 49

3.9.4 Examination of Michael Reaction Catalysis

The ring-closing process of the aza-Diels-Alder reaction to form piperidine products is generally accepted to go *via* a Michael reaction; a reaction that also needs to be optimised to successfully apply new organocatalysts. Chaudhuri *et al*. have specified that the aza-Michael reaction can be effectively performed in water using boric acid as a catalyst.[210] Taking this as a starting point, this reaction was investigated.

The aza-Michael reaction was successfully performed in water using methyl vinyl ketone **164** and dibenzylamine **522**. In order to see if the boronic acids could also be active catalysts, the same reaction was subsequently attempted using phenylboronic acid as the catalyst, with product **523** isolated in 55% yield (Equation 50) after 12 hours.

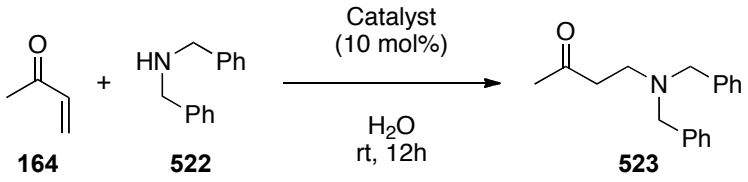

Catalyst	Yield
$B(OH)_3$	48%
$PhB(OH)_2$	55%

Equation 50

When using methyl vinyl ketone **164**, the aminoboronic acid **477** was shown to be effective for this aza-Michael reaction as outlined in Equation 51.

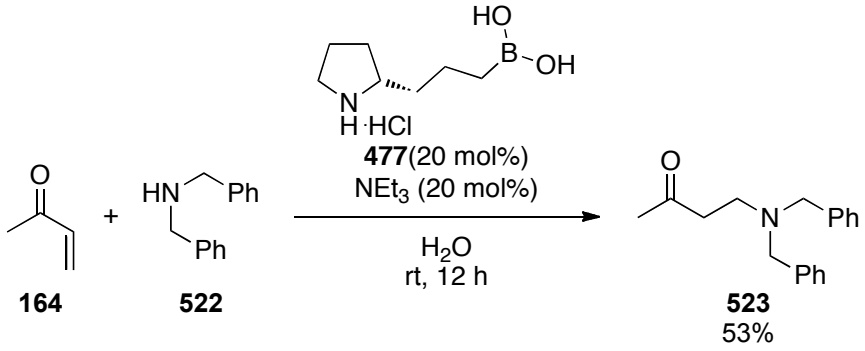

Equation 51

In order to compare the boronic acids **477**, **488**, phenylboronic and boric acid in the Michael reaction between methyl vinyl ketone **164** and dibenzylamine **522**, the reaction was performed in $CDCl_3$ and monitored over time by ^1H NMR analysis. The use of triethylamine on its own was also monitored in order to monitor the catalyst-free background reaction (Table 37). From these studies, it was observed that when using this solvent ($CDCl_3$), complete conversion to the Michael product **523** occurred within half an hour for all the catalysts (Table 37, entries 1-4). Conversely, when monitoring the background reaction using triethylamine as the additive, it took five hours for complete conversion to product **523** to occur thus confirming that the boronic acids are indeed catalysing the reaction.

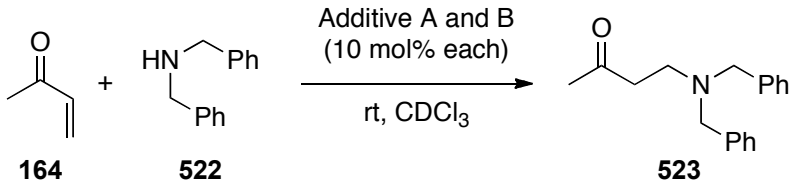

164 **522** **523**

Table 37. Monitoring of the Michael reaction by ^{1}H NMR analysis.

Entry	Additive A (10 mol%)	Additive B (10 mol%)	Time taken for 100% conversion to **523**
1	$B(OH)_3$	-	< 0.5 h
2	$PhB(OH)_2$	-	< 0.5 h
3	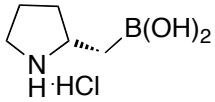 **488**	NEt_3	< 0.5 h
4	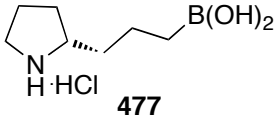 **477**	NEt_3	< 0.5 h
5	NEt_3	-	5 h

These results suggest that aminoboronic acids can catalyse the Michael reaction as effectively as boric and phenylboronic acid and this paves the way for investigating whether chiral aminoboronic acids can cause asymmetric induction within the Michael reaction when using different substituted enones. Hence, this confirms that more research is needed into the Mannich reaction over the Michael reaction when utilising aminoboronic acids as catalysts. The main reason why the Mannich reaction proved to be problematic when using these catalysts could be because the aminoboronic acids in their current form are simply not sufficiently Lewis acidic to catalyse the reaction.

Chapter 4:
CONCLUSIONS AND FUTURE WORK

4. Conclusions and Future Work

It was confirmed that the construction of a robust, efficient and general organocatalytic aza-Diels-Alder process is a real and still ongoing challenge. However, through the screening of different Lewis-acid catalysed aza-Diels-Alder reactions, a few novel cyclisation routes were discovered, dependent on the reagents and reaction conditions used.

When using 4-methoxy-3-buten-2-one, or its (Danishefsky's) diene equivalent, different novel dihydropyridone and dihydropyridine ring systems could be formed when using different imines; each going through a different formal cycloaddition pathway. The acyclic imines were hydrolysed to their amine and aldehyde starting components when reacted with 4-methoxy-3-buten-2-one in the presence of a Lewis acid. It was also found that the stoichiometry and hygroscopic nature of the Lewis acid was important (Scheme 77).

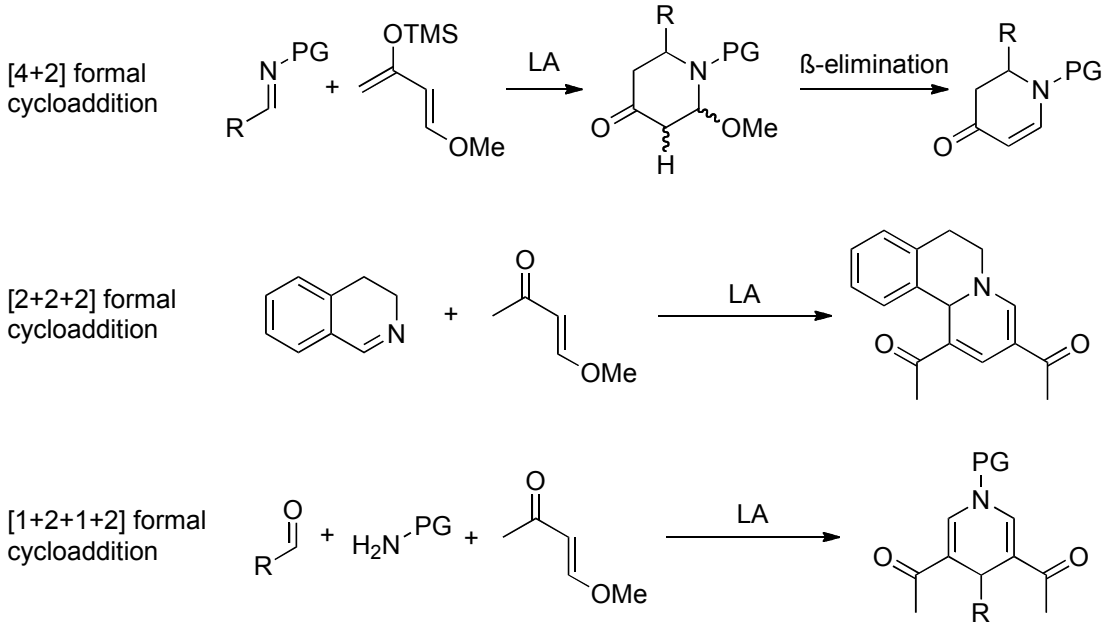

Scheme 77. The different piperidine rings that are obtained when reacting Danishefsky's diene or its enone equivalent with imines.

Further investigation of the formal [4+2]-cycloaddition process provided a greater mechanistic insight into the metal-catalysed aza-Diels-Alder pathway. When using

enones that did not contain a leaving group on the β-position, a formal [4+2]-cycloaddition occurred when the enone was reacted with an imine and a Lewis acid. Dependent on how good a Michael acceptor the enone was dictated whether the mechanism proceeded *via* a Mannich-Michael or a Michael-Mannich pathway (Scheme 78).

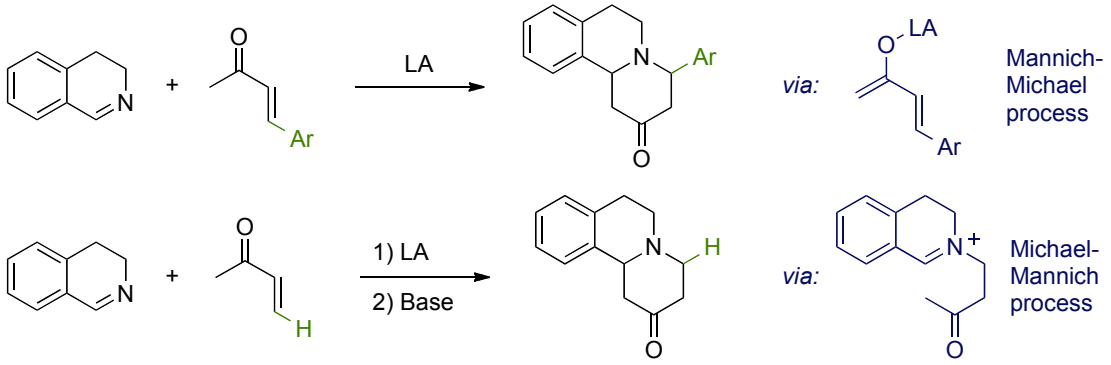

Scheme 78. The different mechanistic pathways within the [4+2]-formal cyclisation when using enones that do not contain a leaving group on the β-position.

Future work with these metal-catalysed cyclisations includes testing out these reactions using an increased substrate database. In addition, it would be beneficial to find the optimum base for the Michael-Mannich formal [4+2]-cycloaddition between methyl vinyl ketone and imines.

The asymmetric syntheses of the aminoboronic acids were successfully accomplished. However, regarding their reactivity, it was concluded that these aminoboronic acids were not sufficiently Lewis acidic to undergo an aza-Diels-Alder reaction. In particular, the catalyst **473** (n = 3) was inactive due to strong intramolecular N-B chelation. Despite this, under very concentrated conditions the catalyst **473** (n = 3) was shown to be active (although slow) in the aldol reaction in order to give predominantly the double aldol product. However, due to the N-B chelation the homoboroproline **493** (n = 1) was deemed to be the optimum aminoboronic acid in terms of the tether distance between the nitrogen and the boron.

Future work regarding the aminoboronic acids includes the construction of a more Lewis acidic aminoboronic acid catalyst in order to test the Mannich reaction, prior to testing on the aza-Diels-Alder reaction. Examples of more Lewis acidic aminoboronic

acids whose syntheses could be attempted include: 1) having two fluorine atoms on the carbon adjacent to the boron (**524**); or 2) attaching strong electron-withdrawing groups such as pentafluorophenol (PFP) to the boron atom (**525**).

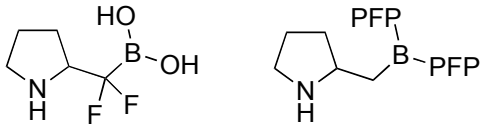

524 **525**

After synthesising the more Lewis acidic aminoboronic acids, their activity can be tested within the aldol, Mannich and Michael reactions, with the ultimate aim of determining whether they can catalyse the aza-Diels-Alder reaction. In addition, the Michael addition reaction can be further investigated regarding the synthesis of chiral products. The kinetics can also be looked at in order to prove the relative reactivities of the different catalysts.

The field of the organocatalytic aza-Diels-Alder reactions has advanced slowly in the past few years. This shows the challenge in constructing a truly robust organocatalytic system for this reaction, one that will no doubt be achieved within the near future. Once developed, these catalysts would be able to be used in an atom-economical aza-Diels-Alder reaction in order to synthesise different biologically active piperidine ring-containing compounds.

Chapter 5:
EXPERIMENTAL

5. Experimental

5.1 General Experimentation

All starting materials, including solvents, were used as received without further purification, unless otherwise stated. All reactions were performed under air unless otherwise specified. Reactions were monitored by TLC analysis carried out on Polygram SIL G/UV_{254} plastic backed silica gel plates, and were visualised under a UV lamp operating at short (254 nm) and long (365 nm) wavelength ranges. Visualisation was aided by staining with I_2 or by dipping plates into an alkaline potassium permanganate or anisaldehyde solution. Flash silica gel column chromatography was carried out on Davisil Silica Gel, 60-200 mesh. 3 Å Molecular sieves were activated by heating to 150 ºC**.** Concentration of the reaction mixture *in vacuo* is the removal of solvent under reduced pressure. ^{1}H NMR spectra were recorded on either Brüker Avance-400, Varian-Mercury 500 or Varian VNMRS 700 MHz spectrometers, operating at ambient probe temperature, unless otherwise stated. Peaks are reported as singlet (s), doublet (d), triplet (t), quartet (q), broad (br), some combinations of these, or multiplet (m), and coupling constants (*J*) in hertz (Hz). ^{13}C NMR spectra were recorded on Varian Brüker Avance-400, Varian Mercury-500 or Varian VNMRS 700 instruments at frequencies of 101, 126 or 176 MHz respectively, unless otherwise stated. The chemical shifts are reported in ppm relative to residual signals of the solvent,[211] and couplings are as follows: s = 0 protons; d = odd number of protons; t = even number of protons, attached to the carbon atom, as determined by ^{13}C DEPT NMR. ^{11}B NMR spectra were recorded on a Brüker Avance-400 instrument at a frequency of 128 MHZ and the chemical shifts are reported in ppm. Deuterated chloroform $CDCl_3$, DMSO and D_2O were used as deuterated solvents for all NMR experiments. Mass spectra for liquid chromatography mass spectrometry (LCMS) were obtained using a Waters LCT spectrometer, and accurate mass spectrometry obtained on a Finnigan LTQ-FT using the electrospray in positive ion mode (ES+) to generate ions, unless otherwise stated. IR spectra were recorded on a Perkin-Elmer Paragon 1000 FT-IR spectrometer. Chiral HPLC analyses

were performed on a Perkin Elmer system equipped with a Perkin Elmer Series 200 pump, a Perkin Elmer Series 200 autosampler and a Perkin Elmer Series 200 Diode array detector. Elemental analysis was performed using an Exeter Analytical E-440 Elemental Analyser. Optical rotations were taken using a JASCO P-1020 polarimeter and $[\alpha]_D$ values are given in deg cm^2g^{-1}. Melting points were measured, where appropriate, with a Gallenkamp Variable Heater melting point apparatus and are uncorrected.

5.2 General Procedures

Procedure for the attempted synthesis of 334 (Scheme 56)

To phenylhydrazine (2 mL, 20 mmol) in hexane (6 mL) under nitrogen at 0 °C was added isobutyraldehyde (1.9 mL, 21 mmol) dropwise. The reaction mixture was stirred at rt for 1 h prior to the slow addition of methanesulfonic acid (9.6 mL, 148 mmol) at 0 °C. The reaction mixture was subsequently stirred at rt overnight, neutralised ($NaHCO_3$) and monitored by LCMS and ^1H NMR. Purification by silica gel chromatography was attempted, however, the compound seemed to be unstable in silica.

Procedure for the one-pot, three-component screening reactions (Table 4)

To a mixture of amine (1 mmol), aldehyde (1 mmol) and enone (4 mmol) in solvent (2 mL) was added the organocatalyst (0.2 mmol) and the reaction mixtures were stirred at rt. The reaction mixtures were monitored after 24 h and 48 h *via* TLC analysis (1:1 to 4:1, EtOAc/hexane, as eluent).

Procedure for the one-pot, three-component screening reactions where the imine was formed *in situ* (Table 5)

A mixture of aldehyde (1 mmol) and amine (1 mmol) in solvent (2 mL) and 3 Å molecular sieves (1 g) was stirred at rt for 12 h prior to the addition of enone (4 mmol and organocatalyst (0.2 mmol). The reaction mixtures were stirred at rt and monitored after 24 h and 48 h *via* TLC analysis (1:1 to 4:1, EtOAc/hexane, as eluent).

Procedure for the imine screening reactions (Table 6)

To a mixture of imine (1 mmol), enone (4 mmol) and 3 Å molecular sieves (1 g) in solvent (3 mL) was added the organocatalyst (0.2 mmol) and the reaction mixtures were stirred at rt. The reaction mixtures were monitored after 24 h and 48 h *via* TLC analysis (1:1 to 2:1, EtOAc/hexane, as eluent).

Procedure for the organocatalysed aza-Diels-Alder reaction (Table 7)

To imine (3.5 mmol) and organocatalyst (20 mol%) in solvent (40 mL) was added enone (14 mmol) and the reaction mixture was stirred at rt. If purified, the mixture was concentrated *in vacuo* and purified by silica gel chromatography (hexane:EtOAc, as eluent).

Procedure for the Lewis acid catalysed aza-Diels-Alder reaction (Table 8)

To imine (1 mmol) and Lewis acid (20 mol%) in solvent (2 mL) was added diene (1.2 mmol) and the reaction mixture was stirred at rt. If purified, the mixture was concentrated *in vacuo* and purified by silica gel chromatography (hexane:EtOAc, as eluent).

Procedure for the formation of $ZnCl_2$•Et_2O

$ZnCl_2$ (0.506 g, 5 mmol) was dissolved in diethyl ether (2.5 mL) whilst stirring at rt for 15 min to form a 1 M solution of $ZnCl_2$•Et_2O.

Procedure for the $ZnCl_2$•Et_2O catalysed aza-Diels-Alder reaction (Table 8)

To $ZnCl_2$•Et_2O (2 M in diethyl ether; 2.5 mL, 5 mmol) and diene **349** (0.218 g, 1 mmol) in solvent (3 mL) was added imine **324** (0.145 g, 1 mmol) and the reaction mixtures were allowed to stir at rt for 48 h.

For an acid-base workup: The reaction mixture was washed with 5% (aq) HCl (2 × 5 mL). Saturated (aq) $NaHCO_3$ (20 mL) was added to the combined aqueous layers and the organics extracted using CH_2Cl_2 (2 × 20 mL), dried ($MgSO_4$) and concentrated *in vacuo*.

For an acid workup: The reaction mixture was quenched with 5% (aq) HCl (5 mL), the organic layer separated and the aqueous layer washed with CH_2Cl_2 (2 × 5 mL). The combined organic layers were dried ($MgSO_4$) and concentrated *in vacuo*.

Procedure for the catalyst screening for the [4+2]-diene cyclisation (Table 10)

To a Lewis acid (20 mol%), 2-ethyl-2-oxazoline (0.016 mL, 0.16 mmol) and 3 Å molecular sieves (1 g) in dry CH_2Cl_2 (0.5 mL) was added imine **243** (0.05 g, 0.4 mmol) and Danishefsky's diene (0.08 mL, 0.4 mmol). The reaction mixtures were flushed with nitrogen, stirred at rt and analysed *via* TLC (EtOAC, as eluent).

Procedure for the phosphine ligand screening for the [4+2]-diene cyclisation (Table 11)

To a phosphine ligand (40 mol%), Lewis acid (20 mol%), and 3 Å molecular sieves (1 g) in dry CH_2Cl_2 (0.5 mL) was added imine **243** (0.05 g, 0.4 mmol) and Danishefsky's diene (0.08 mL, 0.4 mmol). The reaction mixtures were flushed with nitrogen, stirred at rt and analysed *via* TLC (EtOAC, as eluent).

Procedure for the scaled up [4+2]-diene cyclisation (Table 12)

To a Lewis acid (20 mol%), 2-ethyl-2-oxazoline (0.016 mL, 0.16 mmol) and 3 Å molecular sieves (1 g) in dry CH_2Cl_2 (0.5 mL) was added imine **243** (0.05 g, 0.4 mmol) and Danishefsky's diene (0.08 mL, 0.4 mmol). The reaction mixtures were flushed with nitrogen and stirred at rt for 48 h. The reaction mixtures were quenched with 5% (aq) HCl (5 mL), diluted with CH_2Cl_2 (10 mL) and brine (10 mL) and filtered. The mixture was extracted from the filtrate with CH_2Cl_2 (3 × 5 mL) and the combined organics were dried ($MgSO_4$), concentrated *in vacuo* and purified by silica gel chromatography (4:1, EtOAc:hexane, as eluent).

Procedure for the [2+2+2]-screening using trituration to purify (Table 15)

To imine **243** (0.131 g, 1 mmol), 4-methoxy-3-buten-2-one (0.204 mL, 2 mmol) and additive, in solvent (1.5 mL), was added Lewis acid (10 mol%) and the reaction mixture was stirred at rt. After the denoted time, most of the solvent had evaporated, leaving an orange paste. EtOAc was added to the reaction mixture to form a suspension, which was subsequently filtered and the solid washed with EtOAc dropwise.

Procedure for the [2+2+2]-screening using chromatography to purify (Table 16)

To imine **243** (0.131 g, 1 mmol) and 4-methoxy-3-buten-2-one (0.204 mL, 2 mmol) in CH_2Cl_2 (1.5 mL) was added Lewis acid (10 mol%) and the reaction mixture was stirred at rt. After 48 h, the reaction mixtures were purified by silica gel chromatography.

Procedure for the [2+2+2]-cyclisation attempts using different imines (Table 20)

To an imine (1 mmol) and 4-methoxy-3-buten-2-one (0.204 mL, 2 mmol) in CH_2Cl_2 (1.5 mL) was added $Sc(OTf)_3$ (10 mol%). The reaction mixture was stirred at rt and monitored *via* TLC analysis (EtOAc, as eluent).

Procedure for the [1+2+1+2]-cyclisation reaction using imines (Table 21)

To an imine (1 mmol) and 4-methoxy-3-buten-2-one (0.204 mL, 2 mmol) in CH_2Cl_2 (1 mL) was added $Sc(OTf)_3$ (10 mol%). The reaction mixtures were stirred at rt, monitored *via* TLC analysis and purified by silica gel chromatography.

Procedure for the [1+2+1+2]-cyclisation reaction using aldehydes and amines (Table 22)

To an amine (1 mmol), aldehyde (1 mmol) and 4-methoxy-3-buten-2-one (0.204 mL, 2 mmol) in CH_2Cl_2 (1 mL) was added $Sc(OTf)_3$ (10 mol%). The reaction mixtures were stirred at rt, monitored *via* TLC analysis and purified by silica gel chromatography.

Procedure for the biological testing

A549 cells were propagated in DMEM medium (+10% fetal calf serum) in 96 well plates and allowed to grow to 50% confluency at 37 °C in an atmosphere adjusted to 5% CO_2. The medium was removed by aspiration and replaced with DMEM + 2% FCS to mimic conditions used during viral infection. 10 fold serial dilutions of each alkaloid from 100 μM to 1 nM were made and the cells incubated for 96 hours at 33 °C (viral growth conditions). As a control, DMSO was added to cells. Cells were visually monitored using light microscopy for any visible changes in morphology, and viability was analysed using an Almar Blue cytoxicity assay. The IC_{50} was determined empirically and required further refinement to get an absolute.

Procedure for the [1+2+1+2]-mechanism studies (Table 23)

The reagents were reacted in the order shown in the table, using 1 mL of $CDCl_3$ as solvent, where 1 Equiv. corresponds to 1 mmol of reagent, and 2 Equiv. corresponds to 2 mmol of reagent. The reactions were monitored by ^1H NMR analysis over time.

Procedure for the [1+2+1+2]-cyclisation attempts using different enones (Table 24)

To 4-methoxy-3-buten-2-one (0.102 mL, 1 mmol), benzylamine (0.109 mL, 1 mmol) and *p*-nitrobenzaldehyde (0.151 g, 1 mmol) in CH_2Cl_2 (1.5 mL) was added $Sc(OTf)_3$ (10 mol%) and the reaction mixture was stirred at rt. After 24-48 h, an enone (1 mmol) was added to the reaction mixture. The mixture was stirred at rt and monitored *via* TLC and ^1H NMR analysis.

Procedure for the triflic acid reaction (Equation 37)

To imine **243** (0.262 g, 2 mmol) and methyl vinyl ketone (0.162 mL, 2 mmol) in $CDCl_3$ (1.5 mL) was slowly added triflic acid (0.177 mL, 2 mmol) at -70 °C. The reaction mixture was left to warm to rt overnight and monitored by ^1H NMR analysis.

Procedure for the Lewis acid screening in the R = H [4+2]-cyclisation (Table 26)

To a Lewis acid (20 mol%) in CH_2Cl_2 (0.5 mL) was added imine **243** (0.033 g, 0.25 mmol) and methyl vinyl ketone (0.021 mL, 0.25 mmol) and the reaction mixtures were left to stir at rt for 24 h. The LCMS of the crude reaction mixtures were obtained, and the crude ^1H NMR spectra of those deemed to give the most promising results were obtained too.

Procedure for the synthesis of piperidinone 433 (Table 27)

To imine **243** (0.131 g, 1 mmol) and methyl vinyl ketone (0.081 mL, 1 mmol) in solvent (1 mL) was added condition A (Lewis acid). The reaction mixture was stirred at rt overnight prior to addition of condition B (base in excess). The reaction mixture was subsequently stirred at rt overnight, and if quenched with aqueous base (5 mL), the mixture was extracted with CH_2Cl_2 (3 × 10 mL) with the combined organics dried

($MgSO_4$) and concentrated *in vacuo*. The reaction mixtures were purified by silica gel chromatography.

Procedure for the [2+4]-methyl vinyl ketone cyclisation attempts using different imines (Table 30)

To an imine (1 mmol) and methyl vinyl ketone (0.081 mL, 2 mmol) in $CDCl_3$ (1.5 mL) was added $In(OTf)_3$ (40 mol%) and the mixtures were stirred at rt. After 12 h, 20% (aq) NaOH (5 mL) was added to the reaction mixtures and these were monitored *via* TLC and ^1H NMR analysis.

Procedure for reacting 243, 164 and 350 together (Equation 40)

To imine **243** (0.131 g, 1 mmol) and $Yb(OTf)_3$ (0.124 g, 0.2 mmol) in $CHCl_3$ (1.5 mL) under argon was added methyl vinyl ketone **164** (0.081 mL, 1 mmol). After stirring the reaction mixture for 1 h, 4-methoxy-3-buten-2-one **350** (0.102 mL, 1 mmol) was added to the mixture and stirred overnight. Purification by silica gel chromatography (1:1 EtOAc:hexane, to 100%, EtOAc, as eluent) afforded **433** as an beige oil (0.043 mg, 21%). Relative to this value, the crude ^1H NMR showed the presence of **432** (40%) and **350** (>99%).

Procedure for the reaction between 456 and catechol borane (Scheme 67)

456 (0.131 g, 1.5 mmol) and catechol borane (0.176 g, 1.5 mmol) were heated at 100 °C whilst stirring. After 5 h, the reaction mixture was cooled to rt and monitored by ^1H NMR analysis.

Procedure for the hydroboration using IPC borane (Scheme 69)

To (*R*)-alpine-boramine (0.415 g, 1 mmol) in dry THF (2 mL) under nitrogen was added $Et_2O{\bullet}BF_3$ (0.25 mL, 2 mmol) and stirred at rt. Within an hour, a precipitate had formed. **456** (0.211 g, 1 mmol) was added to the reaction mixture at 0 ºC, and the mixture was allowed to warm to rt overnight. Acetaldehyde (0.28 mL, 5 mmol) was added to the reaction mixture at 0 ºC and the reaction mixture was left to stir to rt. The mixture was subsequently concentrated *in vacuo*, treated with 6 N (aq) HCl (5 mL) and stirred at 50 ºC. After 2 h, the mixture was cooled to rt, washed with diethyl ether (2 × 10 mL) and concentrated *in vacuo*. The residue was re-dissolved in water (1 mL),

toluene (5 mL) was added, and the mixture was concentrated *in vacuo*. Azeotroping with toluene was repeated (3 × 5 mL) to afford a brown solid (0.62 g).

Procedure for reaction attempts between imine 243 and 4-methoxy-3-buten-2-one using different organocatalysts (Table 32)

To an organocatalyst HCl salt (20 mol%) and triethylamine (20 mol%) in CH_2Cl_2 (1 mL) was added imine **243** (0.131 g, 1 mmol) and 4-methoxy-3-buten-2-one (0.204 mL, 2 mmol). The reaction mixture was stirred at rt for 2 h and monitored by LCMS ands TLC analysis.

Procedure for the unsuccessful Lewis acid catalysed attempt of ring 496 (Table 33, entry 1)

To *N*-benzylidenebenzenesulfonamide (0.491 g, 2 mmol), $Yb(OTf)_3$ (0.248 g, 0.4 mmol) and 4 Å molecular sieves in $CHCl_3$ (2 mL) under nitrogen was added Danishefsky's diene (0.488 mL, 2.5 mmol) dropwise. The reaction mixture was left to stir at rt.

Procedure for the unsuccessful Lewis acid and thermal catalysed attempt of ring 496 (Table 33, entry 3)

To *N*-benzylidenebenzenesulfonamide (0.491 g, 2 mmol) and $Sc(OTf)_3$ (0.098 g, 0.2 mmol) in toluene (2 mL) under nitrogen was added Danishefsky's diene (0.488 mL, 2.5 mmol) dropwise. The reaction mixture was left to stir at 100 ºC overnight.

Procedure for Table 34 and Table 35 using imine 495

To an organocatalyst HCl salt (20 mol%) and triethylamine (20 mol%) in solvent (2 mL) was added *N*-benzylidenebenzenesulfonamide (0.246 g, 1 mmol) and enone (1 mmol). The reaction mixtures were stirred at the given temperatures and monitored by LCMS analysis.

Procedure for the aldol reactions (Table 36)

To *p*-nitrobenzaldehyde (0.151 g, 1 mmol) and organocatalyst (20 mol%) [and triethylamine (20 mol%) if using the salt of the organocatalyst] in solvent (1 mL) was

added ketone (1 mmol). The reaction mixtures were stirred at rt and monitored *via* TLC analysis.

Procedure for the Mannich reaction between imine 243 and acetone (Equation 46)

To imine **243** (0.131 g, 1 mmol) and acetone (0.73 mL, 1 mmol) in acetonitrile (1 mL) was added L-proline (20 mol%). The reaction mixture was stirred at rt and monitored *via* TLC analysis.

Procedure for an organocatalysed Mannich reaction attempt (Equation 49)

To **473** (0.04 g, 0.2 mmol) and triethylamine (0.028 mL, 0.2 mmol) in toluene (1 mL) was added acetophenone (0.117 mL, 1 mmol) and *N*-benzylidenebenzenesulfonamide (0.246 g, 1 mmol). The reaction mixture was flushed with nitrogen and stirred at rt. After 48 h, the temperature was raised to 70 ºC.

Procedure for the Michael reaction using methyl vinyl ketone (Equation 50 and Equation 51)

To dibenzylamine (0.59 g, 3.0 mmol) and a boronic acid catalyst (20 mol%) [and triethylamine (20 mol%) if the aminoboronic acid catalyst **477** was used] dissolved in water (3 mL) was added methyl vinyl ketone (0.27 mL, 3.3 mmol) and the reaction mixture was stirred at rt overnight. The reaction mixture was extracted with EtOAc (3 × 10 mL), dried ($MgSO_4$), concentrated *in vacuo* and purified by silica gel chromatography (4:1, petroleum ether:diethyl ether, as eluent).

Procedure for the Monitoring of the Michael Reaction (Table 37)

To additive A (10 mol%) and additive B (10 mol%) dissolved in $CDCl_3$ (0.6 mL) was added dibenzylamine (0.115 mL, 0.60 mmol) and methyl vinyl ketone (0.054 mL, 0.66 mmol). The reaction mixture was monitored by ^1H NMR every 0.5 h until the reaction had gone to completion.

Procedure for the Gilman titration method[212]

Titration 1: To distilled water **427** (20 mL) was added *sec*-BuLi **526** (0.5 mL) and phenolphthalein indicator (3 drops). This was titrated against 0.1 M (aq) HCl (8.6 mL) until complete disappearance of the pink colour.

Titration 2: To 1,2-dibromoethane **530** (0.2 mL) in diethyl ether (3 mL) was added at rt *sec*-BuLi **526** (0.5 mL) and the solution was stirred vigorously at rt for 5 min. The reaction mixture was diluted with distilled water **527** (20 mL), phenolphthalein indicator added (2-3 drops) and titrated against 0.1 M (aq) HCl (2.3 mL) with vigorous stirring until the end point was reached (complete disappearance of the pink colour) (Table 38).

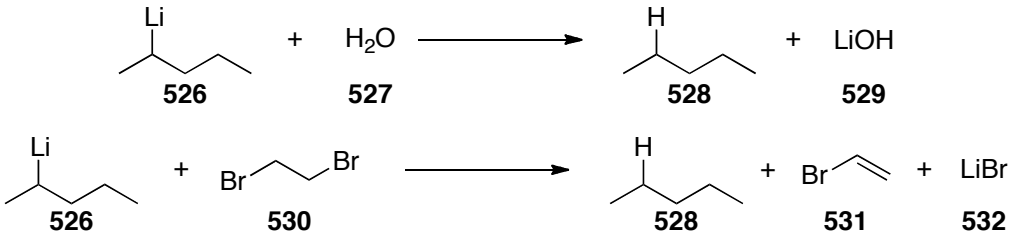

Table 38. Example results from the Gilman double titration procedure.

c(HCl) = 0.1 M	$v(HCl)_1$ = 8.6 mL	$v(HCl)_2$ = 2.3 mL

$v(HCl)_{eff}$ =	$v(HCl)_1 - v(HCl)_2$	
=	8.6 mL - 2.3 mL	= 6.3 mL
c(*sec*-BuLi) =	$(v(HCl)_1 \times v(HCl)_2) / v_{sec\text{-}BuLi}$(aliquot)	
=	(6.3 x 0.1) / 0.5	= 1.26 M
Residual base =	$v(HCl)_{eff} / v(HCl)_1 \times 100$	
=	2.3 / 8.6 x 100	= 27%
Hence, residual base	= 27% 0f 1.26 M	
	= 0.34 M	
Hence, effective *sec*-BuLi base	= 1.26 M - 0.34 M	
	= 0.9 M	

Procedure for the single titration method[213]

To 1,3-diphenylacetone *p*-tosylhydrazone **533** (197 mg, 0.53 mmol) under nitrogen at rt was added dry THF (4 mL). Whilst stirring, the reaction mixture was titrated against *sec*-BuLi **526** (0.59 mL) until the end point was reached (orange-red in colour) (Table 39).

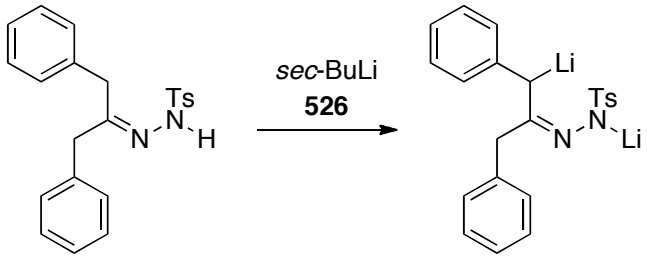

533 534

Table 39. Example results from the single titration procedure.

m(hydrazone) = 0.00053 mol	v(HCl) = 0.59 mL
Hence,	
Molarity of *sec*-BuLi =	1000 x m(hydrazone) / v(HCl)
=	0.53 / 0.59
=	0.9 M

Procedure for drying THF

To THF (1000 mL) and benzophenone (4 spatulas) was slowly added sodium (5/6 small pieces). The mixture was stirred to reflux under argon. The mixture turned from colourless to blue, to deep blue, and finally to a deep purple when all of the THF was dry.

5.3 Synthetic Procedures

1-Methoxy-3-trimethylsiloxy-1,3-butadiene[15]

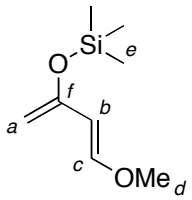

4

Triethylamine (4.18 mL, 30 mmol) was added to a stirred 1 M $ZnCl_2$ solution in diethyl ether (0.40 mL, 0.4 mmol) under nitrogen. After 2 h the resulting suspension was treated with 4-methoxy-3-buten-2-one (1.33 mL, 13 mmol) in diethyl ether (6.5 mL) followed by chlorotrimethylsilane (3.30 mL, 26 mmol). The reaction mixture was stirred at 40 ºC overnight, cooled to rt, diluted with diethyl ether (50 mL), filtered through an alumina pad and concentrated *in vacuo*. Purification by distillation under reduced pressure (32 ºC, 0.5 mbar) afforded **4** as a colourless liquid (1.46 g, 65%): ^{1}H NMR (400 MHz, $CDCl_3$) δ 6.82 (d, *J* = 12.4, 1H, *Hc*), 5.34 (d, *J* = 12.4, 1H, *Hb*), 4.10 (s, 1H, Ha_{trans}), 4.06 (s, 1H, Ha_{cis}), 3.57 (s, 3H, *Hd*), 0.22 (s, 9H, *He*) ppm; ^{13}C NMR (101 MHz, $CDCl_3$) δ 154.1 (s, *Cf*), 150.5 (d, *Cc*), 103.3 (d, *Cb*), 91.2 (t, *Ca*), 56.5 (d, *Cd*), 0.1 (d, *Ce*); IR ν_{max} (neat) 1652 cm^{-1}; LRMS (TOF ES+), 173.10 $[M+H]^+$; HRMS (TOF ES+), calculated for $C_8H_{16}O_2Si+H^+$, 173.0992; found 173.0990. All spectroscopic and analytical properties were identical to those reported in the literature.[214]

2,2-Dimethoxyethylidene-4-methyloxyaniline[61]

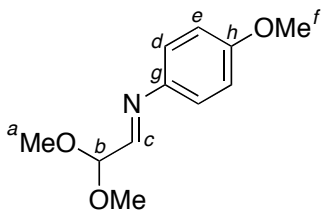

75

To *p*-anisidine (1.23 g, 10 mmol) and 3 Å molecular sieves (10.0 g) in CH_2Cl_2 (40 mL) was added dimethoxyacetaldehyde (60% solution in water) (2.60 g, 15 mmol) and the reaction mixture was stirred at rt overnight. The mixture was filtered and concentrated *in vacuo* to give a crude oil containing **75** and dimethoxyacetaldehyde. The mixture was distilled using a Kugelrohr (100 ºC, 1 mbar) to remove the aldehyde from the product, thus affording **75** as a red oil (1.97 g, 94 %): ^{1}H NMR (400 MHz, $CDCl_3$) δ 7.72 (dd, *J* = 4.3, 1.0 Hz, 1H, *Hc*), 7.13 (d, *J* = 8.9 Hz, 2H, *Hd*), 6.87 (d, *J* = 8.9 Hz, 2H, *He*), 4.86 (dd, *J* = 4.3, 1.0 Hz, 1H, *Hb*), 3.78 (d, *J* = 1.3 Hz, 3H, *Hf*), 3.46 (d, *J* = 1.0 Hz, 6H, *Ha*) ppm; ^{13}C NMR (101 MHz, $CDCl_3$) δ 158.8 (s, *Ch*), 158.2 (d, *Cc*), 143.3 (s, *Cg*), 122.3 (d, *Cd*), 114.4 (d, *Ce*), 103.3 (d, *Cb*), 55.5 (d, *Cf*), 54.1 (d, *Ca*); IR ν_{max} (neat) 2834 (OMe), 1744 (N=C), 1505 (Ar) cm^{-1}; LRMS (TOF ES+), 232.1 $[M+Na]^+$, 210.1 $[M+H]^+$, 178.1; HRMS (TOF ES+), calculated for $C_{11}H_{15}NO_3+H^+$, 210.1130; found 210.1141. All spectroscopic and analytical properties were identical to those reported in the literature.[61]

Ethyl *N*-(*p*-methoxyphenyl)iminoacetate[215]

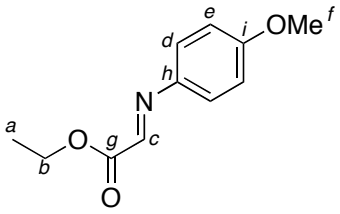

155

To ethyl glyoxylate solution (50% in toluene) (5.11 g, 25 mmol) and 3 Å molecular sieves (5 g) was slowly added a 1M solution of *p*-anisidine (3.08 g, 25 mmol) in toluene (25 mL) over 30 min. The reaction mixture was stirred at rt overnight, washed with CH_2Cl_2, filtered and concentrated *in vacuo*. The oil was filtered to separate the precipitate that was formed, and the filtrate was distilled using a Kugelrohr (175 °C, 0.5 mbar) for 2 h to afford **155** as a thick orange oil (1.18 g, 23%): ^{1}H NMR (400 MHz, $CDCl_3$) δ 7.94 (s, 1H, *Hc*), 7.38-7.34 (m, 2H, *Hd*), 6.95-6.91 (m, 2H, *He*), 4.41 (q, *J* = 7.1 Hz, 2H, *Hb*), 3.84 (s, 3H, *Hf*), 1.40 (t, *J* = 7.1 Hz, 3H, *Ha*) ppm; ^{13}C NMR (101 MHz, $CDCl_3$) δ 163.8 (s, *Cg*), 160.7 (s, *Ci*), 148.2 (d, *Cc*), 141.6 (s, *Ch*), 123.7

(d, *Cd*), 114.7 (d, *Ce*), 62.0 (t, *Cb*), 55.7 (d, *Cf*), 14.4 (d, *Ca*); IR ν_{max} (neat) 2835 (OMe), 1736 (N=C), 1714 (C=O), 1505 (Ar) cm^{-1}; LRMS (TOF ES+), 230.1 $[M+Na]^+$, 208 $[M+H]^+$, 134.1, 124.1; HRMS (TOF ES+), calculated for $C_{11}H_{13}NO_3+H^+$, 208.0974; found 208.0978. All spectroscopic and analytical properties were identical to those reported in the literature.[216]

3,4-Dihydroisoquinoline[217]

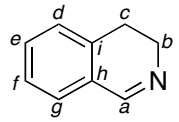

243

Formamide **337** (1.00 g, 6.7 mmol) and polyphosphoric acid (6 g) were heated to 160 ºC overnight whilst stirring. The reaction mixture was poured into ice water and stirred for 3 h. The mixture was basified with 20% (aq) NaOH (50 mL), extracted with diethyl ether (2 × 50 mL), the combined extracts were dried ($MgSO_4$) and concentrated *in vacuo* to afford **243** as an orange oil (0.736 g, 84%): R_f. 0.15 (EtOAc, as eluent); ^{1}H NMR (700 MHz, $CDCl_3$) δ 8.3 (br s, 1H, *Ha*), 7.31 (t, *J* = 7.3 Hz, 1H, *He*), 7.26 (t, *J* = 7.3 Hz, 1H, *Hf*), 7.22 (d, *J* = 7.3 Hz, 1H, *Hg*), 7.11 (d, *J* = 7.3 Hz, 1H, *Hd*), 3.73 (t, *J* = 7.8 Hz, 2H, *Hb*), 2.71 (t, *J* = 7.8 Hz, 2H, *Hc*) ppm; ^{13}C NMR (101 MHz, $CDCl_3$) δ 160.4 (d, *Ca*), 136.4 (s, *Ci*), 131.1 (d, *Ce*), 128.5 (s, *Ch*), 127.4 (d, *Cd*), 127.2 (s, *Cf*), 127.1 (s, *Cg*), 47.4 (t, *Cb*), 25.0 (t, *Cc*); IR ν_{max} (neat) 1626 cm^{-1}; LRMS (TOF ES+), 132.2 (100%) $[M+H]^+$; HRMS (TOF ES+), calculated for $C_9H_9N+H^+$, 132.08078; found 132.08092. All spectroscopic and analytical properties were identical to those reported in the literature.[164, 218]

6,7-Dihydro-1*H*-pyrido[2,1-*a*]isoquinolin-2(11b*H*)-one[219]

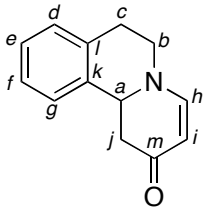

244

To **246** (0.131 g, 1.0 mmol) and $Yb(OTf)_3$ (0.124 g, 0.2 mmol) in CH_2Cl_2 (1.5 mL) under argon was added Danishefsky's diene (0.240 mL, 1.2 mmol) dropwise. The reaction mixture was stirred at rt for 4 h, quenched with 5% (aq) HCl (4 mL) and extracted with CH_2Cl_2 (3 × 5 mL). The combined extracts were dried ($MgSO_4$) and concentrated *in vacuo*. Purification by silica gel chromatography (4:1, EtOAc:hexane, to 100%, EtOAc, as eluent) afforded **244** as a pale orange solid (0.030 g, 15%): m.p. 94-97 °C; R_f. 0.05 (2:1, EtOAc:hexane, as eluent); ^{1}H NMR (400 MHz, $CDCl_3$) δ 7.29-7.17 (m, 4H, *Hd+e+f+g*), 7.16 (dd, *J* = 7.4, 0.9 Hz, *Hh*), 5.08 (dd, *J* = 7.4, 0.9 Hz, 1H, *Hi*), 4.76 (dd, *J* = 16.3, 4.5 Hz, 1H, *Ha*), 3.64 (ddd, *J* = 12.2, 5.1, 2.3 Hz, 1H, Hb_{eq}), 3.45 (td, *J* =12.2, 3.2 Hz, 1H, Hb_{ax}), 3.16 (apparent ddd, *J* = 15.8, 5.1, 0.9 Hz, 1H, *Hc*), 2.87-2.85 (m, 1H, *Hj*), 2.84-2.81 (m, 1H, *Hc*), 2.53 (t, *J* = 16.3 Hz, 1H, *Hj*) ppm; ^{13}C NMR (101 MHz, $CDCl_3$) δ 192.8 (s, *Cm*), 154.2 (d, *Ch*) 135.0 (s, *Cl*), 133.5 (s, *Ck*), 129.5 (d, *Cd*), 127.3 (d, *Cf*), 127.2 (d, *Ce*), 125.7 (d, *Cg*), 98.7 (d, *Ci*), 56.7 (d, *Ca*), 49.8 (t, *Cj*), 44.1 (t, *Cb*), 30.4 (t, *Cc*); IR ν_{max} (thin film) 1630, 1586, 1581 cm^{-1}; LRMS (TOF ES+), 222.2 (100%) $[M+Na]^+$, 200.2 (40%) $[M+H]^+$; HRMS (TOF ES+), calculated for $C_{13}H_{13}NO+H^+$, 200.1075; found 200.1079. All spectroscopic and analytical properties were identical to those reported in the literature.[84, 220]

First alternate procedure:

To **246** (0.131 g, 1.0 mmol) and 3 Å molecular sieves (1 g) under argon was added Danishefsky's diene (0.240 mL, 1.2 mmol) dropwise. The reaction mixture was stirred at rt for 48 h, diluted with CH_2Cl_2 (2 5 mL), filtered and concentrated *in vacuo*. Purification by silica gel chromatography (3:1, EtOAc:hexane, to 100%, EtOAc, as eluent) afforded **244** as a pale orange solid (0.093 g, 47%).

Second alternate procedure:

To **246** (0.131 g, 1.0 mmol), $CeCl_3$ (0.049 g, 0.2 mmol), 2-ethyl-2-oxazoline (0.040 mL, 0.4 mmol) and 3 Å molecular sieves (1 g) under argon in dry CH_2Cl_2 (1.5 mL) was added Danishefsky's diene (0.240 mL, 1.2 mmol) dropwise. The reaction mixture was stirred at rt for 48 h, quenched with 5% (aq) HCl (5 mL), diluted with CH_2Cl_2 (10 mL) and brine (10 mL), filtered and extracted with CH_2Cl_2 (3 × 5 mL). The combined extracts were dried ($MgSO_4$) and concentrated *in vacuo*.

Purification by silica gel chromatography (4:1, EtOAc:hexane, to 100%, EtOAc, as eluent) afforded **244** as a pale orange solid (0.099 g, 49%).

4,9-Dihydro-3*H*-β-carboline[221]

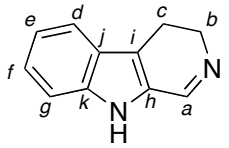

246

To **339** (0.436 g, 2.3 mmol) at 0 °C was slowly added phosphorus(V) oxychloride (4 mL) and the reaction mixture was left to stir at rt. After 12 h, the mixture was quenched with 5% (aq) HCl (20 mL) at 0 °C and basified with 20% (aq) NaOH (50 mL) (pH = 14). The mixture was subsequently warmed to rt, diluted with water (100 mL), extracted with CH_2Cl_2 (3 × 20 mL), dried ($MgSO_4$) and concentrated *in vacuo* to afford **246** as an orange solid (0.329 g, 84%): m.p. 91-92 °C (lit. 92.0-93.5 °C)[222]; ^{1}H NMR (400 MHz, $CDCl_3$) δ 9.06 (s, 1H, *Ha*), 7.53-7.49 (m, 1H, *Hd*), 7.45-7.41 (m, 1H, *Hg*), 7.35-7.30 (m, 1H, *Hf*), 7.13-7.08 (m, 1H, *He*), 3.85 (t, *J* = 9.0 Hz, 2H, *Hb*), 3.06 (t, *J* = 9.0 Hz, 2H, *Hc*) ppm; ^{13}C NMR (101 MHz, DMSO) δ 150.58 (d, *Ca*), 135.5 (135.7)(s, *Ck*), 130.6 (s, *Ch*), 125.1 (127.4)(s, *Cj*), 122.6 (120.2)(d, *Cf*), 117.4 (118.6)(d, *Ce*), 117.0 (118.5)(d, *Cg*), 111.4 (112.7)(s, *Ci*), 110.4 (111.4)(d, *Cd*), 42.5 (47.1)(t, *Cb*), 20.9 (17.7)(t, *Cc*); LRMS (TOF ES+), 171.7 (90%) $[M+H]^+$, 144.4 (100%); HRMS (TOF ES+), calculated for $C_{11}H_{10}N_2+H^+$, 171.0922; found 171.0921. All spectroscopic and analytical properties were identical to those reported in the literature.[165, 166]

Benzylidene-(4-methoxy-phenyl)-amine[223]

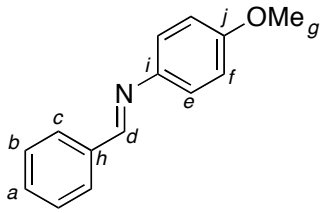

323

To *p*-anisidine (10.0 g, 81 mmol) and $MgSO_4$ (30.0 g) in CH_2Cl_2 (125 mL) was added benzaldehyde (12.4 mL, 122 mmol) and the reaction mixture was stirred at rt overnight. The mixture was filtered, concentrated *in vacuo* and the crude product was recrystalised (hexane) to afford **323** as colourless crystals (12.8 g, 75%): m.p. 70.0-71.0 °C (lit. 70.0-70.5 °C)[224]; ^{1}H NMR (400 MHz, $CDCl_3$) δ 8.49 (s, 1H, *Hd*), 7.91-7.88 (m, 2H, *H*Ar), 7.47-7.46 (m, 3H, *H*Ar), 7.26-7.22 (m, 2H *H*Ar), 6.96-6.92 (m, 2H, *H*Ar), 3.84 (s, 3H, *Hg*) ppm; ^{13}C NMR (101 MHz, $CDCl_3$) δ 158.4 (d, *Cd*), 158.3 (s, Ar), 144.9 (s, Ar), 136.5 (s, Ar), 131.0 (d, Ar), 128.7 (d, Ar), 128.6 (d, Ar), 122.2 (d, Ar), 114.4 (d, Ar), 55.5 (d, *Cf*); IR ν_{max} (neat) 2835 (OMe), 1640 (N=C), 1503 (Ar) cm^{-1}; LRMS (GC EI), 212 (100%) $[M+H]^+$; HRMS (TOF AP+), calculated for $C_{14}H_{13}NO+H^+$, 212.1075; found 212.1066. All spectroscopic and analytical properties were identical to those reported in the literature.[225, 226]

Allyl-benzylidene-amine[223]

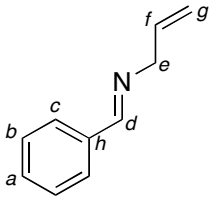

324

To benzaldehyde (15.0 g, 141 mmol) and $MgSO_4$ (50.0 g) in CH_2Cl_2 (150 mL) was added allylamine (11.66 mL, 155 mmol) and the reaction mixture was stirred at rt

overnight. The mixture was filtered, concentrated *in vacuo* and distilled at reduced pressure (120 °C, 46 mbar) to afford **324** as a colourless oil (14.66 g, 72%): ^{1}H NMR (400 MHz, $CDCl_3$) δ 8.30 (t, *J* = 1.5 Hz, 1H, *Hd*), 7.74-7.78 (m, 2H, *Hc*), 7.39-7.45 (m, 3H, $H_{a\&b}$), 6.07 (ddt, *J* = 17.0, 10.0, 5.5 Hz, *Hf*), 5.24 (dq, *J* = 17.0, 1.5 Hz, 1H, Hg_{trans}), 5.16 (dq, *J* = 10.0, 1.5 Hz, 1H, Hg_{cis}), 4.27 (dq, *J* = 5.5, 1.5 Hz, 2H, *He*) ppm; ^{13}C NMR (101 MHz, $CDCl_3$) δ 162.0 (d, *Cd*), 136.2 (s, *Ch*), 135.9 (d, *Cf*), 130.7 (d, C_{para}), 128.6 and 128.1 (d, C_{ortho} and C_{para} or *vice versa*), 116.0 (t, *Cg*), 63.5 (t, *Ce*); IR ν_{max} (neat) 1647 (N=C) cm^{-1}; LRMS (TOF ES+), 146.1 (100%) $[M+H]^+$; HRMS (TOF ES+), calculated for $C_{10}H_{11}N+H^+$, 146.0970; found 146.0960. All spectroscopic and analytical properties were identical to those reported in the literature.[227]

(*E*)-4-methoxy-*N*-(4-nitrobenzylidene)aniline[228]

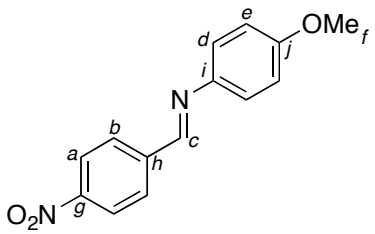

326

p-Nitrobenzaldehyde (1.51 g, 10 mmol), *p*-anisidine (1.23 g, 10 mmol) and $MgSO_4$ (4 g) were dissolved in CH_2Cl_2 (40 mL) and the reaction mixture was stirred at rt. After 24, the mixture was filtered and concentrated *in vacuo* to afford **326** as a yellow solid (2.56 g, 99%): R_f. 0.70 (2:3, EtOAc:hexane, as eluent); m.p. 132-133 °C (lit. 134-135 °C)[229]; ^{1}H NMR (400 MHz, $CDCl_3$) δ 8.58 (s, 1H, *Hc*), 8.33-8.29 (m, 2H, *Ha*), 8.07-8.03 (m, 2H, *Hb*), 7.33-7.29 (m, 2H, *Hd*), 6.98-6.94 (m, 2H, *He*), 3.85 (s, 3H, *Hf*) ppm; ^{13}C NMR (101 MHz, $CDCl_3$) δ 159.4 (s, *Cj*), 154.9 (d, *Cc*), 149.2 (s, *Cg*), 143.8 (s, *Ci*), 142.1 (s, *Ch*), 129.2 (d, *Cb*), 124.1 (d, *Ca*), 122.8 (d, *Cd*), 114.7 (d, *Ce*), 55.7 (d, *Cf*); LRMS (TOF ES+), 257.1 (100%) $[M+H]^+$, 124.0 (50%); HRMS (TOF ES+), calculated for $C_{14}H_{12}N_2O_3+H^+$, 257.0926; observed 257.0931. All spectroscopic and analytical properties were identical to those reported in the literature.[188]

_N_-(2,2-Dimethoxyethylidene)prop-2-en-1-amine

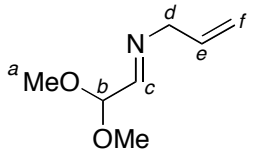

328

To dimethoxyacetaldehyde (60% solution in water) (5.55 g, 32 mmol) and 3 Å molecular sieves (20.0 g) in CH_2Cl_2 (100 mL) was added allylamine (2.63 mL, 35 mmol) and the reaction mixture was stirred at rt overnight. The mixture was filtered and concentrated *in vacuo* to afford **328** as an off-colourless oil (4.43 g, 97%): ^{1}H NMR (400 MHz, $CDCl_3$) δ 7.47 (dt, *J* = 4.3, 1.4 Hz, 1H, *Hc*), 5.92 (ddt, *J* = 17.2, 10.3, 5.9 Hz, 1H, *He*), 5.11-5.08 (m, 2H, *Hf*), 4.65 (d, *J* = 4.3 Hz, 1H, *Hb*), 4.06-4.03 (m, 2H, *Hd*), 3.36 (s, 6H, *Ha*) ppm; ^{13}C NMR (101 MHz, $CDCl_3$) δ 161.3 (d, *Cc*), 135.0 (d, *Ce*), 116.6 (t, *Cf*), 103.1 (d, *Cb*), 63.0 (t, *Cd*), 54.0 (d, *Ca*); IR ν_{max} (neat) 2832 (OMe), 1676 (N=C) cm^{-1}; LRMS (GC CI), 144.1 (100%) $[M+H]^+$, 75.0; HRMS (GC CI), calculated for $C_7H_{14}NO_2+H^+$, 144.1019; found 144.1020.

2-(4-Methoxyphenylimino)-_N_-(4-methoxyphenol)acetamide[163]

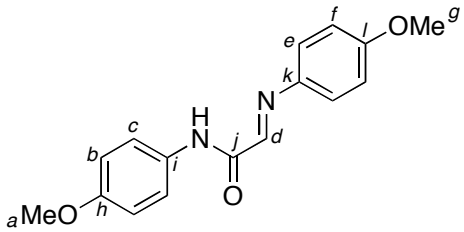

331

To ethyl glyoxylate solution (50% in toluene) (5.11 g, 25 mmol) and 3 Å molecular sieves (5 g) in toluene (25 mL) was added *p*-anisidine (3.08 g, 25 mmol) and the reaction mixture was stirred at rt for 4 h. The reaction mixture was washed with CH_2Cl_2, filtered and concentrated *in vacuo*. The oil was filtered to collect the precipitate that was formed, which was washed with toluene to afford **331** as a green/yellow solid (1.08 g, 21%): m.p. 157-159 °C (lit. 158-159 °C)[163]; R_f. 0.33 (1:1, EtOAc:hexane as eluent); ^{1}H NMR (500 MHz, $CDCl_3$) δ 9.02 (s, 1H, N*H*), 7.94 (s,

1H, *Hd*), 7.64-7.61 (m, 2H, *Hb*), 7.36-7.33 (m, 2H, *Hf*), 6.97-6.94 (m, 2H, *He*), 6.93-6.90 (m, 2H, *Hc*), 3.85 (s, 3H, *Hg*), 3.81 (s, 3H, *Ha*) ppm (addition of D_2O caused the signal at δ 9.02 to disappear); ^{13}C NMR (101 MHz, $CDCl_3$) δ 161.3 (s, *Cj*), 160.5 (s, *Cl*), 156.6 (s, *Ch*), 150.8 (d, *Cd*), 140.2 (s, *Ck*), 130.6 (s, *Ci*), 123.7 (d, *Cf*), 121.4 (d, *Cb*), 114.8 (d, *Ce*), 114.4 (d, *Cc*), 55.7 (d, *Ca*), 55.6 (d, *Cg*); IR ν_{max} (neat) 3308 (NH), 2842 (OMe), 1673 (N=C), 1620 (C=O), 1503 (Ar) cm^{-1}; LRMS (TOF ES-), 283.3 (100%) $[M–H]^-$; HRMS (TOF ES-), calculated for $C_{16}H_{15}N_2O_3$, 283.1083; observed 283.1082; *Anal.* calcd: C, 67.59, H, 5.67, N, 9.85, found: C, 67.57, H, 5.69, N, 9.84. IR properties were identical to those reported in the literature.[163]

2,3,4,5-Tetrahydropyridine[188]

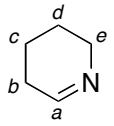

333

To a stirring solution of potassium hydroxide (1.85 g, 33 mmol) in ethanol (30 mL) was slowly added a solution of **341** (1.86 g, 15.6 mmol) in diethyl ether (35 mL) and this was stirred at rt. After 15 h the mixture was filtered and the precipitate washed with ethanol (35 mL). The combined organics were concentrated *in vauo*, diluted with diethyl ether (100 mL) and washed with water (4 × 25 mL). The combined aqueous phases were subsequently washed with diethyl ether (2 × 25 mL). All of the organic phases were combined, dried ($MgSO_4$) and concentrated *in vacuo* to afford **333** as an off-colourless oil, as a mixture of its monomeric, dimeric and trimeric form (0.715 g, 55%): ^1H NMR (400 MHz, $CDCl_3$) δ 7.79 (br s, *Ha*), 3.74-3.48 (m, *monomeric form*), 3.25-3.04 (m, *trimeric form*), 2.93-2.75 (m, *trimeric form*), 2.65-2.44 (m, *dimeric form*), 2.17-2.08 (m, *monomeric form*), 2.05-1.82 (m, *trimeric form*), 1.75-1.44 (m, *trimeric form*), 1.34-1.14 (m, *trimeric form*), 1.00-0.79 (m, *dimeric form*) ppm; ^{13}C NMR (101 MHz, $CDCl_3$) δ 163.3 (d, *Ca*); IR ν_{max} (neat) 2298 (C-H), 2854 (C-H), 1653 (N=C), 1240 (C-N), 1104 (C-C) cm^{-1}; LRMS (TOF ES+), 272.7 (20%) $[trimer+Na]^+$, 250.7 (40%) $[trimer+H]^+$, 248.7 (100%), 167.5 (75%) $[dimer+H]^+$, 84.1 (10%) $[monomer+H]^+$; HRMS (TOF ES+), calculated for $C_{15}H_{27}N_3+Na^+$, 272.2103; found 272.2097 (trimer); calculated for $C_{10}H_{18}N_2+H^+$, 167.1548; found 167.1579

(dimer); calculated for $C_5H_9N+H^+$, 84.0813; found 84.0827 (monomer). All spectroscopic and analytical properties were identical to those reported in the literature.[167, 230]

2-Phenylethanamine[231]

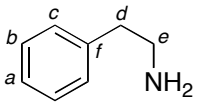

335

An impure commercial sample of 2-phenylethylamine (15 mL, 124 mmol) was purified by distillation under vacuum (53 mbar, 78 °C) to afford **335** as a colourless oil (13.04 g, 87%): ^{1}H NMR (400 MHz, $CDCl_3$) δ 7.33-7.27 (m, 2H, *Hb*), 7.24-7.17 (m, 3H, *Hc*+*a*), 2.97 (t, *J* = 6.9 Hz, 2H, *He*), 2.75 (t, *J* = 6.9 Hz, 2H, *Hd*), 1.18 (br s, 2H, N*H*) ppm (addition of D_2O caused the signal at δ 1.18 to disappear); ^{13}C NMR (101 MHz, $CDCl_3$) δ 140.0 (139.3) (s, *Cf*), 128.9 (128.6) (d, *Cb*), 128.3 (127.9) (d, *Cc*), 126.3 (125.6) (d, *Ca*), 43.7 (43.0) (t, *Ce*), 40.3 (39.6) (t, *Cd*); LRMS (TOF ES+), 122.4 (100%) $[M+H]^+$, 105.6 (55%); HRMS (FTMS ES+), calculated for $C_8H_{11}N+H^+$, 122.0970; found 122.0972; *Anal*. Calcd: C, 79.29, H, 9.15, N, 11.56, found: C, 73.80, H, 8.61, N, 11.82. All spectroscopic and analytical properties were identical to those reported in the literature.[232]

***N*-Phenethylformamide**[233]

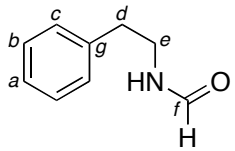

337

2-Phenylethylamine **335** (2.52 mL, 20 mmol) and ethyl formate (4.02 mL, 50 mmol) were stirred and heated to reflux (60 ºC) overnight. The reaction mixture was concentrated *in vacuo* and distilled by Kugelrohr distillation (180 ºC, 2 mbar) to afford **337** as a colourless oil (2.472 g, 83 %): R_f. 0.25 (EtOAc, as eluent); ^{1}H NMR

(400 MHz, $CDCl_3$) δ 5:1 mixture {1H, *Hf* [major isomer: δ 8.11 (s), minor isomer: δ 7.90 (d, *J* = 11.9 Hz)]}, 7.34-7.28 (m, 2H, Ar*H*), 7.27-7.15 (m, 3H, Ar*H*), 5.72 (br s, 1H, N*H*), 5:1 mixture {2H, *He* [major isomer: δ 3.57 (q, *J* = 6.8 Hz), minor isomer: δ 3.47 (d, *J* = 6.7 Hz)]}, 5:1 mixture {2H, *Hd* [major isomer: δ 2.84 (t, *J* = 6.8 Hz), minor isomer: δ 2.81 (d, *J* = 6.7 Hz)]} ppm [addition of D_2O caused the signal at δ 7.90 to turn into a (s), the signal at δ 5.72 to disappear, the signal at δ 3.57 and 3.47 to turn into (t with *J* = 6.9 and 4.8 Hz respectively), and the signal at δ 2.84 and 2.81 to turn into 2.87 and 2.82 (t of *J* = 6.9 and 6.8 Hz respectively)]; ^{13}C NMR (101 MHz, $CDCl_3$) δ (minor rotamer in brackets) 161.4 (164.6)(d, *Cf*), 138.6 (137.7)(s, Ar), 128.7 (128.8)(d, Ar), 128.6 (128.7)(d, Ar), 126.5 (126.8)(d, Ar), 39.2 (43.2)(t, CH_2*Ce*), 35.4 (37.6)(t, *Cd*); IR ν_{max} (neat) 3282, 3028, 1656 (C=O) cm^{-1}; LRMS (TOF ES+), 172.2 (100%) $[M+Na]^+$, 150.2 (24%) $[M+H]^+$, 122.1; HRMS (TOF ES+), calculated for $C_9H_{11}ON+H^+$, 150.09134; found 150.09150. All spectroscopic and analytical properties were identical to those reported in the literature.[164]

_N_-Formyltryptamine[234]

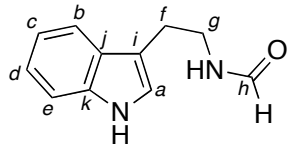

339

Ethyl formate (6 mL) was added to tryptamine (0.48 g, 3 mmol), and the reaction mixture was stirred at 60 ºC. After 12 h, the mixture was cooled to rt and concentrated *in vacuo*. The mixture was subsequently diluted with CH_2Cl_2 (5 mL) and washed with 1 M (aq) HCl (5 mL), sat. K_zCO_3 (5 mL) and brine (5 mL). The organics were dried ($MgSO_4$) and concentrated *in vacuo* to afford **339** as an off-colourless oil (0.467 g, 83%): (3:1 major:minor rotamer, the minor shown in brackets): ^1H NMR (700 MHz, $CDCl_3$) δ 8.13 [7.92 (d, *J* = 12.3 Hz)](s, 1H, *Hh*), 8.10 (br s, 1H, *H*NC=O), 7.69 (7.56)(d, *J* = 7.7 Hz, 1H, *He*), 7.39 (7.39)(d, *J* = 7.7 Hz, 1H, *Hb*), 7.22 (7.22)(t, *J* = 7.7 Hz, 1H, *Hd*), 7.14 (7.15)(t, *J* = 7.7 Hz, 1H, *Hc*), 7.06 (7.04)(s, 1H, *Ha*), 5.59 (br s, 1H, N*H*), 3.67 (3.54)(q, *J* = 6.5 Hz, 2H, *Hg*), 3.02 (2.98)(t, *J* = 6.5 Hz, 2H) ppm (addition of D_2O caused the signals at δ 8.10 and 5.59 to disappear, and the signals at

δ 7.92, 3.67 and 3.54 to change to a s, t and t respectively); ^{13}C NMR (101 MHz, $CDCl_3$) δ 161.3 (164.6)(d, *Ch*), 136.6 (136.6)(s, *Ck*), 127.4 (127.0)(s, *Cj*), 122.5 (122.7)(d, *Ca*), 122.3 (122.6)(d, *Cd*), 119.8 (119.9)(d, *Cc*), 118.8 (118.5)(d, *Ce*), 112.8 (111.8)(s, *Ci*), 111.4 (111.6)(d, *Cb*), 38.5 (42.1)(t, *Cg*), 25.4 (27.6)(t, *Cf*); IR ν_{max} cm^{-1}; LRMS (TOF ES+), 211.5 (100%) $[M+Na]^+$; HRMS (TOF ES+), calculated for $C_{11}H_{12}N_2O+Na^+$, 211.0847; found 211.0851. ^{1}H NMR properties were identical to that reported in the literature.[165]

1-Chloropiperidine[235]

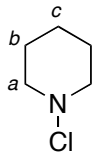

341

To *N*-chlorosuccinimide (2.94 g, 22 mmol) in diethyl ether (100 mL) was added dropwise piperidine (1.98 mL, 20 mmol) and the reaction mixture was stirred at rt. After 3 h, the mixture was filtered, and the precipitate washed with diethyl ether (25 mL). The combined organics were subsequently washed with water (3 × 25 mL), dried ($MgSO_4$) and concentrated *in vacuo* to afford **341** as a colourless oil (1.99 g, 83%): R_f. 0.49 (3:1, hexane:diethyl ether, as eluent); ^{1}H NMR (700 MHz, $CDCl_3$) δ 3.70-2.60 (br m, 4H, *Ha*), 1.74-1.54 (m, 4H, *Hb*), 1.54-1.15 (br m, 2H, *Hc*) ppm; ^{13}C NMR (176 MHz, $CDCl_3$) δ 64.0 (t, *Ca*), 27.6 (t, *Cc*), 23.0 (t, *Cb*); IR ν_{max} (neat) 2940, 2830, 1442, 679 (N-Cl) cm^{-1}; LRMS (EI+) 118.0 (100%) $[M-H]^+$, 119.0 (50%) [M], 120.0 (40%), 121.0 (15%); HRMS (EI-), calculated for C_5H_9NCl, 118.0418; found 118.0420. All spectroscopic and analytical properties were identical to those reported in the literature.[167, 236]

4-Phenyl-3-buten-2-one[237]

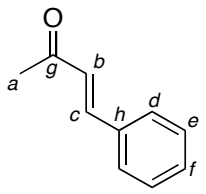

347

To a stirred solution of benzaldehyde (10.61 g, 100 mmol), acetone (20 mL, 0.27 mmol) and water (40 mL) was added dropwise 5% (aq) NaOH (8 mL) and the reaction mixture was stirred at 40 °C for 4 h. The reaction mixture was diluted with EtOAc (100 mL) and the organics extracted with EtOAc (3 × 25 mL), dried ($MgSO_4$) and concentrated *in vacuo* to afford **347** as a yellow liquid (13.35 g, 91%): ^{1}H NMR (400 MHz, $CDCl_3$) δ 7.55-7.51 (m, 3H, *Hd+f*), 7.50 (d, *J* = 16.3 Hz, 1H, *Hc*), 7.40-7.36 (m, 2H, *He*), 6.70 (d, *J* = 16.3 Hz, 1H, *Hb*), 2.34 (s, 3H, *Ha*) ppm; ^{13}C NMR (101 MHz, $CDCl_3$) δ 198.4 (s, *Cg*), 143.4 (d, *Cc*), 134.5 (s, *Ch*), 130.6 (d, *Cf*), 129.0 (d, *Ce*), 128.3 (s, *Cd*), 127.2 (d, *Cb*), 27.6 (d, *Ca*); IR ν_{max} (neat) 1666 (C=C), 1608 (C=O) cm^{-1}; LRMS (TOF ES+), 147.1 $[M+H]^+$; HRMS (TOF ES+), calculated for $C_{10}H_{10}O+H^+$, 147.0810; found 147.0814. All spectroscopic and analytical properties were identical to those reported in the literature.[238, 239]

***trans*-1-Phenyl-3-trimethylsilyloxybutadiene**[240]

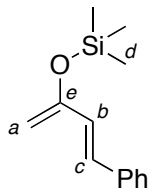

349

To a suspension of zinc(II) chloride (0.2 g, 1.5 mmol) in triethylamine (15 mL, 108 mmol) was added a solution of 4-phenyl-3-but-2-one (7.3 g, 50 mmol) in toluene (15 mL), followed by chlorotrimethylsilane (13 mL, 100 mmol) and the reaction mixture was stirred at 40 °C overnight. The reaction mixture was cooled to rt and diluted with diethyl ether (100 mL). The mixture was filtered, concentrated *in vacuo*

and distilled at reduced pressure (92 °C, 1 mbar) to afford **349** as a yellow liquid (6.10 g, 56%): R_f. 0.57 (2:1, hexane:EtOAc as eluent); ^{1}H NMR (400 MHz, $CDCl_3$) δ 7.43-7.36 (m, 2H, Ar*H*), 7.33-7.29 (m, 2H Ar*H*), 7.24-7.20 (m, 1H Ar*H*), 6.81 (d, *J* = 15.7 Hz, 1H, *Hc*), 6.59 (d, , *J* = 15.7 Hz, 1H, *Hb*), 4.47 (br s, 1H, Ha_Z), 4.43 (br s, 1H, Ha_E), 0.28 (s, 9H, *Hd*) ppm; ^{13}C NMR (101 MHz, $CDCl_3$) δ 155.2 (s, *Ce*), 136.9 (s, Ar), 129.3 (d, *Cc*), 128.7 (d, Ar), 127.8 (d, Ar_{para}), 126.9 (d, Ar), 126.5 (d, *Cb*), 97.2 (t, *Ca*), 0.2 (d, *Cd*); IR ν_{max} (neat) 1670, (C=C), 1610 (Ar), 1252 ($SiCH_3$) cm^{-1}; LRMS (GC EI), 218.1 (68%) [M], 203.1, 128.1, 127.1, 75.1 (100%), 73.1; HRMS (TOF AP+), calculated for $C_{13}H_{18}OSi+H^+$, 219.1205; found 219.1212. All spectroscopic and analytical properties were identical to those reported in the literature.[240, 241]

4-(*p*-Methoxy)-3-buten-2-one[242]

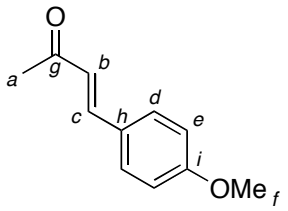

353

To *p*-methoxybenzaldehyde (12.15 mL, 100 mmol), acetone (20 mL, 272 mmol), and water (40 mL) was slowly added 5% (aq) NaOH (8 mL) and the reaction mixture was stirred at 40 °C overnight. The reaction mixture was filtered, the solid dissolved in CH_2Cl_2, dried ($MgSO_4$) and concentrated *in vacuo* to give **353** as a pale yellow solid (15 g, 88%): m.p. 72-73 °C (lit. 72-72.5 °C)[243]; R_f. 0.27 (2:1, hexane:EtOAc as eluent); ^{1}H NMR (400 MHz, $CDCl_3$) δ 7.52-7.48 (m, 2H, *Hd*), 7.48 (d, *J* = 16.2 Hz, 1H, *Hc*), 6.94-6.90 (m, 2H, *He*), 6.61 (d, *J* = 16.2 Hz, 1H, *Hb*), 3.85 (s, 3H, *Hf*), 2.36 (s, 3H, *Ha*) ppm; ^{13}C NMR (101 MHz, $CDCl_3$) δ 198.6 (s, *Cg*), 161.8 (s, *Ci*), 143.4 (d, *Cc*), 130.1 (d, *Cd*), 127.2 (s, *Ch*), 125.2 (d, *Cb*), 114.6 (d, *Ce*), 55.6 (d, *Cf*), 27.6 (d, *Ca*); IR ν_{max} (neat) 2840, (OMe), 1656 (C=C), 1599 (C=O), 1510 (Ar) cm^{-1}; LRMS (TOF ES+), 199.1 (100%) $[M+Na]^+$, 177.2 $[M+H]^+$; HRMS (TOF ES+), calculated for $C_{11}H_{12}O_2+H^+$, 177.09101; found 177.09097. All spectroscopic and analytical properties were identical to those reported in the literature.[238, 244]

4-(*p*-Nitrophenyl)-3-buten-2-one[245]

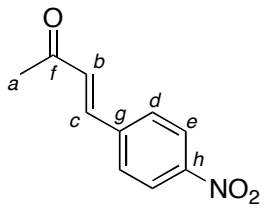

355

To a stirred solution of *p*-nitrobenzaldehyde (3.00 g, 19.9 mmol) in acetone (17.8 mL, 0.68 mol) was added dropwise 0.1 M (aq) NaOH (200 mL) and the reaction mixture was stirred at rt for 1.5 h. The reaction mixture was filtered, the filtrate diluted with EtOAc (120 mL) and the organics extracted with EtOAc (3 × 100 mL), dried ($MgSO_4$) and concentrated *in vacuo*. The crude was purified by silica gel chromatography (2:1, hexane:EtOAc, as eluent) to afford **355** as a yellow solid (1.57 g, 41%): m.p. 105-106 °C (lit. 104-105 °C)[246]; R_f. 0.38 (1:1, EtOAc:hexane, as eluent); ^{1}H NMR (400 MHz, $CDCl_3$) δ 8.28-8.24 (m, 2H, *He*), 7.71-7.68 (m, 2H, *Hd*), 7.53 (d, *J* = 16.3 Hz, 1H, *Hc*), 6.82 (d, *J* = 16.3 Hz, 1H, *Hb*), 2.40 (s, 3H, *Ha*) ppm; ^{13}C NMR (101 MHz, $CDCl_3$) δ 197.6 (s, *Cf*), 148.8 (s, *Ch*), 140.8 (s, *Cg*), 140.2 (d, *Cc*), 130.5 (d, *Cb*), 128.9 (d, *Cd*), 124.4 (d, *Ce*), 28.2 (d, *Ca*); IR ν_{max} (neat) 1690 (C=C), 1594 (C=O), 1511 (Ar), 1342 (NO_2) cm^{-1}; LRMS (TOF ES+), 192.1 (100%) $[M+H]^+$; HRMS (TOF ES+), calculated for $C_{10}H_9NO_3+H^+$, 192.0661; found 192.0672. All spectroscopic and analytical properties were identical to those reported in the literature.[247]

1-Allyl-2,6-diphenyl-piperidin-4-one[94]

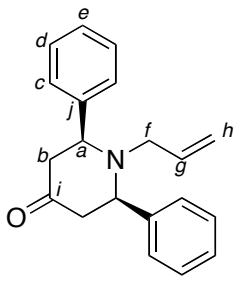

357

To **324** (0.50 g, 3.44 mmol) in MeOH (2 mL) was added 4-phenyl-3-buten-2-one (2.91 g, 13.77 mmol) and L-proline (79 mg, 0.2 mmol). The reaction mixture was stirred at rt overnight. The mixture was concentrated *in vacuo* and purification by silica gel chromatography (8:1, hexane:EtOAc, as eluent) gave a mixture of **357** and benzaldehyde (433 mg). This was dissolved in EtOAc (2 mL) and washed with 5% (aq) HCl (3 × 1 mL). 5% (aq) NaOH (3 mL) was added to the combined aqueous layers and the product extracted using EtOAc (3 × 5 mL), dried ($MgSO_4$) and concentrated *in vacuo* to give **357** as a yellow/orange oil (50 mg, 43%): R_f. 0.61 (1:1, EtOAc:hexane as eluent); ^{1}H NMR (400 MHz, $CDCl_3$) δ 7.47-7.44 (m, 4H, Ar*H*), 7.39-7.36 (m, 4H, Ar*H*), 7.29 (tt, *J* = 2.0, 7.0 Hz, 2H, *He*), 5.75 (ddt, *J* = 17.0, 10.0, 7.0 Hz, 1H, *Hg*), 5.03 (dd, *J* = 10.0, 2.0 Hz, 1H, Hh_{trans}), 4.67 (dd, *J* = 17.0, 2.0 Hz, 1H, Hh_{ciss}), 3.94 (dd, *J* = 12.0, 3.0 Hz, 2H, *Ha*), 2.98 (d, *J* = 7.0 Hz, 2H, *Hf*), 2.75-2.84 (m, 2H, Hb_{trans}), 2.53-2.48 (m, 2H, Hb_{cis}) ppm; ^{13}C NMR (101 MHz, $CDCl_3$) δ 207.4 (s, *Ci*), 142.6 (s, Ar), 130.7 (d, *Cg*), 128.8 (d, Ar), 127.7 (d, *Ce*), 127.4 (d, Ar), 119.6 (t, *Ch*), 64.6 (d, *Ca*), 51.29 (t, *Cf*), 50.93 (t, *Cb*); IR ν_{max} (thin film) 1717 (C=O) cm^{-1}; LRMS (TOF ES+), 292.2 $[M+H]^+$; HRMS (TOF ES+), calculated for $C_{20}H_{21}NO+H^+$, 292.1696; found 292.1712. Both ^{1}H and ^{13}C NMR properties were identical to those reported in the literature.[94]

(*Z*)-4-(Allylamino)but-3-en-2-one[248]

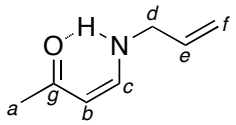

358

To **324** (0.145 g, 1.0 mmol) in MeOH (0.5 mL) was added 4-methoxy-3-buten-2-one (0.255 mL, 2.5 mmol) and $Sc(OTf)_3$ (0.049 g, 0.1 mmol). The reaction mixture was flushed with argon and stirred at rt for 2 days, washed with sat. (aq) $NaHCO_3$ (5 mL) and extracted with CH_2Cl_2 (3 × 7 mL). The combined organics were dried ($MgSO_4$) and concentrated *in vacuo*. Purification by silica gel chromatography (1:9, EtOAc:diethyl ether, to EtOAc, as eluent) afforded **358** as a yellow oil (0.041 g, 33%): R_f. 0.32 (EtOAc, as eluent); ^{1}H NMR (500 MHz, $CDCl_3$) δ 9.77 (v br s, 1H, N*H*), 6.61 (dd, *J* = 12.8, 7.4 Hz, 1H, *Hc*), 5.84 (ddt, *J* = 17.1, 10.4, 5.5 Hz, 1H, *He*),

5.21 (ddd, J = 17.1, 2.9, 1.6 Hz, 1H, Hf_{cis}), 5.16 (10.4, 2.9, 1.6 Hz, 1H, Hf_{trans}), 5.01 (d, J = 7.4 Hz, 1H, *Hb*), 3.78 (ddt, J = 7.1, 5.5, 1.6 Hz, 2H, *Hd*), 2.05 (s, 3H, *Ha*) ppm (addition of D_2O caused the signal at δ 9.77 to disappear); ^{13}C NMR (126 MHz, $CDCl_3$) δ 197.7 (s, *Cg*), 152.4 (d, *Cc*), 134.6 (d, *Ce*), 117.0 (t, *Cf*), 94.4 (d, *Cb*), 50.9 (t, *Cd*), 29.1 (d, *Ca*); IR ν_{max} (thin film) 3264, 3056, 1635 (C=O), 1556, 1487 cm^{-1}; LRMS (TOF ES-), 153.1 (100%), 124.2 (75%) $[M–H]^-$; HRMS (TOF ES-), calculated for $C_7H_{10}NO$, 124.0762; found 124.0759. All spectroscopic and analytical properties were identical to those reported in the literature.[249]

Other procedure:
To allylamine (0.075 mL, 1 mmol) in CH_2Cl_2 (0.5 mL) was added 4-methoxy-3-buten-2-one (0.102 mL, 1 mmol). The reaction mixture was stirred at rt for 24 h and concentrated *in vacuo* to afford **358** as a brown oil (0.124 g, 99%).

_N_-Allyl-2,3-dihydro-2-phenyl-4-pyridone[45]

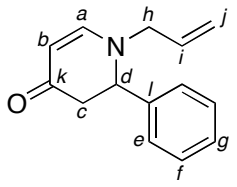

362

To **324** (0.146 g, 1 mmol) and $Yb(OTf)_3$ (0.124 g, 0.2 mmol) in CH_2Cl_2 (1.5 mL) under argon was added Danishefsky's diene (0.240 mL, 1.2 mmol) dropwise. The reaction mixture was stirred at rt overnight, quenched with 5% (aq) HCl (3 mL) and extracted with CH_2Cl_2 (3 × 5 mL). The combined extracts were dried ($MgSO_4$) and concentrated *in vacuo*. Purification by silica gel chromatography (3:1, EtOAc:petroleum ether, as eluent) afforded **362** as an orange oil (0.079 g, 37%): R_f 0.06 (1:1, EtOAc:hexane, as eluent); ^1H NMR (101 MHz, $CDCl_3$) δ 7.41-7.30 (m, 5H, Ar*H*), 7.19 (d, J = 7.7 Hz, 1H, *Ha*), 5.78 (dddd, J = 17.2, 10.2, 7.2, 4.7 Hz, 1H, *Hi*), 5.27 (ddd, J = 10.2, 2.6, 1.2 Hz, 1H, Hj_{trans}), 5.18 (ddt, J = 17.2, 1.7, 1.2 Hz, 1H, Hj_{cis}), 5.09 (d, J = 7.7 Hz, 1H, *Hb*), 4.64 (dd, J = 8.6, 6.9 Hz, 1H, Hd_{ax}), 3.73 (ddt, J = 15.5, 4.7, 1.7 Hz, 1H, *Hh*), 3.59 (ddt, J = 15.5, 7.2, 1.2 Hz, 1H, *Hh*), 2.88 (dd, J = 16.4, 6.9 Hz, 1H, Hc_{eq}), 2.72 (dd, J = 16.4, 8.6 Hz, 1H, Hc_{ax}) ppm; ^{13}C NMR (101

MHz, $CDCl_3$) δ 190.6 (s, *Ck*), 153.9 (d, *Ca*), 132.9 (d, *Ci*), 129.2 (d, *Cf*), 129.0 (s, *Cl*), 128.5 (d, *Cg*), 127.2 (d, *Ce*), 119.3 (t, *Cj*), 99.3 (d, *Cb*), 61.5 (d, *Cd*), 55.7 (t, *Ch*), 44.0 (t, *Cc*); IR ν_{max} (neat) 1633 (C=O), 1588, 1573 cm^{-1}; LRMS (TOF ES+), 236.2 (100%) $[M+Na]^+$, 214.2 (90%) $[M+H]^+$; HRMS (FTMS ES+), calculated for $C_{14}H_{15}NO+H^+$, 214.12264; found 214.12265. All spectroscopic and analytical properties were identical to those reported in the literature.[45]

1-(4-Methoxyphenyl)-2-phenyl-2,3-dihydropyridin-4(1*H*)-one[53]

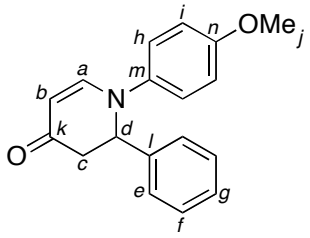

364

To **323** (0.106 g, 0.5 mmol) and $Yb(OTf)_3$ (0.062 g, 0.1 mmol) in toluene (1 mL) was added Danishefsky's diene (0.117 mL, 0.6 mmol). The reaction mixture was stirred at rt overnight, quenched with 5% (aq) HCl (2.5 mL) and extracted with CH_2Cl_2 (3 × 5 mL). The combined extracts were dried ($MgSO_4$) and concentrated *in vacuo*. Purification by silica gel chromatography (1:1, EtOAc:petroleum ether, as eluent) afforded **364** as an orange oil (139 mg, 99%): R_f. 0.09 (1:1, EtOAc:hexane, as eluent); ^{1}H NMR (400 MHz, $CDCl_3$) δ 7.47 (dd, *J* = 7.7, 0.7 Hz, 1H, *Ha*), 7.47-7.16 (m, 5H, Ar*H*), 6.91-6.87 (m, 2H, MeOAr*H*), 6.75-6.71 (m, 2H, MeOAr*H*), 5.16 (dd, *J* = 7.7, 0.7 Hz, 1H, *Hb*), 5.12 (dd, *J* = 7.1, 3.9, 1H, *Hd*), 3.69 (s, 3H, *Hj*), 3.19 (dd, *J* = 16.4, 7.1 Hz, 1H, Hc_{trans}), 2.70 (ddd, *J* = 16.4, 3.9, 0.7 Hz, 1H, Hc_{cis}) ppm; ^{13}C NMR (101 MHz, $CDCl_3$) δ 190.2 (s, *Ck*), 157.1 (s, Ar), 149.7 (d, *Ca*), 138.5 (s, Ar), 138.5 (s, Ar), 129.1 (d, Ar), 128.0 (d, Ar), 126.5 (d, Ar), 121.3 (d, Ar), 114.8 (d, Ar), 101.8 (d, *Cb*), 62.6 (*Cd*), 55.7 (*Cj*), 43.6 (t, *Cc*); IR ν_{max} (neat) 1639 (C=O) cm^{-1}; LRMS (TOF ES+), 280.3 $[M+H]^+$; HRMS (TOF ES+), calculated for $C_{18}H_{17}NO_2+H^+$, 280.1338; found 280.1328. All spectroscopic and analytical properties were identical to those reported in the literature.[250]

1,1'-(7,11b-Dihydro-6*H*-pyrido[2,1-*a*]isoquinoline-1,3-diyl)diethanone

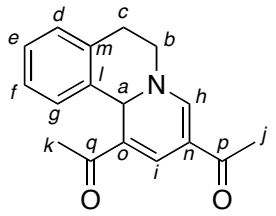

369

To **243** (0.131 g, 1.0 mmol) and $Fe(OTf)_2$ (0.05 g, 0.1 mmol) in CH_2Cl_2 (1 mL) under argon was added 4-methoxy-3-buten-2-one (0.204 mL, 2 mmol). The reaction mixture was stirred at rt for 24 h. Purification by silica gel chromatography (4:1, EtOAc:CH_2Cl_2, as eluent) afforded **369** as a yellow solid (0.234 g, 88%): m.p. 225-230 °C; R_f. 0.1 (2:1, EtOAc:hexane, as eluent); ^{1}H NMR (700 MHz, $CDCl_3$) δ 7.83 (br s, 1H, *Hi*), 7.58 (br s, 1H, *Hh*), 7.18 (t, *J* = 7.2 Hz, 1H, *Hf*), 7.13 (t, *J* = 7.2 Hz, 1H, *He*), 7.10 (d, *J* = 0.4 Hz, 1H, *Hd*), 6.70 (d, *J* = 0.4 Hz, 1H, *Hg*), 5.91 (br s, 1H, *Ha*), 3.94 (dt, 13.1, 7.7 Hz, 1H, Hb_{ax}), 3.79 (ddd, 13.1, 8.1, 4.3 Hz, 1H, Hb_{eq}), 3.19 (dt, *J* = 16.4, 8.1 Hz, Hc_{ax}), 3.09 (ddd, *J* = 16.4, 7.7, 4.3 Hz, 1H, Hc_{eq}), 2.52 (br s, 3H, *Hk*), 2.17 (br s, 3H, *Hj*) ppm; ^{13}C NMR (176 MHz, $CDCl_3$) δ 196.8 (s, *Cq*), 191.0 (s, *Cp*), 151.0 (d, *Ch*), 138.3 (s, *Cm*), 135.4 (d, *Ci*), 132.6 (s, *Cl*), 128.8 (d, *Cd*), 127.5 (d, *Cf*), 126.7 (d, *Ce*), 124.7 (d, *Cg*), 109.0 (s, *Cn*), 55.0 (d, *Ca*), 51.7 (t, *Cb*), 31.0 (s, *Co*), 28.4 (t, *Cc*), 25.0 (d, *Ck*), 24.7 (d, *Cj*); IR ν_{max} (neat) 1644, 1591, 1538 cm^{-1}; UV (MeOH nm) 409 (Σ 5841), 315 (Σ 20076), 228 (Σ 11361), 212 (Σ 13139); LRMS (TOF ES+), 290.3 (100%) $[M+Na]^+$, 268.3 $[M+H]^+$; HRMS (TOF ES+), calculated for $C_{17}H_{17}NO_2$+H^+, 268.1338; found 268.1335; *Anal.* calcd: C, 76.38, H, 6.41, N, 5.24, found: C, 75.85, H, 6.38, N, 5.13.

Alternate procedure:

To **243** (0.131 g, 1.0 mmol) and $Yb(OTf)_3$ (0.124 g, 0.2 mmol) in CH_2Cl_2 (1.5 mL) was added 3-butyn-2-one (0.156 mL, 2 mmol). The reaction mixture was stirred at rt for 48 h and concentrated *in vacuo*. Purification by silica gel chromatography (EtOAc, as eluent) afforded **369** as a yellow solid (0.156 g, 58%).

1,3,5-Triacetylbenzene[251]

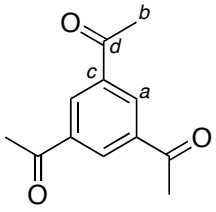

376

To 4-methoxy-3-buten-2-one (0.102 mL, 1.0 mmol) in $CDCl_3$ (0.5 mL) was added $Yb(OTf)_3$ (0.124 g, 0.2 mmol) and the reaction mixture was stirred at rt 7 days. Purification by silica gel chromatography (3:2, diethyl ether:hexane, as eluent) afforded **376** as a white solid (0.030 g, 45%): m.p. 158-159 °C (lit. 158-160 °C)[252]; R_f: 0.16 (2:1, diethyl ether:hexane, as eluent); ^{1}H NMR (400 MHz, $CDCl_3$) δ 8.70 (br s, 3H, *Ha*), 2.71 (br s, 9H, *Hb*) ppm; ^{13}C NMR (101 MHz, $CDCl_3$) δ 196.7 (s, *Cd*), 138.1 (s, *Cc*), 131.9 (d, *Ca*), 27.0 (d, *Cb*); IR ν_{max} (thin film) 1687 (C=O), 1361, 1225 cm^{-1}; LRMS (FTMS NES+), 222.1 (100%) $[M+NH_4]^+$, 205.1 (16%), $[M+H]^+$; HRMS (FTMS ES+), calculated for $C_{12}H_{12}O_3+NH_4^+$, 222.1125; found 222.1127; *Anal.* Calcd: C, 70.57, H, 5.92, found: C, 69.19, H, 5.89. All spectroscopic and analytical properties were identical to those reported in the literature.[253]

1,1'-(1-Allyl-4-phenyl-1,4-dihydropyridine-3,5-diyl)diethanone

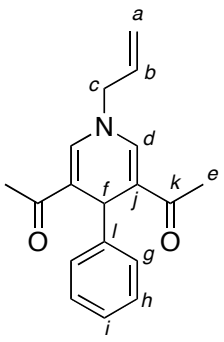

386

To **324** (0.145 g, 1.0 mmol) and $Sc(OTf)_3$ (0.049 g, 0.1 mmol) in $CHCl_3$ (1.5 mL) under argon was added 4-methoxy-3-buten-2-one (0.408 mL, 4.0 mmol). The reaction mixture was stirred at rt for 2 days, washed with sat. (aq) $NaHCO_3$ (5 mL) and

extracted with CH_2Cl_2 (3 × 7 mL). The combined organic extracts were dried ($MgSO_4$) and concentrated *in vacuo*. Purification by silica gel chromatography (1:9, EtOAc:diethyl ether, as eluent) afforded **386** as a yellow oil (0.089 g, 31%): m.p. 118-119 °C; R_f. 0.18 (1:9, EtOAc:diethyl ether, as eluent); ^{1}H NMR (700 MHz, $CDCl_3$) δ 7.30 (d, *J* = 7.7 Hz, 2H, *Hg*), 7.22 (t, *J* = 7.7 Hz, 2H, *Hh*), 7.14-7.11 (m, 1H, *Hi*), 7.13 (s, 2H, *Hd*), 5.94 (ddt, *J* = 17.0, 10.5, 5.6 Hz, 1H, *Hb*), 5.38 (dtd, *J* = 10.5, 1.6, 0.9 Hz, 1H, Ha_{trans}), 5.36 (dtd, *J* = 17.0, 1.6, 0.9 Hz, 1H, Ha_{cis}), 5.18 (s, 1H, *Hf*), 4.10 (dt, *J* = 5.6, 1.6 Hz, 2H, *Hc*), 2.15 (br s, 6H, *He*) ppm; ^{13}C NMR (176 MHz, $CDCl_3$) δ 195.2 (s, *Ck*), 145.9 (s, *Cl*), 138.0 (d, *Cd*), 132.5 (d, *Cb*), 128.3 (d, *Cg*), 128.3 (d, Ch), 126.6 (d, *Ci*), 119.6 (t, *Ca*), 119.5 (s, *Cj*), 57.3 (t, *Cc*), 35.9 (d, *Cf*), 25.7 (d, *Ce*); IR ν_{max} (thin film) 1633 (C=O), 1566 cm^{-1}; LRMS (TOF ES+), 304.3 (100%) $[M+Na]^+$, 282.3 (35%) $[M+H]^+$, 176.2 (20%), 146.2 (20%); HRMS (TOF ES+), calculated for $C_{18}H_{19}NO_2+H^+$, 282.1494; found 282.1495; *Anal.* Calcd: C, 76.84, H, 6.81, N, 4.98, found: C, 76.65, H, 6.84, N, 4.94.

Alternate procedure:

To 4-methoxy-3-buten-2-one (0.204 mL, 2.0 mmol) and benzaldehyde (0.102 mL, 1.0 mmol) in $CHCl_3$ (1 mL), was added $Sc(OTf)_3$ (0.049 g, 0.1 mmol) followed by allylamine (0.075 mL, 1.0 mmol). The reaction mixture was flushed with argon and stirred at rt for 4 days. Purification by silica gel chromatography (1:9, EtOAc:hexane, to 1:9, EtOAc:diethyl ether, as eluent) afforded **386** as a yellow solid (0.135 g, 48%).

1,1'-(1-Allyl-4-(dimethoxymethyl)-1,4-dihydropyridine-3,5-diyl)diethanone

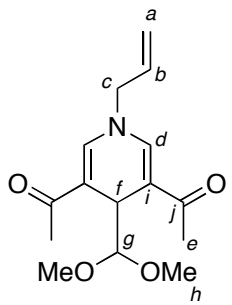

388

To **328** (0.143 g, 1.0 mmol) and $Sc(OTf)_3$ (0.049 g, 0.1 mmol) in $CHCl_3$ (1.5 mL) under argon was added 4-methoxy-3-buten-2-one (0.408 mL, 4.0 mmol). The reaction

mixture was stirred at rt for 2 days, washed with sat. (aq) $NaHCO_3$ (5 mL) and extracted with CH_2Cl_2 (3 × 7 mL). The combined organics were dried ($MgSO_4$) and concentrated *in vacuo*. Purification by silica gel chromatography (1:9, EtOAc:diethyl ether, to EtOAc, as eluent) afforded **388** as a dark orange oil (0.045 g, 20%): R_f. 0.15 (EtOAc, as eluent); ^{1}H NMR (400 MHz, $CDCl_3$) δ 7.09 (s, 2H, *Hd*), 5.86 (ddt, *J* = 16.7, 10.2, 5.0 Hz, 1H, *Hb*), 5.33 (dtd, *J* = 16.7, 1.6, 0.9 Hz, 1H, Ha_{cis}), 5.29 (dtd, *J* = 10.2, 1.6, 0.9 Hz, 1H, Hb_{trans}), 4.45 (d, *J* = 4.0 Hz, 1H, *Hf*), 4.03 (dt, *J* = 5.0, 1.6 Hz, 2H, *Hc*), 3.97 (d, *J* = 4.0 Hz, 1H, *Hg*), 3.22 (br s, 6H, *Hh*), 2.26 (br s, 6H, *He*) ppm; ^{13}C NMR (101 MHz, $CDCl_3$) δ 195.9 (s, *Cj*), 139.9 (d, *Cd*), 132.7 (d, *Cb*), 118.8 (t, *Ca*), 114.9 (s, *Ci*), 107.3 (d, *Cg*), 57.3 (t, *Cc*), 55.9 (d, *Ch*), 33.3 (d, *Cf*), 25.5 (d, *Ce*); IR ν_{max} (thin film) 1639 (C=O), 1567 cm^{-1}; LRMS (TOF ES+), 302.3 (100%) $[M+Na]^+$, 280.3 (60%) $[M+H]^+$, 176.2 (20%), 248.2 (30%); HRMS (TOF ES+), calculated for $C_{15}H_{21}NO_4$+Na^+, 302.1368; found 302.1382.

Alternate procedure:
To allylamine (0.075 mL, 1.0 mmol) in CH_2Cl_2 (1 mL) was added 4-methoxy-3-buten-2-one (0.204 mL, 2 mmol), dimethoxyacetaldehyde (0.174 g, 1 mmol) (60% in water) and $Sc(OTf)_3$ (0.049 mg, 0.1 mmol) and the reaction mixture was stirred at rt for 4 days. Purification by silica gel chromatography (2:1, EtOAc:diethyl ether, as eluent) afforded **388** as a yellow oil (0.064 g, 23%).

***p*-Methoxyphenylamino-4-butene-3-one-2**[254]

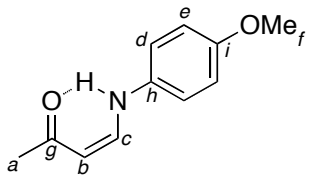

389

To **323** (0.211 g, 1.0 mmol) in $CHCl_3$ (1 mL) was added 4-methoxy-3-buten-2-one (0.255 mL, 2.5 mmol) and $Sc(OTf)_3$ (0.049 g, 0.1 mmol). The reaction mixture was flushed with argon and stirred at rt for 2 days. The crude was concentrated *in vacuo* and purified by silica gel chromatography (1:9, EtOAc:diethyl ether, to EtOAc, as eluent) to afford **389** as an orange oil (0.048 g, 25%): R_f. 0.53 (EtOAc, as eluent); ^{1}H

NMR (400 MHz, $CDCl_3$) δ 11.63 (br d, *J* = 12.0 Hz, 1H, N*H*), 7.15 (dd, *J* = 12.0, 7.6 Hz, 1H, *Hc*), 7.01-6.97 (m, 2H, Ar*H*), 6.90-6.86 (m, 2H, Ar*H*), 5.26, (d, *J* = 7.6 Hz, 1H, *Hb*), 3.80 (s, 3H, *Hf*), 2.15 (s, 3H, *Ha*) ppm (addition of D_2O caused the signal at δ 11.63 to disappear, and the signal at δ 7.15 to change to a d, *J* = 7.6 Hz); ^{13}C NMR (101 MHz, $CDCl_3$) δ 198.5 (s, *Cg*), 156.3 (s, *Ci*), 144.2 (d, *Cc*), 134.2 (s, *Ch*), 117.8 (d, Ar), 115.1 (d, Ar), 96.7 (d, *Cb*), 55.7 (d, *Cf*), 29.5 (d, *Ca*); IR ν_{max} (thin film) 1636 (C=O), 1597, 1569, 1513, 1479 cm^{-1}; LRMS (TOF ES-), 190.2 (100%) $[M–H]^-$, 175.1 (25%); HRMS (TOF ES-), calculated for $C_{11}H_{13}NO_2–H^+$, 190.0868; found 190.0871. All spectroscopic and analytical properties were identical to those reported in the literature.[255]

Alternate procedure:
To *p*-anisidine (0.123 g, 1 mmol) in CH_2Cl_2 (1 mL) was added 4-methoxy-3-buten-2-one (0.102 mL, 1 mmol). The reaction mixture was stirred at rt for 24 h and concentrated *in vacuo* to afford **389** as an off-colourless solid (0.190 g, 99%).

4,4-Dimethoxybutan-2-one[256]

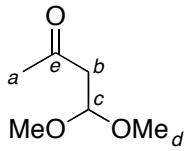

390

To **324** (0.145 g, 1.0 mmol) in MeOH (0.5 mL) was added 4-methoxy-3-buten-2-one (0.255 mL, 2.5 mmol) and $Sc(OTf)_3$ (0.049 g, 0.1 mmol). The reaction mixture was flushed with argon and stirred at rt for 2 days, washed with sat. (aq) $NaHCO_3$ (5 mL) and extracted with CH_2Cl_2 (3 × 7 mL). The combined organics were dried ($MgSO_4$) and concentrated *in vacuo*. Purification by silica gel chromatography (1:9, EtOAc:diethyl ether, to EtOAc, as eluent) afforded **390** as a yellow oil (0.049 g, 20%): R_f. 0.54 (1:1, EtOAc:hexane, as eluent); ^1H NMR (700 MHz, $CDCl_3$) δ 4.77 (td, *J* = 5.6, 2.6 Hz, 1H, *Hc*), 3.35 (d, *J* = 2.6 Hz, 6H, *Hd*$_3$), 2.73 (dd, *J* = 5.6, 2.6 Hz, 2H, *Hb*), 2.17 (d, *J* = 2.6 Hz, 3H, *Ha*) ppm; ^{13}C NMR (176 MHz, $CDCl_3$) δ 205.6 (s, *Ce*), 101.6 (d, *Cc*), 53.9 (d, *Cd*), 47.4 (t, *Cb*), 31.2 (d, *Ca*); IR ν_{max} (thin film) 2938,

2833, 1711 (C=O), 1357 cm^{-1}. All spectroscopic and analytical properties were identical to those reported in the literature.[257]

1,1'-(1-Benzyl-4-(4-nitrophenyl)-1,4-dihydropyridine-3,5-diyl)diethanone

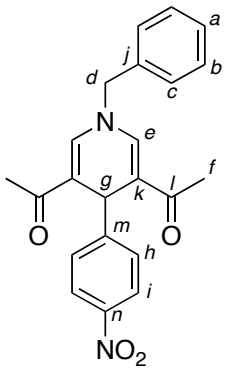

392

To *p*-nitrobenzaldehyde (0.151 g, 1 mmol) in CH_2Cl_2 (1 mL) was added 4-methoxy-3-buten-2-one (0.204 mL, 2 mmol), benzylamine (0.109 mL, 1 mmol) and $Sc(OTf)_3$ (0.049 g, 0.1 mmol) and the mixture was left to stir at rt for 11 d. Purification by silica gel chromatography (1:1, petroleum ether:diethyl ether, to 1:1, diethyl ether:CH_2Cl_2, as eluent) afforded **392** as a yellow solid (0.322 g, 86 %): m.p. 184-185 °C; R_f. 0.16 (2:1, EtOAc:hexane, as eluent); ^{1}H NMR (600 MHz, $CDCl_3$) δ 8.03-8.01 (m, 2H, *Hh*), 7.48-7.45 (m, 2H, *Hb*), 7.44-7.41 (m, 3H, *Ha* + *Hi*), 7.32-7.29 (m, 2H, *Hc*), 7.24 (s, 2H, *He*), 5.29 (s, 1H, *Hm*), 4.72 (s, 2H, *Hd*), 2.13 (s, 6H, *Hf*) ppm; ^{13}C NMR (151 MHz, $CDCl_3$) δ 194.4 (s, *Cl*), 153.0 (s, *Cm*), 146.4 (s, *Cn*), 139.0 (d, *Ce*), 135.4 (s, *Cj*), 129.6 (d, *Cb*), 129.2 (d, *Ci*), 129.1 (d, *Ca*), 127.3 (d, *Cc*), 123.5 (d, *Ch*), 119.0 (s, *Ck*), 58.8 (t, *Cd*), 35.8 (d, *Cg*), 25.2 (d, *Cf*); IR ν_{max} (thin film) 1651, 1624 (C=O), 1573, 1368, 1349 cm^{-1}; LRMS (TOF ES399.236 (100%) $[M+Na]^+$, 377.280 (25%) $[M+H]^+$; HRMS (TOF ES+), calculated for $C_{22}H_{20}N_2O_4+H^+$, 377.14958; observed 377.14939; *Anal.* calcd: C, 70.20, H, 5.36, N, 7.44, found: C, 70.13, H, 5.37, N, 7.48.

1,1'-(1-Benzyl-4-phenyl-1,4-dihydropyridine-3,5-diyl)diethanone[258]

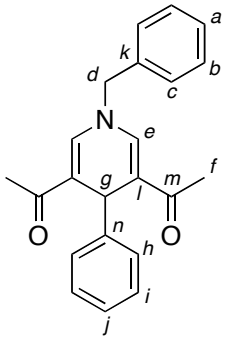

393

To benzaldehyde (0.106 g, 1 mmol) in CH_2Cl_2 (1 mL) was added 4-methoxy-3-buten-2-one (0.204 mL, 2 mmol), benzylamine (0.109 mL, 1 mmol) and $Sc(OTf)_3$ (0.049 g, 0.1 mmol) and the reaction mixture was left to stir at rt for 10 d. Purification by silica gel chromatography (diethyl ether, as eluent) afforded **393** as a yellow solid (0.194 g, 59 %): m.p. 136-137 °C (lit. 136-137 °C)[258]; R_f. 0.23 (2:1, EtOAc:hexane, as eluent); ^{1}H NMR (600 MHz, $CDCl_3$) δ 7.45-7.42 (m, 2H, *Hb*), 7.41-7.38 (m, 1H, *Ha*), 7.30-7.27 (m, 4H, *Hh* + *Hc*), 7.22-7.19 (m, 2H, *Hi*), 7.19 (s, 2H, *He*), 7.13-7.10 (m, 1H, *Hj*), 5.19 (s, 1H, *Hg*), 4.68 (s, 2H, *Hd*), 2.12 (s, 6H, *Hf*) ppm; ^{13}C NMR (151 MHz, $CDCl_3$) δ 195.3 (s, *Cm*), 145.7 (s, *Cn*), 138.2 (d, *Ce*), 135.8 (s, *Ck*), 129.5 (d, *Cb*), 128.8 (d, *Ca*), 128.4 (d, *Ch*), 128.4 (d, *Ci*), 127.3 (d, *Cc*), 126.6 (d, *Cj*), 119.7 (s, *Cl*), 58.8 (t, *Cd*), 35.9 (d, *Cg*), 25.7 (d, *Cf*); IR ν_{max} (thin film) 1628 (C=O), 1565, 1453, 1412, 1366 cm^{-1}; LRMS (TOF ES+), 354.3 (100%) $[M+Na]^+$, 332.3 (30%) $[M+H]^+$; HRMS (TOF ES+), calculated for $C_{22}H_{21}NO_2+H^+$, 332.16451; observed 332.16440; *Anal.* calcd: C, 79.73, H, 6.39, N, 4.23, found: C, 78.84, H, 6.32, N, 4.08.

1,1'-(1-Benzyl-4-(4-methoxyphenyl)-1,4-dihydropyridine-3,5-diyl)diethanone

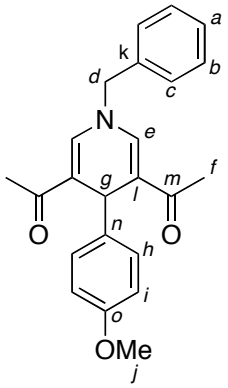

394

To anisaldehyde (0.136 g, 1 mmol) in CH_2Cl_2 (1 mL) was added 4-methoxy-3-buten-2-one (0.204 mL, 2 mmol), benzylamine (0.109 mL, 1 mmol) and $Sc(OTf)_3$ (0.049 g, 0.1 mmol) and the reaction mixture was left to stir at rt for 13 d. Purification by silica gel chromatography (1:1, petroleum ether:diethyl ether, to diethyl ether, as eluent) afforded **394** as a yellow solid (0.212 g, 59 %): m.p. 172-173 °C; R_f. 0.21 (2:1, EtOAc:hexane, as eluent); ^{1}H NMR (600 MHz, $CDCl_3$) δ 7.45-7.42 (m, 2H, *Hc*), 7.40-7.37 (m, 1H, *Ha*), 7.30-7.27 (m, 2H, *Hb*), 7.20-1.18 (m, 2H, *Hi*), 7.18 (s, 2H, *He*), 6.75-6.72 (m, 2H, *Hh*), 5.13 (s, 1H, *Hg*), 4.66 (s, 2H, *Hd*), 3.73 (s, 3H, *Hj*), 2.12 (s, 6H, *Hf*) ppm; ^{13}C NMR (151 MHz, $CDCl_3$) δ 195.3 (s, *Cm*), 158.2 (s, *Co*), 138.3 (s, *Cn*), 138.0 (s, *Ck*), 135.8 (d, *Ce*), 129.4 (d, *Ci*), 129.3 (d, *Cc*), 128.8 (d, *Ca*), 127.3 (d, *Cb*), 119.8 (s, *Cl*), 113.7 (d, *Ch*), 58.7 (t, *Cd*), 55.3 (d, *Cj*), 35.0 (d, *Cg*), 25.7 (d, *Cf*); IR ν_{max} (thin film) 1630 (C=O), 1565, 1511, 1412, 1366 cm^{-1}; LRMS (TOF ES+), 384.3 (100%) $[M+Na]^+$, 254.3 (30%); HRMS (TOF ES+), calculated for $C_{23}H_{23}NO_3+H^+$, 362.17507; observed 362.17507; *Anal.* calcd: C, 76.43, H, 6.41, N, 3.88, found: C, 75.38, H, 6.35, N, 3.75.

1,1'-(1-Benzyl-4-ethyl-1,4-dihydropyridine-3,5-diyl)diethanone

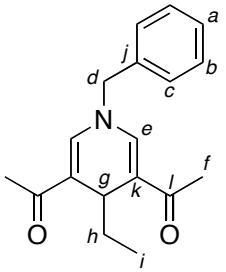

396

To propionaldehyde (0.058 g, 1 mmol) in CH_2Cl_2 (1 mL) was added 4-methoxy-3-buten-2-one (0.204 mL, 2 mmol), benzylamine (0.109 mL, 1 mmol) and $Sc(OTf)_3$ (0.049 g, 0.1 mmol) and the reaction mixture was left to stir at rt for 19 d. Purification by silica gel chromatography (1:1, petroleum ether:diethyl ether, to diethyl ether, to EtOAc, as eluent) afforded a mixture of the vinylagous amide as an orange oil (0.049 g, 28%) and **396** as a yellow oil (0.036 g, 13 %): R_f. 0.22 (2:1, EtOAc:hexane, as eluent); ^{1}H NMR (600 MHz, $CDCl_3$) δ 7.42-7.39 (m, 2H, *Hb*), 7.37-7.34 (m, 1H, *Ha*), 7.24-7.22 (m, 2H, *Hc*), 7.11 (s, 2H, *He*), 4.58 (2, 2H, *He*), 4.16 (t, *J* = 4.9 Hz, 1H, *Hg*), 2.22 (s, 6H, *Hf*), 1.37 (qd, *J* = 7.5, 4.9 Hz, 2H, *Hh*), 0.69 (t, *J* = 7.5 Hz, 3H, *Hi*) ppm; ^{13}C NMR (151 MHz, $CDCl_3$) δ 195.6 (s, *Cl*), 139.7 (d, *Ce*), 135.9 (s, *Cj*), 129.4 (d, *Cb*), 128.6 (d, *Ca*), 127.2 (d, *Cc*), 118.7 (s, *Ck*), 58.6 (t, *Cd*), 30.3 (d, *Cg*), 28.1 (t, *Ch*), 25.4 (d, *Cf*), 9.1 (d, *Ci*); IR ν_{max} (thin film) 1632 (C=O), 1567, 1384 cm^{-1}; LRMS (TOF ES+), 306.324 (100%) $[M+Na]^+$, 284.332 (25%) $[M+H]^+$; HRMS (TOF ES+), calculated for $C_{18}H_{22}NO_2+H^+$, 284.16451; observed 284.16442.

(*Z*)-4-(Benzylamino)but-3-en-2-one[259]

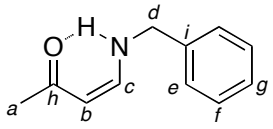

397

To benzylamine (0.019 mL, 1 mmol) in $CHCl_3$ (0.5 mL) was added 4-methoxy-3-buten-2-one (0.12 mL, 1 mmol). The reaction mixture was stirred at rt for 1h and

concentrated *in vacuo* to afford **397** as a brown solid (0.174g, 99%): ^{1}H NMR (700 MHz, $CDCl_3$) δ 10.07 (br s, 1H, N*H*), 7.37-7.34 (m, 2H, *Hf*), 7.30-7.28 (m, 1H, *Hg*), 7.26-7.25 (m, 2H, *He*), 6.71 (dd, *J* = 12.7, 7.4 Hz, 1H, *Hc*), 5.06 (d, *J* = 7.4 Hz, 1H, *Hc*), 5.06 (d, *J* = 7.4 Hz, 1H, *Hb*), 4.38 (d, *J* = 6.1 Hz, 2H, *Hd*), 2.08 (s, 3H, *Ha*) ppm (addition of D_2O caused the signal at δ 10.07 to disappear); ^{13}C NMR (176 MHz, $CDCl_3$) δ 197.8 (s, *Ch*), 152.4 (d, *Cc*), 138.1 (s, *Ci*), 128.9 (d, *Cf*), 127.7 (d, *Cg*), 127.2 (d, *Ce*), 94.5 (d, *Cb*), 52.5 (t, *Cd*), 29.1 (d, *Ca*); IR ν_{max} (thin film) 3262, 3029,1637 (C=O), 1562, 1486 cm^{-1}; LRMS (TOF ES+), 176.5 (100%) $[M+H]^+$, 134.2 (90%); HRMS (TOF ES+), calculated for $C_{11}H_{13}NO+H^+$, 176.10699; found 176.10685. All spectroscopic and analytical properties were identical to those reported in the literature.[259]

1,1'-(1-Benzyl-4-(dimethoxymethyl)-1,4-dihydropyridine-3,5-diyl)diethanone

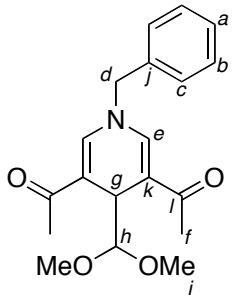

398

To benzylamine (0.109 mL, 1.0 mmol) in CH_2Cl_2 (1 mL) was added 4-methoxy-3-buten-2-one (0.204 mL, 2 mmol), dimethoxyacetaldehyde (0.174 g, 1 mmol) (60% in water) and $Sc(OTf)_3$ (0.049 mg, 0.1 mmol) and the reaction mixture was stirred at rt for 4 days. Purification by silica gel chromatography (1:1, EtOAc:diethyl ether, as eluent) afforded **398** as a yellow solid (0.137 g, 42%): R_f. 0.28 (EtOAc, as eluent); m.p. 142-144 °C; ^{1}H NMR (700 MHz, $CDCl_3$) δ 7.39-7.37 (m, 2H, *Hb*), 7.34-7.32 (m, 1H, *Ha*), 7.28-7.27 (m, 2H, *Hc*), 7.16 (d, *J* = 0.8 Hz, 2H, *He*), 4.65 (s, 2H, *Hd*), 4.49 (dt, *J* = 3.8, 0.8 Hz, *Hg*), 3.99 (d, *J* = 3.8 Hz, 1H, *Hh*), 3.34 (s, 6H, *Hi*), 2.25 (s, 6H, *Hf*) ppm; ^{13}C NMR (176 MHz, $CDCl_3$) δ 195.8 (s, *Cl*), 140.4 (d, *Ce*), 136.2 (s, *Cj*), 129.2 (d, *Cb*), 128.4 (d, *Ca*), 127.0 (d, *Cc*), 114.9 (s, *Ck*), 107.3 (d, *Ch*), 58.7 (t, *Cd*), 56.0 (d, *Ci*), 33.1 (d, *Cg*), 25.3 (d, *Cf*); IR ν_{max} (thin film) 1643 (C=O), 1569

cm^{-1}; LRMS (TOF ES+), 352.2 (100%) $[M+Na]^+$, 298.3 (80%); HRMS (TOF ES+), calculated for $C_{19}H_{23}NO_4+Na^+$, 352.1525; found 352.1526.

1,1'-(4-(4-Nitrophenyl)-1-phenyl-1,4-dihydropyridine-3,5-diyl)diethanone

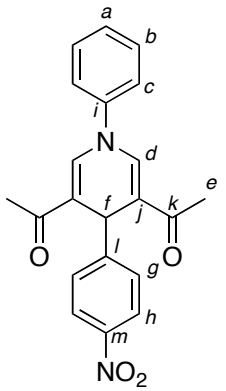

399

To *p*-nitrobenzaldehyde (0.151 g, 1 mmol) in CH_2Cl_2 (1 mL) was added 4-methoxy-3-buten-2-one (0.204 mL, 2 mmol), aniline (0.091 mL, 1 mmol) and $Sc(OTf)_3$ (0.049 g, 0.1 mmol) and the reaction mixture was left to stir at rt for 11 d. Purification by silica gel chromatography (diethyl ether, as eluent) afforded **400** as a yellow solid (0.105 g, 27%) and **399** as a yellow solid (0.113 g, 31%): R_f. 0.34 (2:1, EtOAc:hexane, as eluent); m.p. 217-218 °C; ^{1}H NMR (700 MHz, $CDCl_3$) δ 8.11-8.09 (m, 2H, *Hg*), 7.57 (s, 2H, *Hd*), 7.57-7.53 (m, 4H, *Hc* + *Hh*), 7.44-7.41 (m, 1H, *Ha*), 7.38-7.36 (m, 2H, *Hb*), 5.35 (s, 1H, *Hf*), 2.23 (s, 6H, *He*) ppm; ^{13}C NMR (176 MHz, $CDCl_3$) δ 194.6 (s, *Ck*), 152.7 (s, *Cl*), 146.7 (s, *Cm*), 143.2 (s, *Ci*), 137.5 (d, *Cd*), 130.5 (d, *Cc*), 129.4 (d, *Ch*), 127.7 (d, *Ca*), 123.7 (d, *Cg*), 121.8 (d, *Cb*), 120.4 (s, *Cj*), 36.1 (d, *Cf*), 25.4 (d, *Ce*); IR ν_{max} (thin film) 1644 (C=O), 1594, 1572, 1512, 1495, 1345 cm^{-1}; LRMS (TOF ES+), 385.3 (53%) $[M+Na]^+$, 363.3 (15%), $[M+H]^+$; HRMS (TOF ES+), calculated for $C_{21}H_{18}N_2O_4+H^+$, 363.13393; observed 363.13485.

1,1'-(2-Methoxy-4-(4-nitrophenyl)-1-phenyl-1,2,3,4-tetrahydropyridine-3,5-diyl)diethanone

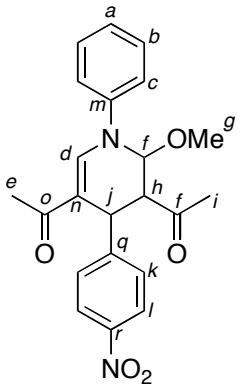

400

To *p*-nitrobenzaldehyde (0.151 g, 1 mmol) in CH_2Cl_2 (1 mL) was added 4-methoxy-3-buten-2-one (0.204 mL, 2 mmol), aniline (0.091 mL, 1 mmol) and $Sc(OTf)_3$ (0.049 g, 0.1 mmol) and the reaction mixture was left to stir at rt for 11 d. Purification by silica gel chromatography (diethyl ether, as eluent) afforded **399** as a yellow solid (0.113 g, 31%) and **400** as a yellow solid (0.105 g, 27%): R_f. 0.26 (2:1, EtOAc:hexane, as eluent); m.p. 195-198 °C; ^{1}H NMR (700 MHz, $CDCl_3$) δ 8.14-8.12 (m, 2H, *Hk*), 7.84 (s, 1H, *Hd*), 7.44-7.41 (m, 4H, *Hc* + *Hl*), 7.32-7.31 (m, 2H, *Hb*), 7.28-7.26 (m, 1H, *Ha*), 5.22-5.21 (m, 1H, *Hf*), 4.71 (br s, 1H, *Hj*), 3.41-3.40 (m, 1H, *Hh*), 2.80 (s, 3H, *Hg*), 2.32 (s, 3H, *Hi*), 2.30 (s, 3H, *He*) ppm; ^{13}C NMR (176 MHz, $CDCl_3$) δ 205.2 (s, *Cp*), 194.0 (s, *Co*), 150.6 (s, *Cq*), 146.5 (s, *Cr*), 145.8 (s, *Cm*), 144.0 (d, *Cd*), 130.0 (d, *Cc*), 128.6 (d, *Cl*), 126.2 (d, *Ca*), 123.5 (d, *Ck*), 121.7 (d, *Cb*), 111.5 (s, *Cn*), 87.2 (d, *Cf*), 55.0 (d, *Cg*), 53.9 (d, *Ch*), 35.4 (d, *Cj*), 28.3 (d, *Ci*), 24.6 (d, *Ce*); IR ν_{max} (thin film) 1709, 1613 (C=O), 1591, 1512, 1494, 1323 cm^{-1}; LRMS (TOF ES+), 417.2 (100%) $[M+Na]^+$, 395.2 (18%), $[M+H]^+$; HRMS (TOF ES+), calculated for $C_{22}H_{22}N_2O_5+H^+$, 395.1607; observed 395.1620.

(*Z*)-4-(Phenylamino)but-3-en-2-one[260]

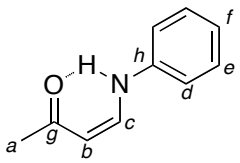

402

To pivalaldehyde (0.086 g, 1 mmol), in CH_2Cl_2 (1 mL), was added 4-methoxy-3-buten-2-one (0.204 mL, 2 mmol), aniline (0.091 mL, 1 mmol) and $Sc(OTf)_3$ (0.049 g, 0.1 mmol) and the reaction mixture was left to stir at rt for 14 d. Purification by silica gel chromatography (1:1, petroleum ether:diethyl ether, to diethyl ether, as eluent) afforded **402** as a beige solid (0.075 g, 45 %): R_f. 0.44 (2:1, EtOAc:hexane, as eluent); ^{1}H NMR (700 MHz, $CDCl_3$) δ 11.58 (br s, 1H, N*H*), 7.32-7.30 (m, 2H, *Hd*), 7.22 (dd, *J* = 12.3, 7.7 Hz, 1H, *Hc*), 7.06-7.02 (m, 3H, *Hf* + *He*), 5.30 (d, *J* = 7.7 Hz, 1H, *Hb*), 2.16 (s, 3H, *Ha*) ppm (addition of D_2O caused the signal at δ 11.58 to disappear); ^{13}C NMR (176 MHz, $CDCl_3$) δ 199.0 (s, *Cg*), 143.2 (d, *Cc*), 140.5 (s, *Ch*), 129.8 (d, *Cd*), 123.5 (d, *Cf*), 116.2 (d, *Ce*), 97.6 (d, *Cb*), 29.7 (d, *Ca*); IR ν_{max} (thin film) 1639 (C=O), 1596, 1568, 1477 cm^{-1}; LRMS (TOF ES-), 160.2 (50%) $[M-H]^-$, 149.0 (100%); HRMS (TOF ES-), calculated for $C_{10}H_{10}NO$, 160.07679; found 160.07690. All spectroscopic and analytical properties were identical to those reported in the literature.[261]

1,1'-(1-Allyl-4-(4-nitrophenyl)-1,4-dihydropyridine-3,5-diyl)diethanone

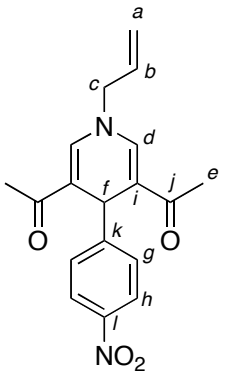

403

To allylamine (0.075 mL, 1 mmol) in CH_2Cl_2 (1 mL) was added 4-methoxy-3-buten-2-one (0.204 mL, 2 mmol), *p*-nitrobenzaldehyde (0.151 g, 1 mmol) and $Sc(OTf)_3$ (0.049 g, 0.1 mmol) and the reaction mixture was left to stir at rt for 8 d. Purification by silica gel chromatography (1:1 to 4:1, EtOAc:Hexane, as eluent) afforded **403** as a yellow solid (0.201 g, 62%): m.p. 106-107 °C; R_f. 0.28 (EtOAc, as eluent); ^{1}H NMR (700 MHz, $CDCl_3$) δ 8.06-8.04 (m, 2H, *Hg*), 7.47-7.45 (m, 2H, *Hh*), 7.16 (s, 2H, *Hd*), 6.00 (ddt, *J* = 17.1, 10.3, 5.6 Hz, 1H, *Hb*), 5.43-5.41 (m, 1H, Ha_{trans}), 5.38 (dtd, *J* =

17.1, 1.6, 0.8 Hz, 1H, *Ha*$_{cis}$), 5.27 (s, 1H, *Hf*), 4.15 (dt, *J* = 5.6, 1.6 Hz, 2H, *Hc*), 2.15 (s, 6H, *He*) ppm; ^{13}C NMR (176 MHz, $CDCl_3$) δ 194.4 (s, *Cj*), 153.2 (s, *Ck*), 146.4 (s, *Cl*), 138.9 (d, *Cd*), 132.2 (d, *Cb*), 129.2 (d, *Ch*), 123.5 (d, *Cg*), 119.9 (t, *Ca*), 118.8 (s, *Ci*), 57.4 (t, *Cc*), 35.9 (d, *Cf*), 25.2 (d, *Ce*); IR ν_{max} (thin film) 1632 (C=O), 1597, 1513, 1368, 1341 cm^{-1}; LRMS (TOF ES+), 349.2 (100%) $[M+Na]^+$, 327.3 (40%) $[M+H]^+$; HRMS (TOF ES+), calculated for $C_{18}H_{18}N_2O_4+H^+$, 327.13393; observed 327.13509.

1,1'-(1-Allyl-4-(4-methoxyphenyl)-1,4-dihydropyridine-3,5-diyl)diethanone

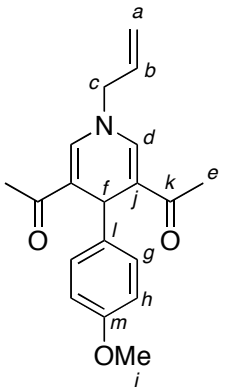

404

To allylamine (0.075 mL, 1 mmol) in CH_2Cl_2 (1 mL) was added 4-methoxy-3-buten-2-one (0.204 mL, 2 mmol), anisaldehyde (0.122 mL, 1 mmol) and $Sc(OTf)_3$ (0.049 g, 0.1 mmol) and the reaction mixture was left to stir at rt for 8 d. Purification by silica gel chromatography (1:1 to 4:1, EtOAc:Hexane, as eluent) afforded **404** as a yellow oil (0.107 g, 34%): R_f. 0.35 (EtOAc, as eluent); ^{1}H NMR (700 MHz, $CDCl_3$) δ 7.22-7.20 (m, 2H, *Hh*), 7.11 (s, 2H, *Hd*), 6.77-6.75 (m, 2H, *Hg*), 5.93 (ddt, *J* = 17.1, 10.3, 5.6 Hz, 1H, *Hb*), 5.39-5.37 (m, 1H, *Ha*$_{trans}$), 5.35 (dtd, *J* = 17.1, 1.6, 0.8 Hz, *Ha*$_{cis}$), 5.11 (s, 1H, *Hf*), 4.08 (dt, *J* = 5.6, 1.6 Hz, 2H, *Hc*)3.73 (s, 3H, *Hi*), 2.14 (s, 6H, *He*) ppm; ^{13}C NMR (176 MHz, $CDCl_3$) δ 195.3 (s, *Ck*), 158.2 (s, *Cm*), 138.4 (s, *Cl*), 137.8 (d, *Cd*), 132.5 (d, *Cb*), 129.3 (d, *Ch*), 119.7 (s, *Cj*), 119.5 (t, *Ca*), 113.7 (d, *Cg*), 57.3 (t, *Cc*), 55.3 (d, *Ci*), 35.0 (d, *Cf*), 25.7 (d, *C*e); IR ν_{max} (thin film) 1638 (C=O), 1568, 1508, 1370 cm^{-1}; LRMS (TOF ES+), 334.3 (100%) $[M+Na]^+$, 204.2 (89%), 126.2 (24%); HRMS (TOF ES+), calculated for $C_{19}H_{21}NO_3+Na^+$, 334.14136; observed 334.14133.

1,1'-(4-Ethyl-1-methyl-1,4-dihydropyridine-3,5-diyl)diethanone

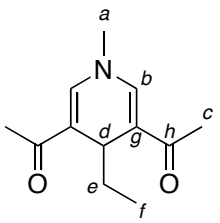

406

To propionaldehyde (0.058 g, 1 mmol) in CH_2Cl_2 (1 mL) was added 4-methoxy-3-buten-2-one (0.204 mL, 2 mmol), methylamine (0.044 mL, 1 mmol) and $Sc(OTf)_3$ (0.049 g, 0.1 mmol) and the reaction mixture was left to stir at rt for 20 d. Purification by silica gel chromatography (1:1, EtOAc:hexane, to EtOAc, as eluent) afforded **376** (0.017 g, 12%) and **406** as a yellow solid (0.057 g, 28 %): m.p. 182-183 °C; R_f. 0.10 (2:1, EtOAc:hexane, as eluent); ^{1}H NMR (400 MHz, $CDCl_3$) δ 7.02 (d, J = 0.5 Hz, 2H, *Hb*), 4.12 (t, J = 4.9 Hz, 1H, *Hd*), 3.24 (s, 3H, *Ha*), 2.25 (s, 6H, *Hc*), 3.53 (qd, J = 7.5, 4.9 Hz, 2H, *He*), 0.68 (t, J = 7.5 Hz, 3H, *Hf*); ^{13}C NMR (101 MHz, $CDCl_3$) δ 195.5 (s, *Ch*), 140.3 (d, *Cb*), 118.4 (s, *Cg*), 41.9 (d, *Ca*), 30.0 (d, *Cd*), 28.2 (t, *Ce*), 25.4 (d, *Cc*), 9.0 (d, *Cf*); IR ν_{max} (thin film) 2960, 1626 (C=O), 1564, 1366 cm^{-1}; LRMS (TOF ES+), 334.3 (100%) $[M+Na]^+$, 204.2 (89%), 126.2 (24%); HRMS (TOF ES+), calculated for $C_{12}H_{17}NO_2+H^+$, 208.1338; observed 208.1338; *Anal.* calcd: C, 69.54, H, 8.27, N, 6.76, found: C, 69.64, H, 8.30, N, 6.62.

(*Z*)-4-(*tert*-Butylamino)but-3-en-2-one[262]

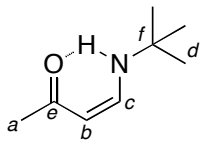

407

To propionaldehyde (0.058 g, 1 mmol) in CH_2Cl_2 (1 mL) was added 4-methoxy-3-buten-2-one (0.204 mL, 2 mmol), *tert*-butylamine (0.105 mL, 1 mmol) and $Sc(OTf)_3$ (0.049 g, 0.1 mmol) and the reaction mixture was left to stir at rt for 17 d. Purification by silica gel chromatography (1:1, petroleum ether:diethyl ether, to diethyl ether, to

EtOAc, as eluent) afforded **407** as a beige solid (0.141 g, 99%): R_f. 0.44 (2:1, EtOAc:hexane, as eluent); ^{1}H NMR (400 MHz, $CDCl_3$) δ 10.13 (br s, 1H, N*H*), 6.8 (dd, *J* = 13.3, 7.4 Hz, 1H, *Hc*), 4.98 (d, *J* = 7.4 Hz, 1H, *Hb*), 2.02 (s, 3H, *Ha*), 1.27 (s, 9H, *Hd*) ppm (addition of D_2O caused the signal at δ 10.13 to disappear); ^{13}C NMR (101 MHz, $CDCl_3$) δ 1970 (s, *Ce*), 148.2 (d, *Cc*), 93.5 (d, *Cb*), 51.9 (s, *Cf*), 30.2 (d, *Cd*), 29.1 (d, *Ca*); IR ν_{max} (neat) 2971, 1631 (C=O), 1555, 1484 cm^{-1}; LRMS (TOF ES+), 164.2 (100%) $[M+Na]^+$, 142.2 (34%) $[M+H]^+$; HRMS (TOF ES+), calculated for $C_8H_{15}NO+Na^+$, 164.10459; observed 164.10442. All spectroscopic and analytical properties were identical to those reported in the literature.[262]

1,1'-(1-(*tert*-Butyl)-4-(4-nitrophenyl)-1,4-dihydropyridine-3,5-diyl)diethanone

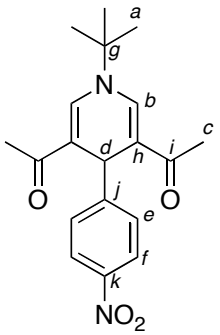

408

To 4-methoxy-3-buten-2-one (0.204 mL, 2 mmol) and *tert*-butylamine (0.105 mL, 1 mmol) in toluene (1 mL) was added $Sc(OTf)_3$ (0.049 g, 0.1 mmol) and *p*-nitrobenzaldehyde (0.151 g, 1 mmol) and the reaction mixture was left to stir at 60 ºC for 7 d. Purification by silica gel chromatography (4:1, hexane:EtOAc, to 2:1, EtOAc:hexane, as eluent) afforded **409** as an orange solid (0.246 g, 59%) and **408** as a yellow oil (0.103 g, 30%): R_f. 0.23 (2:1, EtOAc:hexane, as eluent); ^{1}H NMR (600 MHz, $CDCl_3$) δ 8.06-8.04 (m, 2H, *He*), 7.51 (s, 2H, *Hb*), 7.43-7.40 (m, 2H, *Hf*), 5.27 (s, 1H, *Hd*), 2.18 (s, 6H, *Hc*), 1.55 (s, 9H, *Ha*) ppm; ^{13}C NMR (151 MHz, $CDCl_3$) δ 194.6 (s, *Ci*), 153.2 (s, *Cj*), 146.4 (s, *Ck*), 135.5 (d, *Cb*), 129.0 (d, *Cf*), 123.5 (d, *Ce*), 118.8 (s, *Ch*), 58.4 (s, *Ch*), 36.0 (d, *Cd*), 29.5 (d, *Ca*), 25.3 (d, *Cc*); IR ν_{max} (thin film) 1636 (C=O), 1561, 1513, 1372, 1340 cm^{-1}; LRMS (TOF ES+), 343.3 (35%) $[M+H]^+$; HRMS (TOF ES+), calculated for $C_{19}H_{22}N_2O_4+Na^+$, 365.1477; observed 365.1460.

(3*Z*,5*Z*)-3,5-Bis((*tert*-butylamino)methylene)-4-(4-nitrophenyl)heptane-2,6-dione

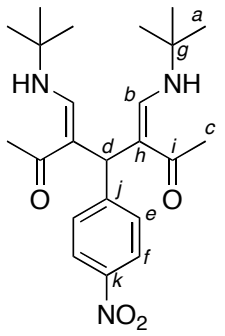

409

To 4-methoxy-3-buten-2-one (0.204 mL, 2 mmol) and *tert*-butylamine (0.105 mL, 1 mmol) in toluene (1 mL) was added $Sc(OTf)_3$ (0.049 g, 0.1 mmol) and *p*-nitrobenzaldehyde (0.151 g, 1 mmol) and the reaction mixture was left to stir at 60 ºC for 7 d. Purification by silica gel chromatography (4:1, hexane:EtOAc, to 2:1, EtOAc:hexane, as eluent) afforded **408** as an orange solid (0.103 g, 30%) and **409** as an orange solid (0.246 g, 59%): m.p. 151-153 °C; R_f. 0.39 (2:1, EtOAc:hexane, as eluent); ^{1}H NMR (700 MHz, $CDCl_3$) δ 7.98-7.96 (m, 2H, *Hf*), 7.63 (d, *J* = 14.2 Hz, 2H, *Hb*), 7.13-7.11 (m, 2H, *He*), 5.54 (s, 1H, *Hd*), 2.18 (br s, 6H, *Hc*), 1.20 (br s, 18H, *Ha*) ppm; ^{13}C NMR (176 MHz, $CDCl_3$) δ 193.7 (br s, *Ci*), 149.5 (s, *Cj*), 148.2 (s, *Ck*), 145.5 (d, *Ce*), 127.8 (d, *Cb*), 122.9 (d, *Cf*), 109.7 (s, *Ch*), 52.8 (s, *Cg*), 35.3 (d, *Cd*), 30.0 (d, *Ca*), 24.5 (br d, *Cc*); IR ν_{max} (thin film) 2970, 1636 (C=O), 1571, 1511, 1490, 1369, 1339, 1321 cm^{-1}; LRMS (ASAP), 416.3 (62%) $[M+H]^+$, 275.1 (100%), 142.1 (32%); HRMS (TOF ES+), calculated for $C_{22}H_{33}N_3O_4+H^+$, 416.2544; observed 416.2545.

1,1'-(1-(4-Methoxyphenyl)-4-(4-nitrophenyl)-1,4-dihydropyridine-3,5-diyl)diethanone

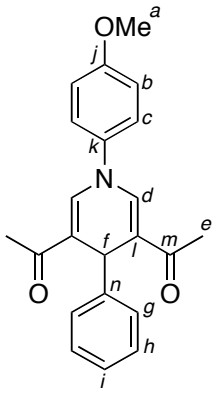

410

To 4-methoxy-3-buten-2-one (0.204 mL, 2 mmol) in $CDCl_3$ (1 mL) was added *p*-anisidine (0.123 g, 1 mmol), $Sc(OTf)_3$ (0.049 g, 0.1 mmol) and benzaldehyde (0.102 mL, 1 mmol). The reaction mixture was stirred at rt for 10 days. Purification by silica gel chromatography (1:1-2:1, diethyl ether/hexane, as eluent) afforded a 2:1 mixture of **410** and the MeOH adduct (0.156 g, 39%). Leaving this in solution ($CDCl_3$) for a month followed by concentration *in vacuo* afforded pure **410** as a yellow solid: R_f. 0.25 (diethyl ether, as eluent); ^{1}H NMR (700 MHz, $CDCl_3$) δ 7.45 (s, 2H, *Hd*), 7.38-7.26 (m, 2H, *Hh*), 7.28-7.26 (m, 2H, *Hb*), 7.26-7.23 (m, 2H, *Hg*), 7.15-7.12 (m, 1H, *Hi*), 7.02-6.99 (m, 2H, *Hc*), 5.23 (s, 1H, *Hf*), 3.86 (s, 3H, *Ha*), 2.18 (s, 6H, *He*) ppm; ^{13}C NMR (176 MHz, $CDCl_3$) δ 195.4 (s, *Cm*), 158.8 (s, *Cj*), 145.7 (s, *Cn*), 137.2 (d, *Cd*), 136.8 (s, *Ck*), 128.4 (d, *Cg*), 128.4 (d, *Ch*), 126.7 (d, *Ci*), 123.7 (d, *Cb*), 120.5 (s, *Cl*), 115.3 (d, *Cc*), 55.8 (d, *Ca*), 35.9 (d, *Cf*), 25.7 (d, *Ce*); LRMS (TOF ES+), 370.3 (100%) $[M+Na]^+$, 348.3 (20%) $[M+H]^+$; HRMS (TOF ES+), calculated for $C_{22}H_{21}NO_3+H^+$, 348.1600; found 348.1598.

4-Phenyl-3,4,6,7-tetrahydro-1*H*-pyrido[2,1-*a*]isoquinolin-2(11b*H*)-one

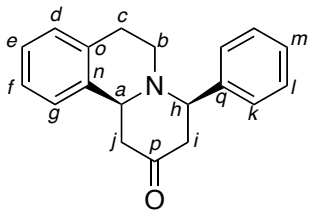

431

To **243** (0.0655 g, 0.5 mmol) in $CHCl_3$ (0.5 mL) was added 4-phenyl-3-buten-2-one (0.264 mL, 1.25 mmol) and $Sc(OTf)_3$ (0.025 g, 0.05 mmol). The reaction mixture was stirred at rt for 3 days and concentrated *in vacuo*. Purification by silica gel chromatography (3% to 10%, EtOAc:hexane, as eluent) afforded a mixture of 4-phenyl-3-buten-2-one and **431** as a colourless oil (0.265 g). A sample of this mixture (0.1 g) was purified by reverse phase HPLC (20% - 100%, H_2O:MeCN, with 1% TFA, as eluent) to give a colourless oil. This was neutralised with $NaHCO_3$ (to pH = 8), and extracted with CH_2Cl_2 (2 × 10 mL). The combined organics were dried ($MgSO_4$) and concentrated *in vacuo* to afford **431** as an off-colourless oil (0.032 g, 61%): R_f. 0.39 (1:3, EtOAc:hexane, as eluent); ^{1}H NMR (700 MHz, $CDCl_3$) δ 7.43-7.39 (m, 4H, *Hk*+*l*), 7.34-7.32 (m, 1H, *Hm*), 7.22-7.18 (m, 2H, *Hf*+*e*), 7.16 (d, *J* = 7.5 Hz, 1H, *Hg*), 7.13 (d, *J* = 7.5 Hz, 1H, *Hd*), 3.87 (d, *J* = 11.6 Hz, 1H, *Ha*), 3.65 (dd, *J* = 11.6, 3.5 Hz, 1H, *Hh*), 3.08 (dt, *J* = 14.1, 2.7 Hz, 1H, *Hj*), 3.05-2.99 (m, 2H, *Hc*+*Hb*), 2.76 (dd, *J* = 14.1, 12.2 Hz, 1H, *Hi*), 2.71 (dd, *J* = 14.1, 12.2 Hz, 1H, *Hj*), 2.64-2.60 (m, 2H, *Hc*+*Hi*), 2.24 (dd, *J* = 12.2, 4.4 Hz, 1H, *Hb*) ppm; ^{13}C NMR (176 MHz, $CDCl_3$) δ 207.6 (s, *Cp*), 142.5 (s, *Cq*), 137.2 (s, *Co*), 135.1 (s, *Cn*), 129.1 (d, *Ck*), 129.0 (d, *Cd*), 127.9 (d, *Cm*), 127.4 (d, *Cl*), 126.7 (d, *Cf*), 126.3 (d, *Ce*), 125.1 (d, *Cg*), 68.5 (s, *Ch*), 62.6 (d, *Ca*), 50.1 (t, *Ci*), 47.6 (t, *Cj*), 47.3 (t, *Cb*), 30.0 (t, *Cc*); IR ν_{max} (thin film) 2807, 1718 (C=O) cm^{-1}; LRMS (TOF ES+), 310.3 (100%), 278.3 (80%) $[M+H]^+$, 276.3 (60%); HRMS (TOF ES+), calculated for $C_{19}H_{19}NO+H^+$, 278.1545; found 278.1539.

2-(3-Oxobutyl)-3,4-dihydroisoquinolin-2-ium trifluoromethanesulfonate

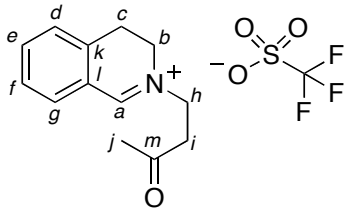

432

To **243** (0.131 g, 1.0 mmol) and $Yb(OTf)_3$ (0.124 g, 0.2 mmol) in CH_2Cl_2 (1.5 mL) under argon was added methyl vinyl ketone (0.162 mL, 2 mmol). The reaction mixture was stirred at rt overnight and concentrated *in vacuo*. Purification by silica gel chromatography (1:1, EtOAc:hexane, to 100%, EtOAc, as eluent) afforded **433** as a white solid (0.051 g, 25%) and **432** as a yellow oil (0.128 g, 37%): R_f. 0.23 (1:1, EtOAc:methanol, as eluent); ^{1}H NMR (700 MHz, $CDCl_3$) δ 9.18 (br s, 1H, *Ha*), 7.87 (dd, *J* = 7.6, 1.1 Hz, 1H, *Hg*), 7.72 (td, *J* = 7.6, 1.1 Hz, 1H, *Hf*), 7.47 (td, *J* = 7.6, 1.1 Hz, 1H, *He*), 7.35 (dd, *J* = 7.6, 1.1 Hz, 1H, *Hd*), 4.32 (t, *J* = 6.0 Hz, 2H, *Hh*), 4.14 (t, *J* = 8.1 Hz, 2H, *Hb*), 3.29 (t, *J* = 6.0 Hz, 2H, *Hi*), 3.27 (t, *J* = 8.1 Hz, 2H, *Hc*), 2.23 (s, 3H, *Hj*) ppm; ^{13}C NMR (176 MHz, $CDCl_3$) δ 206.2 (s, *Cm*), 168.2 (d, *Ca*), 138.6 (d, *Cf*), 136.2 (s, *Ck*), 134.8 (d, *Cg*), 128.9 (d, *Ce*), 128.3 (d, *Cd*), 124.6 (s, *Cl*), 55.5 (t, *Ch*), 49.5 (t, *Cb*), 40.4 (t, *Ci*), 30.1 (d, *Cj*), 25.5 (t, *Cc*); IR ν_{max} (thin film) 1714 (C=O), 1661 cm^{-1}; LRMS (TOF ES+), 203.5 (100%) $[M+H]^+$, 201.7 (70%), 132.1 (25%); LRMS (TOF ES-), 149.0 (100%) $[OTf^-]$; HRMS (FTMS ES+) calculated for $C_{13}H_{15}NO+H^+$, 202.12264; found 202.12262; HRMS (FTMS ES-), calculated for $CF_3O_3S^-$, 148.95257; found 148.95217.

3,4,6,7-Tetrahydro-1*H*-pyrido[2,1-*a*]isoquinolin-2(11b*H*)-one[263]

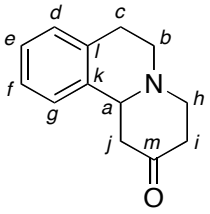

433

To **243** (0.131 g, 1.0 mmol) and $Yb(OTf)_3$ (0.124 g, 0.2 mmol) in CH_2Cl_2 (1.5 mL) under argon was added methyl vinyl ketone (0.162 mL, 2 mmol). The reaction mixture was stirred at rt overnight and concentrated *in vacuo*. Purification by silica gel chromatography (1:1, EtOAc:hexane, to 100% EtOAc, as eluent) afforded **432** as a yellow oil (0.128 g, 37%) and **433** as a white solid (0.051 g, 25%): m.p. 75-77 °C (lit. 76-77 °C)[190]; R_f. 0.18 (EtOAc, as eluent); ^{1}H NMR (600 MHz, $CDCl_3$) δ 7.20-7.13 (m, 3H, *Hd,f,e*), 7.10-7.06 (m, 1H, *Hg*), 3.59 (dd, *J* = 11.9, 3.0 Hz, 1H, *Ha*), 3.28 (ddd, *J* = 10.8, 5.2, 3.0 Hz, 1H, *Hj*), 3.22-3.12 (m, 2H, *Hc,b*), 2.96 (ddd, *J* = 14.6, 3.4, 2.4 Hz, 1H, *Hh*), 2.84-2.80 (m, 1H, *Hc*), 2.75-2.67 (m, 2H, *Hi,j*), 2.63 (td, *J* = 10.6, 3.9 Hz, 1H, *Hb*), 2.50 (ddd, *J* = 14.6, 12.0, 0.9 Hz, 1H, *Hh*), 2.43 (ddd, *J* = 12.0, 3.4, 1.6 Hz, 1H, *Hi*) ppm; ^{13}C NMR (151 MHz, $CDCl_3$) δ 208.7 (s, *Cm*), 136.8 (s, *Ck*), 134.1 (s, *Cl*), 129.1 (d, *Cd*), 126.7 (d, *Cf*), 126.3 (d, *Ce*), 124.9 (d, *Cg*), 61.9 (d, *Ca*), 54.9 (t, *Cj*), 50.8 (t, *Cb*), 47.4 (t, *Ch*), 41.2 (t, *Ci*), 29.9 (t, *Cc*); IR ν_{max} (thin film) 1714 (C=O), 1360 cm^{-1}; LRMS (TOF ES+), 202.2 (100%) $[M+H]^+$; HRMS (FTMS ES+), calculated for $C_{13}H_{15}NO+H^+$, 202.12264; found 202.12264. The enantiomeric ratio of the product was determined by chiral HPLC using OJ-H-Chiralsel column (250 x 4.6 mm), 35 °C, 1 mL/min, 215 nm, hexane:IPA (9:1), t_{R1} = 8.3 min; t_{R2} = 11.9 min. All spectroscopic and analytical properties were identical to those reported in the literature.[219, 264]

4-(3,4-Dihydroisoquinolin-2(1*H*)-yl)butan-2-one[265]

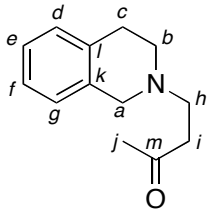

435

To **243** (0.131 g, 1 mmol) in CH_2Cl_2 (1 mL) was added methyl vinyl ketone (0.126 mL, 1.5 mmol) and $In(OTf)_3$ (0.112 g, 0.4 mmol) and the reaction mixture was left to stir at rt. After 4 h, sodium triacetoxyborohydride (0.80 g, 4 mmol) was added to the mixture and this was diluted with CH_2Cl_2 (2 mL) and left to stir over night. The reaction mixture was quenched with water (10 mL), extracted with CH_2Cl_2 (3 ×

10 mL), dried ($MgSO_4$) and concentrated *in vacuo*. Purification by silica gel chromatography (4:1-0:1, hexane:diethylether, as eluent) afforded **433** as a white solid (0.022 g, 11%) and **435** as a cloudy oil (0.069 g, 34%): ^{1}H NMR (400 MHz, $CDCl_3$) δ 7.17-7.06 (m, 3H, *Hd,f,e*), 7.03-6.99 (m, 1H, *Hg*), 3.69 (s, 2H, *Ha*), 2.94-2.84 (m, 4H, *Ha,b*), 2.82-2.75 (m, 4H, *Hh,i*), 2.20 (s, 3H, *Hj*) ppm; ^{13}C NMR (101 MHz, $CDCl_3$) δ 207.6 (s, *Cm*), 133.9 (s, *Ck*), 133.9 (s, *Cl*), 128.8 (d, *Cd*), 126.7 (d, *Cf*), 126.5 (d, *Ce*), 125.9 (d, *Cg*), 55.7 (t, *Ca*), 52.1 (t, *Cb*), 50.7 (t, *Ch*), 41.3 (t, *Ci*), 30.3 (d, *Cj*), 28.5 (t, *Cc*); IR ν_{max} (neat) 2917, 2802, 1710 (C=O), 1357 cm^{-1}; LRMS (TOF ES+), 204.5 (70%) $[M+H]^+$; HRMS (TOF ES+), calculated for $C_{13}H_{17}NO+H^+$, 204.1388; found 204.1409.

1-Allyl-3-cinnamoyl-4-hydroxy-4-methylpiperidin-1-ium trifluoromethanesulfonate

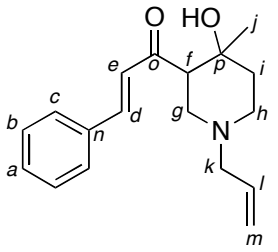

443

To **324** (0.145 g, 1.0 mmol) in $CHCl_3$ (1 mL) was added methyl vinyl ketone (0.203 mL, 2.5 mmol) and $Yb(OTf)_3$ (0.124 g, 0.2 mmol). The reaction mixture was flushed with argon and stirred at rt for 2 days, washed with sat. (aq) $NaHCO_3$ (5 mL) and extracted with CH_2Cl_2 (3 × 7 mL). The combined organics were dried ($MgSO_4$) and concentrated *in vacuo*. Purification by silica gel chromatography (1:1, EtOAc:diethyl ether, to EtOAc, as eluent) afforded **443** as an off-colourless oil (0.015 g, 5%): R_f. 0.14 (EtOAc, as eluent); ^{1}H NMR (700 MHz, $CDCl_3$) δ 7.67 (d, *J* = 16.2 Hz, 1H, *Hd*), 7.57 (dd, *J* = 7.5, 1.6 Hz, 2H, *Hb*), 7.44-7.40 (m, 3H, *Ha+c*), 6.76 (d, *J* = 16.2 Hz, 1H, *He*), 5.88 (ddt, *J* = 17.0, 10.2, 6.6 Hz, 1H, *Hl*), 5.21 (dd, *J* = 17.0, 1.4 Hz, 1H, Hm_{cis}), 5.17 (d, *J* = 10.2 Hz, 1H, Hm_{trans}), 4.28 (d, *J* = 1.8 Hz, 1H, O*H*), 3.23 (dd, *J* = 11.5, 3.4 Hz, 1H, *Hf*), 3.08 (d, *J* = 6.6 Hz, 2H, *Hk*), 2.85 (dd, *J* = 11.4, 2.4 Hz, 1H, *Hg*), 2.74 (d, *J* = 11.4, 1H, *Hh*), 2.51 (td, *J*= 12.2, 3.4 Hz, 1H, *Hh*), 2.47 (t, *J* = 11.5 Hz, 1H, *Hg*), 1.72 (dt, *J* = 13.9, 2.4 Hz, 1H, *Hi*), 1.64 (tdd, *J* = 13.1, 4.3,

1.9 Hz, 1H, *Hi*), 1.23 (s, 3H, H_j) ppm (addition of D_2O caused the signal at δ 4.28 to disappear); ^{13}C NMR (176 MHz, $CDCl_3$) δ 204.4 (s, *Co*), 145.0 (d, *Cl*), 134.7 (d, Ar), 134.1 (s, *Cn*), 131.3 (d, Ar), 129.2 (d, Ar), 128.8 (d, *Ca*), 126.4 (d, *Ce*), 118.7 (t, *Cm*), 68.7 (s, *Cp*), 61.6 (t, *Ck*), 53.7 (d, *Cf*), 52.1 (t, *Cg*), 49.0 (t, *Ch*), 38.3 (t, *Ci*), 29.1 (d, *Cj*); IR ν_{max} (thin film) br 3484 (OH), 2934, 2814, 1674 (C=O), 1636, 1599, 1576, 1450 cm^{-1}; LRMS (TOF ES+), 413.3 (100%), 287.5 (90%), 286.0 (70%) [M]; HRMS (TOF ES+), calculated for $C_{18}H_{23}NO_2+H^+$, 286.1807; found 286.1816.

_N_-Boc-pyrrolidine[266]

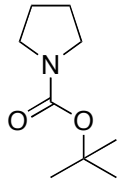

455

To pyrrolidine (4.49 mL, 54 mmol) in ethanol (975 mL) was added dropwise di-*tert*-butyl dicarbonate (18.13 g, 83 mmol) and the reaction mixture was stirred at rt for 15 min. Imidazole (3.66 g, 54 mmol) was added to the reaction mixture and this was stirred at rt for a further 15 min. The reaction mixture was diluted with chloroform (50 mL), concentrated *in vacuo*, dissolved in CH_2Cl_2 (75mL) and washed with 1% (aq) HCl (3 × 50 mL). The combined organics were dried ($MgSO_4$) and concentrated *in vacuo*. Purification by distillation under vacuum (49 mbar, 120 °C) in the presence of CaH_2 afforded **455** a colourless liquid (7.9 g, 86%): R_f. 0.43 (2:1, hexane:EtOAc, as eluent); ^1H NMR (400 MHz, $CDCl_3$) δ 3.30 (br d, J = 0.4 Hz, 4H, *Hb*), 1.82 (br s, 4H, *Ha*), 1.45 (s, 9H, *Hc*) ppm; ^{13}C NMR (101 MHz, $CDCl_3$) δ 154.8 (154.8)(s, *Cd*), 79.0 (s, *Ce*), 46.1 (45.8)(t, *Ca*), 28.7 (d, *Cc*), 25.9 (25.1)(d, *Cb*); IR ν_{max} (neat) 1691 (C=O), 1397 (^{t}Bu) cm^{-1}; LRMS (TOF ES+), 194.2 $[M+Na]^+$, 116.1; HRMS (TOF ES+), calculated for $C_9H_{17}NO_2+Na^+$, 194.1157; found 194.1152. All spectroscopic and analytical properties were identical to those reported in the literature.[267]

***tert*-Butoxycarbonyl 2-propenyl-pyrrolidine**[268]

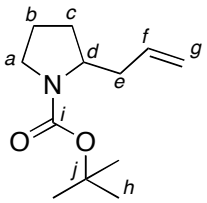

456

To a stirred solution of **455** (0.526 mL, 3 mmol) in dry THF (9 mL) under nitrogen at -78 °C was added dropwise *sec*-BuLi (4 mL, 3.5 mmol). After 4.5 h, allyl bromide (0.260 mL, 3 mmol) was added at -78 °C and the reaction mixture was allowed to warm to rt overnight. The reaction mixture was diluted with diethyl ether (40 mL), quenched with 5% (aq) HCL (30 mL), with the organic layer being separated, dried ($MgSO_4$) and concentrated *in vacuo*. Purification by silica gel chromatography (9:1, hexane:diethyl ether, as eluent) afforded **456** as a colourless liquid (0.510 g, 80%): R_f. 0.38 (3:1, hexane:diethyl, ether as eluent); ^{1}H NMR (500 MHz, $CDCl_3$) δ 5.72 (ddt, *J* = 17.2, 10.2, 7.2 Hz, 1H, *Hf*), 5.05-4.99 (m, 2H, *Hg*), 3.79 (br s, 1H, *Hd*), 3.35 (br s, 1H, *Ha*), 3.30-3.25 (m, 1H, *Ha*), 2.45 (br s, 1H, *He*), 2.15-2.08 (m, 1H, *He*), 1.91-1.66 (m, 4H, *Hc,b*), 1.44 (s, 9H, *Hh*) ppm; ^{13}C NMR (176 MHz, $CDCl_3$) δ 154.4 (s, *Ci*), 135.2 (d, *Cf*), 116.9 (t, *Cg*), 78.9 (br s, *Cj*), 56.6 (d, *Cd*), 46.4 (br t, *Ca*), 38.5 (br t, *Ce*), 29.6 (br t, *Cc*), 28.5 (d, *Ch*), 23.2 (br t, *Cb*); IR ν_{max} (neat) 1690 (C=O) cm^{-1}; LRMS (I.T. ES+), 212.16 (20%) $[M+H]^+$, 156.10 (100%); HRMS (I.T. ES+), calculated for $C_{12}H_{21}O_2N+H^+$, 212.1645; found 212.1645. All spectroscopic and analytical properties were identical to those reported in the literature.[200, 269]

tert-Butyl 2-(3-(4,4,5,5-tetramethyl-1,3,2-dioxaborolan-2-yl)propyl)pyrrolidine-1-carboxylate

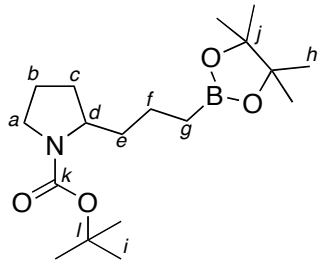

468

To a stirred solution of **456** (0.223 g, 1.1 mmol) in dry THF (0.5 mL) under nitrogen at 0 ºC was added 1 M BH_3 solution in THF (1.1 mL, 1.1 mmol). The reaction mixture was stirred at 0 ºC for 30 min, then at rt for 30 min before being quenched with methanol (0.5 mL). Pinacol (0.201 g, 1.7 mmol) was added and the mixture was stirred at rt for 4 h and concentrated *in vacuo*. Purification by silica gel chromatography (8:2, hexane:diethyl ether, as eluent) afforded **468** as a colourless liquid (70 mg, 20%): R_f. 0.54 (1:1, EtOAc:hexane, as eluent); ^{1}H NMR (500 MHz, $CDCl_3$) δ 3.74-3.59 (m, 1H, *Hd*), 3.38-3.18 (m, 2H, *Ha*), 1.89-1.67 (m, 4H, *Hc*+*b*), 1.66-1.55 (m, 2H, *He*), 1.41 (br s, 9H, *Hi*), 1.37-1.30 (m, 2H, *Hf*), 1.19 (br s, 12H, *Hh*), 0.79-0.68 (m, 2H, *Hg*) ppm; ^{13}C NMR (400 MHz, $CDCl_3$) δ 227.4 (s, *Ck*), 82.9 (s, *Cj*), 78.9 (s, *Cl*), 57.2 (d, *Cd*), 46.4 (46.0)(t, *Ca*), 37.6 (36.9)(t, *Ce*), 30.7 (29.7)(t, *Cc*), 28.6 (br d, *Ci*), 24.9 (24.9)(t, *Ch*), 23.1 (t, *Cb*), 21.0 (t, *Cf*), 11.4 (t, *Cg*); ^{11}B NMR (128 MHz, $CDCl_3$) δ 34.0; IR ν_{max} (thin film) 297.5, 1691 (C=O), 1390 (BO) cm^{-1}; LRMS (TOF ES+), 362.4 (100%) $[M+Na]^+$, 340.4 (45%) $[M+H]^+$, 284.3, 240.3; HRMS (TOF ES+), calculated for $C_{18}H_{34}BNO_4$+Na^+, 361.2515; found 361.2510.

First alternate procedure:

To bis(1,5-cyclooctadiene)diiridium(I) dichloride (0.020g, 0.03 mmol) and 1,2-bis(diphenylphosphino)ethane (0.024 g, 0.06 mmol) in dry CH_2Cl_2 (2 mL) under nitrogen was added **456** (0.422 g, 2 mmol) and pinacolborane (0.350 mL, 2.4 mmol). The resulting reaction mixture was left to stir at rt for 12 h before being quenched with methanol (2 mL) and water (6 mL) and extracted with CH_2Cl_2 (3 × 10 mL). The combined organics were dried ($MgSO_4$) and concentrated *in vacuo*. Purification by

silica gel chromatography (5%-20%, EtOAc:hexane, as eluent) afforded **468** as a colourless oil (0.551g, 81%).

Second alternate procedure:
To tris(triphenylphosphine)rhodium(I)chloride (0.009g, 0.01 mmol) in dry CH_2Cl_2 under nitrogen was added **456** (0.211 g, 1 mmol) and pinacolborane (0.175 mL, 1.2 mmol). The resulting reaction mixture was left to stir at rt for 60 h before being quenched with methanol (1 mL) and water (3 mL) and extracted with CH_2Cl_2 (3 × 5 mL). The combined organics were dried ($MgSO_4$) and concentrated *in vacuo*. Purification by silica gel chromatography (5%-20%, EtOAc:hexane, as eluent) afforded **468** as a colourless oil (0.184g, 54%).

(3-(Pyrrolidin-2-yl)propyl)boronic acid hydrochloride

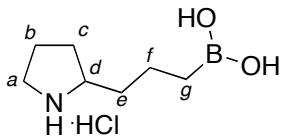

473

To **468** (0.260 g, 0.77 mmol) was added 20% (aq) HCl (1 mL) and the reaction mixture was stirred at 80 °C. After 2 h, the mixture was cooled to rt, diluted with water (5 mL), washed with CH_2Cl_2 (3 × 5 mL) and the aqueous concentrated *in vacuo*, with azeotroping with toluene (3 × 5 mL), to afford **473** as a colourless thick oil (0.147 g, 99%): ^{1}H NMR (700 MHz, D_2O) δ 3.35 (dq, *J* = 9.2, 7.3 Hz, 1H, *Hd*), 3.14-3.06 (m, 2H, *Ha*), 2.01 (dtd, *J* = 13.1, 7.3, 4.0 Hz, 1H, *Hc*), 1.88-1.83 (m, 1H, *Hc*), 1.82-1.75 (m, 1H, *Hb*), 1.57-1.51 (m, 1H, *He*), 1.51-1.46 (m, 1H, *He*), 1.46-1.41 (m, 1H, *Hb*), 1.28 (quin, *J* = 8.0 Hz, 2H, *Hf*), 0.63 (t, *J* = 8.0 Hz, 2H, *Hg*) ppm; ^{13}C NMR (176 MHz, D_2O) δ 60.5 (60.6) (d, *Cd*), 45.0 (t, *Ca*), 34.1 (t, *Ce*), 29.6 (t, *Cc*), 23.0 (t, *Cb*), 20.9 (t, *Cf*), 13.9 (t, *Cg*); ^{11}B NMR (128 MHz, D_2O) δ 32.6; IR ν_{max} (neat) 3350 (br, OH), 2934 (CH), and 1370 (BO) cm^{-1}; LRMS (ES+) 186.17 (100%), 172.15 (95%), 158.13 (35%) $[M+H]^+$, 154.14 (25%), 140.12 (8%); HRMS (ES+), calculated for $C_7H_{16}O_2N^{10}B+H^+$, 157.1383; found 157.1381.

(*R*)-*tert*-Butoxycarbonyl 2-propenyl-pyrrolidine[270]

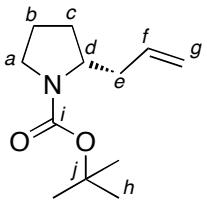

475

To (-)-sparteine (0.28 g, 1.2 mmol) in dry ether (4.8 mL) under argon at -78 ºC was added dropwise *sec*-BuLi (2 mL, 1.2 mmol). After 30 min, **455** (0.174 mL, 1 mmol) was added to the reaction mixture. After 6 h, a solution of $ZnCl_2$ (0.177 g, 1.3 mmol) in dry THF (1.7 mL) was added to the reaction mixture dropwise over 10 min. After 30 min, a solution of CuCN (0.107 g, 1.2 mmol) and LiCl (0.102 g, 2.4 mmol) in dry THF (6 mL) was added rapidly to the reaction mixture. After a further 30 min, allyl bromide (0.261 mL, 3 mmol) was added to the reaction mixture dropwise and was allowed to warm to rt overnight. The reaction mixture was quenched with saturated (aq) NH_4Cl (10 mL) and diluted with diethyl ether (10 mL). After stirring for 5 min, the mixture was filtered, extracted with diethyl ether (3 × 10 mL) and the combined organics dried ($MgSO_4$) and concentrated *in vacuo*. Purification by silica gel chromatography (9:1, hexane:diethyl ether, as eluent) afforded **475** as a colourless oil (0.203 g, 96%, 82% ee): $[\alpha]_D^{22\ ^\circ C}$ = +40.98 (c = 1.00, $CHCl_3$); The enantiomeric ratio of the product was determined by chiral HPLC using OJ-Chiralsel column (250 x 4.6 mm), 25 °C, 0.5 mL/min, 210 nm, hexane:IPA (99.8:0.2), t_R (*R*) = 11.1 min; t_R (*S*) = 12.5 min. All other spectroscopic and analytical properties were identical to the racemic compound **456**.

First alternate procedure:

To (-)-sparteine (0.28 g, 1.2 mmol) in dry ether (4.8 mL) under argon at -78 ºC was added dropwise *sec*-BuLi (2 mL, 1.2 mmol). After 30 min, **455** (0.174 mL, 1 mmol) was added to the reaction mixture. After 1 h, a solution of $ZnCl_2$ (0.177 g, 1.3 mmol) in dry THF (1.7 mL) was added to the reaction mixture dropwise over 10 min. After 30 min, a solution of CuCN (0.107 g, 1.2 mmol) and LiCl (0.102 g, 2.4 mmol) in dry THF (6 mL) was added rapidly to the reaction mixture. After a further 30 min, allyl

bromide (0.261 mL, 3 mmol) was added to the reaction mixture dropwise and was allowed to warm to rt overnight. The reaction mixture was quenched with saturated (aq) NH_4Cl (10 mL) and diluted with diethyl ether (10 mL). After stirring for 5 min, the mixture was filtered, extracted with diethyl ether (3 × 10 mL) and the combined organics dried ($MgSO_4$) and concentrated *in vacuo*. Purification by silica gel chromatography (9:1, hexane:diethyl ether, as eluent) afforded **475** as a colourless oil (0.169 g, 80%, 82% ee);

Second alternate procedure:
To a stirred solution of **455** (0.174 mL, 1.0 mmol) and (-)-sparteine (0.28 g, 1.2 mmol) in dry diethyl ether (4 mL) under nitrogen at -78 °C was added dropwise *sec*-BuLi (1.3 mL, 1.2 mmol). After 1 h, a solution of CuCN (0.045 g, 0.5 mmol) and LiCl (0.043 g, 1.0 mmol) in dry THF (3 mL) was added rapidly to the reaction mixture. After a further hour, allyl bromide (0.0.86 mL, 1 mmol) was added and the reaction mixture was allowed to warm to rt overnight. The reaction mixture was quenched with saturated (aq) NH_4Cl (5 mL) and diluted with diethyl ether (5 mL). After stirring for 5 min, the mixture was filtered, extracted with diethyl ether (3 × 5 mL) and the combined organics dried ($MgSO_4$) and concentrated *in vacuo*. Purification by silica gel chromatography (9:1, hexane:diethyl ether, as eluent) afforded **475** as a colourless oil (0.133 g, 63%, 69% ee);

Third alternate procedure:
To a stirred solution of **455** (0.174 mL, 1.0 mmol) and (-)-sparteine (0.28 g, 1.2 mmol) in dry diethyl ether (4 mL) under nitrogen at -78 °C was added dropwise *sec*-BuLi (1.3 mL, 1.2 mmol).). After 1 h, allyl bromide (0.043 mL, 0.5 mmol) was added and the reaction mixture was allowed to warm to rt overnight. The reaction mixture was quenched with saturated (aq) NH_4Cl (5 mL) and diluted with diethyl ether (5 mL). After stirring for 5 min, the mixture was filtered, extracted with diethyl ether (3 × 5 mL) and the combined organics dried ($MgSO_4$) and concentrated *in vacuo*. Purification by silica gel chromatography (9:1, hexane:diethyl ether, as eluent) afforded **475** as a colourless oil (0.068 g, 64%, 19% ee).

(*S*)-*tert*-Butyl 2-(3-(4,4,5,5-tetramethyl-1,3,2-dioxaborolan-2-yl)propyl)pyrrolidine-1-carboxylate

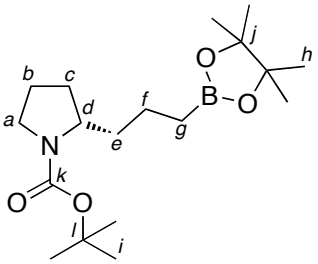

476

To bis(1,5-cyclooctadiene)diiridium(I) dichloride (0.020g, 0.03 mmol) and 1,2-bis(diphenylphosphino)ethane (0.024 g, 0.06 mmol) in dry CH_2Cl_2 (2 mL) under nitrogen was added **475** (0.422 g, 2 mmol) and pinacolborane (0.350 mL, 2.4 mmol). The resulting reaction mixture was left to stir at rt for 12 h before being quenched with methanol (2 mL) and water (6 mL) and extracted with CH_2Cl_2 (3 × 10 mL). The combined organics were dried ($MgSO_4$) and concentrated *in vacuo*. Purification by silica gel chromatography (5%-20%, EtOAc:hexane, as eluent) afforded **476** as a colourless oil (0.551g, 81%): $[\alpha]_D^{22\ °C}$ = 33.94 at c = 1. All other spectroscopic and analytical properties were identical to the racemic compound **468**.

(*S*)-(3-(Pyrrolidin-2-yl)propyl)boronic acid hydrochloride

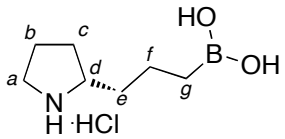

477

To **476** (0.260 g, 0.77 mmol) was added 20% (aq) HCl (1 mL) and the reaction mixture was stirred at 80 °C. After 2 h, the mixture was cooled to rt, diluted with water (5 mL), washed with CH_2Cl_2 (3 × 5 mL) and the aqueous concentrated *in vacuo*, with azeotroping with toluene (3 × 5 mL), to afford **477** as a colourless thick oil (0.147 g, 99%): All spectroscopic and analytical properties were identical to the racemic compound **473**.

(*S*)-(3-(Pyrrolidin-2-yl)propyl)boronic acid

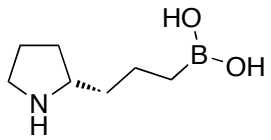

478

To **477** (0.034 g, 0.1 mmol) was added 20% (aq) HCl (2 mL) and the reaction mixture was stirred at 80 °C for 2 h. The reaction mixture was subsequently washed with EtOAc (3 × 5 mL) and the aqueous reaction mixture was concentrated *in vacuo* and azeotroped with toluene (3 × 5 mL). The reaction mixture was diluted in $CDCl_3$ (1 mL), to which was added triethylamine (0.014 mL, 0.1 mmol) and the mixture was stirred under argon overnight to afford a solution containing **478**: ^{11}B NMR = 5 ppm.

2-(Chloromethyl)-4,4,5,5-tetramethyl-1,3,2-dioxaborolane[271]

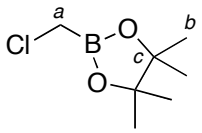

486

To a stirred solution of bromochloromethane (2.00 mL, 31 mmol) and triisopropyl borate (6.46 mL, 28 mmol) in dry THF (28 mL) under argon was added dropwise *n*-BuLi (15 mL, 34 mmol) at -78 ºC and the reaction mixture was stirred for 1 h prior to allowing to warm to rt overnight. The reaction mixture was subsequently quenched with 20% (aq) HCl (6 mL) and extracted with diethyl ether (3 × 10 mL). The combined organics were washed with brine (10 mL), dried ($MgSO_4$) and concentrated *in vacuo* to afford a crude white solid (0.843 g). This was dissolved in diethyl ether (10 mL) prior to adding 0.85 Equivalents of pinacol (0.93 g, 7.9 mmol). The reaction mixture was left to stir at rt overnight and then concentrated *in vacuo*. Purification by distillation under vacuum (32 mbar, 90 ºC) afforded **486** as a colourless oil (1.01 g, 20%): R_f .0.34 (3:1, hexane:diethyl ether, as eluent); ^1H NMR (400 MHz, $CDCl_3$) δ 2.97 (s, 2H, *Ha*), 1.30 (s, 12H, *Hb*) ppm; ^{13}C NMR (101 MHz, $CDCl_3$) δ 84.6 (d, *Ca*), 82.8 (s, *Cb*), 24.8 (d, *Cc*); ^{11}B NMR (128 MHz, $CDCl_3$) δ 31.5; IR ν_{max} (neat) 2979,

1372, 1348 cm^{-1}. All spectroscopic and analytical properties were identical to those reported in the literature.[272]

(*S*)-*tert*-Butyl 2-((4,4,5,5-tetramethyl-1,3,2-dioxaborolan-2-yl)methyl)pyrrolidine-1-carboxylate[161]

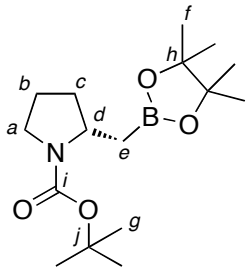

487

To (-)-sparteine (0.87 mL, 3.8 mmol) in dry diethyl ether (20 mL) under argon at -78 ºC was added dropwise *sec*-BuLi (3 mL, 3.8 mmol). After stirring for 20 min, *N*-Boc pyrrolidine (0.522 mL, 3 mmol) was added dropwise to the reaction mixture and stirred for 2 h prior to the dropwise addition of **486** (0.62 g, 3.5 mmol). After 30 min, $ZnCl_2$ (1 M in diethyl ether) (5.6 mL, 5.6 mmol) was added to the reaction mixture and stirred for 45 min before being allowed to warm to rt overnight. The suspension was quenched with 5% (aq) HCl (10 mL), filtered through Celite and washed with 5% (aq) HCl (5 mL). The phases were separated and the aqueous phase extracted with diethyl ether (2 × 8 mL). The combined organics were dried ($MgSO_4$) and concentrated *in vacuo* to afford a crude oil. Purification by silica gel chromatography (5:1, hexane:diethyl ether, as eluent) afforded **487** as a colourless oil (0.391 g, 42%, 96%): R_f. 0.18 (3:1, hexane:diethyl ether, as eluent); $[\alpha]_D^{22\ °C}$ = +33.2 (c = 1.00, CH_2Cl_2); ^{1}H NMR (400 MHz, $CDCl_3$) δ 3.99-3.90 (br m, 1H, *Hd*), 3.38-3.30 (br d, 2H, *Ha*), 2.02 (br s, 1H, *Hc*), 1.87-1.81 (m, 1H, *Hb*), 1.70-1.75 (m, 1H, *Hb*), 1.15 (br s, 1H, *Hc*), 1.45 (s, 9H, *Hg*), 1.23 (s, 12H, *Hf*), 0.84-1.00 (m, 2H, *He*) ppm; ^{13}C NMR (101 MHz, $CDCl_3$) δ 154.7 (s, *Ci*), 83.1 (s, *Ch*), 79.0 (s, *Cj*), 54.3 (d, *Cd*), 46.6 and 46.3 (t, *Ca*), 33.4 and 33.1 (t, *Cc*), 28.7 (d, *Cg*), 25.1 and 24.9 (d, *Cf*), 23.9 and 23.4 (t, *Cb*), 18.5 (t, *Ce*); ^{11}B NMR (128 MHz, $CDCl_3$) δ 32.8; IR ν_{max} (thin film) 2972 (CH), 1693 (C=O), 1389 and 1366 (BO) cm^{-1}; LRMS (TOF ES+), 334.3 (100%) $[M+H]^+$; HRMS (TOF ES+), calculated for $C_{16}H_{30}BNO_4$+Na^+, 334.2202;

found 334.2209. The enantiomeric ratio of the product was determined by GC using CP-Chiralsil-Dex-CB column (35 m x 0.25 mm x 0.25 μm), 128 °C, FID, t_R (*S*) = 124 min; t_R (*R*) = 127 min. All spectroscopic and analytical properties were identical to those reported in the literature.[161]

(*S*)-(Pyrrolidin-2-ylmethyl)boronic acid hydrochloride[161]

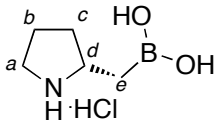

488

To **487** (0.300 g, 0.96 mmol) was added 20% (aq) HCl (1 mL) and the reaction mixture was stirred at 80 °C. After 2 h, the mixture was cooled to rt, diluted with water (5 mL), washed with CH_2Cl_2 (3 × 5 mL) and the aqueous concentrated *in vacuo*, with azeotroping with toluene (3 × 5 mL), to afford **488** as an off-colourless oil (0.155 g, 98%): $[\alpha]_D^{22\ °C}$ = +33.0 (c = 1.00, CH_2Cl_2); ^{1}H NMR (400 MHz, $CDCl_3$) δ 3.77-3.73 (m, 1H, *Hd*), 3.37-3.29 (m, 2H, *Ha*), 2.29-2.25 (m, 1H, *Hc*), 2.12-2.00 (m, 1H, *Hb*), 1.68-1.64 (m, 1H, *Hc*), 1.39 (dd, *J* = 15.4, 7 Hz, 1H, *He*), 1.27 (dd, *j* = 15.4, 9.1 Hz, 1H, *He*) ppm; ^{13}C NMR (101 MHz, $CDCl_3$) δ 18.2 (t, *Ce*), 23.1 (t, *Cb*), 31.5 (t, *Cc*), 44.8 (t, *Ca*), 58.2 (d, *Cd*); ^{11}B NMR (128 MHz, $CDCl_3$) δ 31.0; IR ν_{max} (thin film) 2980 (CH) and 1365 (BO) cm^{-1}. All spectroscopic and analytical properties were identical to those reported in the literature.[161]

***N-tert*-Butoxycarbonyl-L-proline**[273]

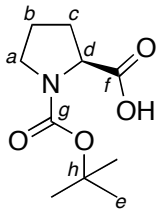

489

To L-proline (1.50 g, 13.0 mmol) at 0 °C in CH_2Cl_2 (30 mL) was added triethylamine (2.36 mL, 16.9 mmol), followed by di-*tert*-butyl-dicarbonate (3.98 g, 18.2 mmol). The reaction mixture was stirred at rt for 2.5 h, quenched with sat. (aq) citric acid (8 mL) and washed with brine (2 × 10 mL) and water (10 mL). The organics were dried ($MgSO_4$) and concentrated *in vacuo*. The crude solid was dissolved in hot EtOAc, followed by the addition of hexane (40 mL). The mixture was crystallised and filtered to afford **489** as a white solid (2.19 g, 78%): m.p. 134-135 °C (lit. 134-135 °C)[274]; ^{1}H NMR (400 MHz, $CDCl_3$) δ 10.9 (br s, 1H, O*H*), 4.36-4.18 (m, 1H, *Hd*), 3.58-3.31 (m, 2H, *Ha*), 2.31-2.17 (m, 1H, *Hc*), 2.15-1.98 (m, 1H, *Hb*), 1.98-1.80 (m, 2H, *Hb*+*c*), 1.40+1.46 (2 x s, 9H, *Hh*) ppm (addition of D_2O caused the signal at δ 10.9 to disappear); ^{13}C NMR (101 MHz, $CDCl_3$) δ 178.8 (175.7) (s, *Cf*), 156.2 (154.1) (s, *Cg*), 81.3 (80.5) (s, *Ch*), 59.1 (d, *Cd*), 47.0 (46.5) (t, *Ca*), 31.0 (29.0) (t, *Cc*), 28.5 (28.4) (d, *Ce*), 24.4 (23.8) (t, *Cb*); IR ν_{max} (neat) 2969 (OH), 1736 (C=O), 1632 (NC=O) cm^{-1}; LRMS (TOF ES+) 238.6 (100%) $[M+Na]^+$, 160.4 (40%), 114.4 (80%), 116.4 (95%); HRMS (TOF ES+), calculated for $C_{10}H_{17}NO_4$+Na^+, 238.1055; found 238.1058. All spectroscopic and analytical properties were identical to those reported in the literature.[275]

(*S*)-*tert*-Butyl 2-(hydroxymethyl)pyrrolidine-1-carboxylate[276]

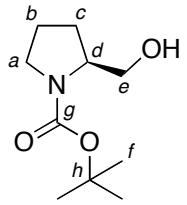

490

To **489** (0.60 g, 2.79 mmol) in dry THF (5 mL) under argon at rt was added dropwise BH_3•DMS (0.306 mL, 3.06 mmol) and refluxed for 2 h. The reaction mixture was cooled to rt, after which was added ice (2.5 g) and the mixture extracted with CH_2Cl_2 (3 × 15 mL). The combined organics were filtered through Celite and the filtrate concentrated *in vacuo* to afford a crude solid. This was washed with cold diethyl ether to afford **490** as a white solid (0.394 g, 70%): m.p. 54-55 ºC (lit. 55-56 ºC)[277]; ^{1}H NMR (400 MHz, $CDCl_3$) δ 4.74 (br s, 1H, O*H*), 3.95 (br s, 1H, *Hd*), 3.64-3.56 (m,

2H, *Ha*), 3.46-3.43 (m, 1H, *He*), 3.32-3.29 (m, 1H, *He*), 2.03-1.98 (m, 1H, *Hc*), 1.86-1.74 (m, 2H, *Hb*), 1.59-1.56 (m, 1H, *Hc*), 1.47 (br s, 9H, *Hf*) ppm (addition of D_2O caused the signal at δ 4.74 to disappear); ^{13}C NMR (101 MHz, $CDCl_3$) δ 157.2 (s, *Cg*), 80.2 (s, *Ch*), 67.7 (t, *Ce*), 60.2 (d, *Cd*), 47.5 (t, *Ca*), 28.7 (t, *Cc*), 28.5 (d, *Cf*), 24.1 (t, *Cb*); IR ν_{max} (neat) 3426 (OH), 2980 (CH), 1652 (C=O), 1403 cm^{-1}; LRMS (TOF ES+), 224.3 (100%) $[M+Na]^+$, 146.2 (80%), 102.2 (70%); HRMS (TOF ES+), calculated for $C_{10}H_{19}NO_3+Na^+$, 224.1263; found 224.1270. All spectroscopic and analytical properties were identical to those reported in the literature.[277, 278]

(*S*)-*tert*-Butyl 2-(iodomethyl)pyrrolidine-1-carboxylate[279]

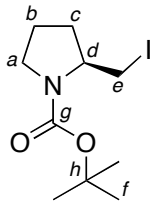

491

To imidazole (0.20 g, 2.98 mmol) and triphenylphosphine (0.59 g, 2.24 mmol) in diethyl ether (4 mL) at 0 °C under argon was added portionwise iodine (0.57 g, 2.24 mmol). The reaction mixture was stirred for 10 min prior to addition of a solution of **490** (0.30 g, 1.49 mol) in CH_2Cl_2 (2 mL). The mixture was stirred at rt for 5 h, filtered and concentrated *in vacuo*. Purification by silica gel chromatography (9:1-3:1, hexane:diethyl ether, as eluent) afforded **491** as a white solid (0.287 g, 62%): m.p. 37-38 °C (lit. 38-40 °C)[280]; ^1H NMR (700 MHz, $CDCl_3$) δ 3.90-3.80 (m, 1H, *Hd*), 3.50-3.11 (m, 4H, *Ha*+*He*), 2.08-2.01 (m, 1H, *Hc*), 1.93-1.75 (m. 3H, *Hb*+*Hc*), 1.46 + 1.44 (2 x s, 9H, *Hf*) ppm; ^{13}C NMR (176 MHz, $CDCl_3$) δ 154.5 (154.2) (s, *Cg*), 80.0 (79.7) (s, *Ch*), 58.2 (58.0) (t, *Cd*), 47.6 (47.2) (d, *Ca*), 31.7 (31.2) (d, *Cc*), 28.6 (t, *Cf*), 23.6 (22.9) (d, *Cb*), 11.1 (10.8) (d, *Ce*); IR ν_{max} (neat) 2974 (CH), 1687 (C=O) cm^{-1}; LRMS (TOF ES+) 242.7 (100%), 234.5 (90%) $[M+Na]^+$; HRMS (TOF ES+), calculated for $C_{10}H_{18}NO_2+Na^+$, 334.0280; found 334.0296. All spectroscopic and analytical properties were identical to those reported in the literature.[202]

(*R*)-*tert*-Butyl 2-((4,4,5,5-tetramethyl-1,3,2-dioxaborolan-2-yl)methyl)pyrrolidine-1-carboxylate[202]

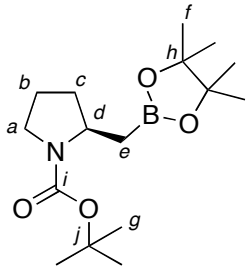

492

To **491** (0.50 g, 1.6 mmol) in dry THF (4 mL) under argon was added B_2pin_2 (0.41 g, 1.6 mmol), LiO^tBu (0.26 g, 3.2 mmol) and CuI (0.175 g, 3.2 mmol). The reaction mixture was stirred at rt for 20 h, quenched with 5% (aq) HCl (5 mL), extracted with diethyl ether (3 × 5 mL) and the combined organics were dried ($MgSO_4$) and concentrated *in vacuo*. Purification by silica gel chromatography (4:1, hexane:EtOAc, as eluent) afforded **492** as a colourless oil (0.170 g, 34%, 97% ee): $[\alpha]_D^{22\ °C}$ = -36.4 (c = 1.00, CH_2Cl_2); The enantiomeric ratio of the product was determined by GC using CP-Chiralsil-Dex-CB column (35 m x 0.25 mm x 0.25 μm), 128 °C, FID, t_R (*S*) = 124 min; t_R (*R*) = 127 min. All other spectroscopic and analytical properties were identical to the opposite enantiomer **487**.

(*S*)-(Pyrrolidin-2-ylmethyl)boronic acid hydrochloride[202]

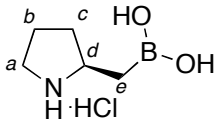

493

To **492** (0.300 g, 0.96 mmol) was added 20% (aq) HCl (1 mL) and the reaction mixture was stirred at 80 °C. After 2 h, the mixture was cooled to rt, diluted with water (5 mL), washed with CH_2Cl_2 (3 × 5 mL) and the aqueous concentrated *in vacuo*, with azeotroping with toluene (3 × 5 mL), to afford **493** as an off-colourless

oil (0.152 g, 96%): $[\alpha]_D^{22\ °C}$ = -33.2 (c = 1.00, CH_2Cl_2). All other spectroscopic and analytical properties were identical to the opposite enantiomer **488**.

2-Phenyl-1-(phenylsulfonyl)-2,3-dihydropyridin-4(1*H*)-one[281]

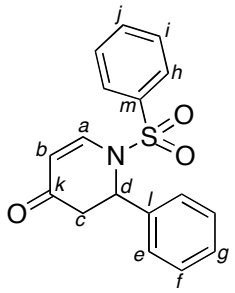

496

To *N*-benzylidenebenzenesulonamide (0.491 g, 2 mmol) in toluene (2 mL) was added Danishefsky's diene **4** (0.5 mL, 2.5 mmol) and the reaction mixture was stirred at 100 °C under nitrogen. After 4 h the mixture was cooled to rt and concentrated *in vacuo*. Purification by silica gel chromatography (5%-35%, EtOAc:hexane, as eluent) afforded **496** as a yellow oil (0.389 g, 62%): ^{1}H NMR (400 MHz, $CDCl_3$) δ 7.83 (dd, *J* = 8.3, 1.5 Hz, 1H, *Ha*), 7.72-7.69 (m, 2H, *Hh*), 7.59-7.55 (m, 1H, *Hj*), 7.46-7.55 (m, 1H, *Hj*), 7.20-7.12 (m, 5H, *He*+*f*+*g*), 5.55 (dt, *J* = 7.2, 1.5 Hz, 1H, *Hd*), 5.43 (dd, *J* = 8.3, 1.2 Hz, 1H, *Hb*), 2.87 (dd, *J* = 16.5, 7.2 Hz, 1H, Hc_{trans}), 2.68 (*J* = 16.5, 1.5, 1.2 Hz, 1H, Hc_{cis}) ppm; ^{13}C NMR (101 MHz, $CDCl_3$) δ 190.5 (s, *Ck*), 142.5 (d, *Ca*), 138.7 (s, *Cl*), 137.0 (s, *Cm*), 133.9 (d, *Cj*), 129.6 (d, *Ci*), 128.9 (d, *Cf*), 128.3 (d, *Cg*), 127.1 (d, *Ch*), 126.4 (d, *Ce*), 108.6 (d, *Cb*), 57.9 (d, *Cd*), 42.0 (t, *Cc*); LRMS (TOF ES+), 336.2 (100%) $[M+Na]^+$, 314.2 (45%) $[M+H]^+$, 242.2 (45%); HRMS (TOF ES+), calculated for $C_{17}H_{15}NO_3S+H^+$, 314.0851; observed 314.0836. All spectroscopic and analytical properties were identical to those reported in the literature.[282]

4-Hydroxy-4-(4-nitrophenyl)butan-2-one[245]

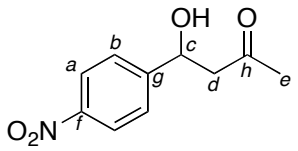

505

To **473** (0.039 g, 0.2 mmol) and triethylamine (0.028 mL, 0.2 mmol) in acetone (1 mL) was added *p*-nitrobenzaldehyde (0.151 g, 1 mmol) and the reaction mixture was left to stir at rt. After 72 h, the mixture was quenched with sat. (aq) NH_4Cl (10 mL), extracted with EtOAc (15 mL), dried ($MgSO_4$) and concentrated *in vacuo*. Purification by silica gel chromatography (1:4-1:0, EtOAc:hexane, as eluent) afforded **507** as an orange solid (0.008 g, 4%), **506** as an off-colourless solid (0.126 g, 69%), and **505** as an off-colourless solid (0.056 g, 27%, 0% ee): R_f. 0.19 (1:1, EtOAc:hexane, as eluent); m.p. 57-59 °C (lit. 58-60 °C)[283]; ^{1}H NMR (400 MHz, $CDCl_3$) δ 8.14-8.09 (m, 2H, *Ha*), 7.51-7.47 (m, 2H, *Hb*), 5.22 (t, *J* = 6.2 Hz, 1H, *Hc*), 3.56 (br s, 1H, O*H*), 2.83 (d, *J* = 6.2 Hz, 2H, *Hd*), 2.18 (s, 3H, *He*) ppm (addition of D_2O caused the signal at δ 3.56 to disappear); ^{13}C NMR (101 MHz, $CDCl_3$) δ 208.5 (s, *Ch*), 150.3 (s, *Cf*), 147.2 (s, *Cg*), 126.5 (d, *Ca*), 123.7 (d, *Cb*), 68.8 (d, *Cc*), 51.6 (t, *Cd*), 30.7 (d, *Ce*); IR ν_{max} (thin film) 3431 (OH), 1710 (C=O), 1514 (Ar), 1343 (NO_2) cm^{-1}; LRMS (TOF ES-), 208.1 (95%) $[M–H]^-$, 190.1 (100%); HRMS (TOF ES-), calculated for $C_{10}H_{10}NO_4$, 208.0610; found 208.0585. The enantiomeric ratio of the product was determined by chiral HPLC using OJ-H-Chiralsel column (250 x 4.6 mm), 15 °C, 1 mL/min, 210 nm, hexane:IPA (9:1), t_R (*S*) = 39.7 min; t_R (*R*) = 45.9 min. All spectroscopic and analytical properties were identical to those reported in the literature.[202]

1,5-Dihydroxy-1,5-bis(4-nitrophenyl)pentan-3-one[284]

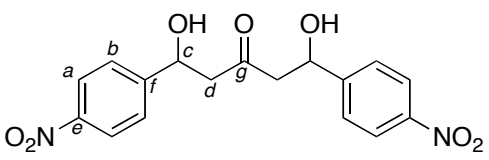

506

To **473** (0.039 g, 0.2 mmol) and triethylamine (0.028 mL, 0.2 mmol) in acetone (1 mL) was added *p*-nitrobenzaldehyde (0.151 g, 1 mmol) and the reaction mixture was left to stir at rt. After 72 h, the mixture was quenched with sat. (aq) NH_4Cl (10 mL), extracted with EtOAc (15 mL), dried ($MgSO_4$) and concentrated *in vacuo*. Purification by silica gel chromatography (1:4-1:0, EtOAc:hexane, as eluent) afforded **507** as an orange solid (0.008 g, 4%), **505** as an off-colourless solid (0.056 g, 27%) and **506** as an off-colourless solid (0.126 g, 69%): R_f. 0.10 (1:1, EtOAc:hexane, as eluent); m.p. 100-101 °C; ^{1}H NMR (400 MHz, $CDCl_3$) δ 8.22-8.18 (m, 4H, *Ha*), 7.56-7.52 (m, 4H, *Hb*), 5.36-5.30 (m, 2H, *Hc*), 3.45 (br s, 2H, *OH*), *2*.98-2.81 (m, 4H, *Hd*) ppm (addition of D_2O caused the signal at δ 3.45 to disappear); ^{13}C NMR (101 MHz, $CDCl_3$) δ 209.4 (209.3) (s, *Cg*), 149.7 (149.8) (s, *Ce*), 147.7 (s, *Cf*), 126.5 (126.6) (d, *Ca*), 124.0 (124.4) (d, *Cb*), 69.1 (69.2) (d, *Cc*), 51.9 (52.0) (t, *Cd*); IR ν_{max} (thin film) 3458 (OH), 1710 (C=O), 1514 (Ar), 1343 (NO_2) cm^{-1}; LRMS (TOF ES-), 359.2 (55%) $[M–H]^-$, 208.0 (100%), 149.0 (20%); HRMS (TOF ES-), calculated for $C_{17}H_{15}N_2O_7$, 359.0879; found 359.0887. ^{1}H NMR spectroscopic properties were identical to those reported in the literature.[285]

(2*R*,6*S*)-2,6-Bis(4-nitrophenyl)dihydro-2*H*-pyran-4(3*H*)-one[286]

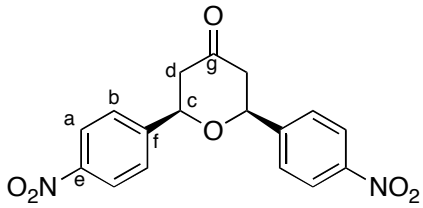

507

To **473** (0.039 g, 0.2 mmol) and triethylamine (0.028 mL, 0.2 mmol) in acetone (1 mL) was added *p*-nitrobenzaldehyde (0.151 g, 1 mmol) and the reaction mixture was left to stir at rt. After 72 h, the mixture was quenched with sat. (aq) NH_4Cl (10 mL), extracted with EtOAc (15 mL), dried ($MgSO_4$) and concentrated *in vacuo*. Purification by silica gel chromatography (1:4-1:0, EtOAc:hexane, as eluent) afforded **505** as an off-colourless solid (0.056 g, 27%), **506** as an off-colourless solid (0.126 g, 69%) and **507** as an orange solid (0.008 g, 4%): R_f. 0.27 (1:1, EtOAc:hexane, as eluent); ^{1}H NMR (700 MHz, $CDCl_3$) δ 8.31-8.28 (m, 4H, *Ha*), 7.66-7.63 (m, 4H, *Hb*),

5.01 (dd, *J* = 11.8, 2.4 Hz, 2H, *Hc*), 2.83 (dd, *J* = 14.7, 2.4 Hz, 2H, Hd_{eq}), 2.67 (dd, *J* = 14.7, 11.8 Hz, 2H, Hd_{ax}) ppm; ^{13}C NMR (151 MHz, $CDCl_3$) δ 203.3 (s, *Cg*), 148.0 (s, *Cf*), 147.1 (s, *Cg*), 126.5 (d, *Cb*), 124.3 (d, *Ca*), 78.1 (d, *Cc*), 49.1 (t, *Cd*); IR ν_{max} (thin film) 1721 (C=O), 1518 (Ar), 1346 (NO_2) cm^{-1}; LRMS (ASAP), 361.1 (20%), 360.1 (100%) $[M+NH_4]^+$, 156.1 (40%); HRMS (ASAP), calculated for $C_{17}H_{14}N_2O_6+NH_4^+$, 360.1190; found 360.1183. All spectroscopic and analytical properties were identical to those reported in the literature.[287]

1-(4-Chlorophenyl)-3-hydroxy-3-(4-nitrophenyl)propan-1-one[208]

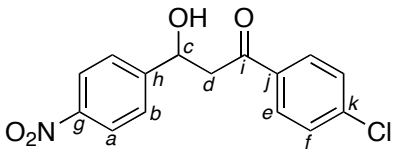

510

To **473** (0.039 g, 0.2 mmol) and triethylamine (0.028 mL, 0.2 mmol) in DMSO (1 mL) was added *p*-chloroacetophenone (0.155 g, 1mmol) and *p*-nitrobenzaldehyde (0.151 g, 1 mmol) and the reaction mixture was left to stir at rt. After 216 h, the mixture was quenched with sat. (aq) NH_4Cl (10 mL), extracted with EtOAc (15 mL), dried ($MgSO_4$) and concentrated *in vacuo*. Purification by silica gel chromatography (1:4-1:0, EtOAc:hexane, as eluent) afforded **511** as an off-colourless solid (0.023 g, 5%) and **510** as an off-colourless solid (0.009 g, 3%): ^{1}H NMR (400 MHz, $CDCl_3$) δ 8.23 (d, *J* = 8.8 Hz, 2H, *Ha*), 7.88 (d, *J* = 8.8 Hz, 2H, *Hb*), 7.61 (d, *J* = 8.7 Hz, 2H, *He*), 7.45 (d, *J* = 8.7 Hz, 2H, *Hf*), 5.43 (dd, *J* = 7.9, 4.2 Hz, 1H, *Hc*), 3.74 (br s, 1H, O*H*), 3.35-3.31 (m, 2H, *Hd*) ppm; LRMS (TOF ES–), 304.1 (80%) $[M–H]^–$, 166.1 (100%); HRMS (TOF ES–), calculated for $C_{15}H_{11}NO_4Cl$, 304.0377; observed 304.0386. All spectroscopic and analytical properties were identical to those reported in the literature.[208]

1-(4-Chlorophenyl)-3-hydroxy-2-(hydroxy(4-nitrophenyl)methyl)-3-(4-nitrophenyl)propan-1-one

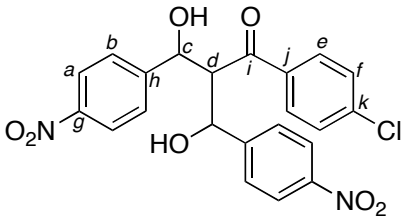

511

To **473** (0.039 g, 0.2 mmol) and triethylamine (0.028 mL, 0.2 mmol) in DMSO (1 mL) was added *p*-chloroacetophenone (0.155 g, 1mmol) and *p*-nitrobenzaldehyde (0.151 g, 1 mmol) and the reaction mixture was left to stir at rt. After 216 h, the mixture was quenched with sat. (aq) NH_4Cl (10 mL), extracted with EtOAc (15 mL), dried ($MgSO_4$) and concentrated *in vacuo*. Purification by silica gel chromatography (1:4-1:0, EtOAc:hexane, as eluent) afforded **510** as an off-colourless solid (0.009 g, 3%) and **511** as an off-colourless solid (0.023 g, 5%): ^{1}H NMR (400 MHz, $CDCl_3$) δ 8.07-8.00 (m, 4H, *Ha*), 7.54-7.46 (m, 4H, *Hb*), 7.24-7.18 (m, 2H, *He*), 7.13-7.07 (m, 2H, *Hf*), 5.57-5.52 (m, 2H, *Hc*), 4.28 (br s, 2H, O*H*), 4.20-4.08 (m, 1H, *Hd*) ppm; LRMS (TOF ES+), 479.2 (80%) $[M+Na]^+$, 304.4 (40%), 185.2 (40%), 139.2 (50%), 130.2 (100%); HRMS (TOF ES+), calculated for $C_{22}H_{17}N_2O_7Cl+Na^+$, 479.0622; observed 479.0623.

(3*S*,4*R*)-3-Hydroxy-4-((4-methoxyphenyl)amino)-4-(4-nitrophenyl)butan-2-one[209]

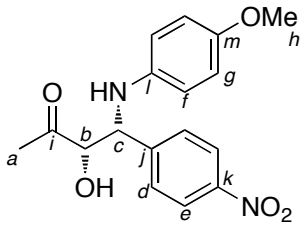

519

To *p*-anisidine (0.135 g, 1.1 mmol) and *p*-nitrobenzaldehyde (0.151 g, 1 mmol) in DMSO (8.1 mL) was added hydroxyacetone (0.9 mL, 10 vol%) and L-proline (0.023 g, 0.2 mmol). The reaction mixture was stirred at rt overnight, quenched with

saturated (aq) NH_4Cl (10 mL), diluted with $CHCl_3$ (20 mL) and separated with EtOAc (3 × 20 mL) with the aid of brine (10 mL). The combined organics were dried ($MgSO_4$) and concentrated *in vacuo* to afford a crude oil. Purification by silica gel chromatography (4:1 to 2:1, hexane:EtOAc, as eluent) afforded **519** as an orange oil (0.274 g, 83 %): R_f 0.46 (2:1, EtOAc:hexane, as eluent); ^{1}H NMR (400 MHz, $CDCl_3$) δ 8.17-8.13 (m, 2H, *He*), 7.56-7.53 (m, 2H, *Hd*), 6.69-6.65 (m, 2H, *Hg*), 6.48-6.44 (m, 2H, *Hf*), 5.04 (d, *J* = 2.4 Hz, 1H, *Hb*), 4.44 (d, *J* = 2.4 Hz, 1H, *Hc*), 4.42 (br s, 1H, N*H*), 3.99 (br s, 1H, O*H*), 3.66 (s, 3H, *Hh*), 2.36 (s, 3H, *Ha*) ppm (addition of D_2O caused the signals at δ 4.42 and 3.99 to disappear); ^{13}C NMR (101 MHz, $CDCl_3$) δ 206.7 (s, *Ci*), 152.8 (s, *Cm*), 147.5 (s, *Cj*), 147.4 (s, *Ck*), 139.3 (s, *Cl*), 128.2 (d, *Cd*), 123.8 (d, *Ce*), 115.2 (d, *Cg*), 115.0 (d, *Cf*), 80.0 (d, *Cb*), 58.8 (d, *Cc*), 55.6 (d, *Ch*), 25.0 (d, *Ca*); LRMS (TOF ES+), 331.2 (50%) $[M+H]^+$, 257.3 (100%); HRMS (TOF ES+), calculated for $C_{17}H_{18}N_2O_5+H^+$, 331.1294; observed 331.1300. All spectroscopic and analytical properties were identical to those reported in the literature.[209]

4-((4-Methoxyphenyl)amino)-4-(4-nitrophenyl)butan-2-one[288]

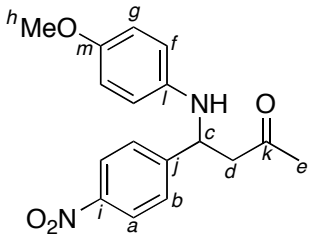

520

To the **473** (0.2 mmol) and triethylamine (0.028 mL, 0.2 mmol) in acetone (1 mL) was added *p*-nitrobenzaldehyde (0.151 g, 1 mmol) and *p*-anisidine (0.123 g, 1 mmol). The reaction mixture was stirred at rt overnight, quenched with (aq) NH_4Cl (10 mL) and extracted with EtOAc (2 × 10 mL). The combined organics were dried ($MgSO_4$) and concentrated *in vacuo*. Purification by silica gel chromatography (10%-100%, EtOAc:hexane, as eluent) afforded **326** as a yellow solid (0.075 g, 29%), **355** as a beige solid (0.015 g, 8%), **505** as a yellow oil (0.036 g, 17%), **506** as an orange oil (0.022 g, 12%) and **520** as a yellow oil (0.020 g, 6%): R_f 0.28 (2:3, EtOAc:hexane, as eluent); ^{1}H NMR (500 MHz, $CDCl_3$) δ 8.18-8.14 (m, 2H, *Ha*), 7.56-7.53 (m, 2H, *hb*),

6.70-6.66 (m, 2H, *Hf*), 6.47-6.44 (m, 2H, *Hg*), 4.85 (t, *J* = 6.3 Hz, 1H, *Hc*), 4.26 (br s, 1H, O*H*), 3.69 (s, 3H, *Hh*), 2.94 (d, *j* = 6.3 Hz, 2H, *Hd*), 2.15 (s, 3H, *He*) ppm; ^{13}C NMR (151 MHz, $CDCl_3$) δ 206.2 (s, *Ck*), 152.9 (s, *Cm*), 150.8 (s, *Cj*), 147.3 (s, *Ci*), 140.3 (s, *Cl*), 127.5 (d, *Ca*), 124.2 (d, *Cb*), 115.5 (d, *Cf*), 114.9 (d, *Cg*), 55.8 (d, *Cc*), 54.8 (d, *Ch*), 50.8 (t, *Cd*), 30.8 (d, *Ce*). All spectroscopic and analytical properties were identical to those reported in the literature.[288]

4-Dibenzylamino-2-butanone[289]

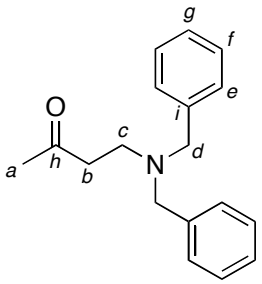

521

To dibenzylamine (0.59 g, 3 mmol) and phenylboronic acid (37 mg, 0.3 mmol) dissolved in water (3 mL) was added methyl vinyl ketone (0.27 mL, 3.3 mmol) and the reaction mixture was stirred at rt overnight. The reaction mixture was extracted with EtOAc (3 × 10 mL), dried ($MgSO_4$) and concentrated *in vacuo*. Purification by silica gel chromatography (4:1, petroleum ether:diethyl ether, as eluent) afforded **521** as a white solid (0.44 g, 55%): m.p. 57-58 °C (lit. 59 °C)[290]; R_f. 0.27 (3:2, petroleum ether:diethyl ether, as eluent); ^{1}H NMR (400 MHz, $CDCl_3$) δ 7.35-7.21 (m, 10H, Ar*H*), 3.55 (s, 4H, *Hd*), 2.77 (t, *J* = 7 Hz, 2H, *Hb*), 2.59 (t, *J* = 7 Hz, 2H, *Hc*), 1.99 (s, 3H, *Ha*) ppm; ^{13}C NMR (101 MHz, $CDCl_3$) δ 208.3 (s, *Ca*), 139.4 (s, *Ci*), 129.0 (d, Ar), 128.4 (d, Ar), 127.1 (d, Ar), 58.5 (t, *Cd*), 48.7 (t, *Cc*), 42.1 (t, *Cb*), 29.8 (d, *Ca*); IR ν_{max} (neat) 1698 (C=O) cm^{-1}; LRMS (TOF ES+), 268.2 (100%) $[M+H]^+$; HRMS (TOF ES+), calculated for $C_{18}H_{21}NO+H^+$, 268.1701; found 268.1706. All spectroscopic and analytical properties were identical to those reported in the literature.[210, 226]

Chapter 6:
REFERENCES

6. References

1. P. D. Bailey, P. A. Millwood and P. D. Smith, *Chem. Commun.*, **1998**, 633-640.
2. M. Amat, N. Llor, J. Hidalgo, C. Escolano and J. Bosch, *J. Org. Chem.*, **2003**, *68*, 1919-1928.
3. N. Asano, R. J. Nash, R. J. Molyneux and G. W. J. Fleet, *Tetrahedron: Asymmetry*, **2000**, *11*, 1645-1680.
4. P. S. Watson, B. Jiang and B. Scott, *Org. Lett.*, **2000**, *2*, 3679-3681.
5. X. G. Huang, A. Q. Zhang, D. L. Chen, Z. H. Jia and X. S. Li, *Bioorg. Med. Chem. Lett.*, **2010**, *20*, 2859-2863.
6. V. H. Lillelund, H. H. Jensen, X. F. Liang and M. Bols, *Chem. Rev.*, **2002**, *102*, 515-553.
7. S. D. Larsen and P. A. Grieco, *J. Am. Chem. Soc.*, **1985**, *107*, 1768-1769; Bertilsson, S. K.; Ekegren; S. K. Bertilsson, J. K. Ekegren, S. A. Modin and P. G. Andersson, *Tetrahedron*, **2001**, *57*, 6399-6406; P. D. Bailey, D. J. Londesbrough, T. C. Hancox, J. D. Heffernan and A. B. Holmes, *J. Chem. Soc.-Chem. Commun.*, **1994**, 2543-2544; D. Ager, N. Cooper, G. G. Cox, F. Garro-Hélion and L. M. Harwood, *Tetrahedron: Asymmetry*, **1996**, *7*, 2563-2566.
8. K. Hattori and H. Yamamoto, *J. Org. Chem.*, **1992**, *57*, 3264-3265.
9. H. Sundén, I. Ibrahem, L. Eriksson and A. Córdova, *Angew. Chem.-Int. Edit.*, **2005**, *44*, 4877-4880.
10. B. List, *Tetrahedron*, **2002**, *58*, 5573-5590.
11. P. Buonora, J. C. Olsen and T. Oh, *Tetrahedron*, **2001**, *57*, 6099-6138.
12. P. I. Dalko and L. Moisan, *Angew. Chem.-Int. Edit.*, **2001**, *40*, 3726-3748.
13. P. I. Dalko and L. Moisan, *Angew. Chem.-Int. Edit.*, **2004**, *43*, 5138-5175.
14. A. Dondoni and A. Massi, *Angew. Chem.-Int. Edit.*, **2008**, *47*, 4638-4660.
15. S. Danishefsky and T. Kitahara, *J. Am. Chem. Soc.*, **1974**, *96*, 7807-7808.
16. S. Danishefsky, C. F. Yan, R. K. Singh, R. B. Gammill, P. M. McCurry, N. Fritsch and J. Clardy, *J. Am. Chem. Soc.*, **1979**, *101*, 7001-7008.
17. S. Danishefsky, J. F. Kerwin and S. Kobayashi, *J. Am. Chem. Soc.*, **1982**, *104*, 358-360.
18. S. Danishefsky and J. F. Kerwin, *J. Org. Chem.*, **1982**, *47*, 3183-3184.
19. J. F. Kerwin and S. Danishefsky, *Tetrahedron Lett.*, **1982**, *23*, 3739-3742.
20. S. Danishefsky, M. E. Langer and C. Vogel, *Tetrahedron Lett.*, **1985**, *26*, 5983-5986.
21. E. R. Larson and S. Danishefsky, *Tetrahedron Lett.*, **1982**, *23*, 1975-1978.
22. S. J. Danishefsky and C. Vogel, *J. Org. Chem.*, **1986**, *51*, 3915-3916.
23. M. M. Midland and J. I. McLoughlin, *Tetrahedron Lett.*, **1988**, *29*, 4653-4656.
24. S. M. Brandstadter and I. Ojima, *Tetrahedron Lett.*, **1987**, *28*, 613-616.
25. L. Lecoz, L. Wartski, J. Seydenpenne, P. Charpin and M. Nierlich, *Tetrahedron Lett.*, **1989**, *30*, 2795-2796.
26. C. Veyrat, L. Wartski and J. Seydenpenne, *Tetrahedron Lett.*, **1986**, *27*, 2981-2984.
27. T. N. Birkinshaw, A. B. Tabor, A. B. Holmes, P. Kaye, P. M. Mayne and P. R. Raithby, *J. Chem. Soc.-Chem. Commun.*, **1988**, 1599-1601.

28. T. N. Birkinshaw, A. B. Tabor, A. B. Holmes and P. R. Raithby, *J. Chem. Soc.-Chem. Commun.*, **1988**, 1601-1602.
29. H. Kunz and W. Pfrengle, *Angew. Chem.-Int. Edit. Engl.*, **1989**, *28*, 1067-1068.
30. M. Weymann, W. Pfrengle, D. Schollmeyer and H. Kunz, *Synthesis*, **1997**, 1151-1160.
31. W. Pfrengle and H. Kunz, *J. Org. Chem.*, **1989**, *54*, 4261-4263.
32. J. T. Randolph, K. F. McClure and S. J. Danishefsky, *J. Am. Chem. Soc.*, **1995**, *117*, 5712-5719.
33. J. Y. Roberge, X. Beebe and S. J. Danishefsky, *Science*, **1995**, *269*, 202-204.
34. I. Paterson, M. Donghi and K. Gerlach, *Angew. Chem.-Int. Edit.*, **2000**, *39*, 3315-3319.
35. D. R. Dragoli, L. A. Thompson, J. O'Brien and J. A. Ellman, *J. Comb. Chem.*, **1999**, *1*, 534-539.
36. G. Zech and H. Kunz, *Chem.-Eur. J.*, **2004**, *10*, 4136-4149.
37. H. Waldmann and M. Braun, *J. Org. Chem.*, **1992**, *57*, 4444-4451.
38. N. T. Anh, *Top. Curr. Chem.*, **1980**, *88*, 145-162.
39. I. Ojima and S. I. Inaba, *Tetrahedron Lett.*, **1980**, *21*, 2081-2084.
40. G. R. Heintzelman, S. M. Weinreb and M. Parvez, *J. Org. Chem.*, **1996**, *61*, 4594-4599.
41. R. Badorrey, C. Cativiela, M. D. Diaz-de-Villegas and J. A. Gálvez, *Tetrahedron*, **1999**, *55*, 7601-7612.
42. G. Babu and P. T. Perumal, *Tetrahedron*, **1998**, *54*, 1627-1638.
43. K. A. Jorgensen, M. Johannsen, S. L. Yao, H. Audrain and J. Thorhauge, *Accounts Chem. Res.*, **1999**, *32*, 605-613.
44. K. Ishihara, M. Miyata, K. Hattori, T. Tada and H. Yamamoto, *J. Am. Chem. Soc.*, **1994**, *116*, 10520-10524.
45. K. Hattori and H. Yamamoto, *Tetrahedron*, **1993**, *49*, 1749-1760.
46. S. Kobayashi, S. Komiyama and H. Ishitani, *Angew. Chem.-Int. Edit.*, **1998**, *37*, 979-981.
47. S. Kobayashi, K. Kusakabe, S. Komiyama and H. Ishitani, *J. Org. Chem.*, **1999**, *64*, 4220-4221.
48. V. Jurčík, K. Arai, M. M. Salter, Y. Yamashita and S. Kobayashi, *Adv. Synth. Catal.*, **2008**, *350*, 647-651.
49. S. L. Yao, S. Saaby, R. G. Hazell and K. A. Jørgensen, *Chem.-Eur. J.*, **2000**, *6*, 2435-2448.
50. F. W. Grevels, W. E. Klotzbucher, G. Russell and K. Schaffner, *Recl. Trav. Chim. Pays-Bas-J. Roy. Neth. Chem. Soc.*, **1995**, *114*, 571-576.
51. J. Savard and P. Brassard, *Tetrahedron Lett.*, **1979**, 4911-4914.
52. M. A. Yawer, I. Hussain, J. P. Gütlein, A. Schmidt, H. J. Jiao, H. Reinke, A. Spannenberg, C. Fischer and P. Langer, *Eur. J. Org. Chem.*, **2008**, 4193-4199.
53. S. Kobayashi, H. Ishitani and S. Nagayama, *Synthesis*, **1995**, 1195-1202.
54. S. Bromidge, P. C. Wilson and A. Whiting, *Tetrahedron Lett.*, **1998**, *39*, 8905-8908.
55. A. Bundu, S. Guillarme, J. Hannan, H. L. Wan and A. Whiting, *Tetrahedron Lett.*, **2003**, *44*, 7849-7850.
56. S. Hermitage, D. A. Jay and A. Whiting, *Tetrahedron Lett.*, **2002**, *43*, 9633-9636.
57. S. Hermitage, J. A. K. Howard, D. Jay, R. G. Pritchard, M. R. Probert and A. Whiting, *Org. Biomol. Chem.*, **2004**, *2*, 2451-2460.

58. T. Akiyama, Y. Tamura, J. Itoh, H. Morita and K. Fuchibe, *Synlett*, **2006**, 141-143.
59. H. F. Du, J. Long, J. Y. Hu, X. Li and K. L. Ding, *Org. Lett.*, **2002**, *4*, 4349-4352.
60. S. Guillarme and A. Whiting, *Synlett*, **2004**, 711-713.
61. L. Di Bari, S. Guillarme, J. Hanan, A. P. Henderson, J. A. K. Howard, G. Pescitelli, M. R. Probert, P. Salvadori and A. Whiting, *Eur. J. Org. Chem.*, **2007**, 5771-5779.
62. C. C. Lin, H. L. Fang, Z. J. Tu, J. T. Liu and C. F. Yao, *J. Org. Chem.*, **2006**, *71*, 6588-6591.
63. H. Mandai, K. Mandai, M. L. Snapper and A. H. Hoveyda, *J. Am. Chem. Soc.*, **2008**, *130*, 17961-17969.
64. J. W. Daly, T. F. Spande, N. Whittaker, R. J. Highet, D. Feigl, N. Nishimori, T. Tokuyama and C. W. Myers, *J. Nat. Prod.*, **1986**, *49*, 265-280.
65. X. D. Lin, R. W. Kavash and P. S. Mariano, *J. Org. Chem.*, **1996**, *61*, 7335-7347.
66. B. Furman and M. Dziedzic, *Tetrahedron Lett.*, **2003**, *44*, 6629-6632.
67. B. Furman, J. Frelek, M. Dziedzic and A. Kamińska, *Pol. J. Chem.*, **2005**, *79*, 1919-1928.
68. A. S. Pilcher, H. L. Ammon and P. Deshong, *J. Am. Chem. Soc.*, **1995**, *117*, 5166-5167.
69. S. K. Lee, U. K. Tambar, N. R. Perl and J. L. Leighton, *Tetrahedron*, **2010**, *66*, 4769-4774.
70. R. Berger, P. M. A. Rabbat and J. L. Leighton, *J. Am. Chem. Soc.*, **2003**, *125*, 9596-9597.
71. G. T. Notte and J. L. Leighton, *J. Am. Chem. Soc.*, **2008**, *130*, 6676-6677.
72. M. Macapinlac, D. D. Biggs, M. Guarino, B. M. Johnson, P. F. Lebowitz and S. F. Su, *Breast Cancer Res. Treat.*, **2006**, *100*, S285-S285.
73. D. Borkin, E. Morzhina, S. Datta, A. Rudnitskaya, A. Sood, M. Török and B. Török, *Org. Biomol. Chem.*, **2011**, *9*, 1394-1401.
74. I. V. Kozhevnikov, *Appl. Catal. A-Gen.*, **2003**, *256*, 3-18.
75. U. Costantino, F. Fringuelli, M. Orrù, M. Nocchetti, O. Piermatti and F. Pizzo, *Eur. J. Org. Chem.*, **2009**, 1214-1220.
76. T. Akiyama, J. Takaya and H. Kagoshima, *Tetrahedron Lett.*, **1999**, *40*, 7831-7834.
77. C. Loncaric, K. Manabe and S. Kobayashi, *Adv. Synth. Catal.*, **2003**, *345*, 475-477.
78. M. Sickert, F. Abels, M. Lang, J. Sieler, C. Birkemeyer and C. Schneider, *Chem.-Eur. J.*, **2010**, *16*, 2806-2818.
79. H. Liu, L. F. Cun, A. Q. Mi, Y. Z. Jiang and L. Z. Gong, *Org. Lett.*, **2006**, *8*, 6023-6026.
80. M. Rueping and C. Azap, *Angew. Chem.-Int. Edit.*, **2006**, *45*, 7832-7835.
81. Z. L. Chen, L. L. Lin, D. H. Chen, J. T. Li, X. H. Liu and X. M. Feng, *Tetrahedron Lett.*, **2010**, *51*, 3088-3091.
82. J. Itoh, K. Fuchibe and T. Akiyama, *Angew. Chem.-Int. Edit.*, **2006**, *45*, 4796-4798.
83. K. A. Jorgensen, *Angew. Chem.-Int. Edit.*, **2000**, *39*, 3558-3588.
84. K. Cheng, L. L. Lin, S. K. Chen and X. M. Feng, *Tetrahedron*, **2005**, *61*, 9594-9599.

85. D. Lanari, F. Montanari, F. Marmottini, O. Piermatti, M. Orrù and L. Vaccaro, *J. Catal.*, **2011**, *277*, 80-87.
86. H. L. Zhang, M. Mifsud, F. Tanaka and C. F. Barbas, *J. Am. Chem. Soc.*, **2006**, *128*, 9630-9631.
87. W. Notz, F. Tanaka, S. Watanabe, N. S. Chowdari, J. M. Turner, R. Thayumanavan and C. F. Barbas, *J. Org. Chem.*, **2003**, *68*, 9624-9634.
88. T. Itoh, M. Yokoya, K. Miyauchi, K. Nagata and A. Ohsawa, *Org. Lett.*, **2003**, *5*, 4301-4304.
89. C. Szántay, G. Blasko, K. Honty, L. Szabó and L. Toke, *Heterocycles*, **1977**, *7*, 155-160.
90. T. Kametani, Y. Hirai, M. Kajiwara, T. Takahashi and K. Fukumoto, *Chem. Pharm. Bull.*, **1975**, *23*, 2634-2642.
91. T. Itoh, M. Yokoya, K. Miyauchi, K. Nagata and A. Ohsawa, *Org. Lett.*, **2006**, *8*, 1533-1535.
92. F. Aznar, A. B. García, N. Quinones and M. P. Cabal, *Synthesis*, **2008**, 479-484.
93. B. Alcaide, P. Almendros, J. M. Alonso and M. F. Aly, *Org. Lett.*, **2001**, *3*, 3781-3784.
94. F. Aznar, A. B. García and M. P. Cabal, *Adv. Synth. Catal.*, **2006**, *348*, 2443-2448.
95. H. Yang and R. G. Carter, *J. Org. Chem.*, **2009**, *74*, 5151-5156.
96. S. Bahmanyar and K. N. Houk, *Org. Lett.*, **2003**, *5*, 1249-1251.
97. H. Yang and R. G. Carter, *Org. Lett.*, **2008**, *10*, 4649-4652.
98. H. Yang and R. G. Carter, *J. Org. Chem.*, **2009**, *74*, 2246-2249.
99. J. Franzén and A. Fisher, *Angew. Chem.-Int. Edit.*, **2009**, *48*, 787-791.
100. K. Jiang, Z. J. Jia, S. Chen, L. Wu and Y. C. Chen, *Chem.-Eur. J.*, **2010**, *16*, 2852-2856.
101. Q. Ding, J.-J. Liu and Z. Zhang, *WO 2007/104714*, **2007**.
102. S. Khaliel, M. V. Nandakumar, H. Krautscheid and C. Schneider, *Synlett*, **2008**, 2705-2707.
103. A. Babtie, N. Tokuriki and F. Hollfelder, *Curr. Opin. Chem. Biol.*, **2010**, *14*, 200-207.
104. M. S. Humble and P. Berglund, *Eur. J. Org. Chem.*, **2011**, 3391-3401.
105. Y. H. He, W. Hu and Z. Guan, *J. Org. Chem.*, **2012**, *77*, 200-207.
106. M. W. Edwards, H. M. Garraffo and J. W. Daly, *Synthesis*, **1994**, 1167-1170.
107. R. S. Aronstam, M. W. Edwards, J. W. Daly and E. X. Albuquerque, *Neurochem. Res.*, **1988**, *13*, 171-176.
108. Y. Yuan, X. Li and K. L. Ding, *Org. Lett.*, **2002**, *4*, 3309-3311.
109. L. H. Liu, S. Y. Zhang, X. F. Fu and C. H. Yan, *Chem. Commun.*, **2011**, *47*, 10148-10150.
110. O. N. Van Buu, A. Aupoix, N. D. T. Hong and G. Vo-Thanh, *New J. Chem.*, **2009**, *33*, 2060-2072.
111. B. Pegot, O. N. Van Buu, D. Gori and G. Vo-Thanh, *Beilstein J. Org. Chem.*, **2006**, *2*, 18.
112. K. Kacprzak and J. Gawronski, *Synthesis*, **2001**, 961-998.
113. Y. Park, E. Park, H. Jung, Y. J. Lee, S. S. Jew and H. G. Park, *Tetrahedron*, **2011**, *67*, 1166-1170.
114. S. M. Paek, N. J. Kim, D. Shin, J. K. Jung, J. W. Jung, D. J. Chang, H. Moon and Y. G. Suh, *Chem.-Eur. J.*, **2010**, *16*, 4623-4628.

115. T. Nemoto, E. Yamamoto, R. Franzén, T. Fukuyama, R. Wu, T. Fukamachi, H. Kobayashi and Y. Hamada, *Org. Lett.*, **2010**, *12*, 872-875.
116. P. R. Girling, T. Kiyoi and A. Whiting, *Org. Biomol. Chem.*, **2011**, *9*, 3105-3121.
117. D. Enders, D. P. Göddertz, C. Beceño and G. Raabe, *Adv. Synth. Catal.*, **2010**, *352*, 2863-2868.
118. X. X. Jiang, X. M. Shi, S. L. Wang, T. Sun, Y. M. Cao and R. Wang, *Angew. Chem.-Int. Edit.*, **2012**, *51*, 2084-2087.
119. J. Vicario, D. Aparicio and F. Palacios, *Tetrahedron Lett.*, **2011**, *52*, 4109-4111.
120. S. L. Zhou, J. L. Li, L. Dong and Y. C. Chen, *Org. Lett.*, **2011**, *13*, 5874-5877.
121. Z.-Q. He, B. Han, R. Li, L. Wu and Y.-C. Chen, *Org. Biomol. Chem.*, **2009**, *8*, 755-757.
122. G. Hirai, H. Oguri, M. Hayashi, K. Koyama, Y. Koizumi, S. M. Moharram and M. Hirama, *Bioorg. Med. Chem. Lett.*, **2004**, *14*, 2647-2651.
123. J. He, X. Q. Chen, M. M. Li, Y. Zhao, G. Xu, X. Cheng, L. Y. Peng, M. J. Xie, Y. T. Zheng, Y. P. Wang and Q. S. Zhao, *Org. Lett.*, **2009**, *11*, 1397-1400.
124. J. L. Li, B. Han, K. Jiang, W. Du and Y. C. Chen, *Bioorg. Med. Chem. Lett.*, **2009**, *19*, 3952-3954.
125. A. Córdova, W. Notz and C. F. Barbas, *J. Org. Chem.*, **2002**, *67*, 301-303.
126. J. L. Li, S. L. Zhou, B. Han, L. Wu and Y. C. Chen, *Chem. Commun.*, **2010**, *46*, 2665-2667.
127. S. M. Sethna and N. M. Shah, *Chem. Rev.*, **1945**, *36*, 1-62.
128. C. A. Kontogiorgis and D. J. Hadjipavlou-Litina, *J. Med. Chem.*, **2005**, *48*, 6400-6408.
129. D. S. Bariana, *J. Med. Chem.*, **1970**, *13*, 544-546.
130. M. Orita, S. Yamamoto, N. Katayama, M. Aoki, K. Takayama, Y. Yamagiwa, N. Seki, H. Suzuki, H. Kurihara, H. Sakashita, M. Takeuchi, S. Fujita, T. Yamada and A. Tanaka, *J. Med. Chem.*, **2001**, *44*, 540-547.
131. S. Robert, C. Bertolla, B. Masereel, J. M. Dogné and L. Pochet, *J. Med. Chem.*, **2008**, *51*, 3077-3080.
132. Y. Watanabe, T. Washio, J. Krishnamurthi, M. Anada and S. Hashimoto, *Chem. Commun.*, **2012**, *48*, 6969-6971.
133. J. Y. Lu and H. D. Arndt, *J. Org. Chem.*, **2007**, *72*, 4205-4212.
134. S. C. Kim, K. M. Choi and C. S. Cheong, *Bull. Korean Chem. Soc.*, **2002**, *23*, 143-144.
135. Y. A. Lee and S. C. Kim, *J. Ind. Eng. Chem.*, **2011**, *17*, 401-403.
136. A. S. L. Devi, Y. S. Rao, M. Satish, G. Jyothi, K. B. Rao and T. Omdutt, *Magn. Reson. Chem.*, **2007**, *45*, 688-691.
137. D. J. Triggle, D. A. Langs and R. A. Janis, *Med. Res. Rev.*, **1989**, *9*, 123-180.
138. D. M. Gotrane, R. D. Deshmukh, P. V. Ranade, S. P. Sonawane, B. M. Bhawal, M. M. Gharpure and M. K. Gurjar, *Org. Process Res. Dev.*, **2010**, *14*, 640-643.
139. S. Samai, G. C. Nandi, S. Chowdhury and M. S. Singh, *Tetrahedron*, **2011**, *67*, 5935-5941.
140. S. R. Kanth, G. V. Reddy, K. H. Kishore, P. S. Rao, B. Narsaiah and U. S. N. Murthy, *Eur. J. Med. Chem.*, **2006**, *41*, 1011-1016.
141. E. M. Grivsky, S. Lee, C. W. Sigel, D. S. Duch and C. A. Nichol, *J. Med. Chem.*, **1980**, *23*, 327-329.

142. D. Heber, C. Heers and U. Ravens, *Pharmazie*, **1993**, *48*, 537-541.
143. L. R. Bennett, C. J. Blankley, R. W. Fleming, R. D. Smith and D. K. Tessman, *J. Med. Chem.*, **1981**, *24*, 382-389.
144. J. Davoll, J. Clarke and E. F. Elslager, *J. Med. Chem.*, **1972**, *15*, 837-839.
145. S. Shigo and I. Hiroshi, *Yakugaku Zasshi*, **1969**, *89*, 266-271.
146. V. K. Ahluwalia, R. Batla, A. Khurana and R. Kumar, *Indian J. Chem. Sect B-Org. Chem. Incl. Med. Chem.*, **1990**, *29*, 1141-1142.
147. H. M. F. Madkour, M. A. I. Salem, T. M. Abdel-Rahman and M. E. Azab, *Heterocycles*, **1994**, *38*, 57-69.
148. E. Gál, C. Cristea, L. Silaghi-Dumitrescu, T. Lovász and A. Csámpai, *Tetrahedron*, **2010**, *66*, 9938-9944.
149. Z. Jia, Y. Ren, C. D. Huo, X. N. Chen, C. X. Tong and X. D. Jia, *Lett. Org. Chem.*, **2012**, *9*, 221-224.
150. S. Palaniappan, B. Rajender and M. Umashankar, *J. Mol. Catal. A-Chem.*, **2012**, *352*, 70-74.
151. K. C. Majumdar, S. Ponra, D. Ghosh and A. Taher, *Synlett*, **2011**, 104-110.
152. S. Ramesh and R. Nagarajan, *Tetrahedron Lett.*, **2011**, *52*, 4857-4860.
153. M. Rodríguez, M. E. Ochoa, R. Santillan, N. Farfán and V. Barba, *J. Organomet. Chem.*, **2005**, *690*, 2975-2988.
154. X. D. Jia, X. E. Wang, C. X. Yang, C. D. Huo, W. J. Wang, Y. Ren and X. C. Wang, *Org. Lett.*, **2010**, *12*, 732-735.
155. R. J. Carra, M. T. Epperson and D. Y. Gin, *Tetrahedron*, **2008**, *64*, 3629-3641.
156. H. Irie, N. Masaki, K. Ohno, K. Osaki, T. Taga and S. Uyeo, *J. Chem. Soc. D: Chem. Commun.*, **1970**, *17*, 1066.
157. R. K. Dieter and F. H. Guo, *J. Org. Chem.*, **2009**, *74*, 3843-3848.
158. S. S. Pakhale and G. B. Maru, *Food Chem. Toxicol.*, **1998**, *36*, 1131-1138.
159. Macconne.Jg, M. S. Baum and H. M. Fales, *Science*, **1970**, *168*, 840-&.
160. T. T. T. Dang and P. J. Facchini, *Plant Physiol.*, **2012**, *159*, 618-631.
161. K. Arnold, A. S. Batsanov, B. Davies, C. Grosjean, T. Schutz, A. Whiting and K. Zawatzky, *Chem. Commun.*, **2008**, 3879-3881.
162. R. Bonnett and T. R. Emerson, *J. Chem. Soc.*, **1965**, 4508-4511.
163. N. A. Akmanova, N. R. Khairullin and Y. V. Svetkin, *Zhurnal Obshchei Khimii*, **1976**, *46*, 704-709.
164. M. C. Elliott and E. Williams, *Org. Biomol. Chem.*, **2003**, *1*, 3038-3047.
165. Y. Mirabal-Gallardo, M. Soriano, J. Caballero, J. Alzate-Morales, M. J. Simirgiotis and L. S. Santos, *Synthesis*, **2012**, *44*, 144-150.
166. D. D. O'Rell, F. G. H. Lee and V. Boekelheide, *J. Am. Chem. Soc.*, **1972**, *94*, 3205-3212.
167. M. R. Monaco, P. Renzi, D. M. S. Schietroma and M. Bella, *Org. Lett.*, **2011**, *13*, 4546-4549.
168. A. King, R. Larsen, T. Li and Y. Lu, *WO 2010/071828*, **2010**.
169. Y. Cui, H. Jiang, Z. T. Li, N. Wu, Z. Yang and J. M. Quan, *Org. Lett.*, **2009**, *11*, 4628-4631.
170. J. Bélanger, N. L. Landry, J. R. J. Paré and K. Jankowski, *J. Org. Chem.*, **1982**, *47*, 3649-3652.
171. C. B. Patil, S. K. Mahajan and S. A. Katti, *J. Pharm. Sci. & Res.*, **2009**, *1*, 11-12.
172. K. Takasu, N. Hosokawa, K. Inanaga and M. Ihara, *Tetrahedron Lett.*, **2006**, *47*, 6053-6056; E. Caballero, J. Figueroa, P. Puebla, R. Peláez, F. Tomé and M. Medarde, *Eur. J. Org. Chem.*, **2008**, 4004-4014; P. D. Bailey, P. D. Smith,

F. Pederson, W. Clegg, G. M. Rosair and S. J. Teat, *Tetrahedron Lett.*, **2002**, *43*, 1067-1070.
173. P. G. Zheng, B. P. Lieberman, S. R. Choi, K. Ploessl and H. F. Kung, *Bioorg. Med. Chem. Lett.*, **2011**, *21*, 3435-3438.
174. C. Zorn, B. Anichini, A. Goti, A. Brandi, S. I. Kozhushkov, A. de Meijere and L. Citti, *J. Org. Chem.*, **1999**, *64*, 7846-7855.
175. E. Winterfeldt and H. Radunz, *Chem. Ber.-Recl.*, **1967**, *100*, 1680-1684.
176. S. Yamada, *Yakugaku Zasshi-J. Pharm. Soc. Jpn.*, **1951**, *71*, 1349-1355.
177. G. M. Sheldrick, *Acta Crystallogr. Sect. A*, **2008**, *64*, 112-122.
178. O. V. Dolomanov, L. J. Bourhis, R. J. Gildea, J. A. K. Howard and H. Puschmann, *J. Appl. Crystallogr.*, **2009**, *42*, 339-341.
179. F. H. Allen, O. Kennard, D. G. Watson, L. Brammer, A. G. Orpen and R. Taylor, *J. Chem. Soc.-Perkin Trans. 2*, **1987**, S1-S19.
180. B. H. O'Connor, *Acta Crystallogr. Sect. B-Struct. Commun.*, **1973**, *B 29*, 1893-1903.
181. B. H. O'Connor and F. H. Moore, *Acta Crystallogr. Sect. B-Struct. Commun.*, **1973**, *B 29*, 1903-1909.
182. J. C. Zhuo, *Magn. Reson. Chem.*, **1997**, *35*, 21-29.
183. J. C. Zhuo, *Magn. Reson. Chem.*, **1997**, *35*, 311-322.
184. E. Fillion and D. Fishlock, *Tetrahedron*, **2009**, *65*, 6682-6695.
185. A. Hantzsch, *Justus Liebigs Ann. Chem.*, **1882**, *215*, 1-82.
186. G. Inouye, *Nippon Kagaku Zassi*, **1959**, *80*, 1061-1063.
187. N. Sugiyama, G. Inouye and K. Ito, *Bull. Chem. Soc. Jpn.*, **1962**, *35*, 927-928.
188. J. Y. Yang, C. Y. Wang, X. Xie, H. F. Li and Y. Z. Li, *Eur. J. Org. Chem.*, **2010**, 4189-4193.
189. P. R. Girling, A. S. Batsanov, H. C. Shen and A. Whiting, *Chem. Commun.*, **2012**, *48*, 4893-4895.
190. J. M. Caroon, R. D. Clark, A. F. Kluge, C. H. Lee and A. M. Strosberg, *J. Med. Chem.*, **1983**, *26*, 1426-1433.
191. I. Georgiou and A. Whiting, *Chim. Oggi-Chem. Today*, **2010**, *28*, IV-VI.
192. H. Charville, D. Jackson, G. Hodges and A. Whiting, *Chem. Commun.*, **2010**, *46*, 1813-1823.
193. I. Georgiou, G. Ilyashenko and A. Whiting, *Accounts Chem. Res.*, **2009**, *42*, 756-768.
194. I. Georgiou and A. Whiting, *Org. Biomol. Chem.*, **2012**, *10*, 2422-2430.
195. A. Pelter, K. Smith and H. C. Brown, *Borane Reagents*, Academic Press, London, 1988.
196. H. C. Brown, J. R. Schwier and B. Singaram, *J. Org. Chem.*, **1978**, *43*, 4395-4397.
197. A. K. Mandal, P. K. Jadhav and H. C. Brown, *J. Org. Chem.*, **1980**, *45*, 3543-3544.
198. S. Pereira and M. Srebnik, *J. Am. Chem. Soc.*, **1996**, *118*, 909-910.
199. Y. Yamamoto, R. Fujikawa, T. Umemoto and N. Miyaura, *Tetrahedron*, **2004**, *60*, 10695-10700.
200. R. K. Dieter, G. Oba, K. R. Chandupatla, C. M. Topping, K. Lu and R. T. Watson, *J. Org. Chem.*, **2004**, *69*, 3076-3086.
201. I. Coldham and D. Leonori, *J. Org. Chem.*, **2010**, *75*, 4069-4077.
202. I. Georgiou and A. Whiting, *Eur. J. Org. Chem.*, **2012**, 4110-4113.
203. J. F. Austin and D. W. C. MacMillan, *J. Am. Chem. Soc.*, **2002**, *124*, 1172-1173.

204. R. Kane, *J. Prakt. Chem.*, **1838**, *15*, 129;R. Kane, *Ann. Phys. Chem. Ser. 2*, **1838**, *44*, 475.
205. T. Mukaiyama, *Org. React.*, **1982**, *28*, 203-331.
206. B. List, R. A. Lerner and C. F. Barbas, *J. Am. Chem. Soc.*, **2000**, *122*, 2395-2396.
207. I. K. Mangion, A. B. Northrup and D. W. C. MacMillan, *Angew. Chem.-Int. Edit.*, **2004**, *43*, 6722-6724.
208. K. Mei, S. Zhang, S. He, P. Li, M. Jin, F. Xue, G. Luo, H. Zhang, L. Song, W. Duan and W. Wang, *Tetrahedron Lett.*, **2008**, *49*, 2681-2684.
209. B. List, P. Pojarliev, W. T. Biller and H. J. Martin, *J. Am. Chem. Soc.*, **2002**, *124*, 827-833.
210. M. K. Chaudhuri, S. Hussain, M. L. Kantam and B. Neelima, *Tetrahedron Lett.*, **2005**, *46*, 8329-8331.
211. H. E. Gottlieb, V. Kotlyar and A. Nudelman, *J. Org. Chem.*, **1997**, *62*, 7512-7515.
212. H. Gilman and F. K. Cartledge, *J. Organomet. Chem.*, **1964**, *2*, 447-454.
213. J. Suffert, *J. Org. Chem.*, **1989**, *54*, 509-510.
214. Y. Yamashita, S. Saito, H. Ishitani and S. Kobayashi, *J. Am. Chem. Soc.*, **2003**, *125*, 3793-3798; P. C. B. Page, S. A. Harkin, A. P. Marchington and M. B. Vanniel, *Tetrahedron*, **1989**, *45*, 3819-3838.
215. E. Borrione, M. Prato, G. Scorrano, M. Stivanello and V. Lucchini, *J. Heterocycl. Chem.*, **1988**, *25*, 1831-1835.
216. Y. Niwa and M. Shimizu, *J. Am. Chem. Soc.*, **2003**, *125*, 3720-3721; M. Shi, G. N. Ma and J. Gaol, *J. Org. Chem.*, **2007**, *72*, 9779-9781; M. Mauksch, S. B. Tsogoeva, S. W. Wei and I. M. Martynova, *Chirality*, **2007**, *19*, 816-825.
217. M. D. Potter and E. P. Taylor, *J. Chem. Soc.*, **1953**, 1320-1321.
218. S. Kodama, J. Yoshida, A. Nomoto, Y. Ueta, S. Yano, M. Ueshima and A. Ogawa, *Tetrahedron Lett.*, **2010**, *51*, 2450-2452; J. C. Pelletier and M. P. Cava, *J. Org. Chem.*, **1987**, *52*, 616-622.
219. S. Cicchi, J. Revuelta, A. Zanobini, M. Betti and A. Brandi, *Synlett*, **2003**, 2305-2308.
220. J. Revuelta, S. Cicchi and A. Brandi, *J. Org. Chem.*, **2005**, *70*, 5636-5642.
221. M. Onda and M. Sasamoto, *Pharmaceutical Bulletin*, **1957**, *5*, 305-10.
222. J. A. Maclaren, *Aust. J. Chem.*, **1987**, *40*, 1617-1618.
223. W. Miller and J. Plöchl, *Chemische Berichte*, **1898**, *31*, 2699-2717.
224. S. E. Denmark, N. Nakajima, C. M. Stiff, O. J. C. Nicaise and M. Kranz, *Adv. Synth. Catal.*, **2008**, *350*, 1023-1045.
225. T. Nakajima, T. Inada, T. Igarashi, T. Sekioka and I. Shimizu, *Bull. Chem. Soc. Jpn.*, **2006**, *79*, 1941-1949.
226. A. Gomtsyan, R. J. Koenig and C. H. Lee, *J. Org. Chem.*, **2001**, *66*, 3613-3616.
227. K. A. Tehrani, T. NguyenVan, M. Karikomi, M. Rottiers and N. De Kimpe, *Tetrahedron*, **2002**, *58*, 7145-7152; N. DeKimpe, D. DeSmaele and Z. Sakonyi, *J. Org. Chem.*, **1997**, *62*, 2448-2452.
228. F. G. Pope and R. Fleming, *J. Chem. Soc.*, **1908**, *93*, 1914-1919.
229. A. W. Johnson and S. C. K. Wong, *Can. J. Chem.*, **1966**, *44*, 2793-2803.
230. C. Darwich, M. Elkhatib, G. Steinhauser and H. Delalu, *Helv. Chim. Acta*, **2009**, *92*, 98-111.
231. P. Spica, *Gazzetta Chimica Italiana*, **1879**, *9*, 555.

232. S. X. Liu, Y. H. Yang, X. L. Zhen, J. Z. Li, H. M. He, J. Feng and A. Whiting, *Org. Biomol. Chem.*, **2012**, *10*, 663-670.
233. A. Bischler and B. Napieralski, *Chemische Berichte*, **1893**, *26*, 1903-1908.
234. C. Schöpf and H. Steuer, *Justus Liebigs Ann. Chem.*, **1947**, *558*, 124-136.
235. E. Lellmann and W. Geller, *Chemische Berichte*, **1888**, *21*, 1921-1923.
236. T. J. Barker and E. R. Jarvo, *J. Am. Chem. Soc.*, **2009**, *131*, 15598-+.
237. L. Claisen and A. Claparède, *Chemische Berichte*, **1881**, *14*.
238. M. McConville, O. Saidi, J. Blacker and J. L. Xiao, *J. Org. Chem.*, **2009**, *74*, 2692-2698.
239. D. Titu and A. Chadha, *Tetrahedron: Asymmetry*, **2008**, *19*, 1698-1701.
240. G. M. Rubottom and J. M. Gruber, *J. Org. Chem.*, **1977**, *42*, 1051-1056.
241. M. E. Jung, N. Nishimura and A. R. Novack, *J. Am. Chem. Soc.*, **2005**, *127*, 11206-11207.
242. A. Einhorn and J. P. Grabfield, *Justus Liebigs Ann. Chem.*, **1888**, *243*, 362-378.
243. M. L. Edwards, H. W. Ritter, D. M. Stemerick and K. T. Stewart, *J. Med. Chem.*, **1983**, *26*, 431-436.
244. Z. H. Wang, G. D. Yin, J. Qin, M. Gao, L. P. Cao and A. X. Wu, *Synthesis*, **2008**, 3675-3681.
245. A. Baeyer and P. Becker, *Chemische Berichte*, **1883**, *16*, 1968-1971.
246. G. P. Schiemenz, J. Becker and J. Stockigt, *Chem. Ber.*, **1977**, 3903-3907.
247. K. Aelvoet, A. S. Batsanov, A. J. Blatch, C. Grosjean, L. G. F. Patrick, C. A. Smethurst and A. Whiting, *Angew. Chem.-Int. Edit.*, **2008**, *47*, 768-770; Y. S. Wu, W. Y. Shao, C. Q. Zheng, Z. L. Huang, J. W. Cai and Q. Y. Deng, *Helv. Chim. Acta*, **2004**, *87*, 1377-1384; A. El-Batta, C. C. Jiang, W. Zhao, R. Anness, A. L. Cooksy and M. Bergdahl, *J. Org. Chem.*, **2007**, *72*, 5244-5259; Y. M. Lin, Z. T. Li, V. Casarotto, J. Ehrmantraut and A. N. Nguyen, *Tetrahedron Lett.*, **2007**, *48*, 5531-5534.
248. N. K. Marakova, Y. A. Zaichenko, A. E. Tsil'ko and I. A. Maretina, *Zhurnal Org. Khimii*, **1984**, *20*, 962-968.
249. Y. S. Kwak and J. D. Winkler, *J. Am. Chem. Soc.*, **2001**, *123*, 7429-7430.
250. K. Manabe, Y. Mori and S. Kobayashi, *Tetrahedron*, **2001**, *57*, 2537-2544.
251. L. Claisen and N. Stylos, *Chemische Berichte*, **1888**, *21*, 1144-1149.
252. J. S. Bajwa and P. J. Sykes, *J. Chem. Soc.-Perkin Trans. 1*, **1979**, 3085-3094.
253. V. Kumbaraci, D. Ergunes, M. Midilli, S. Begen and N. Talinli, *J. Heterocycl. Chem.*, **2009**, *46*, 226-230; S. I. Murahashi, Y. Mitsue and T. Tsumiyama, *Bull. Chem. Soc. Jpn.*, **1987**, *60*, 3285-3290.
254. G. Duuay, *Bulletin de la Societe Chimique de France*, **1974**, 2507-2512.
255. G. Duguay, C. Metayer and H. Quiniou, *Bulletin De La Societe Chimique De France Partie Ii-Chimie Moleculaire Organique Et Biologique*, **1974**, 2507-2512.
256. I. G. Farbenind, *Fortschr. Teerfarbenfabr. Verw. Industriezweige*, **1935**, *24*, 72.
257. D. B. Ramachary and R. Mondal, *Tetrahedron Lett.*, **2006**, *47*, 7689-7693.
258. G. Inoue, *Nippon Kagaku Zasshi*, **1959**, *80*, 1061-1063.
259. G. O. Dudek and G. P. Volpp, *J. Am. Chem. Soc.*, **1963**, *85*, 2697-2700.
260. R. Kaushal, *J. Indian Chem. Soc.*, **1943**, *20*, 54.
261. E. Haak, *Eur. J. Org. Chem.*, **2007**, 2815-2824.
262. J. Dabrowski, A. Skup and S. M., *Organic Magnetic Resonance*, **1969**, *1*, 341-242.

263. D. Beke and C. Szántay, *Chem. Ber.-Recl.*, **1962**, *95*, 2132-2136.
264. L. Cui, Y. Peng and L. M. Zhang, *J. Am. Chem. Soc.*, **2009**, *131*, 8394-8395.
265. A. H. Land, C. Ziegler and J. M. Sprague, *J. Am. Chem. Soc.*, **1947**, *69*, 125-128.
266. P. Beak, S. T. Kerrick, S. D. Wu and J. X. Chu, *J. Am. Chem. Soc.*, **1994**, *116*, 3231-3239.
267. Y. Yoshimi, T. Itou and M. Hatanaka, *Chem. Commun.*, **2007**, 5244-5246;Y. Basel and A. Hassner, *Synthesis*, **2001**, 550-552.
268. T. Shono, J. Terauchi, K. Kitayama, Y. Takeshima and Y. Matsumura, *Tetrahedron*, **1992**, *48*, 8253-8262.
269. K. Narasaka and Y. Kohno, *Bull. Chem. Soc. Jpn.*, **1993**, *66*, 3456-3463.
270. R. K. Dieter, V. K. Gore and N. Y. Chen, *Org. Lett.*, **2004**, *6*, 763-766.
271. P. G. M. Wuts and P. A. Thompson, *J. Organomet. Chem.*, **1982**, *234*, 137-141.
272. G. A. Molander and M. A. Hiebel, *Org. Lett.*, *12*, 4876-4879.
273. G. W. Anderson and A. C. McGregor, *J. Am. Chem. Soc.*, **1957**, *79*, 6180-6183.
274. E. Guibejampel and M. Wakselman, *Synthesis*, **1977**, 772-772.
275. P. Huy, J. M. Neudörfl and H. G. Schmalz, *Org. Lett.*, **2011**, *13*, 216-219.
276. F. Leyendecker, F. Jesser and D. Laucher, *Tetrahedron Lett.*, **1983**, *24*, 3513-3516.
277. E. J. Trybulski, R. H. Kramss, R. M. Mangano and A. Rusinko, *J. Med. Chem.*, **1990**, *33*, 3190-3198.
278. G. Bartoli, M. Bosco, R. Dalpozzo, A. Giuliani, E. Marcantoni, T. Mecozzi, L. Sambri and E. Torregiani, *J. Org. Chem.*, **2002**, *67*, 9111-9114.
279. S. H. Park, H. J. Kang, S. Ko, S. Park and S. Chang, *Tetrahedron: Asymmetry*, **2001**, *12*, 2621-2624.
280. A. Bolognese, O. Fierro, D. Guarino, L. Longobardo and R. Caputo, *Eur. J. Org. Chem.*, **2006**, 169-173.
281. R. A. Abramovitch and J. R. Stowers, *Heterocycles*, **1984**, *22*, 671-673.
282. C. P. Allen, T. Benkovics, A. K. Turek and T. P. Yoon, *J. Am. Chem. Soc.*, **2009**, *131*, 12560-12561.
283. T. A. Connors, W. C. J. Ross and J. G. Wilson, *J. Chem. Soc.*, **1960**, 2994-3007.
284. A. Hosomi, H. Hayashida and Y. Tominaga, *J. Org. Chem.*, **1989**, *54*, 3254-3256.
285. S. Q. Hu, T. Jiang, Z. F. Zhang, A. L. Zhu, B. X. Han, J. L. Song, Y. Xie and W. J. Li, *Tetrahedron Lett.*, **2007**, *48*, 5613-5617.
286. L. Q. Lu, X. N. Xing, X. F. Wang, Z. H. Ming, H. M. Wang and W. J. Xiao, *Tetrahedron Lett.*, **2008**, *49*, 1631-1635.
287. L. Tuchman-Shukron, T. Kehat and M. Portnoy, *Eur. J. Org. Chem.*, **2009**, 992-996.
288. B. List, *J. Am. Chem. Soc.*, **2000**, *122*, 9336-9337.
289. H. Takayama, T. Suzuki and T. Nomoto, *Chem. Lett.*, **1978**, 865-866.
290. L. Lebreton, E. Jost, B. Carboni, J. Annat, M. Vaultier, P. Dutartre and P. Renaut, *J. Med. Chem.*, **1999**, *42*, 4749-4763.

Chapter 7:
APPENDIX

7. Appendix

7.1 List of Publications

P. R. Girling, T. Kiyoi, A. Whiting, "Mannich-Michael *versus* formal aza-Diels-Alder approaches to piperidine derivatives", *Org. Biomol. Chem.,* **2011**, *9*, 3105-3121.

P. R. Girling, A. S. Batsanov, H. C. Shen, A. Whiting, "A multicomponent formal [1+2+1+2]-cycloaddition for the synthesis of dihydropyridines", *Chem. Commun.,* **2012**, *48*, 4893-4895.

7.2 List of Conferences Attended

Date	Meeting	Location	Presentation
12/01/2010	Sheffield Stereochemistry	Sheffield	-
26/01/2010	Thomas Swan & Co. Ltd.	Consett	-
17/03/2010	Life in the Biopharmaceutical Industry	Durham	-
18/03/2010	Catalyst Preparation 4 the 21st Century	London	Poster
15/04/2010	RSC Organic Division Northeast Region Symposium	Durham	Poster
22/04/2010	RSC Bioorganic Meeting	Nottingham	Poster
08/07/2010 – 09/07/2010	USIC (Universities of Scotland Inorganic Conference)	Durham	-
13/10/2010 – 15/10/2010	Dalton Discussion 12: Catalytic C-H and C-X Bond Activation	Durham	-
28/10/2010	1st NORSC (NORthern Sustainable Chemistry) Network Seminar Day	York	Poster
13/01/2011	Stereochemistry at Sheffield	Sheffield	-
06/04/2011	22nd SCI Graduate Symposium	Manchester	-
13/04/2011	RSC Organic Division Northeast Region Symposium	Northumbria	Poster
15/04/2011	RSC Bioorganic Group Postgraduate Symposium	London	-
03/05/2011	22nd SCI Regional Graduate Symposium on Novel Organic Chemistry	Edinburgh	-
04/05/2011	2nd Pre-Grasmere Symposium	York	-
08/08/2011	Merck Medicinal Chemistry Group Meeting	Rahway, New Jersey, USA	Oral
16/08/2011	Merck Summer-Intern Poster Symposium	Rahway, New Jersey, USA	Poster
28/08/2011 – 01/09/2011	242nd ACS Fall Meeting 2011	Denver, USA	-
22/09/2011	RSC Postgraduate Symposium: Heterocyclic and Synthesis Group	AstraZeneca, Alderley Park	Oral

25/10/2011	2nd NORSC Network Seminar Day	York	Oral
02/11/2011	Challenges in Catalysis III	London	Poster
22/11/2011	Durham Synthetic Seminar	Durham	Oral
07/12/2011 – 09/12/2011	29th SCI Process Development Symposium	Cambridge	-
10/01/2012	Stereochemistry at Sheffield	Sheffield	-
25/03/2012 – 29/03/2012	243rd ACS National Meeting and Exposition	San Diego, USA	Oral
12/04/2012	23rd SCI Regional Graduate Symposium on Novel Organic Chemistry	Leeds	Oral
24/04/2012	NEPIC- NORSC Sustainable Chemistry for Industry Event	Ramside Hall, Durham	-
13/06/2012	Durham Postgraduate Symposium	Durham	Oral
03/07/2012	North West Organic Chemistry	Liverpool	Poster
09/09/2012 – 13/09/2012	21st IUPAC International Conference on Physical Organic Chemistry	Durham	-

7.3 ^{1}H-^{1}H 2D NOE (NOESY) Spectrum

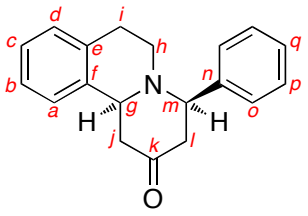

431

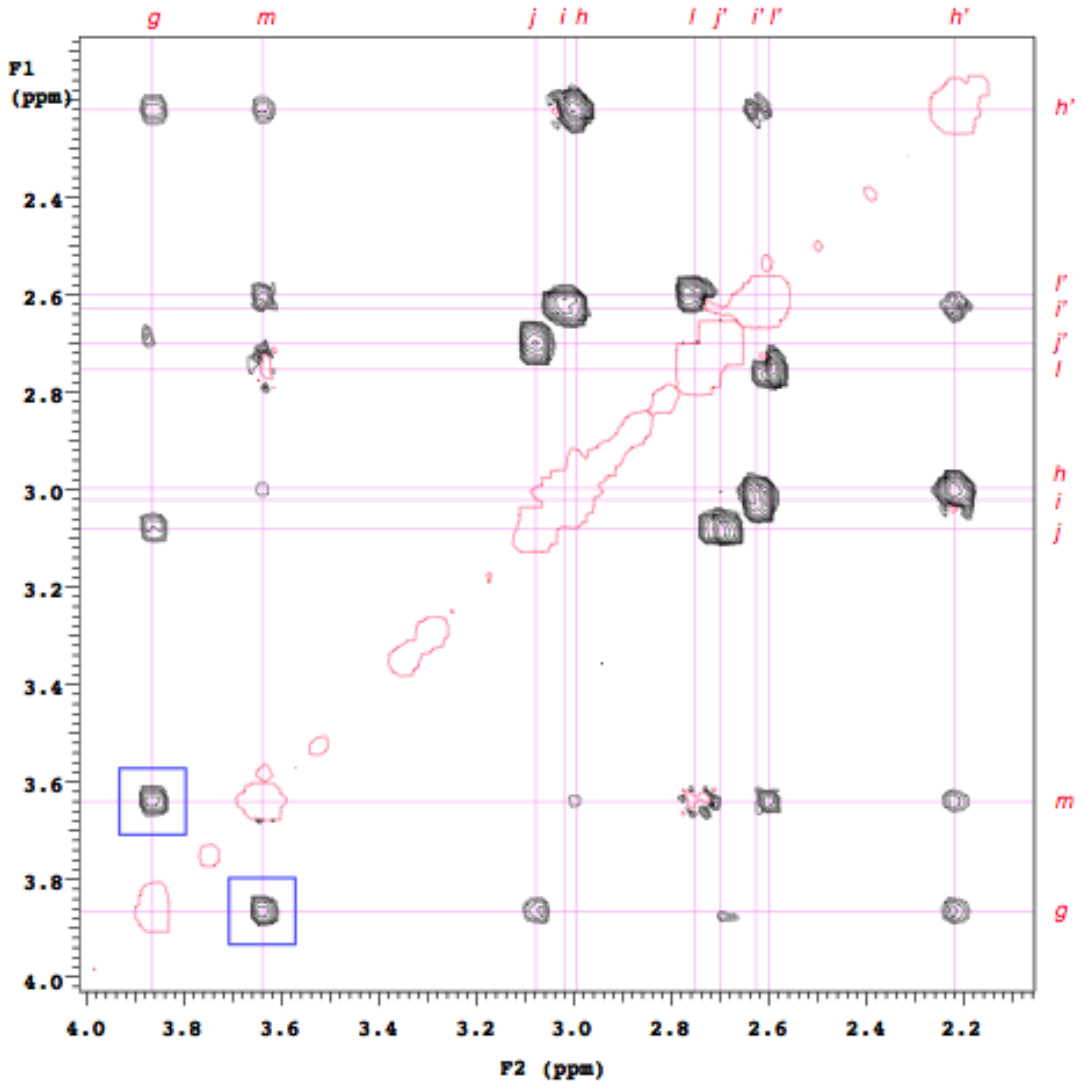

7.4 X-Ray Crystallography Data

Crystallography Data for Compound **369**

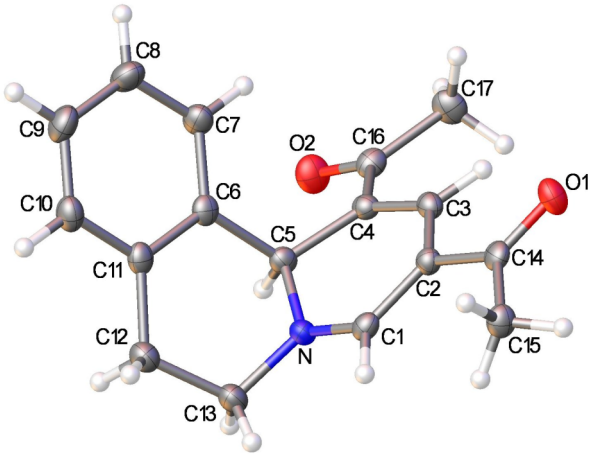

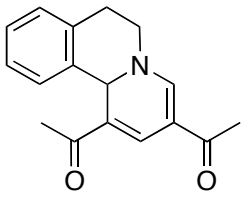

369

Table 1: Crystal data and structure refinement for **369**

Identification code	**369**
Empirical formula	$C_{17}H_{17}NO_2$
Formula weight	267.32
Temperature / K	120.0
Crystal system	orthorhombic
Space group	Pbca
a / Å, b / Å, c / Å	10.5511(4), 8.8537(3), 28.6974(10)
α/°, β/°, γ/°	90.00, 90.00, 90.00
Volume / Å^3	2680.80(17)
Z	8
ρ_{calc} / mg mm^{-3}	1.325
μ / mm^{-1}	0.087
F(000)	1136
Crystal size / mm^3	0.04 × 0.12 × 0.20
Theta range for data collection	1.42 to 49.98°
Index ranges	$-12 \leq h \leq 12$, $-10 \leq k \leq 10$, $-34 \leq l \leq 34$
Reflections collected	25682
Independent reflections	2369[R(int) = 0.0883]
Data/restraints/parameters	2369/0/249

Goodness-of-fit on F^2	0.945
Final R indexes [I>2σ (I)]	$R_1 = 0.0377$, $wR_2 = 0.0812$
Final R indexes [all data]	$R_1 = 0.0734$, $wR_2 = 0.0946$
Largest diff. peak/hole / e $Å^{-3}$	0.178/-0.191

Table 2 Fractional Atomic Coordinates ($\times 10^4$) and Equivalent Isotropic Displacement Parameters ($Å^2 \times 10^3$) for **369**. U_{eq} is defined as 1/3 of of the trace of the orthogonalised U_{IJ} tensor.

Atom	*x*	*y*	*z*	U(eq)
O1	6631.7(12)	1694.5(14)	5105.4(5)	27.3(4)
O2	6609.5(13)	6731.9(15)	6678.0(5)	30.8(4)
N	3834.6(14)	5204.5(17)	5791.1(5)	19.3(4)
C1	4122.9(18)	4179(2)	5470.1(7)	19.8(4)
C2	5274.1(17)	3441(2)	5458.8(6)	18.3(4)
C3	6230.4(18)	3980(2)	5778.7(6)	19.3(4)
C4	5967.5(17)	4974(2)	6120.1(6)	18.5(4)
C5	4600.2(17)	5410(2)	6215.6(6)	19.1(4)
C6	3937.1(18)	4532(2)	6603.2(6)	19.7(4)
C7	4602.8(19)	3755(2)	6945.4(7)	25.2(5)
C8	3966(2)	2940(2)	7283.6(7)	30.6(5)
C9	2650(2)	2906(2)	7283.9(7)	31.3(5)
C10	1985.6(19)	3679(2)	6945.6(7)	27.1(5)
C11	2611.4(18)	4509(2)	6602.8(6)	21.5(5)
C12	1845(2)	5359(3)	6243.5(7)	26.5(5)
C13	2588.5(19)	5928(2)	5820.7(7)	25.2(5)
C14	5586.0(18)	2339(2)	5108.6(6)	20.9(5)
C15	4626(2)	1907(3)	4738.7(7)	24.6(5)
C16	6931.9(18)	5745(2)	6399.8(7)	22.0(5)
C17	8307(2)	5350(3)	6337.7(8)	28.1(5)

Table 3 Anisotropic Displacement Parameters ($Å^2 \times 10^3$) for **369**. The Anisotropic displacement factor exponent takes the form: $-2\pi^2[h^2a^{*2}U_{11}+...+2hka \times b \times U_{12}]$

Atom	U_{11}	U_{22}	U_{33}	U_{23}	U_{13}	U_{12}
O1	19.8(8)	29.0(8)	33.0(8)	-7.0(7)	2.9(6)	1.7(6)
O2	30.9(8)	31.9(8)	29.7(8)	-10.0(7)	-0.7(7)	-2.5(7)
N	16.5(9)	22.1(9)	19.3(9)	1.1(7)	-0.3(7)	2.8(7)
C1	20.1(11)	22.5(11)	16.7(10)	1.6(9)	0.6(9)	-4.0(9)
C2	16.9(10)	20(1)	17.8(10)	0.5(8)	1.4(8)	-0.8(8)
C3	16.8(11)	19.7(10)	21.5(10)	2.2(9)	1.7(9)	0.1(8)
C4	17.2(11)	19.1(10)	19.1(10)	2.8(8)	-0.4(8)	-0.6(8)
C5	19.2(11)	20.7(11)	17.5(10)	-2.3(8)	-1.9(9)	0.7(8)
C6	21.1(11)	19(1)	19(1)	-5.6(9)	1.4(9)	-1.2(8)
C7	19.1(11)	33.4(12)	23.2(11)	0.6(10)	-2.1(10)	-1.5(10)
C8	30.3(13)	40.0(14)	21.6(12)	6.2(10)	-3.1(11)	-0.9(10)
C9	31.2(13)	39.2(14)	23.5(12)	3.1(10)	5.8(11)	-6.3(10)
C10	20.4(11)	34.1(12)	26.7(11)	-3.4(10)	3.8(10)	-2.0(9)
C11	20.1(11)	24.2(11)	20.1(10)	-5.4(9)	2.6(9)	-1.3(8)
C12	21.2(12)	30.3(12)	28.0(12)	1(1)	0.6(10)	3.7(10)
C13	20.1(11)	30.7(12)	24.7(11)	0.6(10)	-0.5(10)	5.4(9)
C14	20.1(11)	22(1)	20.5(11)	4.2(9)	4.8(9)	-3.2(9)
C15	24.1(12)	27.5(12)	22.2(11)	-4.2(10)	0.8(10)	-2.5(11)
C16	25.9(11)	19.1(10)	21.1(10)	0.6(9)	0.4(9)	-3.5(9)
C17	20.5(13)	31.7(13)	32.2(13)	-4.3(11)	-5.6(11)	-3.7(10)

Table 4 Bond Lengths for **369**.

Atom	Atom	Length/Å	Atom	Atom	Length/Å
O1	C14	1.242(2)	C5	C6	1.527(3)
O2	C16	1.232(2)	C6	C7	1.389(3)
N	C1	1.328(2)	C6	C11	1.399(3)
N	C5	1.473(2)	C7	C8	1.383(3)
N	C13	1.465(2)	C8	C9	1.388(3)
C1	C2	1.380(3)	C9	C10	1.379(3)
C2	C3	1.445(2)	C10	C11	1.395(3)
C2	C14	1.439(3)	C11	C12	1.510(3)

C3	C4	1.346(3)	C12	C13	1.529(3)
C4	C5	1.518(3)	C14	C15	1.517(3)
C4	C16	1.465(3)	C16	C17	1.503(3)

Table 5 Bond Angles for **369**.

Atom	Atom	Atom	Angle/°	Atom	Atom	Atom	Angle/°
O1	C14	C2	121.32(17)	C4	C5	C6	115.93(15)
O1	C14	C15	118.18(18)	C4	C16	C17	119.83(17)
O2	C16	C4	119.60(17)	C6	C11	C12	121.89(17)
O2	C16	C17	120.56(18)	C7	C6	C5	122.36(17)
N	C1	C2	122.80(18)	C7	C6	C11	119.94(18)
N	C5	C4	109.91(15)	C7	C8	C9	119.9(2)
N	C5	C6	106.76(15)	C8	C7	C6	120.54(19)
N	C13	C12	111.20(16)	C9	C10	C11	121.17(19)
C1	N	C5	122.16(16)	C10	C9	C8	119.8(2)
C1	N	C13	122.97(17)	C10	C11	C6	118.70(18)
C1	C2	C3	116.30(17)	C10	C11	C12	119.41(18)
C1	C2	C14	122.62(17)	C11	C6	C5	117.69(16)
C2	C14	C15	120.48(18)	C11	C12	C13	115.58(17)
C3	C4	C5	119.57(17)	C13	N	C5	112.98(15)
C3	C4	C16	124.08(17)	C14	C2	C3	120.53(17)
C4	C3	C2	122.31(18)	C16	C4	C5	116.28(16)

Table 6 Hydrogen Atom Coordinates (Å×10^4) and Isotropic Displacement Parameters (Å^2×10^3) for **369**.

Atom	*x*	*y*	*z*	U(eq)
H1	3457(17)	4026(19)	5235(6)	18(5)
H3	7102(18)	3650.0(2)	5721(6)	21(5)
H5	4551(16)	6530.0(2)	6294(6)	23(5)
H7	5527(19)	3770.0(2)	6945(7)	34(6)
H8	4422(17)	2420.0(2)	7521(7)	24(5)
H9	2210(16)	2310.0(2)	7522(7)	22(5)
H10	1051(19)	3660.0(2)	6947(6)	27(5)
H12A	1150.0(2)	4690.0(2)	6128(8)	47(7)
H12B	1438(18)	6200.0(2)	6391(7)	32(6)
H13A	2150(18)	5700.0(2)	5525(7)	26(5)
H13B	2756(18)	7060.0(2)	5853(6)	34(6)

H15A	5080.0(2)	1580.0(2)	4452(8)	47(7)
H15B	4050.0(2)	2700.0(3)	4644(8)	52(7)
H15C	4070.0(2)	1090.0(3)	4840(8)	61(7)
H17A	8550.0(2)	5560.0(2)	6004(8)	48(7)
H17B	8510.0(2)	4280.0(3)	6409(8)	54(7)
H17C	8769(19)	6010.0(2)	6534(7)	31(6

Crystallography Data for Compound **376**

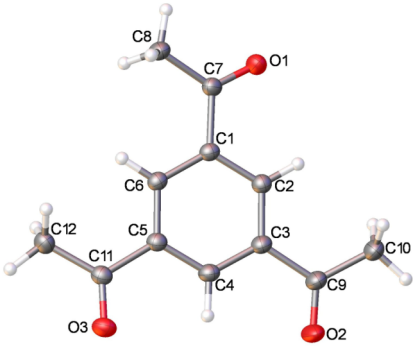

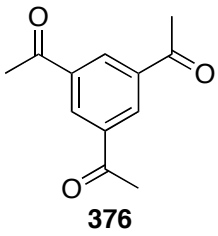

376

Table 1: Crystal data and structure refinement for **376**

Identification code	**376**
Empirical formula	$C_{12}H_{12}O_3$
Formula weight	204.22
Temperature / K	120
Crystal system	monoclinic
Space group	$P2_1/c$
a / Å, b / Å, c / Å	8.3010(3), 16.2516(6), 7.5205(3)
α/°, β/°, γ/°	90.00, 95.383(11), 90.00
Volume / $Å^3$	1010.08(7)
Z	4
ρ_{calc} / mg mm^{-3}	1.343
μ / mm^{-1}	0.096
F(000)	432
Crystal size / mm^3	0.28 × 0.17 × 0.12
Theta range for data collection	2.46 to 54.98°
Index ranges	$-10 \leq h \leq 10$, $-21 \leq k \leq 21$, $-9 \leq l \leq 9$
Reflections collected	11734
Independent reflections	2315[R(int) = 0.0404]

Data/restraints/parameters	2315/0/184
Goodness-of-fit on F^2	1.012
Final R indexes [I>2σ (I)]	R_1 = 0.0444, wR_2 = 0.1198
Final R indexes [all data]	R_1 = 0.0548, wR_2 = 0.1279
Largest diff. peak/hole / e Å^{-3}	0.353/-0.196

Table 2 Fractional Atomic Coordinates ($\times 10^4$) and Equivalent Isotropic Displacement Parameters (Å$^2\times 10^3$) for **376**. U_{eq} is defined as 1/3 of of the trace of the orthogonalised U_{IJ} tensor.

Atom	*x*	*y*	*z*	U(eq)
O1	3397.4(13)	2223.0(6)	2756(2)	55.4(4)
O3	7855.9(11)	3901.6(6)	900.8(13)	32.3(3)
O5	1150.3(11)	5808.5(5)	4543.5(14)	33.1(3)
C1	3334.9(14)	3669.1(7)	2900.5(16)	24.6(3)
C2	4864.0(15)	3733.7(8)	2278.3(17)	24.8(3)
C3	5607.0(14)	4496.1(7)	2122.8(15)	22.5(3)
C4	4799.3(14)	5206.3(7)	2598.2(15)	22.0(3)
C5	3267.8(14)	5152.8(7)	3221.6(15)	21.4(3)
C6	2539.7(15)	4380.5(7)	3369.9(16)	22.9(3)
C11	2604.1(15)	2826.9(8)	3041.2(19)	30.0(3)
C12	896.9(16)	2754.9(8)	3499(2)	34.2(3)
C31	7262.1(14)	4524.2(7)	1463.5(16)	23.8(3)
C32	8145.5(16)	5327.7(8)	1529(2)	29.7(3)
C51	2372.2(14)	5897.0(7)	3786.1(16)	23.3(3)
C52	3009.7(16)	6734.8(8)	3405(2)	28.6(3)

Table 3 Anisotropic Displacement Parameters (Å$^2\times 10^3$) for **376**. The Anisotropic displacement factor exponent takes the form: $-2\pi^2[h^2a^{*2}U_{11}+...+2hka\times b\times U_{12}]$

Atom	U_{11}	U_{22}	U_{33}	U_{23}	U_{13}	U_{12}
O1	38.9(6)	19.0(5)	113.2(11)	0.5(5)	32.8(6)	3.1(4)
O3	31.3(5)	27.4(5)	39.6(5)	-2.6(4)	10.6(4)	5.7(4)
O5	27.9(5)	25.3(5)	48.1(6)	-5.1(4)	14.9(4)	-1.6(4)
C1	25.1(6)	18.9(6)	29.8(6)	1.7(5)	2.7(5)	1.9(4)
C2	26.1(6)	19.9(6)	28.8(6)	0.3(5)	4.0(5)	3.3(5)
C3	22.7(6)	21.4(6)	23.4(6)	0.8(4)	2.3(5)	2.5(4)
C4	23.7(6)	19.3(6)	22.7(6)	0.7(4)	1.7(5)	0.5(4)

C5	23.0(5)	19.0(6)	22.2(6)	-0.2(4)	1.3(5)	1.6(4)
C6	22.6(6)	21.1(6)	25.0(6)	1.4(4)	2.8(5)	0.9(4)
C11	29.2(6)	19.0(6)	42.7(8)	1.0(5)	8.0(5)	0.9(5)
C12	29.5(7)	21.4(7)	52.8(9)	0.2(6)	10.2(6)	-2.0(5)
C31	23.7(6)	24.4(6)	23.5(6)	1.5(5)	2.7(5)	3.4(4)
C32	25.6(6)	29.2(7)	35.4(7)	-2.2(6)	9.0(5)	-0.8(5)
C51	21.3(6)	21.8(6)	26.8(6)	-2.4(5)	1.6(5)	0.9(4)
C52	28.6(7)	19.5(6)	38.4(8)	-0.5(5)	6.4(6)	1.5(5)

Table 4 Bond Lengths for **376**.

Atom	Atom	Length/Å	Atom	Atom	Length/Å
O1	C11	1.2122(16)	C3	C31	1.5044(16)
O3	C31	1.2186(15)	C4	C5	1.3983(16)
O5	C51	1.2175(15)	C5	C6	1.4021(16)
C1	C2	1.3973(17)	C5	C51	1.5016(16)
C1	C6	1.3931(17)	C11	C12	1.4940(18)
C1	C11	1.5048(17)	C31	C32	1.4961(17)
C2	C3	1.3939(17)	C51	C52	1.4982(17)
C3	C4	1.3980(16)			

Table 5 Bond Angles for **376**.

Atom	Atom	Atom	Angle/°	Atom	Atom	Atom	Angle/°
O1	C11	C1	119.66(11)	C3	C4	C5	120.49(11)
O1	C11	C12	121.34(12)	C4	C3	C31	122.27(11)
O3	C31	C3	120.05(11)	C4	C5	C6	119.64(11)
O3	C31	C32	121.55(11)	C4	C5	C51	122.32(10)
O5	C51	C5	119.57(11)	C6	C1	C2	119.30(11)
O5	C51	C52	121.44(10)	C6	C1	C11	122.23(11)
C1	C6	C5	120.32(11)	C6	C5	C51	118.03(10)
C2	C1	C11	118.47(10)	C12	C11	C1	119.00(11)
C2	C3	C4	119.06(11)	C32	C31	C3	118.40(10)
C2	C3	C31	118.66(10)	C52	C51	C5	118.99(10)
C3	C2	C1	121.19(11)				

Table 6 Hydrogen Atom Coordinates (Å×10^4) and Isotropic Displacement Parameters (Å^2×10^3) for **376**.

Atom	*x*	*y*	*z*	U(eq)
H2	5450(17)	3245(9)	1896(19)	27(4)
H4	5288(18)	5744(9)	2529(19)	29(4)
H6	1481(19)	4339(9)	3783(19)	31(4)
H11	170.0(2)	3041(11)	2680.0(2)	45(4)
H12	760.0(2)	3008(12)	4680.0(3)	57(5)
H13	580.0(2)	2171(12)	3550.0(2)	48(5)
H31	8350.0(2)	5510(12)	2730.0(3)	53(5)
H32	9230.0(2)	5285(10)	1010.0(2)	46(4)
H33	7490.0(2)	5760(11)	870.0(2)	50(5)
H51	2350.0(2)	716(1)	3880.0(2)	41(4)
H52	4114(18)	6812(9)	3937(19)	31(4)
H53	3040.0(2)	6810(11)	2170.0(2)	46(5)

Crystallography Data for Compound **386**

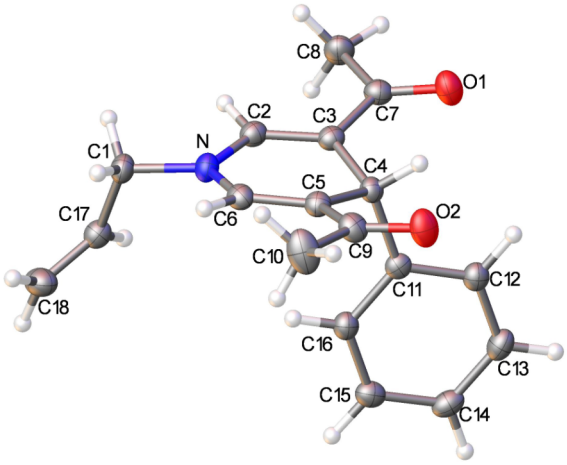

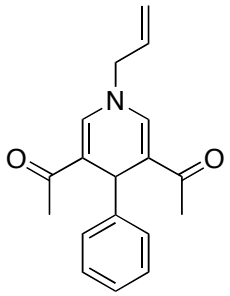

386

Table 1 Crystal data and structure refinement for **385**

Identification code	**385**
Empirical formula	$C_{18}H_{19}NO_2$
Formula weight	281.34
Temperature/K	120
Crystal system	monoclinic
Space group	I2/a
a/Å	16.2061(7)
b/Å	10.9226(4)
c/Å	17.1311(6)
α/°	90.00

β/°	93.915(10)
γ/°	90.00
Volume/Å^3	3025.3(2)
Z	8
ρ_{calc}mg/mm^3	1.235
m/mm^{-1}	0.080
F(000)	1200.0
Crystal size/mm^3	0.22 × 0.16 × 0.16
2Θ range for data collection	4.42 to 55°
Index ranges	-21 ≤ h ≤ 21, -14 ≤ k ≤ 14, -22 ≤ l ≤ 22
Reflections collected	16936
Independent reflections	3486[R(int) = 0.0415]
Data/restraints/parameters	3486/0/266
Goodness-of-fit on F^2	1.034
Final R indexes [I>=2σ (I)]	R_1 = 0.0403, wR_2 = 0.1036
Final R indexes [all data]	R_1 = 0.0545, wR_2 = 0.1123
Largest diff. peak/hole / e Å^{-3}	0.29/-0.21

Table 2 Fractional Atomic Coordinates (×10^4) and Equivalent Isotropic Displacement Parameters (Å^2×10^3) for **385**. U_{eq} is defined as 1/3 of of the trace of the orthogonalised U_{IJ} tensor.

Atom	*x*	*y*	*z*	U(eq)
O1	6394.0(6)	7060.4(9)	3194.2(6)	31.6(2)
O2	3534.6(6)	7215.3(9)	1872.5(6)	33.9(3)
N	4487.6(7)	3827.6(9)	3385.8(6)	23.6(2)
C1	4343.9(9)	2601.0(12)	3699.0(8)	24.8(3)
C2	5240.0(8)	4384.8(12)	3553.5(7)	22.6(3)
C3	5389.4(7)	5554.9(12)	3362.1(7)	20.9(3)
C4	4689.6(7)	6376.2(11)	3037.3(7)	19.9(3)
C5	3987.7(7)	5593.4(12)	2681.9(7)	21.2(3)
C6	3901.5(8)	4417.2(12)	2904.6(7)	22.5(3)
C7	6231.9(8)	6048.6(12)	3456.1(7)	23.7(3)
C8	6907.0(9)	5306.3(14)	3889.1(9)	29.3(3)
C9	3401.8(8)	6172.5(13)	2102.9(7)	26.1(3)
C10	2635.5(11)	5504.9(18)	1791.5(11)	41.2(4)
C11	4398.9(7)	7225.9(11)	3670.8(7)	19.8(3)

C12	4640.8(8)	8449.1(12)	3692.3(8)	23.7(3)
C13	4401.9(8)	9219.6(12)	4278.9(8)	27.3(3)
C14	3915.9(8)	8784.9(13)	4853.4(8)	26.8(3)
C15	3663.0(8)	7571.0(13)	4836.5(8)	25.4(3)
C16	3903.7(8)	6797.3(12)	4247.6(7)	22.7(3)
C17	4107.9(8)	2644.6(12)	4531.4(8)	24.5(3)
C18	3475.5(9)	2058.1(14)	4786.5(9)	33.4(3)

Table 3 Anisotropic Displacement Parameters ($Å^2×10^3$) for **385**. The Anisotropic displacement factor exponent takes the form: $-2\pi^2[h^2a^{*2}U_{11}+...+2hka×b×U_{12}]$

Atom	U_{11}	U_{22}	U_{33}	U_{23}	U_{13}	U_{12}
O1	29.4(5)	31.1(5)	33.9(5)	8.3(4)	-0.3(4)	-4.8(4)
O2	34.1(6)	32.8(6)	33.8(5)	11.5(4)	-6.0(4)	-3.6(4)
N	27.8(6)	18.9(5)	23.8(5)	0.3(4)	0.3(4)	-1.5(4)
C1	31.3(7)	18.4(6)	24.7(6)	0.7(5)	1.7(5)	-0.7(5)
C2	24.2(6)	23.1(6)	20.4(6)	-0.4(5)	1.2(5)	2.8(5)
C3	22.7(6)	22.7(6)	17.3(6)	-1.4(5)	1.0(5)	1.6(5)
C4	22.2(6)	19.7(6)	17.7(6)	1.5(5)	1.1(5)	-1.3(5)
C5	22.8(6)	22.8(6)	17.9(6)	-1.8(5)	0.5(5)	-0.3(5)
C6	24.4(6)	23.7(6)	19.4(6)	-3.4(5)	1.9(5)	-2.3(5)
C7	23.0(6)	27.0(7)	21.1(6)	-0.5(5)	2.3(5)	1.3(5)
C8	23.0(7)	30.7(8)	34.1(8)	2.0(6)	0.5(6)	1.1(6)
C9	27.5(7)	30.7(7)	19.6(6)	1.5(5)	-0.5(5)	-2.5(5)
C10	39.5(9)	46(1)	35.6(9)	10.2(8)	-15.8(7)	-11.7(8)
C11	17.7(6)	22.3(6)	18.7(6)	0.1(5)	-3.3(4)	1.5(5)
C12	23.1(6)	23.2(6)	24.3(6)	1.3(5)	-1.3(5)	-0.2(5)
C13	29.0(7)	20.9(7)	31.3(7)	-2.6(5)	-3.9(5)	1.0(5)
C14	27.7(7)	27.9(7)	24.2(6)	-5.8(5)	-2.4(5)	6.4(5)
C15	23.4(6)	30.6(7)	22.2(6)	1.4(5)	1.5(5)	3.2(5)
C16	23.1(6)	21.9(6)	22.8(6)	1.0(5)	-0.8(5)	-0.8(5)
C17	25.8(7)	23.2(6)	24.0(6)	-1.0(5)	-1.5(5)	1.5(5)
C18	32.0(8)	35.1(8)	33.9(8)	-5.5(6)	8.1(6)	-1.9(6)

Table 4 Bond Lengths for **385**.

Atom	Atom	Length/Å	Atom	Atom	Length/Å
O1	C7	1.2280(16)	C5	C6	1.3501(18)

O2	C9	1.2292(16)	C5	C9	1.4687(17)
N	C1	1.4677(16)	C7	C8	1.5145(18)
N	C2	1.3754(17)	C9	C10	1.506(2)
N	C6	1.3746(16)	C11	C12	1.3922(18)
C1	C17	1.5022(18)	C11	C16	1.3956(17)
C2	C3	1.3455(18)	C12	C13	1.3861(19)
C3	C4	1.5213(17)	C13	C14	1.386(2)
C3	C7	1.4665(18)	C14	C15	1.3875(19)
C4	C5	1.5169(17)	C15	C16	1.3920(18)
C4	C11	1.5268(17)	C17	C18	1.309(2)

Table 5 Bond Angles for **385**.

Atom	Atom	Atom	Angle/°	Atom	Atom	Atom	Angle/°
C2	N	C1	119.22(11)	O1	C7	C3	120.76(11)
C6	N	C1	121.77(11)	O1	C7	C8	119.70(12)
C6	N	C2	118.97(11)	C3	C7	C8	119.53(11)
N	C1	C17	112.03(11)	O2	C9	C5	119.78(12)
C3	C2	N	122.76(12)	O2	C9	C10	119.54(12)
C2	C3	C4	120.47(11)	C5	C9	C10	120.68(12)
C2	C3	C7	120.28(11)	C12	C11	C4	120.14(11)
C7	C3	C4	119.25(11)	C12	C11	C16	118.53(11)
C3	C4	C11	110.91(10)	C16	C11	C4	121.31(11)
C5	C4	C3	109.53(10)	C13	C12	C11	120.65(12)
C5	C4	C11	111.62(10)	C14	C13	C12	120.49(13)
C6	C5	C4	120.81(11)	C13	C14	C15	119.60(12)
C6	C5	C9	121.74(12)	C14	C15	C16	119.88(12)
C9	C5	C4	117.44(11)	C15	C16	C11	120.84(12)
C5	C6	N	122.32(12)	C18	C17	C1	123.87(13)

Table 6 Hydrogen Atom Coordinates ($Å \times 10^4$) and Isotropic Displacement Parameters ($Å^2 \times 10^3$) for **385**.

Atom	*x*	*y*	*z*	U(eq)
H1A	3904(9)	2209(14)	3360(9)	27(4)
H1B	4876(9)	2145(14)	3688(8)	27(4)
H2	5654(9)	3832(13)	3772(8)	26(4)
H4	4898(8)	6918(12)	2633(8)	15(3)

H6	3449(9)	3912(13)	2720(8)	23(4)
H8A	7422(10)	5808(15)	3916(9)	38(4)
H8B	6745(10)	5146(15)	4437(10)	41(5)
H8C	6988(11)	4526(17)	3646(11)	47(5)
H10A	2396(13)	5909(19)	1356(13)	63(6)
H10B	2265(17)	5380(20)	2179(17)	99(9)
H10C	2761(15)	4680(30)	1628(15)	91(8)
H12	4982(9)	8755(14)	3272(9)	31(4)
H13	4568(10)	10075(15)	4282(9)	35(4)
H14	3755(10)	9322(15)	5272(10)	37(4)
H15	3320(9)	7241(14)	5249(9)	28(4)
H16	3744(9)	5965(15)	4239(8)	26(4)
H17	4470(10)	3105(14)	4894(9)	31(4)
H18A	3099(11)	1572(16)	4418(10)	44(5)
H18B	3351(11)	2048(16)	5352(11)	48(5)

Crystallography Data for Compound **392**

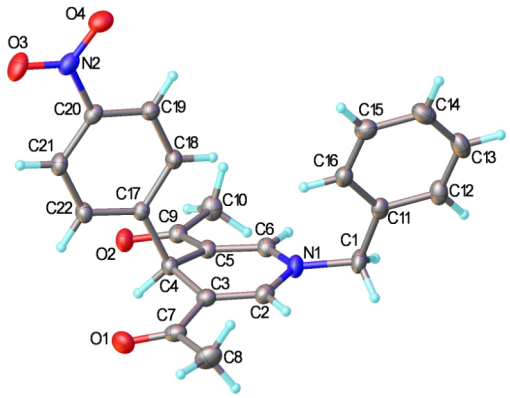

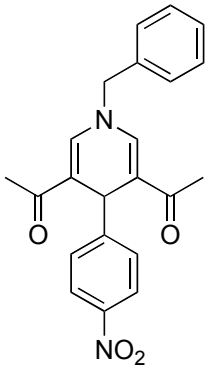

392

Table 1 Crystal data and structure refinement for **392**

Identification code	**392**
Empirical formula	$C_{22}H_{20}N_2O_4$
Formula weight	376.40
Temperature/K	120
Crystal system	monoclinic
Space group	C2/c
a/Å	12.4631(6)
b/Å	11.0700(5)
c/Å	26.6746(12)

α/°	90.00
β/°	99.542(7)
γ/°	90.00
Volume/Å^3	3629.3(3)
Z	8
ρ_{calc}mg/mm^3	1.378
m/mm^{-1}	0.096
F(000)	1584.0
Crystal size/mm^3	0.84 × 0.27 × 0.03
2Θ range for data collection	4.96 to 59.98°
Index ranges	-17 ≤ h ≤ 17, -15 ≤ k ≤ 15, -37 ≤ l ≤ 37
Reflections collected	31575
Independent reflections	5306[R(int) = 0.0307]
Data/restraints/parameters	5306/0/257
Goodness-of-fit on F^2	1.025
Final R indexes [I>=2σ (I)]	R_1 = 0.0413, wR_2 = 0.1068
Final R indexes [all data]	R_1 = 0.0540, wR_2 = 0.1170
Largest diff. peak/hole / e Å^{-3}	0.42/-0.20

Table 2 Fractional Atomic Coordinates (×10^4) and Equivalent Isotropic Displacement Parameters (Å^2×10^3) for **392**. U_{eq} is defined as 1/3 of of the trace of the orthogonalised U_{IJ} tensor.

Atom	*x*	*y*	*z*	U(eq)
O1	5255.6(7)	8577.0(8)	1598.1(4)	31.8(2)
O2	2094.4(7)	7173.0(7)	2405.7(3)	25.47(18)
O3	782.6(8)	9227.7(9)	-196.2(3)	35.1(2)
O4	583.4(7)	7327.1(9)	-383.6(3)	30.9(2)
N1	4505.3(8)	4440.3(8)	1808.8(4)	22.47(19)
N2	936.9(8)	8152.5(10)	-95.3(4)	24.3(2)
C1	4862.2(10)	3187.7(10)	1769.8(4)	25.7(2)
C2	5093.5(9)	5377.2(11)	1645.9(4)	22.1(2)
C3	4780.1(9)	6541.5(10)	1650.4(4)	20.4(2)
C4	3683.9(8)	6887.5(9)	1789.3(4)	18.30(19)
C5	3244.7(9)	5847.3(9)	2064.7(4)	18.6(2)
C6	3625.3(9)	4706.5(10)	2038.5(4)	19.9(2)
C7	5487.2(9)	7523.0(11)	1522.8(4)	24.5(2)
C8	6498.3(10)	7230.9(13)	1299.5(5)	33.7(3)

C9	2368.6(9)	6116.7(10)	2352.6(4)	19.9(2)
C10	1783.9(10)	5104.4(11)	2574.1(5)	27.1(2)
C11	4482.6(9)	2609.3(10)	1257.5(4)	21.2(2)
C12	4581.8(10)	1358.4(10)	1214.3(5)	25.5(2)
C13	4270.5(10)	788.6(11)	749.8(5)	30.7(3)
C14	3857.9(10)	1464.7(12)	323.5(5)	31.9(3)
C15	3766.5(10)	2709.5(11)	361.5(5)	27.9(2)
C16	4077.9(9)	3282.2(10)	826.8(4)	22.8(2)
C17	2897.7(8)	7231.2(9)	1307.4(4)	17.53(19)
C18	2389.3(9)	6336.1(10)	983.2(4)	20.6(2)
C19	1741.1(9)	6631.3(10)	524.6(4)	21.8(2)
C20	1594.6(8)	7837.8(10)	397.8(4)	20.0(2)
C21	2059.3(9)	8755(1)	714.5(4)	22.8(2)
C22	2716.2(9)	8440.3(10)	1168.8(4)	21.6(2)

Table 3 Anisotropic Displacement Parameters ($Å^2 \times 10^3$) for **392**. The Anisotropic displacement factor exponent takes the form: $-2\pi^2[h^2a^{*2}U_{11}+...+2hka \times b \times U_{12}]$

Atom	U_{11}	U_{22}	U_{33}	U_{23}	U_{13}	U_{12}
O1	31.6(5)	24.9(4)	37.8(5)	0.8(4)	2.1(4)	-6.6(3)
O2	28.8(4)	21.3(4)	27.1(4)	-1.2(3)	6.5(3)	5.4(3)
O3	43.4(5)	32.8(5)	28.5(4)	9.9(4)	4.0(4)	14.8(4)
O4	29.8(4)	39.4(5)	22.0(4)	-0.6(4)	-0.1(3)	3.1(4)
N1	27.7(5)	17.6(4)	22.8(4)	1.5(3)	6.1(3)	5.3(4)
N2	22.4(4)	30.8(5)	20.2(4)	4.5(4)	5.4(3)	6.9(4)
C1	33.2(6)	19.4(5)	24.2(5)	1.8(4)	4.1(4)	9.6(4)
C2	21.0(5)	25.2(5)	19.9(5)	0.2(4)	3.1(4)	2.9(4)
C3	19.6(5)	22.6(5)	18.4(5)	1.3(4)	1.2(4)	-0.8(4)
C4	21.5(5)	16.0(4)	17.3(4)	0.6(4)	2.7(4)	1.1(4)
C5	21.7(5)	18.1(5)	15.8(4)	0.5(4)	2.3(4)	0.7(4)
C6	24.0(5)	19.2(5)	16.5(4)	1.1(4)	3.1(4)	0.9(4)
C7	20.8(5)	28.4(6)	22.5(5)	3.0(4)	-1.4(4)	-3.5(4)
C8	22.9(5)	42.9(8)	35.9(7)	8.2(6)	6.4(5)	-3.1(5)
C9	22.8(5)	20.8(5)	15.7(4)	0.2(4)	1.7(4)	1.9(4)
C10	29.9(6)	25.7(6)	28.1(6)	2.5(4)	11.7(4)	0.4(4)
C11	19.6(5)	19.6(5)	25.9(5)	1.0(4)	8.1(4)	1.8(4)

C12	27.3(5)	19.8(5)	31.5(6)	4.0(4)	11.3(4)	1.3(4)
C13	31.9(6)	19.5(5)	42.4(7)	-3.5(5)	11.6(5)	-4.5(4)
C14	30.7(6)	30.8(6)	34.0(6)	-8.6(5)	4.5(5)	-6.9(5)
C15	25.0(5)	29.6(6)	28.3(6)	1.4(5)	1.5(4)	-1.6(5)
C16	21.3(5)	20.2(5)	27.0(5)	1.7(4)	4.5(4)	1.2(4)
C17	18.3(4)	17.6(5)	17.1(4)	1.0(4)	4.4(3)	1.9(4)
C18	22.8(5)	17.1(5)	21.5(5)	0.7(4)	2.0(4)	1.5(4)
C19	21.4(5)	21.8(5)	21.6(5)	-0.9(4)	2.2(4)	0.9(4)
C20	19.0(5)	24.5(5)	17.0(4)	3.6(4)	4.5(4)	4.6(4)
C21	27.6(5)	18.8(5)	22.7(5)	3.5(4)	6.0(4)	4.4(4)
C22	27.0(5)	17.1(5)	20.8(5)	-0.2(4)	4.3(4)	1.1(4)

Table 4 Bond Lengths for **392**.

Atom	Atom	Length/Å	Atom	Atom	Length/Å
O1	C7	1.2265(15)	C5	C9	1.4659(15)
O2	C9	1.2330(13)	C7	C8	1.5152(18)
O3	N2	1.2284(13)	C9	C10	1.5095(16)
O4	N2	1.2280(14)	C11	C12	1.3968(15)
N1	C1	1.4651(14)	C11	C16	1.3916(16)
N1	C2	1.3811(15)	C12	C13	1.3872(18)
N1	C6	1.3742(14)	C13	C14	1.3868(19)
N2	C20	1.4715(14)	C14	C15	1.3878(18)
C1	C11	1.5123(16)	C15	C16	1.3904(16)
C2	C3	1.3474(15)	C17	C18	1.3961(15)
C3	C4	1.5226(15)	C17	C22	1.3969(15)
C3	C7	1.4739(16)	C18	C19	1.3887(15)
C4	C5	1.5161(14)	C19	C20	1.3825(15)
C4	C17	1.5297(14)	C20	C21	1.3849(16)
C5	C6	1.3548(15)	C21	C22	1.3897(15)

Table 5 Bond Angles for **392**.

Atom	Atom	Atom	Angle/˚	Atom	Atom	Atom	Angle/˚
C2	N1	C1	120.34(10)	O2	C9	C5	119.85(10)
C6	N1	C1	120.59(10)	O2	C9	C10	119.87(10)

C6	N1	C2	118.93(9)	C5	C9	C10	120.26(10)
O3	N2	C20	117.97(10)	C12	C11	C1	118.40(10)
O4	N2	O3	123.83(10)	C16	C11	C1	122.39(10)
O4	N2	C20	118.19(10)	C16	C11	C12	119.18(11)
N1	C1	C11	114.31(9)	C13	C12	C11	120.60(11)
C3	C2	N1	123.08(10)	C14	C13	C12	119.85(11)
C2	C3	C4	121.05(10)	C13	C14	C15	119.98(12)
C2	C3	C7	121.19(10)	C14	C15	C16	120.25(12)
C7	C3	C4	117.76(10)	C15	C16	C11	120.14(11)
C3	C4	C17	109.49(8)	C18	C17	C4	120.37(9)
C5	C4	C3	109.72(9)	C18	C17	C22	118.64(10)
C5	C4	C17	111.33(8)	C22	C17	C4	120.91(9)
C6	C5	C4	121.69(10)	C19	C18	C17	121.10(10)
C6	C5	C9	120.94(10)	C20	C19	C18	118.48(10)
C9	C5	C4	117.35(9)	C19	C20	N2	118.61(10)
C5	C6	N1	122.35(10)	C19	C20	C21	122.28(10)
O1	C7	C3	119.83(11)	C21	C20	N2	119.10(10)
O1	C7	C8	120.07(11)	C20	C21	C22	118.33(10)
C3	C7	C8	120.10(11)	C21	C22	C17	121.13(10)

Table 6 Torsion Angles for **392**.

A	B	C	D	Angle/°	A	B	C	D	Angle/°
N1	C1	C11	C16	15.62(16)	C2	N1	C1	C11	-84.78(13)

Table 7 Hydrogen Atom Coordinates (Å×10^4) and Isotropic Displacement Parameters (Å^2×10^3) for **392**.

Atom	*x*	*y*	*z*	U(eq)
H1A	4590	2701	2034	31
H1B	5667	3165	1842	31
H2	5750	5192	1525	26
H4	3787	7603	2021	22
H6	3271	4068	2184	24
H8A	6811	7980	1191	59(3)
H8B	6306	6695	1006	59(3)
H8C	7032	6830	1557	59(3)
H10A	1349	5438	2816	49(3)

H10B	2318	4533	2750	49(3)
H10C	1305	4686	2300	49(3)
H12	4865	894	1506	31
H13	4340	-63	724	37
H14	3638	1076	6	38
H15	3490	3172	69	34
H16	4014	4135	851	27
H18	2489	5511	1078	25
H19	1406	6018	303	26
H21	1932	9579	624	27
H22	3047	9058	1389	26

Crystallography Data for Compound **396**

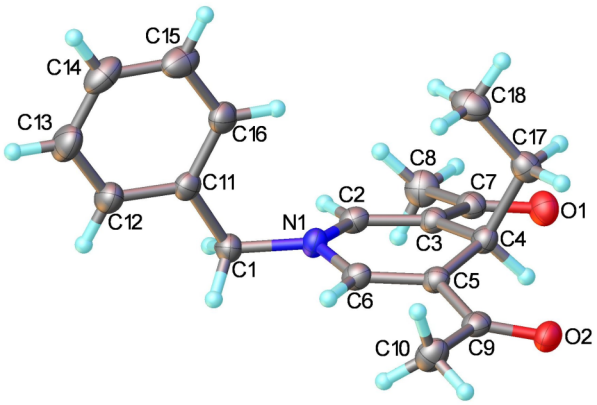

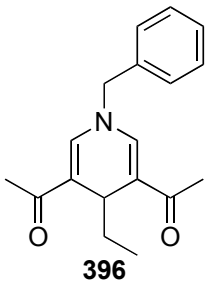

396

Table 1 Crystal data and structure refinement for **396**

Identification code	**396**
Empirical formula	$C_{18}H_{21}NO_2$
Formula weight	283.36
Temperature/K	120
Crystal system	monoclinic
Space group	$P2_1/n$
a/Å	9.3258(9)
b/Å	14.5225(14)
c/Å	11.5197(10)
α/°	90.00
β/°	98.448(19)
γ/°	90.00
Volume/Å^3	1543.2(2)

Z	4
ρ_{calc}mg/mm^3	1.220
m/mm^{-1}	0.079
F(000)	608.0
Crystal size/mm^3	0.19 × 0.08 × 0.06
2Θ range for data collection	4.54 to 50°
Index ranges	-11 ≤ h ≤ 11, -17 ≤ k ≤ 17, -13 ≤ l ≤ 13
Reflections collected	23205
Independent reflections	2717[R(int) = 0.0748]
Data/restraints/parameters	2717/0/195
Goodness-of-fit on F^2	1.024
Final R indexes [I>=2σ (I)]	R_1 = 0.0402, wR_2 = 0.0854
Final R indexes [all data]	R_1 = 0.0746, wR_2 = 0.1020
Largest diff. peak/hole / e Å^{-3}	0.17/-0.18

Table 2 Fractional Atomic Coordinates (×10^4) and Equivalent Isotropic Displacement Parameters (Å^2×10^3) for **396**. U_{eq} is defined as 1/3 of of the trace of the orthogonalised U_{IJ} tensor.

Atom	*x*	*y*	*z*	U(eq)
O1	5728.8(15)	3345.2(9)	2021.7(11)	33.4(4)
O2	1799.0(14)	911.8(9)	2167.0(11)	30.2(3)
N1	4011.9(17)	2504.0(11)	5533.5(13)	26.0(4)
C1	3856(2)	2772.3(13)	6728.9(16)	27.5(4)
C2	4851(2)	3012.9(13)	4885.3(16)	25.4(4)
C3	4937(2)	2839.2(13)	3752.3(16)	24.3(4)
C4	4197(2)	2003.3(13)	3133.6(16)	25.2(4)
C5	3066(2)	1627.3(13)	3831.3(15)	23.9(4)
C6	3072(2)	1859.1(13)	4964.4(16)	25.5(4)
C7	5696(2)	3477.5(13)	3075.3(16)	26.9(4)
C8	6399(2)	4333.3(14)	3649.0(18)	36.0(5)
C9	1934(2)	1020.1(13)	3240.8(16)	25.9(4)
C10	929(2)	516.0(15)	3934.9(18)	35.1(5)
C11	4630(2)	2163.2(13)	7678.5(16)	25.2(4)
C12	4252(2)	2235.0(15)	8795.8(17)	35.6(5)
C13	4935(2)	1715.9(17)	9711.7(18)	43.4(6)
C14	6010(3)	1108.2(15)	9525.0(19)	41.9(6)

C15	6415(2)	1027.4(14)	8430(2)	40.1(5)
C16	5721(2)	1557.4(14)	7499.7(18)	32.7(5)
C17	5295(2)	1246.4(14)	2915.1(17)	30.6(5)
C18	6153(2)	842.4(15)	4017.1(19)	39.8(5)

Table 3 Anisotropic Displacement Parameters ($Å^2×10^3$) for **396**. The Anisotropic displacement factor exponent takes the form: $-2\pi^2[h^2a^{*2}U_{11}+...+2hka×b×U_{12}]$

Atom	U_{11}	U_{22}	U_{33}	U_{23}	U_{13}	U_{12}
O1	40.0(9)	33.4(8)	28.1(8)	4.0(6)	9.9(6)	-0.3(6)
O2	32.9(8)	31.8(8)	24.7(7)	-3.5(6)	0.1(6)	0.9(6)
N1	26.3(9)	31.6(9)	20.0(8)	-1.1(7)	2.8(7)	-3.1(7)
C1	28.1(11)	31.9(11)	22.4(10)	-1.2(8)	3.8(8)	1.4(9)
C2	23.5(10)	25.1(10)	26.7(10)	2.2(8)	0.8(8)	-0.9(8)
C3	24(1)	24.8(10)	23.8(10)	2.5(8)	2.3(8)	1.6(8)
C4	26.5(10)	27.5(10)	21.4(10)	1.7(8)	2.6(8)	-0.6(8)
C5	23.6(10)	25(1)	22.8(10)	3.3(8)	2.3(8)	0.5(8)
C6	23.2(10)	28.2(10)	25(1)	4.5(8)	2.6(8)	-2.2(8)
C7	26.7(11)	26.3(10)	27.9(11)	2.8(9)	4.1(8)	2.9(8)
C8	42.1(13)	29.8(11)	37.1(12)	4.2(9)	8.9(10)	-6.3(9)
C9	24.8(10)	25.2(10)	26.8(11)	1.6(8)	0.2(8)	4.2(8)
C10	32.4(12)	38.9(12)	32.8(12)	2(1)	1.1(9)	-8.6(10)
C11	25.8(10)	25.5(10)	23.3(10)	-2.8(8)	0.3(8)	-4.0(8)
C12	32.5(12)	48.5(13)	25.7(11)	1.7(10)	3.9(9)	2.5(10)
C13	44.1(14)	60.0(16)	25.7(11)	6.5(11)	3.4(10)	-3.3(12)
C14	49.5(14)	36.1(12)	34.9(13)	7.4(10)	-11.2(10)	-4.2(11)
C15	41.7(13)	28.2(11)	46.2(13)	-6(1)	-8.2(10)	5.5(10)
C16	34.8(11)	33.5(11)	28.3(11)	-7.7(9)	-0.4(9)	0.8(9)
C17	30.3(11)	30.0(11)	32.8(11)	-2.2(9)	9.2(9)	-1.9(9)
C18	36.8(13)	36.6(12)	47.8(13)	8.7(11)	12(1)	6(1)

Table 4 Bond Lengths for **396**.

Atom	Atom	Length/Å	Atom	Atom	Length/Å
O1	C7	1.234(2)	C5	C6	1.347(3)
O2	C9	1.235(2)	C5	C9	1.464(3)

N1	C1	1.459(2)	C7	C8	1.511(3)
N1	C2	1.374(2)	C9	C10	1.508(3)
N1	C6	1.381(2)	C11	C12	1.387(3)
C1	C11	1.506(3)	C11	C16	1.383(3)
C2	C3	1.343(3)	C12	C13	1.375(3)
C3	C4	1.521(3)	C13	C14	1.376(3)
C3	C7	1.460(3)	C14	C15	1.374(3)
C4	C5	1.519(3)	C15	C16	1.398(3)
C4	C17	1.548(3)	C17	C18	1.516(3)

Table 5 Bond Angles for **396**.

Atom	Atom	Atom	Angle/°	Atom	Atom	Atom	Angle/°
C2	N1	C1	120.88(16)	O1	C7	C3	120.72(18)
C2	N1	C6	118.64(15)	O1	C7	C8	119.10(17)
C6	N1	C1	118.99(16)	C3	C7	C8	120.13(16)
N1	C1	C11	115.15(16)	O2	C9	C5	120.17(17)
C3	C2	N1	123.18(17)	O2	C9	C10	119.31(17)
C2	C3	C4	121.17(17)	C5	C9	C10	120.52(16)
C2	C3	C7	120.19(17)	C12	C11	C1	118.02(17)
C7	C3	C4	118.59(16)	C16	C11	C1	123.37(17)
C3	C4	C17	112.22(16)	C16	C11	C12	118.59(18)
C5	C4	C3	109.97(15)	C13	C12	C11	121.2(2)
C5	C4	C17	110.99(15)	C12	C13	C14	119.9(2)
C6	C5	C4	121.24(17)	C15	C14	C13	120.2(2)
C6	C5	C9	120.04(17)	C14	C15	C16	119.9(2)
C9	C5	C4	118.70(15)	C11	C16	C15	120.26(19)
C5	C6	N1	122.77(18)	C18	C17	C4	114.78(16)

Table 6 Hydrogen Atom Coordinates (Å×10^4) and Isotropic Displacement Parameters (Å^2×10^3) for **396**.

Atom	*x*	*y*	*z*	U(eq)
H1A	2811	2778	6801	33
H1B	4222	3409	6863	33
H2	5396	3512	5256	30
H4	3685	2210	2353	30
H6	2401	1567	5390	31

H8A	7065	4594	3152	49(4)
H8B	6940	4174	4418	49(4)
H8C	5650	4787	3750	49(4)
H10A	126	248	3396	48(6)
H10B	544	948	4466	48(6)
H10C	1463	24	4394	48(6)
H10D	917	-134	3706	48(6)
H10E	-29	770	3772	48(6)
H10F	1264	577	4760	48(6)
H12	3507	2651	8931	43
H13	4666	1777	10472	52
H14	6473	743	10155	50
H15	7165	613	8304	48
H16	5998	1500	6742	39
H17A	4762	742	2461	37
H17B	5983	1509	2426	37
H18A	6827	377	3801	54(4)
H18B	5487	556	4494	54(4)
H18C	6700	1333	4469	54(4)

Crystallography Data for Compound **398**

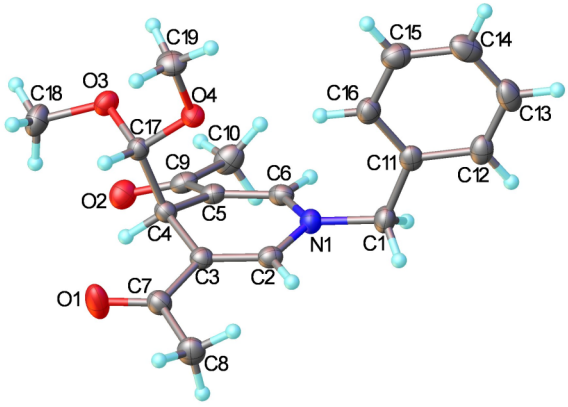

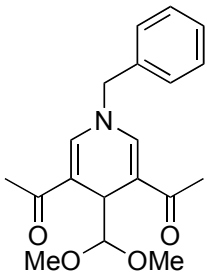

398

Table 1 Crystal data and structure refinement for **398**

Identification code	**398**
Empirical formula	$C_{19}H_{23}NO_4$
Formula weight	329.38
Temperature/K	120
Crystal system	orthorhombic

Space group	Pbca
a/Å	12.0102(2)
b/Å	13.7886(3)
c/Å	20.7109(4)
α/°	90.00
β/°	90.00
γ/°	90.00
Volume/Å^3	3429.80(11)
Z	8
ρ_{calc}mg/mm^3	1.276
m/mm^{-1}	0.089
F(000)	1408.0
Crystal size/mm^3	0.33 × 0.28 × 0.1
2Θ range for data collection	3.94 to 50.06°
Index ranges	-14 ≤ h ≤ 14, -16 ≤ k ≤ 16, -24 ≤ l ≤ 24
Reflections collected	30328
Independent reflections	3028[R(int) = 0.0460]
Data/restraints/parameters	3028/0/221
Goodness-of-fit on F^2	1.028
Final R indexes [I>=2σ (I)]	R_1 = 0.0355, wR_2 = 0.0877
Final R indexes [all data]	R_1 = 0.0480, wR_2 = 0.0941
Largest diff. peak/hole / e Å^{-3}	0.18/-0.18

Table 2 Fractional Atomic Coordinates (×10^4) and Equivalent Isotropic Displacement Parameters (Å^2×10^3) for **398**. U_{eq} is defined as 1/3 of of the trace of the orthogonalised U_{IJ} tensor.

Atom	*x*	*y*	*z*	U(eq)
O1	-286.8(9)	4386.7(8)	3920.3(7)	44.2(3)
O2	359.6(9)	7233.8(8)	2578.6(5)	32.1(3)
O3	886.1(8)	7360.4(7)	4047.8(5)	27.1(2)
O4	2247.2(8)	6317.6(7)	4358.6(5)	25.4(2)
N1	3281.4(9)	5114.3(9)	3110.2(6)	25.0(3)
C1	4423.2(12)	4797.4(11)	2990.5(7)	28.2(3)
C2	2534.9(12)	4505.8(10)	3409.8(6)	23.7(3)
C3	1486.3(11)	4780.8(10)	3552.8(6)	22.3(3)
C4	1138.1(11)	5826.6(10)	3468.7(7)	22.6(3)

C5	1857.3(12)	6306.3(10)	2962.8(7)	23.2(3)
C6	2893.6(12)	5970.6(10)	2850.6(7)	24.4(3)
C7	654.4(12)	4096.7(11)	3799.4(7)	27.2(3)
C8	925.1(13)	3042.7(11)	3884.8(8)	33.5(4)
C9	1366.3(13)	7065.4(10)	2555.3(7)	26.4(3)
C10	2083.6(14)	7612.3(12)	2080.9(8)	35.6(4)
C11	5257.7(12)	5120.3(10)	3491.5(7)	24.7(3)
C12	6380.2(12)	4920.6(11)	3380.0(8)	29.3(3)
C13	7181.2(13)	5183.7(12)	3823.5(8)	36.4(4)
C14	6872.3(14)	5646.9(12)	4390.5(9)	38.2(4)
C15	5767.4(14)	5848.9(12)	4504.0(8)	35.7(4)
C16	4957.4(13)	5588.7(11)	4057.6(8)	29.3(4)
C17	1170.4(12)	6363.9(10)	4117.8(7)	22.7(3)
C18	-283.0(13)	7515.6(12)	4054.0(8)	36.1(4)
C19	2324.0(13)	6644.5(12)	5013.3(7)	32.2(4)

Table 3 Anisotropic Displacement Parameters ($Å^2 \times 10^3$) for **398**. The Anisotropic displacement factor exponent takes the form: $-2\pi^2[h^2a^{*2}U_{11}+...+2hka \times b \times U_{12}]$

Atom	U_{11}	U_{22}	U_{33}	U_{23}	U_{13}	U_{12}
O1	24.1(6)	31.2(6)	77.4(9)	9.5(6)	10.7(6)	0.2(5)
O2	33.3(6)	30.7(6)	32.4(6)	2.7(5)	-2.0(5)	6.8(5)
O3	29.0(6)	21.3(5)	31.2(6)	-0.6(4)	1.0(4)	4.5(4)
O4	22.5(5)	28.4(6)	25.3(5)	-3.5(4)	-1.4(4)	0.2(4)
N1	21.1(6)	25.2(6)	28.8(7)	-0.9(5)	2.6(5)	1.1(5)
C1	23.6(8)	28.9(8)	32.2(8)	-1.0(6)	5.4(6)	3.5(6)
C2	26.1(8)	20.4(7)	24.7(7)	-0.4(6)	-2.5(6)	0.5(6)
C3	22.8(7)	21.3(7)	22.9(7)	-0.4(6)	-2.2(6)	0.1(6)
C4	19.6(7)	21.8(7)	26.4(8)	0.2(6)	-1.4(6)	-1.2(6)
C5	26.7(8)	19.9(7)	23.2(7)	-2.6(6)	-1.0(6)	-1.6(6)
C6	27.3(8)	21.6(7)	24.4(7)	-1.2(6)	0.9(6)	-4.5(6)
C7	24.9(8)	25.3(8)	31.4(8)	1.3(6)	-1.1(6)	-0.7(6)
C8	33.6(9)	24.5(8)	42.5(9)	4.9(7)	3.2(7)	-1.6(7)
C9	34.5(9)	21.3(8)	23.4(8)	-4.0(6)	-1.0(6)	0.7(6)
C10	45.2(10)	27.1(9)	34.6(9)	5.2(7)	5.7(8)	3.7(7)
C11	24.6(8)	17.6(7)	31.9(8)	5.8(6)	2.7(6)	1.3(6)
C12	27.0(8)	24.7(8)	36.3(9)	7.1(7)	5.9(7)	4.5(6)

C13	23.6(8)	33.1(9)	52.4(11)	10.8(8)	-1.1(7)	2.9(7)
C14	34.9(9)	30.6(9)	49.0(11)	5.7(8)	-15.1(8)	-1.3(7)
C15	40.5(10)	29.1(9)	37.4(9)	-3.0(7)	-4.2(7)	2.2(7)
C16	26.2(8)	25.2(8)	36.6(9)	0.8(7)	1.3(7)	3.1(6)
C17	20.5(7)	20.1(7)	27.6(8)	0.4(6)	1.6(6)	0.5(5)
C18	33.3(9)	36.3(9)	38.6(10)	-0.4(7)	3.3(7)	13.1(7)
C19	36.7(9)	34.0(9)	25.8(8)	-2.8(6)	-4.7(7)	-1.4(7)

Table 4 Bond Lengths for **398**.

Atom	Atom	Length/Å	Atom	Atom	Length/Å
O1	C7	1.2249(18)	C4	C5	1.510(2)
O2	C9	1.2320(18)	C4	C17	1.5354(19)
O3	C17	1.4232(16)	C5	C6	1.348(2)
O3	C18	1.4204(18)	C5	C9	1.468(2)
O4	C17	1.3876(17)	C7	C8	1.500(2)
O4	C19	1.4318(17)	C9	C10	1.509(2)
N1	C1	1.4605(18)	C11	C12	1.395(2)
N1	C2	1.3758(18)	C11	C16	1.386(2)
N1	C6	1.3785(19)	C12	C13	1.379(2)
C1	C11	1.510(2)	C13	C14	1.387(2)
C2	C3	1.348(2)	C14	C15	1.376(2)
C3	C4	1.512(2)	C15	C16	1.389(2)
C3	C7	1.466(2)			

Table 5 Bond Angles for **398**.

Atom	Atom	Atom	Angle/°	Atom	Atom	Atom	Angle/°
C18	O3	C17	112.44(11)	O1	C7	C3	119.35(13)
C17	O4	C19	112.70(11)	O1	C7	C8	119.49(14)
C2	N1	C1	120.40(12)	C3	C7	C8	121.12(13)
C2	N1	C6	118.56(12)	O2	C9	C5	120.40(13)
C6	N1	C1	120.48(12)	O2	C9	C10	119.45(13)
N1	C1	C11	114.73(12)	C5	C9	C10	120.09(13)
C3	C2	N1	122.43(13)	C12	C11	C1	118.00(13)
C2	C3	C4	120.10(13)	C16	C11	C1	123.09(13)
C2	C3	C7	122.16(13)	C16	C11	C12	118.90(14)

C7	C3	C4	117.74(12)	C13	C12	C11	120.80(15)
C3	C4	C17	110.64(11)	C12	C13	C14	119.90(15)
C5	C4	C3	109.84(11)	C15	C14	C13	119.72(15)
C5	C4	C17	112.43(11)	C14	C15	C16	120.61(16)
C6	C5	C4	119.82(13)	C11	C16	C15	120.07(14)
C6	C5	C9	121.10(13)	O3	C17	C4	111.75(11)
C9	C5	C4	118.77(12)	O4	C17	O3	107.74(11)
C5	C6	N1	122.60(13)	O4	C17	C4	108.42(11)

Table 6 Hydrogen Atom Coordinates ($Å \times 10^4$) and Isotropic Displacement Parameters ($Å^2 \times 10^3$) for **398**.

Atom	*x*	*y*	*z*	U(eq)
H1A	4661	5047	2564	34
H1B	4434	4080	2968	34
H2	2767	3868	3520	28
H4	352	5833	3310	27
H6	3376	6339	2582	29
H8A	449	2767	4223	50
H8B	1708	2974	4010	50
H8C	795	2698	3478	50
H10A	2221	7206	1701	53
H10B	2795	7778	2285	53
H10C	1701	8208	1949	53
H12	6595	4599	2994	35
H13	7944	5048	3741	44
H14	7421	5824	4699	46
H15	5557	6169	4891	43
H16	4197	5732	4140	35
H17	646	6047	4428	27
H18A	-616	7218	3670	54
H18B	-436	8214	4053	54
H18C	-603	7222	4443	54
H19A	2228	7350	5027	48
H19B	3056	6474	5189	48
H19C	1741	6334	5272	48

Crystallography Data for Compound **399**

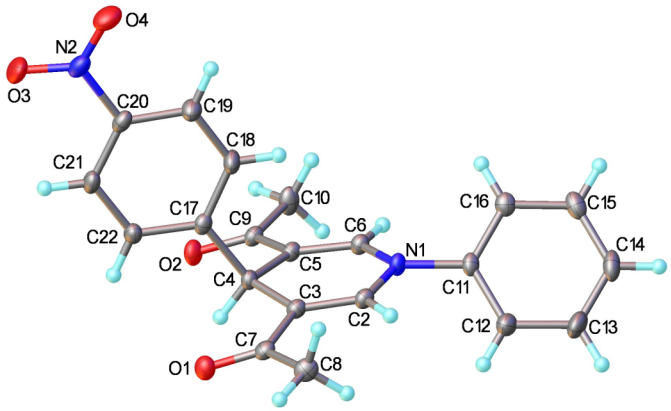

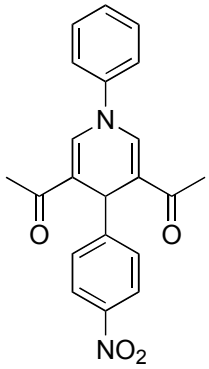

399

Table 1 Crystal data and structure refinement for **399**

Identification code	**399**
Empirical formula	$C_{21}H_{18}N_2O_4$
Formula weight	362.37
Temperature/K	120
Crystal system	triclinic
Space group	P-1
a/Å	8.7082(6)
b/Å	10.1835(5)
c/Å	11.0221(8)
α/°	100.666(5)
β/°	110.831(6)
γ/°	97.843(5)
Volume/Å^3	875.72(9)
Z	2
ρ_{calc}mg/mm^3	1.374
m/mm^{-1}	0.096
F(000)	380.0
Crystal size/mm^3	0.61 × 0.39 × 0.28
2Θ range for data collection	5.14 to 60.08°
Index ranges	$-12 \leq h \leq 11$, $-14 \leq k \leq 13$, $-15 \leq l \leq 15$
Reflections collected	13179
Independent reflections	4593[R(int) = 0.0331]
Data/restraints/parameters	4593/0/248
Goodness-of-fit on F^2	1.042
Final R indexes [I>=2σ (I)]	R_1 = 0.0433, wR_2 = 0.1091
Final R indexes [all data]	R_1 = 0.0519, wR_2 = 0.1175

Largest diff. peak/hole / e Å^{-3}	0.37/-0.28

Table 2 Fractional Atomic Coordinates (×10^4) and Equivalent Isotropic Displacement Parameters (Å^2×10^3) for **399**. U_{eq} is defined as 1/3 of of the trace of the orthogonalised U_{IJ} tensor.

Atom	*x*	*y*	*z*	U(eq)
O1	-2199.3(10)	6262.5(9)	599.8(9)	22.66(19)
O2	2832.9(11)	8926.9(9)	191.8(9)	21.70(19)
O3	272.5(13)	12983(1)	4237.1(11)	37.3(3)
O4	1638.8(13)	12282.6(10)	5968.2(10)	32.6(2)
N1	3240.3(12)	5392.7(10)	2443.3(10)	16.7(2)
N2	964.1(13)	12133(1)	4752.2(11)	23.3(2)
C2	1539.5(14)	5180.9(11)	2189.7(11)	16.2(2)
C3	544.2(14)	5989.4(11)	1632.1(11)	15.7(2)
C4	1236.3(13)	7263.4(11)	1294.9(11)	15.0(2)
C5	3041.6(14)	7296.0(11)	1435.3(11)	15.7(2)
C6	3924.9(14)	6421.7(11)	2001.0(11)	16.4(2)
C7	-1285.5(14)	5645.1(11)	1293.7(11)	17.1(2)
C8	-1997.9(15)	4548.9(13)	1817.0(12)	21.8(2)
C9	3758.0(14)	8288.6(11)	857.3(11)	16.7(2)
C10	5593.9(15)	8512.9(13)	1075.6(14)	24.2(3)
C11	4159.0(14)	4379.4(12)	2854.4(11)	16.8(2)
C12	3443.0(16)	2999.6(13)	2227.5(12)	24.2(3)
C13	4363.6(19)	2025.9(14)	2602.5(14)	30.5(3)
C14	5988.2(18)	2429.0(14)	3573.9(13)	27.6(3)
C15	6683.5(16)	3804.2(14)	4213.9(12)	23.3(3)
C16	5765.5(14)	4784.9(13)	3865.1(12)	19.4(2)
C17	1135.1(14)	8557.7(11)	2192.1(11)	16.2(2)
C18	2164.1(16)	8926.0(13)	3556.7(12)	22.4(3)
C19	2105.4(16)	10092.2(13)	4406.0(12)	22.9(3)
C20	1007.9(14)	10885.8(11)	3858.6(12)	19.1(2)
C21	-21.3(14)	10563.5(12)	2509.9(12)	20.8(2)
C22	44.2(14)	9382.4(12)	1681.4(12)	18.8(2)

Table 3 Anisotropic Displacement Parameters ($Å^2 \times 10^3$) for **399**. The Anisotropic displacement factor exponent takes the form: $-2\pi^2[h^2a^{*2}U_{11}+...+2hka \times b \times U_{12}]$

Atom	U_{11}	U_{22}	U_{33}	U_{23}	U_{13}	U_{12}
O1	18.7(4)	21.4(4)	28.2(4)	7.7(3)	8.0(3)	6.6(3)
O2	22.9(4)	18.9(4)	27.3(4)	12.9(3)	10.1(3)	7.2(3)
O3	35.3(5)	22.3(5)	44.2(6)	0.1(4)	4.2(5)	16.3(4)
O4	43.1(6)	23.6(5)	28.2(5)	-0.6(4)	14.3(4)	6.6(4)
N1	17.7(5)	14.3(4)	21.2(5)	8.5(4)	8.4(4)	5.8(4)
N2	19.9(5)	15.0(5)	32.1(6)	1.1(4)	9.4(4)	3.3(4)
C2	18.4(5)	13.3(5)	18.2(5)	5.0(4)	8.4(4)	2.8(4)
C3	17.4(5)	13.6(5)	17.0(5)	4.0(4)	7.9(4)	2.8(4)
C4	15.8(5)	13.0(5)	17.3(5)	5.8(4)	6.3(4)	4.4(4)
C5	17.6(5)	12.8(5)	17.6(5)	4.4(4)	7.8(4)	3.4(4)
C6	17.3(5)	13.9(5)	19.2(5)	5.2(4)	8.0(4)	3.5(4)
C7	19.1(5)	14.2(5)	18.1(5)	1.5(4)	8.4(4)	3.8(4)
C8	20.8(6)	21.3(6)	25.4(6)	6.3(5)	12.3(5)	2.0(4)
C9	19.9(5)	12.5(5)	19.0(5)	4.2(4)	8.9(4)	3.7(4)
C10	21.2(6)	22.3(6)	35.9(7)	15.9(5)	14.1(5)	6.6(5)
C11	20.7(5)	17.4(5)	18.2(5)	9.7(4)	10.4(4)	8.4(4)
C12	27.7(6)	18.1(6)	23.7(6)	6.1(5)	5.5(5)	6.1(5)
C13	43.7(8)	16.7(6)	31.3(7)	8.5(5)	11.7(6)	12.2(5)
C14	37.1(7)	28.8(7)	28.8(6)	17.2(5)	16.7(6)	21.1(6)
C15	21.9(6)	32.5(7)	22.5(6)	14.2(5)	10.7(5)	12.5(5)
C16	19.7(5)	20.9(6)	21.9(5)	9.0(4)	11.0(4)	6.1(4)
C17	16.5(5)	13.2(5)	21.2(5)	6.6(4)	8.9(4)	3.5(4)
C18	28.1(6)	19.4(6)	21.6(6)	8.3(5)	7.8(5)	12.4(5)
C19	28.3(6)	20.0(6)	19.4(5)	5.1(5)	6.9(5)	9.2(5)
C20	18.9(5)	12.7(5)	26.4(6)	3.3(4)	10.6(4)	3.9(4)
C21	17.3(5)	15.4(5)	28.6(6)	6.2(5)	6.2(5)	6.4(4)
C22	16.3(5)	15.9(5)	21.9(5)	5.0(4)	4.4(4)	4.5(4)

Table 4 Bond Lengths for **399**.

Atom	Atom	Length/Å	Atom	Atom	Length/Å
O1	C7	1.2229(14)	C7	C8	1.5058(16)
O2	C9	1.2283(14)	C9	C10	1.5074(16)
O3	N2	1.2310(14)	C11	C12	1.3912(17)

O4	N2	1.2266(14)	C11	C16	1.3901(16)
N1	C2	1.3836(14)	C12	C13	1.3892(17)
N1	C6	1.3844(14)	C13	C14	1.385(2)
N1	C11	1.4320(14)	C14	C15	1.387(2)
N2	C20	1.4703(15)	C15	C16	1.3876(16)
C2	C3	1.3453(15)	C17	C18	1.3952(16)
C3	C4	1.5196(15)	C17	C22	1.3918(15)
C3	C7	1.4755(15)	C18	C19	1.3886(17)
C4	C5	1.5190(15)	C19	C20	1.3827(16)
C4	C17	1.5278(15)	C20	C21	1.3829(17)
C5	C6	1.3508(15)	C21	C22	1.3903(16)
C5	C9	1.4717(15)			

Table 5 Bond Angles for **399**.

Atom	Atom	Atom	Angle/°	Atom	Atom	Atom	Angle/°
C2	N1	C6	118.23(9)	O2	C9	C10	120.68(10)
C2	N1	C11	120.02(9)	C5	C9	C10	120.50(10)
C6	N1	C11	120.09(9)	C12	C11	N1	119.68(10)
O3	N2	C20	118.05(11)	C16	C11	N1	119.68(10)
O4	N2	O3	123.48(11)	C16	C11	C12	120.64(11)
O4	N2	C20	118.46(10)	C13	C12	C11	119.32(11)
C3	C2	N1	123.49(10)	C14	C13	C12	120.21(12)
C2	C3	C4	121.94(10)	C13	C14	C15	120.18(12)
C2	C3	C7	120.68(10)	C14	C15	C16	120.13(11)
C7	C3	C4	117.37(9)	C15	C16	C11	119.45(11)
C3	C4	C17	110.85(9)	C18	C17	C4	119.28(10)
C5	C4	C3	110.06(9)	C22	C17	C4	121.62(10)
C5	C4	C17	110.59(9)	C22	C17	C18	119.10(10)
C6	C5	C4	122.24(10)	C19	C18	C17	121.02(11)
C6	C5	C9	121.32(10)	C20	C19	C18	118.09(11)
C9	C5	C4	116.37(9)	C19	C20	N2	118.17(11)
C5	C6	N1	122.91(10)	C19	C20	C21	122.68(11)
O1	C7	C3	119.42(10)	C21	C20	N2	119.14(10)
O1	C7	C8	120.99(10)	C20	C21	C22	118.23(10)
C3	C7	C8	119.59(10)	C21	C22	C17	120.88(11)
O2	C9	C5	118.83(10)				

Table 6 Hydrogen Atom Coordinates (Å×10^4) and Isotropic Displacement Parameters (Å^2×10^3) for **399**.

Atom	*x*	*y*	*z*	U(eq)
H2	1048	4424	2422	19
H4	538	7226	341	18
H6	5067	6517	2100	20
H8A	-1561	4840	2798	32(2)
H8B	-1667	3696	1544	32(2)
H8C	-3229	4396	1449	32(2)
H10A	5800	7692	590	48(3)
H10B	6284	8695	2036	48(3)
H10C	5891	9297	742	48(3)
H12	2336	2726	1550	29
H13	3877	1080	2191	37
H14	6628	1762	3803	33
H15	7790	4075	4892	28
H16	6231	5726	4313	23
H18	2916	8370	3910	27
H19	2800	10338	5336	27
H21	-754	11134	2159	25
H22	-665	9135	754	23

Crystallography Data for Compound **400**

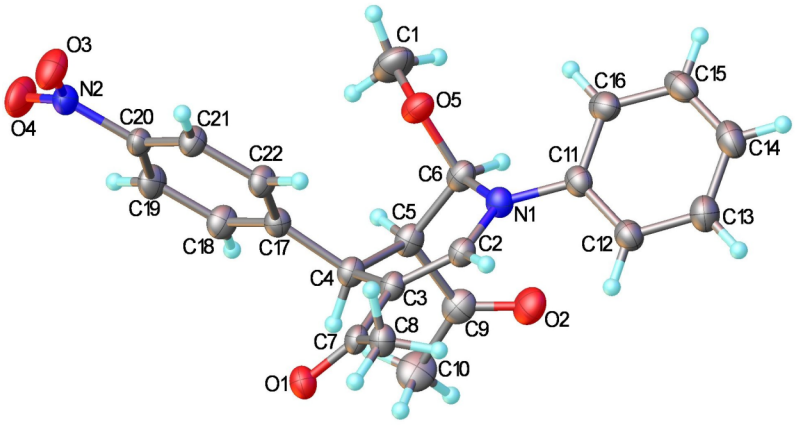

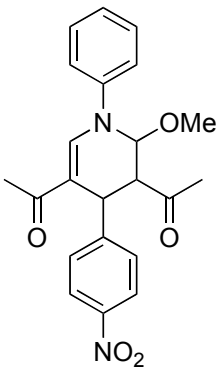

400

Table 1 Crystal data and structure refinement for **400**

Identification code	**400**
Empirical formula	$C_{22}H_{22}N_2O_5$
Formula weight	394.42

Temperature/K	120
Crystal system	monoclinic
Space group	$P2_1/c$
a/Å	11.9899(6)
b/Å	15.0103(8)
c/Å	10.9303(6)
α/°	90.00
β/°	98.151(10)
γ/°	90.00
Volume/Å^3	1947.28(18)
Z	4
ρ_{calc}mg/mm^3	1.345
m/mm^{-1}	0.096
F(000)	832.0
Crystal size/mm^3	0.41 × 0.3 × 0.06
2Θ range for data collection	3.44 to 57°
Index ranges	$-16 \leq h \leq 16$, $-20 \leq k \leq 20$, $-14 \leq l \leq 14$
Reflections collected	24552
Independent reflections	4928[R(int) = 0.0407]
Data/restraints/parameters	4928/0/268
Goodness-of-fit on F^2	1.062
Final R indexes [I>=2σ (I)]	R_1 = 0.0402, wR_2 = 0.1102
Final R indexes [all data]	R_1 = 0.0524, wR_2 = 0.1177
Largest diff. peak/hole / e Å^{-3}	0.33/-0.17

Table 2 Fractional Atomic Coordinates (×10^4) and Equivalent Isotropic Displacement Parameters (Å^2×10^3) for **400**. U_{eq} is defined as 1/3 of of the trace of the orthogonalised U_{IJ} tensor.

Atom	*x*	*y*	*z*	U(eq)
O1	-295.8(7)	4477.4(5)	1793.0(8)	29.1(2)
O2	1896.9(8)	7478.8(6)	1043.7(9)	39.7(2)
O3	2748.8(9)	2646.6(6)	7012.0(9)	43.7(3)
O4	2252.1(9)	3725.8(7)	8115.5(8)	44.9(3)
O5	4028.9(7)	5694.4(6)	3103.9(8)	34.6(2)
N1	3128.1(8)	5795.9(6)	1088.3(9)	27.3(2)
N2	2415.4(9)	3409.5(7)	7121.4(9)	29.9(2)
C1	4518.8(15)	6150.5(11)	4191.4(15)	50.2(4)

C2	2252.5(9)	5217.5(7)	848.7(10)	24.6(2)
C3	1459.8(10)	5080.9(7)	1593.8(10)	23.8(2)
C4	1469.7(10)	5597.5(7)	2773(1)	25.2(2)
C5	2200.1(11)	6445.5(7)	2734.9(11)	28.6(3)
C6	3317.8(11)	6249.2(8)	2270.1(11)	28.9(3)
C7	541.7(10)	4451.9(7)	1262.5(10)	24.0(2)
C8	636.7(11)	3751.5(7)	294.5(11)	27.4(2)
C9	1549.3(11)	7168.4(8)	1945.3(12)	32.5(3)
C10	471.8(13)	7488.5(9)	2348.0(14)	44.2(3)
C11	3793.3(10)	6008.5(8)	145.6(12)	28.0(3)
C12	3294.4(11)	6048.8(8)	-1081.0(12)	31.0(3)
C13	3952.1(12)	6212.6(9)	-2004.2(13)	36.6(3)
C14	5096.7(12)	6363.9(9)	-1708.5(14)	38.4(3)
C15	5580.8(11)	6353.0(8)	-482.7(14)	37.3(3)
C16	4943.4(11)	6169.2(8)	451.0(13)	32.8(3)
C17	1784.2(10)	5024.0(7)	3926.9(10)	24.7(2)
C18	1535.7(11)	5329.8(8)	5060.9(11)	30.2(3)
C19	1741.2(11)	4806.7(8)	6117.8(11)	31.0(3)
C20	2198.5(10)	3970.6(8)	6015.1(10)	25.4(2)
C21	2458.1(10)	3641.2(8)	4904.5(11)	27.7(2)
C22	2249.8(10)	4176.4(8)	3864.1(11)	27.8(3)

Table 3 Anisotropic Displacement Parameters ($Å^2 \times 10^3$) for **400**. The Anisotropic displacement factor exponent takes the form: $-2\pi^2[h^2a^{*2}U_{11}+...+2hka \times b \times U_{12}]$

Atom	U_{11}	U_{22}	U_{33}	U_{23}	U_{13}	U_{12}
O1	32.5(4)	27.0(4)	29.6(4)	0.1(3)	10.7(4)	-1.5(3)
O2	48.2(6)	29.2(5)	41.1(5)	7.4(4)	4.0(4)	-1.5(4)
O3	60.4(7)	37.7(5)	34.2(5)	8.3(4)	11.1(5)	11.3(5)
O4	59.1(7)	55.8(6)	21.7(4)	2.4(4)	12.0(4)	10.5(5)
O5	35.9(5)	32.5(5)	32.9(5)	5.1(4)	-3.8(4)	-3.3(4)
N1	29.8(5)	24.9(5)	27.5(5)	0.0(4)	4.8(4)	-3.2(4)
N2	28.7(5)	38.1(6)	23.7(5)	3.2(4)	6.1(4)	-0.7(4)
C1	51.1(9)	52.7(9)	41.1(8)	3.2(7)	-13.6(7)	-8.3(7)
C2	30.1(6)	19.8(5)	23.7(5)	-0.7(4)	2.8(4)	-0.1(4)
C3	30.0(6)	19.6(5)	21.9(5)	0.5(4)	4.0(4)	0.6(4)
C4	31.3(6)	21.4(5)	23.1(5)	-2.4(4)	4.3(5)	0.4(4)

C5	38.6(7)	21.8(5)	24.8(6)	-3.1(4)	2.7(5)	-2.9(5)
C6	34.5(6)	23.0(5)	28.0(6)	1.2(4)	0.2(5)	-4.7(5)
C7	30.6(6)	20.7(5)	21.0(5)	3.4(4)	5.0(4)	0.3(4)
C8	35.0(6)	23.1(5)	24.9(6)	-1.5(4)	7.2(5)	-3.7(4)
C9	42.6(7)	19.4(5)	34.6(7)	-5.8(5)	1.9(6)	-2.2(5)
C10	57.5(9)	29.5(7)	46.5(8)	-8.0(6)	10.7(7)	11.8(6)
C11	30.1(6)	22.1(5)	32.9(6)	1.7(4)	7.9(5)	-1.0(4)
C12	29.3(6)	30.1(6)	34.4(7)	1.9(5)	7.4(5)	-1.2(5)
C13	41.2(7)	35.7(7)	34.5(7)	1.6(5)	10.8(6)	-2.8(5)
C14	39.3(7)	33.3(7)	46.5(8)	3.5(6)	19.7(6)	-0.7(5)
C15	27.6(6)	30.0(6)	55.7(9)	5.0(6)	10.8(6)	-1.0(5)
C16	30.3(6)	28.1(6)	39.5(7)	4.7(5)	2.6(5)	-0.6(5)
C17	27.6(6)	23.8(5)	23.1(5)	-2.4(4)	4.6(4)	-2.1(4)
C18	39.1(7)	26.2(6)	26.2(6)	-4.9(5)	7.1(5)	3.1(5)
C19	38.4(7)	34.1(6)	21.7(5)	-5.2(5)	8.8(5)	0.6(5)
C20	26.1(6)	30.7(6)	19.8(5)	0.9(4)	4.1(4)	-2.2(4)
C21	32.9(6)	25.9(5)	25.0(6)	-0.8(4)	6.6(5)	3.8(4)
C22	34.8(6)	27.9(6)	22.1(5)	-2.7(4)	8.1(5)	2.8(5)

Table 4 Bond Lengths for **400**.

Atom	Atom	Length/Å	Atom	Atom	Length/Å
O1	C7	1.2293(14)	C5	C9	1.5297(17)
O2	C9	1.2159(16)	C7	C8	1.5073(15)
O3	N2	1.2243(14)	C9	C10	1.502(2)
O4	N2	1.2266(13)	C11	C12	1.3898(18)
O5	C1	1.4243(17)	C11	C16	1.3930(18)
O5	C6	1.4250(15)	C12	C13	1.3878(18)
N1	C2	1.3588(15)	C13	C14	1.383(2)
N1	C6	1.4491(15)	C14	C15	1.383(2)
N1	C11	1.4257(15)	C15	C16	1.3867(19)
N2	C20	1.4664(15)	C17	C18	1.3930(16)
C2	C3	1.3520(16)	C17	C22	1.3950(16)
C3	C4	1.5028(15)	C18	C19	1.3896(17)
C3	C7	1.4564(16)	C19	C20	1.3805(17)
C4	C5	1.5489(16)	C20	C21	1.3863(16)
C4	C17	1.5294(15)	C21	C22	1.3858(16)

C5	C6	1.5277(18)

Table 5 Bond Angles for **400**.

Atom	Atom	Atom	Angle/°	Atom	Atom	Atom	Angle/°
C1	O5	C6	113.04(10)	C3	C7	C8	119.80(10)
C2	N1	C6	119.41(10)	O2	C9	C5	121.54(12)
C2	N1	C11	119.99(10)	O2	C9	C10	121.53(12)
C11	N1	C6	120.39(9)	C10	C9	C5	116.92(11)
O3	N2	O4	122.95(10)	C12	C11	N1	119.90(11)
O3	N2	C20	118.61(10)	C12	C11	C16	119.98(12)
O4	N2	C20	118.44(10)	C16	C11	N1	120.12(11)
C3	C2	N1	124.80(10)	C13	C12	C11	119.86(12)
C2	C3	C4	121.17(10)	C14	C13	C12	120.42(13)
C2	C3	C7	121.31(10)	C15	C14	C13	119.39(13)
C7	C3	C4	117.49(10)	C14	C15	C16	121.07(12)
C3	C4	C5	109.68(9)	C15	C16	C11	119.23(13)
C3	C4	C17	112.83(9)	C18	C17	C4	119.31(10)
C17	C4	C5	114.23(9)	C18	C17	C22	118.81(11)
C6	C5	C4	112.11(9)	C22	C17	C4	121.76(10)
C6	C5	C9	110.51(10)	C19	C18	C17	121.23(11)
C9	C5	C4	110.67(10)	C20	C19	C18	118.14(10)
O5	C6	N1	107.44(9)	C19	C20	N2	118.76(10)
O5	C6	C5	111.93(10)	C19	C20	C21	122.45(11)
N1	C6	C5	110.66(10)	C21	C20	N2	118.79(10)
O1	C7	C3	120.11(10)	C22	C21	C20	118.36(11)
O1	C7	C8	120.06(10)	C21	C22	C17	121.01(10)

Table 6 Hydrogen Atom Coordinates ($Å \times 10^4$) and Isotropic Displacement Parameters ($Å^2 \times 10^3$) for **400**.

Atom	*x*	*y*	*z*	U(eq)
H1A	4847	6713	3962	69(3)
H1B	5109	5779	4648	69(3)
H1C	3936	6273	4714	69(3)
H2	2193	4885	103	30
H4	680	5805	2790	30
H5	2374	6679	3598	34

H6	3715	6825	2169	35
H8A	-66	3410	145	36(2)
H8B	1262	3349	584	36(2)
H8C	775	4039	-475	36(2)
H10A	-151	7106	1987	88(4)
H10B	325	8104	2067	88(4)
H10C	538	7466	3251	88(4)
H12	2505	5964	-1287	37
H13	3614	6221	-2844	44
H14	5546	6474	-2342	46
H15	6363	6474	-277	45
H16	5287	6153	1289	39
H18	1220	5907	5113	36
H19	1572	5019	6889	37
H21	2770	3063	4858	33
H22	2427	3963	3096	33

Crystallography Data for Compound **403**

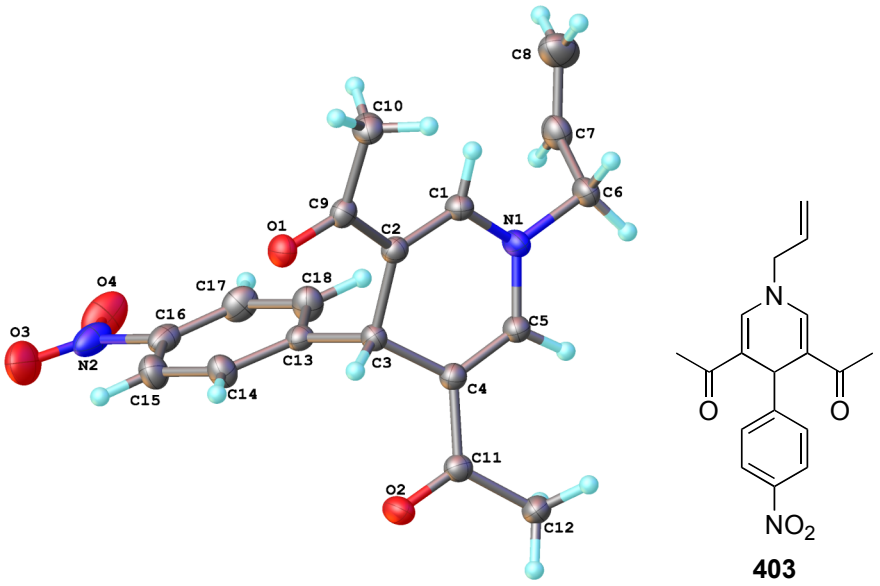

403

Table 1 Crystal data and structure refinement for **403**

Identification code	12srv005
Empirical formula	$C_{18}H_{18}N_2O_4$
Formula weight	326.34
Temperature/K	120
Crystal system	triclinic

Space group	P-1
a/Å	8.0656(3)
b/Å	8.3174(3)
c/Å	12.3033(4)
α/°	95.465(2)
β/°	99.984(2)
γ/°	93.148(2)
Volume/Å^3	807.02(5)
Z	2
ρ_{calc}mg/mm^3	1.343
m/mm^{-1}	0.096
F(000)	344.0
Crystal size/mm^3	0.31 × 0.24 × 0.07
2Θ range for data collection	3.38 to 59°
Index ranges	-11 ≤ h ≤ 11, -11 ≤ k ≤ 11, -17 ≤ l ≤ 17
Reflections collected	13943
Independent reflections	4499[R(int) = 0.0267]
Data/restraints/parameters	4499/0/289
Goodness-of-fit on F^2	1.061
Final R indexes [I>=2σ (I)]	R_1 = 0.0475, wR_2 = 0.1204
Final R indexes [all data]	R_1 = 0.0622, wR_2 = 0.1349
Largest diff. peak/hole / e Å^{-3}	0.42/-0.22

Table 2 Fractional Atomic Coordinates (×10^4) and Equivalent Isotropic Displacement Parameters (Å^2×10^3) for **403**. U_{eq} is defined as 1/3 of of the trace of the orthogonalised U_{IJ} tensor.

Atom	*x*	*y*	*z*	U(eq)
O1	603.7(12)	-922.4(11)	6077.2(8)	26.5(2)
O2	-3487.5(11)	3481.5(11)	5865.0(8)	29.0(2)
O3	-3458.8(17)	-788.4(18)	10559.0(11)	52.4(3)
O4	-2024.8(19)	1325.5(17)	11489.3(10)	54.3(4)
N1	2382.1(13)	4625.6(12)	7053.8(9)	24.0(2)
N2	-2525.9(17)	443.5(17)	10626.1(11)	37.6(3)
C1	2665.9(15)	3003.6(15)	6880.3(10)	22.5(2)
C2	1408.1(15)	1829.8(14)	6614.2(10)	20.8(2)
C3	-405.9(15)	2209.3(14)	6636(1)	20.2(2)
C4	-577.5(15)	3985.9(14)	6485(1)	21.3(2)

C5	770.7(15)	5078.2(15)	6738.5(10)	22.4(2)
C6	3843.1(16)	5818.6(16)	7317.9(12)	25.8(3)
C7	4741.2(18)	5842.7(17)	8492.4(12)	30.9(3)
C8	6297(2)	5431(2)	8770.4(15)	45.2(4)
C9	1746.8(16)	154.4(14)	6275.7(10)	21.9(2)
C10	3527.2(18)	-209.2(17)	6162.1(13)	29.1(3)
C11	-2264.5(15)	4484.9(15)	6059.9(10)	22.5(2)
C12	-2495.8(17)	6234.9(17)	5877.7(13)	28.2(3)
C13	-956.2(15)	1754.8(14)	7698.6(10)	21.3(2)
C14	-2138.3(17)	462.1(17)	7655.4(11)	27.7(3)
C15	-2658.5(18)	19.9(18)	8612.2(12)	32.1(3)
C16	-1972.4(17)	904.5(17)	9610.0(11)	28.5(3)
C17	-785(2)	2185.2(18)	9692.6(12)	32.3(3)
C18	-278.8(19)	2604.4(17)	8724.8(11)	30.1(3)

Table 3 Anisotropic Displacement Parameters ($Å^2 \times 10^3$) for **403**. The Anisotropic displacement factor exponent takes the form: $-2\pi^2[h^2a^{*2}U_{11}+...+2hka \times b \times U_{12}]$

Atom	U_{11}	U_{22}	U_{33}	U_{23}	U_{13}	U_{12}
O1	29.3(5)	21.9(4)	27.8(5)	2.2(3)	5.1(4)	-0.5(3)
O2	21.3(4)	27.8(5)	36.8(5)	3.7(4)	2.6(4)	0.3(4)
O3	49.8(7)	68.7(9)	48.0(7)	28.2(6)	22.4(6)	3.3(6)
O4	83.1(10)	58.6(8)	28.9(6)	10.9(5)	22.4(6)	24.4(7)
N1	19.2(5)	20.6(5)	31.3(5)	2.3(4)	3.1(4)	-0.8(4)
N2	42.5(7)	48.5(8)	29.9(6)	16.9(6)	16.1(5)	22.6(6)
C1	20.1(6)	22.6(6)	25.2(6)	3.6(4)	4.3(4)	3.1(4)
C2	21.5(5)	21.5(5)	20.1(5)	3.8(4)	4.4(4)	3.1(4)
C3	19.3(5)	20.0(5)	21.3(5)	2.6(4)	3.6(4)	0.2(4)
C4	20.8(5)	21.6(5)	22.2(5)	3.9(4)	4.6(4)	2.3(4)
C5	20.9(6)	21.4(5)	25.5(6)	4.1(4)	5.0(4)	2.5(4)
C6	21.6(6)	23.0(6)	32.3(7)	4.0(5)	3.9(5)	-2.8(5)
C7	30.6(7)	28.7(6)	32.1(7)	2.4(5)	5.1(5)	-4.9(5)
C8	34.1(8)	62.2(11)	38.3(9)	14.2(8)	0.1(7)	0.0(7)
C9	26.1(6)	21.7(5)	18.8(5)	4.0(4)	4.9(4)	2.6(4)
C10	28.3(7)	25.2(6)	35.9(7)	3.8(5)	10.5(6)	5.4(5)
C11	21.7(6)	25.5(6)	21.3(5)	3.9(4)	5.4(4)	3.0(4)
C12	23.4(6)	27.3(6)	35.8(7)	10.9(5)	5.3(5)	3.8(5)

C13	20.4(5)	22.2(5)	22.4(5)	4.3(4)	4.9(4)	4.6(4)
C14	27.0(6)	30.0(6)	25.9(6)	2.6(5)	6.3(5)	-3.3(5)
C15	29.8(7)	36.0(7)	33.0(7)	9.1(6)	10.7(5)	-1.4(6)
C16	29.6(6)	35.1(7)	26.0(6)	11.1(5)	11.5(5)	13.6(5)
C17	40.7(8)	33.5(7)	22.1(6)	1.7(5)	3.8(5)	5.8(6)
C18	34.4(7)	29.3(6)	25.0(6)	2.6(5)	2.9(5)	-3.5(5)

Table 4 Bond Lengths for **403**.

Atom	Atom	Length/Å	Atom	Atom	Length/Å
O1	C9	1.2253(15)	C4	C5	1.3509(17)
O2	C11	1.2314(15)	C4	C11	1.4676(17)
O3	N2	1.2250(19)	C6	C7	1.498(2)
O4	N2	1.2246(19)	C7	C8	1.315(2)
N1	C1	1.3835(16)	C9	C10	1.5107(18)
N1	C5	1.3741(16)	C11	C12	1.5103(18)
N1	C6	1.4684(16)	C13	C14	1.3881(17)
N2	C16	1.4748(17)	C13	C18	1.3930(18)
C1	C2	1.3434(17)	C14	C15	1.3906(19)
C2	C3	1.5178(16)	C15	C16	1.379(2)
C2	C9	1.4699(17)	C16	C17	1.377(2)
C3	C4	1.5176(16)	C17	C18	1.392(2)
C3	C13	1.5251(16)			

Table 5 Bond Angles for **403**.

Atom	Atom	Atom	Angle/°	Atom	Atom	Atom	Angle/°
C1	N1	C6	118.55(10)	C8	C7	C6	123.87(15)
C5	N1	C1	118.20(10)	O1	C9	C2	120.63(11)
C5	N1	C6	121.70(10)	O1	C9	C10	120.67(11)
O3	N2	C16	118.44(13)	C2	C9	C10	118.69(11)
O4	N2	O3	123.90(13)	O2	C11	C4	119.98(11)
O4	N2	C16	117.66(14)	O2	C11	C12	120.27(11)
C2	C1	N1	122.75(11)	C4	C11	C12	119.74(11)
C1	C2	C3	120.69(11)	C14	C13	C3	119.99(11)
C1	C2	C9	120.99(11)	C14	C13	C18	118.82(12)
C9	C2	C3	118.32(10)	C18	C13	C3	121.19(11)

C2	C3	C13	111.22(9)	C13	C14	C15	121.14(13)
C4	C3	C2	108.75(9)	C16	C15	C14	118.23(13)
C4	C3	C13	112.36(10)	C15	C16	N2	118.40(13)
C5	C4	C3	121.38(11)	C17	C16	N2	119.03(13)
C5	C4	C11	120.88(11)	C17	C16	C15	122.56(12)
C11	C4	C3	117.75(10)	C16	C17	C18	118.25(13)
C4	C5	N1	122.02(11)	C17	C18	C13	120.99(13)
N1	C6	C7	112.14(11)				

Table 6 Hydrogen Atom Coordinates ($Å \times 10^4$) and Isotropic Displacement Parameters ($Å^2 \times 10^3$) for **403**.

Atom	*x*	*y*	*z*	U(eq)
H1	3830(20)	2811(19)	6930(13)	25(4)
H3	-1160(20)	1524(19)	6007(13)	24(4)
H5	699(19)	6216(19)	6699(13)	24(4)
H6A	3390(20)	6860(20)	7181(15)	35(4)
H6B	4620(20)	5520(20)	6779(15)	36(4)
H7	4100(20)	6220(20)	9051(16)	38(5)
H8A	6820(30)	5510(20)	9556(17)	48(5)
H8B	6970(30)	5040(30)	8210(20)	61(6)
H10A	3510(20)	-1310(20)	5765(15)	37(5)
H10B	4220(30)	-150(20)	6886(18)	48(5)
H10C	4010(20)	580(20)	5751(16)	43(5)
H12A	-2330(20)	6910(20)	6585(18)	48(5)
H12B	-3650(20)	6330(20)	5473(15)	34(4)
H12C	-1640(20)	6670(20)	5471(16)	45(5)
H14	-2590(20)	-150(20)	6927(14)	30(4)
H15	-3510(20)	-880(20)	8563(16)	40(5)
H17	-330(20)	2790(20)	10396(16)	40(5)
H18	590(20)	3510(20)	8772(15)	39(5)

Crystallography Data for Compound **404**

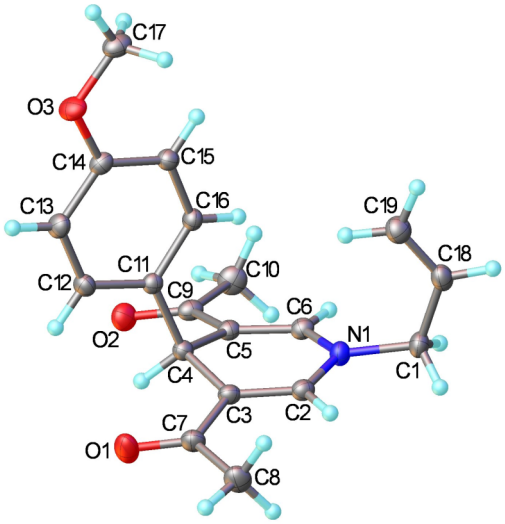

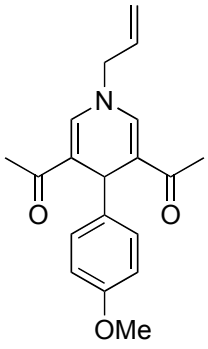

404

Table 1 Crystal data and structure refinement for **404**

Identification code	**404**
Empirical formula	$C_{19}H_{21}NO_3$
Formula weight	311.37
Temperature/K	120
Crystal system	monoclinic
Space group	$P2_1/c$
a/Å	8.5218(6)
b/Å	19.4587(16)
c/Å	9.7216(7)
α/°	90.00
β/°	97.456(9)
γ/°	90.00
Volume/Å^3	1598.4(2)
Z	4
ρ_{calc}mg/mm^3	1.294
m/mm^{-1}	0.087
F(000)	664.0
Crystal size/mm^3	0.7 × 0.4 × 0.3
2Θ range for data collection	4.18 to 60°
Index ranges	$-11 \leq h \leq 11$, $-27 \leq k \leq 27$, $-13 \leq l \leq 13$
Reflections collected	29459
Independent reflections	4652[R(int) = 0.0238]
Data/restraints/parameters	4652/0/222

Goodness-of-fit on F^2	1.068
Final R indexes [I>=2σ (I)]	R_1 = 0.0403, wR_2 = 0.1148
Final R indexes [all data]	R_1 = 0.0458, wR_2 = 0.1209
Largest diff. peak/hole / e Å^{-3}	0.45/-0.21

Table 2 Fractional Atomic Coordinates ($\times 10^4$) and Equivalent Isotropic Displacement Parameters (Å$^2\times 10^3$) for **404**. U_{eq} is defined as 1/3 of of the trace of the orthogonalised U_{IJ} tensor.

Atom	*x*	*y*	*z*	U(eq)
O1	6322.8(9)	1825.6(4)	3828.3(9)	33.7(2)
O2	4190.9(9)	-386.2(4)	1582.1(8)	26.65(16)
O3	378.2(9)	798.5(4)	6733.4(7)	25.03(16)
N1	2386.8(9)	1794.3(4)	-65.0(8)	19.78(16)
C1	1365.2(11)	2194.2(5)	-1095.8(10)	22.72(19)
C2	3402.4(10)	2121.9(5)	936.2(9)	19.19(18)
C3	4272.1(10)	1778.3(4)	1982.5(9)	17.96(17)
C4	4002.5(10)	1015.3(4)	2215.3(9)	16.79(17)
C5	3220(1)	698.7(4)	874.0(9)	17.31(17)
C6	2402(1)	1086.2(5)	-125.8(9)	18.64(17)
C7	5466.4(11)	2143.2(5)	2932.1(10)	22.56(19)
C8	5637.1(13)	2914.8(5)	2808.6(12)	28.5(2)
C9	3345.1(11)	-49.7(5)	711.3(10)	19.82(18)
C10	2422.0(13)	-407.7(5)	-517.5(11)	28.1(2)
C11	3006.2(10)	915.5(4)	3399.2(9)	16.16(16)
C12	3720.5(11)	830.2(5)	4768.1(9)	19.91(18)
C13	2816.5(11)	782.9(5)	5852.8(9)	21.79(19)
C14	1169.0(11)	824.5(5)	5592.2(9)	19.02(18)
C15	431.7(10)	886.9(5)	4236.1(9)	18.60(17)
C16	1360.3(10)	927.7(4)	3159.9(9)	17.65(17)
C17	-1309.2(12)	877.9(5)	6498.2(11)	26.3(2)
C18	-207.1(11)	2370.1(5)	-658.1(10)	23.70(19)
C19	-687.9(13)	2213.4(5)	540.1(11)	26.9(2)

Table 3 Anisotropic Displacement Parameters (Å$^2\times 10^3$) for **404**. The Anisotropic displacement factor exponent takes the form: $-2\pi^2[h^2a^{*2}U_{11}+...+2hka\times b\times U_{12}]$

Atom	U_{11}	U_{22}	U_{33}	U_{23}	U_{13}	U_{12}
O1	28.9(4)	28.3(4)	39.4(4)	8.2(3)	-12.2(3)	-8.4(3)
O2	28.4(4)	19.8(3)	31.5(4)	2.5(3)	2.7(3)	3.4(3)
O3	26.3(4)	31.9(4)	17.9(3)	-1.7(3)	6.8(3)	-3.6(3)
N1	21.2(4)	18.2(4)	19.3(4)	2.4(3)	0.0(3)	1.4(3)
C1	24.9(4)	22.3(4)	20.3(4)	5.7(3)	0.2(3)	2.2(3)
C2	19.1(4)	17.1(4)	21.6(4)	0.7(3)	3.9(3)	-0.9(3)
C3	16.6(4)	16.6(4)	20.9(4)	0.3(3)	3.1(3)	-1.9(3)
C4	16.0(4)	16.3(4)	18.1(4)	0.6(3)	2.1(3)	0.0(3)
C5	17.4(4)	16.9(4)	18.2(4)	-0.3(3)	4.5(3)	-0.3(3)
C6	20.0(4)	19.0(4)	17.4(4)	-0.9(3)	4.2(3)	-0.9(3)
C7	19.4(4)	21.7(4)	26.1(4)	1.4(3)	0.9(3)	-4.3(3)
C8	26.4(5)	21.4(4)	36.0(5)	0.1(4)	-2.6(4)	-5.8(4)
C9	20.3(4)	17.4(4)	23.0(4)	-1.0(3)	7.4(3)	-0.8(3)
C10	33.9(5)	21.3(4)	28.7(5)	-5.6(4)	2.9(4)	-2.9(4)
C11	17.5(4)	13.7(3)	17.3(4)	-0.1(3)	2.2(3)	-0.3(3)
C12	17.9(4)	21.3(4)	19.8(4)	0.1(3)	-0.7(3)	-1.7(3)
C13	23.8(4)	24.8(4)	15.9(4)	0.0(3)	-0.5(3)	-3.1(3)
C14	23.4(4)	17.2(4)	17.0(4)	-1.2(3)	4.5(3)	-2.2(3)
C15	17.9(4)	18.6(4)	19.4(4)	0.3(3)	2.6(3)	-0.1(3)
C16	18.8(4)	18.1(4)	15.7(4)	0.9(3)	1.0(3)	-0.1(3)
C17	28.1(5)	24.1(4)	28.9(5)	0.7(4)	12.6(4)	0.4(4)
C18	22.6(4)	20.3(4)	26.6(5)	2.6(3)	-2.6(3)	1.2(3)
C19	26.3(5)	25.2(5)	29.1(5)	0.8(4)	2.7(4)	3.2(4)

Table 4 Bond Lengths for **404**.

Atom	Atom	Length/Å	Atom	Atom	Length/Å
O1	C7	1.2283(12)	C4	C11	1.5287(12)
O2	C9	1.2274(12)	C5	C6	1.3502(12)
O3	C14	1.3718(11)	C5	C9	1.4703(12)
O3	C17	1.4347(12)	C7	C8	1.5147(14)
N1	C1	1.4632(11)	C9	C10	1.5123(14)
N1	C2	1.3727(12)	C11	C12	1.3996(12)
N1	C6	1.3794(12)	C11	C16	1.3919(12)
C1	C18	1.4972(14)	C12	C13	1.3874(13)
C2	C3	1.3547(12)	C13	C14	1.3963(13)

C3	C4	1.5236(12)	C14	C15	1.3902(12)
C3	C7	1.4658(12)	C15	C16	1.3935(12)
C4	C5	1.5163(12)	C18	C19	1.3196(15)

Table 5 Bond Angles for **404**.

Atom	Atom	Atom	Angle/°	Atom	Atom	Atom	Angle/°
C14	O3	C17	117.04(8)	O1	C7	C8	120.04(9)
C2	N1	C1	120.20(8)	C3	C7	C8	119.75(8)
C2	N1	C6	119.06(8)	O2	C9	C5	119.89(9)
C6	N1	C1	120.66(8)	O2	C9	C10	119.86(9)
N1	C1	C18	113.69(8)	C5	C9	C10	120.25(8)
C3	C2	N1	122.44(8)	C12	C11	C4	121.03(8)
C2	C3	C4	120.94(8)	C16	C11	C4	121.20(8)
C2	C3	C7	120.08(8)	C16	C11	C12	117.74(8)
C7	C3	C4	118.96(8)	C13	C12	C11	120.98(8)
C3	C4	C11	110.17(7)	C12	C13	C14	120.18(8)
C5	C4	C3	109.03(7)	O3	C14	C13	116.04(8)
C5	C4	C11	111.75(7)	O3	C14	C15	124.14(8)
C6	C5	C4	121.37(8)	C15	C14	C13	119.82(8)
C6	C5	C9	120.90(8)	C14	C15	C16	119.09(8)
C9	C5	C4	117.72(8)	C11	C16	C15	122.11(8)
C5	C6	N1	122.27(8)	C19	C18	C1	126.15(9)
O1	C7	C3	120.20(9)				

Table 6 Hydrogen Atom Coordinates ($Å \times 10^4$) and Isotropic Displacement Parameters ($Å^2 \times 10^3$) for **404**.

Atom	*x*	*y*	*z*	U(eq)
H1A	1190	1930	-1972	27
H1B	1917	2625	-1284	27
H2	3499	2608	894	23
H4	5053	789	2477	20
H6	1817	863	-898	22
H8A	5907	3029	1886	50(3)
H8B	6478	3077	3517	50(3)
H8C	4637	3137	2943	50(3)

H10A	2707	-896	-504	58(3)
H10B	2675	-198	-1378	58(3)
H10C	1286	-361	-466	58(3)
H12	4841	804	4957	24
H13	3320	722	6775	26
H15	-690	902	4046	22
H16	854	965	2233	21
H17A	-1726	895	7391	35(2)
H17B	-1779	488	5955	35(2)
H17C	-1575	1305	5988	35(2)
H18	-927	2618	-1304	28
H19A	-16(17)	1957(7)	1250(15)	31(3)
H19B	-1729(18)	2346(8)	757(15)	36(4)

Crystallography Data for Compound **406**

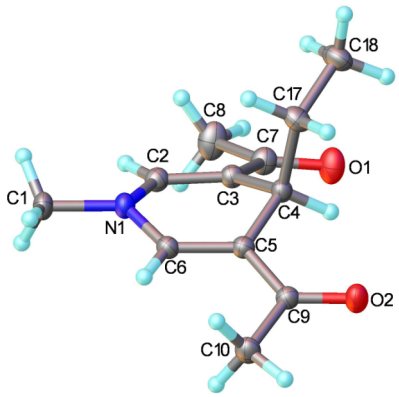

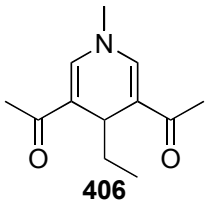

406

Table 1 Crystal data and structure refinement for **406**

Identification code	**406**
Empirical formula	$C_{12}H_{17}NO_2$
Formula weight	207.27
Temperature/K	120
Crystal system	orthorhombic
Space group	$Pna2_1$
a/Å	10.6949(3)
b/Å	9.1552(3)
c/Å	11.6695(4)
α/°	90.00
β/°	90.00

γ/°	90.00
Volume/Å^3	1142.61(6)
Z	4
ρ_{calc}mg/mm^3	1.205
m/mm^{-1}	0.082
F(000)	448.0
Crystal size/mm^3	0.7 × 0.27 × 0.24
2Θ range for data collection	5.66 to 59.98°
Index ranges	-15 ≤ h ≤ 15, -12 ≤ k ≤ 12, -16 ≤ l ≤ 15
Reflections collected	13623
Independent reflections	1736[R(int) = 0.0300]
Data/restraints/parameters	1736/1/144
Goodness-of-fit on F^2	1.058
Final R indexes [I>=2σ (I)]	R_1 = 0.0384, wR_2 = 0.1052
Final R indexes [all data]	R_1 = 0.0407, wR_2 = 0.1077
Largest diff. peak/hole / e Å^{-3}	0.37/-0.14

Table 2 Fractional Atomic Coordinates (×10^4) and Equivalent Isotropic Displacement Parameters (Å^2×10^3) for **406**. U_{eq} is defined as 1/3 of of the trace of the orthogonalised U_{IJ} tensor.

Atom	*x*	*y*	*z*	U(eq)
O1	4178.0(13)	3089.5(14)	7893.9(11)	31.8(3)
O2	3996.0(11)	3163.2(14)	3625.4(11)	27.8(3)
N1	1258.0(11)	247.8(12)	5831.9(13)	21.2(2)
C1	110.7(13)	-622.4(16)	5869.3(16)	25.0(3)
C2	1784.8(14)	748.0(17)	6834.8(13)	20.7(3)
C3	2864.5(13)	1522.5(16)	6841.8(13)	19.2(3)
C4	3615.2(12)	1648.6(14)	5745.9(14)	18.9(3)
C5	2707.6(14)	1660.3(15)	4750.4(13)	19.2(3)
C6	1637.7(13)	869.4(16)	4816.5(13)	19.7(3)
C7	3276.4(15)	2250.3(18)	7892.0(14)	24.7(3)
C8	2556.8(19)	1999(2)	8995.3(15)	35.2(4)
C9	3024.8(13)	2431.9(17)	3692.0(13)	20.1(3)
C10	2140.8(14)	2346.9(19)	2686.7(14)	25.4(3)
C17	4540.4(13)	368.8(17)	5595.8(14)	24.5(3)
C18	5529.3(15)	258(2)	6530.2(18)	31.8(4)

Table 3 Anisotropic Displacement Parameters ($Å^2×10^3$) for **406**. The Anisotropic displacement factor exponent takes the form: $-2\pi^2[h^2a^{*2}U_{11}+...+2hka×b×U_{12}]$

Atom	U_{11}	U_{22}	U_{33}	U_{23}	U_{13}	U_{12}
O1	32.5(6)	37.2(7)	25.8(6)	-5.8(5)	0.4(5)	-12.3(5)
O2	23.5(5)	33.8(6)	26.2(6)	7.2(5)	-2.4(4)	-8.0(4)
N1	17.8(5)	23.3(5)	22.7(6)	1.9(5)	-0.1(5)	-4.2(4)
C1	18.5(6)	26.3(6)	30.2(8)	3.5(6)	0.2(6)	-6.5(5)
C2	21.1(6)	20.7(6)	20.3(7)	0.5(5)	0.9(5)	-0.2(5)
C3	19.3(6)	20.2(6)	18.1(6)	0.6(5)	-0.2(5)	-0.2(4)
C4	16.4(5)	21.4(5)	18.8(6)	2.3(6)	0.0(5)	-1.7(4)
C5	18.0(6)	20.0(6)	19.7(7)	1.8(5)	-0.7(5)	0.2(5)
C6	17.3(6)	21.2(6)	20.5(7)	1.8(5)	-1.5(5)	0.0(5)
C7	26.3(7)	26.9(7)	21.0(7)	-0.5(6)	0.6(6)	-1.8(6)
C8	40.2(9)	42.0(9)	23.4(8)	-5.9(7)	5.9(7)	-11.6(8)
C9	19.4(6)	20.9(6)	20.0(7)	2.1(5)	-0.1(5)	0.0(5)
C10	23.5(7)	31.1(8)	21.4(7)	4.0(6)	-3.2(6)	-2.3(6)
C17	19.5(6)	29.0(7)	25.2(8)	-1.8(6)	-1.1(5)	4.2(5)
C18	24.8(7)	33.2(8)	37.3(9)	1.2(7)	-9.7(6)	4.2(6)

Table 4 Bond Lengths for **406**.

Atom	Atom	Length/Å	Atom	Atom	Length/Å
O1	C7	1.233(2)	C4	C5	1.514(2)
O2	C9	1.2382(18)	C4	C17	1.5436(19)
N1	C1	1.4636(17)	C5	C6	1.3563(19)
N1	C2	1.377(2)	C5	C9	1.463(2)
N1	C6	1.376(2)	C7	C8	1.518(2)
C2	C3	1.355(2)	C9	C10	1.509(2)
C3	C4	1.514(2)	C17	C18	1.522(2)
C3	C7	1.463(2)			

Table 5 Bond Angles for **406**.

Atom	Atom	Atom	Angle/°	Atom	Atom	Atom	Angle/°
C2	N1	C1	119.91(14)	C6	C5	C9	120.10(14)

C6	N1	C1	119.89(14)	C9	C5	C4	120.18(12)
C6	N1	C2	118.26(11)	C5	C6	N1	121.26(14)
C3	C2	N1	121.85(13)	O1	C7	C3	121.39(15)
C2	C3	C4	119.12(13)	O1	C7	C8	119.30(15)
C2	C3	C7	120.00(13)	C3	C7	C8	119.28(14)
C7	C3	C4	120.87(12)	O2	C9	C5	120.58(13)
C3	C4	C17	112.20(12)	O2	C9	C10	120.31(13)
C5	C4	C3	107.98(10)	C5	C9	C10	119.10(12)
C5	C4	C17	109.23(12)	C18	C17	C4	114.48(13)
C6	C5	C4	119.57(13)				

Table 6 Hydrogen Atom Coordinates ($Å \times 10^4$) and Isotropic Displacement Parameters ($Å^2 \times 10^3$) for **406**.

Atom	*x*	*y*	*z*	U(eq)
H1A	-586	-6	6121	49(4)
H1B	218	-1434	6408	49(4)
H1C	-68	-1010	5104	49(4)
H2	1380	544	7542	25
H4	4091	2589	5754	23
H6	1141	742	4149	24
H8A	2986	2490	9629	51(4)
H8B	2509	949	9152	51(4)
H8C	1710	2396	8917	51(4)
H10A	2493	2888	2038	40(4)
H10B	1334	2774	2901	40(4)
H10C	2021	1323	2468	40(4)
H17A	4061	-556	5576	29
H17B	4966	476	4847	29
H18A	6070	-584	6379	48(4)
H18B	5120	137	7276	48(4)
H18C	6034	1152	6537	48(4)

Crystallography Data for Compound **409**

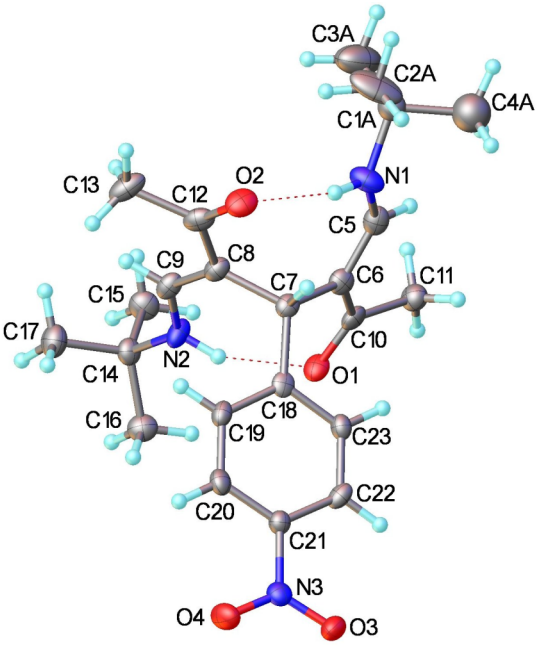

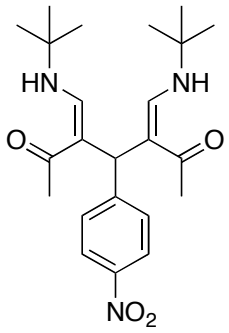

409

Table 1 Crystal data and structure refinement for **409**

Identification code	**409**
Empirical formula	$C_{23}H_{33}N_3O_4$
Formula weight	415.52
Temperature/K	120
Crystal system	monoclinic
Space group	$P2_1$
a/Å	10.565(3)
b/Å	12.104(4)
c/Å	18.684(6)
α/°	90.00
β/°	95.57(3)
γ/°	90.00
Volume/Å^3	2378.0(11)
Z	4
ρ_{calc}mg/mm^3	1.160
m/mm^{-1}	0.080
F(000)	896.0
Crystal size/mm^3	0.22 × 0.19 × 0.09
2Θ range for data collection	5.14 to 50°
Index ranges	$-12 \leq h \leq 12$, $-14 \leq k \leq 14$, $-22 \leq l \leq 22$
Reflections collected	22677
Independent reflections	4407[R(int) = 0.0919]

Data/restraints/parameters	4407/46/559
Goodness-of-fit on F^2	1.045
Final R indexes [I>=2σ (I)]	R_1 = 0.0481, wR_2 = 0.1189
Final R indexes [all data]	R_1 = 0.0598, wR_2 = 0.1291
Largest diff. peak/hole / e $Å^{-3}$	0.22/-0.24

Table 2 Fractional Atomic Coordinates ($\times 10^4$) and Equivalent Isotropic Displacement Parameters ($Å^2 \times 10^3$) for **409**. U_{eq} is defined as 1/3 of of the trace of the orthogonalised U_{IJ} tensor.

Atom	*x*	*y*	*z*	U(eq)
O1	-50(3)	762(3)	4360.3(19)	26.2(8)
O2	617(4)	4709(3)	2838(2)	32.9(9)
O3	5094(4)	2042(3)	6339(2)	30.3(9)
O4	4306(4)	3585(3)	6670(2)	34.4(9)
N1	656(5)	2549(4)	2185(2)	33.2(11)
N2	-1319(4)	2730(4)	4617(2)	26.5(10)
N3	4310(4)	2793(4)	6261(2)	23.7(10)
C1A	370(12)	2637(12)	1392(9)	32.0(18)
C2A	952(16)	3684(13)	1173(8)	65(4)
C3A	-1041(13)	2579(17)	1194(10)	67(4)
C4A	1071(17)	1636(13)	1107(10)	60(5)
C1B	642(13)	2526(11)	1393(9)	32.0(18)
C2B	1770(15)	3186(15)	1188(8)	65(4)
C3B	-577(14)	3154(15)	1125(10)	67(4)
C4B	606(16)	1410(11)	1047(9)	53(4)
C5	421(5)	1695(5)	2600(3)	27.1(12)
C6	466(5)	1718(4)	3335(3)	23.7(11)
C7	815(5)	2809(4)	3714(3)	20.9(11)
C8	-274(5)	3638(4)	3705(3)	24.1(11)
C9	-1221(5)	3535(4)	4150(3)	23.8(11)
C10	110(5)	749(4)	3709(3)	23.3(11)
C11	-52(5)	-352(4)	3322(3)	28.8(13)
C12	-228(5)	4594(5)	3252(3)	27.4(12)
C13	-1198(5)	5505(5)	3278(3)	36.3(14)
C14	-2339(5)	2579(4)	5092(3)	24.0(12)
C15	-3382(5)	1880(5)	4699(3)	31.5(13)
C16	-1750(5)	1970(5)	5756(3)	30.2(13)
C17	-2864(6)	3697(5)	5295(3)	34.6(14)
C18	1633(5)	2722(4)	4434(3)	19.9(11)

C19	1622(5)	3578(4)	4937(3)	21.6(11)
C20	2488(5)	3601(4)	5534(3)	23.5(11)
C21	3349(5)	2747(4)	5647(3)	20.4(11)
C22	3333(5)	1855(4)	5178(3)	22.1(11)
C23	2483(5)	1859(4)	4576(3)	20.8(11)
O5	5898(4)	3924(3)	3297.0(19)	25.6(8)
O6	4582(4)	5459(3)	467.9(19)	32.0(9)
O7	9225(4)	8568(4)	692(2)	38.2(10)
O8	8555(4)	9444(3)	1583(2)	41.3(11)
N4	3381(4)	6199(4)	1659(2)	24.3(10)
N5	5574(5)	2486(3)	2059(2)	28.2(11)
N6	8596(4)	8622(4)	1208(2)	26.4(10)
C24A	2387(12)	7083(11)	1535(7)	29(4)
C25A	1740(12)	6792(11)	770(6)	47(3)
C26A	3041(11)	8167(9)	1512(7)	45(2)
C27A	1391(10)	7030(10)	2051(6)	33(2)
C24B	2325(15)	6901(14)	1425(8)	14(5)
C25B	1362(17)	6309(16)	927(10)	47(3)
C26B	2825(17)	7922(13)	1072(10)	45(2)
C27B	1730(18)	7294(15)	2118(9)	33(2)
C28	3655(5)	5648(4)	2267(3)	22.1(11)
C29	4707(5)	4996(4)	2429(3)	20.0(11)
C30	5706(5)	4818(4)	1904(3)	22.5(11)
C31	5249(5)	4050(4)	1282(3)	26.6(12)
C32	5239(5)	2934(4)	1427(3)	26.5(12)
C33	4915(5)	4466(4)	3121(3)	20.4(11)
C34	3947(5)	4526(4)	3667(3)	25.4(12)
C35	4738(5)	4454(5)	595(3)	30.2(13)
C36	4335(7)	3656(6)	-12(3)	46.4(17)
C37	5496(6)	1313(4)	2270(3)	30.4(13)
C38	4441(6)	1200(5)	2758(4)	41.8(16)
C39	6777(6)	1030(4)	2679(3)	32.6(14)
C40	5251(7)	576(5)	1610(4)	43.8(17)
C41	6407(5)	5854(4)	1691(3)	20.3(11)
C42	6312(5)	6847(4)	2055(3)	22.1(11)
C43	7042(5)	7748(4)	1911(3)	22.6(11)
C44	7848(5)	7660(5)	1381(3)	22.1(11)
C45	7968(5)	6693(5)	1004(3)	27.6(13)

C46	7240(5)	5791(4)	1161(3)	26.6(12)

Table 3 Anisotropic Displacement Parameters ($Å^2 \times 10^3$) for **409**. The Anisotropic displacement factor exponent takes the form: $-2\pi^2[h^2a^{*2}U_{11}+...+2hka \times b \times U_{12}]$

Atom	U_{11}	U_{22}	U_{33}	U_{23}	U_{13}	U_{12}
O1	29(2)	20.0(18)	30(2)	8.2(16)	8.3(17)	1.3(16)
O2	33(2)	31(2)	35(2)	12.5(17)	6.7(19)	-4.0(19)
O3	29(2)	35(2)	27(2)	3.4(17)	2.5(17)	10.8(19)
O4	45(2)	25(2)	30(2)	-6.1(18)	-6.4(19)	0(2)
N1	42(3)	36(3)	22(2)	1(2)	2(2)	-14(2)
N2	23(2)	21(2)	37(3)	9(2)	11(2)	5(2)
N3	28(2)	24(2)	21(2)	3.4(19)	5.8(19)	-2(2)
C2A	73(10)	97(12)	26(4)	9(6)	11(8)	-42(8)
C3A	53(10)	108(15)	40(6)	14(9)	0(7)	1(8)
C2B	73(10)	97(12)	26(4)	9(6)	11(8)	-42(8)
C3B	53(10)	108(15)	40(6)	14(9)	0(7)	1(8)
C5	20(3)	25(3)	37(3)	-3(2)	3(2)	-4(2)
C6	17(3)	26(3)	29(3)	1(2)	4(2)	-3(2)
C7	19(3)	20(2)	24(3)	4(2)	6(2)	-2(2)
C8	21(3)	21(3)	29(3)	2(2)	-1(2)	-1(2)
C9	17(3)	19(3)	35(3)	1(2)	-1(2)	-3(2)
C10	14(2)	24(3)	31(3)	5(2)	0(2)	4(2)
C11	31(3)	23(3)	32(3)	1(2)	2(2)	0(2)
C12	26(3)	24(3)	30(3)	3(2)	-7(2)	-7(2)
C13	25(3)	28(3)	54(4)	15(3)	-8(3)	-4(3)
C14	22(3)	24(3)	28(3)	0(2)	8(2)	-2(2)
C15	28(3)	31(3)	36(3)	-2(3)	2(3)	-8(3)
C16	30(3)	28(3)	32(3)	5(3)	3(2)	-6(3)
C17	35(3)	26(3)	44(4)	-1(3)	10(3)	1(3)
C18	18(3)	19(2)	24(3)	4(2)	10(2)	-4(2)
C19	23(3)	17(2)	26(3)	4(2)	9(2)	3(2)
C20	28(3)	22(3)	22(3)	0(2)	10(2)	1(2)
C21	19(3)	20(3)	23(3)	0(2)	4(2)	-1(2)
C22	18(3)	17(3)	32(3)	7(2)	3(2)	0(2)
C23	22(3)	17(2)	24(3)	-1(2)	7(2)	-1(2)
O5	29(2)	24.2(19)	22.6(19)	2.4(15)	-1.2(16)	4.0(17)
O6	40(2)	32(2)	23(2)	3.1(16)	1.0(18)	0.9(19)

O7	38(2)	40(2)	39(2)	7(2)	18(2)	-6(2)
O8	49(3)	32(2)	45(3)	-8(2)	16(2)	-16(2)
N4	20(2)	29(2)	24(2)	6(2)	2.4(19)	4(2)
N5	39(3)	16(2)	28(2)	-7.2(19)	-5(2)	-2(2)
N6	24(2)	29(3)	25(2)	4(2)	1(2)	0(2)
C28	23(3)	20(3)	23(3)	1(2)	4(2)	-4(2)
C29	21(3)	19(2)	20(3)	1(2)	1(2)	-1(2)
C30	26(3)	20(3)	22(3)	1(2)	0(2)	4(2)
C31	30(3)	24(3)	26(3)	-4(2)	0(2)	-2(2)
C32	34(3)	26(3)	20(3)	-8(2)	2(2)	-2(2)
C33	24(3)	16(2)	20(3)	0(2)	1(2)	-5(2)
C34	26(3)	28(3)	23(3)	7(2)	4(2)	0(2)
C35	37(3)	34(3)	20(3)	-3(2)	3(2)	-4(3)
C36	70(5)	47(4)	20(3)	1(3)	-7(3)	-6(4)
C37	40(3)	16(3)	34(3)	-1(2)	0(3)	0(2)
C38	40(4)	30(3)	56(4)	7(3)	6(3)	-4(3)
C39	37(3)	21(3)	39(3)	0(2)	2(3)	4(3)
C40	56(4)	19(3)	54(4)	-6(3)	-6(3)	-1(3)
C41	24(3)	21(3)	15(2)	1(2)	-2(2)	10(2)
C42	20(3)	27(3)	19(3)	0(2)	4(2)	1(2)
C43	25(3)	21(3)	21(3)	-2(2)	0(2)	1(2)
C44	19(3)	26(3)	21(3)	6(2)	1(2)	-1(2)
C45	26(3)	33(3)	25(3)	0(2)	7(2)	2(3)
C46	33(3)	22(3)	25(3)	-6(2)	7(2)	7(2)

Table 4 Bond Lengths for **409**.

Atom	Atom	Length/Å	Atom	Atom	Length/Å
O1	C10	1.245(6)	O5	C33	1.244(6)
O2	C12	1.244(7)	O6	C35	1.248(7)
O3	N3	1.229(5)	O7	N6	1.226(6)
O4	N3	1.226(5)	O8	N6	1.221(6)
N1	C1A	1.486(17)	N4	C24A	1.503(14)
N1	C1B	1.479(17)	N4	C24B	1.437(18)
N1	C5	1.331(7)	N4	C28	1.326(6)
N2	C9	1.319(7)	N5	C32	1.316(7)
N2	C14	1.473(6)	N5	C37	1.479(7)

N3	C21	1.458(6)	N6	C44	1.461(7)
C1A	C2A	1.483(17)	C24A	C25A	1.564(15)
C1A	C3A	1.502(16)	C24A	C26A	1.487(14)
C1A	C4A	1.543(17)	C24A	C27A	1.497(14)
C1B	C2B	1.514(16)	C24B	C25B	1.494(19)
C1B	C3B	1.537(17)	C24B	C26B	1.520(18)
C1B	C4B	1.497(17)	C24B	C27B	1.567(18)
C5	C6	1.369(7)	C28	C29	1.372(7)
C6	C7	1.527(7)	C29	C30	1.524(7)
C6	C10	1.435(7)	C29	C33	1.442(7)
C7	C8	1.526(7)	C30	C31	1.530(7)
C7	C18	1.530(7)	C30	C41	1.529(7)
C8	C9	1.367(7)	C31	C32	1.378(7)
C8	C12	1.439(7)	C31	C35	1.431(8)
C10	C11	1.519(8)	C33	C34	1.514(7)
C12	C13	1.510(8)	C35	C36	1.519(8)
C14	C15	1.520(7)	C37	C38	1.514(9)
C14	C16	1.523(7)	C37	C39	1.527(8)
C14	C17	1.525(7)	C37	C40	1.524(8)
C18	C19	1.399(7)	C41	C42	1.390(7)
C18	C23	1.387(7)	C41	C46	1.390(7)
C19	C20	1.372(7)	C42	C43	1.378(7)
C20	C21	1.380(7)	C43	C44	1.372(7)
C21	C22	1.390(7)	C44	C45	1.378(8)
C22	C23	1.371(7)	C45	C46	1.384(8)

Table 5 Bond Angles for **409**.

Atom	Atom	Atom	Angle/°	Atom	Atom	Atom	Angle/°
C1B	N1	C1A	12.3(9)	C24B	N4	C24A	11.6(8)
C5	N1	C1A	127.3(7)	C28	N4	C24A	125.6(6)
C5	N1	C1B	125.8(7)	C28	N4	C24B	131.1(7)
C9	N2	C14	126.9(4)	C32	N5	C37	128.2(4)
O3	N3	C21	118.3(4)	O7	N6	C44	118.6(5)
O4	N3	O3	123.2(4)	O8	N6	O7	123.2(5)
O4	N3	C21	118.4(4)	O8	N6	C44	118.2(4)
N1	C1A	C3A	110.1(12)	N4	C24A	C25A	102.6(9)
N1	C1A	C4A	103.3(11)	C26A	C24A	N4	108.3(9)

C2A	C1A	N1	106.6(11)	C26A	C24A	C25A	109.6(10)
C2A	C1A	C3A	113.6(13)	C26A	C24A	C27A	114.5(11)
C2A	C1A	C4A	110.5(12)	C27A	C24A	N4	113.2(9)
C3A	C1A	C4A	112.1(13)	C27A	C24A	C25A	107.9(10)
N1	C1B	C2B	108.1(11)	N4	C24B	C25B	111.5(13)
N1	C1B	C3B	104.1(11)	N4	C24B	C26B	108.7(12)
N1	C1B	C4B	116.5(12)	N4	C24B	C27B	106.9(12)
C2B	C1B	C3B	108.2(12)	C25B	C24B	C26B	111.3(15)
C4B	C1B	C2B	110.8(13)	C25B	C24B	C27B	110.9(14)
C4B	C1B	C3B	108.7(13)	C26B	C24B	C27B	107.2(14)
N1	C5	C6	125.4(5)	N4	C28	C29	125.6(5)
C5	C6	C7	117.8(5)	C28	C29	C30	122.5(4)
C5	C6	C10	119.1(5)	C28	C29	C33	120.2(4)
C10	C6	C7	122.9(4)	C33	C29	C30	117.3(4)
C6	C7	C18	116.1(4)	C29	C30	C31	112.8(4)
C8	C7	C6	114.6(4)	C29	C30	C41	115.8(4)
C8	C7	C18	114.5(4)	C41	C30	C31	115.2(4)
C9	C8	C7	122.0(5)	C32	C31	C30	117.1(5)
C9	C8	C12	120.0(5)	C32	C31	C35	120.2(5)
C12	C8	C7	117.8(5)	C35	C31	C30	122.5(5)
N2	C9	C8	125.4(5)	N5	C32	C31	125.0(5)
O1	C10	C6	122.2(5)	O5	C33	C29	121.4(5)
O1	C10	C11	117.2(5)	O5	C33	C34	116.7(4)
C6	C10	C11	120.5(5)	C29	C33	C34	121.9(4)
O2	C12	C8	121.6(5)	O6	C35	C31	122.4(5)
O2	C12	C13	118.0(5)	O6	C35	C36	117.2(5)
C8	C12	C13	120.4(5)	C31	C35	C36	120.4(5)
N2	C14	C15	108.5(4)	N5	C37	C38	108.2(5)
N2	C14	C16	106.6(4)	N5	C37	C39	106.2(5)
N2	C14	C17	110.2(4)	N5	C37	C40	110.9(5)
C15	C14	C16	110.1(4)	C38	C37	C39	110.3(5)
C15	C14	C17	110.5(5)	C38	C37	C40	110.9(5)
C16	C14	C17	110.9(5)	C40	C37	C39	110.3(5)
C19	C18	C7	120.0(4)	C42	C41	C30	121.5(4)
C23	C18	C7	121.3(4)	C42	C41	C46	118.4(5)
C23	C18	C19	118.5(5)	C46	C41	C30	119.9(5)
C20	C19	C18	120.9(5)	C43	C42	C41	121.4(5)
C19	C20	C21	119.1(5)	C44	C43	C42	118.6(5)
C20	C21	N3	119.4(4)	C43	C44	N6	119.0(5)
C20	C21	C22	121.3(5)	C43	C44	C45	122.0(5)

C22	C21	N3	119.4(4)	C45	C44	N6	119.0(4)
C23	C22	C21	118.8(5)	C44	C45	C46	118.8(5)
C22	C23	C18	121.3(5)	C45	C46	C41	120.8(5)

Table 6 Hydrogen Bonds for **409**.

D	H	A	d(D-H)/Å	d(H-A)/Å	d(D-A)/Å	D-H-A/°
N1	H1N	O2	0.88	2.04	2.888(6)	161.7
N2	H2N	O1	0.88	2.00	2.799(6)	149.7
N4	H4	O6	0.88	2.00	2.814(6)	154.1
N5	H5	O5	0.88	2.06	2.889(5)	157.2

Table 7 Hydrogen Atom Coordinates ($Å \times 10^4$) and Isotropic Displacement Parameters ($Å^2 \times 10^3$) for **409**.

Atom	*x*	*y*	*z*	U(eq)
H1N	829	3185	2401	40
H2N	-711	2231	4648	32
H2A1	595	4306	1422	97
H2A2	779	3783	652	97
H2A3	1872	3650	1302	97
H3A1	-1377	1892	1378	101
H3A2	-1214	2599	670	101
H3A3	-1451	3211	1404	101
H4A1	1981	1693	1264	90
H4A2	946	1631	580	90
H4A3	734	951	1293	90
H2B1	1711	3946	1362	97
H2B2	1768	3189	664	97
H2B3	2558	2848	1405	97
H3B1	-1315	2769	1284	101
H3B2	-658	3191	598	101
H3B3	-535	3903	1323	101
H4B1	1359	989	1234	80
H4B2	600	1491	525	80
H4B3	-162	1018	1158	80
H5A	206	1014	2367	33
H7	1403	3160	3393	25
H9	-1862	4087	4118	29

H111	-766	-305	2947	43(10)
H112	-220	-932	3665	43(10)
H113	729	-527	3102	43(10)
H131	-1095	6038	2893	43(10)
H132	-1075	5880	3745	43(10)
H133	-2054	5188	3213	43(10)
H151	-3027	1171	4566	55(12)
H152	-3733	2269	4265	55(12)
H153	-4058	1752	5014	55(12)
H161	-1072	2422	6003	53(12)
H162	-1394	1267	5610	53(12)
H163	-2405	1829	6081	53(12)
H171	-3328	4034	4870	36(10)
H172	-2161	4181	5475	36(10)
H173	-3441	3595	5669	36(10)
H19	1011	4152	4864	26
H20	2495	4196	5865	28
H22	3905	1255	5273	27
H23	2472	1257	4249	25
H4	3938	6116	1343	29
H5	5888	2941	2398	34
H251	1386	6044	768	71
H252	2379	6835	425	71
H253	1057	7322	634	71
H261	3584	8178	1116	67
H262	3565	8279	1968	67
H263	2410	8760	1443	67
H271	956	6316	1994	50
H272	774	7627	1948	50
H273	1784	7102	2546	50
H254	1002	5674	1161	71
H255	1782	6055	511	71
H256	681	6827	766	71
H264	3345	7705	688	67
H265	3345	8347	1437	67
H266	2110	8376	869	67
H274	1429	6642	2361	50
H275	1009	7781	1974	50
H276	2353	7691	2445	50

H28	3071	5708	2621	27
H30	6381	4378	2189	27
H32	4968	2451	1041	32
H341	4127	5169	3978	38(9)
H342	3994	3852	3959	38(9)
H343	3094	4595	3414	38(9)
H361	4319	4039	-475	70(14)
H362	3486	3368	49	70(14)
H363	4942	3042	0	70(14)
H381	3627	1394	2491	55(12)
H382	4607	1697	3170	55(12)
H383	4406	436	2929	55(12)
H391	6978	1572	3063	43(10)
H392	7439	1047	2347	43(10)
H393	6736	291	2889	43(10)
H401	5917	699	1289	45(10)
H402	4420	755	1357	45(10)
H403	5259	-200	1760	45(10)
H42	5735	6905	2412	26
H43	6987	8416	2172	27
H45	8538	6649	642	33
H46	7311	5122	903	32

Crystallography Data for Compound **506**

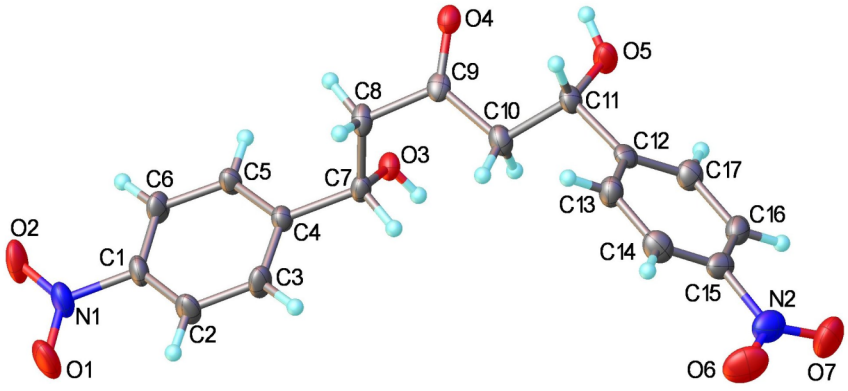

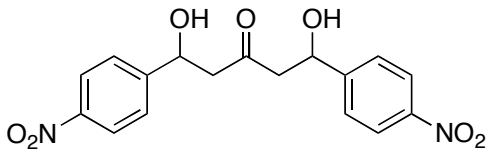

506

Table 1 Crystal data and structure refinement for **506**

Identification code	**506**
Empirical formula	$C_{17}H_{16}N_2O_7$
Formula weight	360.32
Temperature/K	120
Crystal system	monoclinic
Space group	$P2_1/n$
a/Å	4.9791(4)
b/Å	14.3266(8)
c/Å	23.4670(14)
α/°	90
β/°	93.214(6)
γ/°	90
Volume/Å^3	1671.35(19)
Z	4
ρ_{calc}mg/mm^3	1.432
m/mm^{-1}	0.113
F(000)	752.0
Crystal size/mm^3	0.43 × 0.09 × 0.07
2Θ range for data collection	5.688 to 49.996°
Index ranges	$-5 \leq h \leq 5$, $-17 \leq k \leq 17$, $-14 \leq l \leq 28$
Reflections collected	9757

Independent reflections	2467[R(int) = ?]
Data/restraints/parameters	2467/0/239
Goodness-of-fit on F^2	1.079
Final R indexes [I>=2σ (I)]	R_1 = 0.0549, wR_2 = 0.1307
Final R indexes [all data]	R_1 = 0.0780, wR_2 = 0.1420
Largest diff. peak/hole / e Å^{-3}	0.28/-0.20

Table 2 Fractional Atomic Coordinates ($\times 10^4$) and Equivalent Isotropic Displacement Parameters (Å$^2\times 10^3$) for **506**. U_{eq} is defined as 1/3 of of the trace of the orthogonalised U_{IJ} tensor.

Atom	*x*	*y*	*z*	U(eq)
O1	7391(11)	1103(3)	3061(2)	59.3(16)
O2	4745(10)	264(3)	2522.5(17)	45.3(13)
O3	4207(8)	3844(3)	566.0(15)	25.0(9)
O4	-1816(8)	5300(2)	532.2(16)	27.3(10)
O5	531(9)	6865(3)	-29.7(16)	34.3(11)
O6	8858(10)	10145(3)	1578(2)	55.3(15)
O7	9521(12)	10335(3)	684(2)	61.1(16)
N1	5896(12)	1002(3)	2639(2)	36.0(14)
N2	8389(12)	9959(4)	1070(3)	41.9(15)
C1	5370(12)	1796(4)	2254(2)	27.0(14)
C2	6403(13)	2653(4)	2414(2)	32.1(15)
C3	5913(13)	3394(4)	2049(2)	30.4(15)
C4	4446(12)	3280(4)	1537(2)	22.7(13)
C5	3426(12)	2400(4)	1391(2)	25.2(13)
C6	3872(13)	1653(4)	1756(2)	29.2(15)
C7	3892(12)	4101(4)	1141(2)	23.5(14)
C8	1042(12)	4428(4)	1180(2)	26.7(14)
C9	284(12)	5278(4)	819(2)	23.3(13)
C10	2198(13)	6093(4)	843(2)	28.2(14)
C11	959(12)	6981(4)	569(2)	25.5(13)
C12	2829(11)	7798(4)	680(2)	24.0(13)
C13	3083(13)	8178(4)	1227(2)	29.7(14)
C14	4870(13)	8889(4)	1353(3)	34.1(16)
C15	6409(12)	9223(4)	929(3)	29.5(15)
C16	6161(12)	8878(4)	379(3)	30.0(15)
C17	4358(13)	8160(4)	259(2)	29.2(14)

Table 3 Anisotropic Displacement Parameters ($Å^2 \times 10^3$) for **506**. The Anisotropic displacement factor exponent takes the form: $-2\pi^2[h^2a^{*2}U_{11}+...+2hka \times b \times U_{12}]$

Atom	U_{11}	U_{22}	U_{33}	U_{23}	U_{13}	U_{12}
O1	82(4)	44(3)	47(3)	24(2)	-33(3)	-13(3)
O2	79(4)	17(2)	39(3)	9.4(18)	-7(3)	-6(2)
O3	27(2)	22(2)	26(2)	7.3(16)	2.1(18)	-2.6(18)
O4	28(2)	20(2)	34(2)	5.9(17)	2(2)	-1.3(18)
O5	46(3)	25(2)	30(2)	6.3(17)	-11(2)	-13(2)
O6	55(3)	50(3)	60(3)	-24(3)	-8(3)	-15(3)
O7	68(4)	42(3)	73(4)	14(3)	-7(3)	-29(3)
N1	54(4)	23(3)	30(3)	10(2)	-8(3)	-3(3)
N2	39(4)	22(3)	63(4)	-2(3)	-6(3)	-3(3)
C1	36(4)	19(3)	25(3)	9(2)	-1(3)	0(3)
C2	46(4)	26(3)	23(3)	4(2)	-13(3)	-7(3)
C3	44(4)	16(3)	30(3)	1(2)	-6(3)	-10(3)
C4	26(3)	15(3)	26(3)	4(2)	-3(3)	-1(2)
C5	33(3)	17(3)	24(3)	3(2)	-8(3)	-4(3)
C6	41(4)	13(3)	34(3)	1(2)	-3(3)	-5(3)
C7	31(4)	17(3)	23(3)	3(2)	-3(3)	-7(3)
C8	34(4)	17(3)	29(3)	5(2)	8(3)	2(3)
C9	25(4)	17(3)	28(3)	1(2)	9(3)	4(3)
C10	36(4)	21(3)	27(3)	4(2)	-1(3)	2(3)
C11	30(3)	16(3)	31(3)	4(2)	-2(3)	2(3)
C12	23(3)	16(3)	32(3)	4(2)	-5(3)	5(2)
C13	36(4)	24(3)	30(3)	4(3)	0(3)	-4(3)
C14	44(4)	24(3)	33(3)	-3(3)	-6(3)	1(3)
C15	28(4)	15(3)	44(4)	-1(3)	-7(3)	0(3)
C16	29(4)	21(3)	40(4)	7(3)	1(3)	0(3)
C17	36(4)	19(3)	32(3)	-1(3)	-1(3)	0(3)

Table 4 Bond Lengths for **506**.

Atom	Atom	Length/Å	Atom	Atom	Length/Å
O1	N1	1.214(6)	C4	C7	1.515(7)
O2	N1	1.227(6)	C5	C6	1.381(7)
O3	C7	1.417(6)	C7	C8	1.502(9)

O4	C9	1.212(7)	C8	C9	1.518(7)
O5	C11	1.419(6)	C9	C10	1.507(8)
O6	N2	1.232(7)	C10	C11	1.538(7)
O7	N2	1.220(7)	C11	C12	1.509(8)
N1	C1	1.466(7)	C12	C13	1.392(8)
N2	C15	1.468(8)	C12	C17	1.383(8)
C1	C2	1.375(8)	C13	C14	1.374(8)
C1	C6	1.366(8)	C14	C15	1.375(9)
C2	C3	1.379(8)	C15	C16	1.381(8)
C3	C4	1.379(8)	C16	C17	1.385(8)
C4	C5	1.394(7)			

Table 5 Bond Angles for **506**.

Atom	Atom	Atom	Angle/°	Atom	Atom	Atom	Angle/°
O1	N1	O2	122.8(5)	C7	C8	C9	115.0(5)
O1	N1	C1	119.4(5)	O4	C9	C8	120.7(5)
O2	N1	C1	117.9(5)	O4	C9	C10	121.6(5)
O6	N2	C15	117.5(6)	C10	C9	C8	117.7(5)
O7	N2	O6	123.6(6)	C9	C10	C11	112.8(5)
O7	N2	C15	118.9(6)	O5	C11	C10	110.5(4)
C2	C1	N1	118.2(5)	O5	C11	C12	108.6(4)
C6	C1	N1	118.7(5)	C12	C11	C10	109.9(5)
C6	C1	C2	123.0(5)	C13	C12	C11	119.1(5)
C1	C2	C3	117.9(5)	C17	C12	C11	121.7(5)
C2	C3	C4	121.1(5)	C17	C12	C13	119.2(5)
C3	C4	C5	119.3(5)	C14	C13	C12	120.9(6)
C3	C4	C7	120.7(5)	C13	C14	C15	118.8(6)
C5	C4	C7	120.0(5)	C14	C15	N2	118.8(6)
C6	C5	C4	120.3(5)	C14	C15	C16	121.8(6)
C1	C6	C5	118.4(5)	C16	C15	N2	119.4(6)
O3	C7	C4	110.9(4)	C15	C16	C17	118.7(6)
O3	C7	C8	107.1(4)	C12	C17	C16	120.6(5)
C8	C7	C4	110.2(5)				

Table 6 Hydrogen Bonds for **506**.

D	H	A	d(D-H)/Å	d(H-A)/Å	d(D-A)/Å	D-H-A/°
O3	H3	O4[1]	0.77	2.22	2.881(5)	144.6
O5	H5	O3[2]	0.84	2.00	2.801(6)	158.9

[1]1+X,+Y,+Z; [2]-X,1-Y,-Z

Table 7 Hydrogen Atom Coordinates (Å×10^4) and Isotropic Displacement Parameters (Å^2×10^3) for **506**.

Atom	*x*	*y*	*z*	U(eq)
H3	5511	4059	466	38
H5	-990	6626	-103	51
H2	7422	2731	2765	39
H3A	6596	3994	2151	37
H5A	2420	2314	1039	30
H6	3155	1055	1663	35
H7	5156	4622	1250	28
H8A	742	4575	1584	32
H8B	-182	3909	1063	32
H10A	3829	5924	643	34
H10B	2756	6225	1246	34
H11	-800	7113	739	31
H13	2007	7942	1516	36
H14	5039	9145	1727	41
H16	7207	9129	90	36
H17	4170	7913	-117	35